The Cell Biology Of Tetherin Antagonism By HIV-1 Vpu

Kueck, Tonya

Awarding institution:
King's College London

The Cell Biology Of Tetherin Antagonism By HIV-1 Vpu

Tonya Kueck

A thesis submitted to the University of London for the degree of Doctor of Philosophy

Department of Infectious Diseases

King's College London

School of Medicine

Declaration

I, Tonya Kueck, confirm that the work presented in this thesis is my own. Where information has been derived from other sources, I confirm that this has been indicated in the thesis.

3rd March 2014

Tonya Kueck

Für Mama und Papa

Abstract

The HIV-1 accessory protein Vpu counteracts the restriction factor tetherin, and induces its cell surface downregulation and ubiquitin-dependent endosomal degradation.

We have identified an acidic/dileucine based-sorting determinant, **E**xxx**LV**, in the second alpha helix of the Vpu cytoplasmic tail as being required for efficient tetherin antagonism. Mutation of this motif prevents tetherin degradation and downregulation, but not Vpu/tetherin interaction. This effect is similar to Vpu phospho-mutants, which are unable to recruit the SCF-β-TrCP E3 ubiquitin ligase complex. However, **E**xxx**LV** mutants are able to bind to β-TrCP and ESCRT-0 component HRS. Tetherin and **E**xxx**LV** mutants accumulate at the cell surface and in early endosomes implying that post-binding trafficking of Vpu/tetherin complexes is required to prevent tetherin transit to viral assembly sites on the plasma membrane. Our preliminary data shows that the **E**xxx**LV** motif interacts with the trafficking machinery via the clathrin adaptor AP-1 in a manner that is dependent on the tyrosine-based sorting signal in tetherin, although functional redundancy in clathrin trafficking pathways cannot yet rule out other adaptor proteins being involved.

A study performed in our laboratory examined the variation of *vpu* alleles in HIV-1 infection, and identified several variants in which isoleucine residues in the first alpha helix of the cytoplasmic tail were mutated. We show that these isoleucine mutants were defective for inducing tetherin degradation, despite being capable of interacting with tetherin, thus pheno-copying **E**xxx**LV** and phospho-mutants. However, unlike both these mutants, isoleucine mutants fail to interact with HRS, which is required for Vpu-mediated tetherin degradation and antagonism.

Vpu **E**xxx**LV**, isoleucine and phospho-mutants share localisation defects, in which they accumulate at the plasma membrane and in early endosomes. Interestingly, tetherin antagonism, in all of these mutants, can be rescued by C-terminal addition of a clathrin-binding motif. This implies that these mutants might be defective for the same reason: they fail to interact with the clathrin trafficking machinery. Further experiments that will elucidate this hypothesis are underway.

Table of Contents

Table of Figures

Table of Tables

Table of Abbreviations

6HB	Six-helix bundle
AAA ATPase	ATPase-associated with various cellular activities
ADCC	Antibody-dependent cell-mediated cytotoxicity
AGS	Aicardi-Goutières syndrome
AICD	Activation-induced cell death
AIDS	Acquired immunodeficiency syndrome
ALIX	Apoptosis-linked gene-2-interacting protein X
Amp	Ampicillin
AMSH	Associated molecular with SH3 domain of STAM
AP	Adaptor protein
APCs	Antigen-presenting cells
APOBEC3	Apolipoprotein B messenger RNA (mRNA)-editing enzyme catalytic polypeptide-like 3
APS	Ammonium persulfate
Arf	ADP ribosylation factor
ARF	ADP-ribosylation factors 6
ATCC	American Type Culture Collection
ATM	Ataxia-telangiectasia-mutated kinase
ATR	ATM and Rad3-related kinase
AZT	Azidothymidine
BAF	Barrier to auto-integration factor
BFA	Brefeldin A
BGH	Bovine Growth Hormone
BioID	Proximity dependent biotin identification
BirA	Biotin ligase
Bro1	BCK1-like resistance to osmotic shock protein-1
BROX	BRO1 domain and CAAX motif-containing protein
BST-2	Bone marrow stromal cell antigen 2
C-HR	Carboxyl terminal helical region
C-terminal	Carboxyl-terminus
CA	Capsid
CB	Clathrin box
CCD	Catalytic core domain
CCR5	CC chemokine receptor type 5
CCV	Clathrin-coated vesicles
CDK7	Cyclin-dependent kinase 7
CEP55	Centrosomal protein 55kDa
cGAS	Cyclic guanosine monophosphate-adenosine monophosphate (cGAMP) synthase
CHC	Clathrin heavy chain
CHMPs	Charged multivesicular body proteins
CLC	Clathrin light chain
CPSF6	Cleavage and polyadenylation specificity factor subunit 6
CTD	Carboxyl-terminal domain
CTL	Cytotoxic T cell
CXCR4	CXC chemokine receptor type 4
CycT1	Cyclin T1
DCs	Dendritic cells

DMSO	Dulbecco's modified Eagle medium
dNTP	Deoxynucleotide triphosphates
dsDNA	Double stranded DNA
DSIF	DRB sensitivity-inducing factor
DTT	Dithiothreitol
DUBs	Deubiquitinating enzymes
DUIM	Double-sided ubiquitin-interacting motif
E. coli	*Escherichia coli*
EBOV	Ebola virus
ECL	Enhanced chemiluminescence
EDTA	Ethylenediaminetetraacetic acid
EEA1	Early endosome antigen 1
EGF	Epidermal growth factor
EGFR	Epidermal growth factor receptor
eIF	Eukaryotic initiation factor
EM	Electron microscope
Env	Envelope
ER	Endoplasmic reticulum
ERAD	Endoplasmic reticulum-associated protein degradation
ESCRT	Endosomal sorting complex required for transport
F-MuLV	Friend Murine Leukemia Virus
FIV	Feline immunodeficiency virus
Fv-1	Friend virus susceptibility factor-1
FYVE	Fab-1, YGL023, VPS27 and EEA1
GAE	Gamma adaptin ear domain
GALT	Gut-associated lymphoid tissue
GAS	γ-interferon activation site
GAT	GGA and TOM1 domain
GGA	Gamma adaptin ear-containing, ARF-binding
GLUE	GRAM- like ubiquitin-binding in Eap45
gM	Envelope glycoprotein M
GP	Envelope glycoprotein
GPI	Glycosyl-phosphatidylinositol
gRNA	Genomic RNA
HAART	Highly active antiretroviral therapy
HCHO	Formaldehyde
HCMV	Human cytomegalovirus
HDPTP	His domain phosphotyrosine phosphatase
HIV-1	Human immunodeficiency virus type 1
HIV-2	Human immunodeficiency virus type 2
HMGA1	High-mobility group protein A1
HRP	Horseradish peroxidase
HRS	Hepatocyte growth factor- regulated tyrosine kinase substrate
HRV14	Human rhinovirus 14
Hsp90	Heat shock protein 90
HSV-1	Herpes simplex virus 1
Hygrom	Hygromycin
IAV	Influenza A virus
IFI16	IFN-inducible protein 16

IFN	Interferon
ILT7	Immunoglobulin-like transcript 7
ILV	Intraluminal vesicles
IN	Integrase
INR	Initiator
INSTI	Integrase strand transfer inhibitor
IP	Immunoprecipitation
IRES	Internal ribosome entry site
IRF	Interferon regulatory factor
IRF-E	IFN regulatory factor elements
ISG	Interferon stimulatory genes
ISRE	Interferon-stimulated response element
IST1	Increased salt tolerance-1
KIR	Killer immunoglobulin-like receptors
KIR2DL2	Killer immunoglobulin-like receptor, two domains, long cytoplasmic tail, 2
KSHV	Kaposi's sarcoma-associated herpesvirus
L-domain	Late domain
LB	Laemmli buffer
LB	Luria-Bertani
LEDGF	Lens epithelium-derived growth factor
LTR	Long terminal repeat
MA	Matrix
MARV	Marburg virus
MFI	Median fluorescence intensity
MHC	Major histocompatibility complex
MIM	MIT-interacting motif
MIT	Microtubule interacting and trafficking
MITD1	MIT-domain-containing-protein 1
MLV	Murine leukemia virus
Mo-MLV	Moloney Murine Leukemia virus
MOI	Multiplicity of infection
mRNA	Messenger RNA
MVBs	Multivesicular bodies
MX2	Myxovirus resistance 2
N-HR	Amino terminal helical region
NA	Neuraminidase
NC	Nucleocapsid
Nef	Negative factor
NELF	Negative elongation factor
NEM	N-Ethylmaleimide
NES	Nuclear export signal
NF-AT	Nuclear factor of activated T cells
NF-κB	Nuclear factor-κB
NFAT	Nuclear factor of activated T cells
NIS	Nuclear inhibitory signal
NK cells	Natural killer cells
NKT cells	Natural killer T cells
NLRs	Nucleotide oligomerisation domain (NOD)-like receptors

NLS	Nuclear localisation signal
nM	Nanomolar
NNRTI	Non-nucleoside reverse transcriptase inhibitor
NPC	Nuclear pore complexes
NRTI	Nucleoside reverse transcriptase inhibitor
NTB-A	NK-T and B cell antigen
NTD	Amino-terminal domain
Nup	Nucleoporin
P-TEFb	Positive transcription elongation factor b
PAMP	Pathogen-associated molecular pattern
PBMCs	Peripheral blood mononuclear cells
PBS	Primer-binding site
PBS	Phosphate buffered saline
PCE	Posttranscriptional element
PCR	Polymerase Chain Reaction
pDCs	Plasmacytoid dendritic cells
PEI	Polyethylenimine
PIC	Pre-integration complex
PM	Plasma membrane
PPT	Polyurine tract
PR	Protease
PrP	Prion protein
PRR	Pattern recognition receptor
PtdIns(3)P	Endosomal lipid phosphatidylinositol 3-phosphate
PtdIns(4,5)P_2	Phosphatidylinositol 4,5-bisphosphate
Purom	Puromycin
R	Repeat element
RHPN1	Rhophilin 1
RIG-I	Retinoid-inducible gene I
RLRs	Retinoic acid-inducible gene 1 (RIG-I)-like receptors
RLU	Relative light units
RNA Pol II	RNA polymerase II
RPMI	Roswell Park Memorial Institute medium
RRE	Rev responsive element
RT	Reverse transcriptase
RTC	Reverse transcription complex
SAM	Sterile alpha motif
SAMHD1	SAM domain HD domain-containing protein 1
SCF	Skp1-Cullin1-F-Box
SCF^{TrCP}	Skp1-Cullin1-F-Box' (SCF) β-TrCP complex
SDS	Sodium dodecyl sulfate
SFV	Semliki Forest virus
SH3	Src homology-3 domain
shRNA	Small hairpin RNA
siRNA	Small interfering RNA
SIV	Simian immunodeficiency virus
SLAM	Signalling lymphocytic activation molecule
SNX	Sorting nexins
SOUBA	Solenoid of overlapping UBA

SP1	Specificity protein 1
SPG11	Spastic paraplegia 11
SSE	Structure-specific endonuclease
ssRNA	Single stranded RNA
STAM1/2	Signal transducing adaptor molecule 1/2
STAT	Signal transducer and activator of transcription
STING	Stimulator of interferon genes
SU	Surface
TAF	TBP-associated factor
TAR	Transactivation-response region
Tat	Transactivating factor
TCR	T cell receptor
TD	Terminal domain
TEMED	N,N,N′,N′-Tetramethylethylenediamine
TFIIH	Transactivation factor II H
TGN	Trans-Golgi network
TLRs	Toll-like receptors
TM	Transmembrane
TNPO3	Transportin 3
TREX1	Three prime repair exonuclease 1
tRNA	Transfer RNA
TSG101	Tumour susceptibility gene 101
U3	3’ untranslated region
U5	5’ untranslated region
UBA	Ubiquitin-associated
UBAP1	Ubiquitin-associated protein 1
UBPY	Ubiquitin isopeptidase Y
UEV	Ubiquitin E2 variant
UIM	Ubiquitin-interacting motif
UMA	UBAP1-MVB12-associated
VHS	VPS27, HRS and STAM
Vhs	Virion host shut-off protein
Vif	Viral infectivity factor
VLP	Virus-like particle
Vpr	Viral protein R
vps	Vacuolar protein sorting genes
VPS	Vacuolar protein sorting-associated protein 4
Vpu	Viral protein U
VS	Virological synapse
VSV-G	Vesicular stomatitis virus G glycoprotein

Acknowledgements

Thank you to my supervisor **Stuart Neil** for giving me the opportunity to work in such an outstanding lab, for advice whenever I needed it, and for reading this thesis. I've thoroughly enjoyed my time in the lab and learned an awful lot. I look forward to working with you in the nearby future.

Suzy - thank you for always taking the time to help and reading this thesis even during your holidays. You were always happy to answer my countless questions even when you were in the middle of an experiment.

Rui or MacGyver - thank you for being a good neighbour and always being there when I needed your personal as well as scientific advise.

Rafa and **Anna** - despite moving back to France we always stayed in contact, you gave me constructive advice throughout my thesis research and taught me how to be a scientist, for that I am greatly thankful.

Julia - thank you for reminding me that there is a world outside the lab.

Tosh - I enjoyed learning a lot about purifications of recombinant proteins from you. I appreciate that you got us out of the lab and onto the gym floor with a big smile and a lot of energy.

To members of the lab: **Greg**, **Max**, **Jonny**, **Pedro** and **Harry**.

Anne - I couldn't have asked for a better person to meet during the first week of our BSc. I still can't believe that you have left London already and started to work in Vancouver. I hope that some day we will live in the same city or at least country again but we always have Skype.

Joao - For putting up with me during the past 3 months, you never once complained about the paper invasion of our living room, instead you were always there when I needed someone to talk to, even at 6am in the morning. You always took very good care of me during stressful times and I'm very grateful for that.

Mama, **Papa**, **Benjamin** and **Vincent** - I couldn't have done it without your endless support, you were my biggest supporters during the past years and therefore I like to dedicate this thesis to you.

Chapter 1 INTRODUCTION

1.1 HIV-1: the pandemic

1.1.1 HIV/AIDS in context

Acquired immunodeficiency syndrome (AIDS) was first described in 1981 among young homosexual men that presented with unusual opportunistic infections (Gottlieb et al., 1981). Subsequently the human immunodeficiency virus type 1 (HIV-1) was identified as the causative agent of AIDS, which has turned into the most destructive infectious disease worldwide since its discovery more than 30 years ago. In 2008, Luc Montagnier and Françoise Barré-Sinoussi received the Nobel Prize in Physiology and Medicine for the discovery of HIV.

HIV is transmitted through the exchange of bodily fluids including blood, breast milk, semen and vaginal secretions. The most common form of acquiring HIV among adults (approximately 80%) is through sexual transmission. Since the start of the HIV pandemic 75 million people have been infected, with a total number of individuals living with HIV worldwide approximately 35.3 million at the end of 2012 (Figure 1-1). Despite the decrease in new HIV infections and AIDS-related deaths that has been observed in recent years, there are still 2-3 million new infections annually, 30% of them in children. Highly active antiretroviral therapy (HAART) is widely accessible in developed countries (approximately 9.7 million individuals are currently on HAART), which has reduced the number of AIDS-related deaths tremendously. However, even more than 30 years after the discovery of HIV there is no curative treatment, consequently, the HIV/AIDS pandemic will continue to be a threat for decades to come (Source: “2013 Global Report Epidemiology Slides”, obtained from the UNAIDS).

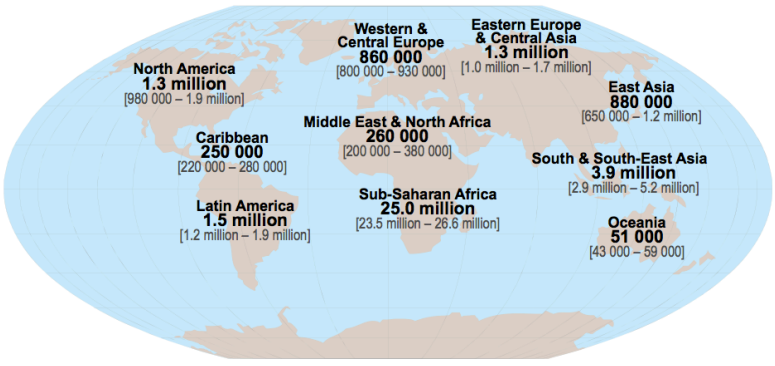

Total: 35.3 million [32.2 million – 38.8 million]

Figure 1-1 HIV global epidemic in numbers

World map displays number of people (adults and children) estimated to be living with HIV in different geographical areas at the end of 2012. The worldwide number of HIV infected individuals is about 35.3 million. Source: “2013 Global Report Epidemiology Slides”, obtained from the UNAIDS.

1.2 HIV-1 genome and structure

The *Retroviridae* are a large viral family of enveloped viruses that store their nucleic acid in the form of positive stranded RNA, and share common features such as: structure, genomic organisation and replication properties. Retroviruses encode reverse transcriptase (RT), which converts the genomic RNA (gRNA) into double-stranded DNA (dsDNA) that is integrated into the host genome by another virally encoded enzyme, integrase (IN). The genus Lentivirus belongs to the family of *Retroviridae*. Lentiviruses are associated with long incubation times and the cause of slow progressive diseases that result in severe immunological or neurological dysfunction (reviewed by (Swanson and Malim, 2008)).

The HIV proviral DNA is approximately 9.7 kb. It is constituted of non-coding sequences that control gene expression as well as protein synthesis, and encodes nine viral genes, including *gag*, *pol* and *env* genes common to all replicating retroviruses (see Figure 1-2). Flanking the retroviral provirus are the long terminal repeats (LTRs). The 5' LTR is a promoter that initiates transcription of the viral genome, while the 3' LTR is important for the polyadenylation signal (poly(A) tail). The *pol* gene encodes three enzymes: reverse transcriptase, which transcribes viral RNA into DNA; IN, which mediates insertion of the DNA template into the host genome to establish the provirus; and protease (PR), which is responsible for maturation into fully infectious virus particles. The HIV genome also encodes two structural genes, *gag* and *env*. The Gag polyprotein is cleaved by PR, resulting in the production of the three main structural proteins: matrix (MA), capsid (CA) and nucleocapsid (NC) (reviewed by (Swanson and Malim, 2008)). The *env* gene encodes two glycoproteins, called surface (SU) gp120 and transmembrane (TM) gp41 subunits. The gp120 protein possesses a high affinity for the CD4 receptor present on the plasma membrane of HIV-1 target cells. Upon binding of gp120 to CD4, a conformational change in the Env spike takes place that allows binding to the co-receptor CCR5 or CXCR4, and in turn activates the fusion mechanism (reviewed by (Wilen et al., 2012)).

In addition to Gag, Pol and Env proteins, HIV also encodes six additional regulatory/ accessory genes: *tat*, *rev*, *vif*, *vpr*, *vpu* and *nef*. The regulatory Tat protein interacts with cellular proteins and binds to the TAR (*trans*-activation response) sequence in the viral RNA to stimulate and promote viral transcriptional elongation. Rev interacts with the Rev responsive element (RRE), a *cis*-acting sequence located in the *env* gene, allowing efficient nuclear export of unspliced and partially spliced viral messenger RNA. The accessory proteins Vif, Vpr, Vpu and Nef regulate innate and adaptive immune functions (reviewed by (Swanson and Malim, 2008)).

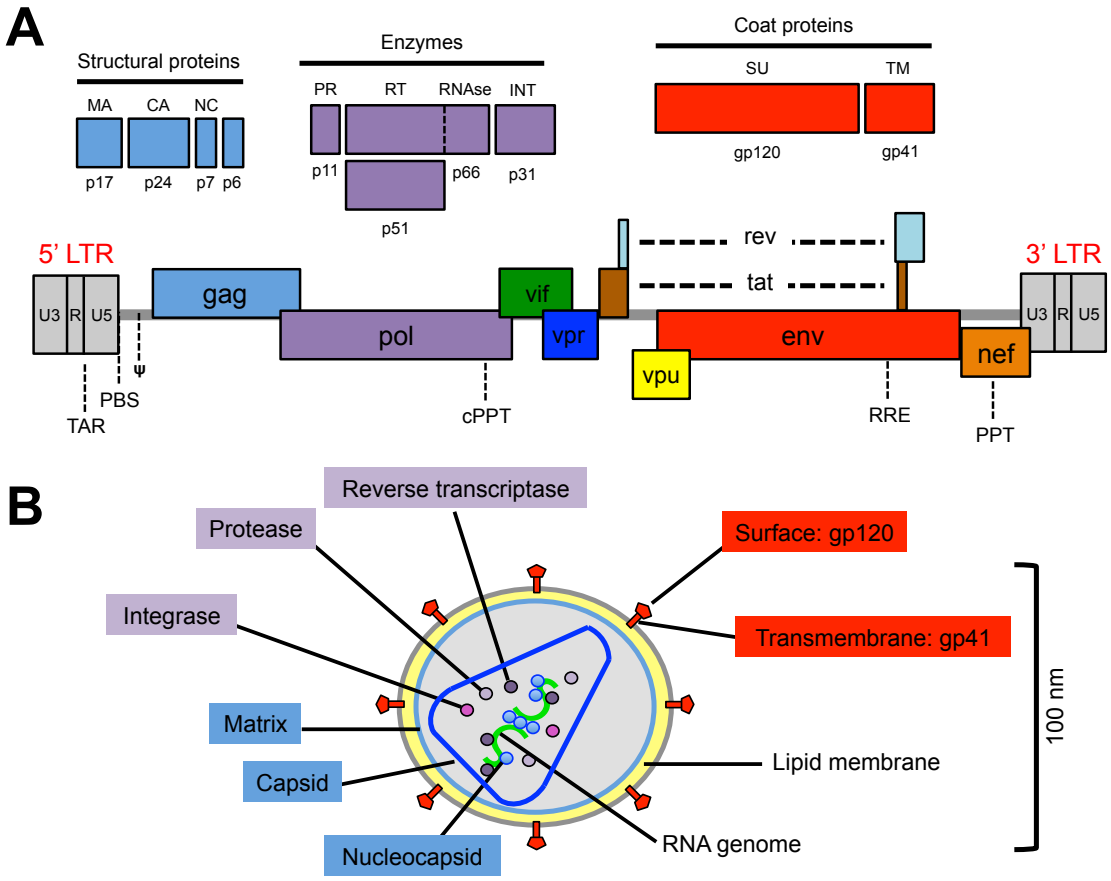

Figure 1-2 Organisation of the HIV-1 proviral genome and virus particle

(A) Schematic representation of the proviral HIV-1 genome. Depicted are the nine open reading frames of HIV-1: *gag*, *pol*, *vif*, *vpr*, *tat*, *rev*, *vpu*, *env* and *nef*. Abbreviations: LTR (long terminal repeat), U5 (5' untranslated region), R (repeat element), U3 (3' untranslated region), MA (matrix), CA (capsid), NC (nucleocapsid), PR (protease), RT (reverse transcriptase), IN (integrase), SU (surface), TM (transmembrane), TAT (*trans*-activator of transcription), ψ (packaging signal), PBS (primer-binding site for tRNA3 (Lys)), RRE (rev response element), PPT (polypurine tract). **(B)** Schematic representation of the HIV-1 virus particle.

The HIV-1 virion is about 100 nm in size and contains two copies of the positive-stranded RNA genome. RNA and RT are enclosed and protected by the core NC protein that in turn is surrounded by the conical shaped CA, which also encloses PR and IN enzymes. The viral CA on the other hand is surrounded by the MA protein, which is connected to the envelope formed from the host cell's lipid bilayer membrane (see Figure 1-2B) (reviewed by (Sundquist and Kräusslich, 2012)).

1.3 HIV-1 replication cycle

The HIV replication cycle can be divided into two parts, the “early” and “late” stages. The early stage encompasses virus entry until integration into the host cell genome, while the late stage occurs from integration of the provirus until viral release and formation of a fully infectious virus particle (see Figure 1-3).

Briefly, HIV predominantly infects CD4-positive T cells through interactions between the viral envelope protein gp120 with cellular CD4 and co-receptors CXC chemokine receptor type 4 (CXCR4) or CC chemokine receptor type 5 (CCR5), leading to membrane fusion-mediated by gp41, which induces release of the viral core into the cytoplasm. The core protects the two copies of single-stranded positive sense RNA genomes, tRNA primers and the viral enzymes IN, PR and RT. Once in the cytoplasm the reverse transcription complex (RTC) mediates reverse transcription of the viral RNA genome into double-stranded cDNA. This results in the formation of the pre-integration complex (PIC), which contains matrix protein p17 and/or capsid protein p24, linear double-stranded DNA, viral IN, RT, accessory protein Vpr and a number of host cell-derived proteins. The virus uses microtubules for retrograde transport, which is dependent on dynein to position itself at the nuclear pore. The pre-integration complex initiates transport into the nucleus followed by integration into the host cell genome through the activity of the host chromatin-binding protein lens epithelium-derived growth factor (LEDGF), or formation of LTR-containing double stranded DNA circles (reviewed by (Coiras et al., 2009) and (Engelman and Cherepanov, 2012)).

Transcription is regulated by the recruitment of host cell transcription factors nuclear factor-κB (NF-κB) and specificity protein 1 (SP1) that initiate the recruitment and binding of the host RNA polymerase II (RNA Pol II) to the TATA box, located at the 5’ LTR, to initiate mRNA transcription. Through the formation of secondary RNA structure, transcription forms the *trans*-activation response element (TAR) that is used by the viral Tat protein to ensure efficient elongation by recruiting the positive transcription elongation factor b (P-TEFb). Viral mRNA is processed by the viral Rev protein, which also regulates nuclear export of spliced mRNA. HIV proteins are then synthesised and processed in the cellular cytoplasm. Subsequently, HIV-1 virions assemble at the host cell plasma membrane, which is followed by budding and maturation of virus particles into their fully infectious form (reviewed by (Coiras et al., 2009) and (Engelman and Cherepanov, 2012)).

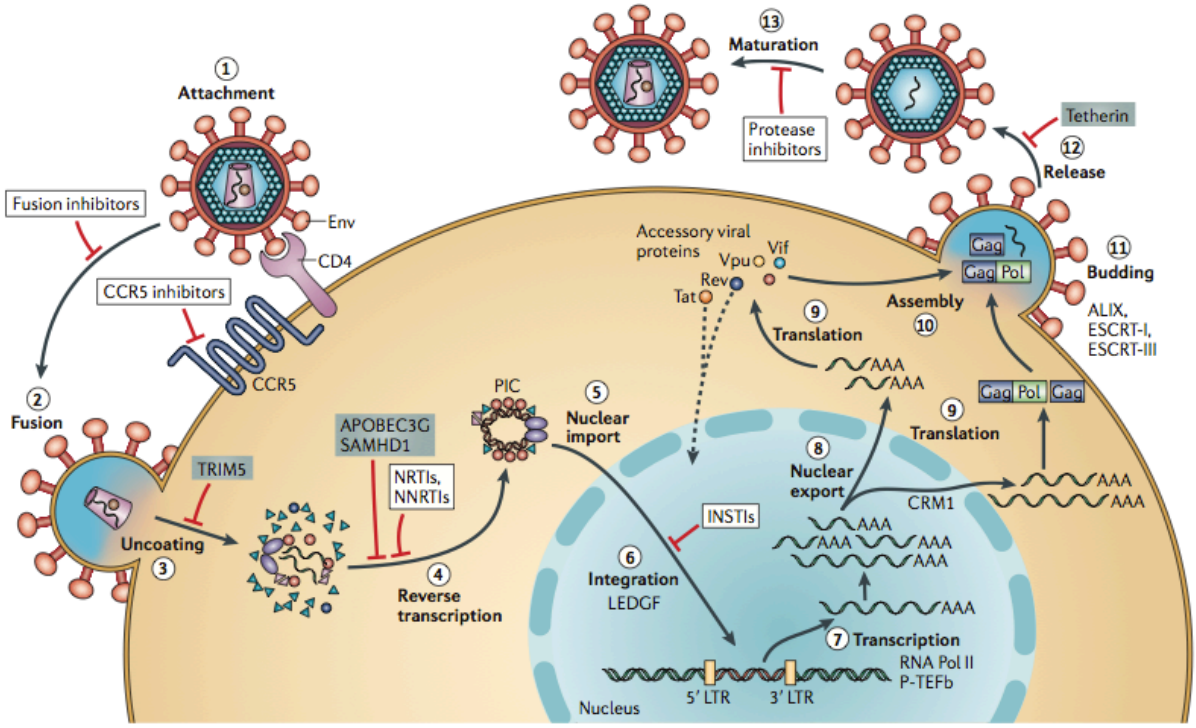

Figure 1-3 The HIV-1 replication cycle

Schematic representation of the HIV-1 replication cycle. **(Step 1)** The viral replication cycle begins with binding of the viral Env coat protein to the cellular CD4 receptor and the co-receptor CCR5 (or CXCR4 not indicated). **(Step 2)** Binding leads to fusion of the virion membrane with the host membrane and entry of the viral core into the cytoplasm. **(Step 3 and 4)** The viral core is uncoated which leads to reverse transcription of the viral RNA into DNA. **(Step 5)** Formation of the pre-integration complex (PIC) leads to nuclear import. **(Step 6)** The viral enzyme integrase mediates formation of the integrated provirus into the host genome with the help of the host chromatin-binding protein lens epithelium-derived growth factor (LEDGF). **(Step 7)** Proviral transcription is mediated by host RNA polymerase II (RNA Pol II) and positive transcription elongation factor b (P-TEFb), resulting in viral mRNAs of different sizes. **(Step 8)** Large viral mRNAs require energy mediated nuclear export by host protein Crm1. **(Step 9)** Viral mRNA serves as template for protein translation. **(Step 10)** Viral proteins and full length genomic RNA is packaged into virus particle at the host cell membrane. **(Step 11)** Budding of the virus is mediated by interaction of Gag with the ESCRT abscission machinery. **(Step 12)** Viral release. **(Step 13)** Maturation of virion into a fully infectious virus particle by viral protease. HIV restriction factor TRIM5, APOBEC3G, SAMHD1 and tetherin (boxed in blue) that act at various stages in the viral lifecycle are indicated. Antiretroviral small molecule inhibitors are indicated (boxed in white) at their site of action. Abbreviations: nucleoside reverse transcriptase inhibitor (NRTI), non-nucleoside reverse transcriptase inhibitor (NNRTI), integrase strand transfer inhibitor (INSTI) (adapted from (Engelman and Cherepanov, 2012)).

1.3.1 Host cell binding and virus entry

The first step in the HIV-1 replication cycle is cell attachment and entry into the host cell. This mechanism plays an important role in determining viral tropism and the ability of HIV to destroy the host immune system. Even before the actual discovery of the HIV virus, Gottlieb and colleagues reported the decline in CD4-positive T cells in four male homosexual patients who presented with unusual opportunistic infections. A few years after the initial observation it was demonstrated that HIV preferentially infects CD4-positive T cells (Dalgleish et al., 1984) (Klatzmann et al., 1984), that CD4 was able to bind to the viral Env protein in co-immunoprecipitation studies (McDougal et al., 1986), and that non-permissive cells could be infected by exogenous expression of CD4 (Maddon et al., 1986).

First, the HIV particle attaches to the host cell membrane, a process that is relatively nonspecific. The viral envelope protein itself or a host transmembrane protein within the virus particle membrane can mediate binding to target cell attachment factors. Attachment factors for the viral envelope protein include the negatively charged heparin sulphate proteoglycans (Saphire et al., 2001) or the $\alpha 4\beta 7$ integrin, resulting in a more specific interaction (Arthos et al., 2008) (Cicala et al., 2009). Nonetheless, attachment factors are not essential for viral replication and their role *in vivo* remains unclear.

The first essential step of virus entry is the binding of the viral Env protein to CD4, its initial host receptor (Kwong et al., 1998). CD4 is a member of the immunoglobulin superfamily and its physiological role is to enhance T cell receptor (TCR)-mediated signalling. The HIV envelope spike is made up of trimers of surface glycoprotein gp120 and transmembrane glycoprotein gp41 that form non-covalently linked heterodimers. The surface gp120 protein subunit is made up of five relatively conserved domains (C1-C5) and five variable regions (V1-V5); where the first four variable regions form loops that contain disulphide bonds at their bases. Variable regions, especially V3, play a major role in immune evasion and co-receptor binding. Upon binding of Env to CD4 a conformational rearrangement of the variable loops V1/V2 and consequently V3 occurs, leading to the formation of the bridging sheet (Kwong et al., 1998) that allows co-receptor binding.

HIV and related viruses have been shown to engage different chemokine receptors, predominately CCR5 (viruses using this receptor are termed R5 tropic) or CXCR4 (viruses using this receptor are termed X4 tropic), but, some viruses can use both co-receptors (termed R5X4 tropic). Co-receptor binding to gp120 leads to the insertion of the hydrophobic fusion peptide, located at the amino terminus of transmembrane gp41 envelope protein, into the target cell membrane (reviewed by (Wilen et al., 2012)).

Insertion of the fusion peptide into the host cell membrane effectively crosslinks viral and host membranes. This initiates folding of each gp41 subunit, bringing the amino terminal helical region (N-HR) and the carboxyl terminal helical region (C-HR) of gp41 together, which results in the formation of a six-helix bundle (6HB) (Chan et al., 1997). Formation of the 6HB brings the two membranes into close proximity, resulting in the formation of a fusion pore and release of the viral core into the host cell cytoplasm (reviewed by (Wilen et al., 2012) and (Melikyan, 2008)).

After the entry mechanism had been solved successfully, research concentrated on the movement of viral particles to sites where efficient entry can occur. HIV virions are thought to travel along the surface of target cells, hijacking cellular transport machineries to reach specific destinations that make entry more effective. For example, some viruses, including HIV, have been shown to travel from distant attachment sites to regions of the cell body in close proximity to the nucleus, where virus entry is thought to be most efficient (Lehmann et al., 2005) (Sherer et al., 2010).

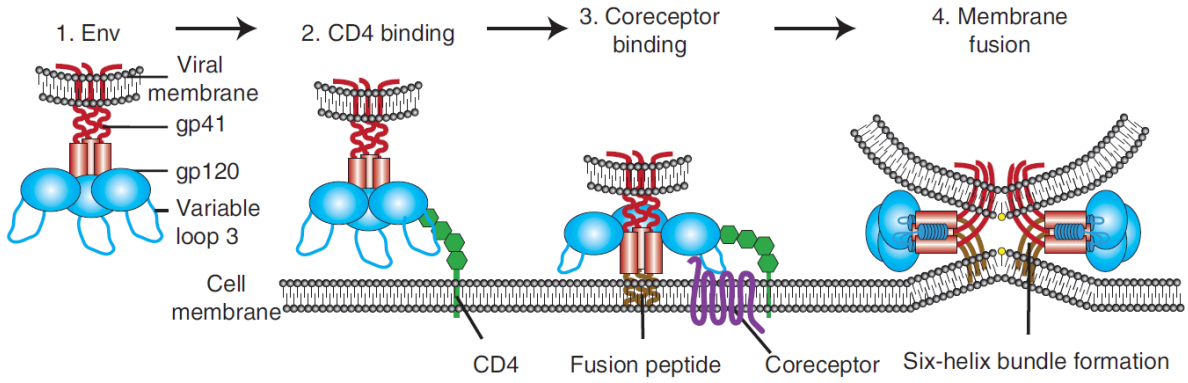

Figure 1-4 Mechanism of HIV-1 entry

Schematic representation of HIV entry. **(1)** HIV-1 Env is made up of gp120 (SU) that contains variable loops and gp41 (TM). **(2)** The gp120 protein binds to host membrane protein CD4, initiating a conformational change in Env. **(3)** This allows co-receptor binding which is facilitated by the variable loop 3 region and insertion of the gp41 fusion peptide into the host membrane. **(4)** Formation of the six-helix bundle and membrane fusion (adapted from (Wilen et al., 2012)).

1.3.2 Reverse transcription

Once the particle has fused with the target cell membrane and released its viral core into the cytoplasm, the single stranded RNA (ssRNA) genome serves as a template for the formation of double stranded DNA (dsDNA). Once integrated into the host chromosome, the viral dsDNA is translated into mRNAs coding for viral proteins and full-length single stranded RNA HIV genome, which together form new HIV particles. In 1975, Howard Temin and David Baltimore received the Nobel Prize in Physiology and Medicine for their discovery of a specific enzyme in RNA tumour viruses that could make DNA out of an RNA copy; this enzyme was later termed reverse transcriptase (RT). The transcription of viral ssRNA into dsDNA is a common feature for all retroviruses and is mediated by the virally encoded enzyme RT in combination with cellular factors. RT has been the subject of extensive study and is a major target for anti-retroviral therapy; the first anti-HIV drug approved was AZT which targets RT (reviewed by (Hu and Hughes, 2012)).

RT is produced from the Gag-Pol polyprotein through cleavage by the viral enzyme PR. The active HIV-1 RT enzyme forms a heterodimer composed of two related subunits: p66 and p51, derived by cleavage of p66 between Phe440 and Tyr441 by PR. The p66 subunit contains both DNA polymerase and RNase H activities (reviewed by (Hu and Hughes, 2012) and (Le Grice, 2012)). The DNA polymerase domain is composed of subdomains that are analogous to a human right hand, containing fingers, palm and a thumb that are connected by subdomains (Kohlstaedt et al., 1992). The same four subdomains in the p55 subunit are folded differently, providing a structural support for the p66 catalytic subunit during tRNA-primed initiation of RT (reviewed by (Le Grice, 2012)).

The mechanism of conversion of the viral ssRNA genome into integration-competent linear dsDNA is well understood, as only purified RT and the HIV RNA genome are required for successful DNA synthesis *in vitro*. However, the mechanism that mediates viral replication is more complicated and involves both cellular and viral elements. The separable steps of HIV DNA synthesis by RT are summarised in a simplified, schematic diagram in Figure 1-5.

To initiate the reverse transcription process, the host cellular-derived tRNA3 (Lys), which is packaged in the virus, whose 3' end (18 nucleotides) is complementary to the primer-binding site (PBS) near the 5' end of the RNA genome, hybridises to the PBS. DNA is then synthesised by RT, creating an RNA-DNA duplex that is targeted for degradation by the RNase H activity of RT, exposing the newly formed minus strand DNA. The long terminal repeats that flank the genomic viral RNA contain identical

direct repeats, called R. The 3' R repeat serves as binding site for the minus strand DNA. After transfer of this strand, synthesis of minus-stranded DNA continues along the entire length of the genomic RNA template, while RNase H degrades the positive-stranded RNA. There are two purine-rich sequences in the HIV genome, polypurine tracts (PPT), where the RNA cannot be degraded by RNase H and serve as primers for the initiation of positive strand DNA synthesis. However, only the 3' PPT and not the central PPT is essential for viral replication. Positive DNA synthesis along the minus strand DNA also leads to the synthesis of the first 18 nucleotides of the transfer (tRNA) Lys3 primer, which is followed by the cleavage of the tRNA one nucleotide away from the 3' terminus, resulting in a single A ribonucleotide appendix. Once the DNA synthesis of the minus-stranded DNA is completed, a second plus strand DNA transfer occurs, in which the PBS from the 3' end anneals to the PBS at the 5' end and DNA synthesis continues on both DNA strands until it is completed, resulting in the synthesis of the complete double-stranded linear viral DNA (reviewed by (Hu and Hughes, 2012) and (Le Grice, 2012)).

Where and when reverse transcription is initiated *in vivo* has been a matter of debate for some time. Some evidence suggests that reverse transcription starts in producer cells through initiation by a small number of nucleotides before the virus particle infects its target cell (Whitcomb et al., 1990). However, the entire double strand DNA synthesis cannot take place in virions due to a limited supply of dNTPs (deoxynucleotide triphosphates) (Lori et al., 1992) (Trono, 1992). Therefore, it is commonly accepted that most of the DNA synthesis takes place in newly infected cells during early stages of the viral replication cycle. DNA synthesis *in vivo* occurs in the reverse transcription complex (RTC) that contains MA, CA, NC, IN and the viral accessory protein Vpr (reviewed by (Hu and Hughes, 2012)). The RTC is the target for cellular restriction factors that are discussed in section 1.5, and the role of Vpr in section 1.5.4. CA and IN proteins provide the structural stability of the RTC. CA might also play a role in transport of the RTC along microtubules to the nuclear pore and in nuclear import (Dismuke and Aiken, 2006) (Lee et al., 2010). The NC protein has been shown to possess nucleic acid chaperone activity, is thought to help RT to overcome secondary structures and assists during the strand transfer process (reviewed by (Hu and Hughes, 2012)).

The structure of the RTC has not yet been solved and the mechanism behind uncoating has been a matter debate. One hypothesis is that uncoating occurs continuously, while the RTC complex changes and DNA synthesis takes place until the PIC has been formed (Forshey et al., 2002) (reviewed by (Craigie and Bushman, 2012)). Another hypothesis is that the viral core remains intact until DNA synthesis has

been completed, providing a confined environment for the RT reaction to take place in. This would direct the RTC towards the nuclear compartment by moving along the microtubule network until the pre-integration complex (PIC) has been formed and penetrated the nuclear membrane (reviewed by (Arhel, 2010)).

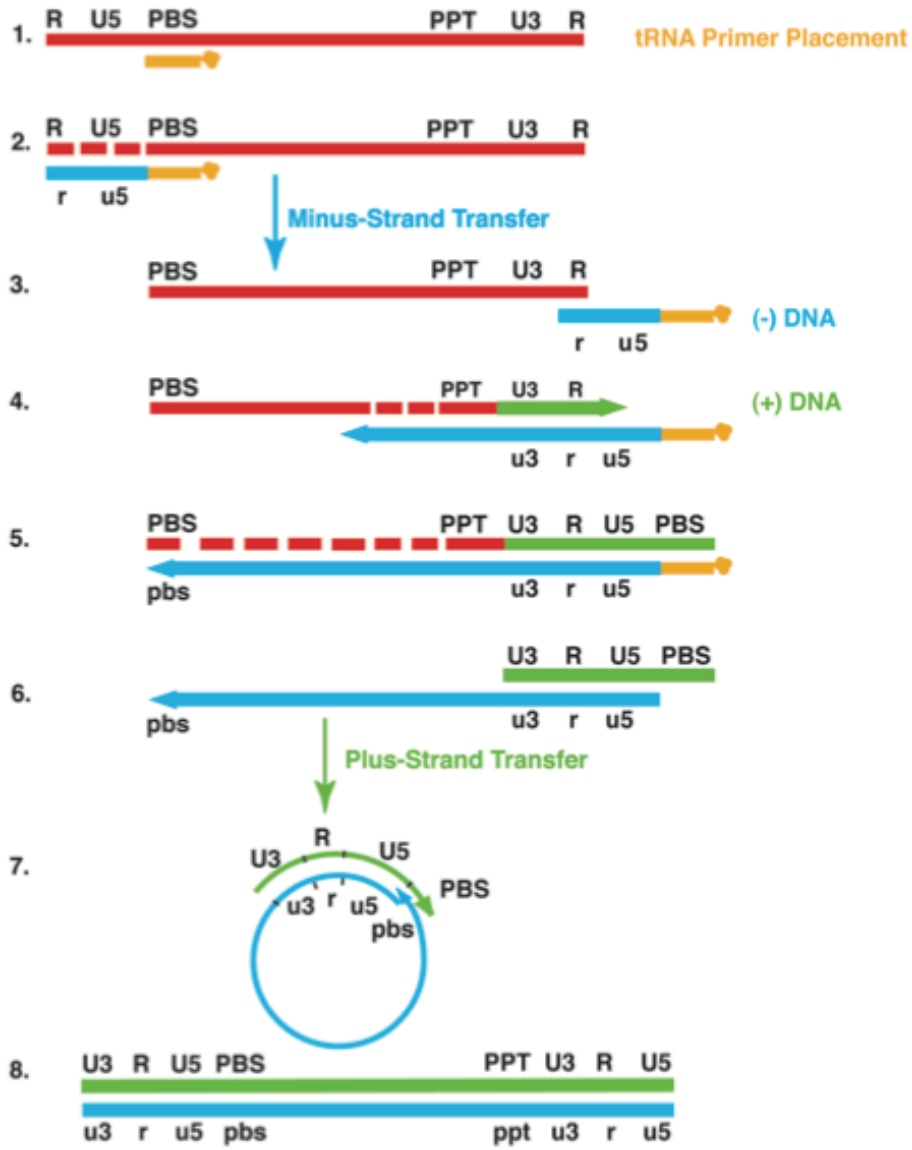

Figure 1-5 Mechanism of conversion of viral single-stranded RNA to double stranded DNA

Simplified schematic representation of the HIV reverse transcription mechanism. **(1)** Reverse transcription is initiated by annealing of the tRNA3 (LYS) primer to the 18 nucleotide overlapping PBS site near the 5' end of the viral positive-strand RNA. Reverse transcriptase starts to catalyse synthesis of negative-strand DNA. **(2)** RNase H activity of RT degrades the positive ssRNA that has been reverse transcribed. **(3)** Minus-strand transfer. **(4)** Elongation of the minus-strand DNA and positive-strand RNA degradation by RNase H resume. The PPT region cannot be degraded by RNase H, and serves as a primer to initiate plus-strand DNA synthesis. **(5)** RT copies the u3, u5 and r regions of the minus-strand DNA, including the tRNA3 (Lys) primer and therefor reconstituting the PBS. **(6)** PPT primers and tRNA3 (Lys) removal by RNase H. **(7)** Plus-strand transfer and circularisation of the two DNA strands. **(8)** Minus- and plus-strand DNA elongation, resulting in a linear dsDNA with a long terminal repeat (LTR) at each end. Viral genomic RNA is shown in red, minus-stranded DNA in blue, plus-strand DNA is shown in green. The tRNA3 (Lys) primer is represented in orange and attached to a 'clover-leaf'. Short red rectangles represent fragments produced by RNase H cleavage of viral genomic RNA (adapted from (Levin et al., 2010)).

1.3.3 Nuclear entry and integration

Once reverse transcription is completed, the linear double-stranded viral DNA associates with IN, and other viral and cellular proteins to form the pre-integration complex (PIC). Lentiviruses are able to replicate in non-dividing cells, which is dependent on the CA protein (Yamashita and Emerman, 2004). Therefore the PIC must be transported through nuclear pores into the nucleus using an active form of transport. However, the exact mechanism is still unclear. Viral components involved in nuclear import have been subject to much debate (reviewed by (Fassati, 2012)). Viral proteins RT, MA, NC and Vpr can be found in PICs in addition to viral DNA and IN. However, none of these proteins was shown to play a specific role in nuclear entry. Cellular proteins can also be packed into PICs or bind to CA directly. Cellular components associated with PICs include LEDGF, which stimulates targeted integration into the host chromosome; high-mobility group protein A1 (HMGA1), which stimulates IN activity; and barrier to auto-integration factor (BAF) a suppressor of auto-integration (reviewed by (Fassati, 2012) and (Craigie and Bushman, 2012)). Since both viral and cellular proteins have been described to play a role in active nuclear import, nuclear import mechanisms might be redundant, or viruses might be are able to hijack different nuclear import pathways.

Several genome-wide siRNA screens have been performed to identify cellular genes that are important for viral replication (Brass et al., 2008) (König et al., 2008). These have identified transportin 3 (TNPO3) and nucleoporins (Nup) 358 and 153 as important for nuclear entry and integration. TNPO3 is a member of the importin β family that serve as nuclear import and export receptors, of which the direction is determined by interaction with RanGTP. TNPO3 mainly affects post-nuclear import steps, and as such is thought to bind to CA and to mediate its nuclear export (Zhou et al., 2011) (De Iaco and Luban, 2011). Nup358 is part of the NPC and contains a Cyp-domain and forms long filaments that protrude into the cytoplasm. The HIV-1 CA protein has been shown to bind the Cyp-domain of Nup358, and Nup358 knockdown results in HIV nuclear import defects (Schaller et al., 2011). Furthermore, the capsid mutant N74, selected by passaging HIV-1 in the presence of dominant negative form of the splicing factor CPSF6, determined the ability of CA to use TNPO3, Nup153 and to some extent Nup358 for nuclear import (Lee et al., 2012). However, knockdown of Nup153 had an evident effect on integration and only a small effect on nuclear import (Matreyek and Engelman, 2011). Nonetheless, the N74 CA mutant is thought to induce premature uncoating, making it unable to interact with Nup153, TNPO3 and Nup358 (reviewed by (Fassati, 2012)). Furthermore, recent data demonstrated that the N74 CA mutant induces type I IFN production through the activation of a cGAS and STING-dependent

innate signalling cascade, suggesting that CPSF6/CA binding is required to cloak HIV replication and to allow evasion of innate immune sensors (Rasaiyaah et al., 2013).

Once inside the nucleus, the viral enzyme IN mediates integration (Figure 1-6) into the host DNA genome. The HIV-1 IN protein is encoded by the Gag-Pol polyprotein and is generated during virion maturation by cleavage of Gag-Pol, which is catalysed by HIV PR. IN is made up of three structural domains: the amino-terminal domain (NTD), the catalytic core domain (CCD) and the carboxyl-terminal domain (CTD) (reviewed by (Craigie and Bushman, 2012)).

During the mechanism of integration, IN removes nucleotides from the 3' end of the viral linear dsDNA in order to generate reactive 3′-hydroxyl groups at both ends. The 3′-hydroxyl ends of the viral DNA will then ligate to the host DNA by binding to a pair of phosphodiester bonds, which are located on different host cell DNA strands, 5 nucleotides apart from each other. This step results in integration intermediates. Completion of integration requires trimming of the last two nucleotides of the 5' viral DNA end and extension from the 3' end of the genomic DNA. The identity of the cellular enzymes required for these processes is still unknown (reviewed by (Craigie and Bushman, 2012)).

With genome-wide high-throughput sequencing becoming broadly available, HIV integration sites have been studied in many different acutely infected cell types, demonstrating that the HIV-1 provirus preferably integrates in active transcription units that are favourable for efficient transcription (Schröder et al., 2002) (Mitchell et al., 2004) (Wang et al., 2007). It is possible that cellular host proteins, such as the cellular transcription factor LEDGF, play an important role in the selection of integration sites within transcribing genes. LEDGF was first identified as a cellular protein that was able to bind tightly to HIV IN using an affinity-based screen (Cherepanov et al., 2003). LEDGF localises to the nucleus and contains a chromatin binding domain, an A/T hook important for DNA binding, and a carboxyl-terminal domain that is responsible for IN interaction (reviewed by (Craigie and Bushman, 2012)). Only a complete depletion of LEDGF results in a decrease of infectivity caused by inhibition of selective integration, as even minute levels of LEDGF can promote integration (Llano et al., 2006). The model for LEDGF-mediated HIV-1 integration is that LEDGF binding to IN tethers the PICs to chromatin at active transcription units, directing integration to a nearby genomic locus.

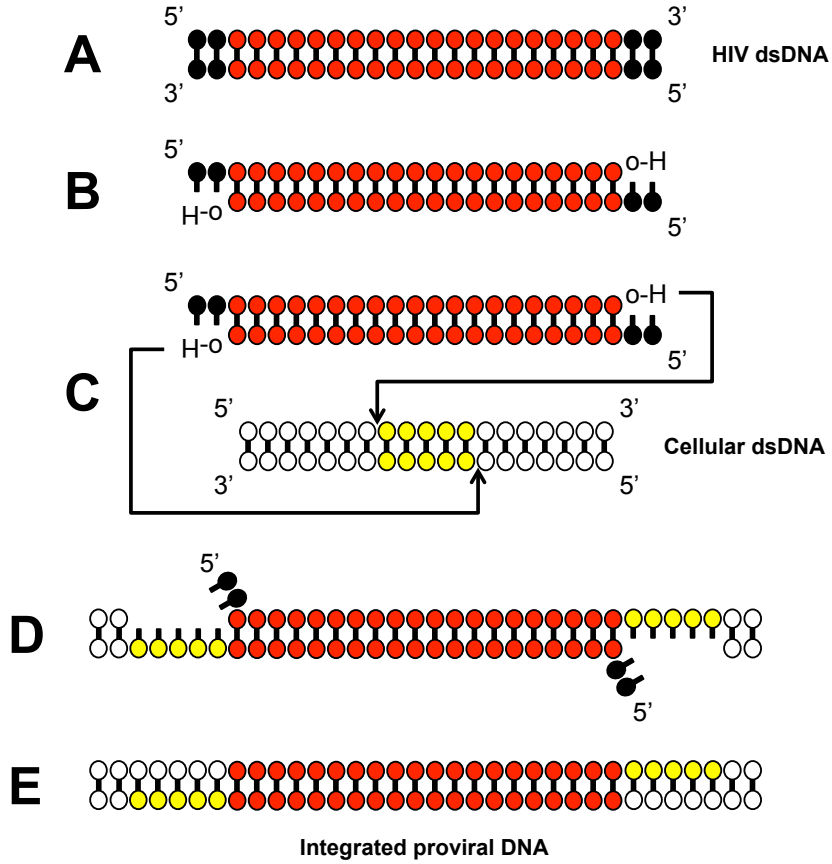

Figure 1-6 HIV-1 provirus integration into target cell chromosome

Schematic representation of the HIV-1 provirus integration process. **(A)** HIV-1 proviral dsDNA. **(B)** IN catalyses 3' terminus processing, generating reactive 3′-hydroxyl groups at both ends of the viral DNA. **(C)** Strand transfer is mediated by the two 3′-hydroxyl viral DNA ends ligating with the host DNA. **(D)** Strand transfer results in a five-base, single-stranded gap and a two-base overhang at the 5′-ends of the viral DNA. **(E)** 5' trimming and DNA repair by cellular repair enzymes.

1.3.4 Transcription and nuclear export

After integration into the host cell genome, the HIV-1 provirus acts like a host gene. Viral mRNA transcription is initiated at the 5' LTR, which contains DNA regulatory elements that serve as binding sites for cellular transcription factors.

The core LTR promoter acts as an extremely efficient transcription initiator and contains several distal (upstream) DNA regulatory elements which mediate binding to cellular transcription initiation factors (Rittner et al., 1995). The core of the LTR promoter is optimally designed for cooperative binding of cellular transcription elements and is comprised of three tandem SP1 binding sites (Jones et al., 1986), a TATA box (Garcia et al., 1989) and a highly active initiator (INR) sequence (Zenzie-Gregory et al., 1993). The additional non-core promoter elements include the transactivation-response region (TAR) and an enhancer region that includes two NF-κB binding motifs (Nabel and Baltimore, 1987), that can interact with both the NF-κB family (Liu et al., 1992) and nuclear factor of activated T cells (NFAT) (Kinoshita et al., 1998), coupling transcription to T cell activation. Furthermore, core promoter elements are important for the binding of multiple subunit transcription factor complexes that contain DNA-helicase and CTD-kinase activities.

During transcription initiation, RNA polymerase II (RNAP II) is recruited to the 5' LTR by transcription factors IID and IIH (TFIID and TFIIH respectively), as well as the co-factor TBP-associated factor (TAF) (Figure 1-7). RNAP II then clears the promoter and starts transcribing along the viral genome. Cyclin-dependent kinase 7 (CDK7) is part of the TFIIH complex and mediates partial phosphorylation of the carboxyl-terminal domain of RNAP II. The partially phosphorylated RNAP II pauses at the transactivation response element (TAR) that forms a highly stable RNA stem-loop. Binding of the negative elongation factor (NELF), which contains an RNA-recognition motif to the stem in TAR, and recruitment of DRB sensitivity-inducing factor (DSIF), ensures that RNAP II does not elongate further (reviewed by (Karn and Stoltzfus, 2012) and (Yankulov and Bentley, 1998)). Next, a larger complex is formed that includes elongation factors such as ELL2, which enhances transcription elongation by preventing RNAP II backtracking.

Although the viral LTR promoter can initiate transcription efficiently, it fails to promote elongation of transcripts due to the low processing capacity of RNAP II. Therefore, in the absence of the viral transcription activator Tat, most viral transcripts terminate prematurely at different positions throughout the proviral genome. The role of Tat is to stimulate RNAP II processivity by causing an increase of transcripts that extend until the 3′ end of the provirus. To this end, Sodroski and co-workers were the first to demonstrate that the 5' LTR serves as an inducible promoter that is dependent on HIV

Tat. Deletion studies of the LTR revealed that Tat function requires TAR (Sodroski et al., 1985a) (Sodroski et al., 1985b). Furthermore, Tat recognises TAR as an RNA element and recruits components of the positive acting elongation factor (P-TEFb) complex. This P-TEFb complex contains the cyclin T1 (CycT1) component that enhances Tat binding to TAR and also recruits the cyclin-dependent kinase 9 (CDK9) to form a stable complex (Marshall et al., 1996) (Wei et al., 1998). After the recruitment of the P-TEFb complex, CDK9 mediates phosphorylation of the elongation suppressor Spt5 in DSIF, converting it into a positive elongation factor, and of NELF, which subsequently dissociates from TAR. CDK9 also completes the phosphorylation of the CTD of RNAP II, thereby modifying RNAP II so that it can bind elongation factors, such as capping enzymes, splicing apparatus and polyadenylation factors, to mediate efficient elongation and viral replication (reviewed by (Karn and Stoltzfus, 2012)and (Yankulov and Bentley, 1998)).

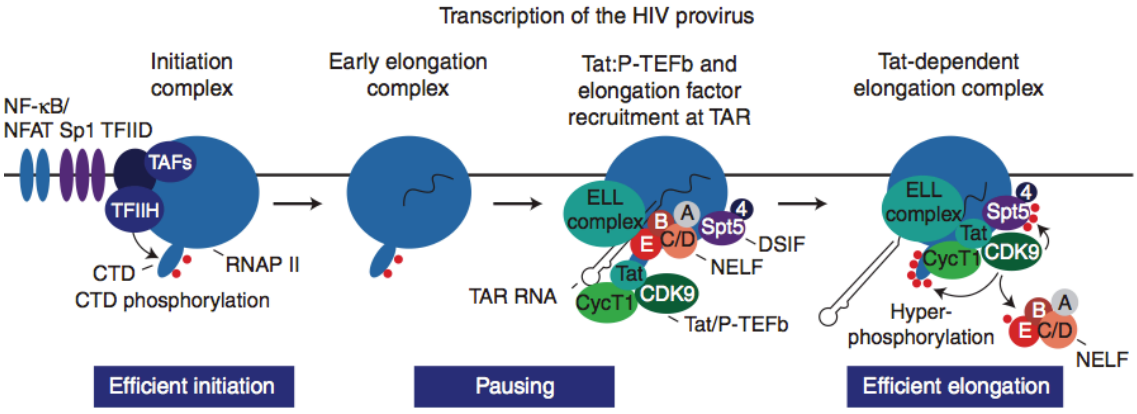

Figure 1-7 HIV-1 transactivation by Tat

Initiation: RNAP II is recruited to the 5' LTR by TFIID, TFIIH and cofactor TAF. The CDK7 subunit of TFIIH mediates phosphorylation of the CTD of RNAP II and elongation is initiated. **Pausing:** After transcription through the TAR element, NELF and DSIF are recruited to the elongation complex and interaction with TAR pauses elongation. **Elongation:** Tat/P-TEFb bind the TAR element and CDK9 induces phosphorylation of NELF that leads to its release, and phosphorylation of Spt5 and RNAP II, which allows enhanced transcription of the full-length transcript (adapted from (Karn and Stoltzfus, 2012)).

Once transcribed, viral pre-mRNA has to be processed by a large complex of cellular factors referred to as the spliceosome, to ensure production of the full range of mRNAs needed to encode all viral proteins. The spliceosome is a large macromolecular complex that contains more than 150 proteins and 5 small nuclear ribonucleoproteins (snRNPs) (U1, U2, U4/U6 ad U5). It removes introns and joins the exons of pre-mRNA, creating an obstacle for HIV-1 because most HIV proteins are translated from incompletely spliced or unspliced transcripts (reviewed by (Karn and Stoltzfus, 2012)). Upon infection, HIV first produces fully spliced ~1.8 kb messenger RNAs (mRNAs) encoding Tat, Rev and Nef proteins, followed by longer ~4 kb unspliced mRNAs encoding Env and viral accessory proteins Vif, Vpr and Vpu, and full-length transcripts that serve as genomic HIV RNA and templates for the Gag-Pol polyprotein (Kim et al., 1989) (Pomerantz et al., 1990). The role of Rev is to protect incompletely spliced and unspliced transcripts from degradation by mediating their nuclear export, achieved through interaction with the Rev-responsive element (RRE), a highly structural RNA element in the HIV *env* gene (Sodroski et al., 1986) (Malim et al., 1989) (Figure 1-8).

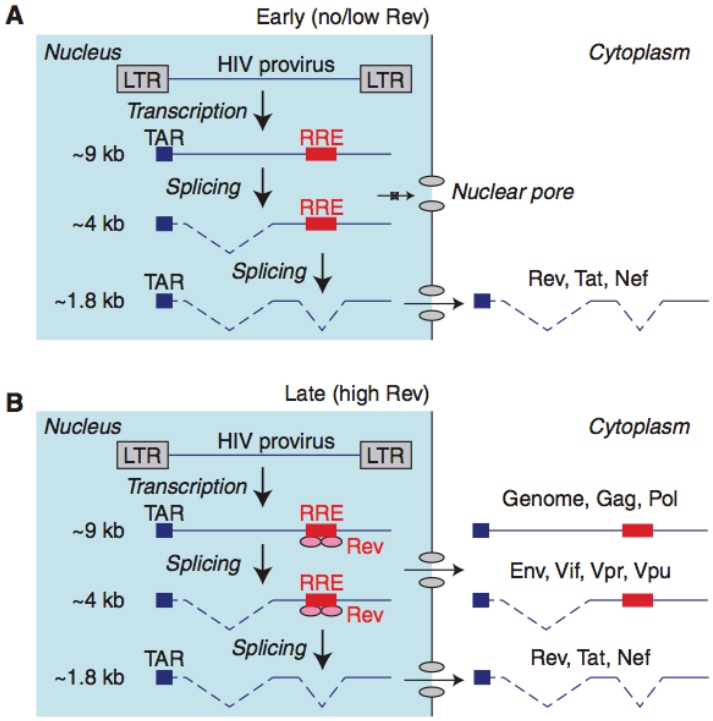

Figure 1-8 HIV-1 mRNA splicing

(A) Early phase of mRNA expression: Only the completely spliced ~1.8 kb mRNA encoding *Tat*, *Rev* and *Nef* is exported into the cytoplasm by the normal nuclear export cellular pathway and translated. The unspliced ~9 kb and incompletely spliced ~4 kb mRNAs are retained in the nucleus where they undergo splicing or degradation. **(B)** Late phase of mRNA expression: When Rev concentrations in the nucleus exceed a threshold, Rev binds to the Rev-responsive element (RRE) in the *env* gene to mediate export to the cytoplasm and translation of ~9 kb and ~4 kb mRNAs (adapted from (Karn and Stoltzfus, 2012)).

Rev is a 19 kDa phosphoprotein that contains three distinct domains. An arginine-rich motif at the N-terminus serves as a nuclear localisation signal (NLS) that is responsible for Rev's nuclear localisation as well as interaction with the RNA stem loop of the RRE. An N-terminal nuclear inhibitory signal (NIS) maintains Rev distribution and activity, and a C-terminal leucine rich sequence serves as nuclear export signal (NES) that interacts with cellular proteins needed for export of viral mRNA, termed the active domain (reviewed by (Suhasini and Reddy, 2009)). Rev-mediated viral mRNA nuclear export (Figure 1-9) requires binding to the RRE, followed by cooperative binding of up to 12 additional molecules of Rev. Transport of HIV mRNA into the cytoplasm requires nuclear pore complexes (NPC), and cellular proteins Crm1 and importin-β. Crm1 interacts with the NES of mRNA-bound Rev in the presence of the GTP-bound form of Ran GTPase (Ran-GTP), bridging Rev to the NPC, which is followed by crossing of the nuclear membrane into the cytosol. The dissociation of Crm1 and Rev/RRE complexes in the cytoplasm requires hydrolysis of Ran-GTP to Ran-GDP, which is mediated by RanGAP1 and RanBP1, causing Crm1 to be released and to return to the nucleus. The NLS in Rev binds directly to the nuclear import factor, importin-β, and Ran-GDP, which mediates the release of the RRE RNA and mediates Rev transport back into the nucleus through the nuclear pore. Once inside the nucleus Ran-GDP is converted into Ran-GTP, which causes Rev to dissociate from importin-β, which returns to the cytoplasm to be imported again, while Rev is able to interact with the next RRE to repeat the transport cycle. This constant shuttling of host and viral factors in and out of the nucleus is efficient, requiring only small amounts of Rev (reviewed by (Suhasini and Reddy, 2009) and (Karn and Stoltzfus, 2012)).

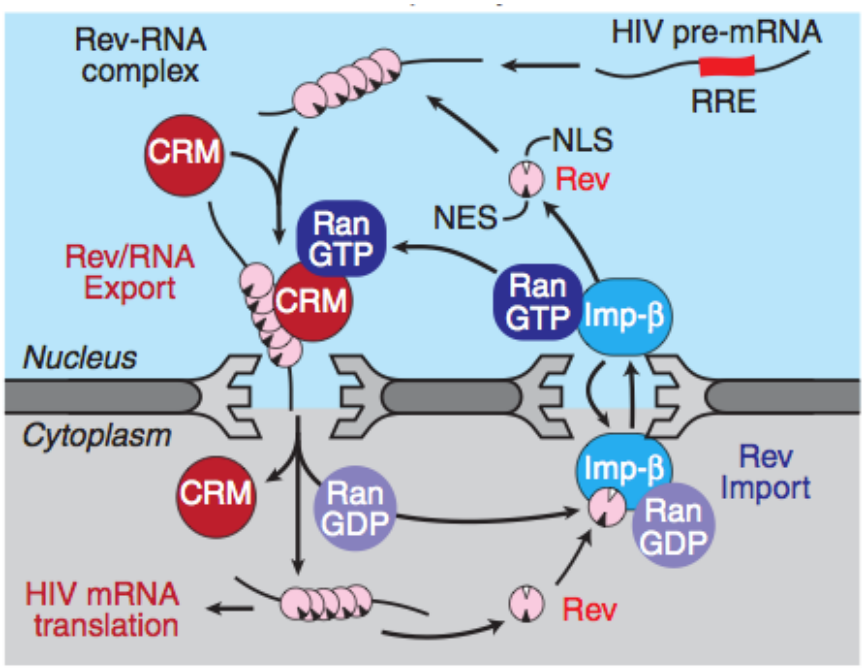

Figure 1-9 Rev-mediated nuclear export of viral mRNA

Rev binds unspliced or incompletely spliced mRNA transcripts through RRE and interacts with Crm1. This complex crosses the nuclear membrane by interaction with nuclear pore proteins. In the cytoplasm, Ran-GTP is converted into Ran-GDP leading to the release of Rev, Crm1 and viral mRNA. Crm1 is transported back into the nucleus and Rev binds to importin-β together with Ran-GDP to facilitate transport back into the nucleus. Once in the nucleus Ran-GDP is converted into Ran-GTP and Rev is released to initiate another nuclear export cycle of viral mRNA (adapted from (Karn and Stoltzfus, 2012)).

1.3.5 Protein translation and viral assembly

HIV-1 protein synthesis relies on the host cell translation machinery to provide ribosomes, tRNAs, amino acids, and initiation, elongation and termination factors. As a product of the cellular RNAP II, the 9.5 kb HIV-1 genomic RNA and all subgenomic mRNAs harbour a 7-methyl-guanosine cap at its 5' end and a poly(A) tail at its 3' terminus. Following nuclear export the genomic RNA is translated on free ribosomes in the cytoplasm of infected host cells to produce viral proteins.

HIV protein synthesis as for eukaryotic protein synthesis, may be divided into four separate phases: (1) the first phase incudes the recruitment of the small charged 43S ribosomal complex to viral mRNA, followed by scanning until it localises to an initiator AUG codon with an appropriate Kozak sequence; (2) the 60S ribosomal subunit joins the complex to form the 80S ribosomal complex, proceeding to elongation wherein the mRNA is decoded by the ribosomes that assemble the appropriate amino acids to synthesise the viral proteins; (3) once the ribosome reaches a termination codon it releases the nascent polypeptides; (4) finally, the ribosome is recycled for the next round of translation (reviewed by (de Breyne et al., 2013)).

Translation initiation is the rate-limiting step in protein synthesis. It involves multiple eukaryotic initiation factors (eIFs) and other proteins that control recruitment of the ribosome, and requires scanning until it localises the authentic AUG start codon. The HIV-1 exon 1 contains multiple highly structured regions and some upstream AUG sequences that interfere with translation initiation. Furthermore, HIV-1 *env* mRNAs are bicistronic and contain an overlapping upstream *vpu* open reading frame. To overcome these impediments two molecular mechanisms have been described, 5' cap-dependent translation initiation and internal ribosome entry sites (IRES). These circumvent inhibition of scanning ribosomes by the complex 5' UTR structure (reviewed by (de Breyne et al., 2013)). Posttranscriptional control elements (PCEs) that bind to cellular RNA binding proteins can also act as enhancers, facilitating translation initiation. For example, translation can be enhanced by the DEIH helicase RHA (Bolinger et al., 2010) as well as by the RNA binding proteins SRp40 and SRp55 (Swanson et al., 2010). Another mechanism that facilitates *env*/*vpu* translation is 5' cap-dependent ribosome shunting in which the ribosome jumps over large regions of mRNA to locate an AUG initiation codon (Krummheuer et al., 2007). To ensure translation of all viral proteins, HIV-1, like all other retroviruses, has evolved programmed frameshifting in which mRNA reading frames can be changed during translation. For instance, in HIV-1 the -1 shift in translation is required to shift from the *gag* to the *pro* and *pol* reading frame using *cis*-acting sequence elements ("slippery" sequence: UUUUUUA) upstream

of the *gag* termination codon, which occurs approximately 5% of the time (reviewed by (Karn and Stoltzfus, 2012)).

HIV-1 virion assembly occurs at the host cell membrane in specialised micro-domains, also called lipid rafts, and is entirely orchestrated by the Gag polyprotein. The roles of Gag include packaging of two copies of full length HIV-1 genomic RNA, binding to the plasma membrane, incorporating the envelope glycoprotein, and interaction with cellular host proteins to mediate formation and release of viral particles (Figure 1-10).

En route to the plasma membrane, Gag NC is responsible for the binding of two full-length viral genomic RNA (gRNA) strands that are non-covalently dimerised at their 5' UTR. gRNA binding occurs via two retroviral zinc finger motifs and several clusters of basic amino acids in NC and the RNA packaging sequence Ψ located in the 5' region, spanning the major splice donor and the Gag start codon (reviewed by (D'Souza and Summers, 2005)). These Gag/gRNA protein complexes then traffic to the plasma membrane where they oligomerise and undergo nucleate assembly (Kutluay and Bieniasz, 2010).

HIV-1 Gag and Gag-Pro-Pol polyproteins are synthesised in the host cytoplasm and trafficked to the plasma membrane using intracellular vesicle trafficking pathways, but the mechanism is still poorly understood. Gag membrane targeting is mediated by its MA domain that undergoes N-terminal myristoylation. MA interaction with the plasma membrane, by binding to phosphatidylinositol 4,5-bisphosphate (PtdIns(4,5)P_2), triggers the exposure of the myristoyl group in MA which then, leads to stabilised anchoring of Gag to the inner leaflet of the membrane (reviewed by (Martin-Serrano and Neil, 2011) and (Sundquist and Kräusslich, 2012)). In the cytoplasm, Gag molecules oligomerise poorly but when they reach the plasma membrane in association with HIV gRNA, Gag molecules are able to form high-order multimers (Kutluay and Bieniasz, 2010). The role of Gag CA domain is to stabilise the formation of the immature lattice by Gag protein-protein interactions involving the carboxyl-terminal domain of CA and the SP1 regions during virus assembly (Forshey et al., 2002).

Env proteins are synthesised in the endoplasmic reticulum (ER) and use the cellular secretory pathway to reach virus assembly domains at the plasma membrane. Env molecules are highly glycosylated, assembled into trimeric complexes and are processed by the cellular protease, of the furin family, into the transmembrane (gp41) and surface (gp120) domains. At the plasma membrane, Gag MA is also responsible for the recruitment of viral Env glycoproteins and ensures incorporation of

approximately 7 to 14 Env trimers per virion (reviewed by (Sundquist and Kräusslich, 2012)).

The Gag p6 protein plays a role in recruitment and incorporation of the accessory protein Vpr (Kondo et al., 1995) and also contains two late-budding domains that are crucial for the recruitment of the endosomal Sorting Complexes Required for Transport (ESCRT) scission machinery and subsequent virus particle release (reviewed by (Martin-Serrano and Neil, 2011)).

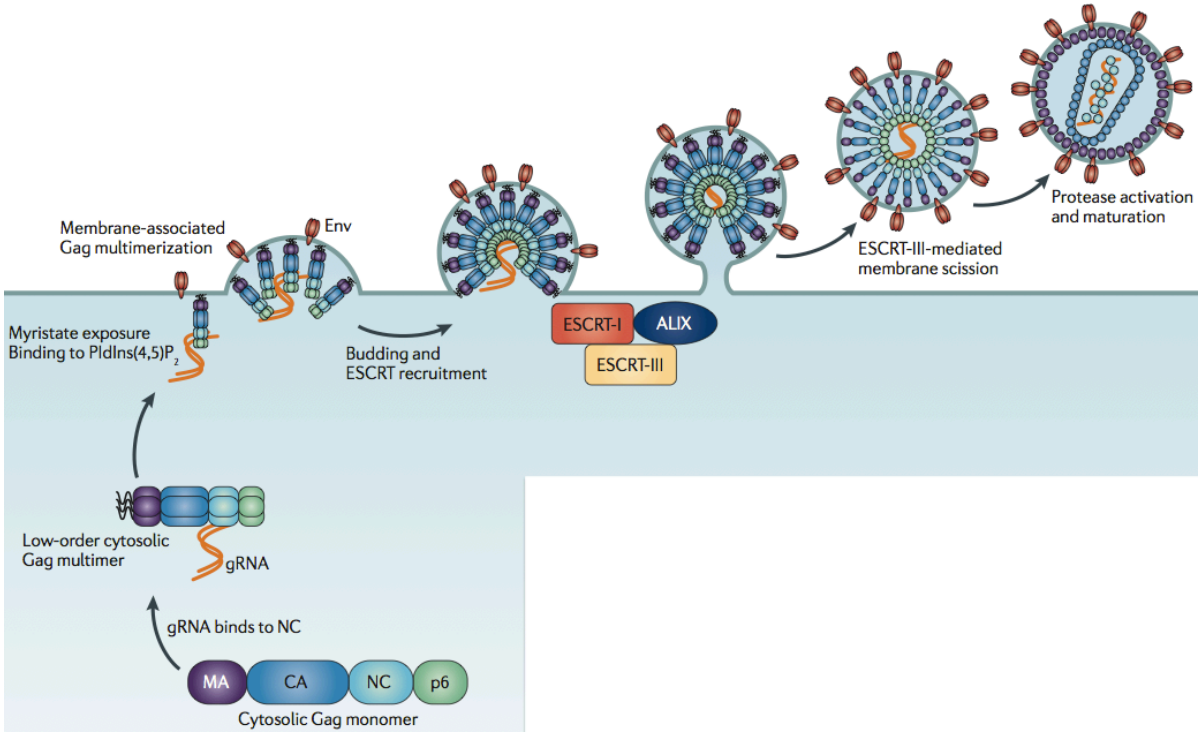

Figure 1-10 Overview of HIV-1 assembly and virus release

Schematic representation illustrating the different stages of HIV-1 assembly, release and maturation. HIV-1 Gag is synthesised in the host cell cytoplasm. Upon binding of two copies of full length HIV-1 genomic RNA, Gag molecules bind to phosphatidylinositol-4,5-bisphosphate (PtdIns(4,5)P_2 and oligomerise at the plasma membrane. The p6 domain of Gag recruits the ESCRT membrane scission machinery that resolves the membrane neck between the cell and the immature virus particle. Gag and Gag-Pol polyprotein multimerisation activates the viral protease enzyme that processes Gag into its subunits; followed by a conformational change that renders the virion fully infectious (adapted from (Martin-Serrano and Neil, 2011)).

1.3.6 HIV-1 budding and virus release

The Gag polyprotein orchestrates virion assembly and incorporation of host factors at the plasma membrane, and recruits the cellular ESCRT machinery using late-domain (L-domain) motifs in HIV-1 p6 in order to terminate Gag multimerisation and to catalyse abscission. The ESCRT machinery mediates topologically equivalent membrane scission events that include vesicle release into multivesicular bodies (MVBs) and membrane scission during cytokinesis (the ESCRT machinery is discussed in detail in 1.9). L-domains encoded by structural proteins of enveloped viruses are short amino acid motifs that are functionally interchangeable and work in a position-independent manner. L-domains are able to promote Gag ubiquitination, but proteasome inhibitors block L-domain function suggesting that ubiquitin and ubiquitin ligases play an important role in retroviral budding. Subsequent discoveries demonstrated that L-domains recruit the ESCRT machinery to mediate membrane scission events. The HIV-1 p6 protein contains two different late-domains, the primary PTAP motif which binds to tumour susceptibility gene 101 (TSG101), and the second YPXL motif which binds to the ESCRT associated factor ALIX (Figure 1-11) (reviewed by (Martin-Serrano and Neil, 2011)).

The primary **P(S/T)AP** motif (Pro-Thr/Ser-Ala-Pro) interacts with TSG101 using an extended groove on the ubiquitin E2 variant (UEV) domain of TSG101. PTAP domains can also be found within the ESCRT-0 component HRS and other related proteins that recruit the ESCRT machinery to endosomal membranes (reviewed by (Ren and Hurley, 2011)). Therefore, HIV-1 p6 mimics the PTAP late domain of a cellular ESCRT-I-recruiting protein. PTAP-dependent membrane scission requires the recruitment of ESCRT-I components VPS28, VPS37 and multivesicular body sorting factor 12 (MVB12). The mechanisms by which TSG101 and ESCRT-I components recruit the core ESCRT-III subunits (namely CHMP2 and CHMP4) and the ATPase VPS4 complexes is not fully understood, and needs to be answered for a complete understanding of HIV-1 budding (Figure 1-11).

The second late domain in HIV-1 p6 **(L)YPX$_n$L** (Tyr-Pro-X-Leu, where "X" can vary in sequence and length) binds to the ESCRT-associated factor ALIX via a conserved hydrophobic groove on arm 2 of the V-domain of ALIX dimers, and is thought to support viral budding in different cell types. In a similar manner to the PTAP domains, it mimics a host cell derived late domain to recruit ALIX. The recruitment of the core ESCRT membrane fission machinery by ALIX is well characterised and occurs through interaction of the Bro1 domain of ALIX with the amphipathic C-terminal helices of CHMP4. This interaction recruits CHMP2 proteins that in turn bind to the MIT domains of the ATPases VPS4 that provides the enzymatic activity for virus release.

Furthermore, the Bro1 domain of ALIX is also able to interact with zinc-fingers in the NC protein of HIV-1 Gag. However, depletion studies of ALIX using short interfering RNA had a minor effect on HIV-1 budding, and other cellular Bro1-containing proteins are thought to compensate by providing alternative NC interactions. Possible Bro1-containing protein candidates that promote virus release by overexpression of their respective Bro1 domains include BROX, HDPTP and rhophilin 1 (Popov et al., 2009); suggesting that Bro1 domains facilitate virus release through interaction with an unknown co-factor/s or by physical interaction with NC. Furthermore, the E3 ubiquitin ligase NEDD4-2 interacts with the carboxy-terminal domain of HIV-1 CA but contributes only modestly to HIV-1 release, suggesting in turn that NEDD4-mediated ubiquitination of Gag might facilitate the p6 L-domain-mediated recruitment of the ESCRT machinery (reviewed by (Martin-Serrano and Neil, 2011) and (Sundquist and Kräusslich, 2012)).

The ESCRT-mediated membrane deformation and abscission events have been an area of extensive research, and three different membrane fission models have been suggested: the spiral, tube and dome models, of which the dome model is the most accepted mechanism of membrane scission. In this model, L-domains in p6 recruit the ESCRT-III components CHMP4 and CHMP2 that form spiralling filaments within the neck of the budding virion. These filaments spiral inwards and form dome-like structures that constrict the opposing membrane stalks and promote abscission. VPS4 is recruited to budding virions immediately before pinching off and is thought to promote dome structure formation and/or ESCRT-III protein removal to promote virus budding (reviewed by (Sundquist and Kräusslich, 2012)).

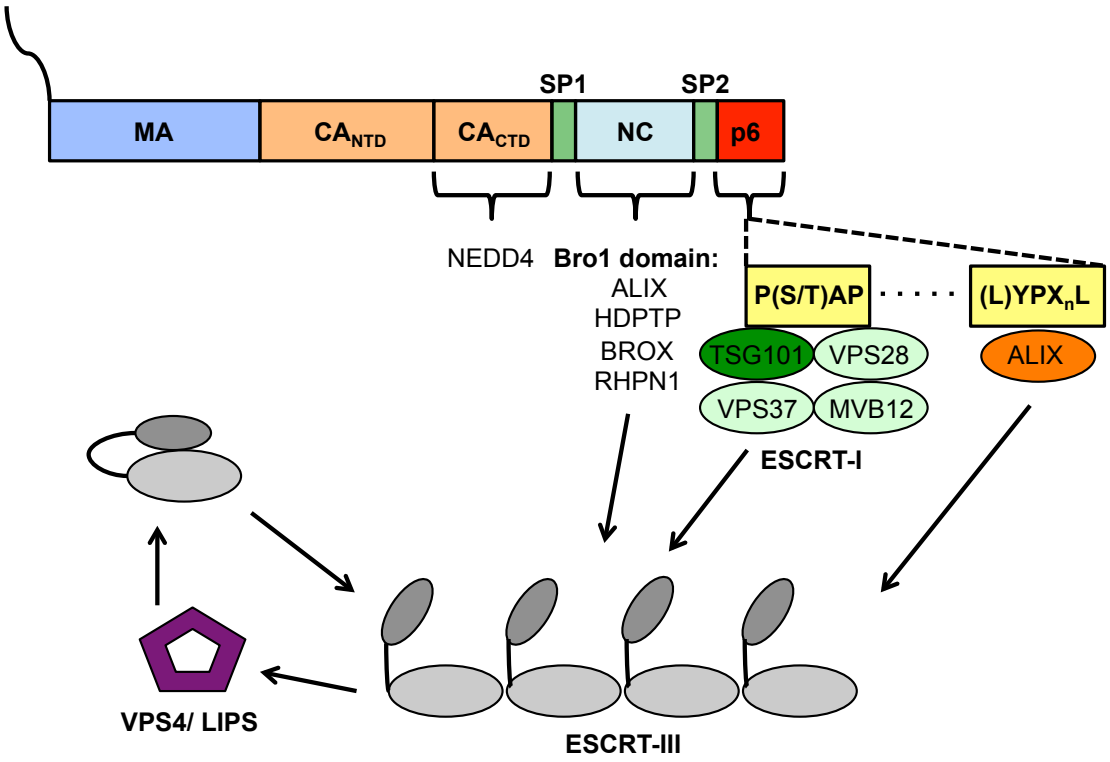

Figure 1-11 Gag-mediated recruitment of cellular host factors required for budding

The HIV-1 Gag protein encodes two late-budding domains (yellow boxes) that recruit the cellular ESCRT machinery through direct interaction with TSG101 (green) and ALIX (red). These ESCRT adaptor proteins recruit the core ESCRT-III machinery and the vacuolar protein sorting-associated protein 4 (VPS4), to mediate virus release. Interactions with Bro1-containing proteins and NEDD4 are also illustrated in this figure. Abbreviations: capsid (CA); carboxyl-terminal domain (CTD); matrix (MA); multivesicular body sorting factor 12 (MVB12); nucleocapsid (NC); amino-terminal domain (NTD); rhophilin 1 (RHPN1); His domain phosphotyrosine phosphatase (HDPTP); BRO1 domain and CAAX motif-containing protein (BROX).

1.3.7 Virion maturation by the viral protease enzyme

The last step of the HIV-1 replication cycle is proteolytic maturation which is essential to form fully infectious virus particles. HIV-1 virions are released from the host cell as non-infectious particles called immature virions. The virus particle then undergoes a dramatic conformational rearrangement that begins concomitant with virus budding, resulting in a mature and infectious virus particle (Figure 1-12). The structural rearrangement is triggered by cleavage of Gag and Gag-Pol polyproteins by the virally encoded enzyme PR. Pol is cleaved into viral enzymes PR, RT and IN, while Gag is cleaved into the structural proteins: MA, CA, NC, p6 and two spacer peptides (p1 and p2) (reviewed by (Sundquist and Kräusslich, 2012)). CA proteins assemble into hexamers to form the core structure. Sporadically, CA can associate into pentamers causing irregularities in the hexameric organisation, resulting in a cone structure (Ganser, 1999) (Briggs et al., 2006) (Ganser-Pornillos et al., 2008).

The catalytically active form of the aspartic acid protease PR consists of a homodimer of two identical subunits that form the substrate-binding pocket at the centre and interact with different Gag and Gag-Pol sequences. The initiation mechanism that activates PR is currently not well understood, but Gag and Gag-Pol multimerisation during budding is required and is thought to allow dimerisation of two PR domains in a process called auto-processing (reviewed by (Fun et al., 2012)). Once activated, PR recognises the overall shape of cleavage sites in Gag-Pol rather than a specific peptide sequence (Prabu-Jeyabalan et al., 2002). Slight differences in the otherwise superimposable secondary structure of the cleavage sites results in distinctive affinities for PR; as a result the cleavage process is highly regulated and occurs in an ordered stepwise process (Wiegers et al., 1998). The in-depth knowledge of HIV-1 protease and substrate structures led to the development of protease inhibitors that inhibit enzymatic activity and prevent cleavage of Gag and Gag-Pol, resulting in the production of immature and non-infectious particles.

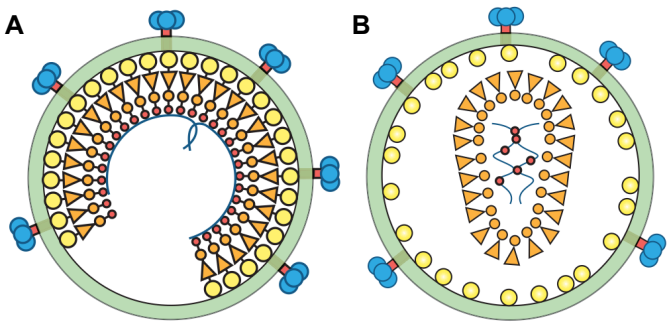

Figure 1-12 Virion maturation

Schematic representation of the organisation of an immature HIV-1 virion **(A)** and a mature HIV-1 virion **(B)** Indicated in yellow (matrix); orange (capsid); and red (nucleocapsid) (adapted from (Sundquist and Kräusslich, 2012)).

1.4 Pathogenesis and innate immune responses to HIV-1 infection

The immune response to HIV consists of an “early” nonspecific innate response, which can be seen as a first line of defence to protect the host against the virus without any prior exposure. The “late” and highly specific adaptive response consists of humoral and T cell-mediated responses (reviewed by (Flint et al., 2009)). This chapter will describe the early phase of infection that results in the activation of a complex network of innate immune factors, and the corresponding innate immune evasion strategies employed by HIV-1.

HIV-1 is most frequently transmitted by sexual contact across mucosal surfaces of genital or rectal tissues. This results in the establishment of a new infection, typically starting from one single virus particle that preferentially infects memory T cells expressing high levels of CD4 and CCR5, inference of transmitted/founder viruses. The infected cells disseminate to lymphoid tissues throughout the body, including the gut-associated lymphoid tissue (GALT) that contains high numbers of CD4+ T cells. A switch in cell tropism occurs with the onset of immunodeficiency, where CXCR4 and macrophage-tropic viruses evolve from CCR5 progenitors. However, both of these variants are not efficiently transmitted (reviewed by (Coffin and Swanstrom, 2013)).

During the early phase of HIV infection the innate immune system is activated. This comprises inflammatory cytokines, an array of different cell types, the complement system and inducible intracellular antiviral proteins. The major cell types critically involved in the innate immune response and production of inflammatory factors are macrophages, dendritic cells (DCs), neutrophils, natural killer cells (NK cells). Most of these cells express various pattern recognition receptors (PRRs) that recognise structurally conserved motifs of proteins, carbohydrates or nucleic acids that are unique to pathogens and not normally produced in human cells. These exogenous motifs are also known as pathogen-associated molecular patterns (PAMPs). The most thoroughly characterised PRRs are: toll-like receptors (TLRs), which are present on the cell surface or endoplasmic compartments and respond to viral glycoproteins, nucleic acids or unmethylated CpG DNA sequences; cytoplasmic (RIG-I)-like receptors (RLRs), which recognise long and short 5’ phosphorylated viral dsRNA; and the nucleotide oligomerisation domain (NOD)-like receptor (NLRs) family, which detects the presence of PAMPs and endogenous molecules in the cytosol. Activation of host receptors by viral ligands leads to downstream signalling events that result in the induction of specific transcription factors that in turn induce the production of inflammatory cytokines and type I interferon (IFN) (reviewed by (Guha and Ayyavoo, 2013)).

Plasmacytoid dendritic cells (pDCs) are specialized in the production of high levels of IFN-α and are the major source of type I IFNs during the early stages of HIV-1 infection. pDCs express a range of surface and endocytic PRRs that detect viral PAMPs. Several lines of evidence suggest that pDCs sense HIV in a TLR-dependent mechanism, particularly by TLR7 and TLR9 (reviewed by (Guha and Ayyavoo, 2013)).

Infection of T cells and macrophages with HIV-1 does not induce interferon expression. This may be due to the presence of the host exonuclease TREX1 (Yan et al., 2010). TREX1 induces the degradation of HIV dsDNA and prevents activation of intrinsic PRRs. HIV DNA can be sensed in the absence of TREX1 or in the presence of high HIV dsDNA concentrations. Excess HIV-1 DNA is sensed by the IFN-inducible protein 16 (IFI16) (Jakobsen et al., 2013); or is sensed by and activates cyclic guanosine monophosphate-adenosine monophosphate (cGAMP) synthase (cGAS) to produce cGAMP (Gao et al., 2013). Both DNA sensors activate the adaptor protein stimulator of interferon genes (STING) to induce transcription of type I IFNs and other cytokines. Other recently identified factors that potentially contribute to the ability of HIV-1 to replicate in macrophages without being sensed are: cleavage and polyadenylation specificity factor subunit 6 (CPSF6) and cyclophilins (Nup358 and CypA) (Rasaiyaah et al., 2013). CPSF6 and CypA bind to the HIV-1 capsid ensuring reverse transcription, uncoating and nuclear entry by cloaking replication. Their binding to HIV-1 capsid allows immune evasion and blocks innate sensors. However, in the absence of CPSF6/CypA and capsid interactions, macrophages are able to activate innate immune signals in a TREX1-independent manner.

NK cells are among the most important innate immune cells involved in the control and clearance of virally infected cells and the regulation of adaptive immune responses. The inflammatory milieu generated during HIV-1 infection, especially following secretion of IFN-α and IL-15, leads to the activation and rapid expansion of NK cells (reviewed by (Biron, 1999)). NK cells largely use a family of germ-line encoded negative or inhibitory killer immunoglobulin-like receptors (KIR) to monitor MHC class I expression on other cells. Many viruses, including HIV-1, downregulate MHC class I molecules from the cell surface of infected cells in order to avoid detection by CD8+ T cells, which in turn puts the infected cell at risk of triggering NK cell activation. However, loss of MHC class I expression on the cell surface of infected cells is not sufficient to trigger NK cell-mediated killing. A second activating signal, achieved through the recognition of stress-ligands is required to induce destruction of infected cells. The HIV-1 accessory protein Nef, for example, can overcome NK cell-mediated killing by selective downregulation of MHC class I molecules and stress-inducible

ligands MIC-A and ULBP-1/2 for the c-type lectin NK-cell (NKG2D) receptor (Cerboni et al., 2007) (reviewed by (Carrington and Alter, 2012)).

Acutely infected HIV-1 patients have high levels of circulating type I IFN (von Sydow et al., 1991), which helps to suppress HIV infection and increases the ability of the adaptive immune response to recognise and eliminate infected cells. Interferon signalling through the Jak-STAT pathway induces the expression of interferon stimulatory genes (ISGs) (reviewed by (Stark and Darnell, 2012)), but, only a small number of these ISGs have been studied. ISGs with anti-HIV activities are: Trim22 which interferes with HIV-1 Gag assembly; ISG15, a small ubiquitin like protein, which conjugates with HIV Gag also interfering with assembly; and the IFITM proteins which block HIV entry (reviewed by (Doehle and Gale, 2012). The most recently characterised member of the group is the myxovirus resistance 2 (MX2) protein, which inhibits nuclear import or destabilises nuclear HIV-1 DNA (Goujon et al., 2013) (Kane et al., 2013) (Liu et al., 2013). Amongst the interferon up-regulated genes are also the well-characterised HIV restriction factors: APOBEC3G, tetherin, SAMHD1 and TRIM5α (discussed in 1.5 below).

1.5 Restriction factors and the role of HIV accessory proteins in their evasion

HIV-1, like all other viruses, hijacks host cellular factors and pathways to complete its own life cycle. In addition to proteins that support viral replication, infected cells can also express a number of inhibitory or dominantly acting proteins that suppress virus replication at various steps.

The concept of retroviral restriction factors was first proposed when murine leukemia virus (MLV) infection was shown to be inhibited by the Friend virus susceptibility factor-1 (*Fv1*) gene. Inbred mice encode two different allelic forms of *Fv1* (*Fv1*^{n} and *Fv1*^{b}). *Fv1*$^{n/n}$ mice are 1000-fold more susceptible to N-tropic MLV than B-tropic MLV strains, and *vice versa* in *Fv1*$^{b/b}$ animals, which are susceptible to B-tropic MLV. Interestingly, heterozygous *Fv1*$^{n/b}$ cells are resistant to both MLV strains, indicating the presence of a dominantly acting restriction factor (Tennant et al., 1974). The *Fv1* gene is located on the mouse chromosome 4 and resembles an endogenous retrovirus *gag*-like gene (Best et al., 1996). Furthermore, Fv1-restricted MLV tropism is determined by sequences within the viral CA. To this end, Fv1 binds to CA and blocks integration of the reverse transcribed retroviral pre-integration complex (Hilditch et al., 2011), however, the exact mechanism is still not well understood.

The identification of additional restriction factors in mammalian cells followed soon after the discovery of *Fv1*. HIV restriction factors, identified to date share common characteristics: they are able to dominantly inhibit HIV replication; show hallmarks of positive selection; their expression is connected to the host cell's innate immune response and is IFN-inducible; and in some cases HIV and its evolutionary predecessors have evolved a potent countermeasure (reviewed by (Harris et al., 2012)). To date, four major HIV restriction factors have been identified that act at different stages of the virus replication cycle, namely APOBEC3G, tetherin, TRIM5α and SAMHD1 (see Figure 1-3 (blue boxes)).

Discussed in this section are APOBEC3G, TRIM5α and SAMHD1, together with viral countermeasures in the form of HIV accessory proteins. Discussed additionally are the roles of HIV-1 Vpr and Nef in virus replication and immune evasion. Tetherin-dependent virus restriction and Vpu-mediated tetherin antagonism are discussed in 1.6.2 and 1.7.3 respectively.

1.5.1 APOBEC3G and Vif

Studies to understand the role of the 192 amino acid Vif protein (viral infectivity factor), during HIV-1 replication in primary cell types showed that it is dispensable in some T cell lines but not in others. Cell fusion experiments of permissive and non-permissive cells suggested the presence of a dominant acting restriction factor (Simon et al., 1998). This phenotype led to the subsequent discovery of apolipoprotein B messenger RNA (mRNA)-editing enzyme catalytic polypeptide-like 3 (APOBEC3G also known as A3G or CEM15) using a cDNA subtraction-based screen (Sheehy et al., 2002). Importantly, the same group also demonstrated that expression of APOBEC3G in permissive T cells was sufficient to render these cells restrictive for viral replication of Vif-deficient HIV-1 (Sheehy et al., 2002).

APOBEC3G is a member of a protein family that possess cytidine deaminase activity, which are expressed in a wide variety of human tissues (in particular in hematopoietic cells) and can be transcriptionally induced by type 1 IFN (Koning et al., 2009). All members of the APOBEC3 family contain at least one copy of a zinc-coordinating deaminase domain (Z domain). APOBEC3G contains two such domains, where the C-terminal Z domain possesses deamination activity, while the non-catalytically active N-terminal Z domain mediates interaction with the NC region of Gag, which is required for APOBEC3G incorporation into viral particles in the absence of Vif. APOBEC3G is packaged into nascent virions by association with NC and viral RNA (Zennou et al., 2004). In the target cell, APOBEC3G associates with the RTC in infected target cells, where it deaminates cytidine residues in single-stranded negative strand viral cDNA, resulting in the production of deoxyuridine that is misread by RT as thymidine. This results in the insertion of adenine instead of guanine in the positive strand. APOBEC3G has a strong intrinsic preference for deaminating 5'-CC**C**A cytidine residues (the underlined cytidine is target for deamination) (reviewed by (Malim and Bieniasz, 2012) and (Harris et al., 2012)). Hypermutations are not the only function of APOBEC3G associated with anti-viral activity, as levels of viral cDNA that accumulate during infection are also reduced. This was initially thought to be a result of uridine-containing DNA degradation induced by cellular host DNA repair mechanisms. However, inhibition of uracil DNA glycosidases had no effect on cDNA levels. Instead, it is now thought that APOBEC3G impedes translocation of viral RT along its RNA template (Bishop et al., 2006) (Gillick et al., 2013), but further experimental evidence is needed to fully explain this observation (reviewed by (Malim and Bieniasz, 2012)).

Expression of Vif enables HIV-1 to overcome the antiviral activities of APOBEC3G by inducing its degradation, thus preventing its incorporation into nascent virions. Vif binds to the catalytically inactive N-terminal Z domain of APOBEC3G and recruits the cellular

ubiquitin ligase complex CRL5. This complex consists of cullin5, elongin B and C, Rbx2 and a to date unidentified E2 conjugating enzyme. This in turn results in poly-ubiquitination and proteasomal degradation of APOBEC3G (see Figure 1-13) (reviewed by(Malim and Bieniasz, 2012)). Furthermore, Vif-induced degradation of APOBEC3G was found to involve the cellular transcription factor CBFβ (Jäger et al., 2012). Recently, one study demonstrated that direct binding of CBFβ to Vif-CRL5 enhances catalytic activity, blocks Vif oligomerisation, and promotes formation of a well-ordered Vif E3 ligase complex (Kim et al., 2013).

In addition to APOBEC3G, other members of the APOBEC3 family have been shown to possess antiviral activity, namely APOBEC3F (A3F), APOBEC3H (A3H) and APOBEC3D (A3D). All four APOBEC3 proteins share common characteristics: they are expressed in CD4+ T cells, packaged into virus particles, possess antiviral activity, are able to induce G to A mutations, and are sensitive to HIV-1 Vif. However, APOBEC3F/H and D cause 5'-T**C** deamination rather than 5'-C**C** and are expressed at lower levels than APOBEC3G, indicating that A3G is the most significant family member as HIV restriction factor (reviewed by (Malim and Bieniasz, 2012) and (Harris et al., 2012)).

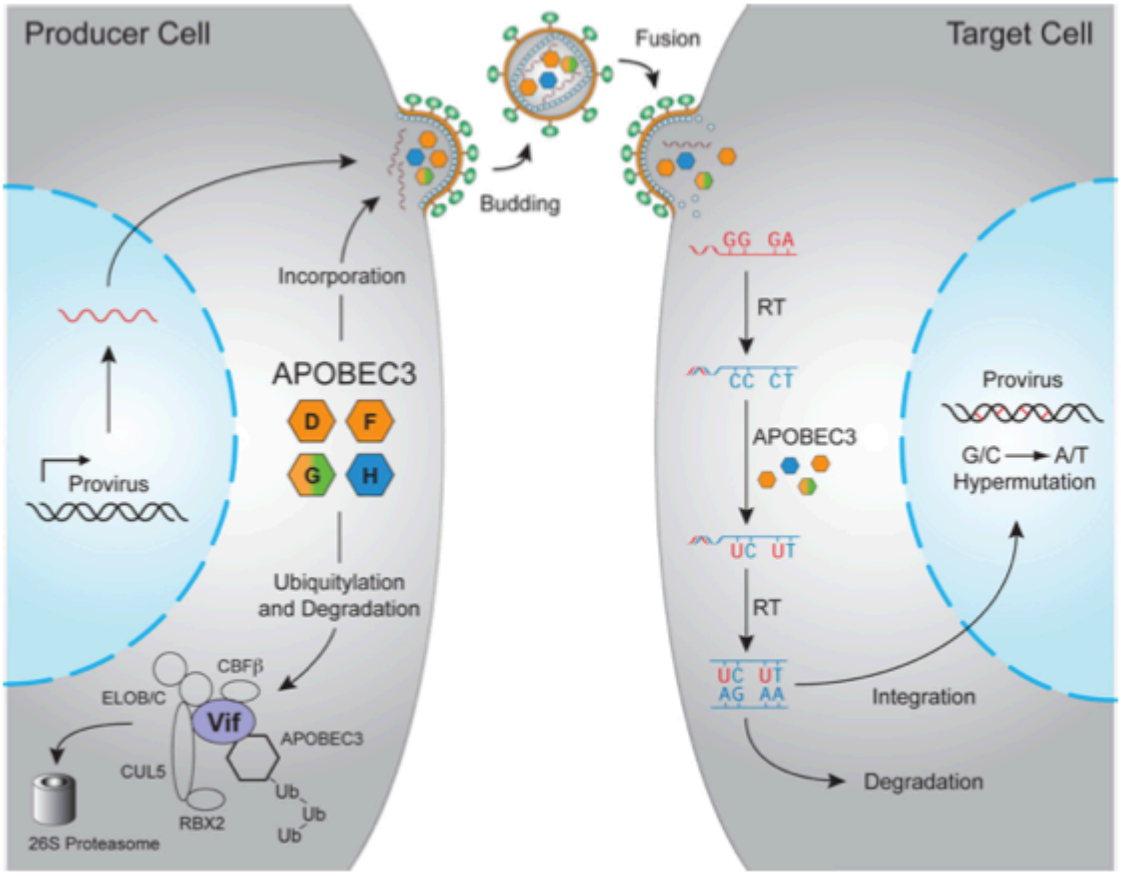

Figure 1-13 Mechanism of HIV-1 restriction by APOBEC3 proteins

Schematic representation of APOBEC3 inhibition of HIV-1 infection and Vif antagonism. APOBEC3 molecules can encapsidate into Vif-deficient HIV virions (left) and infect a target cell (right). In the target cell, APOBEC3 molecules associate with the reverse transcription complex (RTC) and induce deamination of cytidine residues to uridine residues in viral cDNA causing hypermutations. The proviral cDNAs are subsequently degraded or integrated. HIV-1 Vif overcomes APOBEC3-mediated restriction in the producer cell by recruiting an E3 ubiquitin ligase complex to poly-ubiquitinate APOBEC3 molecules and target them for degradation by the 26S proteasome (adapted from (Harris et al., 2012)).

1.5.2 TRIM5α and capsid

Studies from the Sodroski laboratory (Hofmann et al., 1999) demonstrated that infection of non-human primate cells by HIV-1 was inefficient in a manner independent of envelope-mediated entry. The existence of a dominant acting antiviral protein that targets HIV-1, SIV, and other retroviral capsid proteins was predicted by fusion experiments of permissive with non-permissive target cells (Cowan et al., 2002). Interestingly, the resistance phenotypes were very similar to those displayed by *Fv1*, but resistance was also evident in non-murine cells, including humans and monkeys, which lack the *Fv1* gene (Towers et al., 2000) (Besnier et al., 2002). Subsequently, a screen for rhesus macaque genes that were able to restrict HIV-1 infection when expressed in human cells resulted in the identification of TRIM5α (Stremlau et al., 2004).

TRIM5α is a ~500 amino acid cytoplasmic protein that belongs to the tripartite motif (TRIM)-containing protein family. TRIM proteins are involved in various cellular processes, such as proliferation, differentiation, development, apoptosis, oncogenesis and innate immunity. In humans the TRIM family includes close to 100 members that can be classified on the basis of domain organisation. The TRIM family are characterised by an N-terminal RING zinc-finger domain with E3 ubiquitin ligase activity, one or two B-boxes (possibly involved in protein-protein interactions), and a coiled-coil region for homo-multimerisation or hetero-multimerisation. Two-thirds of the human TRIM family proteins also encode a C-terminal SPRY (SplA and ryanodine receptor) domain alone or fused to a PRY forming the PRY-SPRY domain (also referred as B30.2 domain). PRY-SPRY domains have a conserved structure that forms a protein-binding interface (James et al., 2007) (reviewed by (Rahm and Telenti, 2012)).

Unlike rhesus TRIM5α, human TRIM5α only weakly inhibits HIV-1 laboratory adapted strains. However, some primary isolates are more sensitive, and human TRIM5α potently blocks EIAV and N-tropic MLV infection. The difference in specificity between human and rhesus TRIM5α has been mapped to the PRY-SPRY domain of the protein that forms the binding interface for capsid recognition. Once the TRIM5α protein was cloned, it became clear that TRIM5 orthologues in some macaque and owl monkeys were created by LINE1-mediated retrotransposition of cyclophilin A into the TRIM5 locus, resulting in the so-called TRIMCyp protein. Like the rhesus macaque TRIM5α protein, TRIMCyp is able to restrict HIV-1 infection (reviewed by (Grütter and Luban, 2012)).

The mechanism of retroviral inhibition by TRIM5α is not completely understood. However, it is clear that TRIM5α and TRIMCyp bind directly to the HIV-1 capsid via their PRY-SPRY and cyclophilin A domains, respectively, and this leads to a block in reverse transcription and premature disassembly of the viral core (Stremlau et al., 2006). Higher-order TRIM5α multimerisation into hexagonal lattices, which is dependent on its coiled-coil and B-Box-2 domains, may increase efficiency of TRIM5α interaction with the capsid lattice, which in turn promotes antiviral activity (Ganser-Pornillos et al., 2011). The RING domain of TRIM5α confers E3 ubiquitin ligase activity (Xu, 2003), which leads to auto-ubiquitination, explaining its short half-life (Diaz-Griffero et al., 2006). TRIM5α does not induce ubiquitination of viral proteins; instead it is thought to recruit viral components for proteasomal degradation. Inhibition of the proteasome or disruption of the RING domain, however, prevent capsid disassembly and restores reverse transcription but do not allow infection. A possible explanation is that TRIM5α might act at different stages in the replication cycle that lead up to integration into the host DNA (reviewed by (Luban, 2012)).

TRIM5α promotes AP-1 and NF-κB signalling and was recently identified as a pattern recognition receptor (PRR) that is specific for the retroviral capsid lattice (Pertel et al., 2011). In combination with E2 ubiquitin ligases UBC13 and UEV1A, TRIM5α catalyses the formation of K63-linked ubiquitin chains that activate TAK1 which leads to inflammatory cytokine transcription. Other TRIM proteins play an important role in regulating the innate immune response and are up-regulated by type I and II IFNs in CD4+ T cells. For example, TRIM25 promotes ubiquitination of the viral sensor retinoid-inducible gene I (RIG-I) leading to downstream activation of NF-κB (Gack et al., 2007). Another example is the cytosolic antibody receptor TRIM21, which promotes ubiquitination of the interferon regulatory factor (IRF)-8, which in turn leads to the expression of cytokines (McEwan et al., 2013).

Of note, HIV does not encode a TRIM5α countermeasure as it does in case of APOBEC3G, tetherin and SAMHD1, which are antagonised by Vif, Vpu or Vpx respectively. Instead, sequence variations within CA and the recruitment of cellular CypA seem to allow HIV-1 to escape from TRIM5α-induced restriction.

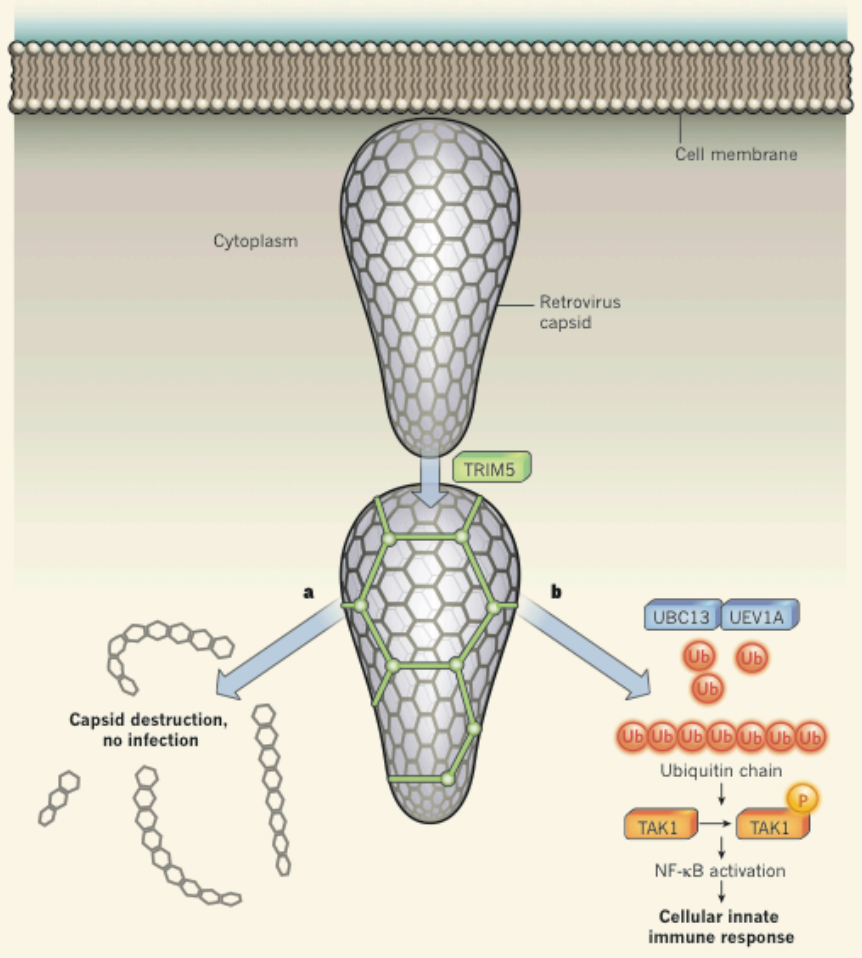

Figure 1-14 Role of TRIM5α in antiviral activity

Schematic representation of TRIM5α-mediated retroviral restriction. **(A)** TRIM5 molecules bind to the viral capsid, causing structural alterations that lead to capsid fragmentation and block in reverse transcription. **(B)** TRIM5 molecules bind to the viral capsid, and together with E2 ubiquitin ligases UBC13 and UEV1A catalyse the formation of K63-linked ubiquitin chains that stimulate TAK1 phosphorylation leading to inflammatory cytokine transcription **(**adapted from (Aiken and Joyce, 2011)).

1.5.3 SAMHD1 and Vpx

The *vpx* (viral protein X) gene is thought to have derived from duplication of the primate lentivirus *vpr* gene. Rhesus macaque SIV (SIVmac) and HIV-2 encode both proteins, while chimpanzee SIV (SIVcpz) and HIV-1 only encode Vpr but not Vpx. However, these closely related proteins have evolved different functions in the viral replication cycle. Vpx and Vpr are unique among lentiviral accessory proteins in that they are present in significant quantities in the virus particle. The packaging of Vpx and Vpr proteins is virus specific and requires a specific interaction with the p6 C-terminal domain of Gag (Yu et al., 1990) (Lu et al., 1993) (Paxton et al., 1993) (Kondo et al., 1995). Studies performed using SIV and HIV-2 Vpx proteins in the context of HIV-1 replication demonstrated that Vpx expression significantly promoted HIV-1 infection in myeloid cells, such as human dendritic cells and macrophages, compared to CD4+ T cells (Goujon et al., 2006). Furthermore, Vpx facilitated the accumulation of full-length HIV cDNA. SIVmac and HIV-2 Vpx proteins were also found to interact with the host cell E3 ubiquitin ligase complex containing DCAF1, CUL4A and DDB1 (Srivastava et al., 2008) (Bergamaschi et al., 2009), suggesting that the unknown factor was being degraded (reviewed by (Wu, 2013)). These findings led to the discovery of the SAM domain HD domain-containing protein 1 (SAMHD1) as a HIV restriction factor in human myeloid cells, by isolation of Vpx-interacting proteins from differentiated human monocytic THP-1 cells (Laguette et al., 2011). At the same time, SAMHD1 was identified as a Vpx interacting protein in HEK 293T cells using a similar proteomic approach (Hrecka et al., 2011).

SAMHD1 is composed of a sterile alpha motif (SAM) that is involved in protein-protein interaction as well as nucleic acid binding; and a dNTP phosphohydrolase domain containing conserved histidine and aspartate residues (also referred to as an HD domain), which is crucial for its enzymatic activity and RNA binding. Multiple phosphorylation sites within SAMHD1 have been identified. In particular residue T592 (Cribier et al., 2013) (White et al., 2013) (Welbourn et al., 2013), which is phosphorylated by cyclin A2 and CDK1, and plays a role in the regulation of SAMHD1 function during the cell cycle. Targeted mutation of residue T592 releases SAMHD1-mediated HIV-1 restriction. Furthermore, mutations in SAMHD1 are associated with the Aicardi-Goutières syndrome (AGS), a rare autoimmune disorder that leads to chronic inflammation through DNA sensing (reviewed by (Sze et al., 2013)).

Identification of SAMHD1 as a restriction factor highlights the importance of metabolic regulation as a restriction mechanism to constrain virus replication. SAMHD1 degrades dNTPs (dATP, dCTP, dTTP and dGTP), the building blocks for DNA synthesis. By diminishing the cellular dNTP pool, SAMHD1 prevents early steps of reverse

transcription thereby blocking full-length cDNA synthesis and efficient HIV-1 replication (Goldstone et al., 2011) (Lahouassa et al., 2012). Furthermore, Vpx induces poly-ubiquitination and proteasomal degradation of SAMHD1 by serving as a scaffolding protein for the DCAF1, DDB1, and CUL4 E3 ubiquitin ligase complex (Laguette et al., 2011) (Hrecka et al., 2011). This function has been predominately recognised in in non-cycling cell types including monocytes (Berger et al., 2011), macrophages (Hrecka et al., 2011), dendritic cells (Laguette et al., 2011), and resting CD4-positive T cells (Baldauf et al., 2012) (reviewed by (Wu, 2013)).

Recently, retroviral DNA intermediates have been associated with innate DNA sensors cGAS (Gao et al., 2013) and IFI16 (Jakobsen et al., 2013), which activate downstream STING resulting in an innate immune response. SAMHD1 activity leads to the accumulation of reverse transcription intermediates in the cytoplasm that can be detected by the innate immune sensing machinery. These can be degraded by the TREX1. TREX1 is also associated with the Aicardi-Goutières syndrome (reviewed by (Sze et al., 2013)). However, more work needs to be done to fully understand the link between retroviral restriction and SAMHD1-mediated innate signalling events.

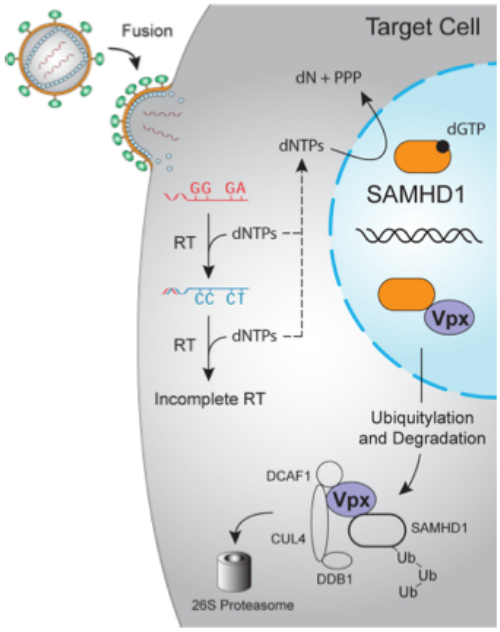

Figure 1-15 Mechanism of HIV-2 restriction by SAMHD1

In myeloid cells, SAMHD1 induces depletion of cellular dNTPs resulting in a block of reverse transcriptase (RT). HIV-2 and SIV Vpx proteins can overcome SAMHD1-mediated restriction by recruiting an E3 ubiquitin ligase complex that poly-ubiquitinates SAMHD1 and targets it for degradation by the 26S proteasome (adapted from (Harris et al., 2012)).

1.5.4 The role of Vpr in HIV and SIV infection

Unlike Vpx, Vpr (viral protein R) is conserved amongst all primate lentiviruses. The Vpr protein contains a flexible N-terminus, three alpha-helical domains and a flexible C-terminal region. Vpr is packaged into mature virions through its interaction with p6, localises to the nucleus and nuclear membrane, and is cytopathic to cells when overexpressed. Some SIV Vpr proteins are able to mediate degradation of SAMHD1, while HIV-1 Vpr proteins are unable to counteract the restriction factor. Many functions have been attributed to Vpr over the years, including nuclear transport of the HIV-1 pre-integration complex, suppression of immune activation, modulation of transcription, stimulation of defects in mitosis and apoptosis, and disruption of cell-cycle control (reviewed by (Romani and Engelbrecht, 2009)). Interestingly, sequence analysis from an accidentally infected laboratory worker, with an HIV strain that encoded a disrupted *vpr* gene, revealed that the gene reverted back to an intact *vpr* open reading-frame two years later (Goh et al., 1998). Furthermore, in studies using rhesus macaques infected with SIVmac239 Vpr minus virus, 3 out of 5 animals reverted to wild-type (reviewed by (Mashiba and Collins, 2012)). Therefore, both studies highlight the importance of Vpr function *in vivo*.

The cell-cycle arrest at the G2/M transition is the only well established phenotype of Vpr. Induction of the G2 arrest in infected cells is thought to provide replication advantages, because transcription levels of the virus are higher during G2 (Goh et al., 1998); and a higher number of HIV-1 infected individuals displayed more CD4+ T cells in the G2 step compared to the healthy control group. Several studies have identified the DDB1-CUL4 E3 ligase complex as a cellular Vpr binding partner to interfere with the DNA replication machinery of infected cells, resulting in cell-cycle arrest (Wen et al., 2007) (Hrecka et al., 2007). As the DDB1-CUL4 E3 ligase complex is involved in proteasomal degradation, it was suggested that Vpr induces the G2 arrest through degradation of an unidentified protein that is needed for progression of cells from G2 arrest to mitosis (Wen et al., 2007).

Recently, the structure-specific endonuclease (SSE) regulator SLX4 complex (SLX4com) has been identified as a Vpr interacting protein using a biochemical approach. This direct interaction leads to the untimely activation of SLX4com by Vpr-mediated recruitment of PLK1 and VPRBP; which activates SLX4-associated endonucleases resulting in DNA cleavage. This in turn results in cell-cycle arrest at the G2/M transition (Laguette et al., 2014). However, there remains the possibility that G2 arrest is a by-product of the degradation of another host factor that plays an important role in cell-cycle progression and a different one in host-mediated viral evasion mechanisms.

1.5.5 HIV-1 Nef and its role in immune evasion

Nef (standing for the misleading name: negative factor) is a ~27 kd myristoylated protein, encoded by all primate lentiviruses. Nef mainly localises to peri-nuclear regions and is associated with cellular membranes. Nef displays diverse functions *in vivo* including downregulation of a number of cell surface molecules, enhancement of viral infection and virus replication capacity, playing a critical role in consistent high plasma viremia and progression to AIDS. The protein structure of Nef can be divided into three domains: a C-terminal flexible loop; a central structured core domain that is involved in protein-protein interactions and encodes multiple intracellular trafficking motifs; and an N-terminal anchor domain that is crucial for membrane binding and localisation into lipid rafts (reviewed by (Foster and Garcia, 2008) and (Mwimanzi et al., 2012)).

CD4 is downregulated from the cell surface by Nef proteins (Guy et al., 1987) (Garcia and Miller, 1991), a common feature of a HIV and SIV Nef proteins, presumably to increase virion release and infectivity, to enhance viral replication and to prevent super-infection. Nef binds to CD4 and recruits the clathrin adaptor AP-2 to induce endocytosis of CD4 via a canonical dileucine motif, **E**xxx**LL**. Furthermore, acidic residues downstream of the trafficking motif are also required for stabilising AP-2 binding (Lindwasser et al., 2008). Endocytosis is followed by the delivery of CD4 to lysosomes for degradation (reviewed by (Foster and Garcia, 2008)). Of note, HIV-1 Vpu is also able to induce CD4 degradation by targeting newly synthesised CD4 in the ER for lysosomal degradation (see 1.7.2).

CD4 binding to gp120 induces conformational changes in gp120 that promote its interaction with the chemokine receptors; result in the exposure of a helical heptad repeat (HR1) segment of the gp41 ectodomain; and expose antibody-dependent cell-mediated cytotoxicity (ADCC) epitopes. Therefore, HIV-1 Nef and Vpu-mediated CD4 cell surface downregulation might help to avoid the killing of HIV-1-infected cells by ADCC (Veillette et al., 2014) (Pham et al., 2014).

Nef also induces downregulation of major histocompatibility complex (MHC) class I molecules HLA-A and B on infected cells, and thereby reduces viral peptide presentation to cytotoxic T cells (CTLs). Two pathways have been described to explain Nef-mediated HLA-I downregulation. In the first model Nef alters the trafficking of HLA-I by interacting with newly synthesised HLA-I molecules within the secretory pathway and redirecting them to the lysosome for degradation. Nef directly binds to AP-1 (Bresnahan et al., 1998) and ß-COP (Piguet et al., 1999), which are important factors in protein transport between the trans-Golgi network (TGN) and endosomes. Interestingly, Nef interacts with the μ subunit of AP-1 only in the presence of HLA-I. A

structural study recently demonstrated that interaction between Nef and AP-1 μ creates a binding pocket in the μ subunit that is capable of binding the **Y**xx**A** motif in HLA-I in order to stabilise the complex (Jia et al., 2012). In the more controversial second model Nef enhances HLA-I turnover. Mechanistically, a series of protein interactions and signalling events lead to the enhanced clathrin-independent endocytosis of HLA-I that requires a small GTPase known as ADP-ribosylation factor 6 (ARF) (Blagoveshchenskaya et al., 2002) (reviewed by (Mwimanzi et al., 2012)).

SIV infections are usually non-pathogenic in their natural host, which correlates with low levels of T cell activation and activation-induced cell death (AICD). HIV-1 infections, however, are characterised by high levels of immune activation and apoptotic cell death. Nef proteins from HIV-2, SIVsm and SIVmac efficiently downmodulate cell surface TCR-CD3 and reduce TCR-induced NFAT activation (Schindler et al., 2006), thereby suppressing the responsiveness of infected T cells to activation and AICD. By contrast, HIV-1 Nef is devoid of this function and this difference has been proposed to govern the pathogenic outcome of lentiviral infections. Thus, demonstrating that Nef exerts an important protective function that was lost during lentiviral evolution. By downmodulating TCR-CD3, SIV Nef proteins might adjust T cell activation to an optimal level to maintain viral persistence in the context of an intact host immune system.

Nef is not only expressed “early” during infection but also at “later” stages of the virus life cycle. This is thought to be important for Nef to enhance the infectivity of virus particles. The mechanism is dependent on the interaction of Nef with the GTPase dynamin 2 that regulates the last step of clathrin-mediated endocytosis. Depletion of dynamin 2 or clathrin by siRNA diminishes the enhancement of Nef-mediated infectivity, indicating the dependence on dynamin 2 and clathrin-mediated membrane invagination for this process (Pizzato et al., 2007). Furthermore, HIV-1 Nef and murine leukemia virus glycoGag similarly enhance the infectivity of HIV-1 virus particles, which is determined by variable regions of HIV-1 gp120 that control Env trimer association and neutralisation sensitivity. This indicates that the effects of Nef and glycoGag on HIV-1 virion infectivity are determined by the quaternary conformation of the apex of the Env trimer (Usami and Göttlinger, 2013). However, how this regulates infectivity is not yet understood.

Although the role of Nef in HIV pathogenesis is not completely understood, it has become increasingly clear that Nef mediates functions that act at different times during the infection course in order to ensure the ultimate goal of viral replication.

Furthermore, SIV Nef but not HIV-1 Nef proteins are able to antagonise the restriction factor tetherin, for more detail see 1.6.4.2.

1.6 Tetherin

Before tetherin (CD317; HM1.24 or bone marrow stromal cell antigen 2 (BST-2)) was discovered as a HIV-1 restriction factor, it was identified in a proteomic screen looking for novel proteins targeted for degradation by K5 (Bartee et al., 2006), a RING-CH (MARCH) ubiquitin ligase from the human Kaposi sarcoma-associated herpesvirus (KSHV). Tetherin protein levels were reduced in K5 expressing cells, which was dependent on the catalytically active form of K5. However, the relevance of tetherin antiviral activity at the time was unclear.

It had been known for a long time, that the HIV-1 accessory protein Vpu is required for efficient release of newly formed viral particles from HIV-1 infected CD4+ T cells and macrophages (reviewed by (Bour and Strebel, 2003)). The Vpu-deficient HIV-1 phenotype was visualised as mature viral particles remaining attached to the cell surface and accumulating in endosomal compartments (Klimkait et al., 1990) (Göttlinger et al., 1993). However, this effect was cell type- and species-specific (Varthakavi et al., 2003) (Neil et al., 2006). Heterokaryon analysis of fusions between cells in which Vpu was required for virus release (restrictive or non-permissive) and these in which Vpu was distensible (permissive) revealed that the requirement for Vpu was dominant. This indicated that Vpu-defective HIV-1 release was hindered by the expression of an unknown dominant acting cellular “restriction” factor, which made virus release dependent on the presence of Vpu (Varthakavi et al., 2003). Transient expression of Vpu in restricted cell types was sufficient to rescue virus release of HIV-1, MLV as well as Ebola virus-like particles (Neil et al., 2006) (Neil et al., 2007) (Göttlinger et al., 1993). The requirement for Vpu in permissive cell types was inducible by treatment with IFNα (Neil et al., 2007). Trapped virions could be released by protease treatment, indicating the presence of a protein-based tether that prevented cell-free virus particle release (Neil et al., 2007). Taken together these findings suggested the presence of an IFN-inducible protein-based tethering mechanism that trapped nascent virions on the cell surface of infected cells.

By comparative gene expression arrays of permissive and non-permissive cell types, Neil and colleagues identified BST-2 as a putative IFN regulated factor. Ectopic expression of BST-2 in permissive cells led to tethered virus particles on the surface of HIV-1 infected cells and was sufficient to induce a requirement for Vpu in HIV-1 release (Neil et al., 2008) (Van Damme et al., 2008). Therefore the novel restriction factor was given the apt name “tetherin” (Neil et al., 2008).

1.6.1 Tetherin: structure and cellular localisation

Tetherin is a type II integral membrane protein whose molecular weight varies between 28 kDa and 36 kDa depending on its glycosylation state (Ohtomo et al., 1999) (Kupzig et al., 2003). Tetherin has an unusual topology in which both ends of the protein are embedded in the cellular membrane (Kupzig et al., 2003); a structure that is only shared by one minor isoform of the prion protein (PrP) (Moore et al., 1999). Tetherin is comprised of a short N-terminal cytoplasmic tail, an alpha helical transmembrane domain, followed by an extracellular coiled-coil domain and a C-terminal glycosyl-phosphatidylinositol (GPI) anchor that covalently anchors tetherin to the outer leaflet of the cellular membrane (Kupzig et al., 2003) (Figure 1-16). Immature tetherin proteins are predicted to contain a C-terminal membrane-spanning helix that is processed into a GPI anchor by the ER-resident enzyme, PIGL. Cells that lack the *pigl* gene fail to modify tetherin's GPI anchor, resulting in retention of unprocessed tetherin proteins in the ER membrane, and therefore preventing tetherin from entering the secretory pathway (Perez-Caballero et al., 2009).

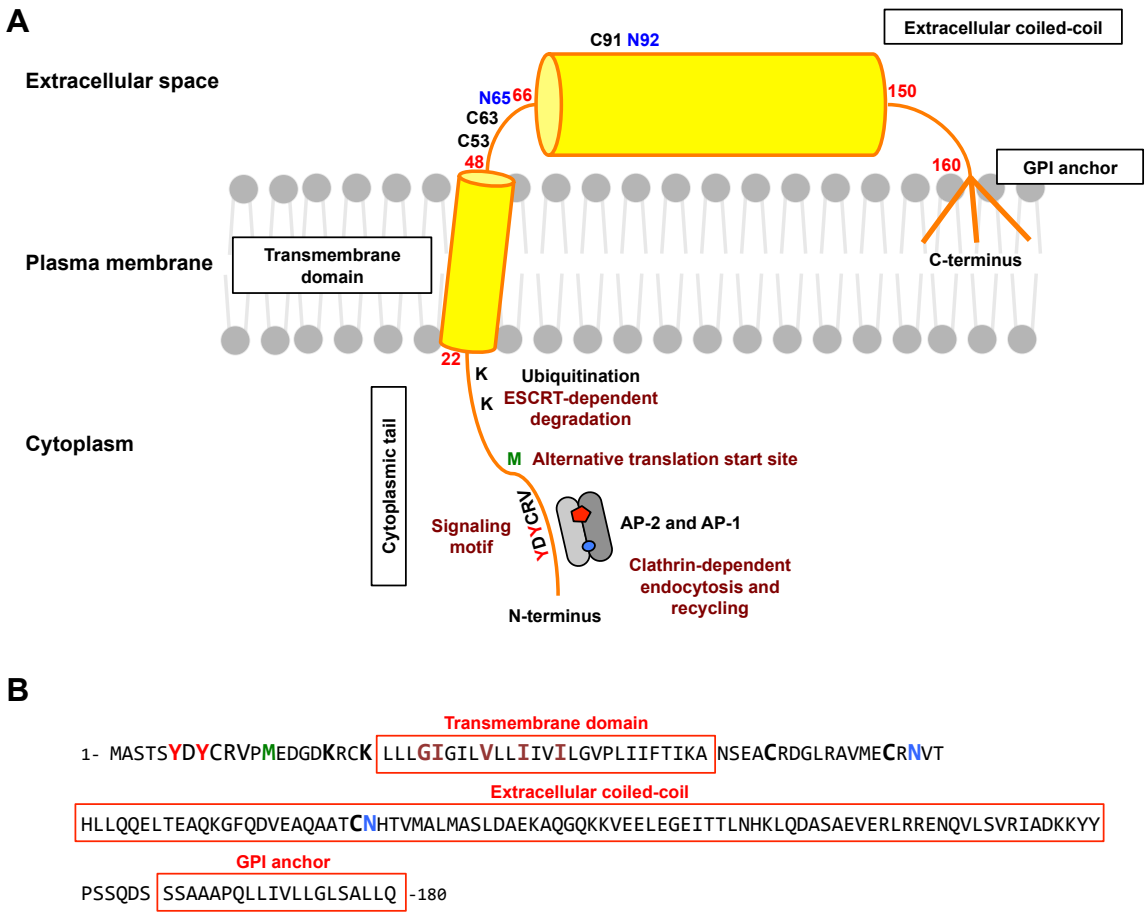

Figure 1-16 Tetherin topology and molecular features

(A) Schematic representation of the predicted secondary structure of tetherin monomer at the plasma membrane, indicated are the major domains of tetherin including the N-terminal cytoplasmic tail, the transmembrane domain, the long α-helical extracellular coiled-coil domain, and the C-terminal GPI anchor. The tyrosine-based endocytosis/signalling (**Y**D**Y**CRV) motif and potential ubiquitin-acceptor lysine residues (K-18 and K-21) are indicated on the cytoplasmic tail. Three cysteine residues (C-53, C-63 and C-91) involved in dimerization and two glycosylation sides (N-65 and N-92) are indicated on the extracellular domain. **(B)** Amino acid sequence of human tetherin. Molecular features from (A) are indicated together with residues within the transmembrane domain that are required for Vpu binding.

The mature form of tetherin exists as a homo-dimer that is linked by disulphide bonds formed by three cysteine residues (C-53, C-63 and C-91) in the N-terminal part of the extracellular domain. The ectodomain also contains two conserved asparagine residues (N-65 and N-92) that serve as N-linked glycosylation sites, which are important for folding of tetherin as well as sub-cellular trafficking in overexpression experiments (Andrew et al., 2009), but the asparagine residues have been shown to be dispensable for tetherin's antiviral function (Perez-Caballero et al., 2009). The crystal structures of human and murine tetherin ectodomains have been solved by several research groups (Figure 1-17) (Hinz et al., 2010) (Schubert et al., 2010) (Yang et al., 2010) (Swiecki et al., 2011), which revealed that two tetherin ectodomains form a parallel dimeric disulphide-linked coiled-coil domain that is hinged at residues A88 and G109 to allow N-terminal flexibility, and to accommodate membrane dynamics during the budding process (Schubert et al., 2010) (Yang et al., 2010). Furthermore, ectodomain integrity is crucial for tetherin molecules to form membrane micro-domain clusters and also allows controlled lateral mobility (Hammonds et al., 2012).

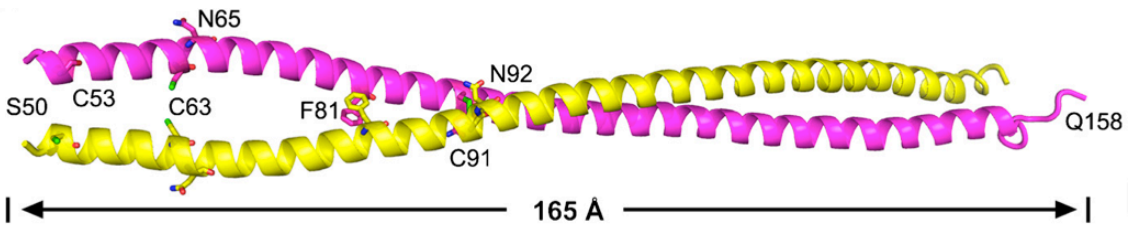

Figure 1-17 Structure of tetherin ectodomain dimer

Tertiary structure of a human tetherin ectodomain dimer based on X-ray crystallography (Yang et al., 2010).

Tetherin localises to the plasma membrane and the TGN, but can also be found in early and recycling endosomes (Kupzig et al., 2003) (Masuyama et al., 2009) (Habermann et al., 2010). In HIV-1 infected cells, tetherin localises to sites of virion assembly at the plasma membrane (Neil et al., 2008) (Lehmann et al., 2011). Furthermore, tetherin is inserted into cholesterol-rich micro-domains (also termed lipid rafts) through its GPI anchor (Kupzig et al., 2003). However, the role of these domains

in tetherin's antiviral function is still unclear at present. One study suggested that tetherin molecules form a "tethered picket fence" between raft and non-raft domains that play a role in the organisation of lipid rafts and distribution of membrane proteins (Billcliff et al., 2013).

The tetherin cytoplasmic tail contains a non-canonical dual tyrosine motif (**Y**x**Y**xxϕ) that serves as an endocytic signal. The internalisation of tetherin is clathrin dependent and requires direct binding of the clathrin adaptor AP-2 μ subunit to the highly conserved endocytic motif (Rollason et al., 2007). The dual tyrosine motif has also been shown to interact with the AP-2 α subunit. However, this interaction has been shown in yeast two-hybrid assays (Masuyama et al., 2009), which are prone to giving false positive results. In fact, tyrosine base endocytic motifs are not known to bind to clathrin adaptor α subunits, and therefore the observed interaction between tetherin and the AP-2 α subunit might be misleading. Following endocytosis, tetherin is transported to endosomes and back to the plasma membrane via the TGN in a process often referred to as the "slow-recycling pathway". Delivery of tetherin from endosomal compartments to the TGN is dependent on binding of the AP-1 μ subunit to the dual tyrosine motif in the cytoplasmic domain of tetherin (Rollason et al., 2007).

In polarized epithelial cells, tetherin localises particularly to the apical surface, where it has been shown to interact indirectly with the sub-apical actin cytoskeleton. The linkage between tetherin and the cytoskeleton is mediated by an interaction through the Rho GTPase-activating protein RICH2; EBP50; and ezrin (Figure 1-18). Knockdown studies of tetherin or RICH2 led to the disappearance of the apical actin network. Furthermore, disruption of tetherin/RICH2 interactions led to the activation of Rac1 and subsequent dissolution of the polarized actin filament (Rollason et al., 2009).

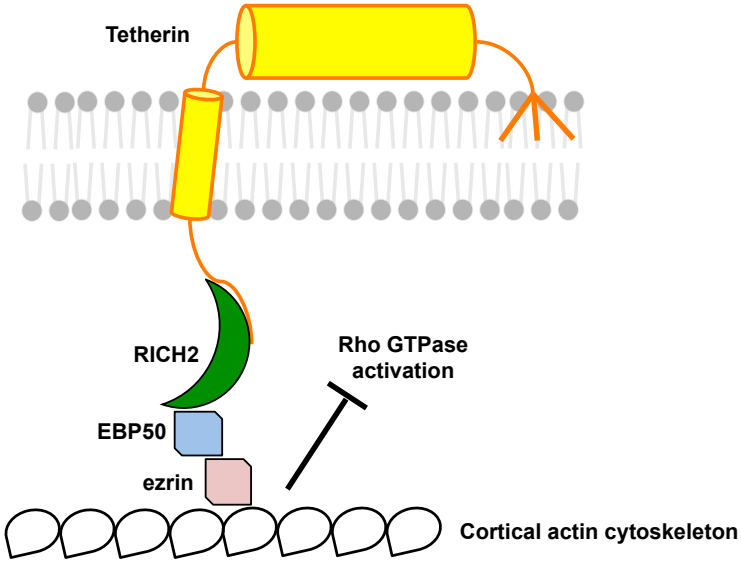

Figure 1-18 Tetherin indirectly interacts with the cortical actin cytoskeleton

Schematic representation of human tetherin at the plasma membrane of polarised cells in indirect association with the cortical actin cytoskeleton by an interaction between its cytoplasmic tail and RICH2, EBP50 and ezrin. Disruption of tetherin/RICH2 interactions activates the Rho GTPase Rac1 leading to the dissolution of the polarized actin filament.

1.6.2 Mechanism of tetherin-mediated virion restriction

Most biochemical, structural and cellular data suggest that tetherin restricts the release of enveloped viruses by directly tethering them to the cell surface, in a model in which tetherin dimers are embedded into the host and viral membranes simultaneously (Figure 1-19). The unusual topology of tetherin enables virus retention, where both membrane anchors, the integrity of the coiled-coil ectodomain and the formation of stable disulphide-linked dimers are essential in for this process (Perez-Caballero et al., 2009) (Hammonds et al., 2012).

This model is supported by several observations. Firstly, tetherin-restricted virus particles can be released by protease treatment, suggesting that tethers consist of proteins (Neil et al., 2008). Interestingly, studies using an artificial tetherin molecule, which contains the same overall topological arrangement as wild-type tetherin, showed that the artificial molecule was also able to trap virions on the plasma membrane. This suggests that it is the unique topology of tetherin, rather than the amino acid sequence *per se*, that confers its retention activity (Perez-Caballero et al., 2009). These data also suggests that no cellular co-factor is required for tetherin-mediated physical particle restriction. Further evidence came from electron microscope (EM) studies that allowed visualisation of electron-dense tethers between virus and host cell membranes or between virions themselves (Figure 1-19 A and B) (Neil et al., 2007) (Neil et al., 2008) (Hammonds et al., 2010). Immunogold labelling EM studies showed that tetherin molecules can be detected at the interface between the host cell membrane and restricted virions (Fitzpatrick et al., 2010) (Hammonds et al., 2010) (Habermann et al., 2010), and super-resolution microscopy revealed that 4 to 7 tetherin dimers cluster at HIV-1 assembly sites (Lehmann et al., 2011).

Taking all data together, a model in which tetherin forms parallel dimers with either N- or C-terminus inserted into the virion membrane (Figure 1-19), is favoured. A recent study suggests that there is a three- to five-fold preference for the insertion of the GPI anchor into viral particles, rather than the transmembrane domain (Venkatesh and Bieniasz, 2013). Indeed, this preference would allow tetherin to activate NF-κB signalling events through a highly conserved **Y**D**Y**CRV motif in its cytoplasmic tail (see 1.6.7). It is currently unknown if the recruitment of tetherin to viral assembly sites requires any signalling events or if the linkage to the actin cytoskeleton recruits tetherin to viral budding zones. However, a recent study suggests that Gag-induced membrane curvature may promote tetherin recruitment to viral budding zones (Grover et al., 2013). Indeed, the relative flexibility of tetherin's extracellular domain would allow recruitment by membrane curvature as tetherin dimers partition into host and virion membranes (Yang et al., 2010) (Schubert et al., 2010).

Following cell surface retention, virions are internalised into endosomal compartments, which most likely results in their degradation. Tetherin mutants that lack the **Y**D**Y**CRV endocytic motif show a reduction in virion accumulation in endosomal compartments, suggesting that tetherin might play a role in virion delivery to endosomes (Galão et al., 2012). Furthermore, internalisation can be blocked by a dominant-negative Rab5 mutant that controls early endosome formation (Neil et al., 2006). The association of tetherin with the actin cytoskeleton through RICH2 (Rollason et al., 2009) might also play a role in virion internalisation. Interestingly, a rare single-nucleotide polymorphism in the *RICH2* gene is associated with HIV-1 disease progression (Le Clerc et al., 2011). Therefore the role of RICH2/tetherin interactions in relation to tetherin's antiviral activity requires further investigation.

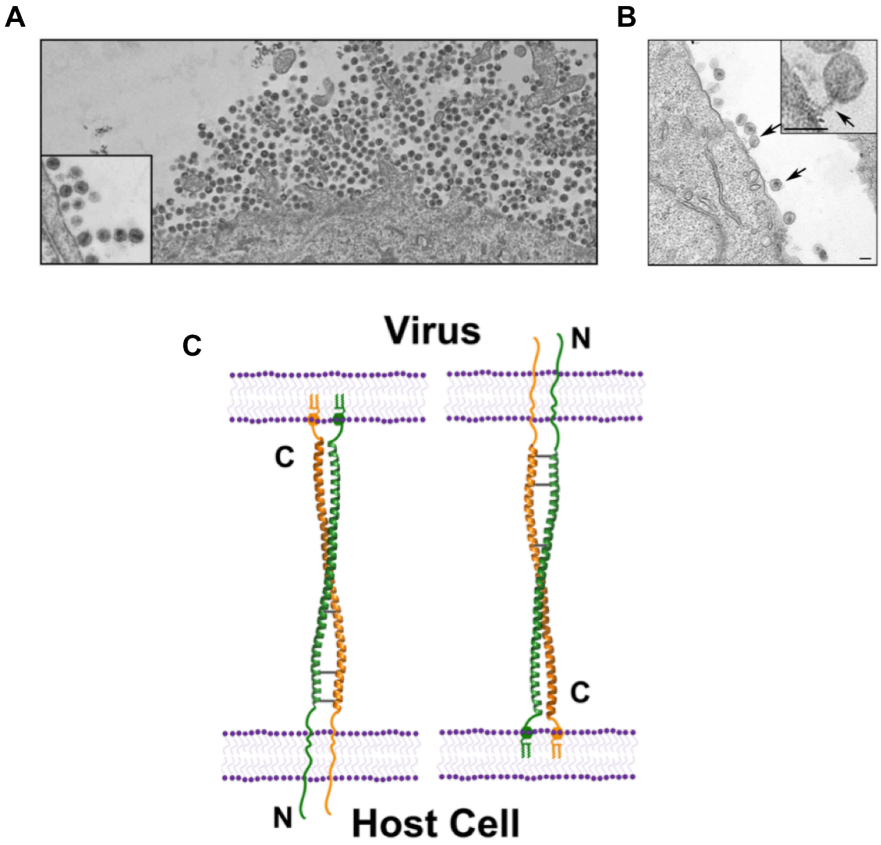

Figure 1-19 Tetherin-mediated restriction of virus particle release

(A) Electron micrographs showing virion surface accumulations of Vpu-defective HIV-1 infected HT1080 cells expressing tetherin (adapted from (Neil et al., 2008)). **(B)** Virus particle tethered to the plasma membrane of Vpu-defective HIV-1 infected Jurkat cells, images visualised using transmission electron microscopy (adapted from (Jolly et al., 2010)). **(C)** Schematic representation of the predicted configuration of tetherin dimers directly inhibiting virus particle release. Tetherin monomers are arranged in a parallel orientation with either the GPI anchors or the N-terminal transmembrane domains inserted into the virion (adapted from (Venkatesh and Bieniasz, 2013)).

1.6.3 Tissue expression and transcriptional regulation of tetherin

BST-2 (tetherin) was initially discovered as a marker of terminally differentiated B cells and bone marrow stromal cells. It has also been identified as a tumour antigen that is expressed on multiple myeloma cells, and it was therefore initially proposed as a selective target for immunotherapy (Goto et al., 1994) (Ishikawa et al., 1995) (Ohtomo et al., 1999). However, a large immunohistochemistry study of human tissues revealed that tetherin is expressed in a broad variety of tissues including hepatocytes, pneumocytes, ducts of major salivary glands, pancreas and kidney, epithelia, plasma cells, bone marrow stromal cells, monocytes, and vascular endothelium (Erikson et al., 2011). This wide constitutive expression suggests that tetherin is not suited as a target for immunotherapy of B cell malignancies. Furthermore, expression of tetherin can also be induced by interferon and other pro-inflammatory stimuli in usually tetherin negative cell types (Neil et al., 2008) (Van Damme et al., 2008) (Bego et al., 2012) (Homann et al., 2011).

Investigations into the nature of the transcriptional regulation of tetherin by type I IFN revealed multiple putative *cis*-regulatory elements for transcription factors in its promoter region including: nuclear factor of activated T cells (NF-AT), signal transducer and activator of transcription (STAT) and NF-κB (Bego et al., 2012). The promoter also possesses an overlapping sequence containing an interferon-stimulated response element (ISRE), an γ-interferon activation site (GAS), IFN regulatory factor elements (IRF-E) and NF-AT (see Figure 1-20). Interestingly, tetherin expression is directly inducible by IRF-3 and IRF-7, independent of its type I IFN-mediated up-regulation. Consistent with this notion, tetherin expression can also be induced downstream of TLR3 and TLR8 (Bego et al., 2012) (Homann et al., 2011). Taken together, these results indicate that pattern recognition can directly induce tetherin expression, suggesting that tetherin plays a crucial role in early anti-viral responses.

Recent evidence suggests that tetherin exists in two isoforms (Cocka and Bates, 2012). Mammalian tetherins have a methionine at position 13, downstream of the tyrosine-base sorting signal. The AUG codons at position 13 as well as the +1 translational initiating codon have weak Kozak consensus sequences, resulting in leaky ribosomal scanning and the expression of both long and short isoforms.

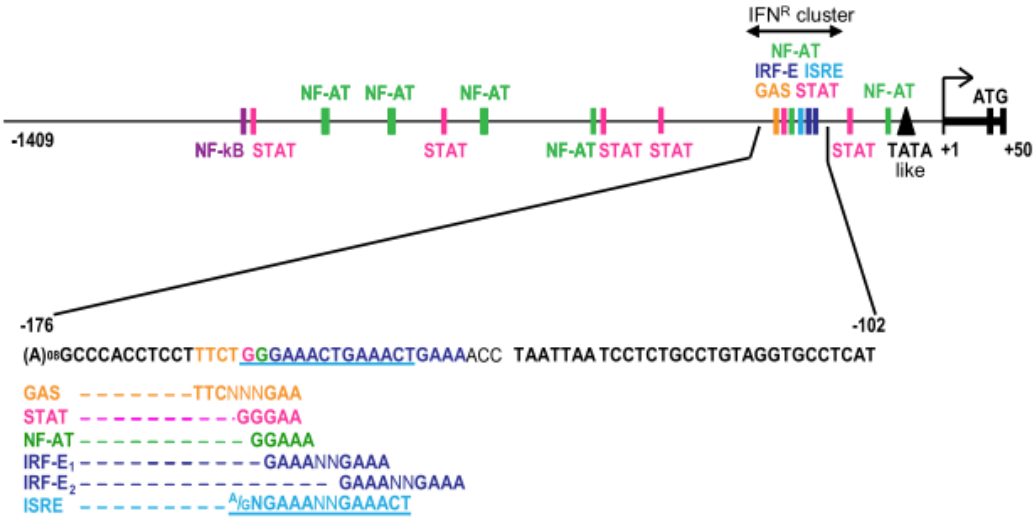

Figure 1-20 Tetherin promoter region

Schematic representation of predicted regulatory elements in the human tetherin promoter region. Abbreviations: GAS (γ-activated site); STAT (signal transducer and activator of transcription); NF-AT (nuclear factor of activated T cells); IRF-E (IFN regulatory factor element); ISRE (IFN-stimulated response element) (adapted from (Bego et al., 2012)).

1.6.4 Viral countermeasures

Tetherin inhibits the release of enveloped virus particles from a variety of viral groups that share little or no homology, thus highlighting tetherin's broad anti-viral function. Mechanistically, tetherin targets the host-derived lipid envelope of viruses, the one component that the virus cannot mutate. There are several examples of mammalian viruses that have evolved tetherin antagonists and most use different mechanisms to induce tetherin cell surface removal. The HIV-1 accessory protein Vpu is used as the prototype countermeasure, but to date seven other virally encoded mammalian counter-tetherin proteins have also been characterised: SIV Vpu; SIV Nef; HIV-2 Env; SIVtan Env; KSHV K5; HSV-1 gM/Vhs; and Ebola GP.

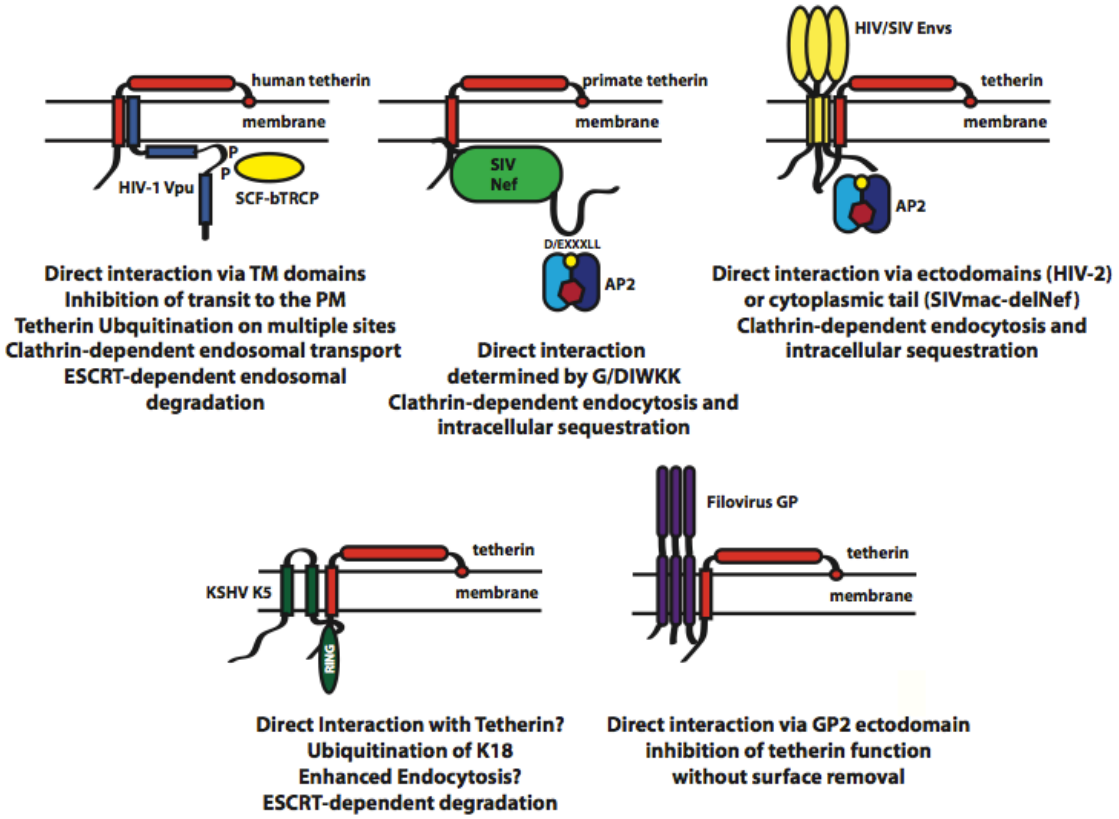

Figure 1-21 Tetherin and its virally encoded antagonists

Schematic representation of the five well characterised tetherin antagonists (as displayed from top left to right bottom): HIV-1 Vpu, SIV Nef, HIV-2/ SIV Envs, KSHV K5 and Filovirus GP. A short summary of mechanistic details is shown under each viral antagonist (Neil, 2013).

1.6.4.1 HIV-1 and SIV Vpu

The HIV-1 accessory protein Vpu is a small N-terminally anchored transmembrane protein that for many years had two known functions: degradation of CD4 and enhancement of virus progeny virions release from certain cell types. The discovery of tetherin as a restriction factor answered the more than 20 year old question regarding the role of Vpu during virus release (Neil et al., 2008) (Van Damme et al., 2008). SIV chimpanzee (SIVcpz) and certain members of the SIV lineage that infect african guenon monkeys including the SIV greater spot-nosed monkeys (SIVgsn), SIV mustached monkey (SIVmus), SIV mona monkey (SIVmon), as well as SIV dents monkey (SIVden), also encode Vpu proteins (reviewed by (Sharp and Hahn, 2011)) which display anti-tetherin activity, at least against their host species orthologous proteins (Sauter et al., 2009).

HIV-1 Vpu reduces tetherin cell surface levels (Van Damme et al., 2008) and re-directs tetherin for ESCRT-dependent degradation in lysosomal compartments (Douglas et al., 2009) (Iwabu et al., 2009) (Mitchell et al., 2009) (Kueck and Neil, 2012) (Agromayor et al., 2012). Vpu antagonises tetherin through direct interactions of their respective transmembrane domains (Kobayashi et al., 2011) (Vigan and Neil, 2010) and displays a species-specificity governed by residues that form the interaction face (McNatt et al., 2009) (Gupta et al., 2009a). The mechanism by which Vpu overcomes tetherin restriction has been studied extensively and will be discussed below (1.7.3)

1.6.4.2 SIV Nef

SIV lineages that do not encode a Vpu protein use their Nef proteins as tetherin antagonists. The Nef accessory proteins of phylogenetically diverse SIVs, including SIVmac (macaque), SIVagm (African green monkey), SIVsmm (sooty mangabey monkey), SIVblu (blu monkey), SIVrcm (red capped monkey) and SIVcpz (chimpanzee), counteract tetherin orthologues derived from their simian hosts (Jia et al., 2009) (Zhang et al., 2009) (Lim et al., 2010). Nef-mediated anti-tetherin activity is primate species-specific, and all SIV Nef proteins fail to antagonise human tetherin. This specificity results from the five amino acid deletion, G/DIWKK, in the cytoplasmic tail of human tetherin (Figure 1-22) (Jia et al., 2009) (Zhang et al., 2009).

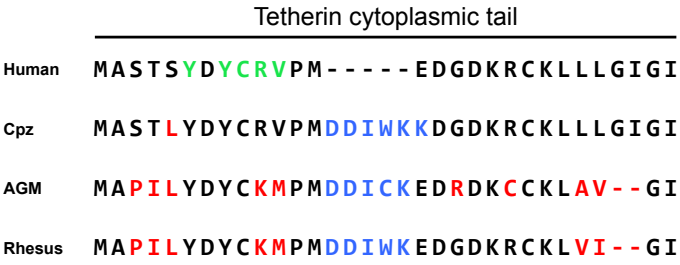

Figure 1-22 Primate tetherin cytoplasmic tail alignment

Amino acid alignment of primate tetherin cytoplasmic tails. Regions differing from human tetherin are depicted in red and blue, the tyrosine-based endocytosis/signalling motif is illustrated in green.

Interestingly, the tryptophan residue in the G/DI**W**KK motif has been under high selective pressure, possibly imposed by Nef-like viral antagonists, which determines species-specificity, and may have forced tetherin molecules to mutate into a resistant form during primate evolution. Insertion of the G/DIWKK motif into human tetherin renders it sensitive to SIV Nef proteins (Lim et al., 2010) (Zhang et al., 2009). Like HIV-1 Vpu, SIV Nef proteins are able to reduce tetherin surface levels, but do not induce tetherin degradation. Mechanistically, Nef targeting to cellular membranes by myristoylation of a glycine residue at position 2 is required for tetherin cell surface downregulation (Zhang et al., 2011a). The core domain of Nef has been shown to directly interact with the N-terminus of rhesus tetherin. However, the interaction is also stabilized by residues in the N-terminal and flexible loop region of Nef that are thought to affect membrane association or the recruitment of unknown cellular co-factors (Serra-Moreno et al., 2013). A highly conserved acidic dileucine motif (**D**/**E**)xxx**L**(**L**/**M**) and supporting acidic residues in Nef proteins bind to the clathrin adaptor AP-2, which is crucial for tetherin removal from virus assembly zones (Zhang et al., 2011a) (Serra-Moreno et al., 2013). AP-2-mediated endocytosis is also required for Nef to induce cell surface downmodulation of the HIV-1 entry receptor CD4 (Lindwasser et al., 2008). However, the mechanism of tetherin antagonism by SIV Nef is otherwise genetically separable from additional functional activities of Nef, like CD4 and MHC downregulation (Serra-Moreno et al., 2013).

1.6.4.3 HIV-2 and SIV envelopes

HIV-2 is a zoonotic infection of SIV from sooty mangabey monkeys (SIVsmm) transmitted to humans. The low virus loads and transmission rates in humans make HIV-2 less pathogenic than HIV-1. Interestingly, HIV-2 does not encode a *vpu* gene (reviewed by (Sharp and Hahn, 2011)).

The ability of the HIV-2 envelope protein to promote virus release in certain cell lines, in a Vpu-like manner, was recognised before this effect was attributed to the counter-action of tetherin (Bour and Strebel, 1996) (Bour et al., 2003). Subsequently, it has been shown that the HIV-2 ROD10 envelope glycoprotein interacts with tetherin via ectodomain interactions, and is able to mediate its cell surface removal, whereas HIV-2 ROD14 and the SIVmac Env proteins do not (Bour et al., 2003) (Le Tortorec and Neil, 2009) (Hauser et al., 2010). HIV-2 Env also displays a broader species-specificity for tetherin than Vpu but the Env antagonism is less potent than Vpu or Nef, at least in *in vitro* assays (Hauser et al., 2010). HIV-2 Env removes tetherin from virus assembly sites by inducing intracellular sequestration in TGN-associated compartments, but like SIV Nef, does not induce tetherin degradation (Le Tortorec and Neil, 2009) (Hauser et al., 2010).

The exact determinants required for tetherin antagonism in HIV-2 Env are still under investigation. However, the highly conserved membrane-proximal binding site for the AP-2 μ subunit, G**Y**xxϕ, is essential for tetherin endocytosis (Abada et al., 2005) (Noble et al., 2006) (Le Tortorec and Neil, 2009). Tantalus SIV (SIVtan) Env, like HIV-2 Env, counteracts human and several primate tetherin orthologues. The SIVtan Env protein also relies on the AP-2 binding site in its cytoplasmic tail to induce tetherin cell surface downregulation (Gupta et al., 2009b). However, SIVtan is a laboratory adapted strain and was co-cultured in tantalus monkey and human CD4+ T cells before isolation, and may not reflect tetherin antagonism in the natural host. However, another SIV Env protein has been reported to be able to antagonise tetherin, isolated from experimentally infected rhesus macaques, with Nef-deleted SIVmac viruses, that reverted to pathogenicity (Serra-Moreno et al., 2011). Upon investigation of the determinants it was shown that the Env protein had acquired activity against rhesus tetherin by a five amino acid substitution in the gp41 cytoplasmic tail. Like the HIV-2 Env mechanism of counteraction, this Env was able to interact with rhesus tetherin and removed tetherin from sites of viral assembly in the presence of an intact G**Y**xxϕ sorting motif in its cytoplasmic tail. The ectodomain of this Env protein was dispensable for tetherin antagonism, as gp41/CD4 chimeric proteins sufficiently antagonised tetherin, with physical association mediated by gp41. In terms of tetherin itself, Nef-deficient SIVmac Env-mediated tetherin targeting is highly species-specific and is

determined by differences in residues that flank the dual tyrosines (PIL**Y**D**Y**(R/C)KM versus STS**Y**D**Y**CRV) between rhesus and human tetherin molecules respectively (see Figure 1-22).

Proteolytic processing of the envelope protein into the subunits gp120 and gp41 is also required for tetherin antagonism (Bour et al., 2003) (Le Tortorec and Neil, 2009). The HIV-2 Env extracellular domain is likely to be involved in tetherin interaction, as exchange of the gp41 transmembrane domain and cytoplasmic tail with SIVmac did not abolish anti-tetherin function (Le Tortorec and Neil, 2009). In further support of ectodomain interactions, a substitution of a single positively selected amino acid in human tetherin, A100D, rendered tetherin resistant to SIVtan Env without compromising antiviral activity or sensitivity to Vpu (Gupta et al., 2009b).

1.6.4.4 HSV-1 encodes two tetherin antagonists: gM and Vhs

The herpes simplex virus 1 (HSV-1) is a large DNA virus that belongs to the alpha-herpesvirus family. Like all *Herpesviridae*, HSV-1 has a complex assembly pathway, in which the final envelopment occurs at membranes derived from TGN compartments (Flint et al., 2009).

Two recent publications demonstrated that HSV-1 particle release is restricted by tetherin overexpression (Zenner et al., 2013) (Blondeau et al., 2013). One group identified the viral envelope glycoprotein M (gM) as a moderate anti-tetherin factor (Blondeau et al., 2013) (Nathan and Lehner, 2009). They demonstrated that gM expression reduced cell surface tetherin levels and induced tetherin intracellular localisation to TGN46-positive compartments. Furthermore, the HSV-1 gM glycoprotein specifically rescued Vpu deficient HIV-1 virus particle release. However, gM only had minor effects on HSV-1 replication, and tetherin degradation was found to be independent of gM. Thus, this raised the possibility that HSV-1 may encode another partially redundant tetherin antagonist. A second research group identified the virion host shut-off protein (Vhs) as a tetherin countermeasure (Zenner et al., 2013). Vhs is an endoribonuclease that causes destabilization of a broad spectrum of mRNA molecules and has been shown to antagonise both innate and adaptive immune responses. This group demonstrated that Vhs is able to overcome tetherin restriction by reducing tetherin mRNA levels, and potentially avoiding tetherin-mediated NF-κB signalling events. This is a novel mechanism that has never been described before. However, more work is needed to clarify the role of HSV-1 gM and Vhs proteins in tetherin antagonism and to explore tetherin-induced signalling events in HSV-1 infection.

1.6.4.5 KSHV K5

K5 is a membrane attached RING-CH (MARCH) domain E3 ubiquitin ligase encoded by the gamma herpesvirus Kaposi's sarcoma-associated herpesvirus (KSHV), and has been shown to downregulate a number of different cell surface proteins including NK receptor ligands, MHC class I and II as well as adhesion proteins (reviewed by (Nathan and Lehner, 2009). Before tetherin was recognised as an HIV-1 restriction factor, it had been identified in a proteomic screen for novel K5 targets (Bartee et al., 2006). K5 counteracts tetherin activity in a species-specific manner and promotes ESCRT-dependent lysosomal degradation of tetherin similar to the degradation seen with HIV-1 Vpu (Mansouri et al., 2009) (Pardieu et al., 2010) (Agromayor et al., 2012). Knockdown of the ESCRT-I component ubiquitin-associated protein 1 (UBAP1) results in the accumulation of ubiquitinated tetherin molecules in late endosomal compartments

(Agromayor et al., 2012). Furthermore, it has also been shown that dominant negative VPS4 is able to block cell surface down-modulation of tetherin by K5 (Pardieu et al., 2010), suggesting that K5 is, like Vpu, able to redirect tetherin from the cell surface to late endosomes and routes tetherin for lysosomal degradation. Interestingly, K5 selectively ubiquitinates the lysine residue at position 18 in tetherin's cytoplasmic tail, and this ubiquitination is absolutely required for K5 to counteract tetherin (Mansouri et al., 2009) (Pardieu et al., 2010).

Unlike HIV, herpes viruses undergo two envelopments to complete assembly, the first at the nuclear membrane and the second in TGN-associated compartments that leads to virion egress via the secretory pathway (Mettenleiter et al., 2006). Tetherin is thought to inhibit KSHV virion release in TGN-associated compartments, which gives rise to the question whether other herpes virus families are restricted by tetherin and encode countermeasures.

1.6.4.6 Ebola envelope glycoprotein

The highly pathogenic Ebola virus (EBOV) was first described in 1976 and is the causative agent of severe viral haemorrhagic fever outbreaks in humans and non-human primates. EBOV is a negative single-stranded RNA virus, forms filamentous virions and belongs, like Marburg virus (MARV), to the *Filoviridae* family. To date five different EBOV species have been identified, which vary in sequence and mortality rates (Flint et al., 2009).

Vpu is able to enhance the release of EBOV virus-like particles (VLPs) from tetherin expressing cells, demonstrating that filovirus virions are sensitive to tetherin-mediated restriction (Neil et al., 2007). Indeed, the EBOV envelope glycoprotein (GP) is able to antagonise tetherin function (Kaletsky et al., 2009), an ability which is conserved in the *Filoviridae* family, given that the MARV GP is also able to rescue Vpu deficient HIV-1 release (Kühl et al., 2011). The EBOV GP, unlike HIV-1 Vpu and most other tetherin antagonists, is able to counteract human, primate and murine tetherin molecules (Lopez et al., 2010). This broad activity might be due to the breadth of mammalian host species infected by EBOV. The exact mechanism of GP-mediated tetherin antagonism is unclear but requires direct interaction of GP and tetherin via its GP2 subunit (Kaletsky et al., 2009) (Kühl et al., 2011). Tetherin is not removed from the cell surface in the presence of EBOV GP and remains associated with lipid rafts (Lopez et al., 2010) (Lopez et al., 2012), which is surprising to some extent as EBOV GP has been shown to induce downregulation of other cell surface molecules like MHC class I and the epidermal growth factor receptor (EGFR) (Simmons et al., 2002). Therefore, GP

might physically interfere with tetherin restriction of virions at the plasma membrane, however, it does not rely on a specific domain in tetherin, because it is able to antagonise a completely synthetic tetherin molecule (Lopez et al., 2010). Tetherin levels remain constant in EBOV infected cells, indicating that GP does not induce tetherin degradation, unlike HIV-1 Vpu and KSHV K5. However, tetherin has no effect on EBOV spread using infectious EBOV replication assays (Radoshitzky et al., 2010), which could be a result of a cell type specific function of GP (Kühl et al., 2011). Clearly, more studies are required to fully understand the mechanism of EBOV GP-mediated tetherin antagonism.

1.6.5 Tetherin and other viruses

To date, tetherin has been shown to restrict the virus particle release of all retroviruses tested as well as filoviruses (Ebola virus and Marburg virus), arenaviruses (Lassa virus and Machupo virus), paramyxoviruses (Nipah virus, Hendra virus and Sendai virus), gamma-herpesviruses (KSHV), alpha-herpesviruses (HSV-1), rhabdoviruses (vesicular stomatitis virus) and flaviviruses (Dengue virus) (reviewed by (Le Tortorec et al., 2011) and (Neil, 2013)). The capability of tetherin to restrict such a broad range of viruses resides in its ability to trap enveloped viruses that bud from cellular membranes by incorporation into the host-derived envelope. However, some viruses that are highly sensitive to tetherin expression *in vitro* do not encode a tetherin countermeasure. Tetherin might not be expressed in their natural target cells or the assembly mechanism of these enveloped viruses itself might be insensitive to tetherin restriction.

Studies performed with influenza A virus (IAV) showed opposing results regarding the sensitivity to tetherin. Initial observations revealed that tetherin was unable to restrict IAV budding, excluding tetherin incorporation into virions (Watanabe et al., 2011). However, the same group also reported that tetherin expression inhibited influenza VLP release, which could be overcome by HIV-1 Vpu expression. At the same time the neuraminidase (NA) protein of some IAV strains was reported to possess a Vpu-like function on VLP release (Yondola et al., 2011). An independent study showed that ectopic expression of tetherin strongly inhibited the release of newly formed IAV particles and could be overcome by the influenza virus NS1 protein, which reduced IFN-mediated up-regulation of ISGs including tetherin (Mangeat et al., 2012). However, two different reports have challenged these results since (Winkler et al., 2012) (Bruce et al., 2012). One research group used microscopic imaging techniques to demonstrate that filamentous and spherical assembly of various IAV strains was unaffected by tetherin, suggesting that IAV may possess a mechanism to exclude tetherin from

budding of filamentous virions (Bruce et al., 2012). Thus, more work needs to be done to clarify the effects of tetherin on IAV.

Interestingly, tetherin was suggested to act as an entry co-factor for the beta-herpesvirus human cytomegalovirus (HCMV) (Viswanathan et al., 2011). Tetherin expression enhanced viral entry, as more virions were released into tetherin positive cells compared to tetherin negative cells. Therefore, the authors suggested that tetherin is incorporated into virions and is able to interact with monomeric tetherin molecules expressed at the surface of their target cells, which leads to enhancing HCMV entry. However, the underlying mechanism of these observations remains to be determined.

1.6.6 Tetherin and cell to cell transmission

HIV-1 and other human enveloped viruses can disseminate within an infected host by two mechanisms: cell-free virus release and virus transfer by physical interaction between infected donor and uninfected target cells (reviewed by (Sattentau, 2008) and (Mothes et al., 2010)). The latter mechanism is called cell-to-cell transfer and is thought to be up to 10-100 times more efficient than cell-free virus spread. There are several advantages in direct cell-to-cell transfer that can be exploited by viruses. First, direct cell-to-cell spread is more rapid because it reduces rate-limiting early steps in the virus life cycle. Second, the limited exposure time to extracellular space may help viruses to evade elements of the innate immune system, such as neutralising antibodies and complement. A supramolecular structure, termed the virological synapse (VS), was shown to mediate the cell-to-cell dissemination of HTLV-I and HIV-1 (Igakura et al., 2003) (Jolly et al., 2004). For HIV-1 the VS is formed by binding of the Env protein, which is displayed at the surface of infected cells, to its entry receptors expressed on the target cell membrane (Jolly et al., 2004) (Chen et al., 2007). Cytoskeletal rearrangements and a variety of adhesion molecules, including LFA-1, ICAM-1 and ICAM-3, are required to maintain the stability of the virological synapse (Jolly et al., 2004) (Jolly et al., 2007). The relative contribution of cell-free and cell-to-cell HIV-1 dissemination *in vivo* is still unclear. However, a recent study that examined the migratory behaviour of HIV-1 infected T cells in lymph nodes of humanised mice discovered that infected T cells are motile and are the major route of virus dissemination to distal tissues (Murooka et al., 2012).

Some studies that have addressed the role of HIV-1 Vpu in cell-to-cell transmission were performed before the discovery of tetherin as a viral restriction factor, and replication studies performed with Vpu-deleted HIV-1 suggested that cell-free virion

accumulation in the supernatant was reduced while spread within the culture was unimpaired (Strebel et al., 1989) (Terwilliger et al., 1989) (Klimkait et al., 1990) (Yao et al., 1992) (Schubert et al., 1995). Consistent with this notion, selection for HIV-1 variants that spread more efficiently by cell-to-cell dissemination resulted in viruses with mutation in their *vpu* gene (Gummuluru et al., 2000). However, since viruses restricted by tetherin are fully infectious, the question whether these viruses can be transferred by cell-to-cell contact through virological synapses remained.

Studies that have directly addressed the role of tetherin in cell-to-cell spread have reported opposing results. There is agreement that tetherin co-localises with Env at virological synapses. Furthermore, VS formation in T cells infected with Vpu-defective HIV-1 was increased compared to wild-type. But the consequences of tetherin-mediated virus retention on cell-to-cell spread have been controversial (Jolly et al., 2010) (Casartelli et al., 2010). One study demonstrated that tetherin-mediated retention of virions could promote cell-to-cell spread between Jurkat T cells infected with Vpu-defective HIV-1 and primary CD4+ T cells, presumably by providing immobilised and infectious virions at the contact side (Jolly et al., 2010). This effect could be reversed by siRNA-mediated depletion of tetherin. However, two other studies reported that tetherin expression reduced cell-to-cell transfer (Casartelli et al., 2010) (Kuhl et al., 2010). These contradictory results might be explained by differences in tetherin expression levels between cell types used in the different studies. HeLa and tetherin-inducible 293T cells express higher amounts of tetherin than Jurkat and primary CD4+ T cells. It is possible, that at high tetherin expression levels cell-to-cell transfer is impaired whereas at low expression levels cell-to-cell transfer is increased. Jolly et al showed that increased tetherin expression by IFN treatment had only minor effects on cell-to-cell spread. Furthermore, the Vpu 2/6 phospho-mutant, which is strongly impaired in its ability to antagonize tetherin, replicates less efficiently in macrophages, which express high levels of tetherin, compared to primary CD4+ T cells (Schindler et al., 2010). Another possible explanation for the contradictory results is that the dynamics of cell-to-cell spread may be dependent on specific features in donor and target cell types (Zhong et al., 2013).

Another interesting possibility is that tetherin itself might be involved in the formation and stabilisation of virological synapses. To this end, depletion of tetherin impaired wild-type HIV-1 cell-to-cell dissemination (Jolly et al., 2010), suggesting that reduced tetherin levels at the cell surface might negatively affect HIV-1 transmission. Tetherin was shown to indirectly interact with the actin cytoskeleton, in polarised epithelial cells, via the BAR-RacGAP protein RICH2 (Rollason et al., 2009). This interaction physically links tetherin molecules to the apical actin network, which enables tetherin to contribute

to the organisation of lipid rafts (Billcliff et al., 2013). HIV-1 assembles in lipid rafts and the integrity of these rafts as well as the underlying actin cytoskeleton is required for efficient cell-to-cell spread (reviewed by (Ono, 2010)). Thus, it remains to be solved which role tetherin plays in the organisation of lipid rafts during HIV assembly.

1.6.7 Tetherin as a viral immune sensor

Tetherin concentrates virus particles at the surface of infected cells. Therefore one might speculate that: (1) tetherin enhances antibody opsonisation and clearance of infected cells by the recruitment of complement or natural killer cells through Fc receptor recognition; (2) tetherin increases MHC class II antigen presentation and therefore provides a link between innate and adaptive immunity; or (3) tetherin acts as pattern-recognition receptor to activate immune signalling pathways (Figure 1-23). Indeed, before its discovery as a restriction factor, tetherin was identified in a genome wide cDNA screen, looking for factors that induce NF-κB activation (Matsuda et al., 2003).

Recently, the potential importance of tetherin in regulating immune responses to viral infection has started to emerge as tetherin was found to be able to stimulate NF-κB activation and trigger antiviral responses (Cocka and Bates, 2012) (Galão et al., 2012) (Tokarev et al., 2013). Cross-linking of surface tetherin by antibody, budding of tetherin-sensitive HIV-1 and EBOV particles (Galão et al., 2012), and overexpression of tetherin, enhanced NF-κB activation (Cocka and Bates, 2012) (Galão et al., 2012) (Tokarev et al., 2013). Furthermore, human primary CD4+ T cells infected with Vpu-defective HIV-1 produced high levels of pro-inflammatory cytokines, including CXCL10, IL-6 and type I IFN, in a tetherin-dependent manner, suggesting that tetherin acts as a PRR for enveloped viruses (Galão et al., 2012). However, tetherin-mediated endocytosis of virions is not required to trigger NF-κB activation. Unpublished data from our laboratory (personal communication with Galao, Pickering and Neil) indicates that the tyrosine residues within the **Y**D**Y**CRV signalling motif in the cytoplasmic tail of tetherin are phosphorylated by a member of the Src family kinase, which leads to the subsequent recruitment of a signalling complex that includes TRAF6, TRAF2 and Ubc13. This in turn leads to an Ubc13-dependent activation of TAK1 through polymerisation of K63-linked ubiquitin chains. Polymerisation leads to IKK phosphorylation and IκB degradation, allowing translocation of NF-κB and expression of pro-inflammatory genes (Galão et al., 2012). Interestingly, the signalling activity of tetherin might be an evolutionary recent acquired function, as it has only been observed in human and chimpanzee tetherin orthologues (Galão et al., 2012). HIV-1 Vpu and KSHV K5, thus far, are the only known antagonists of human tetherin that induce its degradation, therefore it is tempting to speculate that only the final degradation of tetherin ensures inhibition of tetherin-mediated immune activation.

Viral retention and re-routing of tethered virions to endosomal compartments may also promote the availability of virus components to other host pathogen recognition factors including endosomal TLRs, cytoplasmic PRRs and DNA sensors. Indeed, tetherin-

mediated IFN responses in infected CD4+ T cells can be blocked by inhibition of the TLR3 adaptor protein TRIF. This suggests that tetherin may also be able to indirectly enhance the expression of type I IFNs and pro-inflammatory cytokines via the IRF pathway.

Finally, tetherin was proposed to bind to the immunoglobulin-like transcript 7 (ILT7) (Cao et al., 2009). ILT7 is a negative regulatory receptor that is found on resting pDCs, and which downregulates TLR responses after viral stimulation (Cho et al., 2007). Therefore, it was proposed that tetherin/ILT7 interaction may downregulate TLR-mediated IFN and cytokine responses in a negative-feedback manner (reviewed by (Cao and Bover, 2010)). However, blockade of tetherin/ILT7 interactions, in peripheral blood mononuclear cell cultures, did not affect the ability of ILT7 to dampen TLR9 responses (Tavano et al., 2013), suggesting that tetherin/ILT7 interactions might act as a homeostatic regulatory mechanism on immature pDCs, rather than a negative-feedback mechanism.

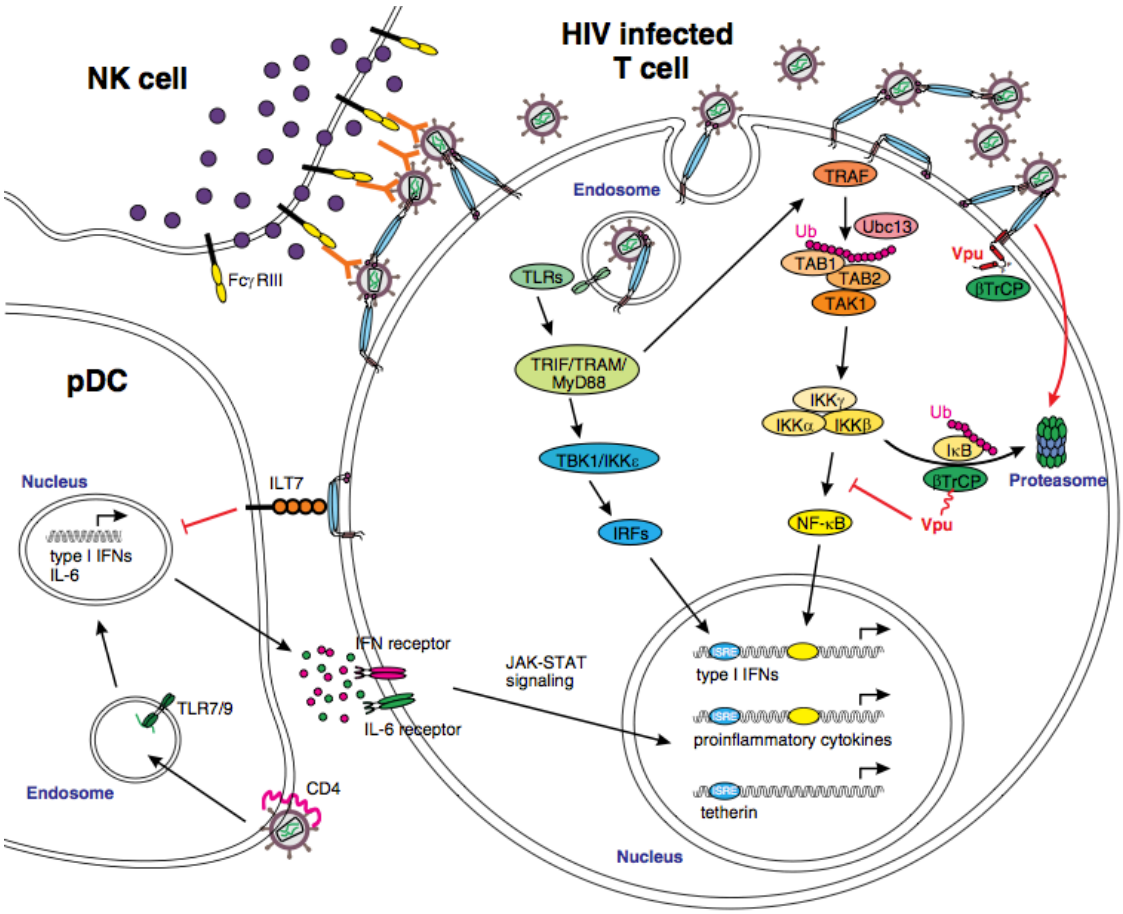

Figure 1-23 Reported roles of tetherin in immune signalling events

HIV-1 virus particles bind to CD4 on the surface of plasmacytoid dendritic cells (pDC), followed by their endocytosis and recognition of viral RNA by TLR7/9 in endosomal compartments. This leads to the expression of type I IFN and IL-6 that bind to their subsequent receptors on T cells to mediate transcription of interferon-induced genes (including tetherin), pro-inflammatory cytokines, and type I IFN, through the JAK-STAT signalling pathway. At the plasma membrane, tetherin molecules restrict the release of mature virus particles, which induces TRAF- and Ubc13-dependent ubiquitin-mediated activation of TAK1 that in turn induces IKK-mediated phosphorylation, followed by proteasomal degradation of IκB to allow NF-κB-dependent gene expression. HIV-1 Vpu interferes with this process by mediating tetherin degradation and/or sequestering β-TrCP. Internalisation of tetherin-retained virions for degradation may increase the recognition of virus particle-associated PAMPs by endosomal pattern recognition receptors, promoting the expression of antiviral genes such as type I IFN and pro-inflammatory cytokines, via the IRF pathway. Tetherin interaction with ILT7, expressed on the surface of pDCs, induces an inhibitory feedback loop that reduces TLR-mediated expression of type I IFN and pro-inflammatory cytokines. Tetherin may also facilitate antibody opsonisation by increasing the number of viral antigens at the cell surface, which might lead to the recognition of antibodies by Fc receptors expressed on the surface of NK cells, leading to subsequent cytokine release and destruction of infected T cell (adapted from (Hotter et al., 2013)).

1.6.8 Tetherin and viral pathogenesis *in vivo*

The role of tetherin in pathogenesis and antiviral immune responses *in vivo* has so far addressed only in murine systems. One study used tetherin knockout mice infected with Moloney murine leukemia virus (Mo-MLV) or a pathogenic MLV strain LP-BM5, and showed that tetherin plays a direct antiviral role *in vivo* (Liberatore and Bieniasz, 2011). Extensive immuno-phenotyping of tetherin -/- mice showed that tetherin is not required for the development of the functional adaptive immune system. Initially, Mo-MLV infection did not induce tetherin expression on target cells and type I IFN treatment of tetherin -/- mice was required to reveal the anti-Mo-MLV activity of tetherin. However, tetherin-deficient mice infected with LP-BM5 had higher levels of plasma viremia and induced exaggerated pathology reminiscent of HIV/AIDS, indicating that tetherin plays a direct antiviral role *in vivo*. Another study identified a single nucleotide polymorphism in the *tetherin* gene of NZW/LacJ (NZW) mice. This homozygous polymorphism leads to the exclusive expression of short-tetherin isoforms that lack the tyrosine-based endocytic motif (**Y**x**Y**xxϕ) (Barrett et al., 2012). Cell surface tetherin expression on lymphoid and myeloid cells in these mice was increased compared to control C57BL/6 mice expressing full-length tetherin. Increased surface tetherin expression in NZW mice correlated with a decrease in Friend murine leukemia virus (F-MuLV) replication and pathogenesis. A humanised NOD-SCID IL2Rγ^{null} (NSG) mouse model of acute HIV infection has also been used to assess the role of Vpu-mediated tetherin antagonism in establishing plasma viremia and viral dissemination in lymphoid tissues (Dave et al., 2013). This study demonstrated that optimal tetherin antagonism by HIV-1 Vpu is critical for the establishment of efficient plasma viremia and dissemination during acute infection.

Further compelling evidence for the importance of tetherin in human HIV/AIDS disease comes from the adaptation of a fully functional Vpu protein that correlates with efficient spread of group M (Sauter et al., 2009), and the characterisation of a group N Vpu protein that has evolved to become a tetherin antagonist (Sauter et al., 2012). Recently, single genome analysis of *vpu* alleles from HIV-1 clade B infected individuals showed that despite extensive amino acid diversity of the Vpu protein, anti-tetherin function of Vpu was rarely impaired (Pickering et al., 2014). Therefore, highlighting the importance of maintaining anti-tetherin function throughout HIV-1 infection. Another study tested the association of *tetherin* gene variants with disease progression and reported a faster HIV-1 disease progression in individuals with a 19 base-pair insertion or a single-nucleotide polymorphism in their *tetherin* genes (Laplana et al., 2013).

1.7 HIV-1 Vpu

The accessory protein Vpu was first identified in 1988 as a previously undetected open reading frame located between the first exon of the *tat* gene and the *env* gene of HIV-1 (Cohen et al., 1988) (Strebel et al., 1988). This was also when the gene was given its name *vpu*, standing for: viral protein *unique*. Antibodies to the newly identified protein could be detected in patient serum from infected HIV-1 individuals. Interestingly, Vpu distinguished HIV-1 isolates from HIV-2 and some SIV (SIVsmm and SIVmac) isolates, as these viruses do not encode an equivalent protein (Cohen et al., 1988) (Strebel et al., 1988). With time, homologues have been identified in SIVcpz, SIVmon, SIVgsn, SIVmus, SIVden and SIVgor (reviewed by (Sharp and Hahn, 2011)). Initial studies ascribed Vpu with a functional property of facilitating virus release from infected cells. However, since the identification of Vpu its list of functions has increased. To date the major roles attributed to Vpu are: rapid degradation of the cell surface receptor CD4, enhancement of virus particle release by counteraction of tetherin, and downmodulation of CD1d and NTB-A.

1.7.1 Structure and cellular localisation of Vpu

HIV-1 Vpu is a small 77-86 amino acid type I integral membrane protein capable of homo-oligomerisation (Maldarelli et al., 1993). Vpu is translated from a Rev-dependent bicistronic mRNA, which also encodes the viral envelope glycoprotein (Schwartz et al., 1990). The prototype NL4.3 Vpu protein is predicted to have a short luminal N-terminal domain, an N-terminal hydrophobic transmembrane domain (residues 4-27) followed by 54 amino acids that form the C-terminal cytoplasmic tail (residues 27-81) (Figure 1-24) (Maldarelli et al., 1993) (reviewed by (Bour and Strebel, 2003)). The crystal structure of the full-length Vpu protein is yet to be solved. However, several NMR structures of both TM and cytoplasmic tails have been determined (Henklein et al., 1993) (Federau et al., 1996) (Wray et al., 1995). The N-terminal membrane-spanning domain is predicted to form an alpha helix with an average tilt angle of 13 degrees in a lipid environment (Park et al., 2003) (Park and Opella, 2005). Interestingly, the transmembrane domain of Vpu is also critical for oligomerisation and the pentameric structure has been predicted to form a cation-selective ion channel (Schubert et al., 1996a) (Lopez et al., 2002) (Hussain et al., 2007). Notably, the ion channel activity of Vpu does not appear to be required for anti-tetherin or anti-CD4 function.

The cytoplasmic tail of Vpu comprises two predicted alpha helices, the first of which is thought to be partially submerged in the lipid bilayer by virtue of a juxta-membrane hinge. The flexible and highly conserved region between the cytoplasmic alpha helices

forms a loop-like structure. The location of the second helix still remains unclear. Upon interaction with cellular host factors CD4 or tetherin the tertiary structure of Vpu is thought to undergo conformational change (reviewed by (Bour and Strebel, 2003)).

The flexible cytoplasmic domain contains a region bearing a highly conserved D**S**GNE**S** motif. The pair of serine residues (S52 and S56) is constitutively phosphorylated by casein kinase II (Schubert et al., 1992) (Schubert and Strebel, 1994) (Friborg et al., 1995). This phosphorylation mediates binding to β-TrCP and the cytosolic Skp1-Cullin1-F-Box (SCF) E3 ubiquitin ligase complex (SCF^{TrCP}) (Margottin et al., 1998).

The laboratory-adapted NL4.3 Vpu protein and those encoded by other subtype B strains localise to internal membrane structures, predominantly the trans-Golgi network, as well as endosomes and endoplasmic reticulum, little or no accumulation of Vpu is detected at the cell surface (Varthakavi et al., 2006) (Dubé et al., 2009). An important domain for the TGN localisation was mapped to residues R30 and K31 in the first alpha helix of subtype-B Vpu (Dubé et al., 2009). These residues are part of a putative overlapping tyrosine **Y**xxϕ and acidic/dileucine motif in the hinge region between the transmembrane domain and cytoplasmic tail (Figure 1-24B). The second alpha helix bears a putative acidic/dileucine-based sorting motif, **E**xxx**LV,** that is required for efficient virus release from interferon treated CD4+ T cells, tetherin cell surface downregulation and ESCRT-dependent degradation of Vpu/tetherin complexes (Kueck and Neil, 2012). The evidence for this is presented in Chapter 4 of this thesis. In addition, it has been shown that certain strains of HIV-1 subtype C possess a di-leucine based (**D**/**E**)xxx**L**(**L**/**I**/**V**) transmembrane proximal sorting signal and localise predominantly to the plasma membrane (Ruiz et al., 2008). The fact that rare defective primary isolates of HIV-1 harbour *vpu* genes with mutations within these trafficking motifs (Pickering et al., 2014) raises the possibility that subcellular localisation of Vpu and subsequent biological activities might present the virus with selective advantages.

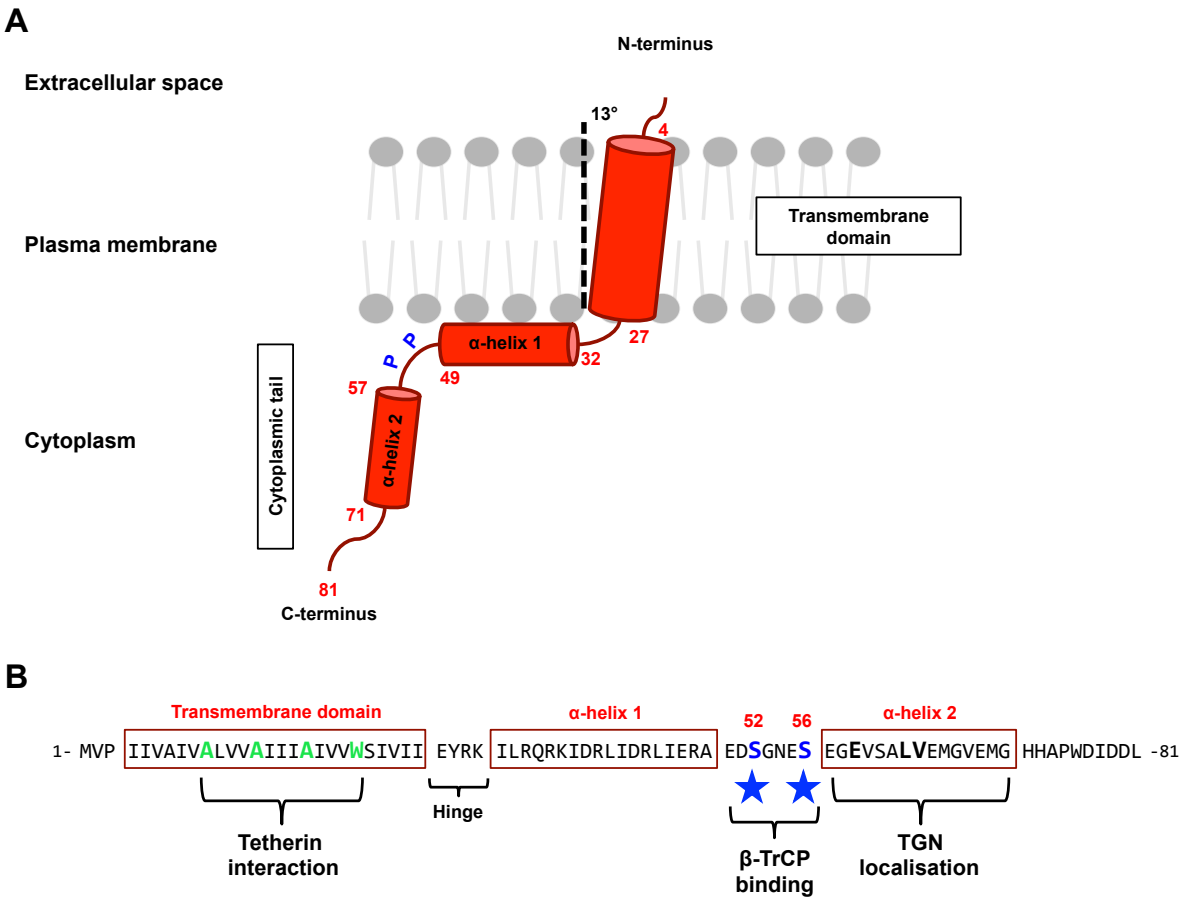

Figure 1-24 Vpu topology and molecular features

(A) Predicted secondary structure of the prototype NL4.3 Vpu protein. Indicated are: the N-terminal transmembrane domain with the predicted 13° angle; the cytoplasmic tail containing two α-helices and phosphorylated serine residues (S52 and S56, highlighted in blue). **(B)** NL4.3 Vpu topology. The red boxes indicate the transmembrane domain and α-helices. Highlighted in green is the alanine face (AxxxAxxxAxxxW) located in the TM domain. Highlighted in blue are phosphorylated serine residues within the D**S**GNE**S** β-TrCP-binding motif. Also depicted is the hinge region containing the putative overlapping trafficking motif and the ExxxLV motif in the second α-helix.

1.7.2 Vpu and CD4 degradation

Despite its compact genome, HIV-1 dedicates two accessory proteins, Nef and Vpu, to reducing CD4 levels at the plasma membrane, implying that surface downregulation of CD4 plays an important role in HIV-1 replication. Indeed, newly synthesised CD4 molecules are able to retain the envelope precursor gp160 in the ER, therefore preventing Env incorporation into virions, resulting in non-infectious virus particles. CD4 expression on the surface of infected cells promotes super-infection, which is known to inhibit efficient virus particle release (Wildum et al., 2006). Furthermore, very recent studies suggest that in the absence of Vpu and Nef, CD4-induced epitopes of gp120 are exposed on infected cell surfaces, sensitising the cell to enhanced antibody-dependent cytotoxicity (Veillette et al., 2014) (Pham et al., 2014). Early during infection, Nef enhances endocytosis of mature CD4 proteins at the cell surface in a mechanism that is dependent on clathrin and AP-2, followed by the delivery of CD4 molecules to lysosomes. Vpu on the other hand is expressed later during the viral replication cycle and induces rapid degradation of newly synthesised CD4 proteins in the ER (reviewed by (Dubé et al., 2010a) and (Andrew and Strebel, 2010)).

Vpu-mediated degradation of CD4 molecules in the ER is well characterised and thought to be initiated by Vpu/CD4 physical interactions via their respective cytoplasmic tails. While Vpu and CD4 transmembrane domains are thought not to be required for binding (Bour et al., 1995) (Schubert et al., 1996b), their hydrophobic nature might stabilise Vpu/CD4 interactions (Magadán et al., 2010). The cytoplasmic determinant required for direct Vpu binding in CD4 has been mapped to a short motif (414 LSEKKT 419) and a α-helix located in the membrane proximal region (Bour et al., 1995) (Lenburg and Landau, 1993) (Vincent et al., 1993) (Willey et al., 1994) (Yao et al., 1995). The first alpha helix of the Vpu cytoplasmic tail was thought to be required for CD4 binding (Hill et al., 2010) (Tiganos et al., 1997), however recent NMR data suggests that both cytoplasmic helices are involved in CD4 binding (Singh et al., 2012). Physical interaction between either alone is not sufficient for CD4 degradation.

The highly conserved di-phosphoserine (D**S**GNE**S)** motif in Vpu is required to interact with β-TrCP1/2 (Margottin et al., 1998) (Butticaz et al., 2007). β-TrCP is a F-box adaptor protein that is part of the cytosolic SCF E3 ubiquitin ligase complex (Margottin et al., 1998). The phosphorylated serine residues bind directly to the WD-repeat in the β-propeller of β-TrCP, creating a CD4/Vpu/β-TrCP ternary complex that allows poly-ubiquitination of CD4 on lysine as well as serine/threonine residues (Binette et al., 2007) (Magadán et al., 2010), thus targeting CD4 for degradation by the cytosolic proteasome.

Although it is now well established that Vpu induces CD4 degradation via a proteasomal-dependent pathway, it is still unclear how CD4 is trans-located from the ER membrane into the cytoplasm for ubiquitin ligase-mediated degradation. This degradation appears to be through some form of the endoplasmic reticulum-associated protein degradation (ERAD) pathway, that targets misfolded membrane and luminal proteins for degradation in the cytosol. Vpu-induced CD4 degradation is distinct from the classical ERAD pathway in that Vpu relies on the SCF^{TrCP} complex rather than on the typical ER membrane-bound E3 ubiquitin ligases, including the HRD1-SEL1L complex, TEB4/MARCH-VI, and the GP78-RMA1 complex (reviewed by (Dubé et al., 2010a) and (Andrew and Strebel, 2010)). However, like classical ERAD, it has been shown that the VCP-UFD1L-NPL4 complex, that includes the AAA-ATPase p97/VCP, is recruited to provide the energy for the extraction or dislocation of Vpu-induced CD4 degradation from the ER membrane (Binette et al., 2007) (Magadán et al., 2010). Therefore, Vpu bypasses the early substrate recognition stage of ERAD but joins the pathway at later steps. Taken together a model emerges in which Vpu binds newly synthesised CD4 molecules in the ER membrane, recruits the SCF^{TrCP} complex, induces CD4 poly-ubiquitination followed by dislocation into the cytosol and degradation by the proteasome (Figure 1-25).

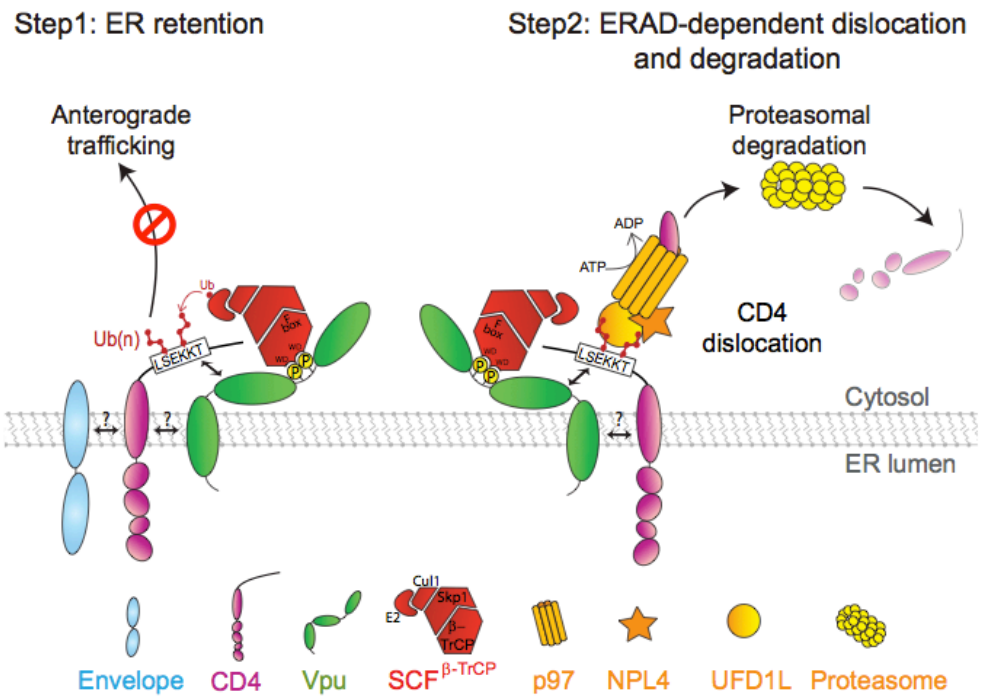

Figure 1-25 Vpu-mediated ERAD-dependent degradation of CD4

Schematic representation of Vpu-mediated CD4 degradation. Vpu retains CD4 in the endoplasmic reticulum by interaction through their transmembrane domains. The formation of Env/CD4 complexes might contribute to Vpu capture of CD4 molecules. The cytoplasmic tail of Vpu (mediated by the first alpha helix) interacts with CD4 (residues 414-LSEKKT-419) and recruits the SCF-β-TrCP E3 ubiquitin ligase complex, which induces poly-ubiquitination of CD4 and targets CD4 for proteasomal degradation. This targeting involves a dislocation step mediated by the ERAD associated p97-UFD1L-NPL4 complex, through the recognition of K-48-linked ubiquitin chains on the CD4 cytosolic tail by UFD1L. The ATPase activity of p97(VCP) mediates dislocation of CD4 from the ER membrane into the cytosol where CD4 becomes readily accessible for proteasomal degradation (adapted from(Dubé et al., 2010a)).

1.7.3 Vpu-mediated tetherin antagonism

Vpu-mediated tetherin antagonism is distinct from CD4 degradation as tetherin inactivation takes place outside the ER, but the exact mechanism still remains somewhat unclear. Artificial retention of Vpu in the ER results in its inability to counteract tetherin-mediated virus restriction (Schubert and Strebel, 1994) (Skasko et al., 2011) (Vigan and Neil, 2011). However, it is known that Vpu downmodulates cell surface tetherin (Van Damme et al., 2008) and decreases total cellular tetherin levels (Goffinet et al., 2009). This is achieved by redirecting tetherin to endosomal compartments for lysosomal degradation through an ESCRT-dependent mechanism (Douglas et al., 2009) (Janvier et al., 2011) (Agromayor et al., 2012).

1.7.3.1 Vpu and tetherin interaction

Vpu and tetherin directly interact via their respective TM domains, and this physical interaction is essential for Vpu-mediated tetherin antagonism (Iwabu et al., 2009) (Mangeat et al., 2009) (Perez-Caballero et al., 2009) (Dubé et al., 2010b) (Vigan and Neil, 2010) (McNatt et al., 2013). This interaction is also species-specific and explains the inability of HIV-1 Vpu to counteract other primate tetherins with the exception of chimpanzee and gorilla (McNatt et al., 2009) (Gupta et al., 2009a). In particular the species-specific amino acids I34, L37 and L41 in the TM domain of tetherin are crucial for direct interaction with HIV-1 Vpu, and mutations at any of these residues make tetherin molecules resistant to Vpu activity (Kobayashi et al., 2011) (McNatt et al., 2009) (Gupta et al., 2009a). The residues I34, L37 and L41 also lie along one face of the tetherin TM helix (Figure 1-26), suggesting that they present a binding interface between the two proteins (Dubé et al., 2010b) (Kobayashi et al., 2011). In addition to the TM residues, a threonine at position 45 in the transmembrane/ectodomain boundary of tetherin is essential for tetherin/Vpu interaction (Gupta et al., 2009a) (McNatt et al., 2009) (Kobayashi et al., 2011).

Extensive mutagenesis studies of the transmembrane domain of HIV-1 NL4.3 Vpu identified three amino acid positions A14, A18 and W22 that are required for direct tetherin binding. Interestingly, these residues are part of a highly conserved “alanine face” in the TM domain of Vpu, $A_{10}xxx(A/V)_{14}xxxA_{18}xxxW_{22}$ (Figure 1-26). Amino acids important for direct interaction in both proteins lie on the same helical interface, suggesting that Vpu molecules target tetherin as a monomer (Vigan and Neil, 2010) (Kobayashi et al., 2011) (Skasko et al., 2011). The alanine face is conserved in HIV-1 subgroups M and N, but subgroup O Vpu lacks it (Vigan and Neil, 2010). Furthermore,

in the predicted multimeric form of Vpu (Park et al., 2003), the alanine face would be obstructed by neighbouring monomers (Vigan and Neil, 2010).

The tryptophan residue at position 22 in the Vpu TM domain has been suggested to regulate the transition of Vpu between monomeric and multimeric forms inside the ER (Magadán and Bonifacino, 2012). According to this study, Vpu induces CD4 degradation in its monomeric form, mutations of W22 stabilise multimeric complexes and therefore inhibit CD4 degradation. Whether this scenario is also true for tetherin antagonism by Vpu remains to be determined.

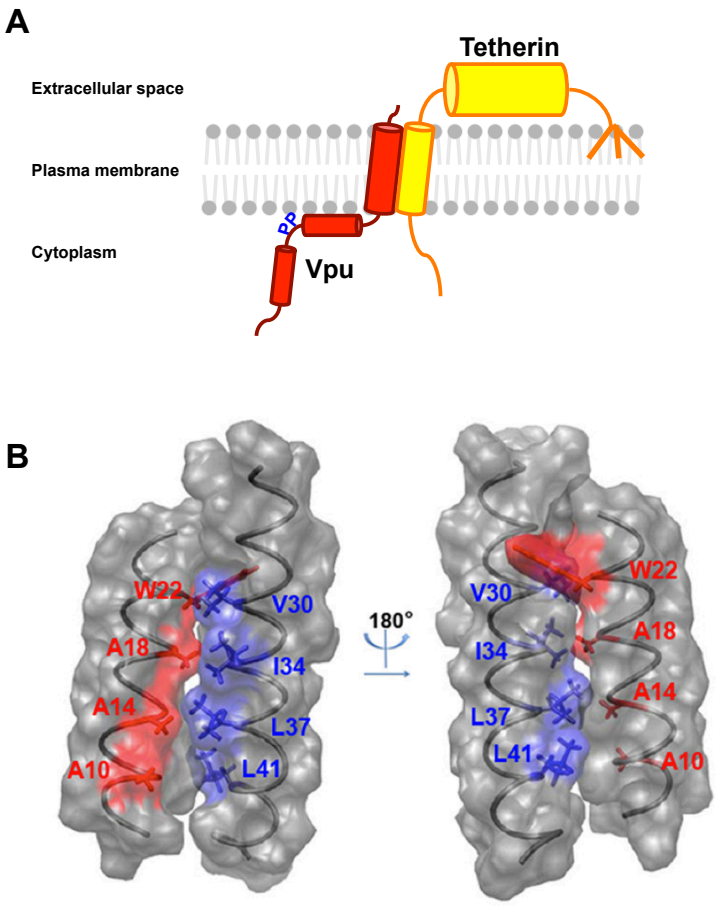

Figure 1-26 Vpu and tetherin transmembrane domains directly interact

(A) Schematic representation of direct binding between Vpu and tetherin transmembrane domains. **(B)** NMR-based model of Vpu and tetherin transmembrane domain interactions. Highlighted in red are residues in the Vpu alanine face; highlighted in blue are residues in tetherin that are important for physical Vpu interaction (adapted from (Skasko et al., 2012)).

1.7.3.2 Subversion of tetherin's trafficking by Vpu

Vpu induces tetherin cell surface downmodulation, and this is required for tetherin antagonism at high surface expression levels. However, the endocytosis rate of tetherin is not increased by Vpu expression (Mitchell et al., 2009) (Miyagi et al., 2009) (Dubé et al., 2010b) (Schmidt et al., 2011), neither does Vpu remove tetherin from lipid rafts (Fritz et al., 2012) (Lopez et al., 2012), highlighting the importance of differential trafficking and sequestration of tetherin in cellular compartments like the TGN and/or endosomes as a mechanism of Vpu activity (Varthakavi et al., 2006). Tetherin degradation is dispensable in some systems for the ability of Vpu to antagonise its function, indicating that alteration of cellular tetherin trafficking and/or recycling by Vpu is the key to keeping tetherin away from the site of virus particle release. Multiple studies have demonstrated that Vpu and tetherin co-localise predominantly in the TGN and endosomal compartments where tetherin appears to be sequestered (Dubé et al., 2010b) (Dubé et al., 2011) (Schmidt et al., 2011). Furthermore, Vpu mutants that are not able to localise in the TGN have an intermediate effect on tetherin antagonism, again suggesting that re-direction of tetherin into the TGN is important for Vpu-mediated antagonism (Dubé et al., 2009).

As discussed in section 1.6.1, clathrin adaptors AP-2 and AP-1 are involved in tetherin endocytosis and its subsequent delivery to the TGN for recycling. Inhibition of tetherin endocytosis by AP-2 knockdown or overexpression of dominant negative dynamin 2 rescues tetherin cell surface levels in Vpu-expressing cells to some extent (Iwabu et al., 2009) (Mitchell et al., 2009) (Lau et al., 2011). However, this treatment also interferes with the natural turnover and recycling of tetherin, making these results difficult to interpret. Treatment of cells with monensin, an inhibitor of the fast recycling route, indicated that tetherin recycles through a slow-recycling pathway (Figure 1-27A) (Dubé et al., 2011) (Schmidt et al., 2011). Therefore, Vpu potentially has to antagonise two different tetherin pools in infected cells: newly synthesised and slow-recycling tetherin. By using the anti-malaria drug primaquine, a lysosomotropic amine, tetherin cellular trafficking can be subverted and HIV-1 virus release can be rescued similar to Vpu's effect on tetherin, implicating that Vpu alters tetherin trafficking/recycling as well as anterograde trafficking pathways (Figure 1-27B) (Schmidt et al., 2011). Another study highlighted the trafficking subversion effect of tetherin by Vpu using brefeldin A (BFA) (Lau et al., 2011), a reagent that increases the retrograde protein transport from the Golgi network to the endoplasmic reticulum by causing the collapse of the Golgi network, and therefore induces protein accumulation in the ER (Miller et al., 1992). Vpu inhibits tetherin recycling to the plasma membrane in BFA treated cells, suggesting an inhibition of endosomal recycling of tetherin (Lau et al., 2011).

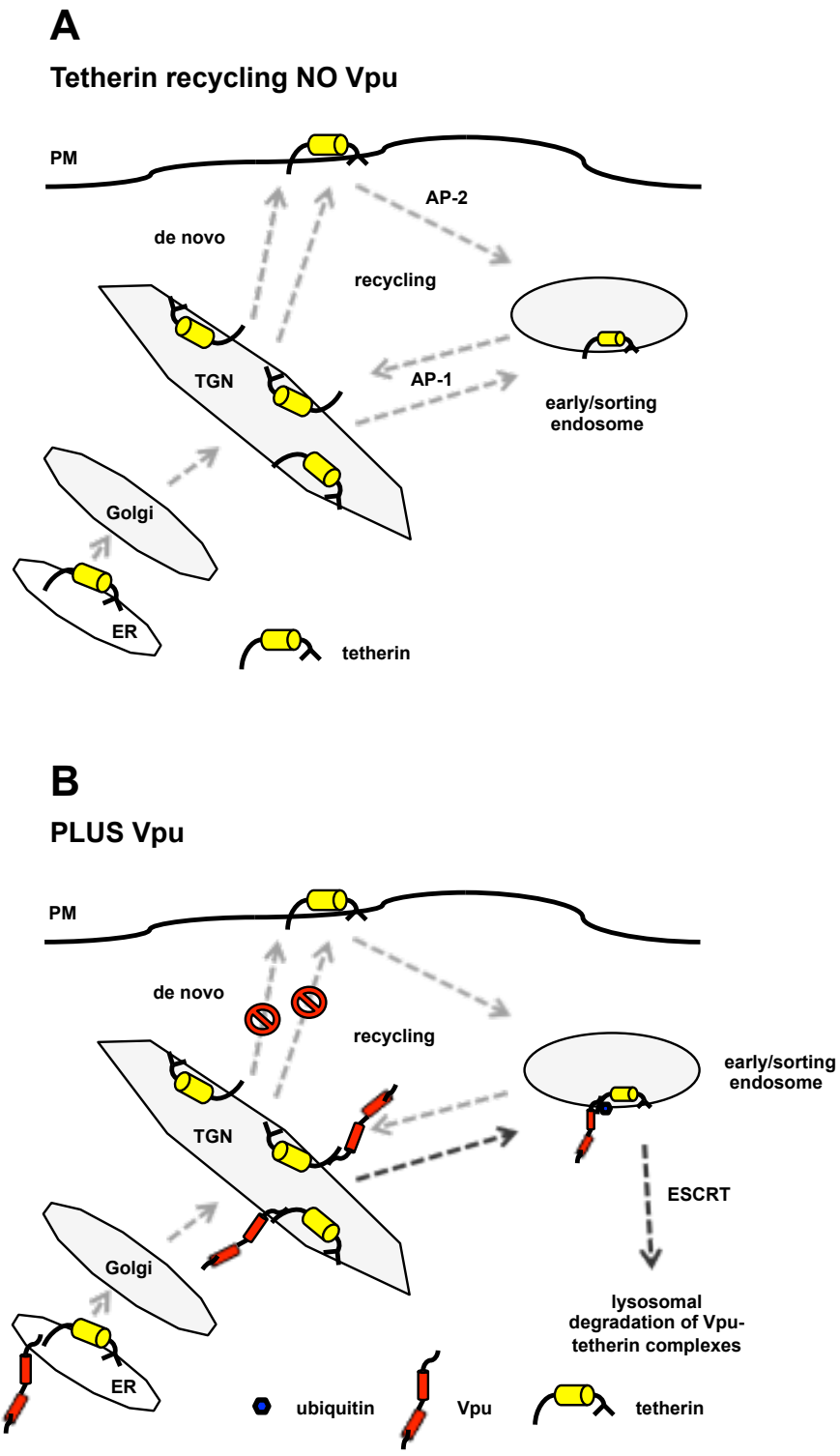

Figure 1-27 Model of Vpu-mediated cell surface downmodulation of tetherin

(A) Schematic representation of tetherin trafficking/recycling in the absence of Vpu. Tetherin reaches the plasma membrane through the anterograde trafficking pathway. Tetherin is endocytosed in AP-2-mediated clathrin-coated pits, transported to the TGN through the interaction with AP-1, and recycles back to the cell surface. **(B)** Schematic representation of tetherin trafficking/recycling in the presence of Vpu. Vpu interacts with tetherin in the endoplasmic reticulum (ER) or Golgi compartments, thereby targeting either newly synthesized or recycling tetherin molecules. Vpu/tetherin complexes are then targeted to endosomal compartments, simultaneously Vpu-mediated recruitment of SCF-β-TrCP leads to the ubiquitination of tetherin on multiple cytoplasmic tail residues. In early/sorting endosomal compartments, ubiquitin-dependent recruitment of HRS promotes sorting of Vpu/tetherin complexes for ESCRT-dependent degradation in lysosomes.

Overexpression experiments with the C-terminal domain of the clathrin sequestering protein AP180, demonstrated a requirement for clathrin in the cellular redistribution of tetherin molecules and counteraction by Vpu (Lau et al., 2011) (Kueck and Neil, 2012). Further evidence for the importance of differential trafficking of tetherin in the TGN and/or recycling compartments comes from the identification of an acidic di-leucine trafficking motif, **E**xxx**LV**, in the second alpha helix of Vpu. This motif is required for efficient virus release from interferon-treated CD4+ T cells, tetherin cell surface downregulation and ESCRT-dependent degradation of tetherin/Vpu complexes (Kueck and Neil, 2012). However, the **E**xxx**LV** motif is missing in the second alpha helix in HIV-1 subgroup C and F Vpu proteins, and instead both Vpu proteins contain **E**xxx**LL** motifs in their first alpha helices (Ruiz et al., 2008). Whether these putative trafficking motifs also play a role in tetherin antagonism is not yet known. The exact role of clathrin in this mechanism remains unclear and requires further investigation. There are still open questions about the mechanism of Vpu-mediated tetherin antagonism, including where within the cellular compartments Vpu redirects tetherin molecules for degradation and directions of trafficking *per se*. Results presented in Chapter 4 and Chapter 6 concentrate on answering some of the above-mentioned questions and will give a more detailed insight into Vpu/tetherin complex trafficking.

1.7.3.3 Degradation of tetherin mediated by Vpu

Vpu diminishes cell surface tetherin levels and induces subsequent tetherin degradation in both HIV-1 infected cells as well as in cells expressing Vpu *in trans* (Van Damme et al., 2008). It has been under debate whether this degradation is proteasomal or endo-lysosomal as inhibitors for both pathways restore cellular tetherin levels. However, reports that tetherin was degraded by the proteasome were subsequently shown to be artificial (reviewed by (Le Tortorec et al., 2011)).

Furthermore, tetherin degradation by Vpu has been shown to be ubiquitin-dependent, but there have been conflicting reports about which residues in the tetherin cytoplasmic tail are ubiquitinated and important for antagonism. Tetherin undergoes mono-ubiquitination on lysine residues 18 and/or 21 (Pardieu et al., 2010), and mutation of these residues completely blocks Vpu-mediated tetherin degradation (Goffinet et al., 2010). Further studies also demonstrated the importance of serine and threonine residues, in the tetherin cytoplasmic tail, as poly-ubiquitin acceptors required for cell surface downregulation and efficient virus particle release (Tokarev et al., 2011). However, another study showed that mutation of all the above-mentioned possible ubiquitin acceptor residues still led to ubiquitination and subsequent tetherin degradation, indicating that Vpu might also target tyrosine residues within the cytoplasmic tail or the NH2 terminus of tetherin for ubiquitination (Gustin et al., 2012). Taken together, these results demonstrate the involvement of ubiquitin in Vpu-mediated tetherin cell surface downregulation, degradation and subsequent virus particle release. However, this appears to be a complex process that requires further clarification.

The ubiquitination of tetherin is thought to be dependent on the phosphorylation of two serine residues within the conserved D**S**GNE**S** motif in cytoplasmic tail of Vpu and subsequent recruitment of the E3 ubiquitin ligase complex SCF^{TrCP} (Margottin et al., 1998) (Butticaz et al., 2007) (Mangeat et al., 2009) (Douglas et al., 2009) (Mitchell et al., 2009) (Iwabu et al., 2009) (Goffinet et al., 2009). Targeted mutagenesis of the two serine residues leads to the disruption of Vpu and β-TrCP interactions, resulting in a partial block of tetherin surface down-modulation. However, this Vpu phospho-mutant still retains some capacity to promote virus particle egress (Van Damme et al., 2008) (Mitchell et al., 2009), indicating that other cellular pathways such as protein trafficking might also play an important role in Vpu-mediated tetherin antagonism. Therefore, one could conclude that Vpu-mediated tetherin antagonism is not solely dependent on the degradation of the restriction factor and further studies are required to clear discrepancies.

Evidence for an endo-lysosomal degradation of tetherin by Vpu comes from studying Rab GTPases, which are required for diverse membrane trafficking events. The GTPase Rab7A plays a role in the organisation and maturation of endocytic compartments as well as fusion of endosomes and phagosomes with lysosomal compartments (reviewed by (Huotari and Helenius, 2011)). Rab7A is involved in Env processing and therefore required for HIV-1 virus release and virus particle infectivity. Importantly, depletion of Rab7A leads to the accumulation of virions at the cell surface. This implies a role for Rab7A in the late stages of the HIV-1 replication cycle and highlights the importance of multi-vesicular trafficking events during the HIV-1 propagation cycle (Caillet et al., 2011).

The ESCRT machinery is required for natural tetherin turnover. In particular, the ESCRT-0 component HRS, which binds ubiquitinated transmembrane cargo molecules and induces sorting of these ubiquitin-tagged molecules for lysosomal degradation (Raiborg and Stenmark, 2009). Janvier and colleagues demonstrated that HRS is required for efficient virus particle release and Vpu-mediated tetherin cell surface downregulation as well as degradation (Janvier et al., 2011). The recently discovered UBAP1, a subunit of the human ESCRT-I complex, which is required for the endosomal degradation of ubiquitinated proteins but not for any other ESCRT-I-related functions (Stefani et al., 2011) (Agromayor et al., 2012), makes it possible to differentiate between Vpu-mediated tetherin antagonism and subsequent tetherin degradation (results are presented in Chapter 5) (Agromayor et al., 2012). Depletion of cellular UBAP1 levels resulted in a block of tetherin degradation and an increase of highly ubiquitinated tetherin forms in HIV-1 infected cells, suggesting that, in the presence of Vpu, tetherin is sorted for degradation by an ubiquitin-dependent multivesicular body (MVB) pathway (Agromayor et al., 2012). Therefore, despite increased cellular tetherin levels in UBAP1 depleted cells, the release of infectious virus from cells infected with wild-type HIV-1 is not affected, suggesting that Vpu inactivates tetherin by shuttling it into endosmal compartments from which it cannot escape (Agromayor et al., 2012). In other words, the commitment of Vpu/tetherin complexes for degradation is enough to enhance virus particle release but the final degradation is dispensable for Vpu-mediated antagonism of tetherin.

1.7.3.4 Tetherin, a significant barrier to SIV zoonoses

The chimpanzee simian immunodeficiency virus (SIVcpz) was generated by recombination events between two SIV lineages that infect old world monkeys (Figure 1-28). The 3' end of the SIVcpz genome including the *nef* gene is closely related to SIV red-capped mangabeys (SIVrcm), while the *vpu*, *tat*, *rev* and *env* genes are related to SIVs that infect several species, including SIV greater spot-nosed (SIVgsn), SIV mustached (SIVmus) and SIV mona (SIVmon) monkeys (reviewed by (Sharp and Hahn, 2011)). This complex mosaic genome suggests that chimpanzees obtained SIV by hunting and killing of other monkeys. In turn, there have been at least four independent cross-species transmission events that transferred SIVcpz into humans, resulting in distinct lineages of HIV-1 called groups M, N, O and P. While groups M and N are derived from SIVcpz strains found in *Pan troglodytes troglodytes* (SIVcpzPtt), group P is derived from SIV gorilla (SIVgor) and the origins of group O remain unclear (Figure 1-28) (reviewed by (Sharp and Hahn, 2011)). The HIV-1 group M gave rise to the AIDS pandemic whereas group O represents less than 1% of global HIV-1 infections, while for group N and group P only a limited number of sequences is available due to a low number of incidences and/or documented cases.

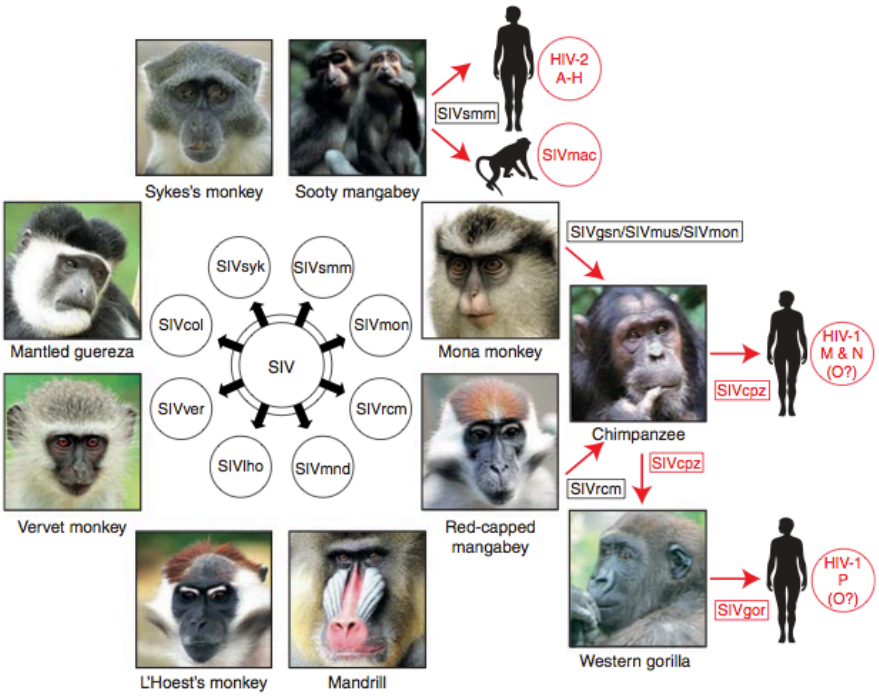

Figure 1-28 Human immunodeficiency virus origins

Schematic representation of the origins of HIV viruses. Old work monkeys are naturally infected with more than 40 different simian immunodeficiency viruses (SIVs), the suffix denotes their primate species of origin, for example SIVsmm stands for sooty mangabey. Highlighted in red are known cross-species transmissions as well as the resulting viruses (Sharp and Hahn, 2011).

HIV-1 and viruses from the SIVgsn/mus/mon lineage use their Vpu protein to bind to the tetherin transmembrane domain and to induce cell surface removal and degradation (Sauter et al., 2009). Yet, despite encoding a *vpu* gene, SIVcpz uses its Nef protein to counteract tetherin restriction. Upon cross-species transmission into humans, however, the SIVcpz Nef protein was inactive against the human tetherin protein due to the deletion of the Nef target motif in human tetherin (G/DIWKK) that occurred at least 800,000 years ago, as the deletion was present in Neanderthals and Denisovans (Sauter et al., 2011a). During cross-species transmission, only HIV-1 group M switched from Nef to Vpu to enhance virus release in its new human host. On the other hand, HIV-2, which originated from SIV sooty mangabey monkeys (SIVsmm) (Figure 1-29) and does not encode a *vpu* gene, switched from Nef to its Env glycoprotein to suppress tetherin restriction. This switch might have come at a price, as Env is a major structural protein that is required for virus entry and has evolved to downregulate tetherin from the cell surface and to sequester tetherin in intracellular compartments, which might reduce the number of Env molecules incorporated into virus particles. One could speculate that this is one of the reasons why HIV-2 is less virulent than HIV-1.

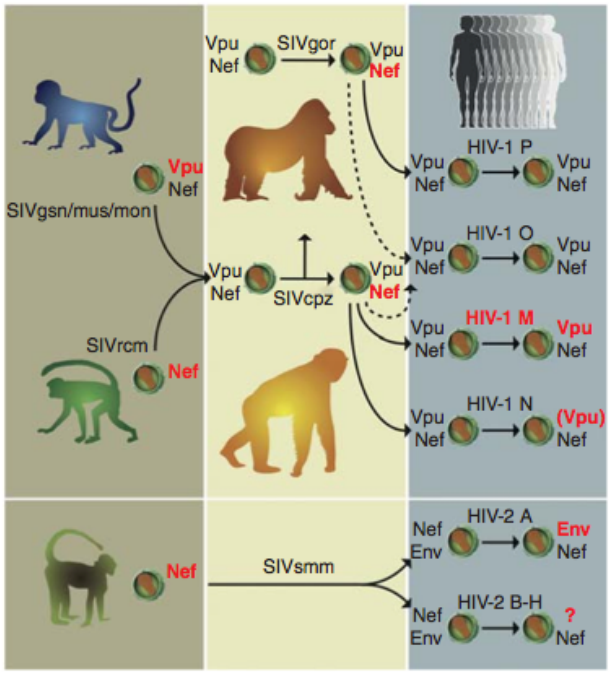

Figure 1-29 Tetherin antagonists in primate hosts

Schematic representation of tetherin antagonists in HIV-1 and HIV-2 as well as in their predecessors. SIVcpz acquired its *vpu* gene from the SIVgsn/mus/mon lineage and its *nef* gene from the SIVrcm lineage. During adaptation in chimpanzees, Nef has evolved to become a tetherin countermeasure. Both SIVgor and SIVsmm also use their Nef proteins to antagonise tetherin function. During adaptation in humans, SIVcpz, SIVgor, and SIVsmm Nef proteins were unable to counteract human tetherin due to a five amino acid deletion in tetherins cytoplasmic tail. In HIV-1 group M, Vpu has evolved to regain efficient anti-tetherin function. Both Nef and Vpu proteins of HIV-1 groups O and P are poor tetherin countermeasures, while the HIV-1 group N Vpu protein regained modest anti-tetherin function. HIV-2 group A has evolved to use Env to counteract tetherin function. Highlighted in red are proteins that are able to antagonise tetherin (Sharp and Hahn, 2011).

Of note, HIV-1 group M is the only group that successfully regained Vpu-mediated anti-tetherin function (Figure 1-29). HIV-1 group O Vpu proteins have no anti-tetherin activity due to their lacking of the tetherin-interacting alanine face in their TM domain (Yang et al., 2011) (Vigan and Neil, 2011). So far, only two group P Vpu proteins have been isolated and tested for their ability to antagonise tetherin and both fail to inactivate tetherin function. Nor can group P Nef or Env proteins remove tetherin from virus budding zones (Sauter et al., 2011b) (Yang et al., 2011). However, both groups O and P Vpu proteins maintain the ability to induce CD4 degradation (Sauter et al., 2009) (Sauter et al., 2011b). Most group N Vpu proteins are also poor tetherin antagonists (Sauter et al., 2009), yet, in contrast to group O, Vpu proteins from group N have the above-mentioned alanine face and interact with tetherin (Vigan and Neil, 2010). However, most N Vpu proteins lack the D**S**GNE**S** phosphorylation and **E**xxx**LV** trafficking motifs rendering them unable to degrade CD4 and tetherin (Sauter et al., 2012). Interestingly, one group N Vpu has undergone adaptation to tetherin, which has been associated with pathogenesis. This new N Vpu has been isolated from an individual returning to France from a trip to Togo, a country with no prior record of non-group M HIV-1 infections. The adaptation determinants map to residues in the transmembrane domain, and repair of the D**S**GNE**S** and **E**xxx**LV** motifs, resulting in a highly efficient N Vpu protein that is able to reduce tetherin surface expression and to induce degradation (Sauter et al., 2012). This case demonstrates that the HIV-1 group N is under strong host-specific pressure, and that adaptation to acquire an effective tetherin countermeasure may increase viral fitness. Thus, the general inability of HIV-1 groups N, O and P to efficiently antagonise human tetherin might explain the limited spread of these viruses in the human population.

1.7.4 Vpu suppresses cellular innate immune responses by downmodulation of NTB-A and CD1d

NK cells play an important role in the innate immune system. They possess the ability to produce immunoregulatory cytokines and to mediate target cell lysis through the release of cytoplasmic lytic granules in a process called degranulation. The ability of NK cells to destroy virus-infected cells is dependent on interactions between NK cell surface receptors and their corresponding ligands presented on the surface of target cells. NKG2D is one such NK cell activation receptor that recognises stress-induced molecules, such as MIC-A, as well as ULBP-1 and -2. Activation of NK cells via NKG2D (referred to as signal 1 in Figure 1-30) is necessary but not sufficient to induce production of lytic granules. Degranulation also requires the concomitant activation of a co-receptor (referred to as signal 2) (reviewed by (Bryceson et al., 2006)). The NK-T and B cell antigen (NTB-A (also termed SLAMF6)) serves as such an activation co-receptor to mediate the release of lytic granules. NTB-A is a type 1 transmembrane protein that functions as a homotypic ligand-co-activator of NK receptors and belongs to the signalling lymphocytic activation molecule (SLAM) family.

HIV has developed strategies to regulate various NK cell ligands, making the infected cell surprisingly refractory to NK cell lysis (Bonaparte and Barker, 2003). This is baffling because the HIV-1 accessory protein Vpr is able to enhance expression levels of ligands for NKG2D (Ward et al., 2009), and Nef is able to remove the inhibitory ligands HLA-A and -B from the surface of infected cells (Cohen et al., 1999).

A recent study demonstrated that the HIV-1 Vpu protein interferes with NK cell degranulation by reducing NTB-A cell surface levels of infected cells (Shah et al., 2010). NTB-A downregulation by Vpu is mechanistically distinct from CD4 and tetherin cell surface downmodulation. The reduction of surface NTB-A levels was shown to be independent of β-TrCP recruitment and Vpu did not affect steady-state levels of NTB-A. However, Vpu/NTB-A interaction was dependent on Vpu's transmembrane domain, and Vpu did not increase the endocytosis rate of NTB-A to reduce cell surface expression. Therefore the authors suggested a mechanism in which Vpu alters the trafficking and/or recycling of NTB-A and sequesters NTB-A in an intracellular compartment. Indeed, Vpu has been shown to affect the glycosylation pattern of newly synthesised NTB-A molecules by a post-ER mechanism, suggesting that Vpu interferes with the anterograde transport of NTB-A in the TGN (Bolduan et al., 2013). Therefore, Vpu-induced downmodulation of NTB-A might provide an explanation for the inability of NK cells to mediate killing of virus-infected cells despite their strong activation status. However, *in vivo* studies using humanized mouse models of acute HIV infection demonstrated that NTB-A was not significantly downregulated from the cell surface in a

Vpu-dependent manner, unlike CD4 and tetherin (Sato et al., 2012) (Dave et al., 2013). More studies are required to understand how HIV-1 balances activation and inhibition of degranulation *in vivo*.

Polymorphisms in the HIV-1 Vpu/Env overlapping coding region have been associated with the inhibitory receptor killer immunoglobulin-like receptor, two domains, long cytoplasmic tail, 2 (KIR2DL2) and its ligand HLA-C. This link suggested that the polymorphisms enhance the ability of the inhibitory receptor KIR2DL2 to bind to HIV-1-infected cells, providing a strong inhibitory signal to KIR2DL2 positive NK cells and thereby protecting HIV-1 infected cells (with Vpu/Env polymorphisms) from lysis by NK cells (Alter et al., 2011).

Vpu has also been reported to downmodulate CD1d from the surface of HIV-1 infected DCs (Figure 1-30) (Moll et al., 2010). CD1d is a MHC class I-like membrane-associated protein expressed by antigen-presenting cells (APCs). The role of CD1d during a viral infection is to present pathogen-derived lipid antigens to CD1d-restricted natural killer T (NKT) cells, resulting in the mutual activation of both cells and subsequent initiation of cellular immune responses. Activated NKT cells rapidly secrete T helper type 1 and 2 cytokines to activate and regulate various other cell types, including DCs, NK cells, B cells and conventional T cells. As observed with NTB-A, Vpu did not enhance CD1d endocytosis or induced rapid CD1d degradation. Instead, Vpu was found to interact with CD1d and to inhibit CD1d recycling from endosomal compartments back to the cell surface by retaining CD1d in early endosomes. Therefore, preventing antigen loading of CD1d in late endosomes strongly inhibits the ability of infected DC to activate CD1d-restricted NKT cells.

The increasing number of membrane-associated cell surface receptors involved in innate immune responses, and targeted by HIV-1 Vpu, promotes the potential role of Vpu as a key regulator in the evasion of innate immune responses.

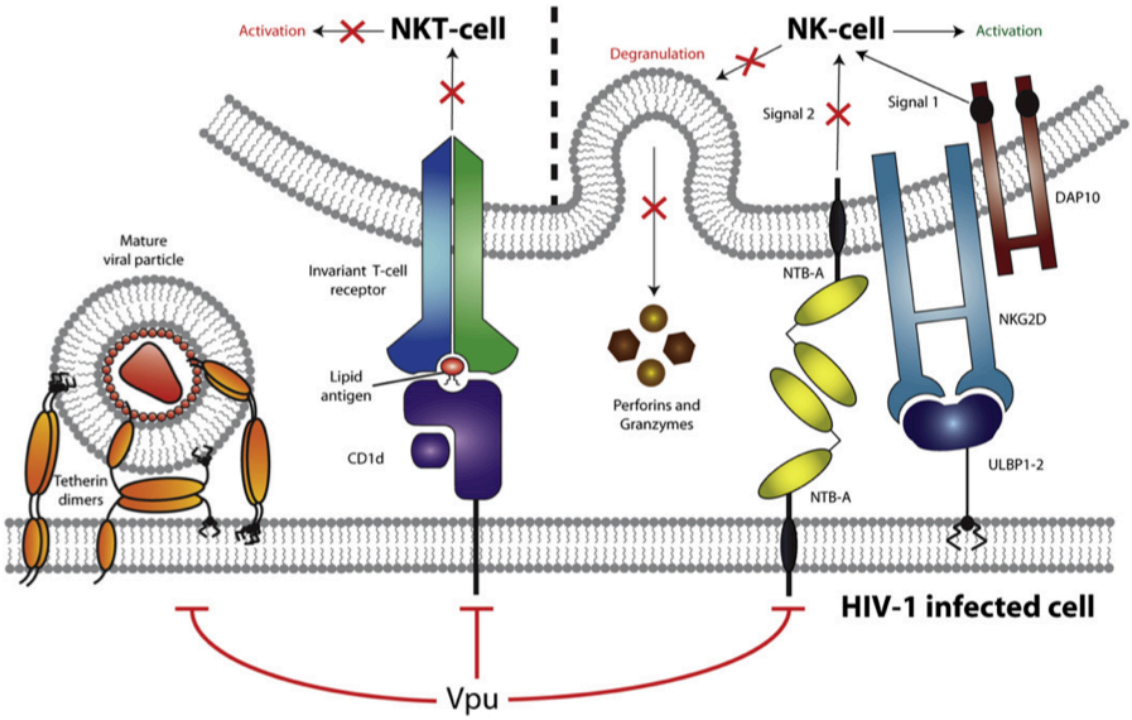

Figure 1-30 Vpu induces CD1d and NTB-A cell surface downregulation

Vpu expression leads to the cell surface downmodulation of tetherin (left), CD1d (middle) and NTB-A (right). Reduced CD1d cell surface levels prevent the presentation of lipid antigens to CD1d-restricted NKT cells, therefore avoiding their activation. Reduced cell surface levels of NTB-A protect infected cells from NK-cell-mediated killing, since both NTB-A- and NKG2D-triggered signals are required for NK-cell-mediated killing by degranulation of perforins and granzymes (adapted from (Richard and Cohen, 2010)).

1.8 The clathrin adaptor machinery and its role in cellular vesicle trafficking

1.8.1 Clathrin coats involved in vesicular transport

Clathrin-coated vesicles (CCVs) are important for lipid and soluble macromolecule transport between membrane-bound compartments. Vesicles bud from a cellular donor compartment and fuse with an acceptor compartment. Selection of cargo molecules and vesicle budding are mediated by coat-proteins that are recruited from the cytoplasm to assemble at membranes; the most common scaffolding coat protein is clathrin. Sites of clathrin assembly are differentially marked by either phosphoinositides and/or Arf proteins, which recruit adaptor proteins (APs). Adaptor proteins bind to signals present within cytosolic domains of transmembrane cargo molecules and simultaneously serve as clathrin anchors for coat formation, leading to the capture of cargo proteins at sites of vesicle formation (Figure 1-34). The donor membrane curves and a spherical clathrin-coated vesicle is formed, the role of which is to transport cargo molecules to their corresponding destination (Canagarajah et al., 2013). The GTPase dynamin 2 mediates the pinching of CCVs at the donor membrane, by formation of a spiral around the neck of the vesicle that is restrained through GTP hydrolysis (Bonifacino and Traub, 2003). The clathrin adaptor machinery plays an important role in the biogenesis and function of endosomes and lysosomes. The correct transport orientations are crucial: at the plasma membrane proteins can be endocytosed and delivered to endosomes; at the TGN there is the choice between transport to the plasma membrane or endosomes; and at endosomes proteins can be recycled, delivered back to the TGN, or delivered to lysosomes for degradation (Figure 1-31). This complicated system is highly regulated by sorting signals and the different highly specialised clathrin adaptor proteins that mediate delivery of cargo proteins to their intracellular destination.

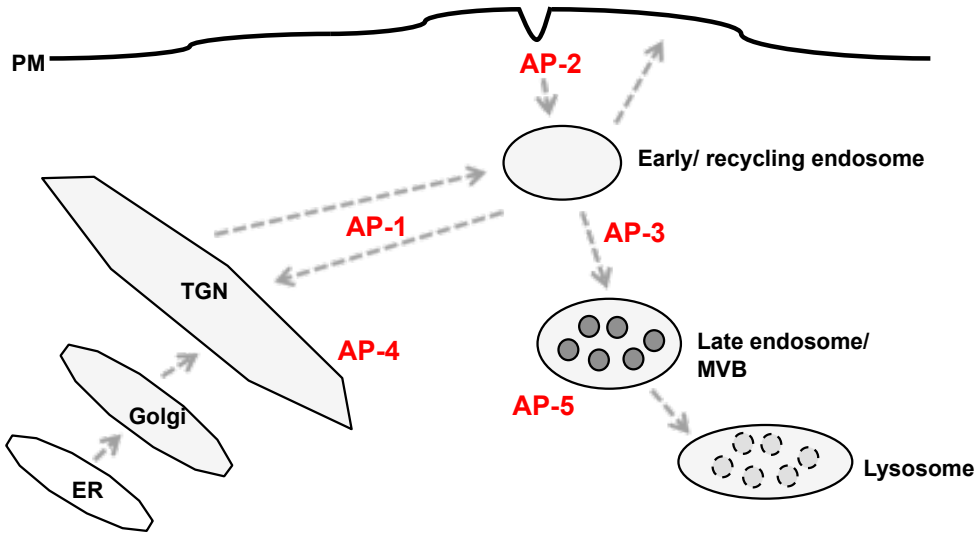

Figure 1-31 Adaptor protein sorting pathways

Simplified representation of adaptor protein sorting pathways leading to endosomal and lysosomal compartments. The assumed cellular localisation and sites of action of different adaptor proteins are indicated next to the corresponding cellular organelle or arrows.

Abnormalities in clathrin adaptor transport pathways can lead to a variety of diseases including Huntington's disease, leukaemia, Alzheimer's disease, Hermansky Pudlack syndrome and familial hypercholesterolemia (Lafer, 2002). Viruses hijack clathrin-mediated trafficking pathways both to gain entry into host cells and for immune evasion.

1.8.2 Clathrin-binding and coat formation

At least 20 clathrin-binding proteins have been identified in the last few years, including well-characterised adaptor proteins AP-1, AP-2, HRS, AP180 and gamma adaptin ear-containing, ARF-binding (GGA) proteins. All adaptor proteins contain long unstructured regions that contain one or more mostly short and linear clathrin-binding motifs.

These motifs interact with the β-propeller head of clathrin, which is located at the N-terminus of the clathrin heavy chain (CHC), called the terminal domain (TD). The nature of these interactions is of a relatively weak binding strength and short half-life (K_d= 1-100 μM and $t_{1/2}$= 1-10 seconds respectively) (Edeling et al., 2006). Clathrin-binding peptides are often called "clathrin boxes". As more and more clathrin boxes are discovered it becomes increasingly difficult to find a common consensus sequence. However, when all known clathrin-binding sequences are aligned the best consensus match is ρLϕρϕρ (ρ= polar residue and ϕ= aliphatic hydrophobic residue) in which position 2, 3 and 4 show the least number of deviations (Lafer, 2002).

The unassembled cytosolic form of clathrin is comprised of 3 heavy and 3 light chain molecules, which is termed a triskelion. As the triskelia assemble, they form basket like structures with pentagonal and hexagonal faces. The light chains regulate clathrin-coated vesicle dynamics (Figure 1-32 A and B) (Lafer, 2002).

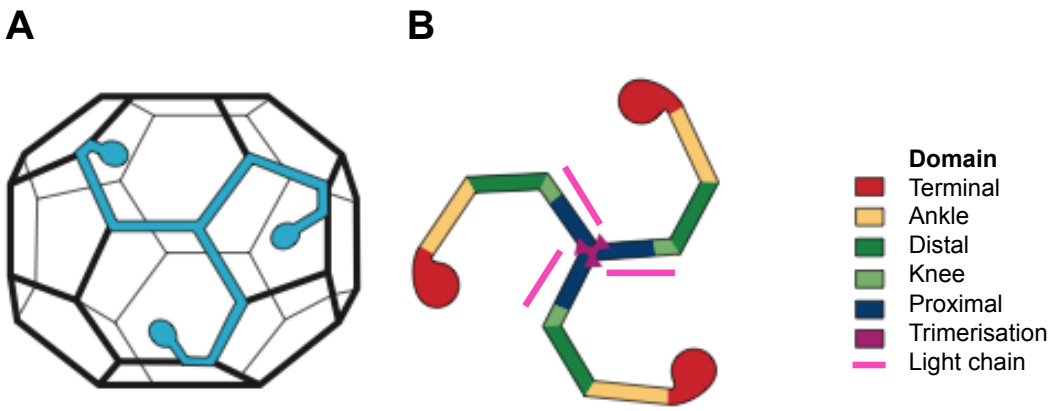

Figure 1-32 The clathrin triskelion

(A) Schematic representation of a clathrin basket with a single triskelion highlighted in blue. **(B)** Clathrin triskelion representation. Three clathrin heavy chains are depicted and highlight the various heavy chain domains using different colours (see key) (adapted from (Edeling et al., 2006)).

1.8.3 Structure and function of adaptor protein complexes

Adaptor proteins (APs) play a major role in selecting cargo molecules designated for intracellular transport via clathrin-coated vesicles. The first identified and best-characterised clathrin adaptor proteins are AP-1 and AP-2. They are part of a larger heterotetrameric adaptor complex family that also includes AP-3, AP-4 and newly identified AP-5. All five adaptor protein complexes are made up of two large, one medium and one small subunit. All complexes form a large core domain with two unstructured joint segments, each ending with an ear or appendage region (Figure 1-33) (Canagarajah et al., 2013). The medium μ subunit is part of the core and has been shown to swing out of the core upon activation of the complex on membranes. The μ subunit and the small σ subunit form the core complex and are responsible for binding of tyrosine-based and acidic dileucine-based sorting signals respectively (binding to the interface of AP-1 γ-σ and AP-2 α-σ subunits). The hinge or joint domains contain direct clathrin-binding sequences that are known to bind to the clathrin heavy chain terminal domain (Canagarajah et al., 2013).

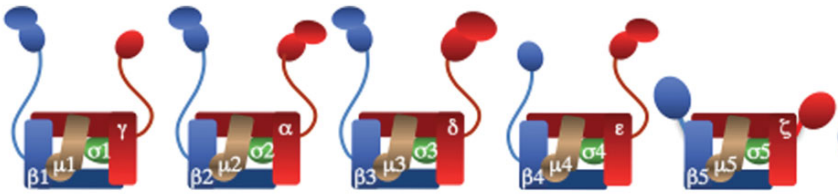

Adaptor	AP-1	AP-2	AP-3	AP-4	AP-5
Scaffold	Clathrin	Clathrin	Clathrin ?	?	SPG11 ?
Signals	Yxxϕ [DE]xxxL[LI]	Yxxϕ [DE]xxxL[LI]	Yxxϕ [DE]xxxL[LI]	Yxxϕ Yx[FYL][FL]E	?
Localisation	TGN/ endosomes	Plasma membrane	Endosomes	TGN	Late endosomes

Figure 1-33 Adaptor protein (AP) complexes

Schematic representation of all members of the heterotetrameric adaptor protein machinery. Listed properties include the scaffolding protein with which they are known to associate, the sorting signals that they interact with, and their intracellular localisation (adapted from (Canagarajah et al., 2013)).

The **AP-1** complex (consisting of subunits: β, γ, μ and σ) machinery has mainly been described to mediate bi-directional transport between the TGN and endosomes. The GTPase Arf1 targets AP-1 to membranes and induces an allosteric change in AP-1, therefore activating the complex. The phosphoinositide, PI(4)P, might complement Arf1-mediated activation of the AP-1 complex (Figure 1-34) (reviewed by (Canagarajah et al., 2013)). The **AP-2** complex (consisting of subunits: β, α, μ and σ) has been shown to be exclusively responsible for endocytosis of transmembrane cargo proteins and subsequent delivery to endosomal compartments. AP-2 is activated on membranes by interaction with the phosphoinositide, $PI(4,5)P_2$, however the mechanism is still unclear (Figure 1-34) (reviewed by (Canagarajah et al., 2013)).

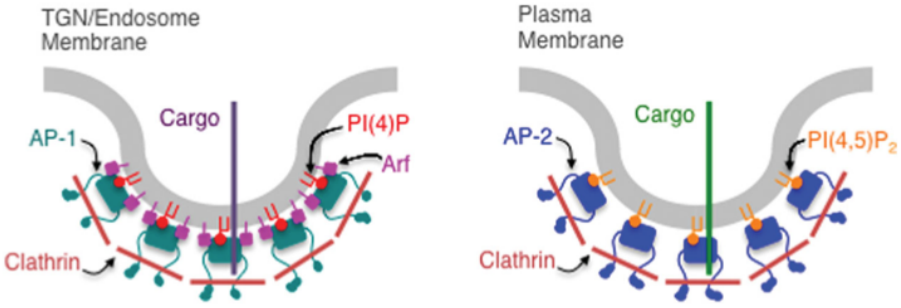

Figure 1-34 Clathrin coat formation

Schematic representation of clathrin coat formation in case of AP-1 and AP-2. **Left diagram:** AP-1 is recruited to membranes by interaction with GTP-bound Arf1 and PI(4)P which are located at TGN or endosomal compartments. **Right diagram:** AP-2 is recruited to membranes by interaction with $PI(4,5)P_2$ which is located at the plasma membrane. Recruitment to membranes positions the adaptor proteins to interact with transmembrane cargo proteins, and the adaptor proteins also serve as attachment sites for formation of clathrin into a polyhedral coat (adapted from (Canagarajah et al., 2013)).

The mammalian **AP-3** complex (consisting of subunits: β, δ, μ and σ) has been shown to bind to clathrin in vitro and to co-localise with clathrin in vivo, however the exact function of AP-3 is still unclear. It is thought to play a role in clathrin-independent sorting from tubular endosomes to late endosomes and lysosomes (Hirst et al., 2011). The **AP-4** complex (consisting of subunits: β, ε, μ and σ) localises to the TGN and contains putative clathrin-binding sequences, however, no binding to clathrin has been detected to date. AP-4 is thought to be part of a non-clathrin coat associated with the TGN (Lafer, 2002) and has been shown to traffic the amyloid precursor protein from the TGN to endosomes (Hirst et al., 2011). Whether AP-3 and AP-4 are involved in clathrin-dependent sorting requires further research. The recently identified and probably final member of the clathrin adaptor family is **AP-5** (consisting of subunits: β, ζ, μ and σ), which has been shown to localise to late endosomal compartments and is a component of non-clathrin coats. AP-5 is thought to participate in endosomal sorting and is linked to hereditary spastic paraplegia, which is a human genetic disorder that causes progressive spasticity (Hirst et al., 2011).

1.8.4 Tyrosine-based sorting signals

The best-characterised tyrosine-based sorting signals are **Y**xxϕ motifs. This clathrin adaptor binding site is known to mediate rapid endocytosis from the plasma membrane; targeting of cargo proteins for lysosomal degradation; and cargo trafficking from the TGN to endosomes, and *vice versa*. The Y position is indispensable and cannot be replaced by other aromatic amino acids. The residue ϕ at position 4 can accommodate different bulky hydrophobic residues, which are thought to specify the nature of the signal. Positions 2 and 3 can be flexible but tend to be hydrophilic residues. Residues flanking the **Y**xxϕ motif can also contribute specificity and strength of the signal. **Y**xxϕ motifs have been shown to interact with clathrin adaptors AP-1, AP-2, AP-3 and AP-4. They bind to the core subunit μ with relatively weak affinity (K_d= 0.05-100 μM). The binding of APs to the tyrosine-based sorting signal is dependent on the Y and ϕ residues. The different μ subunits tend to bind to distinctive sets of **Y**xxϕ motifs (Bonifacino and Traub, 2003).

There is also flexibility in the distal end of tyrosine-based sorting motifs. For example, the tetherin cytoplasmic tail contains a **Y**x**Y**xxϕ tyrosine sorting motif (discussed in 1.6.1) that has been shown to bind to the large AP-2 α subunit (Masuyama et al., 2009) and to the AP-1 and AP-2 μ subunits (Rollason et al., 2007).

1.8.5 Dileucine-based sorting signals

The most studied acidic dileucine-based sorting signal is the (**D**/**E**)xxx**L**(**L**/**I**) motif. This clathrin adaptor motif is known to mediate rapid endocytosis as well as vesicle transport to endosomal and lysosomal compartments. The first leucine residue is critical for function. The second leucine residues can be replaced by isoleucine without loss of function. An acidic residue at the first position is thought to be responsible for the targeting of cargo proteins to late endosomal and lysosomal compartments. A second acidic residue or a serine residue further downstream of the (**D**/**E**)xxx**L**(**L**/**I**) motif can add potency to the signals. The position of the motif within the protein, for example, close to the plasma membrane domains (6-11 residues) or close positioning to the C-terminus can influence the nature of the signal and is thought to enable optimal binding conditions for AP complexes (Bonifacino and Traub, 2003). Some (**D**/**E**)xxx**L**(**L**/**I**) motifs are recognised by the core of AP complexes at the interface of the small σ and the large γ subunit of AP-1; the large α subunit of AP-2; or the large δ subunit of AP-3 (Canagarajah et al., 2013). Binding of dileucine-based sorting motifs to μ subunits of AP-1, -2, and -3 has also been demonstrated, but, dileucine motifs bind to different sites at the μ subunit than tyrosine-based sorting signals (Bonifacino and Traub, 2003).

The HIV-1 accessory protein Nef contains two acidic (**D**/**E**)xxx**L**(**L**/**I**) motifs that have been shown to bind to μ subunits of AP-1, -2, and -3 and to the σ- α hemi-complex of AP-2, and are important for the downregulation of CD4 (Janvier et al., 2003) (Chaudhuri et al., 2007) (Lindwasser et al., 2008) (Ren et al., 2014).

Another distinct class of dileucine-based sorting signals are the **D**xx**LL** motifs, important in mediating cargo transport between the TGN and endosomes. The position 1, 4 and 5 (D, L and L respectively) are strictly required, while the residues 2 and 3 are less important for function. **D**xx**LL** motifs are unable to bind to traditional clathrin AP complexes. Instead they have been shown to interact with the VHS domain of human monomeric clathrin-binding GGA proteins (Bonifacino and Traub, 2003).

1.9 ESCRT pathway and MVB biogenesis

The conserved ESCRT machinery was first identified in yeast and later on in mammalian cells. Early studies performed in yeast knock-out systems identified a crucial role for the “class E” vacuolar protein sorting (*vps*) genes in delivery of cargo molecules to the yeast vacuole and endsosome morphology (Raymond et al., 1992). These studies helped to characterise the ESCRT-I complex and its role in sequestering ubiquitinated cargo at the endosomal membrane and its subsequent delivery into multivesicular bodies, (Katzmann et al., 2001) as well as ESCRT-II and -III complexes as mediators for the delivery of ubiquitinated cargo to the yeast vacuole (Babst et al., 2002a) (Babst et al., 2002b). Interestingly, the ESCRT machinery induces invaginations that bulge away from the cytoplasm, in a process that is topologically inverted from the clathrin-mediated vesicle budding pathways. To date the ESCRT machinery consists of five complexes (ESCRT-0, -I, -II, -III and the AAA ATPase VPS4), and was found to be involved in topologically-related membrane scission events. These can occur during sorting of ubiquitin-labelled membrane proteins into invaginations of endosomal membranes, cytokinesis, viral budding of a number of enveloped viruses, exosome secretion and autophagy (Figure 1-35) (reviewed by (Henne et al., 2011)).

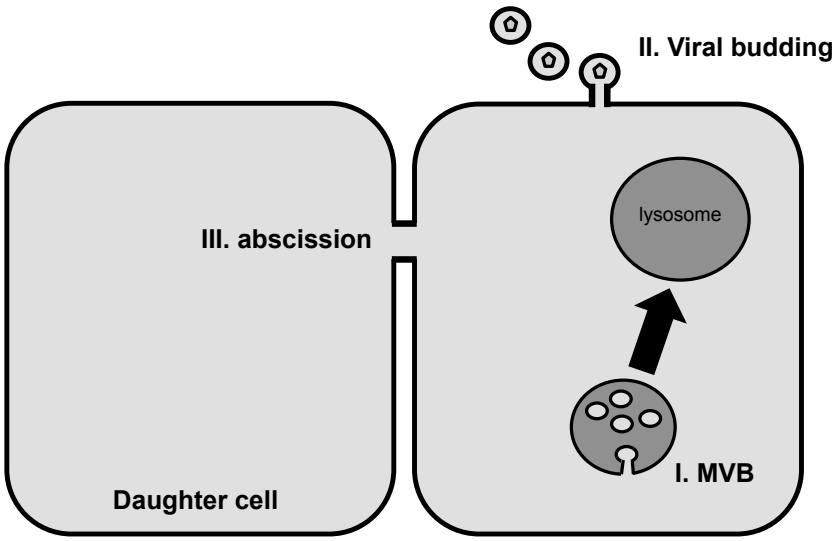

Figure 1-35 Divers roles of ESCRT-mediated processes

The ESCRT machinery plays a role in at least three distinct pathways in mammalian cells **(I)** MVB formation, which delivers ubiquitinated transmembrane cargo proteins to the lysosome for degradation. **(II)** Budding of enveloped viruses like HIV-1 and MLV. **(III)** Abscission, final stages of cell cytokinesis.

During sorting of ubiquitinated membrane proteins into MVBs all five ESCRT complexes are required to be recruited in a sequential manner (see Figure 1-37). The **ESCRT-0** complex consists of two subunits, HRS (hepatocyte growth factor- regulated tyrosine kinase substrate) (for HRS schematic see Figure 5-9A top lane) and STAM1/2 (signal transducing adaptor molecule 1/2), which interact via their respective coiled-coil domains in a 1:1 ratio. The unique feature of ESCRT-0 component HRS is a FYVE (Fab-1, YGL023, VPS27 and EEA1) zinc finger domain that binds to the endosomal lipid phosphatidylinositol 3-phosphate (PtdIns(3)P), providing specificity and membrane recruitment. Both HRS and STAM1/2 have been shown to contain several ubiquitin-binding motifs. HRS binds mono- and lysine 63-linked poly-ubiquitinated cargo via a double-sided ubiquitin-interacting motif (DUIM) (Hirano et al., 2006) and a N-terminal VHS (VPS27, HRS and STAM) domain (demonstrated *in vitro* only) (Ren and Hurley, 2010). STAM1/2 also contains an ubiquitin-binding domain and an amino-terminal VHS domain for ubiquitin binding. It is unclear why the ESCRT-0 complex contains distinct ubiquitin interaction domains, but several explanations have been suggested, namely to sequester of several different cargo molecules simultaneously, binding of one cargo molecule very tightly via multiple interactions, or to engage poly-ubiquitinated cargo membrane proteins with high affinity (Ren and Hurley, 2010). In addition to using ubiquitin-interacting motifs, ESCRT-0 complexes may also interact with cargo molecules through the clathrin machinery. Both HRS and STAM1/2 contain clathrin-binding motifs. HRS has been shown to bind to the clathrin heavy chain at the endosomal membrane, resulting in recruitment into flat clathrin lattice micro-domains (Raiborg et al., 2006). There has also been debate as to whether HRS and STAM1/2 are the only ESCRT-0 components which are able to sort ubiquitinated cargo for lysosomal degradation, as there are structurally similar proteins that might provide an alternative into the ESCRT machinery (Figure 1-36). Potential candidates are members of the GGA protein family and TOM1 or TOM1L1-like proteins which all share common molecular features such as VHS domains, ubiquitin-binding motifs, clathrin-binding boxes and PSAP/PTAP ESCRT-I-binding motifs (reviewed by (Raiborg and Stenmark, 2009)).

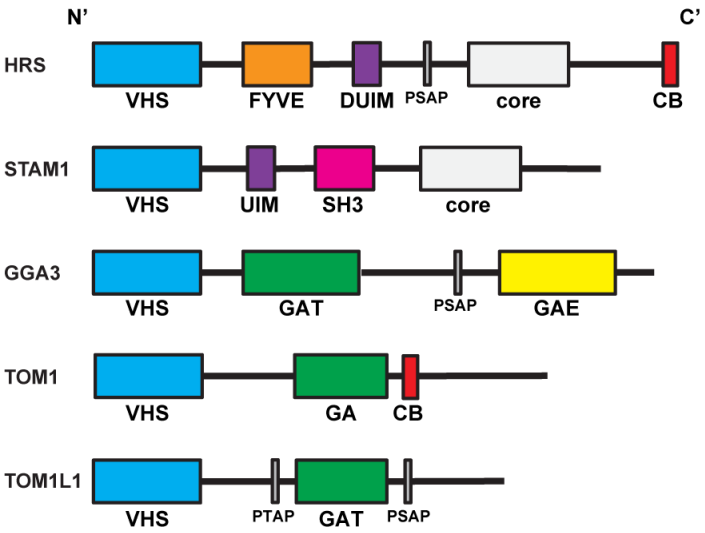

Figure 1-36 Schematic representation of selected VHS domain containing proteins

Schematic representation of ESCRT-0 VHS domain containing proteins HRS and STAM1 as well as other potential ESCRT-0 proteins: GGA3 (GGA1 and GGA2 are similar to GGA3), TOM1 and TOM1L1. In blue VHS domain (VPS27, HRS and STAM), in orange FYVE domain (Fab-1, YGL023, VPS27 and EEA1), in purple UIM or DUIM motif (double-sided or ubiquitin-interacting motif), in red CB (clathrin box), in pink SH3 (Src homology-3 domain), in green GAT or GA domain (GGA and TOM1), in yellow GAE (gamma adaptin ear) domain, and PSAP and PTAP are ESCRT-I binding motifs. ESCRT-0 core and GAT regions are responsible for heterodimerisation.

The **ESCRT-I** complex consists of TSG101, VPS28, VPS37 and either MVB12 or UBAP1 (in a 1:1:1:1 ratio), and is recruited by HRS to the endosome. This recruitment is crucial for cargo molecule sorting for lysosomal degradation because ESCRT-I is unable to bind to membrane lipids directly. The PSAP motif in HRS binds to the ubiquitin E2 variant domain (UEV) at the N-terminus of TSG101. However, as is the case with HRS and STAM1/2, ESCRT-I proteins TSG101, MVB12 and UBAP1 have been shown to bind ubiquitin. Unlike ESCRT-0, ESCRT-I is not thought to be involved in the capture of ubiquitinated cargo proteins. All described ESCRT ubiquitin-binding domains bind to the same hydrophobic isoleucine residue 44 of ubiquitin with roughly the same low affinity. Therefore ubiquitinated cargo proteins are thought to be passed over in a sequentially specific manner from complex to complex (reviewed by (Raiborg and Stenmark, 2009)).

The **ESCRT-II** complex consists of EAP45, EAP30 and EAP20 (in a 1:1:2 ratio). The direct link between ESCRT-I and ESCRT-II in mammalian cells remains unknown. However, ESCRT-II recruitment is dependent on the ESCRT-I VPS28 C-terminal domain through a helix that is C-terminal to the GLUE domain (reviewed by (Raiborg and Stenmark, 2009)). The GRAM-like ubiquitin-binding in Eap45 (GLUE) domain in VPS36 binds to ubiquitin and engages PtdIns(3)P lipids and therefore provides specific localisation to cellular membranes in a similar manner to the FYVE domain in HRS only in a less strong manner.

The mammalian **ESCRT-III** complex consists of four major "core" subunits called charged multivesicular body proteins (CHMP6; 4; 3; 2 and their isoforms). The auto-inhibited, "closed" conformation and therefore inactive monomeric forms do not localise to the endosome. During membrane sculpting events the ESCRT-III components recruit one another transiently in a sequential manner to endosomes, where the physical contact between subunits induces a conformational change and activates the subunits. However, the initial trigger for ESCRT-III subunit release from auto-inhibition is still unknown (reviewed by (Henne et al., 2013)). In addition to the "core" subunits, there are apoptosis-linked gene-2 interacting protein X (ALIX) and CHMP1 subunits that are necessary for MVB sorting and cytokinesis, and increased salt tolerance-1 (IST1) which is important in cytokinesis only. ESCRT-III lacks the ability to bind ubiquitin. However, recently ALIX has been shown to bind to ubiquitin directly, and its yeast homolog BCK1-like resistance to osmotic shock protein-1 (Bro1) has been shown to function as a cargo recognition subunit for ubiquitinated proteins (Dowlatshahi et al., 2012) (Pashkova et al., 2013).

Before cargo proteins are delivered to the lysosome, they must be de-ubiquitinated, a process which is important to maintain cellular ubiquitin pools constant. The DUBs associated molecular with SH3 domain of STAM (AMSH) and ubiquitin isopeptidase Y (UBPY) are recruited by ESCRT-III and ALIX, as well as by the ESCRT-0 component STAM. AMSH interacts with both ESCRT-0 and ESCRT-III and has been shown to only recognise Lys-63-linked poly-ubiquitin chains, while UBPY interacts only with ESCRT-0 and has been shown to recognise Lys-63-linked and Lys-48-linked poly-ubiquitin chains. The DUBs are thought to de-ubiquitinate cargo proteins that are wrongly sorted into the MVB pathway, or to relieve auto-inhibitory mono-ubiquitination of ESCRT-0 components and remodelling of ubiquitin chains (reviewed by (Raiborg and Stenmark, 2009)).

Once the ESCRT-III complex is assembled at the endosomal membrane it requires energy to dissociate from the membrane. The only known energy input in MVB membrane scission events is provided by the AAA ATPase **VPS4**. VPS4 binds to ESCRT-III components via an microtubule-interacting and trafficking (MIT) domain that recognises MIT-interacting motif (MIMs) in ESCRT-III subunits. The role of VPS4 in membrane fission is not clear. A possible model for the role of VPS4 involves the recycling of ESCRT-III components after abscission, or the stepwise removal of ESCRT-III to generate constrictive forces that are crucial for abscission (reviewed by (Henne et al., 2011)).

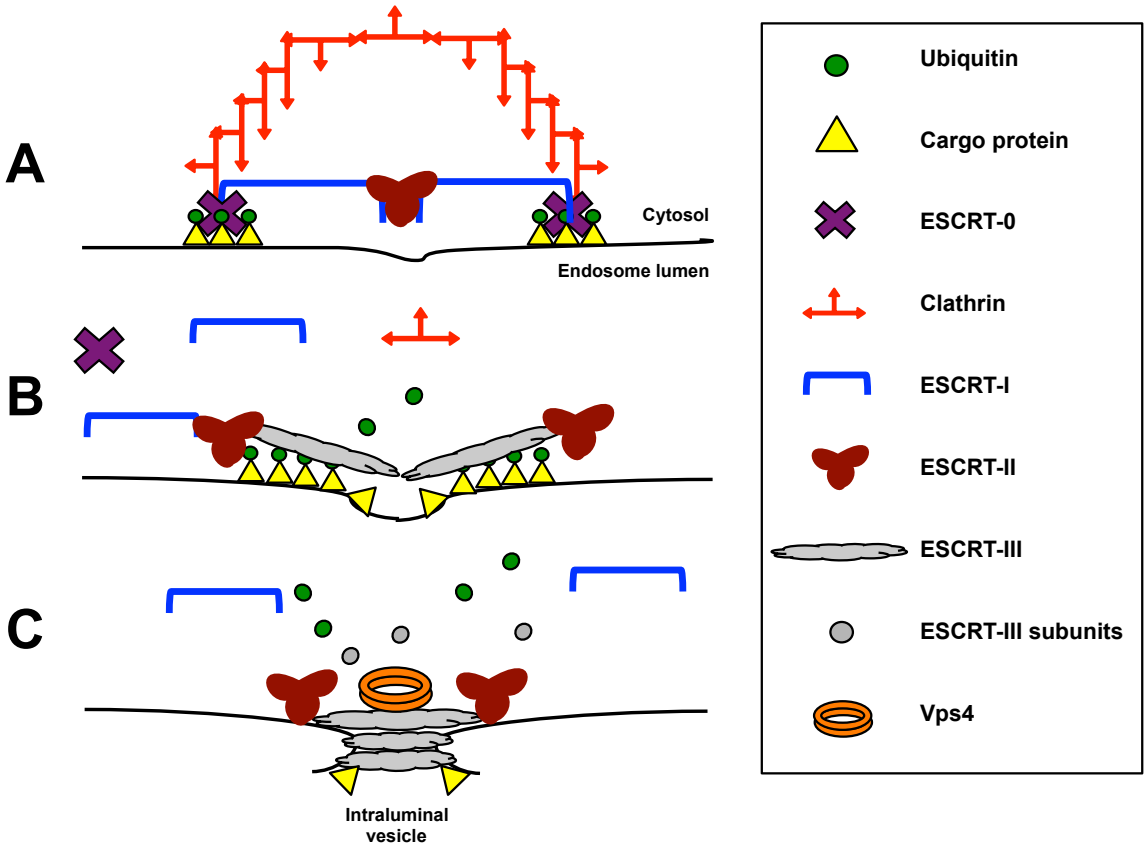

Figure 1-37 ESCRT machinery and sorting of ubiquitinated cargo proteins

(A) Recognition of ubiquitinated transmembrane cargo proteins by ESCRT-0, which are sorted and concentrated in clathrin-coated micro-domains. ESCRT-0 recruits ESCRT-I that in turn recruits ESCRT-II, this process might initiate membrane involution. **(B)** ESCRT-III complexes are activated and recruited by binding to the ESCRT-II subunit EAP20. Leading to the formation of spiral formed filaments that gate cargo proteins into invaginations. Cargo proteins are also de-ubiquitinated by DUBs recruited by ESCRT-III. **(C)** VPS4 disassembles ESCRT-III filaments into its subunits that are being recycled. Followed by membrane abscission.

In short, during the final stages of cytokinesis the centrosomal protein 55 (CEP55) is recruited to the midbody, in turn recruiting ESCRT-I and ALIX. In the absence of ESCRT-II, this functions as a platform to activate and recruit ESCRT-III to the midbody. The details of the release of auto-inhibition of ESCRT-III subunits are not known, but three models of ESCRT-III-mediated abscission have been proposed. The “spiral-ingression” model, where ESCRT-III subunit-containing spirals form around and narrow the intracellular bridge to initiate final abscission. The “sliding model”, which is similar to the above but spirals slide along the midbody to induce abscission. And the “vesicle-mediated ingression” model, where vesicles derived from the recycling endosome cause narrowing of the midbody by fusion with the plasma membrane. VPS4 activity is essential during final stages of cell division. The AAA ATPase VPS4 has been shown to be recruited by IST1, which can be negatively regulated MIT-domain-containing-protein 1 (MITD1). Interestingly, IST1 activity is dispensable for MVB formation and viral budding. Recruitment of VPS4 accords with membrane cutting and is therefore

thought to generate constrictive forces for membrane severing, or as discussed above it might disassembles ESCRT-III subunits that serve as a recycling pool (reviewed by (Henne et al., 2013)).

In short (see 1.3.6 for more detail), during HIV-1 budding, Gag, the major HIV-1 structural protein recruits ESCRT-I and ESCRT-III complexes through its C-terminal p6 late-budding domain (L-domains). The p6 P(S/T)AP motif binds the ESCRT-I complex TSG101 that in turn recruits ESCRT-III, therefore bypassing the need to bind ESCRT-0 component HRS. Similarly, the (L)YPX_nL motif in p6 provides another platform to recruit the ESCRT machinery by binding ALIX. Failure to recruit the ESCRT machinery leads to the accumulation of budding deficient virions at the plasma membrane of infected cells (reviewed by (Martin-Serrano and Neil, 2011)).

Chapter 2 AIM OF THESIS RESEARCH

One of the best-characterised examples that illustrate the role of HIV-1 Vpu in antagonising cellular innate immune defences is the restriction factor tetherin. The studies of the mechanism by which Vpu antagonises the anti-viral function of tetherin provide a powerful tool to understand the complex interactions between virus and host. In that regard, the aim of this thesis is to contribute to the understanding of the mechanism by which Vpu targets tetherin. This thesis includes three chapters of experimental data that aim to demonstrate:

1. The role of the second alpha helix of HIV-1 Vpu in tetherin antagonism. We identified a putative sorting signal, **E**xxx**LV**, which is required for post-binding trafficking of Vpu/tetherin complexes and inhibition of antiviral activity in primary CD4+ T cells.

2. The importance of the hydrophobic residues in Vpu cytoplasmic helix 1, essential for Vpu/HRS interaction, which is dependent on residues that bind ubiquitin in the DUIM of HRS.

3. The cytoplasmic tail mutants Vpu ELV, Vpu LILI and Vpu 2/6A all have the same defect, as these mutants appear to fail to interact with the cellular clathrin trafficking machinery.

Chapter 3 MATERIALS AND METHODS

3.1 WORKING WITH DNA

3.1.1 Polymerase Chain Reaction (PCR)

PCR is an *in vitro* method designed to amplify short DNA fragments. It is used to replicate the original DNA sample using an enzyme called DNA polymerase, which produces new complementary DNA strands. Two primer pairs are required which determine the beginnings of the region to be amplified. This method consists of a repetition of a series of cycles and each cycle consists of three different steps. First, the double stranded DNA is separated in the denaturation step. The next step is the annealing where the primers bind to the single stranded DNA templates. In the last step DNA polymerase catalyses the synthesis of DNA and extends between primer pairs using the complementary DNA strand as a template. These three steps make up one cycle, which can be repeated up to 30 times.

The **standard PCR** method was used mainly for subcloning of DNA fragments into expression vectors with different multiple cloning sites. All proteins in pCR3.1 were generated with a Kozak consensus (GCCACC) sequence located immediately upstream of the ATG start codon, and all primers were synthesised by MWG Eurofins. For Vpu subcloning, the forward primer encoded an EcoRI cloning site. The reverse primer encoded a XhoI or NotI cloning site, and if required contained a TAG or TGA stop codon. Standard PCR reactions were carried out as described in Table 1 and PCR machine (Eppendorf Mastercycler) was set to below described cycle conditions (Table 2).

Overlapping PCR was used to generate pCR3.1 Vpu ELV and pCR3.1 CD8-CI-M6PR expression vectors. In case of the Vpu ELV mutant wild-type Vpu was used as a template for the first of two separate PCR reactions. Standard setting were used to carry out overlapping PCR (Table 1 and Table 2) in which forward and reverse oligonucleotides containing the desired ELV mutation were used in combination with Vpu full-length forward and reverse primers to generate two small DNA fragments. Subsequently specific fragments were gel purified as described in 3.1.7. and 10 μl of each was used as template DNA in a second PCR reaction with full-length forward and reverse Vpu primers.

Site directed mutagenesis, also termed **QuickChange** was employed to generate Vpu triple alanine mutants in the second alpha helix of Vpu using forward and reverse complementary oligonucleotide, containing the desired mutation. The required mutation is located in the middle of the oligonucleotides with 10-15 bases on either side. Primers were between 25 and 50 bases in length with a desired melting temperature (T_m) of ≥78°C, a minimum GC content of 40%, and terminate in one or more G or C bases. PCR reactions were carried out as described in Table 1 and PCR machine (Eppendorf Mastercycler) was set to the below described cycle conditions for QuickChange (Table 2).

Table 1 PCR reaction setup

Reagent	Final concentration
Primer forward	1 pmol (standard PCR) 100 ng (QuickChange)
Primer reverse	1 pmol (standard PCR) 100 ng (QuickChange)
dNTPs (Sigma)	0.2 mM
DNA template	200 ng (standard PCR) 10 ng (QuickChange)
Phusion ® High-Fidelity DNA Polymerase (New England Biolabs)	1 µl (2 units)
Phusion HF buffer (New England Biolabs)	1x
ddH_2O	x µl
Total	50 µl

Table 2 PCR cycle conditions

Step	Temperature	Time	Cycle repeats
Denaturation	95°C	30 seconds	1x
Denaturation	95°C	30 seconds	30x (standard PCR) 18x (QuickChange)
Primer annealing	55°C	30 seconds (standard PCR) 1 minute (QuickChange)	
Extension	72°C	30 seconds (standard PCR) 7 minutes (QuickChange) (Phusion DNA Polymerase extension time: 15 seconds per 1 kb of DNA)	
Extension	72°C	5 minutes	1x
Cooling	4°C	10 minutes or endless until stopped manually	

3.1.2 Extraction and purification of DNA fragments

Agarose gel electrophoresis was used to separate DNA fragments by molecular weight after PCR or restriction digest. For a 1% agarose gel, 0.5 g of electrophoresis grade agarose (Invitrogen) was added to 50 ml of 1x TAE buffer (1x TAE buffer: 40 mM Tris-acetate, 1 mM EDTA, 0.114% glacial acetic acid pH 8.2-8.3) and heated until completely dissolved. Once cooled down 2 μl of ethidium bromide (Sigma) was added and the solution poured into a gel cast to set. Subsequently, samples were loaded alongside a 2-log DNA ladder (New England BioLabs) and samples and run in 1x TAE buffer at 100 volt (V). DNA bands were visualised using Chemi Doc UV system (Bio-Rad).

Gel purification. The DNA band was cut out from the agarose gel and DNA was extracted using a Quickgel Extraction Kit (QIAGEN). The Quickgel Extraction Kit follows a bind-wash-elute procedure. Briefly, the DNA was absorbed to the silica membrane of the spin-column, the impurities were then washed away and the pure DNA was eluted, see manufacturer's instructions for detailed protocol.

3.1.3 DNA digest by restriction endonucleases

Restriction endonucleases are used to cleave DNA at specific nucleotide sequences in order to isolate fragments of interest or confirm the presence of a ligated insert. The choice of enzyme depends upon the following: specific sequence sites available, easily distinguishable sizes of fragments (when separated), conditions under which the enzymes cut most efficiently, and if blunt or sticky ends are required (sticky ends are easier to ligate into a vector).

XhoI, NotI, NheI, EcoRI, EcoRV and DpnI (New England BioLabs) were commonly used enzymes and ratios of reagents used in the restriction digest mix are shown in Table 3. Once combined the mix was left incubating at 37°C for 2 hours, and if necessary the 5' phosphatase group of the linearized expression vector was removed by Antarctic Phosphatase (New England BioLabs), to prevent recirculation or self-ligation of DNA. In these cases, 1x of Antarctic buffer (New England BioLabs) and 5 units of Antarctic Phosphatase enzyme (New England BioLabs) were added to the reaction-mixture and incubation was continued for another 30 minutes.

Table 3 Restriction digest setup

Reagent	Final volume
Buffer (appropriate for enzymes used)	5 μl
BSA	1x
Restriction enzyme 1	10 units
Restriction enzyme 2	10 units
DNA (2.5 μg)	x μl
ddH_2O	x μl
Total	50 μl

3.1.4 DNA ligation

Ligation of DNA fragments into expression vectors (Table 6) was carried out using T4 DNA Ligase (New England BioLabs). In short, DNA inserts were previously generated by PCR, isolated by agarose gel electrophoresis and purified. DNA and expression vectors were cut with restriction enzymes (New England BioLabs) in order to produce sticky ends and linear vectors.

Ratios of the reagents used for the ligation reaction are shown in Table 4. Once all reagents were mixed the solution was left incubating at room temperature for 1 hour. For the negative control the insert was replaced with sterile water to detect the number of background colonies, due to self-ligation of the expression vector.

Table 4 Ligation setup

Reagent	Final volume
Vector	x μl
DNA insert	x μl (3-fold molar excess of insert)
T4 Ligase Buffer 10x	2 μl
T4 DNA Ligase	1 μl
ddH_2O	x μl
Total	20 μl

3.1.5 Preparation of chemically competent cells

The DH10 (Invitrogen) *Escherichia coli* (*E.coli*) cells were grown in 10 ml of Luria-Bertani (LB) medium and incubated in a shaking incubator at 220 rpm and 37°C for 16 hours. 50 ml of LB broth was inoculated with 0.5 ml of overnight culture and incubated in a shaking incubator at 220 rpm and 37°C until OD_{550}=0.45. Cells were then chilled on ice for 10 minutes to stop growth and pelleted in a pre-chilled bench top centrifuge

at 3000 x g. Cells were resuspended in 20 ml of filter-sterilized buffer 1 (Table 5) and incubated on ice for 5 minutes before pelleting as described above. Next, cells were resuspended in filter-sterilized buffer 2 (Table 5) and incubated for 10 minutes on ice. The now chemically competent *E.coli* cells were snap-frozen on dry ice in 100 µl aliquots and stored at -80 °C.

Table 5 List of buffers for chemically competent cells

Buffer 1	Buffer 2
30 mM KAc	10 mM PIPES
100 mM RbCl	75 mM CaCl2
10 mM CaCl2	10 mM RbCl
50 mM MnCl2	15% glycerol
15% glycerol	

3.1.6 Transformation of plasmid DNA into competent *E.coli* cells

50 µl of chemically competent DH10 *E.coli* cells were thawed and stored on ice before being incubated with 5-50 ng of plasmid DNA or with 3 µl of the ligation reaction mix. After 20 minutes incubation on ice, the cells were heat shocked for 45 seconds at 42°C and immediately put back on ice. The bacteria were then incubated with 200 µl of fresh LB broth for 45 minutes at 30°C or 37°C in a shaking incubator at 220 rpm. The bacterial solution was spread onto a LB/amp (100 µl/ml) agar plate and placed into an incubator at 30°C or 37°C overnight. Retroviral vectors were grown at 30°C to avoid genetic recombination. Single colonies were picked and transferred into a 2 ml LB/amp culture in order to amplify the bacterial clone. This culture was either used directly to screen colonies by PCR, for plasmid extraction (mini-prep) to screen of colonies by restriction digest or sequencing, or used as a starter culture to inoculate 50 ml of LB/amp for large-scale plasmid amplification.

3.1.7 Plasmid amplification and purification

100 µl of a 2 ml starter culture was used to inoculate 50 ml LB/amp and incubated overnight in a 500 ml flask at 30°C or 37°C in a shaking incubator at 220 rpm. Cells were harvested by centrifugation in a bench top centrifuge at 6000 x g for 15 minutes at 4°C. Plasmid extraction from pelleted bacterial cells was performed using a Plasmid Midi kit (QIAGEN), which follows a simple bind-wash-elute method. Briefly, bacterial cultures were lysed followed by centrifugation and the cleared lysates were applied to a

QIAprep column where the plasmid DNA is absorbed by the silicagel membrane. Subsequently, impurities were washed out and plasmid DNA was eluted. The elution buffer/DNA solution was supplemented with isopropanol to precipitate plasmid DNA by centrifugation. Finally, the eluted DNA was washed in 70% ethanol and resuspended in ddH_2O.

Alternatively, plasmid extraction was carried out from 2 ml overnight cultures obtained from 3.1.6. The method is based on the above-described principle using the QIAprep Spin Miniprep kit (QIAGEN). See manufacturer handbooks for detailed protocols on midi-prep and mini-prep plasmid DNA extraction.

3.1.8 DNA sequencing and vector features

DNA concentrations of plasmid preparations (list of all DNA vectors displayed in Table 6) were measured using a Nanodrop ND-100 Spectrophotometer (Labtech International) and 15 µl of a 50-100 ng/µl plasmid DNA solution in ddH_2O was sent for sequencing to Eurofins MWG Operon.

The T7 primer site was used for forward sequencing and BGH was used for reverse sequencing in pCR3.1. Sequencing primers for NL4.3, pCMS28, pLHCX and pAIP were directed against down- and up-stream sequences of the respective multiple cloning sites.

Table 6 List of DNA vectors and proviruses used in this study

Vector	Source	Features
pCR3.1	Invitrogen	Encodes Ampicillin resistance gene and pUC origin for selection in *E. coli*. Large multiple cloning site is downstream of the human cytomegalovirus (CMV) promoter region. Encodes Bovine Growth Hormone (BGH) polyadenylation signal and transcription termination sequence for enhanced mRNA stability.
NL4.3	NIH AIDS Reagent Program	Full-length, replication and infection competent chimeric HIV-1 DNA molecular clone.
NL4.3 delVpu	Stuart Neil	Derived from NL4.3 by replacing the ATG start codon of the *vpu* ORF with BamHI restriction site to intoduce a frame shift (Neil et al., 2006).
pLHCX	Clonetech	Retroviral based vector, contains elements derived from Moloney murine leukemia and Moloney murine sarcoma viruses. 5' viral LTR contains promoter sequences that control expression of the hygromycin resistance gene. The multiple cloning site is immediately downstream of the human cytomegalovirus (CMV) promoter region.
pCMS28	M. Malim	Derived from pMigR1 retroviral based vector, encodes puromycin resistance gene linked via an IRES to the multi-cloning site.
pAIP	Andrea Cimarelli	Retroviral based vector, encodes puromycin resistance gene, contains human cytomegalovirus (CMV) promoter region.

Table 7 List of DNA plasmids

Gene	Vector	Restriction sites	Tag	Resistance gene	Source
YFP	pCR3.1		No tag	Amp	Paul Bieniasz
GFP	pCR3.1		No tag	Amp	Paul Bieniasz
eGFP	pCMS28		IRES (N-terminus)	Amp/ Purom	Anna Le Tortorec
Cherry	pCR3.1		No tag	Amp	Paul Bieniasz
Tetherin wt	pCR3.1 pLHCX pCR3.1 pLHCX	XhoI/NotI XhoI/NotI XhoI/NotI XhoI/NotI	HA (position 463) HA (position 463) No tag No tag	Amp Amp/ Hygrom Amp Amp/ Hygrom	Stuart Neil Stuart Neil Stuart Neil Stuart Neil
Tetherin Y6,8A	pCR3.1 pLHCX	 XhoI/NotI	No tag No tag	Amp Amp/ Hygrom	Anna Le Tortorec Anna Le Tortorec
Tetherin delGPI	pLHCX	XhoI/NotI	No tag	Amp/ Hygrom	Rui Pedro Galao
Tetherin STS	pLHCX	XhoI/NotI	No tag	Amp/ Hygrom	Julia Weinelt
Vpu	pCR3.1 pCR3.1 pCR3.1 NL4.3	EcoRI/XhoI EcoRI/XhoI EcoRI/NotI	No tag HA (C-terminus) GFP (C-terminus) No tag	Amp Amp Amp Amp	Klaus Strebel Subcloning Subcloning NIH AIDS Reagent Program
delVpu	NL4.3		No tag	Amp	Stuart Neil
Vpu	pCMS28		IRES/ GFP (C-terminus)	Amp/ Purom	Anna Le Tortorec
Vpu2/6A	pCR3.1 NL4.3	EcoRI/XhoI	HA (C-terminus) No tag	Amp Amp	Stuart Neil Stuart Neil
Vpu 59-61A	pCR3.1	EcoRI/XhoI	HA (C-terminus)	Amp	Site directed mutagenesis
Vpu 60-62A	pCR3.1	EcoRI/XhoI	HA (C-terminus)	Amp	Site directed mutagenesis
Vpu 61-63A	pCR3.1	EcoRI/XhoI	HA (C-terminus)	Amp	Site directed mutagenesis
Vpu 62-64A	pCR3.1	EcoRI/XhoI	HA (C-terminus)	Amp	Site directed mutagenesis
Vpu 63-65A	pCR3.1	EcoRI/XhoI	HA (C-terminus)	Amp	Site directed mutagenesis
Vpu 64-66A	pCR3.1	EcoRI/XhoI	HA (C-terminus)	Amp	Site directed mutagenesis
Vpu 65-67A	pCR3.1	EcoRI/XhoI	HA (C-terminus)	Amp	Site directed mutagenesis
Vpu 66-68A	pCR3.1	EcoRI/XhoI	HA (C-terminus)	Amp	Site directed mutagenesis
Vpu 67-69A	pCR3.1	EcoRI/XhoI	HA (C-terminus)	Amp	Site directed mutagenesis
Vpu 68-70A	pCR3.1	EcoRI/XhoI	HA (C-terminus)	Amp	Site directed mutagenesis
Vpu ELV	pCR3.1 pCR3.1 NL4.3	EcoRI/XhoI EcoRI/NotI	HA (C-terminus) GFP (C-terminus) No tag	Amp Amp Amp	Overlapping PCR Subcloning Overlapping PCR
Vpu 64I	pCR3.1	EcoRI/XhoI	HA (C-terminus)	Amp	Site directed mutagenesis
Vpu 64M	pCR3.1	EcoRI/XhoI	HA (C-terminus)	Amp	Site directed mutagenesis
Vpu 64L	pCR3.1	EcoRI/XhoI	HA (C-terminus)	Amp	Site directed mutagenesis
Vpu EntsLL	pCR3.1	EcoRI/XhoI	HA (C-terminus)	Amp	Site directed mutagenesis
Vpu-Nef	pCR3.1 pCR3.1	EcoRI/XhoI EcoRI/XhoI	HA (C-terminus) Cherry (C-terminus)	Amp Amp	Standard PCR (long primer) Subcloning
Vpu-Nef-mu	pCR3.1 pCR3.1	EcoRI/XhoI EcoRI/XhoI	HA (C-terminus) Cherry (C-terminus)	Amp Amp	Standard PCR (long primer) Subcloning
Vpu LILI	pCR3.1 NL4.3	EcoRI/XhoI	HA (C-terminus) No tag	Amp Amp	Site directed mutagenesis Site directed mutagenesis
Vpu LILI + ELV	pCR3.1 NL4.3	EcoRI/XhoI	HA (C-terminus) No tag	Amp Amp	Site directed mutagenesis Site directed mutagenesis
Vpu A14L W22A	pCR3.1 NL4.3		HA (C-terminus) No tag	Amp Amp	Raphael Vigan Raphael Vigan
BirA	pAIP	XhoI/NotI	Myc (N-terminus)	Amp/ Purom	BirA provided by: Kyle J. Roux pAIP provided by: Andrea Cimarelli
B Vpu	pAIP	XbaI/XhoI	Myc/ BirA (C-terminus)	Amp/ Purom	Synthesised and subcloned

B Vpu ELV	pAIP	XbaI/XhoI	Myc/ BirA (C-terminus)	Amp/ Purom	Synthesised and subcloned
B Vpu 3/7A	pAIP	XbaI/XhoI	Myc/ BirA (C-terminus)	Amp/ Purom	Synthesised and subcloned
B Vpu I+I	pAIP	XbaI/XhoI	Myc/ BirA (C-terminus)	Amp/ Purom	Synthesised and subcloned
Vpu HRS CB	pCR3.1	EcoRI/XhoI	No tag	Amp	Standard PCR (long primer)
Vpu HRS CB mut	pCR3.1	EcoRI/XhoI	No tag	Amp	Standard PCR (long primer)
Vpu ELV CB	pCR3.1	EcoRI/XhoI	No tag	Amp	Standard PCR (long primer)
Vpu ELV CB mut	pCR3.1	EcoRI/XhoI	No tag	Amp	Standard PCR (long primer)
Vpu LILI CB	pCR3.1	EcoRI/XhoI	No tag	Amp	Standard PCR (long primer)
Vpu LILI CB mut	pCR3.1	EcoRI/XhoI	No tag	Amp	Standard PCR (long primer)
Vpu 2/6A CB	pCR3.1	EcoRI/XhoI	No tag	Amp	Standard PCR (long primer)
Vpu 2/6A CB mut	pCR3.1	EcoRI/XhoI	No tag	Amp	Standard PCR (long primer)
CI-M6PR	pCR3.1	EcoRI/NotI	CD8 (N-terminus)	Amp	Matthew Seaman
Beta-TrCP2	pCR3.1	BamHI/XhoI	Myc (N-terminus)	Amp	Cloned from HeLA cDNA
HRS	pCR3.1 pCR3.1	XhoI/NotI XhoI/NotI	HA (N-terminus) Myc (N-terminus)	Amp Amp	Juan Martin-Serrano Subcloning
HRS delCB	pCR3.1	XhoI/NotI	Myc (N-terminus)	Amp	Standard PCR
HRS 1-500	pCR3.1	XhoI/NotI	Myc (N-terminus)	Amp	Standard PCR
HRS 1-280	pCR3.1	XhoI/NotI	Myc (N-terminus)	Amp	Standard PCR
HRS 1-250	pCR3.1	XhoI/NotI	Myc (N-terminus)	Amp	Standard PCR
HRS W25A L29D	pCR3.1	XhoI/NotI	Myc (N-terminus)	Amp	Site directed mutagenesis
HRS A266/268Q	pCR3.1	XhoI/NotI	Myc (N-terminus)	Amp	Site directed mutagenesis
GGA1	pCR3.1	EcoRI/XhoI	Myc (N-terminus)	Amp	cDNA from
GGA2	pCR3.1	EcoRI/NotI	Myc (N-terminus)	Amp	cDNA from
GGA3	pCR3.1	EcoRI/XhoI	Myc (N-terminus)	Amp	cDNA from
Ubiquitin	pCR3.1		HA (N-terminus)	Amp	Juan Martin-Serrano
DN dynamin 2	pCR3.1	NotI/ NotI	HA (C-terminus)	Amp	Stuart Neil
WT dynamin 2	pCR3.1	NotI/ NotI	HA (C-terminus)	Amp	Stuart Neil
AP180c	pCR3.1		Flag (N-terminus)	Amp	Heinrich Gottlinger
VSV-G	pCMV		No tag	Amp	Paul Bieniasz
MLV gag-pol	pCAGGS		No tag	Amp	Paul Bieniasz
HIV gag-pol	pVRC1		No tag	Amp	Paul Bieniasz

3.2 WORKING WITH CELLS

3.2.1 Cell Culture

All adherent cells were maintained at 37°C and 5% CO_2 under sterile conditions in Dulbecco's Modified Eagle Medium (DMEM) (Invitrogen) supplemented with 10% fetal calf serum (FBS, Invitrogen – heat-inactivation for 30 minutes at 56°C) and 0.02 mg/ml gentamycin (Invitrogen). T-cell lines were grown at 37°C and 5% CO_2 under sterile conditions in Roswell Park Memorial Institute medium (RPMI) supplemented with 10% fetal calf serum and 0.02 mg/ml gentamycin. Cell density was monitored daily and cells were passaged every two days or when required. Adherent cells lines were first washed in 5 ml of 1x phosphate buffered saline (PBS) and detached from the tissue culture plate using 1 ml of Trypsin (TrpLE Express + phenol red, Invitrogen). Cells were resuspended in warm DMEM and appropriate aliquots of the cell suspensions were transferred into a fresh tissue culture plate. T cell lines were passaged by aspiration of tissue culture medium (containing cells) and addition of fresh RPMI.

For long time storage, detached cells were pelleted by centrifugation at 1500 rpm and resuspended in a 10% DMSO (Sigma) and 90% FBS (Invitrogen) solution. Cells were immediately placed in the -80°C freezer for 5 days before being transferred into a liquid nitrogen tank. All cell lines used can be seen in Table 8.

Table 8 Cell lines used in this study

Cell line	Origin	Source	Culture medium	Characteristics
HeLa	Adenocarcinoma cell line, isolated from human cervix tissue	ATCC	DMEM (adherent cells)	- Endogenously express tetherin
HeLa-TZMbl	Adenocarcinoma cell line, isolated from human cervix tissue	NIH AIDS Reagent Program	DMEM (adherent cells)	- Endogenously express tetherin - Express HIV-1 receptor CD4 and CCR5
HT1080	Isolated from human fibrosarcoma connective tissue	ATCC	DMEM (adherent cells)	- Do not express tetherin
HEK-293T	Isolated from human embryonic kidney tissue, express SV40 T-antigen	ATCC	DMEM (subconfluent cells)	- Do not endogenously express tetherin but can be induced by IFN
Jurkat	CD4+ T lymphocyte (leukemia)	ATCC	RPMI (confluent cells)	- Endogenously express tetherin - Express HIV-1 receptor CD4 and CXCR4
AP-1 μ1A -/-	Mouse fibroblast	Peter Schu	DMEM (adherent cells)	Express human tetherin-HA under hygromycin selection

AP-3 δ -/- (*pearl*)	Mouse fibroblast	Andrew Peden	DMEM (adherent cells)	Express human tetherin-HA under hygromycin selection
HEK-293T tetherin	Isolated from human embryonic kidney tissue, express SV40 T-antigen	Generated from HEK-293T cells	DMEM (subconfluent cells)	Stably express human tetherin under hygromycin selection
HEK-293T tetherin Y6,8A	Isolated from human embryonic kidney tissue, express SV40 T-antigen	Generated from HEK-293T cells	DMEM (subconfluent cells)	Stably express human tetherin Y6,8A mutant under hygromycin selection
HEK-293T tetherin delGPI	Isolated from human embryonic kidney tissue, express SV40 T-antigen	Generated from HEK-293T cells	DMEM (subconfluent cells)	Stably express human tetherin truncated at GPI anchor under hygromycin selection
HT1080/tetherin-HA	Isolated from human fibrosarcoma connective tissue	Generated from HT1080 cells	DMEM (adherent cells)	Stably express human tetherin-HA under hygromycin selection

3.2.2 Transient transfection

Cells were plated at a density of $5x10^5$ in a 6-well plate or at $1.2x10^5$ in a 24-well plate and grown for 24 hours to achieve a confluency of 50-60% at the time of transfection. For each transfection plasmid DNA concentrations were measured and appropriate amounts of pCR3.1 and/or NL4.3 expression vector were diluted in DMEM and mixed gently. The transfection reagent was diluted in DMEM and incubated at room temperature for 5 minutes before being combined with the diluted DNA, mixed gently, and incubated at room temperature for a further 20 minutes. The transfection mix was then added drop-wise to the cells, and medium was replaced 6 hours post transfection. Cells were incubated for 48 hours before analysis by Western blot or FACS.

HeLa and HeLa-TZMbl cells were transfected according to manufacture's instructions using Lipofectamine 2000 (Invitrogen), 293T and 293T tetherin cells were transfected using a 1 mg/ml polyethylenimine (PEI) solution (pH 7), while mouse fibroblasts were transfected according to manufactures instructions using FuGENE (Promega). The above transfection reagents facilitate cell entry of negative charged DNA through endocytosis. The DNA usually does not integrate into the genome and will be degraded or diluted through mitosis.

3.2.3 Generation of stable cell lines using retroviral vectors

Subconfulent 293T cells were plated in a 6-well plate and transfected with 1 μg of proviral plasmid (pLHCX or pCMS28) containing the protein of interest in combination with 200 ng of VSV-G and 1 μg of MLV gag-pol. 24 hours post-transfection, the medium was replaced and cells were incubated for another 24 hours. The supernatant containing virus like particles (VLPs) were filtered (0.45 μm) (Millipore) and used to transduce target 293T, HT1080 or murine fibroblasts cells. Spinoculation was used to enhance delivery of VLPs into target cells. Tissue culture plates were centrifuged for 3 hours at 1500 rpm at room temperature and placed back into tissue culture incubator. 48 hours post-transduction cells were split into 10 cm dishes, placed under antibiotic selection (usually at 100 μg/ml for Hygromycin B and 1 μg/ml for Puromycin) and incubated at 37°C and 5% CO_2 to allow selection of stably expressing cells.

3.2.4 Gene silencing by siRNA

293T tetherin cells were seeded at a density of $2x10^5$ cells per well in a 12-well plate. After 6 hours the first transfection was performed. For each well 2 μl of Dharmafect (Thermo Scientific) was added to 98 μl of Opti-MEM (Life Technologies), this solution was added to 5 μl of 20 μM siRNA in 95 μl of Opti-MEM according to manufacturers instructions. For HRS knockdown a siRNA oligonucleotide against HGS targeting the CCGGAACGAGCCCAAGTACAA sequence (QIAGEN) was used alongside a non-targeting siRNA as control (Dharmafect). For a complete list of oligonucleotides see Table 9. The cells were subsequently re-seeded into a 24-well plate on day 2 and a second transfection was performed according to manufacturers instructions. The cells were then infected 3 hours post transfection with VSV-G-pseudotyped NL4.3 HIV-1 wt, HIV-1 delVpu at an MOI of 0.8 and harvested 48 hours later. Infectivity of viral supernatants was determined by infecting HeLa-TZMbl reporter cells as described in 3.4.5. Cell lysates and viral particles were subjected to SDS-PAGE as described in 3.4.4, and Western blot assays were performed using rabbit anti-HSP90 antibody (Santa Cruz Biotechnologies), monoclonal mouse anti-HIV-1 p24CA antibody (kindly provided by B Chesebro through the NIH AIDS Reagent Program), rabbit polyclonal anti-HRS (HGS) antibody (Millipore), a polyclonal rabbit anti-UBAP1 antibody (Proteintech) and a monoclonal mouse anti-TSG101 antibody (Abcam).

Alternatively for clathrin adaptor and VPS27 knockdown, 293T tetherin or HeLa cells were seeded at a density of $2x10^5$ cells per well in a 12-well plate. After 3 hours the first transfection was performed. For each well 3 μl of Oligofectamine (Invitrogen) was added to 10 μl of Opti-MEM (Life Technologies), this solution was then added to 5 μl of 20 mM siRNA in 85 μl of Opti-MEM according to manufacturer's instructions. For AP-1 knockdown HeLa cells stably expressing doxycycline-inducible pTRIPZ shRNA directed against AP-1 γ1 (OpenBiosystems) were used in combination with siRNA oligonucleotides directed against AP-1 γ1. For AP-3 knockdown, SMARTpool siRNA targeting the AP-3 μ1 subunit was used in combination with SMARTpool siRNA targeting the AP-3 δ1 subunit (Dharmacon). Oligonucleotides used for AP-2 and VPS27 silencing are displayed in Table 9. After 24 hours the cells were re-seeded into a 24-well and a second transfection was performed according to manufacturers instructions. The cells were then infected 3 hours post the second transfection with VSV-G-pseudotyped HIV-1 wt or HIV-1 delVpu at a MOI of 0.8. In the case of AP-2 knockdown the second transfection of oligonucleotides was performed in combination with indicated NL4.3 proviral plasmid using Lipofectamine 2000 (Invitrogen). The infectivity of viral supernatants was determined by infecting HeLa-TZMbl cells as described in 3.4.5. Cell lysates and viral particles were subjected to SDS-PAGE as described in 3.4.4, and Western blotted for appropriate proteins.

Table 9 Sequences of siRNA oligonucleotides

Protein	Type	Source	Target sequence
UBAP1 (Q3)	siRNA	QIAGEN	CTCGACTATCTCTTTGCACAT
UBAP1 (Q4)	siRNA	QIAGEN	CAGCTAAAGTTGGTCTACCTA
TSG101	siRNA	Dharmacon	CCUCCAGUCUUCUCUCGUC
ALIX	siRNA	Dharmacon	GAAGGAUGCUUUCGAUAAAUU
HRS	siRNA	QIAGEN	CCGGAACGAGCCCAAGTACAA
AP-1 γ1	siRNA	QIAGEN	AAGAAGATAGAATTCACCTTT
AP-1 γ1	doxycycline-inducible shRNA in pTRIPZ	OpenBiosystems	No sequence information available. Oligo ID: V2THS_201653
AP-2 μ1	siRNA SMARTpool	Dharmacon	GAACCGAAGCUGAACUACA AGUUUGAGCUUAUGAGGUA GCGAGAGGGUAUCAAGUAU GUUAAGCGGUCCAACAUUU
AP-3 μ1	siRNA SMARTpool	QIAGEN	AAGGATAGCCCTTACACTCAT
AP-3 δ1	siRNA SMARTpool	Dharmacon	CUACAGGGCUCUGGAAUAUU GGACGAGGCAAAAUACAUA GAAGGACGUUCCCAUGGUA CAAAGUCGAUGGCAUUCGG
VPS27	siRNA	QIAGEN	AACCACCTATCCTGATGTTAA
Non-targeting control	siRNA SMARTpool	Dharmacon	No sequence information available. Order number: D-001810-10-20

3.2.5 Isolation of CD4+ T lymphocytes from Peripheral Blood Mononuclear Cells (PBMCs)

Fresh venous blood was drawn from healthy volunteers by a phlebotomist. Total peripheral blood mononuclear cells were isolated using a density gradient centrifugation method. First, blood was collected in heparin-coated tubes (BD Bioscience) and diluted by addition of an equal volume of 1x PBS. 30 ml of diluted blood was carefully layered over 15 ml of Lymphoprep (Axis-Shield) in a 50 ml Falcon tube and centrifuged for 30 minutes at 1000 x g (without brake) at room temperature. After centrifugation the PBMCs form a separate band (buffy coat) at the blood/Lymphoprep interface and cells were collected using a Pasteur pipette. This fraction was diluted in 40 ml of 1x PBS and cells were pelleted by centrifugation for 10 minutes at 300 x g. This step was repeated three times or until supernatant became clear.

CD4+ T lymphocytes were purified from PBMCs by negative isolation using the Dynabeads Untouched human CD4 T cells kit (Invitrogen). Isolation was performed according to manufacturers instructions. Briefly, PBMCs were depleted from CD8+ T cells, B cells, NK cells, monocytes, platelets, dendritic cells, granulocytes and erythrocytes by a mixture of mouse IgG antibodies directed against the non-CD4+ T cells and capture of antibody-labelled cells by magnetic Dynabeads. Only negatively selected and untouched CD4+ T cells are left in the samples that have not been in contact with the Dynabeads. Once selected a small portion of CD4+ T cells was kept to check purity by FACS using an anti-CD4 antibody coupled to an APC fluorochrome (BD Pharmingen).

Purified CD4+ T cells were then activated for 48 hours using Dynabeads Human T-Activator CD3/CD28 (Invitrogen) according to manufacturers instructions. Dynabeads mimic physiological T cell activation by antigen-presenting cells, providing both TCR and co-stimulating signals. After removal of the beads, cells were maintained in rhIL-2 (30 U/ml) (Roche) before infection with VSV-G-pseudotyped HIV-1.

3.3 WORKING WITH PROTEINS

3.3.1 SDS-PAGE and Western blotting

The resolving gel was made up as described in Table 10 and the solution was pipetted quickly into a glass plate sandwich situated in a casting frame. The resolving gel was covered with isopropanol (Fischer) and allowed to set. Next, the gel was rinsed with ddH_2O to remove excess isopropanol. The stacking gel was made up as described in Table 10 and the solution was pipetted on top of the resolving gel, a plastic comb (15 wells/ 0.75 mm) was inserted and the solution was allowed to polymerize. The gel cassette was then placed into Mini- PROTEAN Tetra Cell electrophoresis system (Bio-Rad) and filled up with running buffer containing 0.1% SDS, 25 mM Tris-Base and 200 mM glycine pH 8.8. Samples were resuspended in 2x LB (20% glycerol, 4% SDS, 100 mM Tris-HCl pH 6.8, 200 mM β-mercaptoethanol, 0.2% bromophenol blue) and boiled at 100°C for 10 minutes to denature proteins. 10 µl of each protein sample was loaded per well alongside 5 µl of molecular size marker (Prestained Protein Marker, broad range (7-175 kDa), New England Biolabs). The gel was subsequently run at 80V for about 10-15 minutes until samples started to migrate through the separating gel, and switched to 100V until the end of the run.

Separated proteins were then transferred onto a 0.45 µm nitrocellulose membrane (Hybond ECL nitrocellulose membrane, GE-Amersham Biosciences) using a Criterion Blotter with Plate Electrodes (Bio-Rad). Transfer was conducted in transfer buffer containing 20% ethanol, 25 mM Tris-Base and 200 mM glycine pH 8.8 and run at 100V for 1 hour or at 18V for 16 hours. The membrane was then incubated in blocking solution (5% milk (Marvel) in 1x PBS/ 0.1% Tween 20) on a shaker for 30 minutes at room temperature or at 4°C overnight. Next, the membrane was probed with primary antibody (see Table 11) diluted in blocking solution for 1 hour at room temperature or at 4°C overnight. The primary antibody solution was subsequently removed and the membrane was washed 3 times for 10 minutes with 1x PBS/ 0.1% Tween 20. The membrane was then incubated with the secondary antibody (see Table 12) diluted in blocking solution for 1 hour at room temperature and washed 3 times for 10 minutes with 1x PBS/ 0.1% Tween 20. Membranes incubated with secondary antibodies conjugated to IRDye 800-700 were rinsed in 1x PBS and scanned using the LI-COR Odyssey infrared imaging system (LI-COR Biosciences). In contrast membranes incubated with horseradish peroxidase (HRP) conjugated secondary antibodies for detection by enhanced chemiluminescence (ECL) were incubated with SuperSignal West Pico Chemiluminescent solutions (Thermo Scientific) in a 1:1 ratio for 2 minutes and visualised using the ImageQuant LAS 400 mini system (GE Healthcare).

Table 10 SDS-Page set-up

Separating gel	10%	12%	Stacking gel	
dH_2O	5 ml	4.5 ml	**dH_2O**	3.25 ml
1.5 M Tris pH 8.8	2.5 ml	2.5 ml	**0.5 M Tris pH 6.8**	1.25 ml
Acrylamide (40%)	2.5 ml	3 ml	**Acrylamide (40%)**	465 µl
APS (10%)	50 µl	50 µl	**APS (10%)**	25 µl
TEMED	10 µl	10 µl	**TEMED**	5 µl
SDS (10%)	100 µl	100 µl	**SDS (10%)**	50 µl

Table 11 Primary antibodies used for Western blotting

Antibody	Species	Antigen	Source	Dilution
α-HSP90	Rabbit	Human HSP90	Santa Cruz Biotechnology	1:5000
α-Vpu	Rabbit	NL4.3 Vpu (amino acids 33-81)	NIH AIDS Reagent Program	1:5000
α- HIV-1 p24-CA	Mouse	183-H12-5C (Hybridoma supernatant)	NIH AIDS Reagent Program	1:75
α-HA	Mouse	CYP**YDVPDYA**SL HA.11 clone 16B12	Covance	1:5000
α-HA	Rabbit	HA epitope tag	Rockland	1:5000
α-myc	Mouse	Clone 9E10	Covance	1:1000
α-BST-2 (tetherin)	Rabbit	Human BST-2	NIH AIDS Reagent Program	1:1000
α-HRS (HGS)	Rabbit	Epitope against SNX1 region	Millipore	1:1000
α-UBAP1	Rabbit	Human UBAP1	Proteintech	1:1000
α-TSG101	Mouse	TSG101 residues 167-374 Clone 4A10	Abcam	1:1000
α-ALIX	Rabbit	Human ALIX	W. Sundquist	1:1000
α-AP-1 γ1	Mouse	Derived from 100/3 hybridoma, AP-1 adaptor from bovine brain was used as immunogen	Sigma	1:1000
α-AP50 (AP-2 µ1)	Mouse	Mouse AP50 residues 110-230	BD Bioscience	1:250
α-AP-3 δ1	Mouse	Human adaptin δ residues 627-731	BD Bioscience	1:750
α-AP-3 µ1	Rabbit	Di vs47p affi	M.S. Robinson	1:750
α-VPS27	Rabbit	Synthetic peptide derived from within residues 300 to the C-terminus of human VPS27	Abcam	1:500

Table 12 Secondary antibodies used for Western blotting

Antibody	Conjugation	Source	Dilution
Goat α-mouse	HRP	Cell Signalling	1:5000
Goat α-rabbit	HRP	Cell Signalling	1:5000
Goat α-mouse	IRDye 680	LI-COR Bioscience	1:5000
Goat α-rabbit	IRDye 800	LI-COR Bioscience	1:5000

3.3.2 Immunoprecipitation (for HRS/Vpu)

Immunoprecipitation was performed as previously described (Kueck and Neil, 2012). In short 293T or 293T tetherin cells were plated into a 6-well plate and transfected with 600 ng of pCR3.1 myc-HRS or indicated mutants/ truncations in combination with pCR3.1 Vpu-HA or indicated mutant or GFP expression plasmids. 48 hours post transfection cells were lysed on ice for 30 minutes in buffer containing 50 mM Tris pH 7.4, 150 mM NaCl, 200 μM sodium orthovanadate, 5 mM NEM, complete protease inhibitors (Roche) and 1% digitonin. After removal of the nuclei by centrifugation supernatants were immunoprecipitated with 5 μg/ml monoclonal mouse anti-myc antibody (Covance) and protein G agarose beads (Invitrogen) for 3 hours and washed four times in lysis buffer containing 0.01% digitonin. Cell lysates and immunoprecipitates were subjected to SDS-PAGE and Western blotted using a polyclonal rabbit anti-HA antibody (Rockland) and rabbit polyclonal anti-HRS (HGS) antibody (Millipore). Proteins were subsequently visualised by ImageQuant (GE) using corresponding HRP-linked secondary antibodies (Cell Signalling).

3.3.3 Immunoprecipitation (for tetherin/Vpu)

Immunoprecipitation was performed as indicated above. In these experiments 293T tetherin cells were transfected twice over 48 hours with siRNA oligonucleotides directed against UBAP1 targeting CTCGACTATCTCTTTGCACAT or non-targeting siRNA as control (Dharmacon). The cells were then infected with VSV-G-pseudotyped NL4.3 HIV-1 wt, HIV-1 delVpu, HIV-1 Vpu LILI or HIV-1 Vpu A14L W22A at an MOI of 2 or transfected with 600 ng of pCR3.1 Vpu or indicated mutant or pCR3.1 GFP expression plasmids. 48 hours post infection cells were lysed on ice for 30 minutes in buffer containing 50 mM Tris pH 7.4, 150 mM NaCl, complete protease inhibitors (Roche) and 1% digitonin (Calbiochem). After removal of the nuclei by centrifugation supernatants were immunoprecipitated with 5 μg/ml mouse monoclonal anti-BST2 antibody (eBiosciences) and protein G agarose beads (Invitrogen) for 3 hours before washing four times in lysis buffer containing 0.01% digitonin. Western blot assays of cell lysates and immunoprecipitates were performed using a rabbit anti-Vpu antibody (kindly provided by K. Strebel through the NIH AIDS Reagent Program), polyclonal rabbit anti-tetherin antibody (kindly provided by K. Strebel through the NIH AIDS Reagent Program), polyclonal rabbit anti-UBAP1 antibody (Proteintech) and visualised by ImageQuant using corresponding HRP-linked secondary antibodies (Cell Signalling).

3.3.4 Cross-linking immunoprecipitations

293T cells were co-transfected with 600 ng of pCR3.1 myc-β-TrCP2 and with either pCR3.1Vpu-HA, pCR3.1 Vpu LILI-HA, pCR3.1 Vpu 2/6A-HA or GFP expression plasmids. 48 hours post transfection cross-linking immunoprecipitation was performed as previously described (Niranjanakumari et al., 2002). In short cells were trypsinised, washed in 1x PBS and cross-linking was performed with 0.05% HCHO. Subsequently cells were lysed in buffer containing 150 mM NaCl, 10 mM Hepes pH 7, 6 mM MgCl2, 2 mM DTT, 10% glycerol, 0.5% NP40, 200 µM sodium orthvanadate and complete protease inhibitors (Roche). Cleared lysates were immunoprecipitated with with 5 µg/ml of mouse anti-myc monoclonal antibody (Covance) and protein G agarose beads (Invitrogen). Cross-linking was reversed with 10 mM EDTA, 5 mM DTT and 1% SDS and cell lysates and immunoprecipitates were subjected to SDS-PAGE, and Western blotted using a polyclonal rabbit anti-HA antibody (Rockland) and mouse monoclonal anti-myc antibody (Covance). Visualisation of proteins was conducted by ImageQuant (GE) using corresponding HRP-linked secondary antibodies (Cell Signalling).

3.3.5 BioID assay using BirA R118G (Roux et al., 2012)

293T or 293T tetherin cells were plated into a 10cm dish and transfected with 5 ug of empty BirA vector, Vpu-myc-BirA or indicated mutant using polyethylenimine (PEI). 8 hours post transfection medium was changed and cells were treated overnight with 100 nM of Concanamycin A (Invitrogen) to prevent tetherin degradation, and 150 µM free biotin (life technologies) to induce biotinylation of surrounding proteins. Cells were then trypsinised, washed in 1x PBS and lysed in 1 ml of 50 mM Tris pH 7.4, 500 mM NaCl, 0.4% SDS, 5 mM EDTA, 1 mM DTT and complete protease inhibitor (Roche). Next samples were sonicated for 20 seconds prior to the addition of Triton X-100 to 2% final concentration and an equal volume of 50 mM Tris pH 7.4. Lysates were cleared by centrifugation (5 minutes at maximum speed) and supernatants were incubated with 200 µl avidin agarose (Pierce) for 3 hours. Avidin agarose beads were collected and washed twice with lysis buffer over chromatography columns (Bio-Rad) and were resuspended in 100 µl of 2x LB supplemented with biotin. Cell lysates and precipitates were subjected to SDS-PAGE, and Western blotted using HRP-conjugated streptavidin (Invitrogen), mouse monoclonal anti-myc antibody (Covance), mouse monoclonal anti-AP-1 γ1 antibody (Sigma). Proteins were subsequently visualised by ImageQuant (GE) using corresponding HRP-linked secondary antibodies (Cell Signalling).

3.3.6 Immunofluorescence microscopy

Cells were grown on coverslips and either infected with VSV-G-pseudotyped NL4.3 HIV-1 wt, indicated mutants or transfected with indicated protein expression vectors. 48 hours or 16 hours later cells were fixed in 4% paraformaldehyde, washed with 10 mM glycine and permeabilised in 1% bovine serum albumin/ 0.1% Tritin-X100 for 15 minutes. Cells were then stained with primary antibodies diluted in 1% bovine serum albumin/ 0.01% Tritin-X 100 for 1 hour. Next, cells were stained for example using anti-rabbit polyclonal Vpu (kindly provided by K. Strebel through the NIH AIDS Reagent Program) in combination with sheep anti-human TGN46 (AbD Serotec), mouse anti-EEA1 (BD Biosciences), mouse anti-CD63 (Developmental Studies Hybridoma Bank, University of Iowa) or mouse polyclonal anti-BST-2 (Abnova) followed by appropriate secondary antibodies conjugated to Alexa 488 or 594 fluorophores (Molecular Probes, Invitrogen); for a list of primary and secondary antibodies see Table 13 and Table 14. The cells were then washed and mounted on glass slides using ProLong AntiFade-49,6-diamidino-2-phenylindole (DAPI) mounting solution (Molecular Probes, Invitrogen). Cells were visualised with a Leica DM-IRE2 confocal microscope (63x oil immersion lens) and images were analysed using the Leica Confocal Software and ImageJ. Alternatively, Z stacks were taken with a Nikon ESCLIPSE Ti inverted microscope (100x oil immersion lens), images were deconvoluted using AutoQuant X3 and analysed using the ImageJ software.

Table 13 Primary antibodies used in immunofluorescence microscopy

Antibody	Species	Antigen	Source	Dilution
α-Vpu	Rabbit	NL4.3 Vpu (amino acids 33-81)	NIH AIDS Reagent Program	1:5000
α-HA	Mouse	CYP**YDVPDYA**SL HA.11 clone 16B12	Covance	1:1000
α-HA	Rabbit	HA epitope tag	Rockland	1:1000
α-BST-2 (tetherin)	Mouse	Human BST-2 residues 40-181	Abnova	1:200
α-CD8	Mouse	Human thymocytes/Sezary T cells	Ancell	1:200
α-TGN46	Sheep	Human TGN46	AbD Serotec	1:100
α-EEA1	Mouse	Human EEA1 residues 3-281	BD Biosciences	1:200
α-CD63	Mouse	Human CD63 (Hybridoma supernatant)	Developmental Studies Hybridoma Bank, University of Iowa	1:10

Table 14 Secondary antibodies used for immunofluorescence microscopy

Antibody	Conjugation	Source	Dilution
Donkey α-mouse	Alexa Fluor 488	Molecular Probes (Invitrogen)	1:500
	Alexa Fluor 594	Molecular Probes (Invitrogen)	1:500
	Alexa Fluor 630	Molecular Probes (Invitrogen)	1:500
Goat α-mouse	Alexa Fluor 488	Molecular Probes (Invitrogen)	1:500
	Alexa Fluor 594	Molecular Probes (Invitrogen)	1:500
	Alexa Fluor 630	Molecular Probes (Invitrogen)	1:500
Donkey α-Rabbit	Alexa Fluor 488	Molecular Probes (Invitrogen)	1:500
	Alexa Fluor 594	Molecular Probes (Invitrogen)	1:500
	Alexa Fluor 630	Molecular Probes (Invitrogen)	1:500
Donkey α-Sheep	Alexa Fluor 594	Molecular Probes (Invitrogen)	1:500

3.3.7 Detection of tetherin surface levels: Flow cytometry (FACS)

HeLa or HeLa-TZMbl cells were transfected with 400 ng of pCR3.1 GFP and 400 ng of pCR3.1 Vpu-HA or indicated mutants. 48 hours post transfection the cells were harvested and stained for surface tetherin using a monoclonal anti-BST2 IgG2a antibody (Abnova) and a goat-anti-mouse IgG2a-Alexa633 conjugated secondary antibody (Molecular Probes, Invitrogen, UK). The cells were detached for the tissue culture plate using 5 mM EDTA and washed in FACS buffer containing 1% BSA and 0.1% sodium azide in 1x PBS. Cells were subsequently stained with primary antibody in FACS buffer for 1 hour on ice. Cells were then washed three times and incubated with the secondary antibody in FACS buffer on ice for 1 hour. Cells were washed twice in FACS buffer and once in 1x PBS. Tetherin expression on GFP positive cells was then analysed using a BD FACSCanto II flow-cytometer (Becton Dickinson) or FACSCalibur flow-cytometer (Becton Dickinson) and FlowJo software.

3.3.8 Tetherin downregulation in AP-1 and AP-3 knockout fibroblasts

Murine fibroblasts (knockout for: AP-1 μ1A -/- or AP-3 δ-/-) stably expressing human tetherin-HA were transduced with the pMigR1 based retroviral vector pCMS28-IRES-eGFP or a derivative expressing the NL4.3 Vpu protein. 48 hours post transduction the cells were stained as described in 3.3.7 and analysed for surface HA versus GFP expression levels using FACSCalibur flow-cytometer (Becton Dickinson) and FlowJo software.

3.4 WORKING WITH VIRUSES

3.4.1 Preparation of VSV-G-pseudotyped HIV-1 virus stocks

For the production of full-length HIV-1 NL4.3 wt, NL4.3 delVpu, NL4.3 Vpu LILI, NL4.3 Vpu ELV, NL4.3 LILI ELV, NL4.3 Vpu 2/6A and NL4.3 Vpu A14L W22A virus stocks pseudotyped with the Vesicular Stomatitis Virus Glycoprotein (VSV-G) the following protocol was followed: $5x10^5$ 293T cells were plated in a 6-well plate and transfected with 2 μg of proviral plasmid in combination with 200 ng of VSV-G using 5 μg/ml polyethyleneimine (Polysciences). 24 hours post-transfection the medium was replaced and cells were incubated for another 24 hours before being harvested. The supernatant containing virions was filtered (0.45 μm) (Millipore), aliquoted and stored at -80°C. Viral endpoint titres were determined on HeLa-TZMbl cells as described previously (Le Tortorec and Neil, 2009) and in 3.4.2.

3.4.2 Determination of virus stock titres on HeLa-TZMbl cells

NL4.3 HIV-1 VSV-G-pseudotyped virus stocks prepared as in 3.4.1 were titrated on HeLa-TZMbl cells to determine virus titres. HeLa-TZMbl reporter cells were plated at a density of 10^4 per well in a 96-well plate and infected with 40 μl of serial dilutions (from 10^0 to 10^{-8}) of virus stocks. 48 hours post transfection, cells were fixed in 0.5% glutaraldehyde for 15 minutes, washed in 1x PBS and incubated overnight at 37°C with X-Gal substrate solution containing 1 mg/ml X-gal-dimethylformamide in 5 mM K ferrocyanide, 5 mM ferricyanide, 2 mM $MgCl_2$, 0.02% NP40, 0.01% Triton-X 100 in 1x PBS. Infected cells will tern blue as a result of the β-galactosidase activity induced by the HIV-1 Tat protein expression. End point titres (pfu/ml) were determined by counting blue colonies using a light microscope.

Multiplicity of infection (MOI): The infectious virus particle yield per cell can be calculated from the titres obtained above and is displayed in the multiplicity of infection (MOI). MOI of 1 means that the number of infectious virus particles resembles the number of target cells. This value varies among different viruses and virus-host cell combinations. The Poisson distribution is used to calculate the distribution of virus particles per cell.

Poisson distribution: $P(k)=e^{-m}m^k/k!$

Where $P(k)$ is the fraction of cells infected with k virus particles and m resembles the MOI (reviewed in (Flint et al., 2009)).

3.4.3 Virus release assay

For virus release assays using transient transfection subconfluent 293T cells were plated in a 24-well plate and transfected with 500 ng of NL4.3 proviral plasmid in combination with increasing concentrations of tetherin (0 ng, 25 ng, 50 ng and 100 ng), and 25 ng of Vpu-HA or mutants using 1 μg/ml polyethyleneimine (Polysciences) per well. Alternatively, 293T tetherin cells were plated in a 24-well plate and transfected with 500 ng of NL4.3 proviral plasmid, in combination with increasing concentrations or 25 ng of Vpu-HA or indicated mutant using 1 μg/ml polyethyleneimine (Polysciences) per well. The medium was replaced 8 hours post transfection, cells and supernatants containing virions were harvested after 48 hours and analysed for physical virus particle release (as in 3.4.4) and infectious virus particle release using HeLa-TZMbl reporter cells (as in 3.4.5).

3.4.4 Biochemical analysis of physical virus particle release

The viral supernatant containing virus particles was harvested from each well using a syringe-driven filter unit (0.22 μm) (Millipore) and was transferred into a fresh 24-well plate. The syringe-driven filter unit removes cells and cell debris that the supernatant might contain. To harvest the virions 500 μl of the filtered supernatant was added slowly onto 500 μl of cold 1x PBS/20% sucrose in a microcentrifuge tube and centrifuged for 1.5 hours at 14,000 rpm and 4°C. The supernatant was carefully aspirated and the invisible pellet was resuspended in 30 μl of 2x LB followed by denaturation for 10 minutes at 100°C. Virions and corresponding cell lysates were then subjected to SDS-PAGE and Western blotted for rabbit anti-HSP90 (Santa Cruz Biotechnologies), monoclonal mouse anti-HIV-1 p24CA (kindly provided by B Chesebro through the NIH AIDS Reagent Program), monoclonal mouse anti-HA (Covance), polyclonal rabbit anti-HA (Rockland) and/ or polyclonal rabbit anti-Vpu antibody (kindly provided by K. Strebel through the NIH AIDS Reagent Program). Proteins were subsequently visualised by LiCor apparatus using fluorophores conjugated secondary antibodies (IRDye 800 Goat anti-rabbit, IRDye 680 Goat anti-mouse).

3.4.5 Determination of infectious virus particle release

The release of infectious virus particles from viral supernatants was determined by infecting HeLa-TZMbl, a HIV-1 β-galactosidase reporter cell line. HeLa-TZMbl reporter cells were plated at a density of 10^4 per well in a 96-well plate and infected with 20 μl of viral supernatant obtained from 3.4.3. 48 hours post transfection cells were lysed in 50 μl of Tropix Galacto-Star Lysis solution (Applied Biosystems) for 30 minutes at room temperature. 10 μl of cell lysates were transferred into a white luminescence 96-well plate and incubated with 45 μl of a 1:50 dilution of Tropix Galacto-Star Substrate in Reaction Buffer Diluent (Applied Biosystems) for 15 minutes before measuring the β-galactosidase induced light signal using a luminescence counter (Victor Light 1420-Perkin Elmer) and Wallac 1420 software.

3.4.6 Tetherin degradation assay

$1.5x10^5$ 293T tetherin cells (per well in a 24-well plate) were plated, infected with VSV-G-pseudotyped NL4.3 HIV-1 wt, HIV-1 delVpu, HIV-1 Vpu LILI, HIV-1 Vpu ELV or HIV-1 Vpu 2/6A at a MOI of 2 to ensure that approximately 90% of the cells were infected. The medium was replaced 4 hours after infection and 48 hours post infection cell were harvested in 250 μL 2x LB. Lysates were subsequently subjected to SDS-PAGE and Western blotted using rabbit anti-HSP90 (Santa Cruz Biotechnologies) and polyclonal rabbit anti-tetherin antibody (kindly provided by K. Strebel through the NIH AIDS Reagent Program), and visualised by LiCor apparatus using fluorophores conjugated secondary antibodies (IRDye 800 Goat anti-rabbit, IRDye 680 Goat anti-mouse).

Alternatively, HT1080 cells stably expressing tetherin-HA were infected with VSV-G-pseudotyped NL4.3 HIV-1 wt, HIV-1 delVpu or HIV-1 Vpu ELV virus stocks at a MOI of 2. The medium was replaced 4 hours after infection, and 48 hours post infection, cell lysates were harvested and processed as above, using a mouse anti-HA antibody (Covance) to detect tetherin levels.

3.4.7 One round virus release assay

293T tetherin, Jurkat or CD4+ T cells were infected with VSV-G-pseudotyped NL4.3 HIV-1 wt, HIV-1 delVpu or HIV-1 Vpu ELV at an MOI of 0.5-1. 16 hours post infection medium was replaced and cells (treated or not with 5000 U/ml of universal type-1 interferon (PBL InterferonSource)) were cultured for a further 24 hours. The cells were harvested and infectivity of viral supernatants was determined by infecting HeLa-TZMbl (as described in 3.4.5) and biochemical analysis of physical virus particle release was performed as in 3.4.4.

3.4.8 Intracellular p24 staining plus tetherin levels

Jurkat or CD4+ T cells were infected with VSV-G-pseudotyped NL4.3 HIV-1 wt, HIV-1 delVpu or HIV-1 Vpu ELV at an MOI of 1. 48 hours post infection, cells were stained for surface tetherin expression as in 3.3.7, then fixed and permeabilized for 20 minutes in Fixation/Permeabilization solution (Cytofix/cytoperm Fixation/Permeabilization kit, BD Biosciences) and stained for intracellular HIV-1 p24CA using the KC57 antibody conjugated to PE (Beckman-Coulter) in BD Perm/Wash buffer (Cytofix/cytoperm Fixation/Permeabilization kit, BD Biosciences). The cells were then washed and analysed by or FACSCalibur flow-cytometer (Becton Dickinson) and FlowJo software.

Chapter 4 A cytoplasmic tail determinant in Vpu mediates targeting of tetherin for degradation and counteracts restriction

Most of the results presented in this chapter were published as “A Cytoplasmic Tail Determinant in HIV-1 Vpu Mediates Targeting of Tetherin for Endosomal Degradation and Counteracts Interferon-Induced Restriction” (Kueck and Neil, 2012).

4.1 INTRODUCTION

Downregulation of cell surface immunomodulatory proteins is a common theme in the evasion of innate and adaptive immune responses by mammalian viruses. One host molecule targeted by diverse enveloped viruses is tetherin, an interferon-induced dimeric type II membrane protein, which inhibits the release of nascent virions from the cell surface (Neil et al., 2008) (Van Damme et al., 2008). The HIV-1 accessory protein Vpu antagonises tetherin anti-viral function. Vpu is a small integral membrane phospho-protein, which directly associates with tetherin through interactions between the transmembrane domains of both proteins (Iwabu et al., 2009) (Kobayashi et al., 2011) (Dubé et al., 2010b) (Vigan and Neil, 2010).

Recent evidence demonstrates that tetherin degradation is dependent on the ESCRT pathway (Janvier et al., 2011), however, tetherin degradation is not strictly required for Vpu activity (Goffinet et al., 2010) (Miyagi et al., 2009). Recruitment of the ESCRT-0 subunit HRS by Vpu is essential to counteract tetherin activity (Janvier et al., 2011). Coupled with recent evidence that dysregulation of the entire late endosomal compartment by mutants of Rab7a (Caillet et al., 2011), this suggests an emerging picture in which Vpu alters tetherin trafficking to counteract its antiviral activity prior to lysosomal delivery. While HIV-2 and SIV tetherin antagonists Env and Nef promote tetherin internalisation through their interactions with AP-2, (Noble et al., 2006) (Le Tortorec and Neil, 2009) (Zhang et al., 2011b), Vpu does not enhance the rate of tetherin endocytosis (Dubé et al., 2010b) (Mitchell et al., 2009). Rather it is thought that Vpu/tetherin interactions preclude both the recycling of tetherin back to the cell surface and the transit of newly synthesized tetherin to the PM by trapping it in intracellular compartments, notably the TGN (Dubé et al., 2010b). Consistent with this, the ability of Vpu to localise to the TGN correlates with tetherin antagonism (Dube et al., 2009), and disruption of the recycling compartment by a dominant Rab11a mutant compromises Vpu activity (Varthakavi et al., 2006). Truncations of the Vpu cytoplasmic tail, particularly the second alpha helix, lead to aberrant localisation and a reduction in its

anti-tetherin activity, suggesting it harbours a domain required for Vpu function (Dube et al., 2009). Amino acid sequence analysis of the cytoplasmic domain of HIV-1 Vpu revealed the presence of a putative trafficking signal in the second alpha helix that harbours a degree of amino acid variation among Vpu alleles from different subtypes (Dubé et al., 2010a). This signal resembles a variant of an acidic dileucine sorting signal (**D**/**E**)xxx**L**(**L**/**I**) found in the cytoplasmic tails of membrane proteins that traffic through endosomal compartments. Acidic dileucine trafficking motifs have been shown to bind to canonical clathrin adaptor proteins AP-1, AP-2 and AP-3. Clathrin adaptors are responsible for trafficking of transmembrane cargo proteins from the plasma membrane to early/recycling endosomes, transport between TGN/endosome and trafficking from early/recycling endosomes to late endosomal compartments (see 1.8). Interestingly, subtype C Vpu has been shown to bear a functional overlapping putative tyrosine and dileucine-based sorting **EY**xx**L**(**L**/**I**) motif in the membrane proximal region of its cytoplasmic tail. It has been shown model subtype C Vpu localises to the PM rather than the TGN and that this is in part due to this motif (Ruiz et al., 2008). Therefore, we investigated the role of clathrin adaptor proteins AP-1, AP-2 and AP-3 in Vpu subcellular trafficking that is required for tetherin counteraction, especially in context of the **E**xxx**LV** sorting motif in Vpu cytoplasmic tail.

In this chapter we have examined the role of the second alpha helix of HIV-1 Vpu in tetherin antagonism. We identify a putative sorting signal, **E**xxx**LV**, which is required for post-binding trafficking of Vpu/tetherin complexes and inhibition of antiviral activity in primary CD4+ T cells. Moreover, because residual activity of the **E**xxx**LV** mutant requires an intact recycling signal in tetherin, we propose that the second alpha helix mutant is selectively defective for routing tetherin into an endosomal degradation pathway thereby inhibiting its transit to the PM and incorporation into nascent virions. Furthermore, we have examined the nature of the **E**xxx**LV** sorting singal in HIV-1 Vpu. While this motif can be functionally replaced by a clathrin adaptor binding peptide derived from HIV-1 Nef, however, Vpu activity does not require the canonical adaptors AP-1, AP-2 or AP-3 as determined by depletion and knockout studies.

4.2 RESULTS

4.2.1 Determinants of tetherin inactivation in the second alpha helix of the Vpu cytoplasmic tail

Truncations of the Vpu cytoplasmic tail lead to aberrant localisation and a reduction in its anti-tetherin activity (Dube et al., 2009). To further study the determinants within the second alpha helix of Vpu that account for TGN localisation, we performed overlapping triple-alanine mutagenesis through the second alpha helix of a codon optimized HIV-1 NL4.3 Vpu construct bearing a C-terminal HA tag (Figure 4-1A). We then assayed these Vpu mutants for their ability to rescue Vpu-defective HIV-1 from tetherin restriction. 293T cells were transfected with wild-type HIV-1 (HIV-1 wt) or Vpu-defective HIV-1 (HIV-1 delVpu) proviruses in combination with a fixed dose of a human tetherin expression vector, and 25 ng of Vpu-HA or indicated mutant. 48 hours after transfection, cell lysates and supernatants were harvested and analysed for physical viral yield by Western blot (Figure 4-1B) or supernatant infectivity of HeLa-TZMbl indicator cells (Figure 4-1C). As expected, in the absence of Vpu, both supernatant particle yield and infectivity of HIV-1 delVpu was profoundly reduced in the presence of tetherin, expression of Vpu *in trans* rescued virus production to wild-type levels. By contrast, mutations encompassing residues E59 or L63 and V64, but not the intervening or subsequent amino acids, displayed defective rescue of HIV-1 delVpu (Figure 4-1 B and C). All Vpu mutants with the exception of Vpu 67-69A-HA were expressed equivalently. Vpu 63-65A-HA appeared to display a dominant interfering activity on HIV-1 wt titre, but this was not reflected as apparently in particle yield.

These results suggested a functional requirement for residues E59 and L63/V64 in tetherin antagonism by Vpu. To confirm this we mutated these residues to alanine in the context of an HIV-1 NL4.3 provirus (NL4.3 Vpu ELV) and examined viral release from 293T cells in the presence of increasing expression levels of tetherin. Because this part of Vpu overlaps with start of the Env open reading frame in the provirus, these mutations were rendered silent in the +1 reading frame and displayed no defect in virus release in the absence of tetherin (Figure 4-1 D and E). In agreement with the virus rescue by Vpu expression *in trans*, NL4.3 Vpu ELV release was markedly defective in the presence of increasing tetherin doses, although it did display a residual antagonism of tetherin when compared to the Vpu-defective NL4.3 (Figure 4-1 D and E).

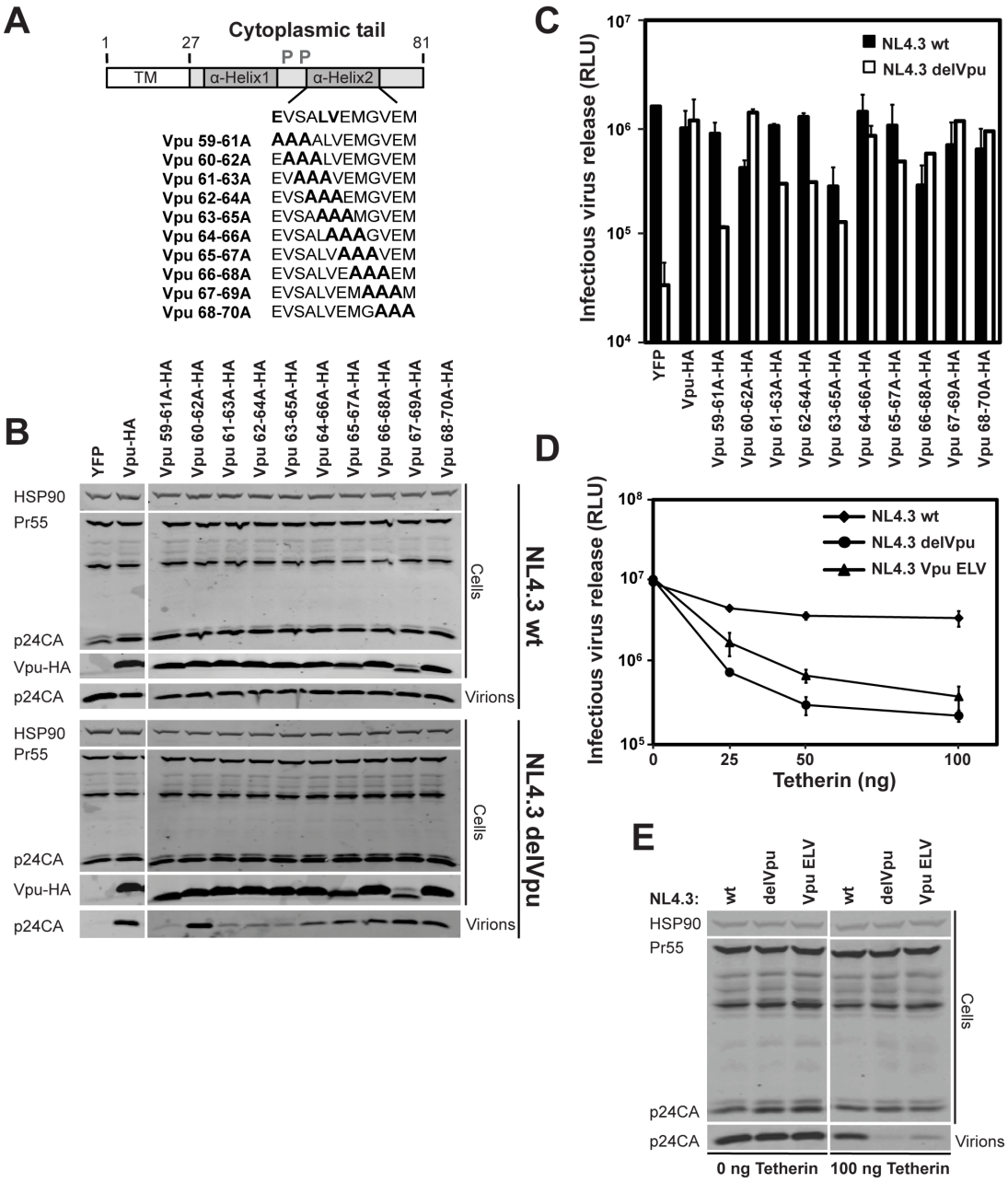

Figure 4-1 Residues E59, L63 and V64 in Vpu are required for efficient counteraction of tetherin

(A) Schematic representation of alanine scan mutagenesis in the second alpha helix of the codon-optimized HIV-1 NL4.3 Vpu protein. **(B)** 293T cells were transfected with NL4.3 wt or NL4.3 delVpu proviruses in combination with tetherin and the indicated pCR3.1 Vpu-HA expression vectors. 48 hours post transfection, cell lysates and pelleted supernatant virions were harvested and subjected to SDS-PAGE and analysed by Western blotting for HIV-1 p24CA, Vpu-HA and Hsp90 serving as loading control, and analysed by LiCor quantitative imager. **(C)** Viral supernatants from (B) were assayed for infectivity using HeLa-TZMbl reporter cells. Infectious virus release is plotted on a log scale as β-galactosidase activity in relative light units (RLU). Error bars represent standard deviations of the means of three independent experiments. **(D)** E59A, L63A and V64A mutations were inserted into the *vpu* gene of the NL4.3 provirus referred to as NL4.3 Vpu ELV. 293T cells were transfected with NL4.3 wt, NL4.3 delVpu or NL4.3 Vpu ELV proviral plasmids together with increasing doses of tetherin expression vector. The resulting infectivity was determined as in (C), error bars represent standard deviations of the means of three independent experiments. **(E)** Cell lysates and pelleted viral supernatants from 0 ng and 100 ng tetherin input from (D) were subjected to SDS-PAGE and analysed by Western blotting for HIV-1 p24CA and Hsp90, and analysed by LiCor quantitative imager.

We next examined the phenotypic basis for the defect in tetherin antagonism by Vpu ELV. Vpu stimulates the ubiquitin-dependent degradation of tetherin, most likely in lysosomal compartments (Douglas et al., 2009) (Mitchell et al., 2009). To this end, we infected HT1080 cells stably expressing human tetherin bearing an HA-tag in the extracellular domain (HT1080 tetherin-HA) with VSV-G-pseudotyped HIV-1 wt, HIV-1 delVpu or HIV-1 Vpu ELV at an MOI of 2 to ensure >90% cell infection. 48 hours later, cells were lysed and Western blotting performed for relative tetherin-HA levels (Figure 4-2A). As expected, cells infected with HIV-1 wt showed reduced steady state levels of tetherin that was not apparent in those infected with HIV-1 delVpu. Similarly, in cells infected with HIV-1 Vpu ELV there was no evidence of tetherin degradation, but interestingly there appeared to be enhanced levels of tetherin, perhaps suggesting stabilization of the protein in the presence of the mutant Vpu. Thus, E59, L63, V64 mutations abolish the ability of Vpu to induce tetherin degradation.

We then examined the ability of Vpu ELV mutants to downregulate surface tetherin levels. We first transfected HeLa cells (that express tetherin constitutively) with Vpu-HA or indicated mutant expression vectors in combination with a GFP reporter. 48 hours later, surface tetherin was assayed by flow cytometry in the GFP positive cells. As expected, wild-type Vpu expression reduced cell surface tetherin levels. Vpu mutants bearing E59A, L63A, V64A mutations, or the full ELV mutant all displayed a reduced capacity to downregulate surface tetherin levels (Figure 4-2 B and C). To confirm this in infected cells, we infected HeLa cells with HIV-1 wt, HIV-1 delVpu, HIV-1 Vpu ELV or HIV-1 Vpu 2/6A. 48 hours post infection, cells were stained for surface tetherin and co-stained for intracellular p24CA as a marker of infection (Figure 4-3A). Cells infected with HIV-1 wt showed a dramatic downregulation of tetherin on the surface of p24CA positive cells. While, tetherin was not downregulated from the surface of either HIV-1 delVpu, HIV- 1 Vpu 2/6A or HIV-1 Vpu ELV infected cells. We also performed the same experiment in a more relevant cell-type. To this end, we infected CD4-positive Jurkat T cells and analysed them for surface tetherin levels (Figure 4-3B). To discriminate between truly infected cells, and those that acquired p24+ debris by exposure of cells to high titre (MOI 1) of viral inoculum, we compared to cells exposed to virus in the presence of 50 mM AZT (Figure 4-3C). Cultures infected with HIV-1 wt showed clear downregulation of tetherin on the surface of p24CA positive cells. By contrast, tetherin was not downregulated from the surface of either HIV-1 delVpu, HIV- 1 Vpu 2/6A or HIV-1 Vpu ELV infected cells. Rather, tetherin levels were raised on some infected cells, perhaps reflecting accumulation of tethered virions on the cell surface. Although in HeLa cells, we could not detect enhanced tetherin surface levels on cells infected with Vpu mutants (Figure 4-3A), likely due to their endocytic removal from the surface.

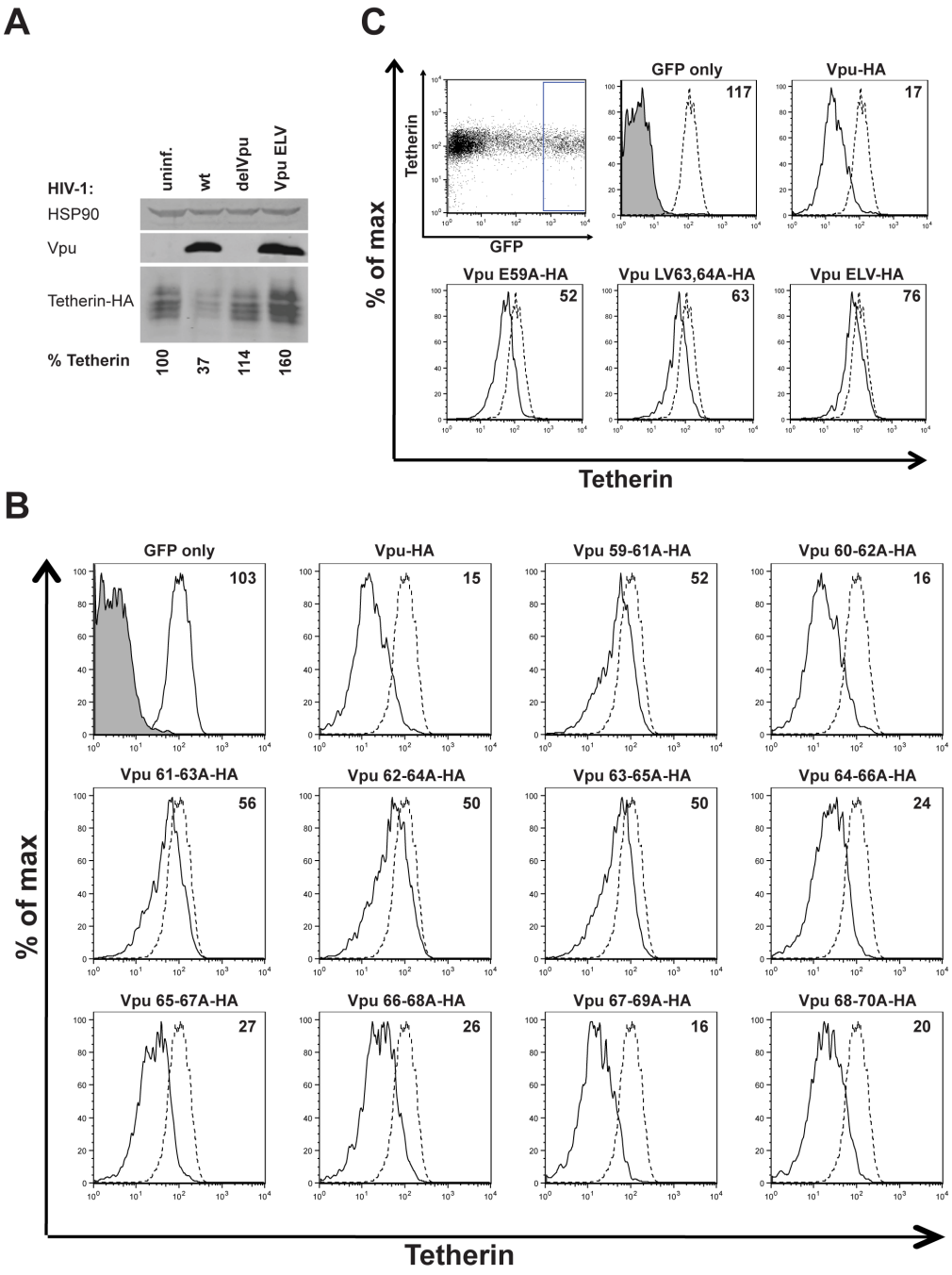

Figure 4-2 Vpu ELV mutants are defective for tetherin degradation and downregulation

(A) HT1080 cells stably expressing tetherin-HA were infected with VSV-G-pseudotyped HIV-1 wt, HIV-1 delVpu or HIV-1 Vpu ELV at an MOI of 2. 48 hours post infection, cells were harvested and subjected to SDS-PAGE and analysed by Western blotting for tetherin-HA, Vpu and Hsp90, and analysed by LiCor quantitative imager. Relative tetherin-HA levels are indicated below each lane. The blot shown is a representative example of 3 independent experiments. **(B)** HeLa cells were co-transfected with pCR3.1 Vpu-HA or indicated Vpu mutant in combination with a GFP expression construct. Cell surface staining for endogenous tetherin was analysed by flow cytometry 48 hours post transfection. GFP positive cells were gated and tetherin levels (solid lines) were compared to those of un-transfected HeLa cells (dotted lines). Numbers indicate median fluorescence intensities of surface tetherin on transfected cells. The solid peak in the upper left histogram represents the binding of the isotype control. **(C)** HeLa cells were treated and analysed as in (B) and transfected with Vpu E59A-HA, Vpu LV63,64AA-HA or Vpu ELV-HA.

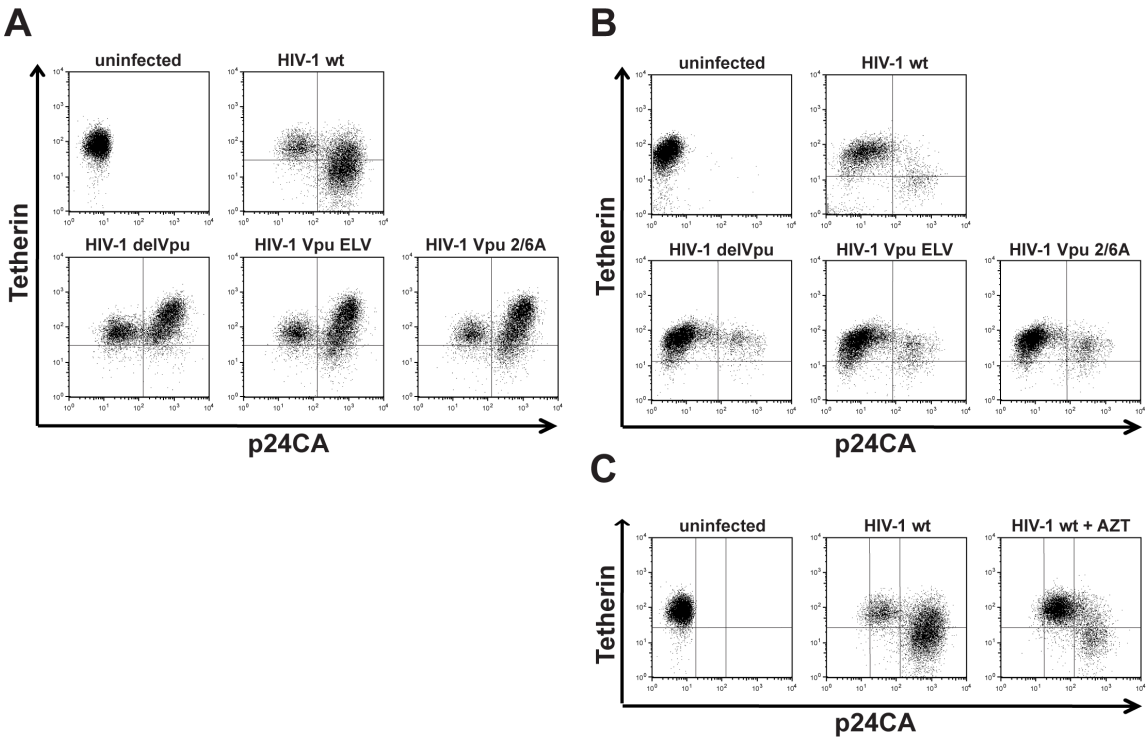

Figure 4-3 Vpu ELV mutants are defective for tetherin downregulation in infected Jurkat T-cells

(A) HeLa cells were infected with VSV-G-pseudotyped HIV-1 wt, HIV-1 delVpu, HIV-1 Vpu ELV or HIV-1 Vpu 2/6A at an MOI of 1. 48 hours post infection, cells were stained for cell surface tetherin and intracellular p24CA, and analysed by flow cytometry **(B)** Jurkat cells were infected as in (A). Productively infected cells were identified by comparing with cultures infected with the same MOI in the presence of 50 mM AZT to control for p24CA uptake of the inoculum **(C)**.

4.2.2 Vpu ELV mutants localise to early endosomal compartments

The **E**59xxx**L**63**V**64 motif in Vpu resembles an acidic dileucine sorting signal (**D**/**E**)xxx**L**(**L**/**I**) found in the cytoplasmic tails of membrane proteins that traffic through endosomal compartments (reviewed by (Bonifacino and Traub, 2003)). We therefore addressed whether mutation of this motif affected Vpu subcellular localisation. To this end, we infected 293T expressing tetherin or not, as well as Jurkat and HeLa cells with VSV-G-pseudotyped HIV-1 NL4.3 and NL4.3 Vpu ELV and stained them for Vpu in combination with several subcellular markers 48 hours later. As expected, in all cells, the predominant localisation of wild-type Vpu was in association with the TGN, with between 20-50% of the Vpu immunoreactivity visible in TGN46-positive compartments (Figure 4-4 A-D). The proportion of the Vpu ELV mutant in TGN46-positive compartments was significantly reduced in 293T tetherin, Jurkat and HeLa, and appeared as ‘‘endosome-like’’ punctae in the cytoplasm and associated on or near the plasma membrane (Figure 4-4 A-C and E). Interestingly, in the parental 293T cells, which lack tetherin expression, Vpu and Vpu ELV localisation was indistinguishable, and predominantly associated with TGN46-positive compartments (Figure 4-4 D and E). Thus, the difference in Vpu ELV localisation appeared to be tetherin dependent. The nature of these extra-TGN compartments was further analysed in HeLa cells and revealed that Vpu ELV accumulated in EEA1-positive early/sorting endosomal compartments, but not CD63-positive late endosomes (Figure 4-4F). Thus, mutation of the **E**xxx**LV** motif leads to endosomal and surface localisation of Vpu consistent with it being required for modulating the trafficking of tetherin.

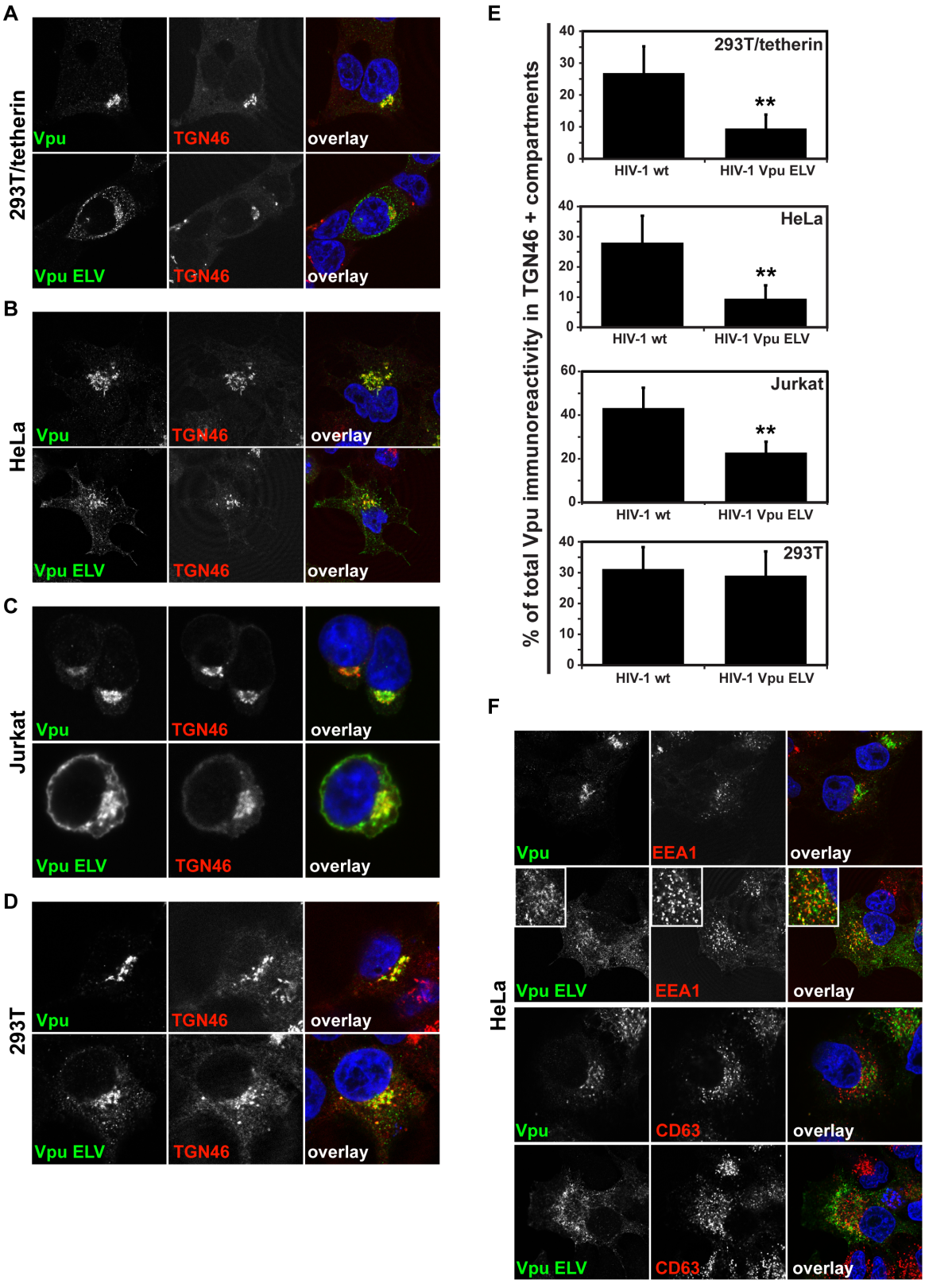

Figure 4-4 ExxxLV mutants localise to early endosomal compartments

(A) 293T tetherin, **(B)** HeLa, **(C)** Jurkat or **(D)** parental 293T were infected with HIV-1 wt or HIV-1 Vpu ELV at an MOI of 1. 48 hours later, cells were fixed and stained for Vpu (green) and the TGN marker TGN46 (red) and examined by confocal microscopy. Panels are of representative examples. **(E)** The percentage of the total Vpu immunoreactivity localised to TGN46+ compartments was calculated for cells (n=20) from (A–D) using the Leica Confocal Software. Results were analysed by unpaired 2-tailed t-test - ** $P=10^{-8}$ or lower. **(F)** HeLa cells as in B were stained for Vpu (green) and the early endosomal marker EEA1 or late endosomal marker CD63 (red).

4.2.3 Vpu ELV mutants interact with cellular host factors as well as tetherin and are incorporated into virions

Since tetherin degradation is dependent on Vpu binding to β-TrCP2 via a phosphorylated pair of serine residues in the Vpu cytoplasmic tail (S52 and S56) (Margottin et al., 1998) (Mitchell et al., 2009) (Mangeat et al., 2009), we tested whether Vpu ELV mutants were defective for interaction with β-TrCP2 in co-immunoprecipitations from transfected cells (Figure 4-5A). Myc-β-TrCP2 was co-immunoprecipitated with Vpu-HA and Vpu ELV-HA, but as expected, not the phospho-mutant Vpu 2/6-HA, ruling out this defect in Vpu ELV. Recent data suggests that ESCRT-mediated degradation of tetherin in the presence of Vpu is mediated by interaction of Vpu with HRS (ESCRT-0) (Janvier et al., 2011). We could further show that both Vpu and Vpu ELV also co-precipitated with HA-HRS from transfected 293T cells (Figure 4-5B) indicating that an inability to recruit ESCRT-0 does not explain the defect in Vpu ELV-mediated degradation of tetherin.

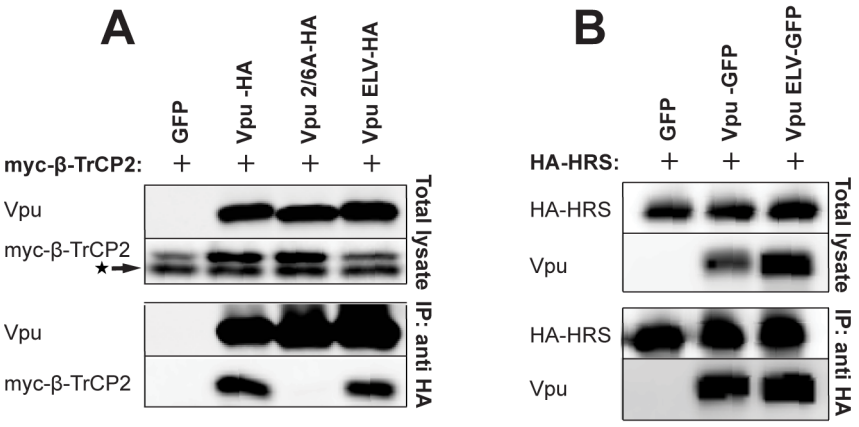

Figure 4-5 Vpu ELV interaction with cellular co-factors essential for tetherin antagonism

(A) 293T cells were transfected with pCR3.1 Vpu-HA, Vpu 2/6A-HA, or Vpu ELV-HA in combination with pCR3.1 myc-b-TrCP2. 48 hours post transfection, cells were lysed and immunoprecipitated with anti-HA antibody. Lysates and precipitates were subjected to SDS-PAGE and analysed by Western blotting for Vpu and myc-b-TrCP2, and analysed by ImageQuant. The star represents an unspecific band. **(B)** Similarly, 293T cells were transfected with pCR3.1 HA-HRS in combination with Vpu-GFP or Vpu ELV-GFP expression constructs. Cell lysates were precipitated with an anti-HA antibody and analysed as in (A).

As a putative trafficking signal, the **E**xxx**LV** motif may exert its effect on tetherin antagonism in two ways. Firstly, the sequence may be required to permit Vpu to traffic to a compartment where it can interact with tetherin; secondly, the sequence may be required for post-interaction trafficking of Vpu/tetherin complexes such that tetherin is not incorporated into budding virions and expression on the cell surface is reduced. A potential confounding factor in investigating, however, is that wild-type Vpu induces tetherin degradation, while Vpu ELV does not. Whilst a Vpu 2/6 control maybe

applicable, controversies surrounding the nature of its phenotype in terms of tetherin counteraction also make it problematic. To alleviate these issues, we took advantage of our recent observations with the novel ESCRT-I subunit, UBAP1 (Stefani et al., 2011) (Agromayor et al., 2012), (data presented in 5.2.1). Interestingly, UBAP1 is essential for Vpu-mediated degradation of tetherin, but is not required for Vpu-mediated tetherin antagonism, implying that commitment of tetherin into a degradative pathway by Vpu, but not ESCRT-I function itself, counteracts tetherin activity (Agromayor et al., 2012). We therefore first examined whether Vpu or Vpu ELV interacted with tetherin in immunoprecipitations from infected cells in the presence or absence of siRNA-mediated silencing of UBAP1. To this end, 293T tetherin cells were treated twice over a period of 48 hours with non-coding siRNA or two different siRNA oligonucleotides directed against UBAP1, and infected with HIV-1 wild-type or HIV-1 delVpu. 48 hours post infection, cells were lysed and tetherin was immunoprecipitated and visualised by Western blotting (Figure 4-6A). As expected, UBAP1 siRNA treatment rescued tetherin levels from Vpu-mediated degradation, but also further enhanced total cellular levels of tetherin (Agromayor et al., 2012), consistent with the known role of ESCRT in tetherin's natural turnover (Janvier et al., 2011). Interestingly, UBAP1 siRNA also enhanced the total cellular content of wild-type Vpu to that of the Vpu ELV mutant (approximately 4/5-fold). Immunoprecipitation of tetherin from the lysates from these cells revealed a similar picture. Wild-type Vpu was detected associated with residual tetherin precipitated from cells, and this was markedly increased upon UBAP1 knockdown. This data strongly suggests that Vpu itself may be co-degraded with tetherin in endosomal compartments. The Vpu ELV mutant efficiently co-precipitated with tetherin irrespective of UBAP1 knockdown, and as expected the Vpu A14L/W22A tetherin binding mutant (Vigan and Neil, 2010) failed to co-precipitate under either condition. Interestingly, however, the ratio of relative band intensities between of Vpu or Vpu ELV precipitated with tetherin in the presence UBAP1 siRNA was equivalent, indicating that Vpu ELV was not defective for physical tetherin interaction, suggesting that the Vpu ELV mutant's defect in tetherin antagonism is due to an inability to mediate post-binding trafficking of Vpu/tetherin complexes into an ESCRT-dependent pathway in which both proteins are degraded. Consistent with this notion, Vpu ELV co-localised with tetherin in infected HeLa and 293T tetherin, both in peripheral endosomal structures and at the cell surface (Figure 4-6B). By contrast, the little tetherin visible in cells infected with wild-type virus co-localised with Vpu in peri-nuclear areas.

Vpu is not a constituent of HIV-1 particles. We therefore reasoned that if the **E**xxx**LV** motif was required to prevent tetherin trafficking to viral budding sites and commit it for degradation, interaction with tetherin itself might lead to Vpu ELV mutant accumulation

in nascent viral particles. To test this hypothesis we took advantage of a tetherin mutant lacking its GPI anchor (tetherin delGPI), which despite its high surface expression, does not restrict virus particle release, but accumulates in virus particles and is sensitive to Vpu (Perez-Caballero et al., 2009). 293T tetherin delGPI cells were mock-transfected or transfected with NL4.3 wt, NL4.3 Vpu ELV, and NL4.3 delVpu. 48 hours later, cell supernatants were centrifuged through a sucrose cushion and analysed for tetherin incorporation by Western blot (Figure 4-6 C and D). As expected, high levels of tetherin delGPI could be detected in NL4.3 delVpu viral pellets, but not in pelleted supernatants from mock-transfected cells. Tetherin delGPI incorporation was reduced in the wild-type virus consistent with tetherin removal from the cell surface. The level of tetherin incorporation in NL4.3 Vpu ELV particles was similar to that of the Vpu-defective mutant. Interestingly, NL4.3 Vpu ELV particles contained detectable levels of Vpu (in this case Vpu appears as a doublet band, which we suggest may be due to exposure to active HIV-1 protease in the particle). By contrast, no Vpu was detectable in any viral particles derived from 293T cells, indicating that Vpu ELV incorporation into viral particles was tetherin dependent. Taken together, these data indicate that the **E**xxx**LV** motif is required for efficient tetherin antagonism, by modulating the trafficking of tetherin such that it cannot become efficiently incorporated into nascent viral particles.

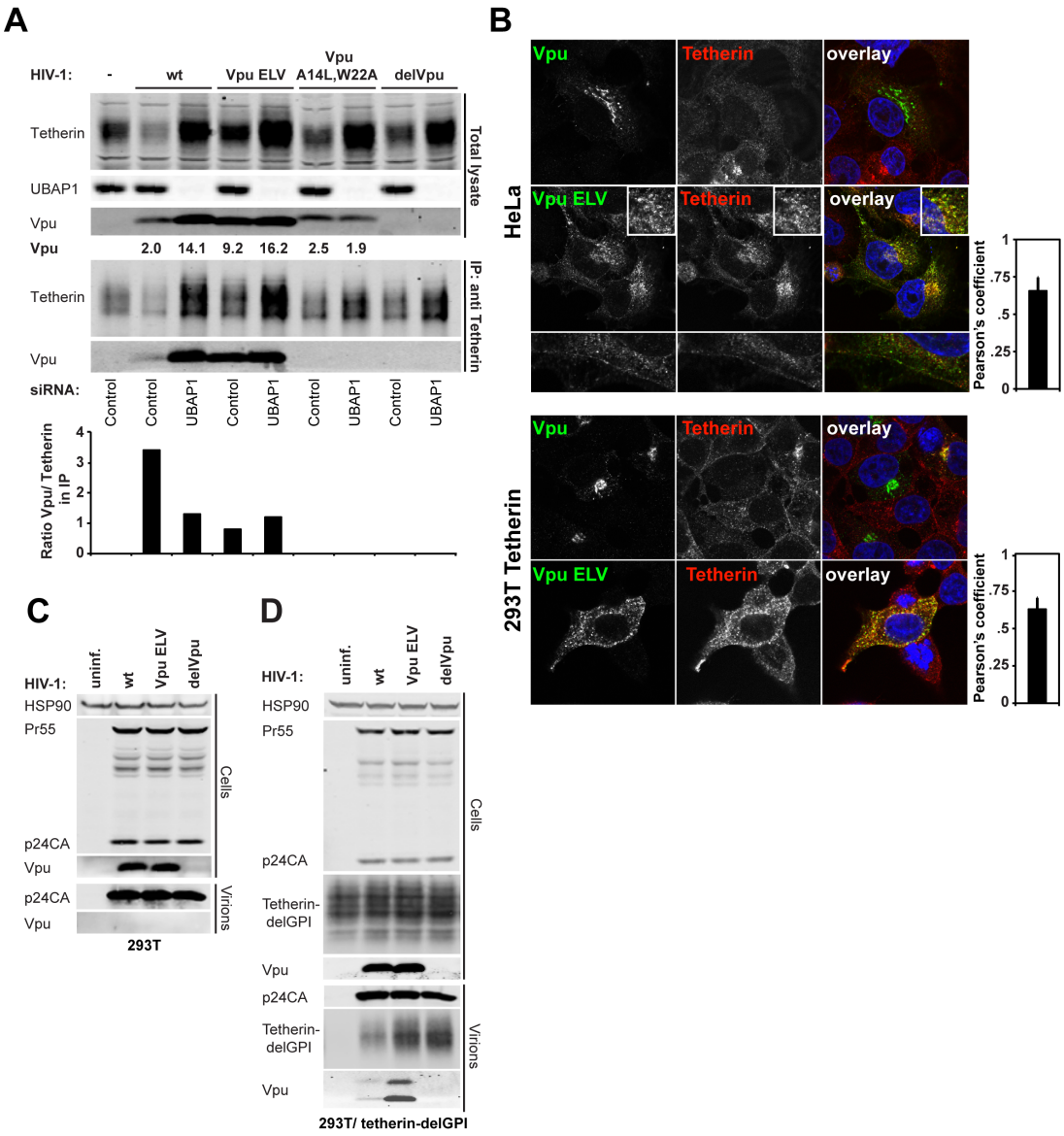

Figure 4-6 Vpu ELV interacts with tetherin and is incorporated into nascent virions

(A) 293T tetherin cells were transfected twice over 48 hour with siRNA oligonucleotide directed against UBAP1 or Non-targeting control. The cells were then infected with the indicated virus at an MOI of 2. 48 hours later, cell lysates were immunoprecipitated with an anti-tetherin monoclonal antibody. Lysates and immunoprecipitates were separated by SDS-PAGE and blotted for tetherin, UBAP1 or Vpu using LiCor quantitative Western blotting. Numbers under the Vpu lanes of the cell lysate represent relative band intensities. The histogram below the IP represents the ratio of tetherin band intensity to that of Vpu in the co-immunoprecipitation. **(B)** HeLa and 293T tetherin cells were infected as in Figure 4-4, and stained for Vpu (green) and tetherin (red) and examined by confocal microscopy. Adjacent histograms quantify the degree of co-localisation of Vpu ELV and tetherin (Pearson's Correlation Coefficient calculated using ImageJ) for 20 individual cells. **(C and D)** 293T or 293T cells stably expressing tetherin delGPI were infected with HIV-1 wt, HIV-1 Vpu ELV or HIV-1 delVpu at an MOI of 1. 48 hours post infection, cells were harvested and viral supernatants were pelleted through a 20% sucrose cushion. Cells and virions were subjected to SDS-PAGE and Western blotting for tetherin delGPI, Vpu, HIV-1 p24CA and Hsp90 and analysed by LiCor quantitative imager.

Recent data suggests that Vpu blocks both the transit of de novo synthesized tetherin to the cell surface as well as the recycling of endocytosed tetherin from the plasma membrane, with the relative importance of these processes currently a matter of debate (Tervo et al., 2011) (Schmidt et al., 2011). Tetherin recycling requires a dual tyrosine **Y**x**Y**xxϕ motif in its cytoplasmic tail that acts as a binding site for AP-2 (for internalisation) and AP-1 (for recycling via the Golgi) (Rollason et al., 2007) (Masuyama et al., 2009). Mutation of this motif enhances tetherin surface expression, but only has minor effects on its ability to restrict virus release or its sensitivity to Vpu (Iwabu et al., 2009) (Dubé et al., 2010b). Given that the **E**xxx**LV** motif was defective for post-binding inactivation of tetherin, but retained a low residual activity against tetherin in transient transfection assays, we asked whether Vpu ELV was differentially defective against tetherin mutants bearing lesions in its own sorting sequence. We infected 293T tetherin and 293T tetherin Y6,8A cells with HIV-1 wt, HIV-1 delVpu and HIV-1 Vpu ELV at a fixed dose (MOI 1) and measured viral release 48 hours later (Figure 4-7 A and B). Vpu-defective viral release was approximately 35-fold reduced from 293T tetherin cells compared to the wild-type virus, and as expected NL4.3 Vpu ELV had an intermediate phenotype in this assay (6-fold less release than wt). However, in 293T tetherin Y6,8A all residual antagonistic activity of Vpu ELV was abolished with viral release equivalent to that of the Vpu deleted virus. By contrast, the wild-type virus retained the majority of its anti-tetherin activity. This again was not due to a defect of Vpu interaction with tetherin, as immunoprecipitation of tetherin after UBAP1 siRNA treatment demonstrated equivalent levels of Vpu and Vpu ELV co-precipitation from both tetherin and tetherin Y6,8A expressing cells (Figure 4-7C). Thus, residual activity of Vpu ELV requires that tetherin retains its capacity to recycle from the PM.

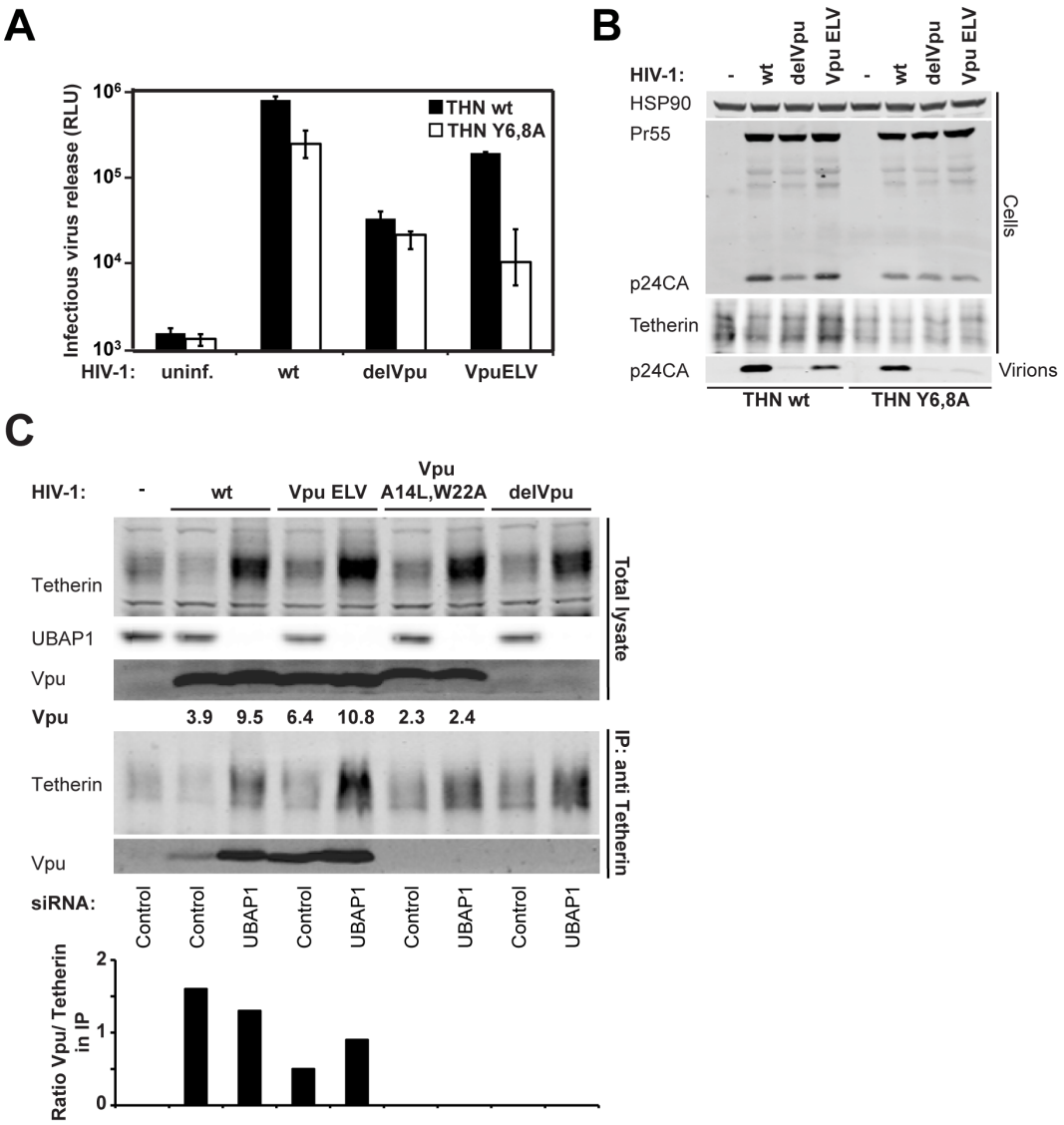

Figure 4-7 Residual activity of Vpu ELV mutants requires an intact recycling signal in tetherin

(A) 293T tetherin or 293T tetherin Y6,8A mutant were infected with VSV-G-pseudotyped HIV-1 wt, HIV-1 delVpu or HIV Vpu ELV at an MOI of 0.5. Supernatants and cell lysates were harvested 48 hours later and analysed for infectious virus release on HeLa-TZMbl as Figure 4-1. Error bars represent the standard deviation of three independent experiments. **(B)** Corresponding Western blots of cell lysates and virions from A. **(C)** 293T tetherin Y6,8A cells treated with control or UBAP1 specific siRNAs were infected with VSV-G-pseudotyped HIV-1 wt, HIV Vpu ELV, HIV-1 Vpu A14L/W22A or HIV-1 delVpu at an MOI of 2. 48 hours post infection, cells were lysed and immunoprecipitated with an anti-tetherin antibody. Lysates and immunoprecipitates were subjected to SDS-PAGE and analysed by Western Blotting for tetherin, UBAP1 and Vpu, and analysed by LiCor quantitative imager. Ratios of Vpu/ tetherin band intensities in the co-immunoprecipitation are plotted on the histogram below.

4.2.4 Tetherin antagonism by Vpu is clathrin-dependent

The implication of putative clathrin adaptor sites in Vpu-mediated tetherin antagonism led us to first test whether inhibition of overall clathrin function inhibits Vpu activity. Overexpression of the C-terminal fragment of the neuronal adaptor AP180 (AP180c) that inhibits clathrin/membrane interactions (Ford et al., 2001), was recently shown to inhibit tetherin downregulation from the surface (Lau et al., 2011). To this end, 293T tetherin expressing cells were transfected with increasing concentrations of AP180c in combination with NL4.3 wt or NL4.3 delVpu. 48 hours post transfection, cells and supernatant containing virions were harvested and analysed by Western Blot. Overexpression of AP180c specifically blocked Vpu-dependent particle release (Figure 4-8A), indicating clathrin-dependent subcellular trafficking is essential for Vpu activity. Infectious yield could not be determined in this experiment because AP180c overexpression inhibits envelope processing and blocks clathrin incorporation into particles, which has been shown to play a role in retroviral particle infectivity (Popov et al., 2011) (Zhang et al., 2011b). Interestingly AP180c expression, like UBAP1 siRNA treatment (Figure 4-6A), enhanced total Vpu expression levels, indicating that clathrin-dependent transport is involved in the turnover of Vpu. Visualization of Vpu-YFP localisation in 293T tetherin cells overexpressing AP180c showed vesicular rather than peri-nuclear localisation similar to that seen in the same cells infected with HIV-1 Vpu ELV (Figure 4-8B), and this was not apparent in the parental tetherin negative 293T cells, suggesting again this difference was driven by interaction with tetherin.

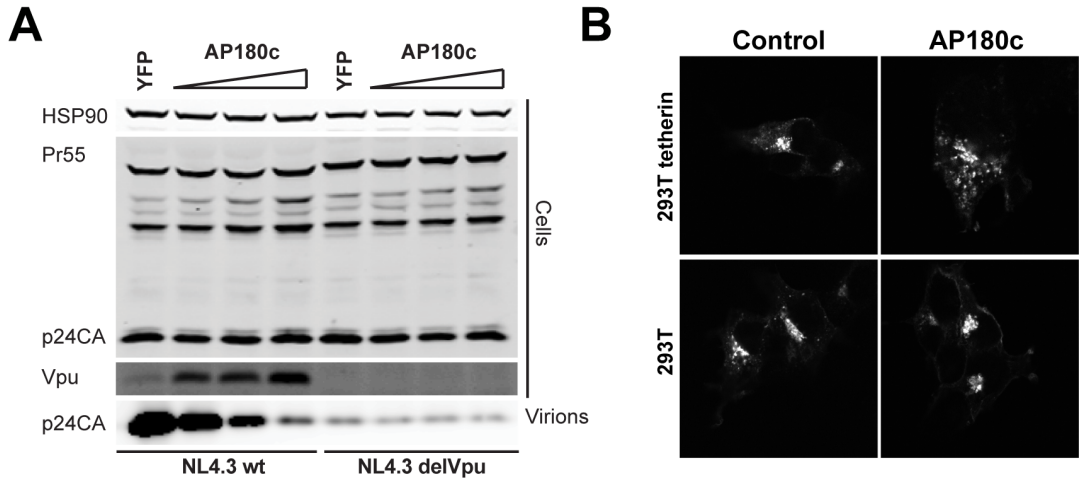

Figure 4-8 AP180c inhibits Vpu-mediated tetherin antagonism

(A) 293T tetherin were transfected with NL4.3 wt or NL4.3 delVpu proviral plasmids in combination with either YFP or increasing doses of an AP180c expression vector. 48 hours post transfection, cell lysates and pelleted supernatant virions were harvested and subjected to SDS-PAGE and analysed by Western blotting for HIV-1 p24CA, Vpu and Hsp90 serving as loading control, and analysed by LiCor quantitative imager. **(B)** 293T or 293T tetherin cells were transfected with pCR3.1 Vpu-YFP with or without AP180c co-expression, fixed after 48 hours and examined by confocal microscopy.

The dominant negative mutant of the GTPase dynamin 2 (K44A) has also been described to have an intermediate effect on tetherin counteraction by Vpu, compared to the complete disruption of HIV-2 Env function which, like SIV Nef, is dependent on AP-2 and endocytosis (Lau et al., 2011). We transfected increasing doses of HA-tagged dominant negative dynamin 2 or the wild-type protein along with HIV-1 proviruses into 293T tetherin and parental cells (Figure 4-9 A-C). In agreement with Lau *et al* (Lau et al., 2011) dominant negative dynamin 2, but not equivalent levels of the wild-type dynamin 2, partially blocked the release of wild-type HIV-1 (Figure 4-9 A-C). Furthermore, dominant negative dynamin 2 expression levels in these assays were sufficient to block transferrin uptake in parallel cultures tested by fluorescence imaging (Figure 4-9D). Interestingly, dominant negative dynamin 2 also blocked residual Vpu ELV-mediated and even the low level Vpu-defective viral release proportionally (7x, 4x and 8x for WT, Vpu-defective or Vpu ELV respectively), suggesting that this effect was independent of the ELV motif. Given that dominant negative dynamin 2 inhibits tetherin endocytosis (Lau et al., 2011), this data suggests that its effect on restriction may be due more to the build up of tetherin at the cell surface that cannot be turned over rather than a direct effect on Vpu function itself.

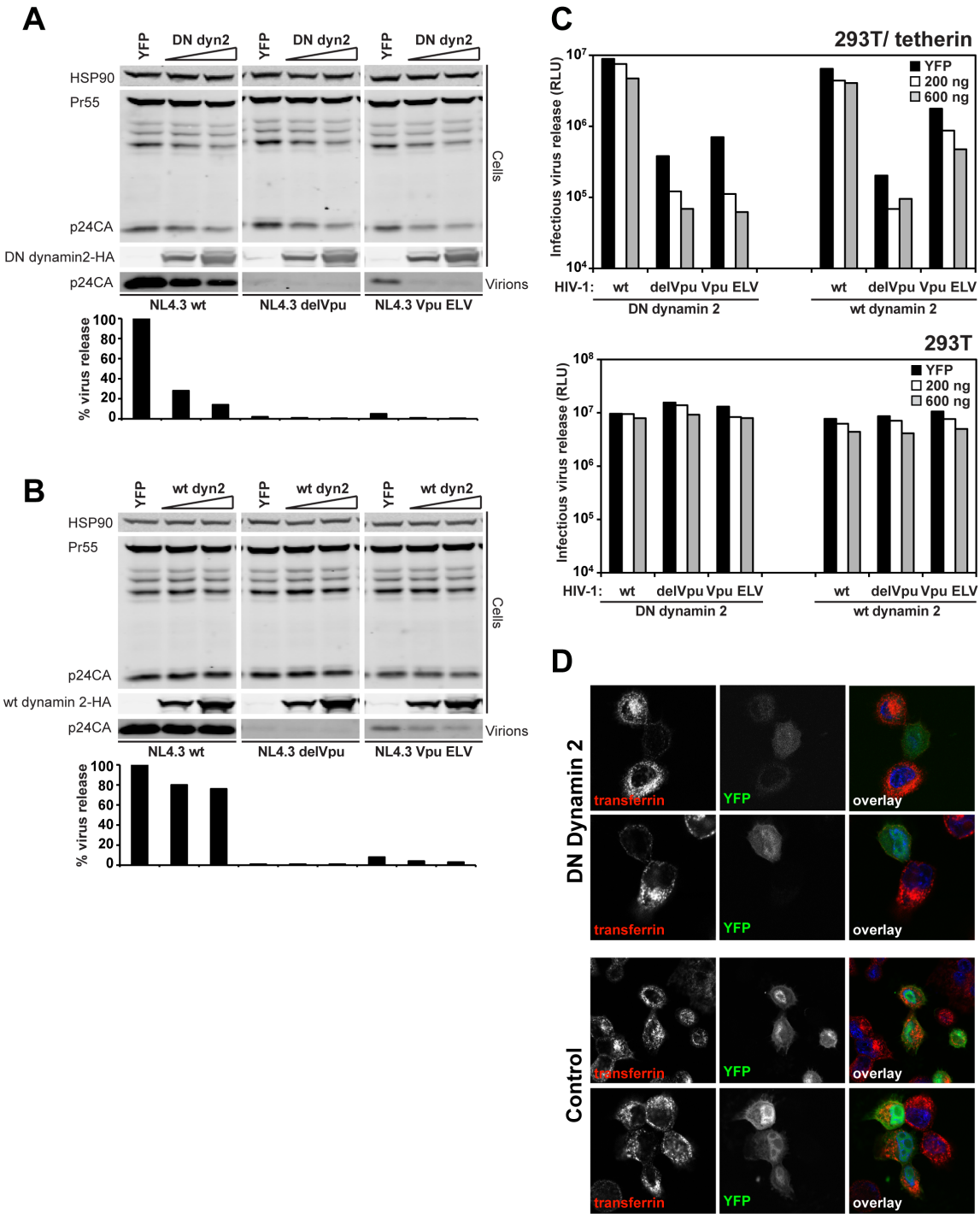

Figure 4-9 Effects of dominant negative dynamin 2 on Vpu-mediated HIV-1 release

(A and B) 293T tetherin cells were transfected with the indicated HIV-1 provirus and increasing doses of HA-tagged dominant negative dynamin 2 (A) or the wild-type protein (B). 48 hours later, cell lysates and viral supernatants were harvested and subjected to SDS-PAGE and analysed by Western blotting for HIV-1 p24CA, dynamin 2-HA and Hsp90, and analysed by LiCor quantitative imager. Histograms below the blots indicate particle release efficiency compared to wild-type virus release in the absence of dynamin 2 or increasing doses of dynamin 2 expression vector. **(C)** Corresponding infectivity of viral supernatants from (A and B) on HeLa-TZMbl cells alongside those from a parallel experiment in parental 293T cells. **(D)** 293T tetherin cells were transfected with pCR3.1 YFP with or without increasing doses of dominant negative dynamin 2. 48 hours later, cells were starved in serum-free medium for 30 minutes and then treated for a further 15 minutes with 10 µg/ml Alexa-594-conjugated transferrin, before fixation and imaging by confocal microscopy.

4.2.5 Second alpha helix can be functionally replaced by D/ExxxLL-containing peptide from HIV-1 Nef

Acidic dileucine-based sorting signals, **D**/**E**xxx**L**(**L**/**I**), act as binding sites for a hemi-complex of sigma and adaptin subunits of the canonical clathrin adaptors AP-1, AP-2 and AP-3, and are required for endocytic and endosomal/Golgi trafficking (see 1.8). While the requirement for the acidic and first leucine residues are absolute, the third position is less well conserved, and can be L, I or on occasion V or M. Analysis of the cytoplasmic tails of Vpu sequences from most clades of HIV-1 group M, show that a putative **E**xxx**L**(**V**/**M**/**I**) is well conserved in the second alpha helix (Figure 4-10A). In contrast to other HIV-1 subgroups, Clade C and F isolates have an **E**xxx**LL** motif juxtaposed to the plasma membrane in helix 1 (not shown), which has been previously suggested to be a determinant of Clade C Vpu localisation to the PM (Ruiz et al., 2008). In subgroup B, the V64 position is usually V or M, although occasional I or L residues are found at this position. We mutated position 64 to M, L or I in NL4.3 Vpu and examined the mutant Vpu proteins for tetherin antagonism and their ability to downregulate tetherin form the cell surface. To study antagonism, 293T cells expressing tetherin were transfected with Vpu-HA or indicated mutant in combination with wild-type HIV-1 provirus NL4.3 (NL4.3 wild-type) or Vpu-defective NL4.3 (NL4.3 delVpu). 48 hours after the transfection cell lysates and supernatants containing viral particles were harvested and analysed for physical virus yield by Western blot (Figure 4-10B). To study downregulation, HeLa cells were transfected with a GFP reporter in combination with Vpu-HA or indicated mutant protein. 48 hours post transfection, cell surface levels of tetherin were analysed by flow cytometry (Figure 4-10C). We found no defect in the mutant proteins abilities to counteract or downregulate tetherin from the surface (Figure 4-10 B and C), in agreement with the above data demonstrating that this position is the least important of the three, and consistent with the role of this motif as a sorting signal.

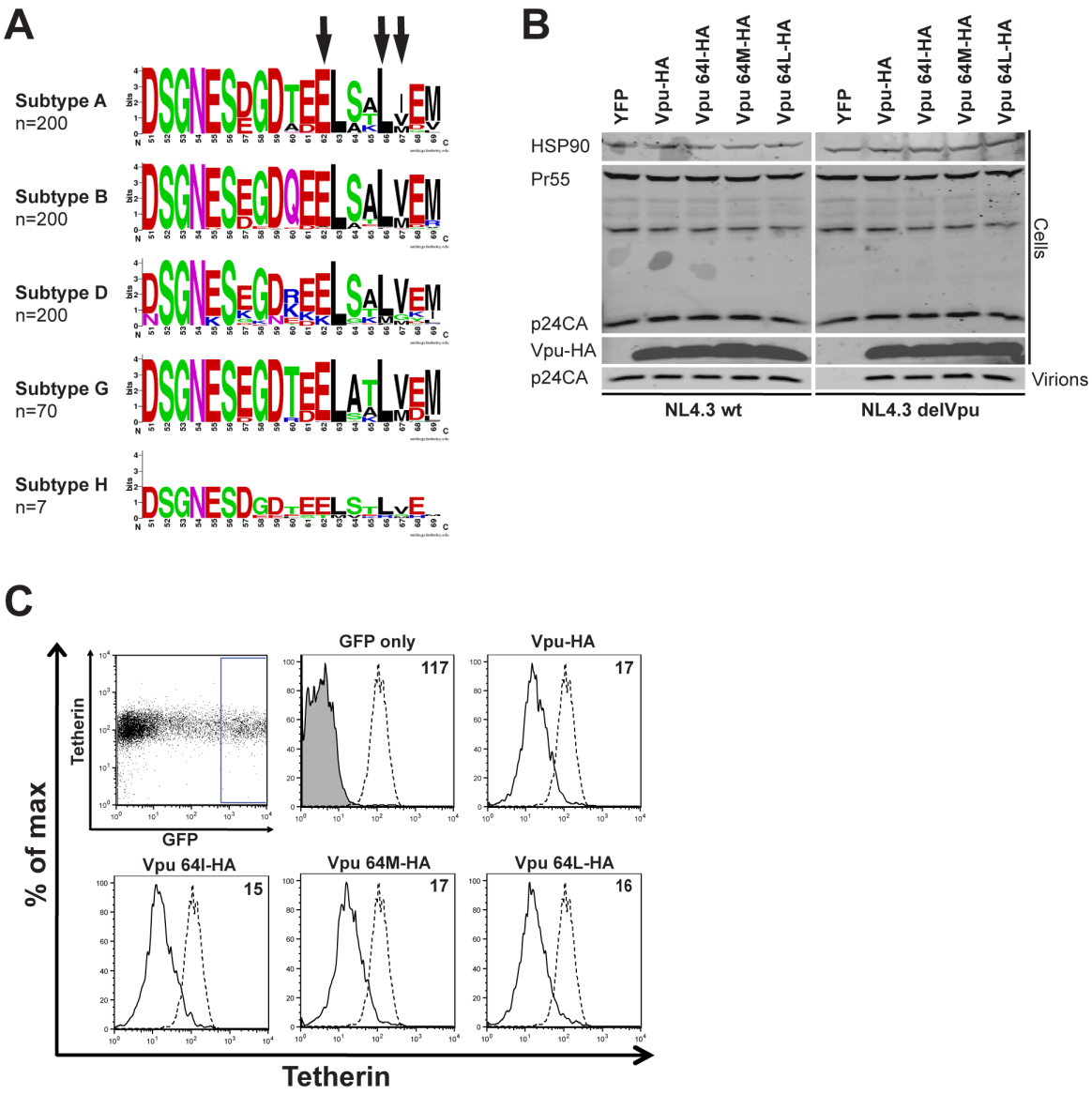

Figure 4-10 Vpu Exxx(V/M/I/L) is conserved in most HIV-1 clades

(A) LogoPlots of Vpu cytoplasmic tail portions encompassing the conserved phosphorylation motif (D**S**GNE**S**) and helix 2 from HIV-1 subgroup M clades A, B, D, G and H generated from sequences obtained from the Los Alamos database (www.hiv.lanl.gov). **(B)** 293T cells were transfected with NL4.3 or NL4.3 delVpu proviruses in combination with tetherin and Vpu-HA, Vpu 64I-HA, Vpu 64M-HA or Vpu 64L-HA expression vectors. 48 hours post transfection, cell lysates and pelleted supernatant virions were harvested and subjected to SDS-PAGE and analysed by Western blotting for HIV-1 p24CA, Vpu-HA and Hsp90, and analysed by LiCor quantitative imager. **(C)** HeLa cells were co-transfected with Vpu or indicated Vpu mutant and a GFP expression construct. Cell surface staining for endogenous tetherin was analysed by flow cytometry 48 hours post transfection, as in Figure 4-2.

The Nef proteins of primate immunodeficiency viruses are also multifunctional adaptor proteins, targeting a variety of immune regulatory cell surface molecules for downregulation and degradation (reviewed by (Kirchhoff, 2010)). Nef interacts promiscuously with AP-1, AP-2 and AP-3 through a conserved C-terminal **D**/**E**xxx**LL** motif (Janvier et al., 2003) (Chaudhuri et al., 2007). The interaction of AP-2 with this site is essential for Nef targeting of CD4 for ESCRT-dependent lysosomal degradation (Chaudhuri et al., 2007), but Nef-mediated downmodulation of class I MHC molecules

requires AP-1 (Lubben et al., 2007). Importantly, several SIV Nef proteins are also tetherin antagonists (Jia et al., 2009) (Zhang et al., 2009) and again this is dependent on the **D**/**E**xxx**LL** motif (Zhang et al., 2011a). We therefore asked whether the C-terminus of HIV-1 Vpu could be functionally substituted with a known AP-binding site from these proteins. The **E**VSA**LV** motif of NL4.3 Vpu was first replaced with the core AP-binding site from NL4.3 Nef, **E**NTS**LL** (Figure 4-11A), and this Vpu protein was as functional as the wild-type protein in virus rescue experiments (Figure 4-11 B and C). We then replaced the entire cytoplasmic tail of Vpu from residue 58 with a 19 amino acid stretch derived from Nef including the **E**NTS**LL** and a downstream dual-aspartic acid motif that has been previously shown to stabilize AP-2 interactions (Lindwasser et al., 2008). Remarkably, when we tested the ability of these proteins to antagonise tetherin function, the Vpu-Nef chimeric protein substantially recovered tetherin antagonistic activity (Figure 4-11 B and C). Moreover, this chimera also displayed improved tetherin downregulation from the surface of transfected HeLa cells (Figure 4-11 D). This activity was entirely dependent on the key amino acids required for AP-interaction as a chimera in which E, LL and DD positions were mutated to alanine was unable to counteract tetherin or downregulate it from the surface (Figure 4-11 B-D). Examination of the subcellular distribution of Vpu-Nef or the mutant fused to CherryFP suggested that the mutant was localised more prominently to the PM consistent with a defect in trafficking imparted by the mutation (Figure 4-11E). Thus, Vpu function can be substantially recovered by replacing its entire second alpha helix with a promiscuous AP-binding (**D**/**E**)xxx**L**(**L**/**I**) sorting signal, indicating that linking Vpu directly to the clathrin trafficking machinery can restore its activity in the absence of the second alpha helix.

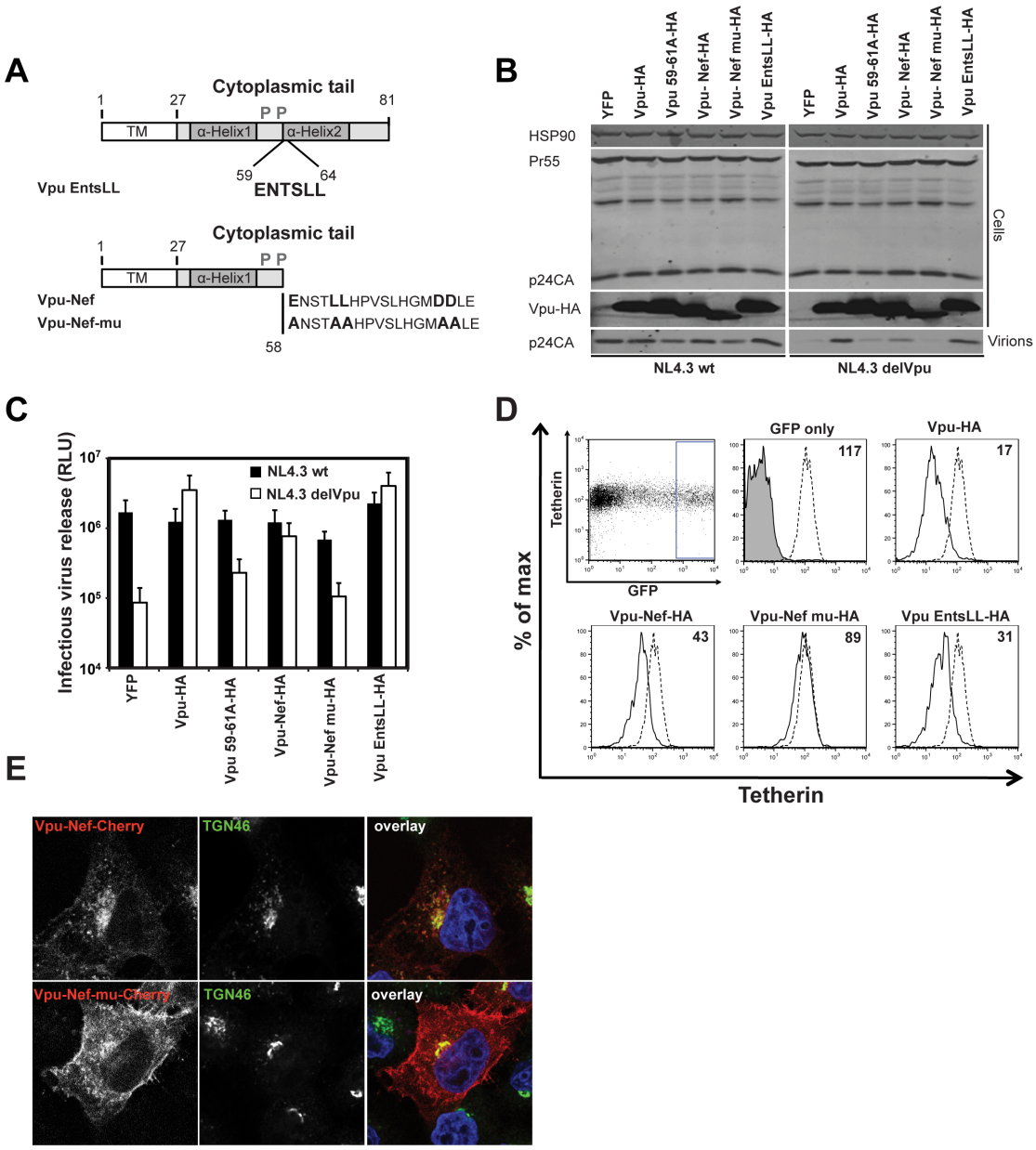

Figure 4-11 The second alpha helix of Vpu can be functionally replaced by D/ExxxLL endocytic signal from HIV-1 Nef

(A) Schematic representation of Vpu ENTSLL and Vpu-Nef chimeric constructs. **(B)** 293T cells were transfected with NL4.3 wt or NL4.3 delVpu proviral plasmids in combination with tetherin and indicated pCR3.1 Vpu-HA or Vpu-Nef-HA chimera. 48 hours post transfection, cell lysates and pelleted supernatant virions were harvested and subjected to SDS-PAGE and analysed by Western blotting for HIV-1 p24CA, Vpu-HA and Hsp90, and analysed by LiCor quantitative imager. **(C)** Infectivity of viral supernatants from (B) was determined on HeLa-TZMbl cells as in Figure 4-1. Error bars represent standard deviation of three independent experiments. **(D)** HeLa cells were co-transfected with Vpu or indicated Vpu mutant and a GFP expression construct. Cell surface staining for endogenous tetherin was analysed by flow cytometry 48 hours post transfection, as in Figure 4-2. **(E)** HeLa cells were transfected with Vpu-Nef or Vpu-Nef-mu CherryFP fusions (red) and counterstained for TGN46 (green) and DAPI (blue) and examined by confocal microscopy.

4.2.6 Vpu-mediated tetherin antagonism is independent of canonical adaptor proteins

The similarities between the **E**xxx**LV** motif and acidic dileucine sorting signals, and its functional replacement with the promiscuous **E**NTS**LL** motif in HIV-1 Nef led us to test whether the major known adaptors involved in trafficking of membrane proteins between the PM, endosomes and Golgi compartments were required for Vpu-mediated tetherin antagonism. Clathrin-mediated endocytosis requires AP-2, whereas AP-3 controls early to late endosomal/lysosomal trafficking. AP-1 plays a role in trafficking of cargo between early endosomes and the TGN, with evidence that it can function in either direction, discussed 1.8. To this end we examined the effects of siRNA-mediated silencing of AP-1 (AP-1 γ1), AP-2 (AP-2 μ1), AP-3 (AP-3 μ1/AP-3 δ1). HeLa or 293T tetherin expressing cells were treated twice over a period of 48 hours with non-coding siRNA or indicated siRNA oligos directed against the clathrin adaptors, and infected or transfected with HIV-1 wild-type or HIV-1 delVpu. 48 hours post infection, cells were lysed and analysed by Western blot. For AP-1, siRNA-mediated silencing was inefficient in 293T tetherin cells (not shown) and we therefore constructed a HeLa cell line containing a doxycycline-inducible shRNA hairpin against AP-1 γ1. Induction of this hairpin coupled with simultaneous depletion of AP-1 γ1 by oligonucleotide transfection led to approximately 95% knockdown efficiency. This treatment had no specific effect on Vpu-dependent virus particle yield in HeLa cells indicating that tetherin antagonism again was not compromised (Figure 4-12A), and furthermore tetherin surface downregulation was not defective in mouse AP-1 μ1a -/- fibroblasts (Figure 4-12B) (Zizioli et al., 1999). Similarly AP-3 μ1 and AP-3 δ1 co-depletion had no detectable effect on tetherin activity or Vpu-mediated counteraction (Figure 4-12C). Furthermore, human tetherin could also be downregulated from the surface of mouse fibroblasts defective in AP-3 δ1 when transduced to express Vpu (Peden et al., 2002) (Figure 4-12D). Depletion of AP-2 by RNAi in 293T tetherin cells had only minor effects on Vpu-dependent virus particle release, suggesting that unlike SIV Nef and HIV-2 Env, and consistent with the reports that Vpu does not enhance tetherin endocytosis, AP-2 activity is dispensable for Vpu-mediated tetherin antagonism (Figure 4-12E).

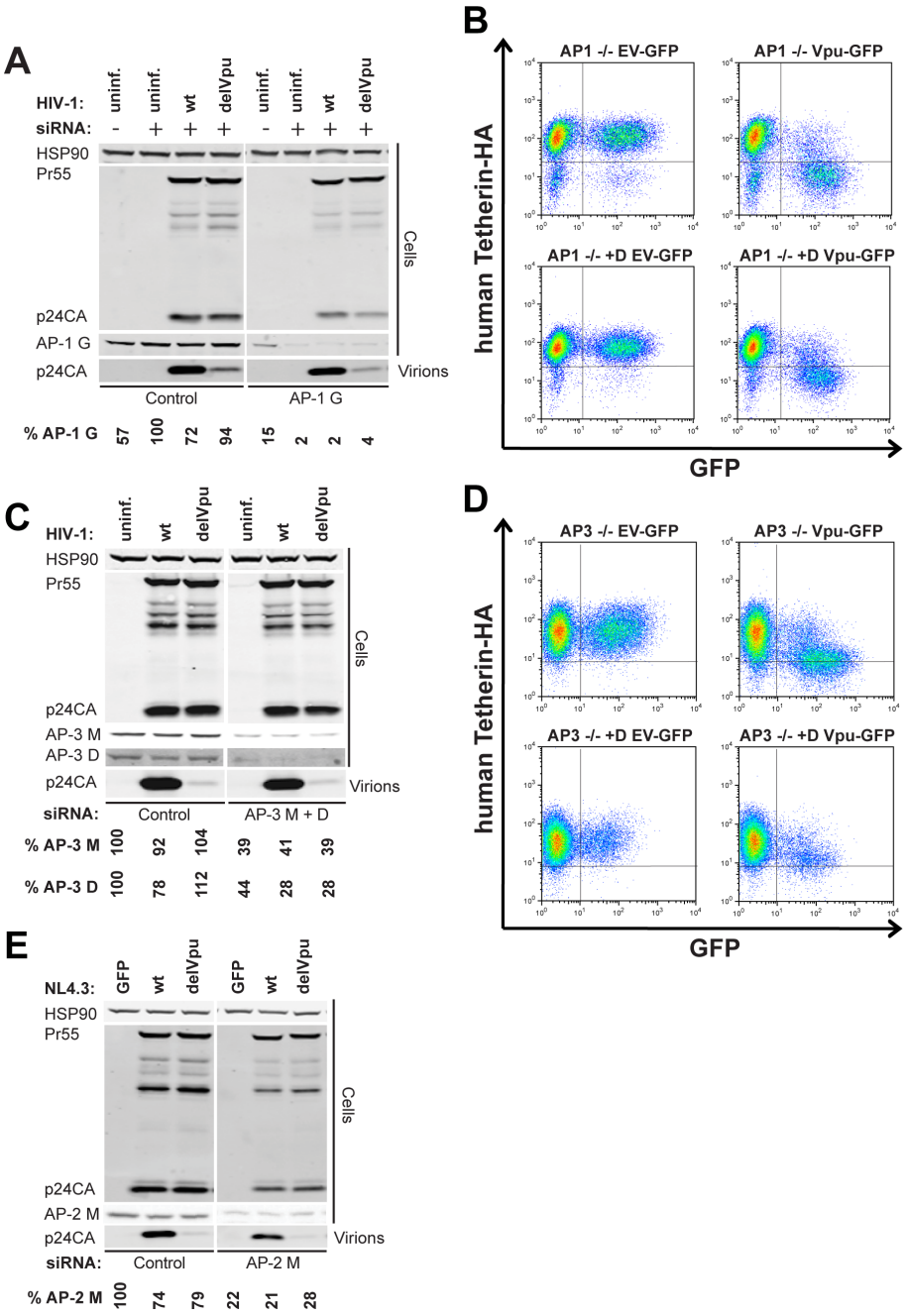

Figure 4-12 Clathrin adaptor AP-1, AP-2 and AP-3 are dispensable for Vpu-mediated tetherin antagonism

(A) HeLa cells expressing a doxycycline-inducible shRNA hairpin against AP-1 γ1 were transfected twice with pooled control or siRNA pools against AP-1 γ1. 4 hours post the second transfection the cells were infected with VSV-G-pseudotyped HIV-1 wt or HIV-1 delVpu virus stock at an MOI of 1. 48 hours post infection, cell lysates and pelleted supernatant virions were harvested and subjected to SDS-PAGE and analysed by Western blotting for HIV-1 p24CA, AP-1 γ and Hsp90 serving as loading control, and analysed by LiCor quantitative imager. The percentage of AP-1 γ1 knockdown was determined by the relative band intensity and is indicated below the blot panel. **(B)** Fibroblasts from AP-1 μ1A −/− mice or their reconstituted counterparts were transduced to express human tetherin bearing an extracellular HA-tag. The cells were then transduced with retroviral vector constructs encoding IRES-linked Vpu GFP. 48 hours later, cells were surface stained for human tetherin expression using anti-HA antibodies and analysed by flow cytometry. **(C)** 293T cells stably expressing tetherin were transfected twice with pooled control or siRNA pools against AP-3 δ1 and AP-3 μ1. 4 hours post the second transfection, cells were infected with VSV-G-pseudotyped HIV-1 wt or HIV-1 delVpu virus stock at an MOI of 1. Cells were harvested and analysed as in (A). **(D)** Fibroblasts from pearl AP3 δ −/− mice or their reconstituted counterparts were treated and analysed as in (B). **(E)** 293T cells stably expressing tetherin were transfected twice with pooled control or AP-2 μ1 siRNA and co-transfected with NL4.3 wt, NL4.3 delVpu or GFP expression vectors. Cells were harvested and analysed as in (A).

Finally, we examined whether there was any role for the retromer complex, in Vpu-mediated tetherin antagonism. Retromer regulates retrieval and recycling of endosomal proteins to the TGN and is known to act co-operatively or antagonistically with AP-1 (reviewed by (Attar and Cullen, 2010)). The retromer complex consists of several sorting nexins (SNX), and a core complex containing cargo binding component, VPS34, and two essential co-factors, VPS26 and VPS29. We performed siRNA-mediated knockdown of VPS26 (Figure 4-13A). At levels of knockdown that were sufficient to re-localise the CD8-cation-independent mannose-6-phosphate receptor (CD8-CI-M6PR) (Figure 4-13B), disruption of retromer had no detectable effect of Vpu-mediated HIV-1 release from 293T tetherin cells.

Taken together these results demonstrate that neither depletion of individual cellular adaptor proteins known to bind to (**D**/**E**)xxx**L**(**L**/**I**) motifs, nor disruption of retromer-mediated endosome-to-TGN retrieval, were sufficient to recapitulate the phenotype of the Vpu ELV mutant.

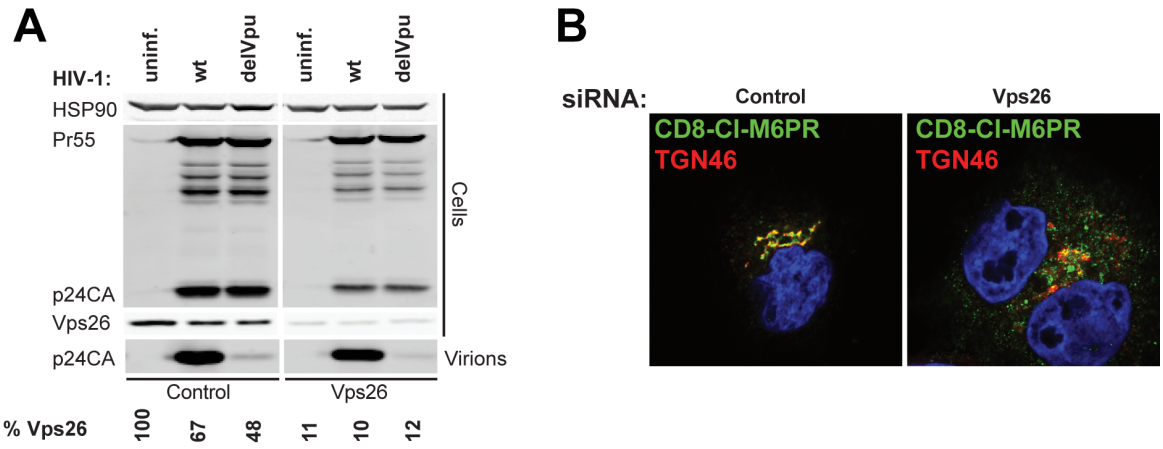

Figure 4-13 The retromer complex is dispensable for Vpu-mediated tetherin antagonism

(A) 293T cells stably expressing tetherin were transfected twice with pooled control or siRNA pools against the retromer subunit VPS26 and co-transfected with NL4.3 wt, NL4.3 delVpu or GFP expression vectors. 48 hours post transfection, cell lysates and pelleted supernatant virions were harvested and subjected to SDS-PAGE and analysed by Western blotting for HIV-1 p24CA, VPS26 and Hsp90 serving as loading control, and analysed by LiCor quantitative imager. The percentage of VPS26 knockdown was determined by the relative band intensity and is indicated below the blot panel. **(B)** HeLa cells stably expressing the CD8-CI-M6PR were treated with control or VPS26 siRNA. 48 hours later, cells were fixed and stained for CD8 (green) and TGN46 (red) and analysed by confocal microscopy.

4.2.7 AP-1 binding to Vpu/tetherin complexes is dependent on the ExxxLV motif in biochemical studies

The context dependency of (**D**/**E**)xxx**L**(**L**/**I**) motifs that governs which adaptor they bind to *in vivo* is poorly defined at present, meaning that RNAi depletion is the most reliable method for identifying the cellular factor involved. While individual depletion of AP-1, 2 or 3 in our experiments had no effect on Vpu-mediated tetherin antagonism, replacement of the second alpha helix with the promiscuous AP-binding peptide from HIV-1 Nef and treatment with AP180c did recover function, underscoring that linking Vpu to the clathrin trafficking machinery promotes its ability to counteract tetherin. We have so far been unable to demonstrate direct interaction between the Vpu **E**xxx**LV** motif and adaptors AP-1, 2 or 3. The low affinity of these interactions, their transient nature, and the complex interactions of the adaptor protein with membrane lipids means that adaptor binding is rarely measurable in co-precipitations from cells.

However, data presented at the 2013 Cold Spring Harbour Meeting on Retroviruses (this study is currently under revision) demonstrated that Vpu/tetherin complexes bind to the clathrin adaptor AP-1 (Figure 4-14). The Yong Xiong laboratory performed crystal structure studies in which they fused Vpu and tetherin cytoplasmic tails to bring them in close proximity. They were able to show that, σ and γ subunits of AP-1 bind to the **E**xxx**LV** motif in Vpu while the μ subunit binds to the **Y**D**Y**xxϕ motif in tetherin, which in turn recruits the β subunit, resulting in a Vpu/tetherin/AP-1 complex.

This data is in agreement with our Vpu **E**xxx**LV** results, in which this trafficking motif is required for post-binding trafficking of Vpu/tetherin complexes and inhibition of antiviral activity. Moreover, because residual activity of the **E**xxx**LV** mutant requires an intact recycling signal in tetherin, **Y**D**Y**xxϕ, we proposed that the second alpha helix mutant is selectively defective for routing tetherin into an endosomal degradation pathway, and thereby inhibiting its transit to the PM and incorporation into nascent virions.

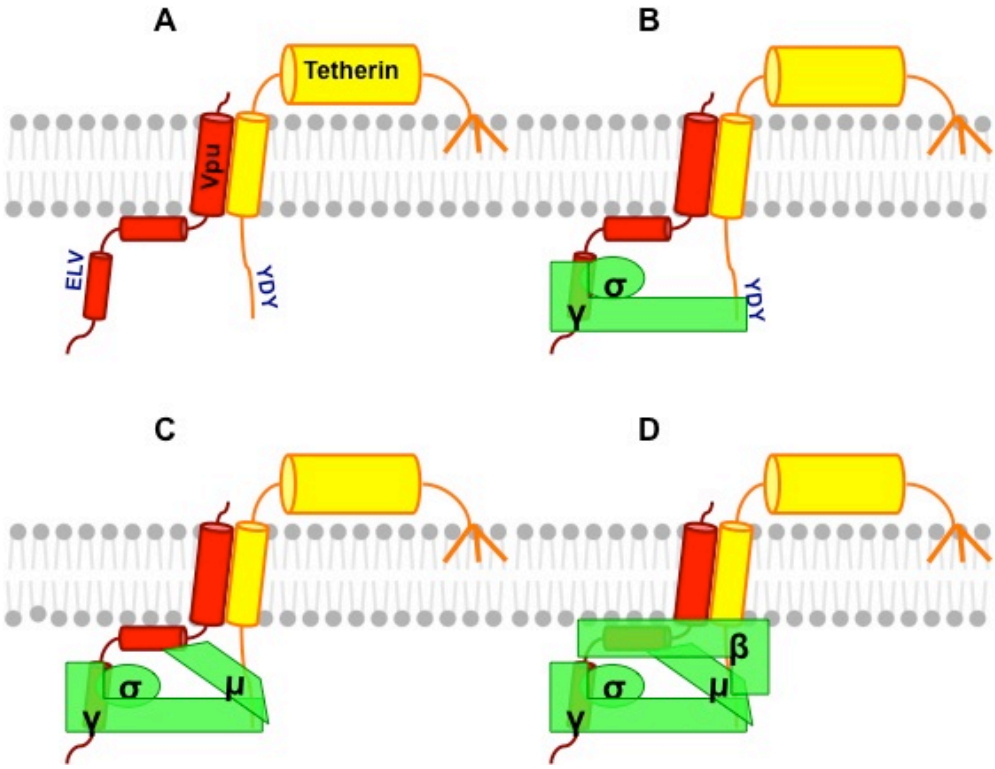

Figure 4-14 Clathrin adaptor AP-1 binds Vpu/ tetherin complexes (CSH 2013 Yong Xiong lab)

The Yong Xiong lab fused Vpu cytoplasmic tail with the cytoplasmic tail of tetherin and performed crystallography studies. They obtained crystal structures, which revealed that the σ and γ subunits of AP-1 bind to the Vpu **E**xxx**LV** motif while the **Y**D**Yxx**ϕ motif in tetherin binds to the μ subunit which in turn recruits the β subunit of the AP-1 complex (unpublished data).

We therefore took advantage of a new technique to identify proteins in close proximity, called proximity dependent biotin identification (BioID) (Roux et al., 2012). This technique makes use of a highly promiscuous form of the *E. coli* biotin R113G ligase (BirA), which when fused to a protein of interested biotinylates proximate proteins. This allows harsh lysis conditions, biotinylated proteins can be affinity purified and analysed by Western blot or mass spectrometry. To this end, we fused BirA to myc-tagged consensus subgroup B Vpu wild-type and ELV mutant and expressed the fusion proteins in 293T tetherin cells. The cells were treated overnight with free biotin and concanamycin A to block tetherin degradation, followed by affinity purification and Western blot analysis for avidin, Vpu-myc-BirA and AP-1. Using the new BioID technique we were able to demonstrate that AP-1 interacts with Vpu wild-type in tetherin positive cells (Figure 4-15 A and B). Interestingly, this interaction was dependent on an intact **E**xxx**LV** trafficking motif in Vpu (Figure 4-15A), confirming the crystal structure data form Yong Xiong's laboratory, suggesting a role of AP-1 in Vpu-mediated tetherin antagonism.

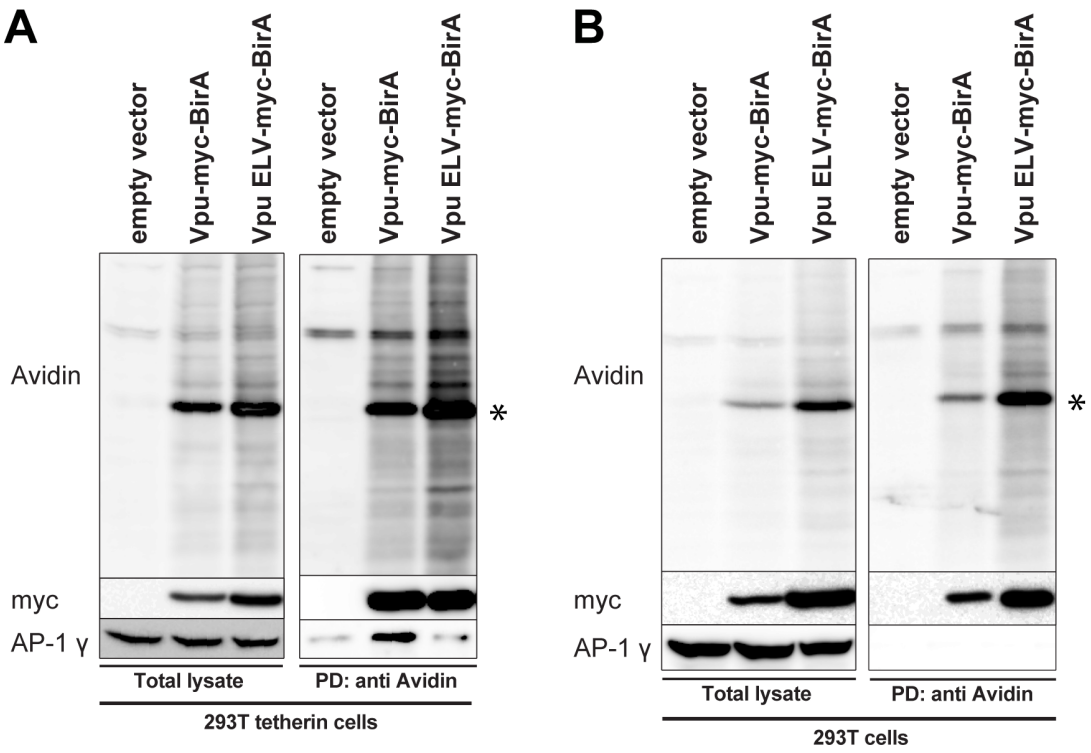

Figure 4-15 AP-1 interaction with Vpu is dependent on intact ExxxLV motif

(A) 293T tetherin cells were transfected with subgroup B Vpu-myc-BirA, Vpu ELV-myc-BirA or empty vector control. 6 hours post transfection, cells were treated with 10 nM concanamycin A in the presence of 150 μM free Biotin. 16 hours later, cells were washed, lysed, sonicated and biotinylated proteins were recovered on streptavidin-conjugated beads and analysed by Western blot for avidin, Vpu-myc-BirA and AP-1 γ. Asterisk: Vpu-myc-BirA band. **(B)** Same as in (A) but with 293T cells (performed together with Dr Toshana Foster). Same data set as presented in Figure 6-6; Western blot is cut for simplicity reasons.

4.2.8 Vpu ELV is defective for tetherin antagonism in CD4+ T cells after treatment with type I interferon

The results presented hitherto have demonstrated a requirement for the Vpu ELV motif in counteracting tetherin in cells stably expressing it or mutants thereof, and that it is required in constitutively-expressing target cells such as Jurkat to reduce surface tetherin levels. However, some studies have cast doubt as to whether tetherin degradation and/or surface reduction is essential for Vpu function (Tervo et al., 2011) (Schmidt et al., 2011). Furthermore, in contrast to 293T tetherin, release of HIV-1 Vpu ELV from HeLa was only 3-fold less efficient than wild-type in one round release (Figure 4-16A).

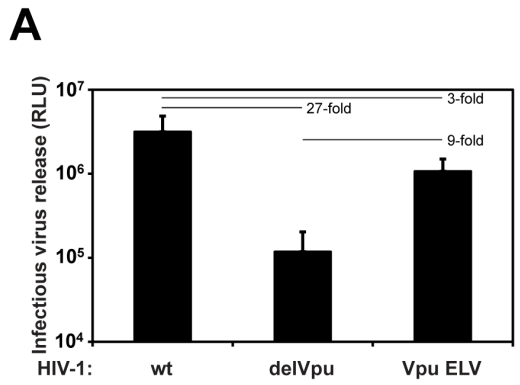

Figure 4-16 Effect of ELV mutants on HIV-1 infectious virus particle release

(A) HeLa cells were infected with VSV-G-pseudotyped stocks of the indicated virus at an MOI of 0.5. 48 hours later, the cell supernatants were harvested and infectivity determined on HeLa-TZM cells. Error bars represent the standard deviation of three independent experiments.

We therefore explored whether there was a requirement for the ELV motif in HIV-1 release from physiologically relevant target cells, namely Jurkat or primary human CD4+ T cells, particularly after treatment with type I IFN which upregulates tetherin. Infection of Jurkat at an MOI of 1 resulted in a partial defect in release of the HIV-1 Vpu ELV mutant compared to the controls (Figure 4-17 A and B). However, induction of higher tetherin expression by overnight treatment with universal type I IFN effectively reduced HIV-1 Vpu ELV particle release to levels similar to that of the Vpu-defective control while only reducing the wild-type release moderately. Similarly, interferon treatment of purified activated human CD4+ T cells led to a selective defect in the production of cell-free HIV-1 Vpu ELV virions (Figure 4-17C) consistent with a concomitant up-regulation of surface tetherin levels (Figure 4-17D), and the lack surface tetherin downregulation (Figure 4-17E). Taken together with results presented above, these data demonstrate that the ability to downregulate and degrade tetherin imparted by the **E**xxx**LV** motif is required for cell-free virion release from relevant

primary HIV target cells, and becomes essential when tetherin expression is enhanced by an antiviral stimulus.

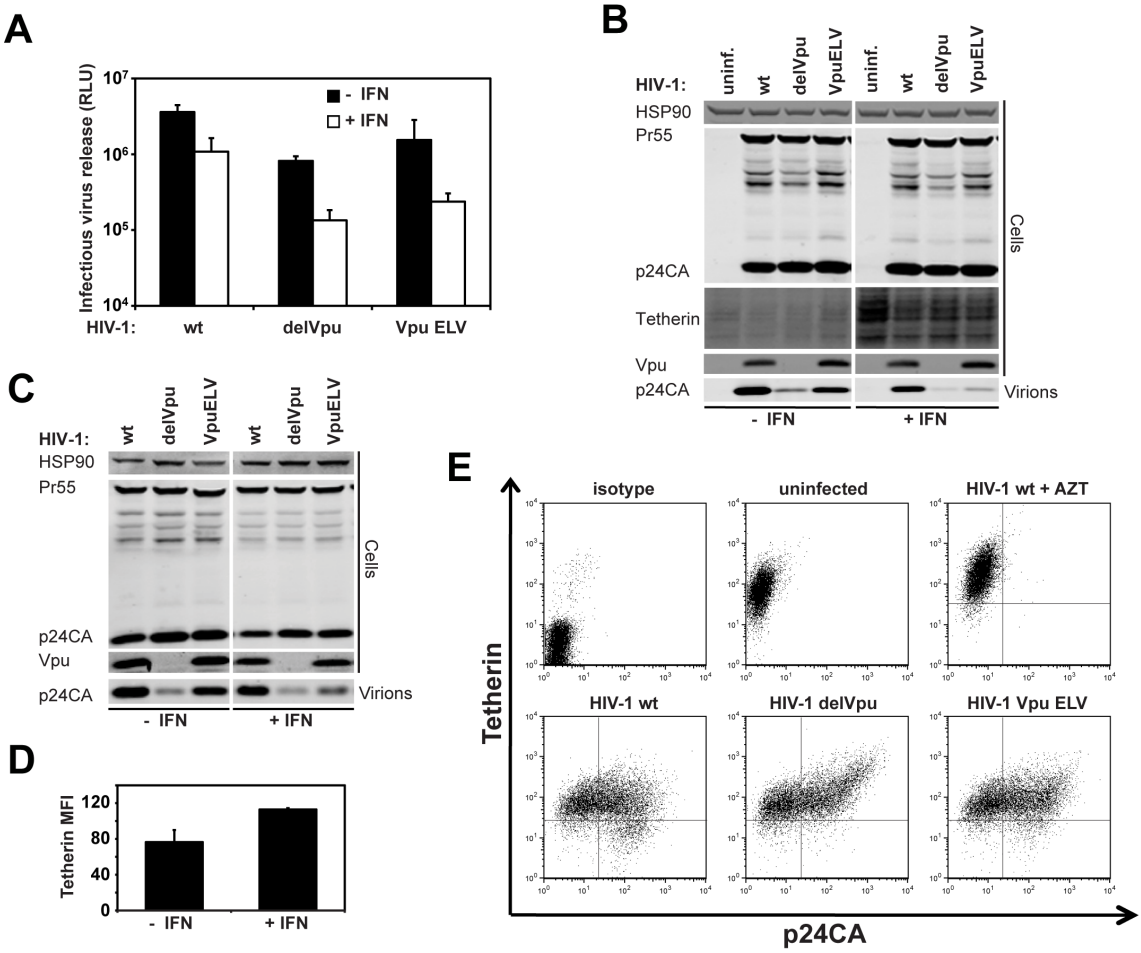

Figure 4-17 Residues E59, L63 and V64 are essential to counteract tetherin-mediated restriction of cell-free HIV-1 particle release from CD4+ T cells treated with interferon

(A and B) Jurkat cells were infected with the indicated HIV-1 mutant at an MOI of 1. 16 hours later, the cells were treated or not with 5000 U/ml universal type I IFN. Cell lysates and viral supernatants were harvested a further 24 hours later and analysed for infectivity on HeLa-TZMbl or physical particle yield and cellular viral and tetherin expression by quantitative Western blotting. Error bars represent the standard deviation of three independent experiments. **(C)** A representative example of primary human CD4+ T cells treated as in (A and B). **(D)** MFI of surface tetherin levels on these cells with or without 24 hours type I IFN treatment as analysed by flow cytometry. Error bars represent the standard deviation of three independent experiments. **(E)** Human CD4+ T cells were infected with the indicated virus. 48 hours later, cells were stained for surface tetherin and intracellular p24CA and analysed by flow cytometry.

4.3 DISCUSSION

In this chapter we have identified a determinant within the second alpha helix of the cytoplasmic tail of HIV-1 NL4.3 Vpu, **E**59xxx**L**63**V**64, which is required for efficient antagonism of tetherin. Mutation of this site blocks the ability of Vpu to mediate tetherin downregulation from the cell surface and its ESCRT-dependent degradation, but does not abolish its interaction with tetherin, nor recruitment of β-TrCP2 or the ESCRT-0 component HRS. Importantly, this motif is required to counteract tetherin in CD4+ T cells, particularly after their exposure to type I IFN. Vpu ELV mutants localise to the cell surface and early/recycling endosomal compartments rather than the TGN by virtue of their interaction with tetherin. This is consistent with a role for this determinant in Vpu-mediated inhibition of the transit of newly synthesized and/or recycling tetherin to the cell surface, its internal sequestration and targeting for endo/lysosomal degradation. Residual Vpu ELV activity against tetherin was entirely dependent on an intact recycling motif in tetherin's cytoplasmic tail, suggesting that this motif differentially affects antagonism of newly synthesized tetherin rather than pre-existing pools recycling to the PM. There has been much debate as to whether the reduction of tetherin levels at the plasma membrane is required to counteract its antiviral activity, particularly in CD4+ T cells (reviewed in (Le Tortorec et al., 2011)). In our hands, tetherin surface levels are reduced in HIV-1 infected primary T cells and Jurkat cells. However, under these conditions, the viral release phenotype of the Vpu ELV mutant is only a few fold different than the wild-type protein. Interestingly this changes upon treatment of the cells with type I IFN, which upregulates tetherin expression levels. In this case Vpu ELV mutant release is reduced almost to that of the Vpu-defective virus, but only minor further reductions are observed for the wild-type virus. This therefore indicates that the requirement for surface reduction/degradation of tetherin becomes much more important at higher expression levels of the restriction factor (something that has been suggested previously by Goffinet *et al* (Goffinet et al., 2009)). The fact that tetherin antagonism is a highly conserved attribute amongst primate immunodeficiency viruses implies its importance *in vivo*. Since interferon treatment of CD4+ T cells magnifies the defective phenotype of a Vpu ELV mutant, the ability to mediate tetherin's surface reduction and target it for endosomal degradation is likely to be essential for the virus to avoid restriction under pro-inflammatory conditions it is likely to encounter *in vivo*, particularly during acute infection (Stacey et al., 2009) (Jacquelin et al., 2009).

It is now clear that Vpu-mediated tetherin degradation is ubiquitin-dependent and occurs in lysosomes rather than early reports of proteasomal processing (Douglas et al., 2009) (Mitchell et al., 2009), and that this process requires the ESCRT pathway

(Janvier et al., 2011). Depletion of both TSG101 and VPS4 inhibits Vpu-mediated tetherin degradation, and recruitment of HRS has been reported to be required for Vpu-mediated tetherin antagonism (Janvier et al., 2011), as has ubiquitination on multiple residues in the tetherin cytoplasmic tail (Tokarev et al., 2011) (Gustin et al., 2012). However, tetherin's ultimate degradation itself is not essential for Vpu or other lentiviral countermeasures to inactivate its function. Our recent observations with the novel ESCRT-I subunit, UBAP1, (Chapter 5 and the results presented herein), demonstrate that ESCRT-I function is unlikely to be required for tetherin antagonism, but its commitment to endosomal degradation is. Interestingly, the concomitant enhancement of wild-type Vpu levels, both co-precipitating with tetherin and at steady state, suggest that Vpu is likely co-degraded with its target. Alongside the current literature our data suggests that Vpu interaction with tetherin leads to a differential trafficking of tetherin in the TGN and/or recycling compartments rather than enhancing tetherin internalisation (Figure 7-1). This inhibits forward trafficking of either recycling or newly synthesized tetherin to the PM, and commits it to a pathway that ultimately targets it to endo/lysosomal compartments for degradation. We suggest that it is this commitment, regulated by the **E**xxx**LV** motif in second helix, rather than degradation *per se*, that is principally responsible for antagonizing tetherin. Where Vpu interacts with tetherin in the cell is likely to be related temporally to the viral replication cycle, tetherin expression level, and its natural turnover rate. Vpu is expressed ''late'' in replication from the same mRNA as Env (reviewed by (Dubé et al., 2010a)), at the time new virions are being built. Thus, Vpu must deal with two pools of tetherin: pre-existing protein in the periphery recycling via the TGN (Rollason et al., 2007) and *de novo* synthesized tetherin trafficking through the Golgi *en route* from the ER to the surface. Therefore we predict that Vpu must interact with tetherin in TGN associated compartments to engage these two pools of tetherin, although our recent data suggests that binding to newly synthesized tetherin may occur prior to this in the ER (Vigan and Neil, 2010). Thereafter, a sorting event determined by the second alpha helix, **E**xxx**LV** motif, precludes Vpu/tetherin complexes transiting to the PM. This intracellular sequestration of tetherin is further coupled to late endosomal targeting and ESCRT-dependent degradation through the recruitment of HRS and tetherin ubiquitination (Tokarev et al., 2011) (Janvier et al., 2011). In line with this, global disruption of early to late endosomal transition by dominant negative Rab7a also appears to inhibit Vpu activity (Caillet et al., 2011). Interestingly, ubiquitinated cargo destined for ESCRT-dependent degradation via HRS recruitment has been shown to partition differentially to areas of early/sorting endosomal membranes rich in flat clathrin lattices, thereby anchoring it away from the recycling machinery (Raiborg et al., 2006). Recruitment of tetherin into such structures in the sorting compartment may be

sufficient to antagonize its function. In the absence of the **E**xxx**LV** motif, tetherin is not committed to this differential sorting in the TGN, and Vpu/tetherin complexes are targeted to the cell surface and thereafter back into the recycling system, accounting for the localisation of Vpu ELV in infected cells and its incorporation into virions. Therefore, in addition to acting as an adaptor for the recruitment of ESCRT-0 and E3 ubiquitin ligase activity to tetherin, we propose that through the **E**xxx**LV** motif, Vpu directly chaperones associated tetherin molecules into an endosomal compartment from which they cannot recycle to the PM. **E**xxx**LV** mutants retain some residual antagonistic activity that is entirely dependent on the AP-1/AP-2-binding motif in tetherin. This would suggest that the action of the **E**xxx**LV** motif does not solely account for the inhibition of tetherin by Vpu. Vpu ELV still interacts with β-TrCP2, suggesting that tetherin ubiquitination, which is important for counteracting its activity (Tokarev et al., 2011), may still take place during the recycling process and effect antiviral function. Also physical interaction between Vpu and tetherin may be sufficient to interfere with some level tetherin function provided tetherin can still associate with the clathrin-dependent endocytic machinery.

Furthermore, we were able to functionally complement Vpu function by grafting the **D**/**E**xxx**L**(**L**/**I**/**M**) motif from HIV-1 Nef in place of helix-2, we could detect no effect of depletion of the canonical clathrin adaptor proteins AP-1, AP-2 or AP-3 on Vpu-mediated tetherin antagonism. The inhibition by AP180c overexpression, however, implicates clathrin function in Vpu-mediated tetherin antagonism. These results are in contrast to the recent study by Lau e*t al* who were unable to demonstrate a phenotype for an LV63,64AA mutant despite interfering with Vpu activity with AP180c (Lau et al., 2011). Given that we have demonstrated phenotypes in several cellular systems including CD4+ T cells for the Vpu ELV mutant, the reason for this discrepancy is unclear.

The **D**/**E**xxx**L**(**L**/**I**/**M**) motif is conserved in Vpu proteins from HIV-1 M group subtypes A, B, D, G and H (Figure 4-10A). While Group O Vpus cannot antagonize tetherin (Sauter et al., 2009), this maps to defective TM domain-mediated interaction and the membrane proximal hinge region. When replaced by those from a Group M Vpu these are sufficient to confer tetherin inactivation implying that C-terminal determinants retain function (Vigan and Neil, 2011). In Group M clades C and F, the equivalent position is (**D**/**E**)xxx**L**(**S**/**A**) respectively, suggesting that the site may not be functional in those Vpus, with the caveat that the second position in the dileucine motif is less important. Intriguingly, both these subtypes bear **EY**xx**L**(**L**/**I**) motifs in the membrane proximal region of their cytoplasmic tails that encompass both a putative tyrosine and dileucine-based sorting sequence. Evidence from Ruiz *et al* (Ruiz et al., 2008) has shown that a

model subtype C Vpu localises to the PM rather than the TGN and that this is in part due to this motif. While LL mutations in this subtype C Vpu confer T cell line replication phenotypes suggestive of a failure to downmodulate tetherin, no direct experiments on the role of this motif in tetherin-mediated HIV-1 release have been thus far performed, nor whether this site can bind known clathrin adaptors.

The context dependency of **D**/**E**xxx**L**(**L**/**I**) motifs that governs which adaptor they bind to *in vivo* is poorly defined at present, meaning that RNAi depletion is the most reliable method for identifying the cellular factor involved. While individual depletion of AP-1, 2 or 3 in our experiments had no effect on Vpu-mediated tetherin antagonism, replacement of the second alpha helix with the promiscuous AP-binding peptide from HIV-1 Nef did recover function. This site in Nef is essential for several functions including CD4 and MHC class I downregulation, the former being AP-2-dependent (Chaudhuri et al., 2007), the latter requiring AP-1 (Lubben et al., 2007). Importantly, binding of AP-2 to this site in SIV Nef proteins is required for their counteraction of non-human primate tetherins (Zhang et al., 2011a). Thus, there are several possibilities. The **E**xxx**LV** motif in Vpu might be a promiscuous AP-binding site and adaptor usage may be redundant. The subcellular localisation of tetherin/Vpu ELV complexes in EEA1-positive endosomes and the partial effect of dominant negative dynamin 2 would argue against a significant role for AP-2, the major regulator of clathrin-mediated transport from the plasma membrane. However, toxicity associated with simultaneous knockdown of multiple adaptors has precluded us from addressing this possibility so far. A novel approach to study clathrin adaptor-mediated trafficking using a rapamycin induced protein dimerisation together with trapping these proteins on mitochondria named “knocksideways” has been described by Margret Robinson (Robinson et al., 2010). This method overcomes artefacts induced by prolonged clathrin adaptor knockdown, in which other adaptor proteins are able to compensate and mask the real phenotype. However, this method requires rapamycin treatment that is toxic to cells if used for a longer period of time, which would be necessary to study Vpu-mediated virus particle release.

Vpu activity was insensitive to retromer (VPS26) depletion, which is essential for endosome to TGN retrieval and recycling (reviewed by (Attar and Cullen, 2010)), we suggest that Vpu targets tetherin into the ESCRT-dependent degradative pathway from the TGN to endosomal compartments, and an ensuing swift degradation accounts for the observed sequestration in TGN46-positive compartments. In the absence of the **E**xxx**LV** motif, tetherin is not committed to this differential sorting in the TGN, and Vpu/tetherin complexes are targeted to the cell surface and thereafter back into the

recycling system, accounting for the localisation of Vpu ELV in infected cells and its incorporation into virions.

Alternatively, replacement of the second alpha helix with the Nef peptide recovers function because it confers AP-2 binding to Vpu, thus allowing Vpu to counteract tetherin in a manner similar to SIV Nef and HIV-2/SIV Envs that both require AP-2 interactions (Noble et al., 2006) (Le Tortorec and Neil, 2009) (Zhang et al., 2011a) (Serra-Moreno et al., 2011). However, these data do underscore that linking Vpu to the clathrin trafficking machinery promotes its ability to counteract tetherin. If Vpu-mediated tetherin antagonism is clathrin-dependent, but independent of AP-1, AP-2 or AP-3, what other adaptors might be important? Two further heterotetrameric adaptors, AP-4 and AP-5, have been identified, but understanding of their role in subcellular trafficking is limited, siRNA depletion of AP-4 or AP-5 had no effect virus particle release (data not shown), and at present they are not known to bind to acidic dileucine motifs or to control clathrin-mediated transport (reviewed by (Bonifacino and Traub, 2003)) (Hirst et al., 2011). The monomeric GGA1, -2, and -3 proteins also function as clathrin adaptors that regulate Golgi to endosome transport are potentially attractive candidates, whose dysregulation has been reported to inhibit HIV-1 assembly (Joshi et al., 2008). However, known GGA binding motifs in cellular cargoes correspond to a **D**xx**LL** consensus where the spacing of the leucines from the acidic residue is thought critical and overexpression of GGA1, GGA2 or GGA3 had only minor effects on Vpu-mediated virus particle release (Chapter 6).

We have so far been unable to demonstrate direct interaction between the Vpu **E**xxx**LV** motif and adaptors AP-1, 2 or 3 that are known to bind acidic dileucine signals via a hemicomplex of their σ and adaptin subunits (reviewed by (Bonifacino and Traub, 2003)). These interactions have been demonstrated in yeast 3-hybrid assays previously for HIV-1 Nef (Janvier et al., 2003) (Chaudhuri et al., 2007), but not all interactions are amenable to this method and in our hands the Vpu cytoplasmic tail is a constitutive activator of transgene expression precluding its use. Furthermore, the low affinity of these interactions, their transient nature, and the complex interactions of the adaptor protein with membrane lipids means that adaptor binding is rarely measurable in co-precipitations from cells.

Crystal structure data presented at the 2013 CSH Retrovirology meeting revealed that the σ and γ subunits of AP-1 bind to the Vpu **E**xxx**LV** motif while the **Y**D**Y** motif in tetherin binds to the μ subunit which in turn recruits the β subunit of the AP-1 complex. We therefore applied the new technique BioID to study Vpu/tetherin and AP-1 interactions. Vpu was able to interact with AP-1 in the presence of tetherin that was

dependent on an intact **E**xxx**LV** motif in the second alpha helix of Vpu. Advantages using this technique are: detection of protein interactions in their cellular context, biotinylation occurs before solubilisation therefore it should detect both weak and transient interactions Disadvantages are: interactions might be indirect or even vicinal and biotinylation might not be able to cross-link proteins that interact via their transmembrane domains. Clearly, a more detailed analysis of the functional requirements of these clathrin adaptors in particular AP-1 in Vpu/tetherin complex trafficking is required and siRNA depletion studies particularly of clathrin adaptors should always be combined with biochemical approaches.

Chapter 5 HIV-1 Vpu-mediates ESCRT-dependent degradation of tetherin

Some of the results presented in this chapter were published in collaboration with Monica Agromayor from Juan Martin-Serrano's research group as "The UBAP1 Subunit of ESCRT-I Interacts with Ubiquitin via a SOUBA Domain" (Agromayor et al., 2012).

5.1 INTRODUCTION

Recently, HIV-1 Vpu-mediated tetherin lysosomal degradation has been shown to be dependent on the ESCRT machinery (Janvier et al., 2011). The ESCRT-0 component HRS (also known as hepatocyte growth factor-regulated tyrosine kinase substrate (HGS)) recognizes ubiquitinated cargo proteins in the endosome membrane and prevents their cellular recycling and retrograde trafficking. HRS then recruits the ESCRT-I component TSG101 via a PSAP motif and therefore induces deformation of the endosomal membrane, invagination of cargo proteins and final abscission forming intraluminal vesicles (ILVs) (discussed in detail in 1.9). However, HRS is not required for HIV-1-related budding events (Pornillos et al., 2003). Another group was able to demonstrate that tetherin itself is routed for ESCRT-dependent lysosomal degradation, and upon Vpu expression this degradation is enhanced. They were also able to show that HRS interacts with both Vpu and tetherin in co-immunoprecipitation studies. Knockdown of HRS revealed a role in tetherin surface downregulation, degradation as well as tetherin-mediated restriction of virus particle release (Janvier et al., 2011). Data from the same group showed that the late endosomal small GTPase Rab7A, which is key regulatory protein which is important for biogenesis and maintenance of the structure of late endosomal and lysosomal compartments, plays a role in Vpu-mediated antagonism of tetherin (Caillet et al., 2011).

In this chapter we have examined the role of the ESCRT pathway in endosomal sorting of tetherin-mediated by HIV-1 Vpu, concentrating on the newly identified mammalian ESCRT-I component UBAP1. UBAP1 contains a region that is highly conserved in MVB12 and this region has been termed a UBAP1-MVB12-associated (UMA) domain (de Souza and Aravind, 2010). UBAP1 has been shown to be part of a complex with ESCRT-I subunits TSG101 and VPS37, and be involved in endosomal sorting of ubiquitinated cargo but not in cytokinesis (Stefani et al., 2011). A postdoctoral fellow in the laboratory, Dr Suzanne Pickering, performed a single genome analysis of *vpu*

genes from individuals infected with HIV-1 and tested all unique Vpus for their ability to downregulate CD4 and antagonise tetherin (Pickering et al., 2014). In this chapter we also investigate the virological phenotype of one naturally occurring HIV-1 clade B Vpu that bears mutants in the first alpha helix that are important for Vpu anti tetherin function.

Our results show that newly identified ESCRT-I component UBAP1 is essential for Vpu-mediated tetherin lysosomal degradation and that Vpu is able to counteract tetherin virus restriction in UBAP1 depleted cells. Furthermore, in this chapter we were able to show that the hydrophobic residues in Vpu cytoplasmic helix 1 are essential for Vpu/HRS interaction and that this interaction is dependent on residues that bind ubiquitin in the double ubiquitin-binding motif (DUIM) of HRS. Interestingly, Vpu/HRS interaction in the presence or absence of tetherin is independent of β-TrCP2, the only know E3 ubiquitin ligase known to interact with HIV-1 Vpu. Additionally, we were able to demonstrate, by siRNA interference that ALIX, and by overexpression that GGA1, -2 and -3 do not affect Vpu-mediated tetherin degradation and countermeasures.

5.2 RESULTS

5.2.1 ESCRT-I component UBAP1 is essential for tetherin degradation

The ESCRT machinery plays a role in sorting of ubiquitinated membrane proteins for lysosomal degradation and virus budding (see 1.9). Here we test the role of a novel ESCRT-I component UBAP1 in Vpu-mediated tetherin degradation. UBAP1 has recently been shown to interact with ESCRT-I components TSG101, VPS28, and VPS37, and to be required for ESCRT-mediated endosomal sorting of the EGFR but not cytokinesis (Stefani et al., 2011) (Agromayor et al., 2012). Furthermore, recent data has shown that Vpu-mediated tetherin degradation is dependent on ESCRT-I component TSG101 and ATPase VPS4 (Janvier et al., 2011). VPS4 is thought to mediate stepwise removal of ESCRT-III and generates constrictive forces that are crucial for abscission. TSG101 is also recruited to sites of budding virions by interacting with the major structural virus protein gag, which in turn recruits ESCRT-III. Failure to recruit TSG101 leads to accumulation of budding-deficient virus particles at the plasma membrane.

To this end, 293T tetherin cells were treated twice over a period of 48 hours with non-coding siRNA or two different siRNA oligonucleotides directed against UBAP1, and infected with HIV-1 wild-type or HIV-1 delVpu. 48 hours post infection, cells were lysed and tetherin was immunoprecipitated, de-glycosylated, and visualised by Western blot. As expected, cells transfected with non-targeting control and infected with HIV-1 wild-type had greatly reduced tetherin levels (Figure 5-1A). However, in cells depleted for UBAP1 and infected with HIV-1 wild-type tetherin degradation was prevented and tetherin amounts similar to uninfected cells could be detected. Tetherin levels in cells infected with HIV-1 delVpu and treated with siRNA directed against UBAP1 were, as expected, also high and similar to uninfected cells. Next, we looked at post-translational modifications of tetherin in cells depleted for UBAP1, using a similar approach as above with cells transfected also with a fixed dose of HA-ubiquitin. Tetherin was highly ubiquitinated in cells infected with HIV-1 wild-type and depleted for UBAP1 when compared to cells treated with non-targeting control (Figure 5-1B). This data suggests that ubiquitin-dependent sorting of tetherin by the ESCRT-dependent MVB pathway is inhibited when UBAP1 is depleted.

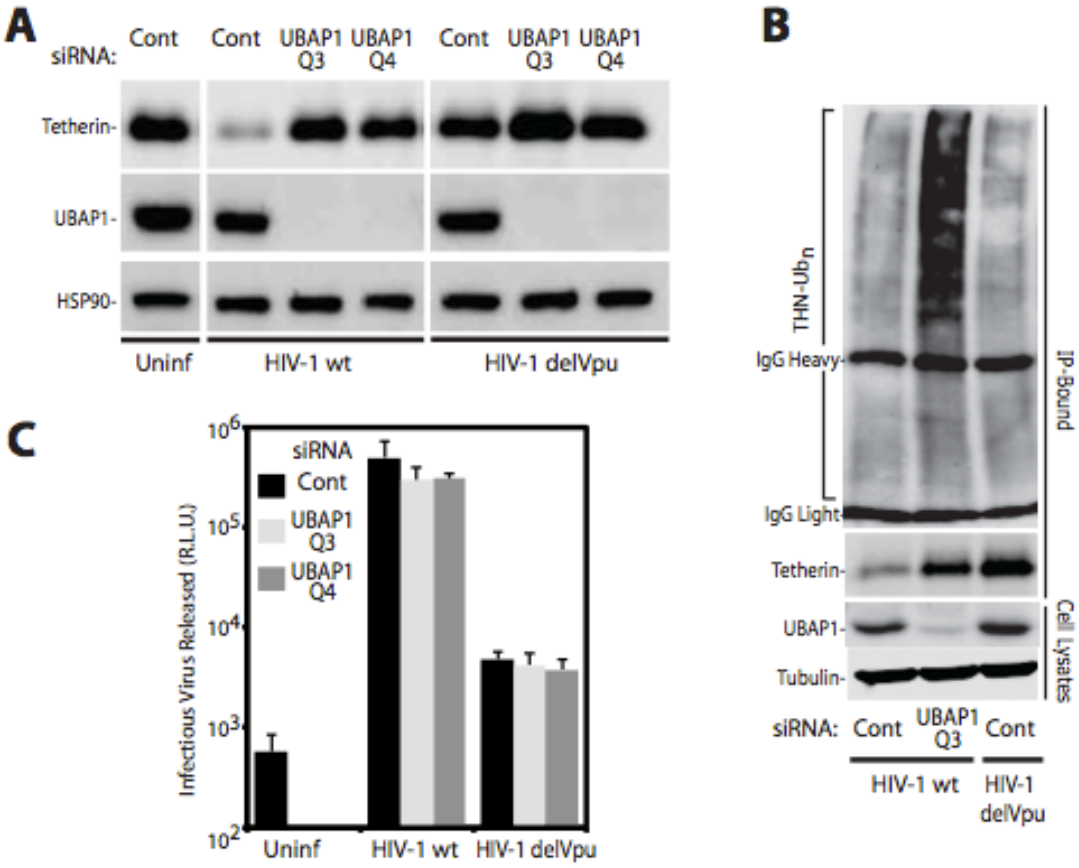

Figure 5-1 UBAP1 is essential for Vpu-mediated degradation of tetherin

(A) 293T tetherin expressing cells were transfected twice over a 48 hour period with siRNA oligonucleotides directed against UBAP1 or non-targeting control. The cells were then infected with HIV-1 wild-type or HIV-1 delVpu at an MOI of 2. 48 hours later, cells were lysed, immunoprecipitated with anti-tetherin antibody and de-glycosylated. Total cell lysates and precipitates were subjected to SDS-PAGE and analysed by Western blotting for tetherin, UBAP1 and HSP90, and analysed by ImageQuant. **(B)** 293T tetherin cells were treated as in (A) and cells were then transfected with a HA-ubiquitin expression vector and infected with HIV-1 wild-type or HIV-1 delVpu at an MOI of 2. 48 hours later, cells were lysed, immunoprecipitated with anti-tetherin antibody and de-glycosylated. Total cell lysates and precipitates were subjected to SDS-PAGE and analysed by Western blotting for tetherin, UBAP1 and Tubulin, and analysed by ImageQuant. **(C)** 293T tetherin cells were treated as in (A) and infected with HIV-1 wild-type or HIV-1 delVpu at an MOI of 0.8. 48 hours post infection, infectivity of viral supernatants was assayed on HeLa-TZMbl reporter cells. Infectious virus release was plotted as β-galactosidase activity in relative light units (RLU). Error bars represent the standard deviation of three independent experiments.

The infectivity of supernatant containing virions from cells treated with UBAP1 siRNA and infected with HIV-1 wild-type or HIV-1 delVpu at an MOI of 0.8 was measured on HeLa-TZMbl indicator cells. Surprisingly, despite the block of tetherin degradation in UBAP1 depleted cells infected with wild-type HIV-1, release of infectious virus particles was not affected (Figure 5-1C). However, virus particle release from HIV-1 delVpu infected cells was approximately 100-fold less compared to HIV-1 wild-type infected tetherin expressing cells (Neil et al., 2008), and UBAP1 knockdown did not affect virus release.

Another approach to determine to role of UBAP1 in Vpu induced tetherin degradation, was to visualise cellular localisation of tetherin in UBAP1 depleted cells. To this end, 293T tetherin cells were treated twice over a period of 48 hours with non-coding siRNA or siRNA directed against UBAP1, and infected with HIV-1 Nef IRES GFP. 48 hours post infection, cells were fixed and stained for tetherin in combination with CD63 (late endosomes) or FK2 (ubiquitin) subcellular markers. As expected, tetherin levels in HIV-1 infected cells treated with non-targeting siRNA were largely reduced. Consistent with inhibition of tetherin degradation and accumulation of ubiquitinated forms of tetherin in UBAP1 depleted cell, as shown in Figure 5-1 A and B, tetherin accumulated in intracellular structures that show co-localisation with the late endosomal marker CD63 (Figure 5-2A) and with the ubiquitin marker FK2, which detects both mono- and poly-ubiquitinated proteins but not free ubiquitin (Figure 5-2B). Collectively, Vpu-mediated ESCRT degradation of tetherin is dependent on UBAP1, while ultimate degradation of tetherin is separable from the ability of Vpu to counteract the anti-viral activity of tetherin. These results suggest, that Vpu interacts with tetherin prior to the recruitment of ESCRT-I, and inactivates tetherin by committing it to an early/late endosomal pathway from which it cannot escape.

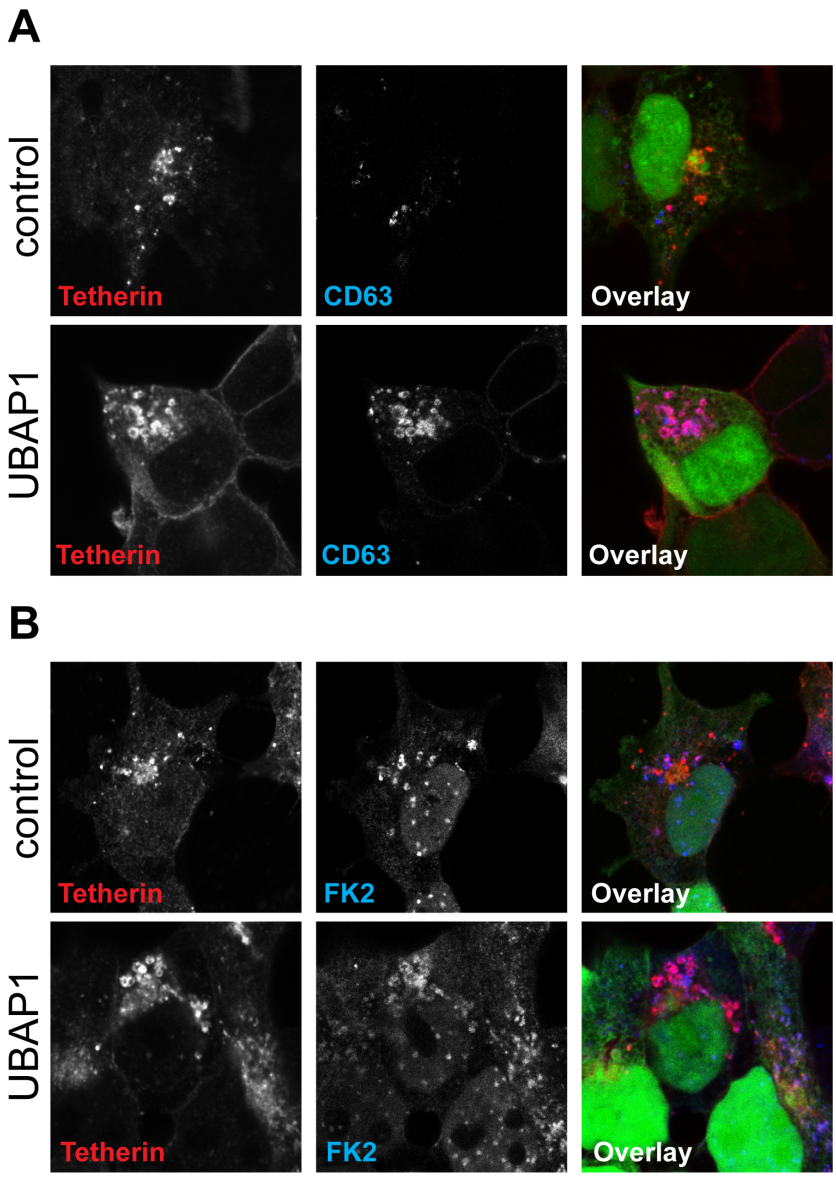

Figure 5-2 UBAP1 depletion induces tetherin accumulation in late endosomal compartments

(A) 293T tetherin cells were transfected twice over a 48 hour period with siRNA oligonucleotides directed against UBAP1 or non-targeting control and infected with VSV-G-pseudotyped HIV-1 Nef IRES GFP at an MOI of 0.5. 24 hours post transfection, cells were fixed and stained for tetherin (red) and late endosomes (CD63 antibody) (blue) and examined by fluorescent microscopy. Panels are of representative examples. **(B)** HeLa cells were transfected as in (A) and stained for tetherin (red) and ubiquitin (FK2 antibody) (blue) and examined by fluorescent microscopy. Panels are representative examples of 10 visualised cells.

5.2.2 A derivative of naturally occurring HIV-1 clade B Vpu mutant is unable to counteract tetherin function

Single genome analysis of *vpu* genes from individuals infected with HIV-1 clade B revealed that two isoleucine residues (I43 and I46) in the first alpha helix are important for Vpu anti-tetherin function (Figure 5-3, I43/I46 mutant is encircled in red). To investigate the effects of these naturally occurring helix 1 Vpu mutants on tetherin function, in a replicating competent molecular clone, we replaced hydrophobic amino acids leucine/isoleucine 41/42 and leucine/isoleucine 45/46 in the HIV-1 NL4.3 Vpu protein with nonpolar alanine residues.

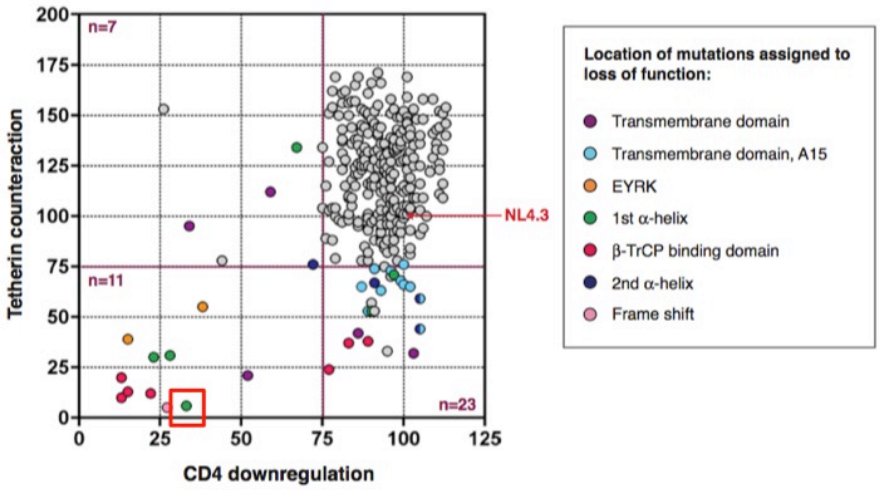

Figure 5-3 Functional analysis of HIV-1 clade B patient Vpu proteins

Functional profiles for 304 tested HIV-1 clade B patient Vpus shown as tetherin antagonism vs CD4 downregulation. Functionality was measured as percentage of NL4.3 Vpu activity (see red arrow). Defects are pinpointed to responsible amino acid changes and each defective Vpu protein is colour-coded according to the location of inactivating amino acid change, as shown in the key (adapted from (Pickering et al., 2014))

We then assayed these Vpu mutants, termed Vpu LILI, for their ability to counteract tetherin restriction. 293T cells were transfected with a fixed dose of either wild-type HIV-1 provirus NL4.3 (NL4.3 wild-type), Vpu-defective NL4.3 (NL4.3 delVpu), Vpu LILI mutant (NL4.3 Vpu LILI), Vpu ELV trafficking mutant (NL4.3 Vpu ELV) or Vpu S52/56A phosphorylation mutant (NL4.3 Vpu 2/6A) (Figure 5-4A) and examined for viral release in the presence of increasing tetherin concentrations. 48 hours after transfection, cell lysates and supernatants containing viral particles were harvested and analysed for viral infectivity on HeLa-TZMbl reporter cells (Figure 5-4B) or physical virus yield by Western blot (Figure 5-4C). As expected, the infectivity and supernatant viral particle yield were both profoundly reduced with increasing tetherin expression in NL4.3 Vpu deficient provirus compared to the NL4.3 wild-type counterpart. NL4.3 Vpu LILI provirus was prominently defective in the presence of increasing amounts of tetherin,

comparable to the trafficking and phosphorylation defect of NL4.3 Vpu ELV and Vpu 2/6A respectively. All tested Vpu mutants however displayed a residual activity against tetherin when compared to the Vpu deletion mutant (Figure 5-4 B and C). Next we wanted to know if the hydrophobic amino acids could be found in multiple HIV-1 clades. Sequences were obtained from the Los Alamos database (www.hiv.lanl.gov), and we generated LogoPlots covering the first alpha helix of HIV-1 subgroups A, B, C, D, G and H. This revealed that the leucine and isoleucine residues are highly conserved throughout different HIV-1 group M clades (Figure 5-4D). However, these amino acid sequences slightly deviate from the NL4.3 Vpu protein as this Vpu contains an additional isoleucine residue.

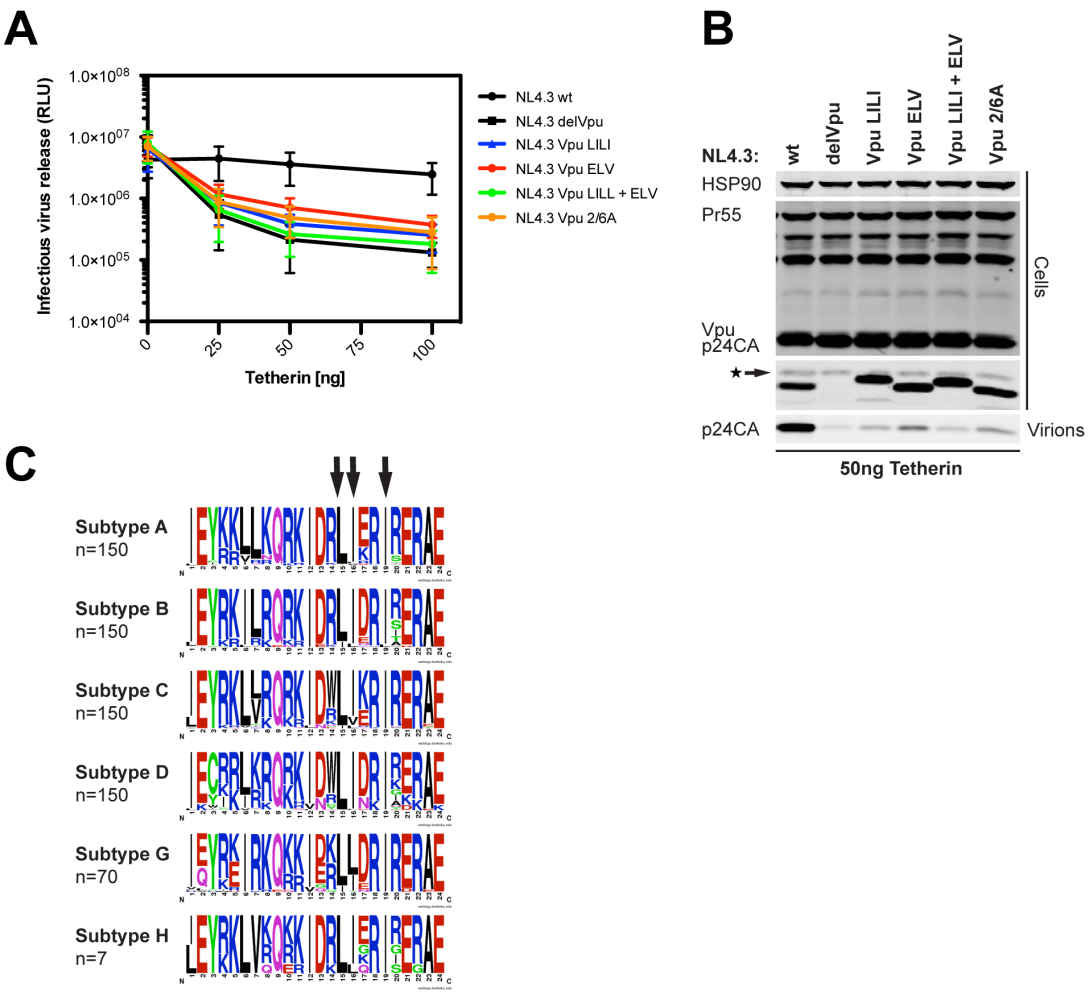

Figure 5-4 Naturally occurring Vpu LILI mutant is required for tetherin antagonism

(A) L41A I42A L45A I46A mutations were introduces into the NL4.3 *vpu* gene referred to as NL4.3 Vpu LILI. 293T cells were transfected with NL4.3 wild-type, NL4.3 delVpu, NL4.3 Vpu LILI, NL4.3 Vpu ELV or NL4.3 Vpu 2/6A together with increasing concentrations of pCR3.1 tetherin-HA expression plasmid. Infectivity of viral supernatants was assayed on HeLa-TZMbl reporter cells. Infectious virus release was plotted as β-galactosidase activity in relative light units (RLU). Error bars represent the standard deviation of three independent experiments. **(B)** Cell lysates and sucrose purified viral supernatants form 50 ng tetherin input were subjected to SDS-PAGE and analysed by Western blotting for Hsp90, HIV-1 p24CA and Vpu, and analysed by LiCor quantitative imager. **(C)** LogoPlots of first alpha helix of the Vpu cytoplasmic tail from HIV-1 subgroup M clades A, B, C, D, G and H generated from sequences obtained from the Los Alamos database (www.hiv.lanl.gov).

We then characterized the phenotype of Vpu LILI mutants further and examined the ability of Vpu LILI to down-modulate tetherin from the plasma membrane. HeLa-TZMbl cells were transfected with the indicated Vpu-HA expression vectors in combination with a GFP expression plasmid. 48 hours post transfection, tetherin surface levels were analysed by flow cytometry in GFP positive cells (Figure 5-5A). As expected, Vpu wild-type reduced tetherin levels at the plasma membrane, but Vpu LILI mutants were defective in reducing tetherin surface levels. The Vpu LILI defect on tetherin cell surface down-regulation was more apparent than the deficiencies of mis-localised Vpu ELV or Vpu 2/6A mutants, which is unable to recruit the E3 ubiquitin ligase β-TrCP2 (Figure 5-5A). It has been demonstrated that Vpu stimulates ubiquitination and ESCRT-dependent degradation of tetherin via lysosomal compartments. Therefore we examined the ability of Vpu LILI to induce tetherin degradation. 293T cells stably expressing tetherin were infected with VSV-G-pseudotyped HIV-1 wild-type, HIV-1 delVpu, HIV-1 Vpu LILI, HIV-1 Vpu ELV or HIV-1 Vpu 2/6A at an MOI of 2 to ensure high infection rates. The cells were lysed 48 hours after infection and Western blotting was performed for cellular tetherin levels (Figure 5-5B). As expected, tetherin levels at steady state were reduced in cells infected with HIV-1 wild-type compared to uninfected cells and cells infected with HIV-1 delVpu. Interestingly, tetherin levels in cells treated with HIV-1 Vpu LILI were not reduced (Figure 5-5B), implicating that Vpu LILI is unable to induce tetherin degradation like the Vpu ELV and 2/6A mutants.

The failure of Vpu LILI mutants to degrade tetherin molecules may be due to the inability of LILI mutants to bind to tetherin or other known cellular co-factors. To address the first question we took advantage of the fact that tetherin degradation, but not antagonism, is completely dependent on the ESCRT-I component UBAP1 (Agromayor et al., 2012). Using siRNA directed against UBAP1 we were able to block Vpu-mediated tetherin degradation and perform immunoprecipitation studies using infected cells (Figure 5-5C). 293T tetherin expressing cells were treated twice over a period of 48 hours with non-coding siRNA or siRNA oligonucleotides directed against UBAP1 and infected with HIV-1 wild-type, HIV-1 Vpu LILI, HIV-1 del Vpu or HIV-1 Vpu A14L W22A, a Vpu mutant that renders mutations in the Vpu interface which is important for tetherin binding (Vigan and Neil, 2010) (Skasko et al., 2012). 48 hours post infection, cells were lysed, tetherin immunoprecipitated and analysed by Western blotting for Vpu (Figure 5-5C). As shown in the previous chapter, Vpu wild-type was detected in cells associated with tetherin, blocking of Vpu/tetherin complex degradation using UBAP1 depletion enhanced this effect, whereas Vpu A14L/W22A failed to interact with tetherin under these conditions. The amount of Vpu LILI precipitated in cells treated with non-targeting siRNA was (approximately 4-fold) higher compared to

the wild-type protein. Interestingly, the relative band intensity ratio determined by Western blotting of Vpu LILI and wild-type Vpu in cells depleted for UBAP1 and immunoprecipitated for tetherin was the same. This demonstrates that Vpu LILI mutants are able to interact with tetherin to the same extent as the wild-type protein. Indicating that the defect in tetherin degradation and surface downregulation is independent of tetherin binding. Since tetherin degradation has also been shown to be dependent on the ubiquitination of the tetherin intracellular domain by the E3 ubiquitin ligase β-TrCP2, which binds to Vpu via a phosphorylated pair of serine residues in the cytoplasmic tail of Vpu (S52 and S56) (Figure 5-4A) (Margottin et al., 1998) (Mitchell et al., 2009) (Mangeat et al., 2009), we tested binding of Vpu LILI mutants to the E3 ubiquitin ligase β-TrCP2 next (Figure 5-5D). 293T cells were transfected with myc-β-TrCP2 in combination with Vpu-HA or indicated mutant. 48 hours post transfection, cells were lysed and immunoprecipitated using an anti myc antibody and analysed by Western blot. As expected, Vpu was co-immunoprecipitated with myc-β-TrCP2 while the phosphorylation mutant Vpu 2/6A was not. Interestingly, Vpu LILI was co-precipitated with a similar efficiency to the wild-type Vpu protein (Figure 5-5D), therefore ruling out a defect in tetherin/β-TrCP2 interaction as a cause for the Vpu LILI phenotype defect.

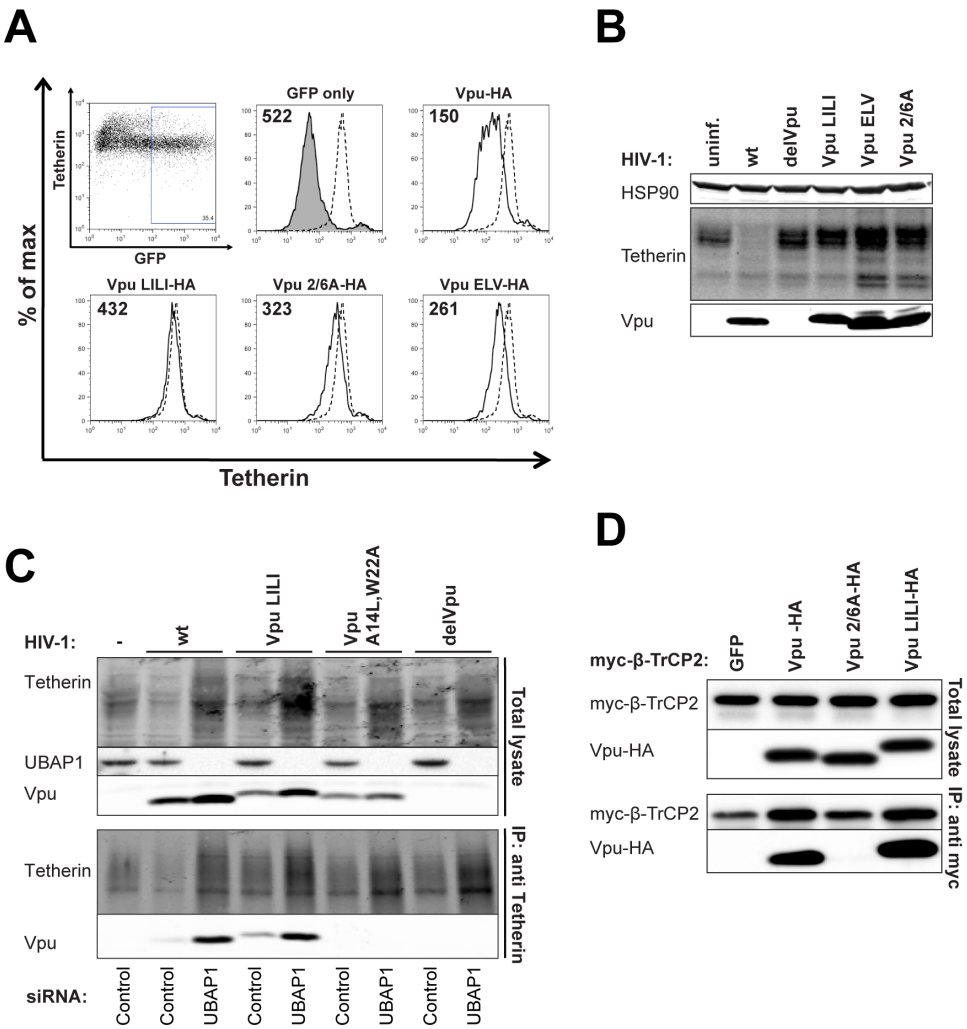

Figure 5-5 Vpu LILI mutants are defective for tetherin cell surface downregulation and degradation

(A) HeLa-TZMbl cells were co-transfected with pCR3.1 Vpu-HA or indicated mutant and a GFP expression vector. Cell-surface tetherin levels were analysed 48 hours post transfection by flow cytometry. GFP positive cells were gated and tetherin levels (solid lines) were compared to un-transfected cells or transfected with indicated Vpu (dotted lines). Numbers indicate median fluorescence intensities of endogenous tetherin surface levels. The solid peak in the upper histogram in the middle of the panel represents binding of the isotype control. **(B)** HeLa cells were infected with VSV-G-pseudotyped HIV-1 wild-type, HIV-1 delVpu, HIV-1 Vpu LILI, HIV-1 Vpu ELV or HIV-1 Vpu 2/6A at an MOI of 2. 48 hours post infection, cell lysates were subjected to SDS-PAGE and analysed by Western blotting for Hsp90, tetherin and Vpu, and analysed by LiCor quantitative imager. **(C)** 293T tetherin expressing cells were transfected twice over a 48 hour period with siRNA oligonucleotide directed against UBAP1 or non-targeting control. The cells were then infected with HIV-1 wild-type, HIV-1 Vpu LILI, HIV-1 Vpu A14L W22A or HIV-1 delVpu at an MOI of 2. 48 hours later, cells were lysed and immunoprecipitated with anti-tetherin antibody. Total cell lysates and precipitates were subjected to SDS-PAGE and analysed by Western blotting for tetherin, UBAP1 and Vpu, and analysed by ImageQuant. **(D)** 293T cells were transfected with pCR3.1 Vpu-HA or indicated mutant in combination with a pCR3.1 myc-β-TrCP2 expression vector. 48 hours post transfection, cells were lysed and immunoprecipitated with anti-myc antibody. Total cell lysates and precipitates were subjected to SDS-PAGE and analysed by Western blotting for myc-β-TrCP2 and Vpu-HA, and analysed by ImageQuant.

5.2.3 ESCRT-0 component HRS is involved in Vpu-mediated virus release

HRS binds to ubiquitinated cargo proteins that are delivered for lysosomal degradation, and Vpu has been shown to promote tetherin ubiquitination and to co-precipitate with HRS (Janvier et al., 2011). We therefore tested whether Vpu LILI mutants were defective for interaction with HRS in co-immunoprecipitations in transfected 293T or 293T cells stably expressing tetherin. As expected, Vpu wild-type and Vpu ELV were co-precipitated with HRS in the presence or absence of tetherin (Figure 5-6 A and B). As Vpu interacts with HRS in the absence of tetherin, it might induce ESCRT-dependent degradation of an unknown cellular factor, or Vpu itself directly interacts with HRS. Vpu LILI mutants were unable to interact with HRS in both the presence or the absence of tetherin (Figure 5-6 A and B), indicating that Vpu LILI is unable to recruit ESCRT-0. This could explain the defect in tetherin degradation and virological phenotype demonstrated in Figure 5-4 A and B and in Figure 5-5 A and B. Since HRS has been shown to orchestrate degradation of ubiquitinated membrane proteins, we decided to include the phospho-mutant Vpu 2/6A in our analysis. Vpu 2/6A is unable to recruit the SCF E3 ubiquitin ligase complex containing β-TrCP2, which has been shown to induce tetherin ubiquitination. Surprisingly, Vpu 2/6A mutants retained the ability to interact with HRS (Figure 5-6 A and B), indicating that Vpu and Vpu/tetherin complex interaction with HRS is independent of β-TrCP2 ligase recruitment.

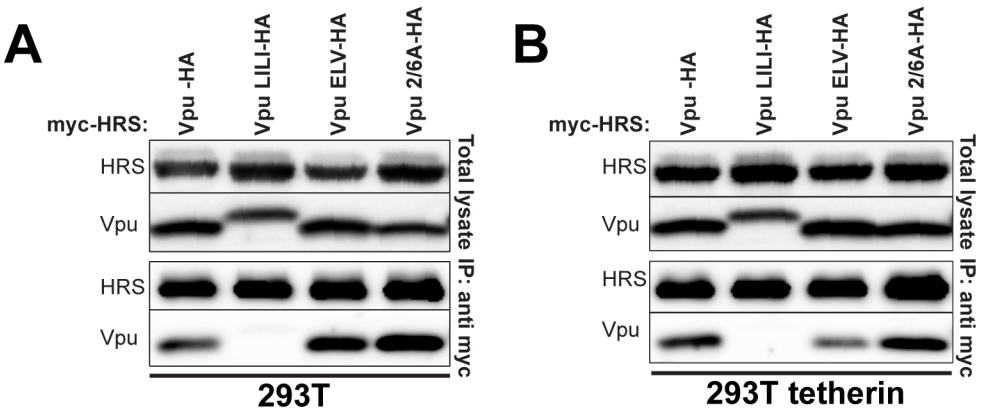

Figure 5-6 Vpu LILI mutants are defective for HRS interaction

(A and B) 293T or 293T tetherin cells were transfected with pCR3.1 Vpu-HA or indicated mutant in combination with a pCR3.1 myc-HRS expression vector. 48 hours post transfection, cells were lysed and immunoprecipitated with anti-myc antibody. Total cell lysates and precipitates were subjected to SDS-PAGE and analysed by Western blotting for HRS and Vpu, and analysed by ImageQuant.

Next, we tested the effect of HRS knockdown on virus release using oligonucleotides. 293T tetherin cells were treated twice over a period of 48 hours with non-coding siRNA or siRNA directed against HRS, and against downstream ESCRT-I components UBAP1 or TSG101, and cells were then infected with HIV-1 wild-type or HIV-1 delVpu. 48 hours post infection, cells were lysed and analysed by Western blot, and viral infectivity was measured on HeLa-TZMbl indicator cells. Knockdown efficiencies of ESCRT components were monitored in every individual experiment; see Figure 5-7A for a representative example. First, we tested the role of HRS in virus particle release. Depletion of HRS led to a small decrease in physical virus particle release (4.8-fold), whereas depletion of TSG101, as expected, inhibited budding of virus particles from the plasma membrane (Figure 5-7B). Notably knockdown of HRS enhanced total cellular levels of Vpu similarly to what has been observed with UBAP1 depletion, indicating that Vpu is most likely co-degraded with tetherin via the lysosome (Kueck and Neil, 2012). The effect of HRS knockdown on infectious virus particle release was equally mild (2-fold decrease) when compared to wild-type levels. As expected, TSG101 depletion resulted in a 20-fold decrease while UBAP1 levels remained unaffected (Figure 5-7C). Next, we tested the role of HRS in Vpu-mediated tetherin degradation in infected cells. 293T tetherin cells were treated as above and infected with a MOI of 2 to ensure a > 90% cell infection rate. As expected, tetherin levels were considerably reduced in cells infected with wild-type virus compared to both uninfected cells and cells infected with Vpu deletion virus (Figure 5-7D). As expected, natural turnover of tetherin was affected by depletion of HRS in uninfected cells (about 30% more compared to control siRNA). However, tetherin levels were rescued from degradation in cells depleted for HRS and infected with wild-type virus (about 50% more compared to control siRNA), while there was no difference in tetherin levels in HIV-1 delVpu infected cells (Figure 5-7 D and E). Our results show additionally that rescue of tetherin from ESCRT-mediated degradation was significantly higher in cells treated with UBAP1 or TSG101 siRNA oligonucleotides (Figure 5-7D), suggesting that HRS depletion in our system only partially blocks Vpu-mediated virus particle release and tetherin degradation, or that HRS depletion obtained was high enough. The above-observed defect of Vpu LILI mutants therefore cannot be explained by HRS recruitment alone.

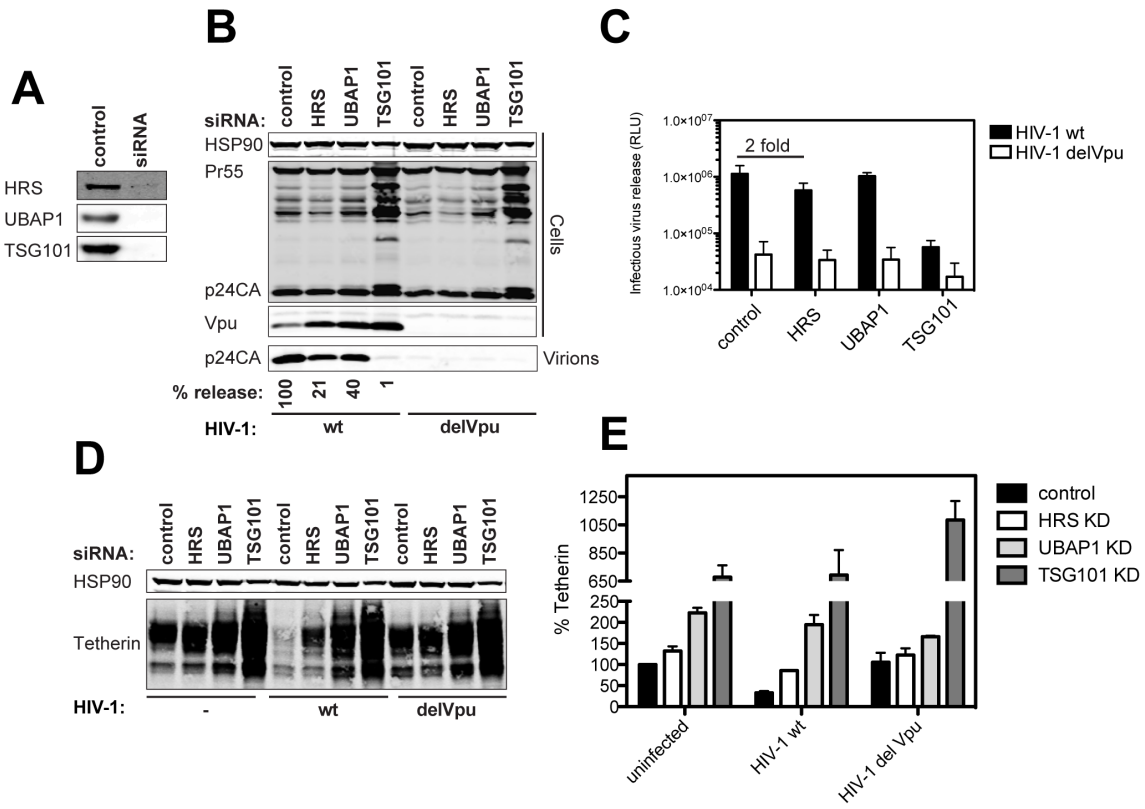

Figure 5-7 HRS knockdown partially blocks virus particle release and tetherin degradation

(A) Representative example of siRNA knockdown efficiencies. 293T tetherin expressing cells were transfected twice over a 48 hour period with siRNA oligonucleotide directed against HRS, UBAP1, TSG101 or non-targeting control. **(B)** 293T tetherin cells were treated as in (C), cells were then infected with HIV-1 wild-type or HIV-1 delVpu at an MOI of 0.8. Cell lysates and sucrose purified viral supernatants form (D) were subjected to SDS-PAGE and analysed by Western blotting for Hsp90, HIV-1 p24CA and Vpu, and analysed by LiCor quantitative imager. **(C)** Infectivity of viral supernatants form C was assayed on HeLa-TZMbl reporter cells. Infectious virus release was plotted as β-galactosidase activity in relative light units (RLU). Error bars represent the standard deviation of three independent experiments. **(D)** Cells were treated like in (D) but infected with an MOI of 2. Cell lysates were subjected to SDS-PAGE and analysed by Western blotting for Hsp90 and tetherin, and analysed by LiCor quantitative imager. **(E)** Percentage of tetherin in cells transfected with HRS or non-targeting siRNA oligonucleotides and infected with HIV-1 wild-type or HIV-1 del Vpu. Error bars represent the standard deviation of three independent experiments.

5.2.4 Vpu LILI mutants localise to early endosomal compartments

In Vpu LILI mutants the hydrophobic leucine and isoleucine residues were replaced with non-polar residues. This might have an effect on the conformation of the first alpha helix, which in wild-type Vpu is thought to be embedded into the plasma membrane (Maldarelli et al., 1993) (Wray et al., 1995) and result in a mis-folded and/or mis-trafficked Vpu LILI protein. Most mis-folded secretory proteins might remain in the ER until routed for ERAD degradation, and therefore never reaching the trans-Golgi network where wild-type Vpu can be found (Varthakavi et al., 2006) (Dubé et al., 2009). To this end, we decided to look at the cellular localisation of Vpu LILI mutants using fluorescent microscopy. 293T tetherin cells were transfected with Vpu-HA, Vpu LILI-HA or Vpu ELV-HA, 16 hours post transfection and then fixed and stained for Vpu-HA in combination with TGN46 or EEA1 subcellular markers. As expected, wild-type Vpu localises mainly to TGN46-positive compartments (Figure 5-8 A and B). The proportion of Vpu LILI mutants in TGN46-positive compartments was significantly reduced and surprisingly resembled the amount of Vpu ELV trafficking mutants typically found in the TGN (Figure 5-8 A and B). Both Vpu LILI and ELV mutants appeared more as “endosome-like” punctate structures within the cytoplasm and associated on or close to the plasma membrane (Figure 5-8A). It has been shown previously that some of these punctate structures in the case of Vpu ELV mutants were EEA1-positive early/sorting endosomal compartments (Kueck and Neil, 2012). When we further analysed the puncta in the case of Vpu LILI mutants we observed that they appeared to be EEA1 positive compartments, indicating that Vpu LILI mutants were pheno-copying Vpu ELV localisation (Figure 5-8C), and in turn showing that Vpu LILI mutants accumulate in EEA1-positive early/sorting endosomal compartments to which HRS is known to localise (Raiborg et al., 2001). Therefore Vpu LILI mutants accumulate in the cellular compartment where HRS is present but they do not interact. Vpu LILI mutants pheno-copy the early endosomal localisation of ELV trafficking mutants and display a similar defect in tetherin antagonism. However, Vpu ELV mutants retain the ability to bind to ESCRT-0 component HRS (Figure 5-6 A and B) (Kueck and Neil, 2012).

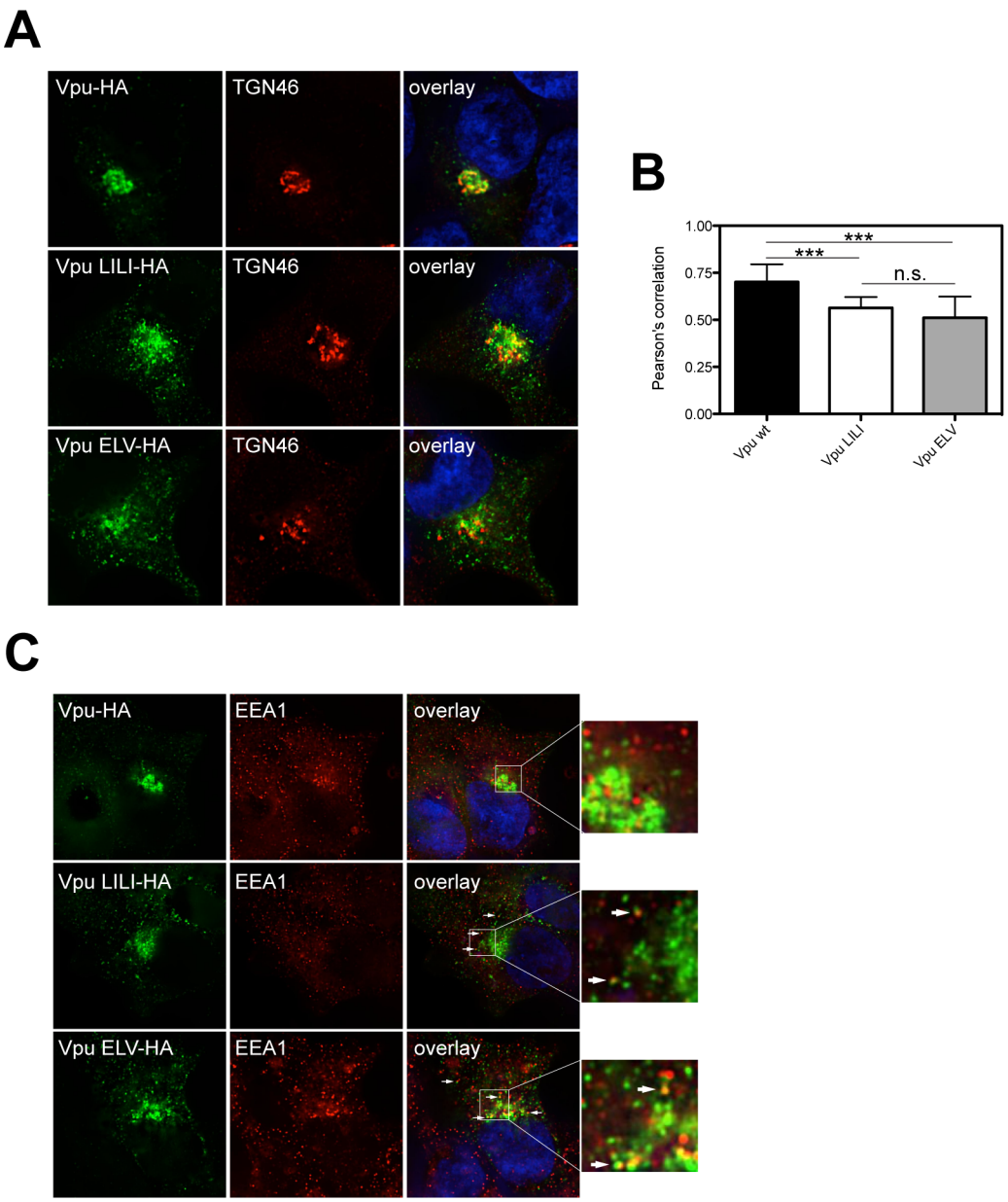

Figure 5-8 Vpu LILI mutants pheno-copy Vpu ELV early endosomal localisation

(A) 293T tetherin expressing cells were transfected with 75 ng of pCR3.1 Vpu-HA and indicated mutants. 16 hours post transfection, cells were fixed and stained for HA (green) and the TGN marker TGN46 (red) and examined by fluorescent microscopy. Panels are of representative examples. **(B)** Z stacks were taken of all cells (n=15), images were deconvoluted using the AutoQuant X3 software and Pearson's correlations were calculated for all Z stacks using ImageJ. Results were analysed by unpaired 2-tailed t-test - *** P = 10^{-5} or lower. **(C)** 293T tetherin cells were transfected as in (A) and stained for HA (green) and the early endosome using the marker EEA1 (red) and examined by fluorescent microscopy. Panels are representative examples. Same data as set presented in Figure 6-1 (Vpu 2/6A mutant is left out for clarity).

5.2.5 Vpu/HRS interaction is dependent on the ubiquitin binding motif (DUIM) in HRS

We next decided to study the nature of Vpu and HRS interaction in greater detail and concentrated on the mechanistic features in HRS that are required for Vpu interaction. To this end, we created a series of C-terminal HRS truncations, starting with truncating the clathrin-binding box (HRS delCB), the unstructured domain (HRS 1-500), the PSAP motif (which links HRS to ESCRT-I component TSG101) (HRS 1-280), and the double ubiquitin-binding motif (DUIM) (HRS 1-250) (Figure 5-9A). 293T cells were transfected with myc-HRS or indicated truncation in combination with Vpu-HA. 48 hours post transfection, cells were lysed and immunoprecipitated using an anti-myc antibody and analysed by Western blot. As expected, Vpu was co-immunoprecipitated with myc-HRS (Figure 5-9B). Interestingly, when we truncated beyond the DUIM of HRS, Vpu was not co-precipitated efficiently, suggesting that the ability of HRS to bind to ubiquitin is important for Vpu interaction. Therefore we point mutated residues in the DUIM and VHS domains that previously have been shown to bind ubiquitin (Hirano et al., 2006) (Ren and Hurley, 2010) and performed another co-immunoprecipitation. Vpu was not precipitated with point mutations in the DUIM of HRS which Vpu was precipitated with point mutations in the VHS domain (Figure 5-9C), indicating that Vpu/HRS interactions are dependent on residues 266 and 268 in the DUIM that bind directly to ubiquitin.

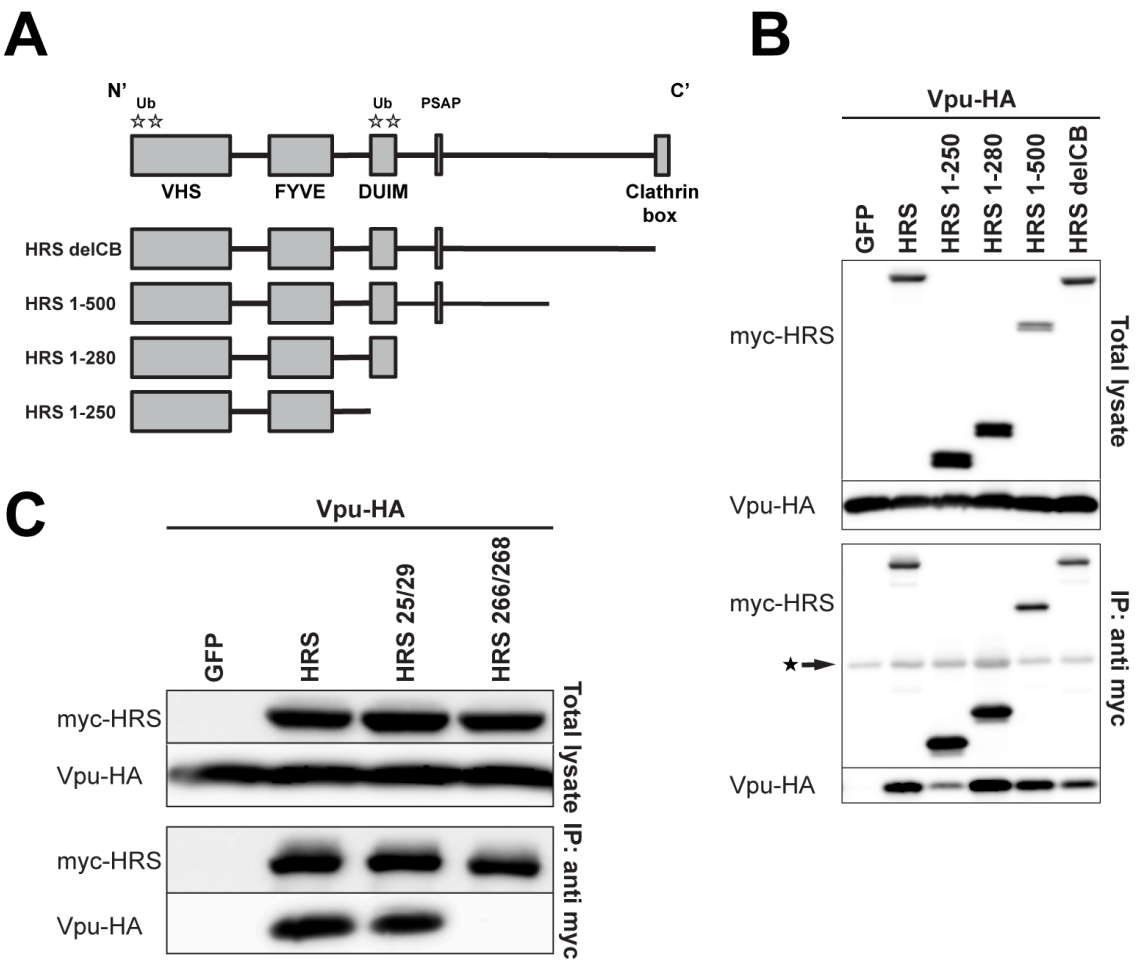

Figure 5-9 Vpu/HRS interaction is dependent on residues in the DUIM of HRS that bind ubiquitin

(A) Schematic representation of HRS C-terminal truncations. **(B)** 293T cells were transfected with pCR3.1 Vpu-HA in combination with a pCR3.1 myc-HRS or myc-HRS truncation expression vector. 48 hours post transfection cells were lysed and immunoprecipitated with anti-myc antibody. Total cell lysates and precipitates were subjected to SDS-PAGE and analysed by Western blotting for myc-HRS and Vpu, and analysed by ImageQuant. Start/asterisk: Heavy chain from myc antibody. **(C)** Immunoprecipitation was performed like in (B) but with myc-HRS W25A L29D (VHS domain) and myc-HRS A266Q A268Q (DUIM domain) mutants.

5.2.6 Role of other potential ESCRT-0 components

Depletion of HRS partially blocks virus particle release and tetherin degradation. Proteins that share molecular characteristics with the ESCRT-0 subunit HRS might also function as ubiquitin receptors for cargo protein sorting into multivesicular endosomes. One recently suggested candidate is ALIX, which has been shown to bind to ubiquitinated cargo and to be responsible for sorting of these cargo molecules into multivesicular endosomes (Dowlatshahi et al., 2012) (Pashkova et al., 2013).

Next, we therefore tested the effect of ALIX knockdown on virus release and tetherin degradation. 293T tetherin cells were treated twice over a period of 48 hours with either non-coding siRNA or siRNA directed against ALIX and HRS, alone or in combination, and infected with HIV-1 wild-type or HIV-1 delVpu. 48 hours post infection, viral infectivity was measured on HeLa-TZMbl indicator cells. Depletion of ALIX caused no decrease in physical virus particle release (see Figure 5-10A), which is consistent with functional studies demonstrating that ALIX is not required for P(S/T)AP-dependent viral budding (reviewed by (Martin-Serrano and Neil, 2011)). Depletion of HRS led to a small decrease in physical virus particle release (3-fold) when compared to wild-type levels which was also observed in Figure 5-7C. Both, ALIX and HRS have been shown to sort ubiquitinated cargo into MVBs for lysosomal degradation. As such they might have additive effects on each other, and depletion of one alone might not be enough to unravel a strong phenotype regarding virus particle release phenotype. To this end, ALIX and HRS were depleted in combination, but no effect on virus particle release was observed (see Figure 5-10A). Next, we tested the role of ALIX in Vpu-mediated tetherin degradation in infected cells. 293T tetherin cells were treated as above and infected with a MOI of 2 to ensure a > 90% cell infection rate. 48 hours post infection, cells were lysed and analysed by Western blot. As expected, tetherin levels were considerably reduced in cells infected with wild-type virus when compared to uninfected and cells infected with Vpu deletion virus. Tetherin levels were rescued from degradation in cells depleted for HRS and infected with wild-type virus, while there was no difference in tetherin levels in HIV-1 delVpu infected cells (see Figure 5-10B). However, tetherin levels were not rescued from ESCRT-mediated degradation in ALIX depleted. Rescue of tetherin levels in cells co-depleted of ALIX and HRS was similar to the degradation rescue in HRS knockdown cells (see Figure 5-10B), suggesting that HIV-1 Vpu induced ESCRT degradation of tetherin is independent of ALIX function.

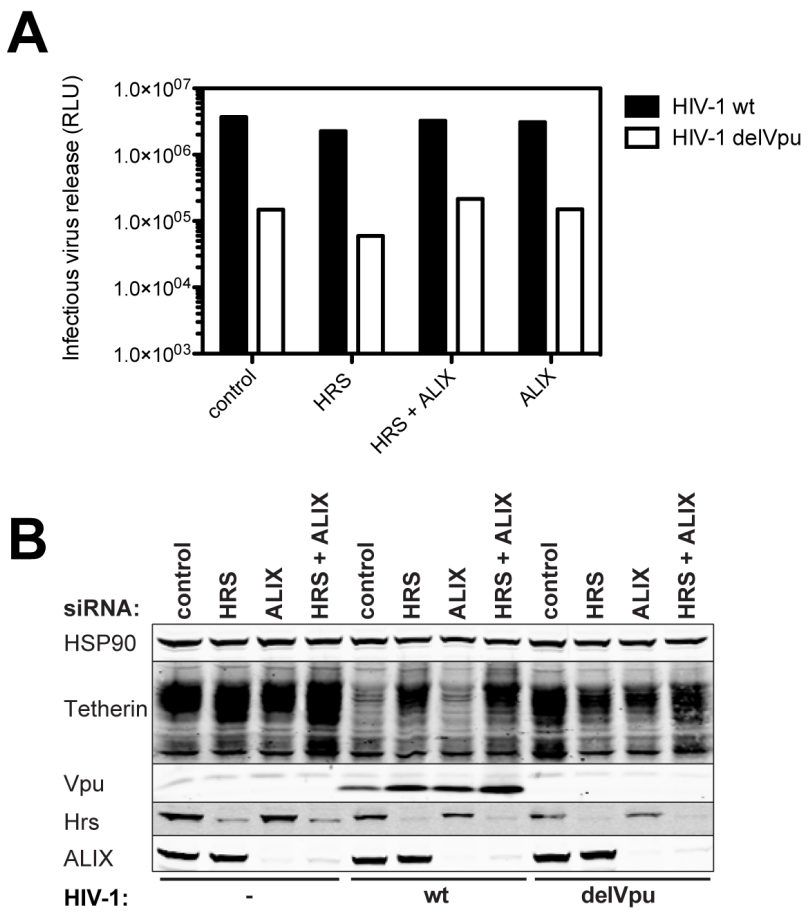

Figure 5-10 Vpu-mediated tetherin degradation is independent of ALIX

(A) 293T tetherin expressing cells were transfected twice over a 48 hour period with siRNA oligonucleotide directed against HRS, ALIX or non-targeting control. The cells were then infected with HIV-1 wild-type or HIV-1 delVpu at an MOI of 0.8. Infectivity of viral supernatants form C was assayed on HeLa-TZMbl reporter cells. Infectious virus release was plotted as β-galactosidase activity in relative light units (RLU). **(B)** Cell lysates and sucrose purified viral supernatants form (A) were subjected to SDS-PAGE and analysed by Western blotting for Hsp90, HIV-1 p24CA, Vpu, HRS and ALIX and analysed by LiCor quantitative imager.

Another group of potential ESCRT-0 complex candidates are the monomeric clathrin adaptor GGA proteins, These proteins function in cargo trafficking between the TGN and endosomes, which could be consistent with Vpu's ability to subvert tetherin trafficking. Furthermore, overexpression of these proteins has been shown to induce accumulation of cellular compartments containing TSG101 and HRS and lead to disruption in endosomal sorting (Joshi et al., 2009).

Next, we tested the effect of GGA overexpression on tetherin-mediated virus particle release. To this end, 293T tetherin cells were transfected with increasing concentrations of GGA1, GGA2 or GGA3 in combination with a fixed dose of NL4.3 wild-type or NL4.3 delVpu provirus. 48 hours after the transfection, cell lysates and supernatants containing viral particles were harvested and analysed for viral infectivity on HeLa-TZMbl reporter cells (Figure 5-11A), or physical virus yield by Western blot

(Figure 5-11B). As expected, virus particle release in NL4.3 delVpu expressing cells is about 23-fold lower than virus release from NL4.3 wild-type cells. GGA1 overexpression results in a dramatic decrease in infectious virus release in both wild-type and delVpu treated cells, with levels close to the detection limit of the dynamic range of the β-galactosidase-based assay. However, GGA2 overexpression in NL4.3 wild-type transfected cells resulted in 19-fold decrease, and in NL4.3 delVpu transfected cells in a 13-fold decrease in infectious virus particle release could be observed when compared to control cells. GGA3 overexpression resulted in a 46-fold decrease in wild-type and 15-fold decrease in delVpu transfected cells (Figure 5-11A). Notably, overexpression of GGA1 has been shown to inhibit virus assembly and release by disrupting ADP ribosylation factor (Arf) protein activity, therefore disrupting Gag binding to membranes (Joshi et al., 2008). GGA overexpression induced accumulation of cellular compartments containing TSG101, HRS and poly-ubiquitin, which in turn led to disruption in endosomal sorting (Joshi et al., 2009). Next, we looked at physical virus particle release and Gag processing by Western blot. GGA1 overexpression induced a slight degradation of the viral structural protein Gag, resulting in a drastic decrease in virus release, while overexpression of GGA2 and GGA3 had no effect on Gag processing (Figure 5-11B). Overexpression of GGA2 and GGA3 in NL4.3 wild-type cells resulted in a decrease in virus particle release of 5 and 25-fold respectably, while the effect in NL4.3 delVpu was residual (Figure 5-11B). Next, we tested the effect of GGA overexpression in tetherin negative 293T cells, which were treated as above and transfected with 250 ng of GGA1, GGA2 or GGA3. As expected, virus particle release from wild-type and delVpu was unchanged (Figure 5-11C). While particle release in GGA overexpressed cells was dramatically reduced, there was no difference between NL4.3 wild-type or delVpu transfected cells (Figure 5-11C).

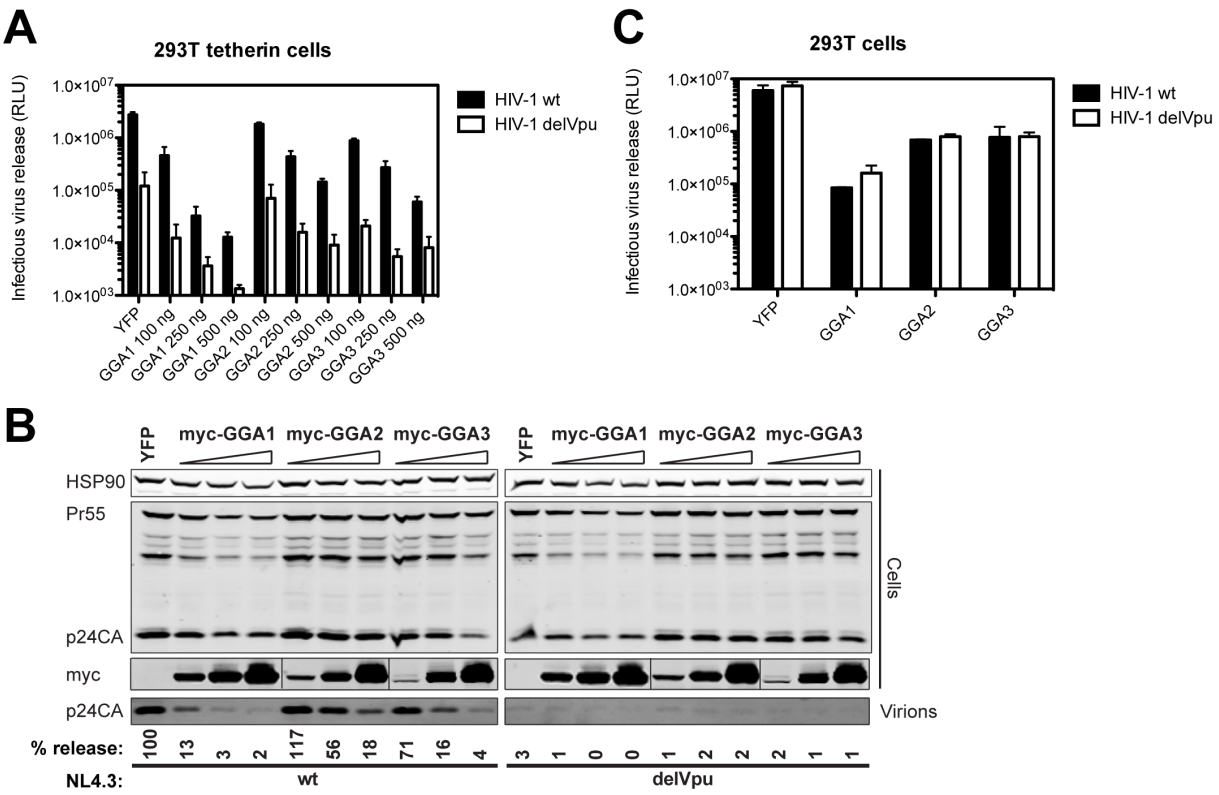

Figure 5-11 Role of GGA proteins in tetherin antagonism by Vpu

(A) 293T tetherin cells were transfected with increasing concentrations of pCR3.1 myc-GGA1, GGA2 or GGA3 expression vector (100 ng, 250 ng and 500 ng) or YFP expression plasmid together with NL4.3 wild-type or NL4.3 Vpu delVpu. Infectivity of viral supernatants was assayed on HeLa-TZMbl reporter cells. Infectious virus release was plotted as β-galactosidase activity in relative light units (RLU). Error bars represent the standard deviation of three independent experiments. **(B)** Cell lysates and sucrose purified viral supernatants were subjected to SDS-PAGE and analysed by Western blotting for Hsp90, HIV-1 p24CA, Vpu, myc and analysed by LiCor quantitative imager. **(C)** 293T cells or 293T tetherin cells were transfected as in (A) and transfected with a fixed dose of myc-GGA1, GGA2 or GGA3. Error bars represent the standard deviation of three independent experiments.

5.3 DISCUSSION

In this chapter we have identified the role of the newly identified ESCRT-I subunit UBAP1 in Vpu-mediated tetherin degradation, which was part of a project that resulted in a publication in Structure (Agromayor et al., 2012). In this manuscript, we were able to show that UBAP1 forms a complex with TSG101, VPS28 and VPS37 with a 1:1:1:1 stoichiometry. Co-depletion studies demonstrated that binding to TSG101 stabilizes endogenous UBAP1 and that UBAP1 is able to recruit ESCRT subunits in a TSG101-dependent manner. This evidence suggested that UBAP1 is part of the human ESCRT-I complex, which is consistent with results published earlier by Woodman and colleagues (Stefani et al., 2011). We were able to demonstrate that UBAP1 is able to bind to ubiquitin using its novel C-terminal solenoid of overlapping ubiquitin-associated (SOUBA) domain to increase ESCRT-I interaction with ubiquitin. The SOUBA domain consist of three ubiquitin-associated (UBA) domains that bind to three mono-ubiquitin molecules adjacent to one another. All three UBAs bind to the hydrophobic region of ubiquitin that includes residues isoleucine 44 and valine 70. ESCRT-I subunit UBAP1 is essential for ESCRT-mediated degradation of ubiquitinated cargo via the lysosome but dispensable for HIV-1 budding and cytokinesis. The KSHV ubiquitin ligase K5 induces endo/lysosomal degradation of tetherin via the lysine 18 amino acid residue in the tetherin cytoplasmic tail (Mansouri et al., 2009) (Pardieu et al., 2010), and this degradation is dependent on the ESCRT-I subunit UBAP1. The HIV-1 accessory protein Vpu targets tetherin for lysosomal degradation (Douglas et al., 2009) (Iwabu et al., 2009) (Mitchell et al., 2009), a process that is dependent on the ESCRT-0 subunit HRS (Janvier et al., 2011). We were able to demonstrate that UBAP1 is essential for Vpu-mediated tetherin degradation, which is nevertheless dispensable for Vpu anti-tetherin activity. Furthermore, in UBAP1 depleted cells, ubiquitinated tetherin proteins accumulate in late endosomal structures, which are not affecting the efficiency of Vpu to antagonise tetherin. This knowledge provides us with a powerful tool to study the mechanism of Vpu-mediated counteraction of tetherin without using lysosomal inhibitors that can be toxic when used for a prolonged period of time. While UBAP1 activity is dispensable for cell division and virus budding, depleted cells remain healthy after a 72 hour treatment with siRNA oligonucleotides. However, UBAP1 could stabilise binding of multiple mono-ubiquitinated cargo molecules or clustered mono-ubiquitinated cargo. Further studies are needed to understand the in detail nature of ubiquitin binding of cargo proteins designated for lysosomal degradation via the SOUBA domain.

In this chapter we also identified hydrophobic residues in the first alpha helix of the cytoplasmic tail of the HIV-1 NL4.3 Vpu, LI 41/42 AA LI 45/46 AA, which are required

for the antagonism of tetherin restriction. Naturally occurring mutations of these residues were also found in a single genome sequencing study of HIV-1 infected individuals (Pickering et al., 2014). Mutation of these residues blocks the ability of Vpu to mediate tetherin surface downregulation and induce ESCRT-dependent degradation of tetherin. Vpu LILI mutants retain the ability to interact with tetherin via their respective transmembrane domains, and to recruit the ubiquitin ligase SCF-β-TrCP2 complex via a pair of phosphorylated serine residues in the highly conserved region between cytoplasmic helix 1 and 2. Vpu LILI mutants pheno-copy the cellular localisation of trafficking Vpu ELV mutants in which they localise to early/recycling endosomal structures and the plasma membrane rather than the TGN.

A previous study has demonstrated that both Vpu and tetherin interact with the ESCRT-0 component HRS and that HRS is important for tetherin cell surface downregulation and degradation (Janvier et al., 2011). Interestingly, Vpu LILI mutants failed to co-precipitate with HRS. This loss of interaction might explain why Vpu LILI mutants are unable to antagonise tetherin function. Another possibility is that Vpu LILI mutants are defective in tetherin antagonism for unrelated reasons. For example, LILI mutants fail to interact with the clathrin adaptor AP-1, and on top of that are unable to recruit HRS (see Chapter 6 for further characterisation of Vpu mutants). Vpu/HRS interaction is likely to occur via ubiquitin, as mutation of the residues known to bind to ubiquitin in the DUIM motif in HRS completely abolished co-precipitation of Vpu. We were unable to find any evidence of ubiquitinated forms of Vpu in our immunoprecipitations, despite performing our experiments in the presence of de-ubiquitinase inhibitors, and potentially enriching for ubiquitinated proteins by precipitating myc-HRS. This means that Vpu/HRS interaction is likely to be indirect. Interestingly, Vpu wild-type interacts with HRS in the presence or absence of tetherin, indicating a role for another cellular factor that is being ubiquitinated and is “bridging” between Vpu and HRS. This cellular factor is unlikely to be the lipid-antigen presenting protein CD1d or the natural killer cell ligand NTB-A, as degradation of these proteins is not induced by HIV-1 Vpu (Moll et al., 2010) (Shah et al., 2010). In addition, CD1d and NTB-A are not expressed in 293T cells, which were used in the co-immunoprecipitation studies. We found that the phospho-mutant Vpu 2/6A which is unable to recruit the only E3 ubiquitin ligase known to induce tetherin as well as CD4 ubiquitination, is able to interact with HRS in both presence and absence of tetherin. Vpu/HRS interaction is independent of β-TrCP2 but dependent on ubiquitin, highlighting the potential role of a to date unknown ligase which ubiquitinates Vpu’s target membrane proteins for degradation. The importance of the D**S**GNE**S** phosphorylation motif and subsequent recruitment of the E3 ubiquitin ligase β-TrCP2 in Vpu-mediated tetherin antagonism

has been subject to debate, as β-TrCP is not strictly required for Vpu-mediated tetherin antagonism (Tervo et al., 2011) (Schmidt et al., 2011). Tetherin is ubiquitinated on multiple residues within its cytoplasmic tail. This ubiquitination has been shown to be crucial for degradation (Tokarev et al., 2011) (Gustin et al., 2012) and might be induced by ligases other than β-TrCP2. However, the type of ubiquitination (mono-ubiquitination and/or poly-ubiquitination), as well as the nature of chain linkages still needs to be evaluated. Different ubiquitin patterns can have detrimental effects on the fate of recycling membrane proteins. Multiple mono-ubiquitination and lysine 63-linked poly-ubiquitination function as sorting motifs in early/recycling endosomes for lysosomal degradation, whereas lysine 48-linked poly-ubiquitination leads to proteosomal degradation (reviewed by (Raiborg and Stenmark, 2009)).

Depletion studies of HRS using siRNA showed a partial phenotype for virus particle release and tetherin degradation. HRS knockdown could have an effect on HIV-1 envelope trafficking to the plasma membrane. Therefore affecting the infectious virus particle release, analysed by β-galactosidase-based reporter assay, might be lower than the physical particle yield analysed by Western blot. Furthermore, there are discrepancies between our results and published data (Janvier et al., 2011): we show a partial phenotype for virus particle release and tetherin degradation while Janvier *et al* propose that Vpu-mediated tetherin degradation is dependent on HRS and that HRS depletion induces a tetherin phenotype on efficient virus release. These differences might be due to the nature of assays or cell lines used in the knockdown experiments. We present our virus particle release results in “fold differences” while Janvier *et al* used “percentages”, which tends to make small differences appear more significant. Therefore one could argue if there are differences in actual results obtained, or only differences in presentation and subsequent interpretation of these results.

There has been a debate as to whether HRS is the only ESCRT-0 component which is able to sort ubiquitinated cargo or if there are structurally similar proteins that might be able to act as an alternative way into the ESCRT machinery. Potential candidates are members of the GGA protein family and TOM1 or TOM1L1-like proteins as all share common features with HRS: VHS domains, ubiquitin-binding motifs, clathrin-binding boxes and PSAP/PTAP ESCRT-binding motifs (reviewed by (Raiborg and Stenmark, 2009)). Furthermore, GGA3 has also been shown to interact with ESCRT-I subunit TSG101 (Puertollano and Bonifacino, 2004). Another report highlighted the potential role of ALIX as an ESCRT-0 component, binding to ubiquitinated cargo and sorting these into multivesicular endosomes (Dowlatshahi et al., 2012) (Pashkova et al., 2013). We tested this hypothesis and depleted ALIX alone or in combination with HRS and performed a virus release and tetherin degradation assay. However, we were unable to

see any effect of ALIX depletion on Vpu-mediated virus particle release or infectivity and tetherin degradation in preliminary experiments. Overexpression of monomeric alternative clathrin adaptors GGA1, GGA2 and GGA3 indicated that there might be a Vpu and tetherin specific role in infectious virus particle release for GGA2 and GGA3 in initial experiments. GGA proteins are monomeric alternative clathrin adaptor proteins that function in cargo trafficking between the TGN and endosomes (reviewed by (Lafer, 2002)), which is consistent with Vpu's ability to subvert tetherin trafficking to the plasma membrane and re-routing it for ESCRT-dependent endo/lysosomal degradation. Overexpression has been shown to induce accumulation of cellular compartments containing TSG101, HRS and poly-ubiquitin, which in turn lead to disruption in endosomal sorting (Joshi et al., 2009). Furthermore, overexpression studies of GGA proteins have been shown to induce artificial intracellular compartments that in case of GGA1 sequester HIV-1 gag and virus particles. Additionally, GGA proteins have been shown to be important modulators of retrovirus release, and overexpression of these proteins impairs the trafficking of gag to the plasma membrane (Joshi et al., 2008). Therefore it is important to perform further studies using knockdown techniques of especially GGA2 and GGA3 to evaluate their role in Vpu-mediated tetherin antagonism, cell surface downregulation and degradation. As GGA proteins play a role in gag trafficking, siRNA studies should be performed without full-length virus in order to unmask any GGA-dependent effect on Vpu-mediated tetherin antagonism. Due to the high degree of homology between GGA1, GGA2, and GGA3 initial depletion studies revealed that knockdown of one of the GGA proteins can have an effect on expression levels of other GGA family members. Therefore it is important to monitor expression levels of all three GGA proteins closely. It is also important to perform cellular localisation studies for both GGA overexpression and depletion studies to detect any effect on subcellular trafficking of Vpu and tetherin proteins.

While there is no full-length crystal structure of Vpu, structural studies using transmembrane or cytoplasmic domains have revealed that the first alpha helix of Vpu is embedded into the host plasma membrane due to its charged and hydrophilic nature (Maldarelli et al., 1993) (Wray et al., 1995). Mutating isoleucine and leucine residues into nonpolar alanine residues in the first alpha helix might weaken the helix structure, which might be important for Vpu interaction with ESCRT-0 HRS or other cellular factors.

Chapter 6 Further studies on the relationship between Vpu mutants and the clathrin machinery

6.1 Introduction

We have noticed that Vpu ELV (Chapter 4) and LILI (Chapter 5) cytoplasmic tail mutants, as well as the previously characterised Vpu 2/6A phospho-mutant, predominately localise to punctate structures within the cytoplasm (Figure 6-1), which we predict to be early/recycling endosomal compartments. Therefore, Vpu LILI and Vpu 2/6A mutants pheno-copy the localisation defect of Vpu ELV mutants, which is unable to interact with the clathrin adaptor AP-1, and as a result accumulate in endosomal compartments. We consequently asked the question if Vpu LILI and Vpu 2/6A mutants are also defective for AP-1 interaction.

Data presented in Chapter 4 implicates a function of clathrin in Vpu-mediated tetherin antagonism. However, we could not detect any effects of depletion of the canonical clathrin adaptor proteins AP-1, AP-2 or AP-3 on Vpu-mediated tetherin antagonism. This is potentially suggestive of redundancy in the clathrin adaptor pathway, thus making depletion experiments difficult to interpret. By replacing the second alpha helix of Vpu cytoplasmic tail, containing a trafficking motif with the **D**/**E**xxx**L**(**L**/**I**/**M**) motif from HIV-1 Nef that has been demonstrated to bind canonical clathrin adaptors AP-1, AP-2 and AP-3 (Janvier et al., 2003) (Chaudhuri et al., 2007), we were able to indirectly link Vpu to the clathrin machinery and to functionally complement Vpu function.

Acidic amino acid residues or phosphorylated serine residues downstream of acidic dileucine-based sorting motifs can add potency to the signals and enhance clathrin adaptor binding (Mauxion et al., 1996). Interestingly, immediate upstream of the **E**xxx**LV** sorting signal in HIV-1 Vpu, is a highly conserved D**S**GNE**S** motif containing a pair of serine residues that are phosphorylated by casein kinase II. In the Vpu 2/6A mutant these serine residues are mutated, potentially leading to the destabilisation of Vpu/AP-1 complexes mediated by the **E**xxx**LV** motif in the second alpha helix of Vpu.

Vpu LILI mutants display a defect in tetherin antagonism that renders it unable to interact with the ESCRT-0 component HRS, responsible for binding to ubiquitinated transmembrane cargo molecules and delivers them for endo/lysosomal degradation. HRS also sequesters cargo molecules into micro-domains in early endosomal compartments by directly binding to flat clathrin lattices. Therefore, inhibiting the recycling of cargo molecules designated for degradation back to the plasma membrane. Flat clathrin lattices are organised differently from clathrin-coated pits at the plasma membrane. Clathrin-coated pits or vesicles are curved and contain a one-

layered and well-organised coat, while HRS containing endosomal clathrin lattices are flat and bi-layered (Raiborg et al., 2002).

Therefore, Vpu ELV, Vpu LILI and Vpu 2/6A mutants indirectly interact or potentially stabilise binding to the cellular clathrin machinery, but these clathrin interactions occur in different cellular compartments. One could argue that Vpu/tetherin complexes have to interact with the clathrin machinery independent of cellular localisation in order to be sorted for lysosomal degradation.

In this chapter we have examined the effect of fusing the clathrin-binding box of HRS to the C-terminus of different Vpu mutants, including ESCRT-0 interaction mutant (Vpu LILI), phospho-mutant (Vpu 2/6A) and trafficking mutants (Vpu ELV). Interestingly, all mutants, when fused to a direct clathrin-binding motif, rescue tetherin antagonism. This indicates that interaction with the clathrin machinery within the cell is critical for Vpu to exclude tetherin away virus budding sites at the plasma membrane, and into the degradative ESCRT-dependent pathway.

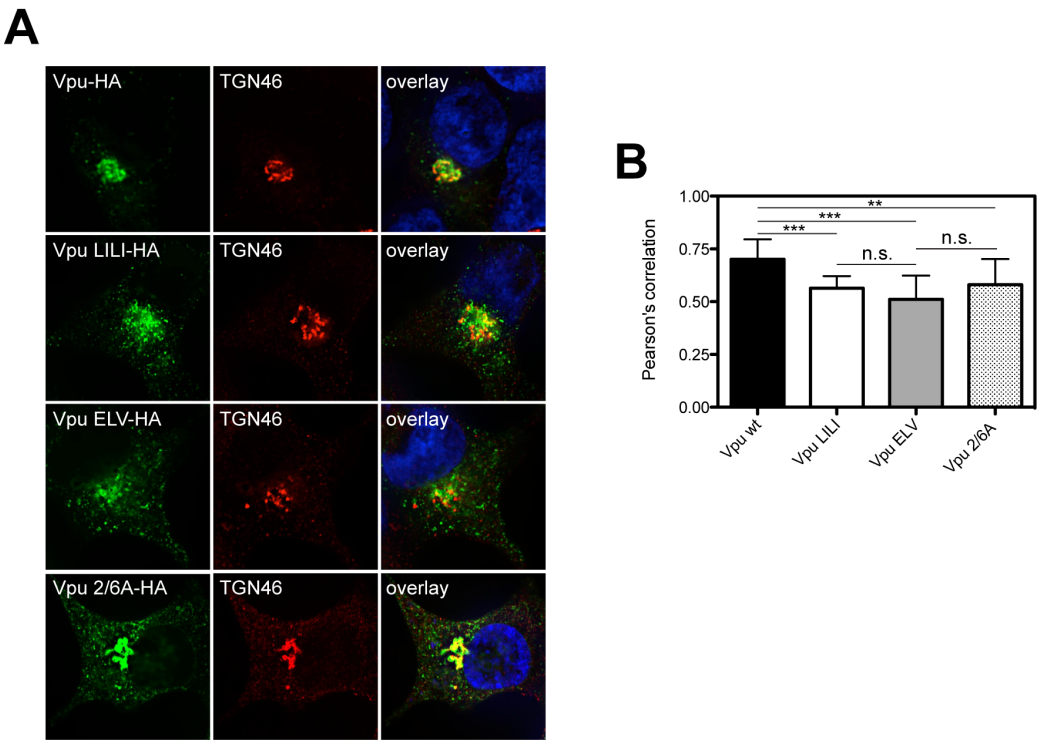

Figure 6-1 Comparison of Vpu mutant subcellular localisation

(A) 293T tetherin expressing cells were transfected with 75 ng of pCR3.1 Vpu-HA and indicated mutants. 16 hours post transfection, cells were fixed and stained for HA (green) and the TGN marker TGN46 (red) and examined by fluorescent microscopy. Panels are of representative examples. **(B)** Z stacks were taken of all cells (n=15), images were deconvoluted using the AutoQuant X3 software and Pearson's correlations were calculated for all Z stacks using ImageJ. Results were analysed by unpaired 2-tailed t-test - *** P = 10^{-5} or lower. Data for: Vpu wt, Vpu LILI and Vpu ELV is the same as presented in **5.2.4.** Same data set as presented in Figure 5-8.

6.2 Results

6.2.1 Vpu cytoplasmic tail mutants can be functionally rescued by a clathrin-binding motif

Vpu ELV, Vpu LILI and Vpu 2/6A mutants have the same localisation defect, so we reasoned that they all have defective interactions with clathrin. If so, then we hypothesised that bypassing the defect and linking Vpu directly to clathrin might restore anti-tetherin function. We therefore decided to fuse the C-terminal clathrin-binding box of HRS to the cytoplasmic tail mutants Vpu LILI, Vpu 2/6A and Vpu ELV, and study their ability to counteract tetherin restriction. To this end, we fused the AQ**LI**SFD clathrin heavy chain-binding motif of HRS or corresponding mutant to the carboxyl-terminus of Vpu cytoplasmic tail mutants (Figure 6-2A). 293T tetherin cells were co-transfected with increasing concentrations of a tetherin expression vector and indicated Vpu clathrin box chimeras in combination with a fixed dose of NL4.3 delVpu provirus. 48 hours after the transfection, cell lysates and supernatants containing viral particles were harvested and analysed for physical virus yield by Western blot (Figure 6-2 B and C) and viral infectivity on HeLa-TZMbl reporter cells (Figure 6-2 D until F). Remarkably, when we tested the ability of these proteins to antagonise tetherin function, all Vpu cytoplasmic tail mutant clathrin box chimeric proteins substantially recovered tetherin anti-viral activity (Figure 6-2 B and C). This effect could also be observed with two different clathrin-binding motifs from GGA2 (preliminary results). Moreover, these chimeras also displayed improved tetherin downregulation from the surface of transfected HeLa-TZMbl cells that were analysed for tetherin cell surface levels by flow cytometry (Figure 6-3 A until E). This activity was entirely dependent on the key amino acids required for clathrin interaction as chimeras in which L and I positions were mutated to alanine were unable to counteract tetherin or to induce tetherin cell surface downregulation (Figure 6-2 and Figure 6-3). Thus, Vpu function can be substantially recovered by fusing Vpu cytoplasmic tail ESCRT-0, phospho- and trafficking mutants to a clathrin-binding signal AQ**LI**SFD, indicating that linking Vpu directly to the clathrin trafficking machinery can restore its activity.

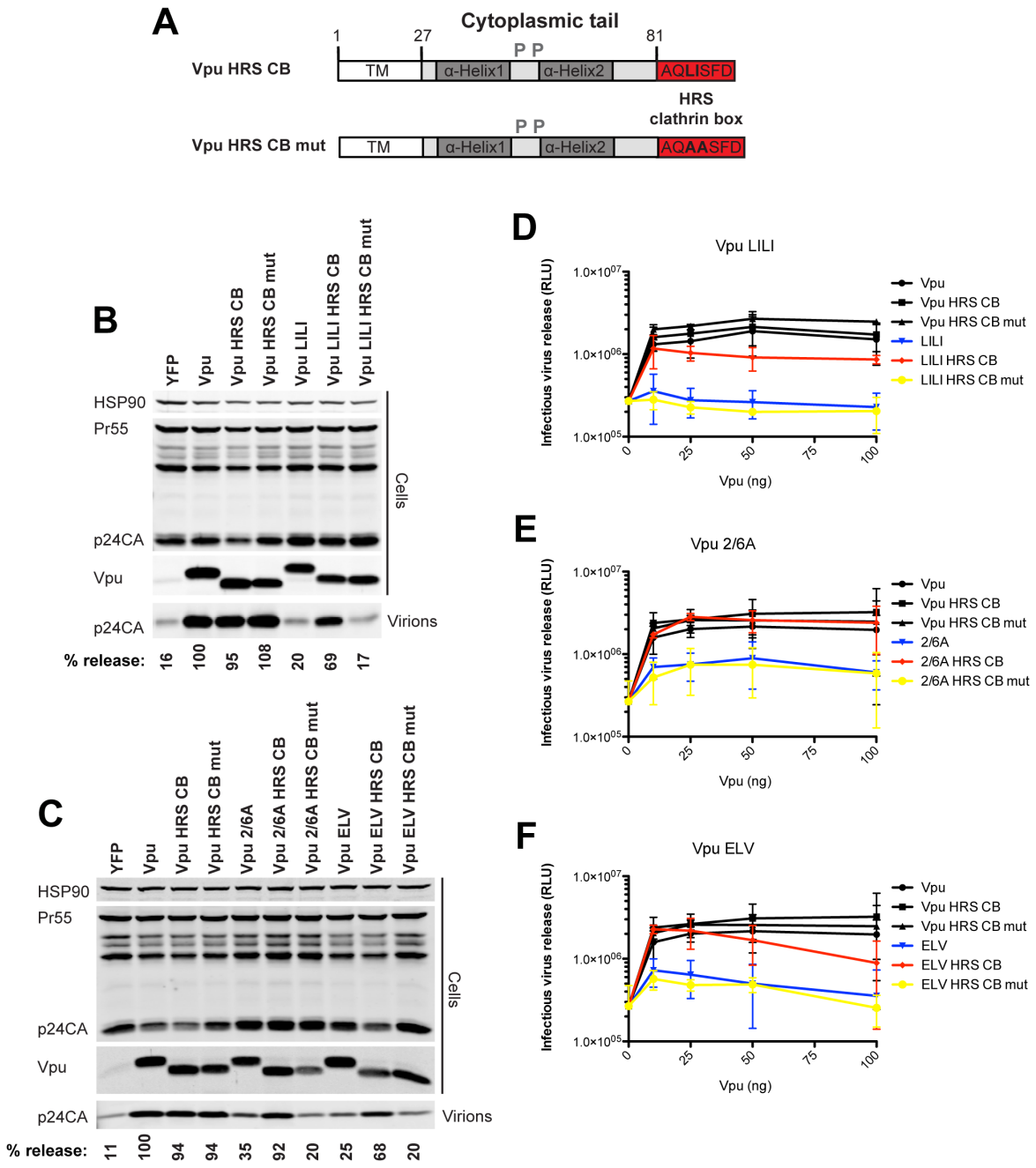

Figure 6-2 Virus particle release of Vpu cytoplasmic tail mutants can be rescued by clathrin-binding motif of HRS

(A) Schematic representation of Vpu HRS CB chimera constructs (Jonathon Sumner contributed to the cloning process of the indicated constructs). **(B)** 293T tetherin cells were transfected with NL4.3 delVpu proviral plasmid in combination with YFP expression vector, pCR3.1 Vpu, pCR3.1 Vpu HRS CB, pCR3.1 Vpu HRS CB mut or indicated Vpu LILI CB chimera construct. 48 hours post transfection, cell lysates and pelleted supernatant virions were harvested and subjected to SDS-PAGE and analysed by Western blotting for HIV-1 p24CA, Vpu and Hsp90, and analysed by LiCor quantitative imager. **(C)** Same experiment as in (A) but with pCR3.1 Vpu 2/6A or pCR3.1 Vpu ELV CB chimera as indicated. **(D)** Infectivity of viral supernatants from (B) was determined on HeLa-TZMbl cells as in Figure 4-1. Error bars represent standard deviation of three independent experiments. **(E)** Infectivity of viral supernatants from (C) using pCR3.1 Vpu 2/6A constructs. Error bars represent standard deviation of three independent experiments. **(F)** Infectivity of viral supernatants from (C) using pCR3.1 Vpu ELV constructs. Error bars represent standard deviation of three independent experiments.

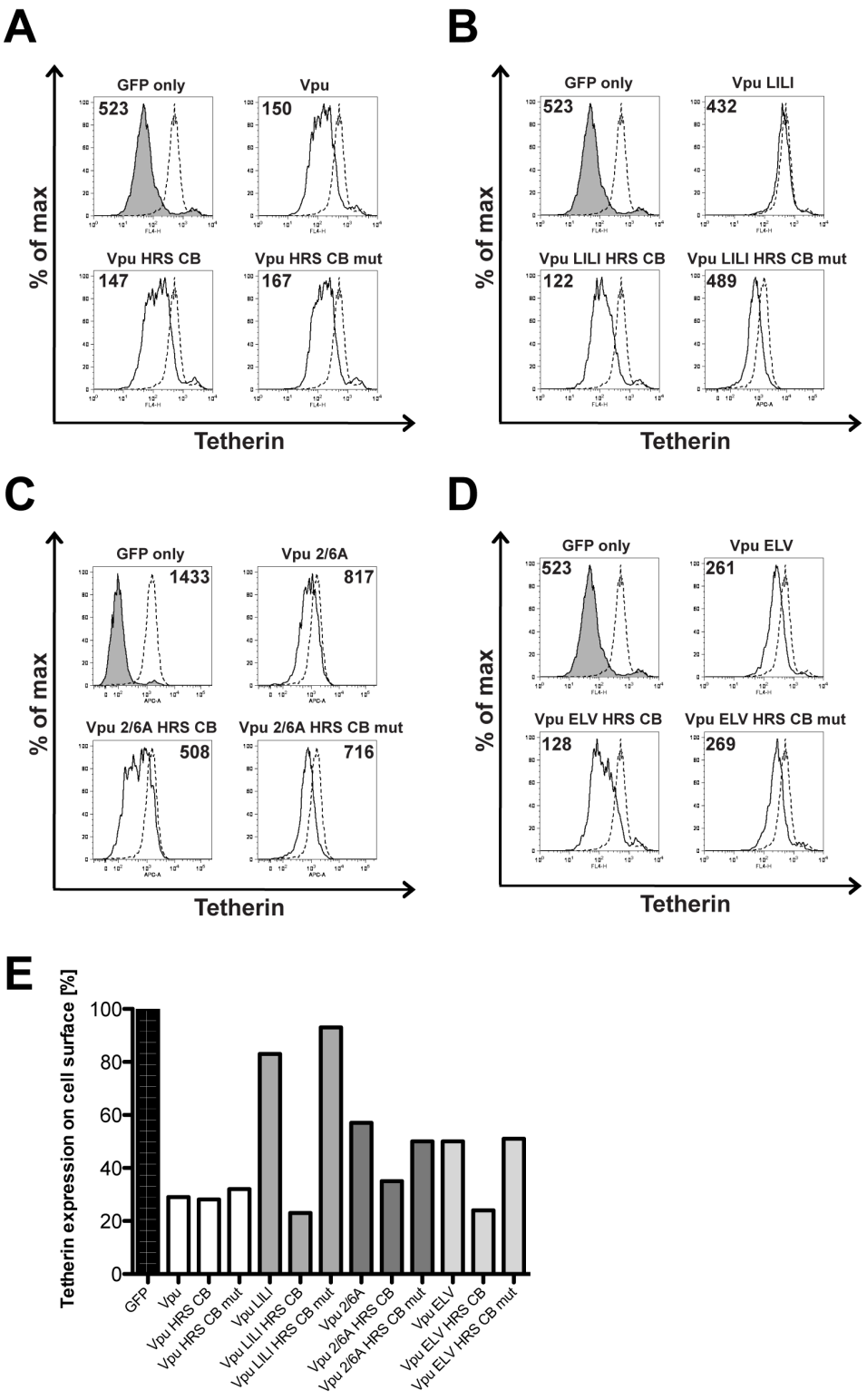

Figure 6-3 Vpu cytoplasmic tail mutants fused to a clathrin-binding box are able to downregulate tetherin from the plasma membrane

(A) HeLa-TZMbl cells were co-transfected with pCR3.1 Vpu or indicated mutant and a GFP expression vector. Cell-surface tetherin levels were analysed 48 hours post transfection by flow cytometry. GFP positive cells were gated and tetherin levels (solid lines) were compared to mock-transfected cells or transfected with indicated Vpu (dotted lines). Numbers indicate median fluorescence intensities of endogenous tetherin surface levels. The solid peak in the upper left histogram represents binding of the isotype control. **(B)** Same as in (A) but transfected with pCR3.1 Vpu LILI or indicated mutant. **(C)** Same as in (A) but transfected with pCR3.1 Vpu 2/6A or indicated mutant. **(D)** Same as in (A) but transfected with pCR3.1 Vpu ELV or indicated mutant. **(E)** Percentages of tetherin surface expression levels calculated from median fluorescence intensities from (A-D).

Recent data suggests that Vpu blocks both the transit of *de novo* synthesised tetherin to the cell surface as well as the recycling of endocytosed tetherin molecules from the plasma membrane. Tetherin recycling requires a dual tyrosine **Y**x**Y**xxϕ motif in its cytoplasmic tail that acts as a binding site for AP-2 (for internalisation) and AP-1 (for recycling via the Golgi) (Rollason et al., 2007) (Masuyama et al., 2009). Mutation of this motif enhances tetherin surface expression, but only has minor effects on its ability to restrict virus release or its sensitivity to Vpu (Iwabu et al., 2009) (Dubé et al., 2010b). Since tetherin is degraded by an ubiquitin-dependent process, and Vpu-mediated recruitment of the SCF-β-TrCP E3 ubiquitin ligase complex has been shown to induce tetherin ubiquitination at multiple residues in its cytoplasmic tail, one being a serine/threonine motif (STS) (Tokarev et al., 2011), we asked whether Vpu LILI, 2/6A and ELV clathrin box chimeras were differentially defective against tetherin mutants bearing changes in its sorting sequence and ubiquitination motif. We transfected 293T tetherin STS mutant and 293T tetherin Y6,8A cells with NL4.3 delVpu in combination with increasing concentrations of indicated Vpu clathrin box chimera expression vectors, and measured viral release 48 hours later (Figure 6-4 A until F). Vpu ESCRT, phospho- and trafficking mutants when fused to the HRS clathrin box displayed the ability to antagonise tetherin function to levels similar to the wild-type Vpu protein in tetherin cells defective for the serine/threonine motif (Figure 6-4 A until C). These levels were also comparable with rescue of virus release obtained in wild-type tetherin cells (Figure 6-2 D until F). Interestingly, mutant Vpu clathrin box chimeras failed to rescue virus particle release from tetherin mutant cells bearing lesions in its sorting motif **Y**x**Y**xxϕ (Figure 6-4D until F), suggesting that the rescue of three different Vpu mutants by addition of a C-terminal clathrin-binding motif requires tetherin to retain its capacity to recycle from the PM.

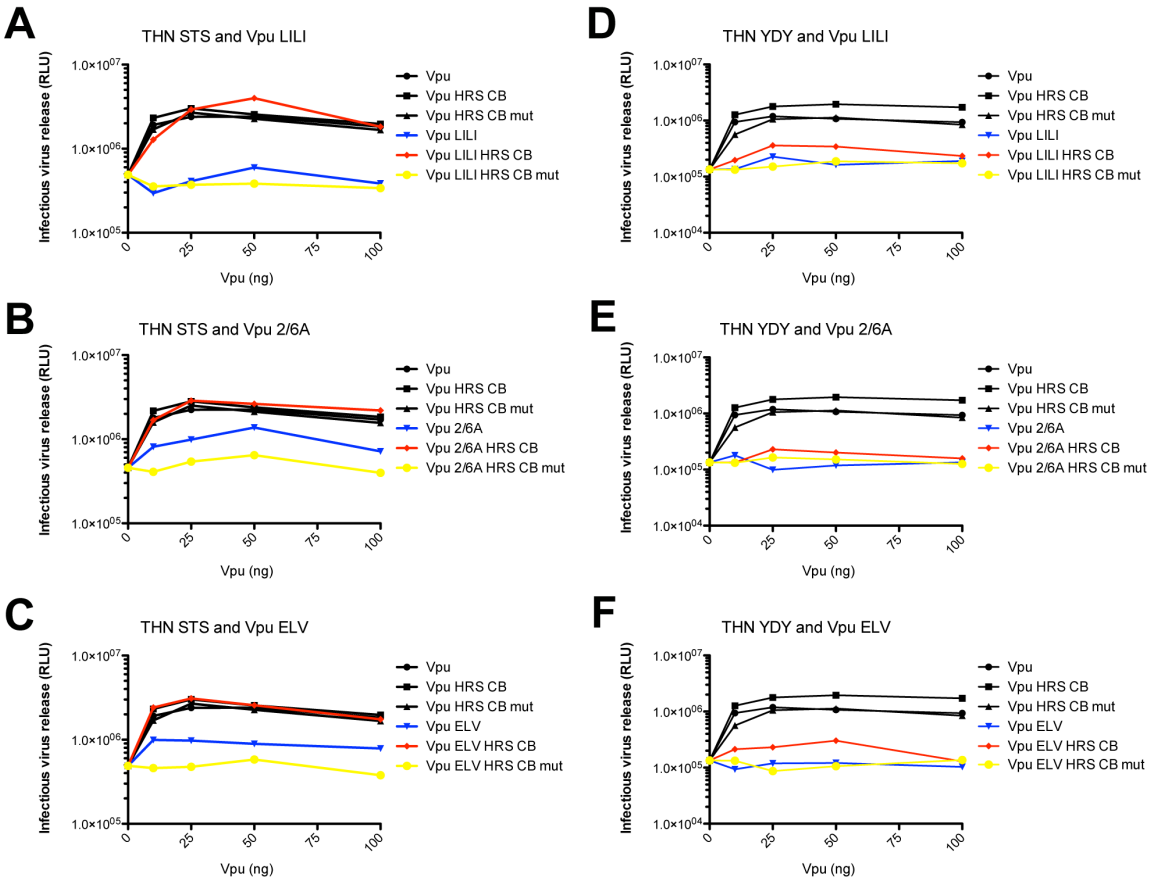

Figure 6-4 Virus particle release rescue is dependent on an intact YxYxxϕ motif in tetherin

(A) 293T tetherin STS cells were transfected with NL4.3 delVpu proviral plasmid in combination with YFP expression vector, pCR3.1 Vpu, pCR3.1 Vpu HRS CB, pCR3.1 Vpu HRS CB mut or Vpu LILI CB chimera. 48 hours post transfection, infectivity of viral supernatants from was determined on HeLa-TZMbl. **(B)** Same as in (A) but with pCR3.1 Vpu 2/6A CB chimera constructs. **(C)** Same as in (A) but with pCR3.1 Vpu ELV CB chimera constructs. **(D)** 293T tetherin Y6,8A cells were transfected with NL4.3 delVpu proviral plasmid in combination with YFP expression vector, pCR3.1 Vpu, pCR3.1 Vpu HRS CB, pCR3.1 Vpu HRS CB mut or Vpu LILI CB chimera. 48 hours post transfection, infectivity of viral supernatants from was determined on HeLa-TZMbl. **(E)** Same as in (D) but with pCR3.1 Vpu 2/6A CB chimera constructs. **(F)** Same as in (D) but with pCR3.1 Vpu ELV CB chimera constructs.

Next, we tested if the rescue of tetherin antagonism demonstrated in Figure 6-2 and Figure 6-3 was sensitive to inhibition of overall clathrin function. We therefore performed an overexpression experiment using the C-terminal fragment of the neuronal adaptor AP180 (AP180c) that inhibits clathrin/membrane interactions (Ford et al., 2001), co-transfected with NL4.3 delVpu and indicated Vpu clathrin box chimera, and tested physical virus particle release from tetherin positive cells (Figure 6-5A). As expected, physical virus particle release from wild-type Vpu transfected cells was blocked upon AP180c expression by approximately 7-fold, while release from mock-infected cells was unchanged. AP180c expression had only minor effects on Vpu LILI, 2/6A or ELV mutants (2-, 3- and 5-fold respectively). Interestingly, the rescue of Vpu mutants by fusion to a clathrin-binding motif was sensitive to relative available cellular clathrin. Virus release from Vpu LILI, 2/6A and ELV was dramatically decreased by AP180c expression (6-, 5- and 6.5-fold respectively). Interestingly, AP180c expression enhanced total Vpu levels (like observed in Figure 4-6), indicating a clathrin-dependent transport in natural turnover of Vpu proteins. Thus, Vpu function can be substantially recovered by fusing Vpu cytoplasmic tail LILI, 2/6A and ELV mutants to a clathrin-binding signal, indicating that linking Vpu directly to the clathrin trafficking machinery can restore its activity. Furthermore, the recovery observed is dependent on cellular clathrin levels.

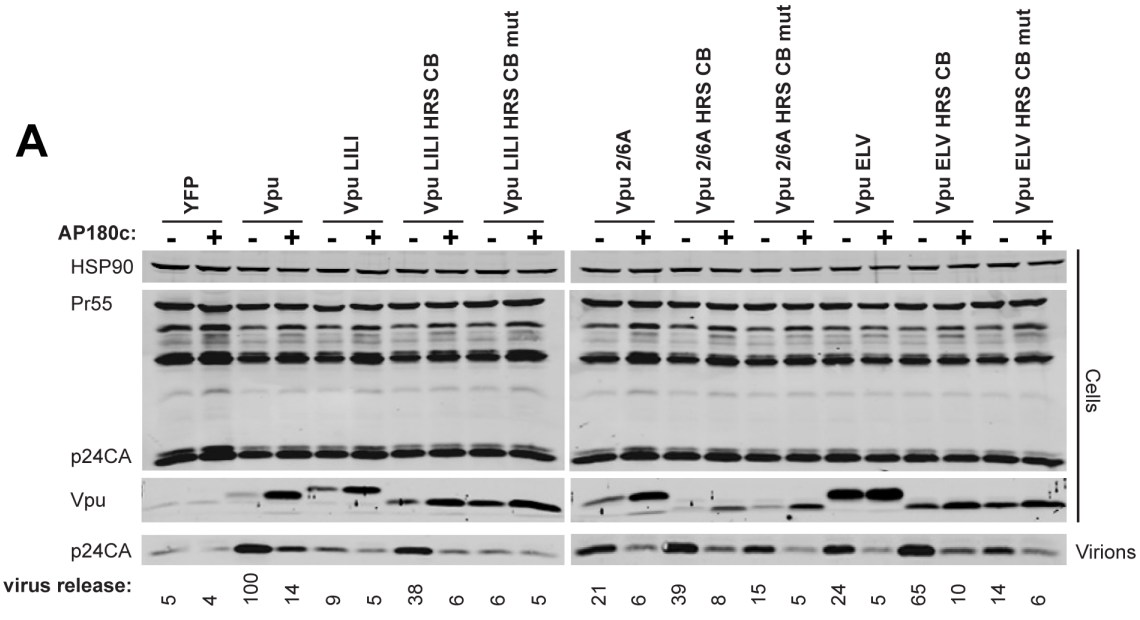

Figure 6-5 Functional rescue of Vpu cytoplasmic tail mutants is dependent on clathrin

(A) 293T tetherin expressing cells were co-transfected with NL4.3 delVpu proviral plasmid and YFP, Vpu, Vpu HRS CB, Vpu HRS CB mut expression vector or indicated mutant in combination with AP180c. 48 hours post transfection, cell lysates and pelleted supernatant virions were harvested and subjected to SDS-PAGE and analysed by Western blotting for HIV-1 p24CA, Vpu and Hsp90, and analysed by LiCor quantitative imager.

6.2.2 Are Vpu ESCRT-0-binding mutant, phospho-mutant, and trafficking mutant defective for the same reason?

Next, we wanted to explore why tetherin antagonism by Vpu ESCRT-0 and phosho-mutants was rescued by C-terminal fusion to the HRS clathrin-binding motif. Since these Vpu mutants are defective in their interaction with both the ESCRT-0 component HRS and the SCF E3 ubiquitin ligase complex, which binds to two phosphorylated serine residues in Vpu cytoplasmic tail, and have not been associated with the clathrin machinery. While it is not surprising that Vpu ELV trafficking mutants are able to interact with clathrin adaptor AP-1 (Figure 4-15), these are being rescued by introduction of a direct clathrin-binding sequence, therefore bypassing the need for an adaptor protein. To get a better understanding of the cellular implications of the ESCRT-binding and phospho-mutant we made use the BioID assay. To this end, we fused BirA to myc-tagged subgroup B Vpu 3/7A (resembles phospho-mutant) and Vpu I+I (ESCRT-0 binding mutant) and transfected 293T tetherin cells with either mutant, wild-type or ELV Vpu proteins. As expected, using this new BioID assay we were able to demonstrate that AP-1 interacts with wild-type Vpu. However, Vpu I+I mutants failed to interact with AP-1 similarly to the defect observed in Vpu ELV mutants, while Vpu 3/7A interaction with AP-1 was impaired. These results allow us to conclude that AP-1 interaction with Vpu is highly sensitive and dependent on an overall intact Vpu cytoplasmic tail structure.

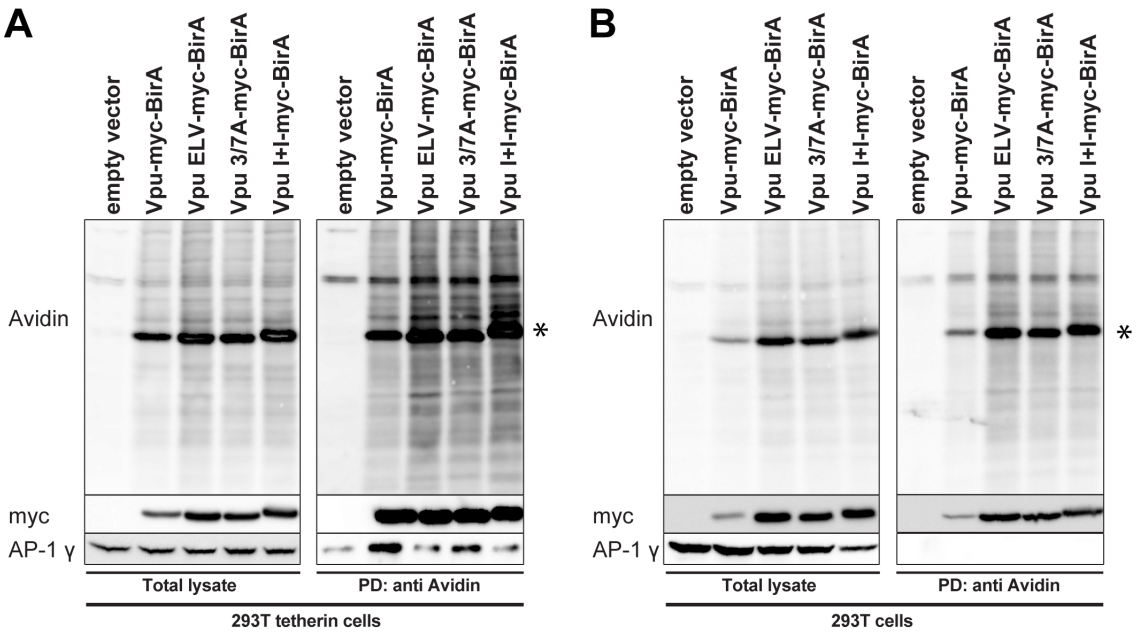

Figure 6-6 Vpu phospho-mutant and ESCRT-0 interaction mutant are defective for AP-1 interaction in tetherin positive cells

(A) 293T tetherin cells were transfected with subgroup B Vpu-myc-BirA, B Vpu ELV-myc-BirA, B Vpu 3/7A-myc-BirA (phospho-mutant), B Vpu I+I-myc-BirA (naturally occurring ESCRT interaction mutant) or empty vector control. 6 hours post transfection, cells were treated with 10 nM concanamycin A in the presence of 150 μM free Biotin. 16 hours later, cells were washed, lysed, sonicated and biotinylated proteins were recovered on streptavidin-conjugated beads and analysed by Western blot for avidin, Vpu-myc-BirA and AP-1 γ. Asterisk: Vpu-myc-BirA band. **(B)** Same as in (A) but with 293T cells (performed together with Dr Toshana Foster). Same data set as presented in Figure 4-15,

6.3 Discussion

In this chapter we have been able to functionally substitute Vpu LILI, 2/6A and ELV mutants with a direct clathrin heavy chain-binding motif of the ESCRT-0 component HRS, which is highly conserved among HRS homologues in yeast, nematodes and flies. By fusing the clathrin-binding sequence to the C-terminus of Vpu cytoplasmic tail mutants we were able to rescue infectious virus particle release in a clathrin-dependent manner, as well as tetherin cell surface downregulation to almost wild-type Vpu levels. We were also able to confirm these results with a different clathrin heavy chain-binding motif from GGA2 (RN**LL**DLL) that is not located at either C- or N-terminus of the protein. This indicates that the observed rescue is dependent on clathrin heavy chain-binding *per se* and not specific clathrin-binding motif peptides. To date there is no full-length crystal structure of Vpu or Vpu and tetherin complexes, making it difficult to predict the impact of an additional C-terminal clathrin-binding motif on the structural integrity of the cytoplasmic tail of Vpu, which is thought to be dynamic. Since we were able to rescue all tested Vpu mutants to similar levels, one could speculate that the additional 7 residues of the clathrin-binding box lead to an alteration of the structure of the cytoplasmic tail, blocking host cell protein interactions and therefore making all Vpu mutants dependent on the clathrin interaction despite their different underlying defects.

We were able to functionally rescue the Vpu 2/6A phospho-mutant with the addition of a clathrin-binding motif but without restoring binding to the SCF-β-TrCP E3 ubiquitin ligase complex. This and previous studies suggest that serine phosphorylation and recruitment of SCF-β-TrCP may be dispensable for tetherin antagonism (Tervo et al., 2011). Indeed, a dual function of the D**S**GNE**S** motif has been suggested in accordance with previous demonstrations that β-TrCP is not strictly required for tetherin trafficking by Vpu (Schmidt et al., 2011), and that Vpus with N55H or E56G mutations within the D**S**GNE**S** motif affected tetherin counteraction but were still able to bind to β-TrCP (Pickering et al., 2014). It is possible that these residues are required to facilitate access to either of the two cytoplasmic helices. In this regard, acidic dileucine trafficking motifs, such as the **E**xxx**LV** signal of Vpu, have been associated with upstream serine phosphorylation in the trafficking of the CI-M6PR (Mauxion et al., 1996).

The clathrin box-mediated rescue of tetherin antagonism by Vpu is dependent on an intact trafficking signal (**Y**x**Y**xxϕ) in the tetherin cytoplasmic tail but independent of the ubiquitination motif STS. As demonstrated in Chapter 4 residual activity of Vpu ELV mutants is dependent on an intact **Y**x**Y**xxϕ motif in tetherin and Vpu ELV mutants fail to re-route tetherin to endosomal compartments for degradation, resulting in Vpu ELV

mutants being dragged to the plasma membrane by tetherin where they are being incorporated into budding virions. Therefore it would be interesting to see if all Vpu cytoplasmic tail mutants and/or Vpu clathrin box chimeras are being incorporated into virions like ELV mutants.

We propose that ESCRT-0, phospho- and trafficking Vpu mutants are defective for the same reasons, namely that they are unable to interact with the cellular clathrin machinery. To this end, our preliminary data suggests that as expected Vpu ELV mutants are defective in interacting with AP-1, and interestingly Vpu ESCRT-0 and phospho-mutants also displayed a defect in AP-1 binding. However, more work needs to be done to answer questions like: whether other clathrin adaptors like AP-2 are able to interact with Vpu additionally to AP-1. Due to technical problems we were unable to demonstrate direct binding of Vpu clathrin box chimeras to the clathrin heavy chain using recombinant proteins, but more experiments are being performed to answer this question.

Vpu-mediated ESCRT-dependent degradation of tetherin is defective for Vpu LILI, 2/6A and ELV mutants. Therefore it would be interesting to see if addition of the clathrin-binding sequence restores tetherin degradation. Another important unanswered question is the subcellular localisation of the Vpu clathrin box chimeras. Especially, if the chimeras accumulate at endosomal compartments, as the HRS clathrin-binding sequence has been shown to be important for scaffolding of HRS into clathrin rich dynamic micro-domains, important for the degradation of the endocytosed epidermal growth factor (EGF) (Raiborg et al., 2006). To date, these clathrin-binding motif induced micro-domains have only been observed on endosomal membranes (Raiborg et al., 2002).

By fusing the clathrin-binding box directly to the C-terminus of Vpu we might have introduced an additional (**D**/**E**)xxx**L**(**L**/**I**) motif starting at residue D80 which is highly conserved and important for tetherin antagonism (Pickering et al., 2014). We therefore introduced a short linker sequence between Vpu and the clathrin box and repeated the experiments to ensure that the observed effect is due to direct binding to the clathrin heavy chain and not due to interaction with clathrin adaptors. Preliminary data suggest that the rescue in virus particle release is only mildly affected by introducing a linker between Vpu and the clathrin box to disrupt a potential clathrin adaptor-binding motif.

Chapter 7 GENERAL CONCLUSION AND FUTURE DIRECTIONS

Since Vpu was first discovered in 1988 its list of functions has increased steadily. To date the major roles attributed to Vpu include rapid degradation of the cell surface receptor CD4, enhancement of virus particle release by counteraction of tetherin and downmodulation of CD1d and NTB-A. Vpu targets these membrane-associated proteins to allow HIV-1 to escape immune activation and to create optimal condition for virus replication. However, the importance of Vpu during HIV-1 infection might still be incomplete. *In vivo* there is selective pressure for maintaining a functional *vpu* gene, as for example monkeys infected with a Vpu-defective SHIV variant carrying an ATG to ACG mutation revert back to a functional open reading frame during the course of infection (McCormick-Davis et al., 1998). Furthermore, a single genome analysis of *vpu* alleles from HIV-1 clade B infected individuals showed that despite extensive amino acid diversity of the Vpu protein, the Vpu functions of targeting CD4 and counteracting both physical virus restriction and NF-κB activation by tetherin are rarely impaired (Pickering et al., 2014). These observations highlight the importance of maintaining Vpu function throughout HIV-1 infection. It is intriguing that Vpu, an 81 amino acid protein, can interact with a broad range of cellular target proteins sharing little or no homology. One of the best-characterised examples to illustrate the role of Vpu in antagonising cellular innate immune defences is the restriction factor tetherin. The studies of the mechanism by which Vpu antagonises the anti-viral function of tetherin provide a powerful tool to understand the complex interactions between virus and host.

Towards a unified mechanistic model of tetherin antagonism by HIV-1 Vpu

In Chapter 4, through mutational analysis of the second alpha helix of HV-1 Vpu (NL4.3), we have identified a determinant, **E**59xxx**L**63**V**64, which is required for efficient antagonism of tetherin. Importantly, this motif is required to counteract tetherin in CD4+ T cells, particularly after their exposure to type I IFN. Mutation of this site blocks the ability of Vpu to mediate downregulation of tetherin cell surface expression and its ESCRT-dependent degradation, but does not abolish its interaction with tetherin, nor recruitment of β-TrCP2 or the ESCRT-0 component HRS. Vpu ELV mutants localise to the cell surface and early/recycling endosomal compartments rather than the TGN by virtue of their interaction with tetherin. Residual Vpu ELV activity against tetherin was entirely dependent on an intact recycling motif in tetherin's cytoplasmic tail, suggesting that this motif differentially affects antagonism of newly synthesized tetherin rather than pre-existing pools recycling to the PM. Using the new BioID technique we were able to demonstrate that Vpu interacts with AP-1 in the presence of tetherin, and that this interaction is dependent on an intact **E**xxx**LV** motif in the second alpha helix of Vpu. This data is in agreement with an unpublished crystal

structure, presented at the 2013 CSH Retrovirology meeting, that shows that the σ and γ subunits of AP-1 bind to the Vpu **E**xxx**LV** motif while the **Y**D**Y** motif in tetherin binds to the μ subunit which in turn recruits the β subunit of the AP-1 complex.

Therefore, in the presence of an intact **E**xxx**LV** motif, Vpu mediates the inhibition of transit of newly synthesised and/or recycling tetherin to the cell surface, its internal sequestration and targeting for endo/lysosomal degradation occuring via an AP-1-dependent mechanism. In the absence of an intact **E**xxx**LV** motif, Vpu/tetherin complexes recycle via the plasma membrane dependent on the **Y**x**Y**xx**V** sorting motif in the tetherin cytoplasmic tail, which interacts with AP-2 and AP-1. During the recycling process, physical interaction of Vpu and/or modification by ubiquitin ligases, such as SCF-β-TrCP2, may further interfere with tetherin function to a variable degree in the absence of cell-surface downregulation (Figure 7-1).

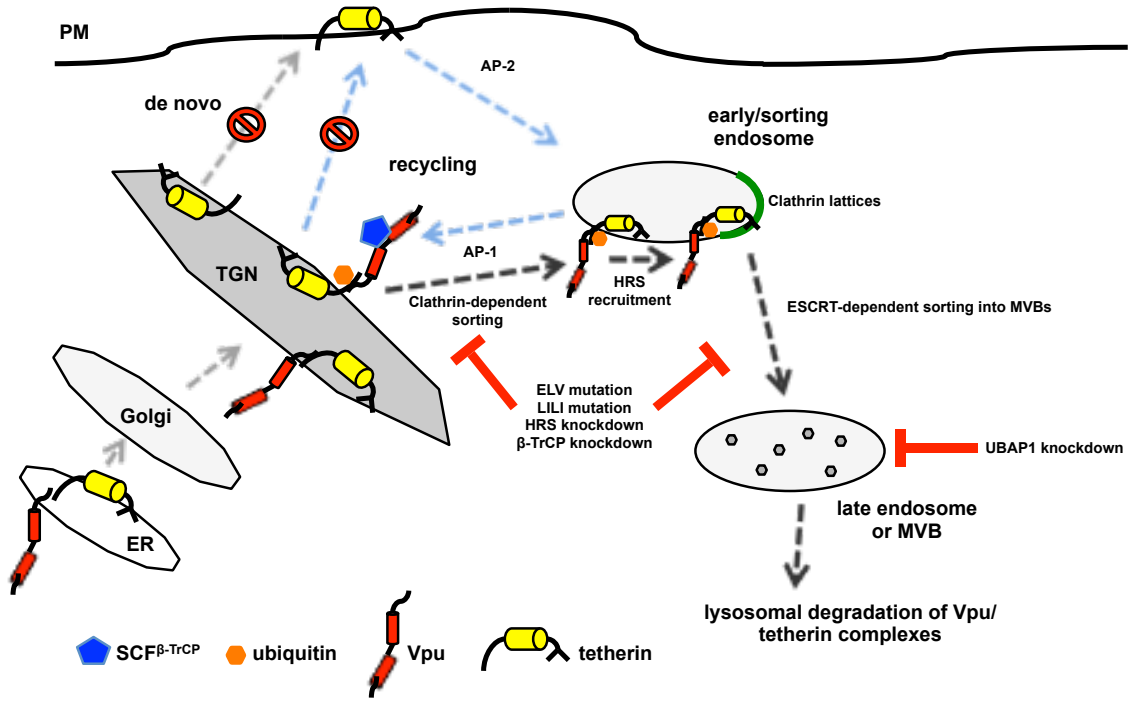

Figure 7-1 Unified mechanistic model of tetherin antagonism by HIV-1 Vpu

Newly synthesised tetherin molecules reach the plasma membrane by using the secretory pathway. At the plasma membrane tetherin incorporates into viral particles or recycles constitutively via early/sorting endosomal compartments and the TGN. Vpu interacts with recycling tetherin in the TGN (and with newly synthesised tetherin molceules perhaps earlier) through transmembrane domain-mediated interactions. Vpu/tetherin complexes are targeted to early endosomal compartments by a clathrin-dependent transport mechanism. During this process, physical interaction of Vpu and/or modification by ubiquitin ligases, such as SCF-β-TrCP2, lead to ubiquitination of tetherin on multiple cytoplasmic tail residues. In early/recycling endosomes ubiquitin-dependent recruitment of HRS promotes sorting of Vpu/tetherin complexes for ESCRT-dependent degradation in lysosomes. In the absence of an **E**xxx**LV** motif, Vpu/tetherin complexes recycle via the PM, which is dependent on the **Y**x**Y**xxϕ sorting sequence in the tetherin cytoplasmic tail that interacts with AP-2 and AP-1. Blue arrows indicate normal tetherin recycling; black arrows indicate Vpu-mediated tetherin transport for ultimate degradation; and red bars indicate Vpu mutations or siRNA treatments that disturb this process.

In Chapter 5, we have identified a role for the ESCRT-I component UBAP1 in Vpu-mediated tetherin degradation (Figure 7-1). However, degradation *per se* is dispensable for Vpu-induced anti-tetherin activity. Furthermore, we have identified naturally occurring hydrophobic residues in the first alpha helix of the cytoplasmic tail of the HIV-1 NL4.3 Vpu, LI 41/42 AA LI 45/46 AA, which are required for the antagonism of tetherin restriction. Mutation of these residues blocks the ability of Vpu to mediate tetherin surface downregulation and induce ESCRT-dependent degradation of tetherin. Vpu LILI mutants retain the ability to interact with tetherin and to recruit the ubiquitin ligase SCF-β-TrCP2 complex. Interestingly, Vpu LILI mutants pheno-copy the cellular localisation of trafficking mutants, in which they localise to early/recycling endosomal structures and the plasma membrane rather than the TGN.

Taking all data together, we propose the following model for Vpu-mediated ESCRT-dependent tetherin and/or target protein degradation (Figure 7-2A): HIV-1 Vpu binds to its target designated for lysosomal degradation, where the target protein can be tetherin or an yet unidentified cellular interaction partner. Vpu induces ubiquitination of its target by β-TrCP2, and potentially by another to date unknown ubiquitin ligase. The Vpu/target protein complexes are shuttled to endosomal compartments where the ubiquitinated target membrane protein interacts with ESCRT-0 component HRS via the double ubiquitin-binding motif (DUIM) in the HRS cytoplasmic tail. Clathrin and HRS form a matrix, which allows the trapping and concentrating of ubiquitinated transmembrane proteins on the surface of recycling/sorting endosomes. ESCRT-I, including the newly identified subunit UBAP1, and ESCRT-II and -III complexes are then sequentially recruited, delivering Vpu/target complexes to the intracellular lumen of late endosomal structures also called multivesicular bodies, which in turn fuse to lysosomes leading to the degradation of the internalised cargo.

A

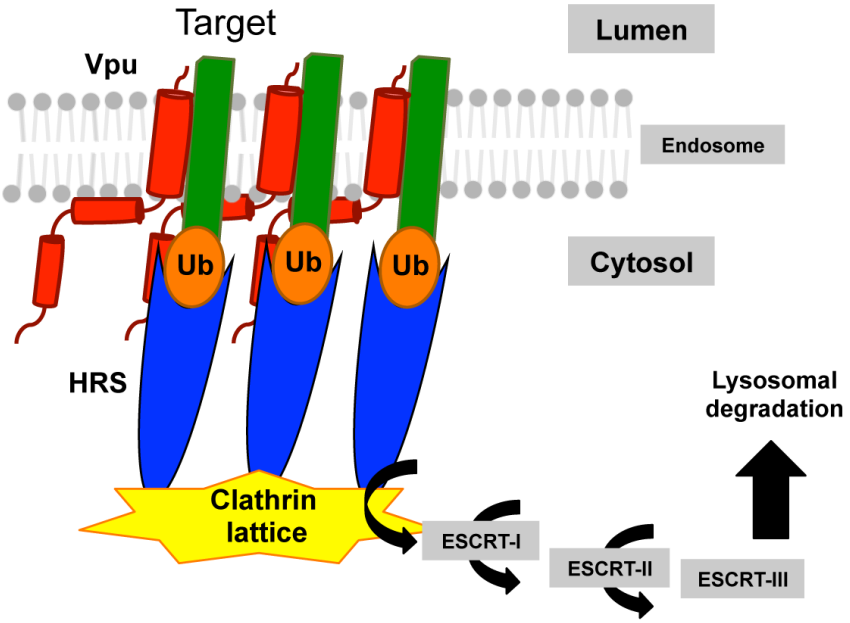

Figure 7-2 Model for Vpu-mediated ESCRT-dependent tetherin degradation

HIV-1 Vpu binds to its target (tetherin or potentially other proteins) designated for lysosomal degradation, the target protein could be tetherin or a unidentified cellular interaction partner. Vpu induces ubiquitination of its target by β-TrCP2 and potentially another to date unknown ubiquitin ligase. The Vpu/target protein complexes are shuttled to endosomal compartments where the ubiquitinated target membrane protein interacts with ESCRT-0 component HRS via the double ubiquitin-binding motif (DUIM) in the HRS cytoplasmic tail. ESCRT-I, -II and -III complexes are being sequentially recruited, delivering Vpu/target complexes to the intracellular lumen of late endosomal structures also called multivesicular bodies (MVBs) which in turn fuse to lysosomes leading to the degradation of the internalised cargo.

Future directions

Vpu ELV, LILI and 2/6A cytoplasmic tail mutants predominately localise to punctate structures within the cytoplasm, which are most likely early/recycling endosomal compartments. Therefore, Vpu LILI and Vpu 2/6A mutants pheno-copy the localisation defect of Vpu ELV mutants that are unable to bind the clathrin adaptor AP-1. We consequently asked the question if Vpu LILI and Vpu 2/6A mutants are also defective for clathrin adaptor binding. In Chapter 6, we were able to functionally substitute Vpu LILI, 2/6A and ELV mutants. By fusing a clathrin-binding motif to the C-terminus of these mutants we were able to rescue infectious virus particle release in a clathrin-dependent manner, as well as tetherin cell surface downregulation. Interestingly in case of the Vpu 2/6A clathrin-binding motif chimera we were able to rescue anti-tetherin function in the absence of recruitment of the SCF-β-TrCP E3 ubiquitin ligase complex. We concluded from this data that Vpu ELV, LILI and 2/6A mutants are defective for the same reason, which is that they fail to induce binding to the cellular clathrin adaptor machinery.

Viral proteins, including HIV-1 Vpu, often target numerous cellular factors. A diversified set of protein conformational subpopulations is required for productive interaction with multiple targets. Since there is no full-length crystal structure of Vpu, Vpu/tetherin complexes, or Vpu in combination with cellular binding partners it is difficult to predict the conformation of the cytoplasmic tail. However, Vpu conformation might adapt for interactions with various cellular proteins. The Vpu cytoplasmic tail exhibits a certain degree of structural flexibility in NMR studies (Wittlich et al., 2009), which lead us to propose the following hypothesis: In a closed confirmation, the second alpha helix **E**xxx**LV** motif is embedded within the tertiary structure. The conserved W at amino acid position 76 (Pickering et al., 2014) (Jafari et al., 2014) folds back and interacts with acidic residues within the D**S**GNE**S** motif, to keep the cytoplasmic tail locked in an auto-inhibited position. However, upon phosphorylation; change in cellular environment, for example pH; or binding to tetherin or a cellular binding partner, Vpu undergoes a conformational change and adapts an open configuration in which the **E**xxx**LV** motif is accessible to bind AP-1 (Figure 7-3). Mutations within the LILI and D**S**GNE**S** motifs or the conserved W interfere with tertiary structural rearrangements and render Vpu defective in tetherin counteraction.

Currently, we are planning a series of experiments that will help us to understand the impact of phosphorylation on cytoplasmic tail rearrangements. To this end, we are planning to make use of the Vpu cytoplasmic tail mutant clathrin-binding box chimeras. If our hypothesis is true, CKII phosphorylation inhibitors will affect Vpu wild-type ability to counteract tetherin, but not Vpu wild-type clathrin-binding box equivalent, as this construct is able to link Vpu to the clathrin machinery directly without having to undergo a conformational change. Furthermore, CKII inhibitors will abrogate binding of wild-type Vpu to AP-1 in BioID pull-down assays.

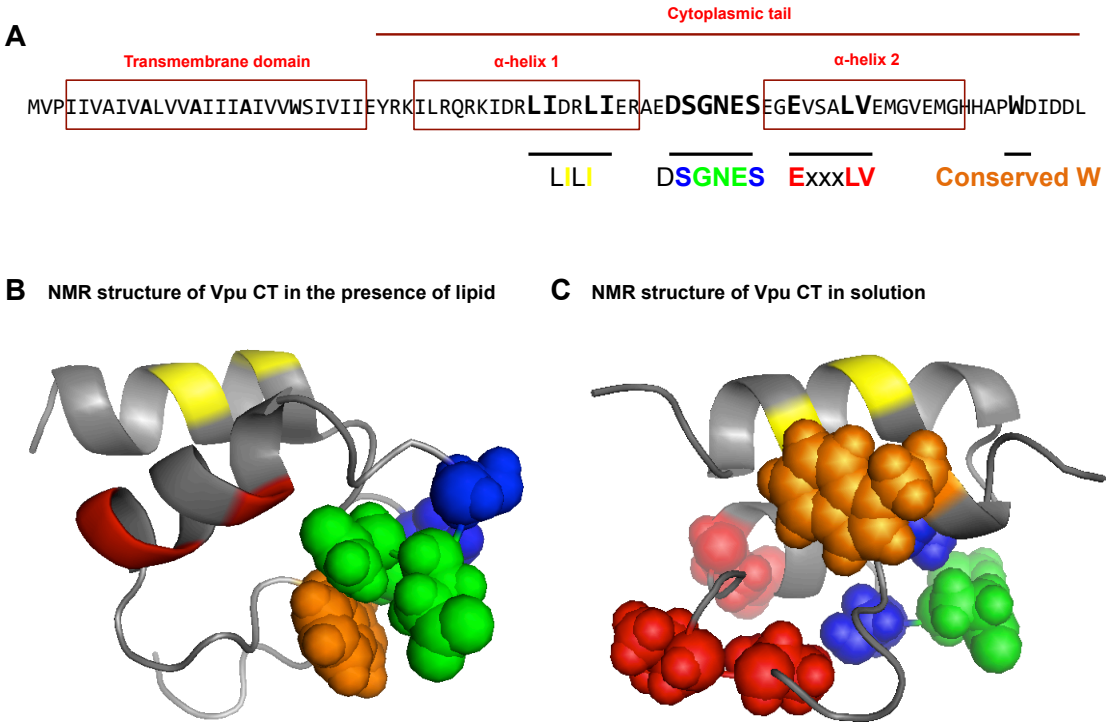

Figure 7-3 Does serine phosphorylation expose the ExxxLV motif?

(A) NL4.3 Vpu amino acid sequence. Highlighted are conserved motifs within the cytoplasmic tail that are required for tetherin antagonism. **(B)** Structure of the Vpu CT in the presence of membrane simulating dodecylphosphatidylcholine (DPC) micelles obtained by high-resolution liquid state NMR adapted from (Wittlich et al., 2009). **(C)** Structure of the Vpu CT in aqueous buffer obtained by high-resolution liquid state NMR adapted from (Wittlich et al., 2009). Highlighted and colour-coordinated are motifs from (A) (images produced by Stuart Neil using PyMOL version 1.7, personal communication).

REFERENCES

Abada, P., Noble, B., and Cannon, P.M. (2005). Functional Domains within the Human Immunodeficiency Virus Type 2 Envelope Protein Required To Enhance Virus Production Functional Domains within the Human Immunodeficiency Virus Type 2 Envelope Protein Required To Enhance Virus Production. J. Virol. *79*, 3627–3638.

Agromayor, M., Soler, N., Caballe, A., Kueck, T., Freund, S.M., Allen, M.D., Bycroft, M., Perisic, O., Ye, Y., McDonald, B., et al. (2012). The UBAP1 subunit of ESCRT-I interacts with ubiquitin via a SOUBA domain. Structure *20*, 414–428.

Aiken, C., and Joyce, S. (2011). TRIM5 does double duty. Nature *472*, 305–306.

Alter, G., Heckerman, D., Schneidewind, A., Fadda, L., Kadie, C.M., Carlson, J.M., Oniangue-Ndza, C., Martin, M., Li, B., Khakoo, S.I., et al. (2011). HIV-1 adaptation to NK-cell-mediated immune pressure. Nature *476*, 96–100.

Andrew, A., and Strebel, K. (2010). HIV-1 Vpu targets cell surface markers CD4 and BST-2 through distinct mechanisms. Mol. Aspects Med. *31*, 407–417.

Andrew, A.J., Miyagi, E., Kao, S., and Strebel, K. (2009). The formation of cysteine-linked dimers of BST-2/tetherin is important for inhibition of HIV-1 virus release but not for sensitivity to Vpu. Retrovirology *6*, 80.

Arhel, N. (2010). Revisiting HIV-1 uncoating. Retrovirology *7*, 96.

Arthos, J., Cicala, C., Martinelli, E., Macleod, K., Van Ryk, D., Wei, D., Xiao, Z., Veenstra, T.D., Conrad, T.P., Lempicki, R. a, et al. (2008). HIV-1 envelope protein binds to and signals through integrin alpha4beta7, the gut mucosal homing receptor for peripheral T cells. Nat. Immunol. *9*, 301–309.

Attar, N., and Cullen, P.J. (2010). The retromer complex. Adv. Enzyme Regul. *50*, 216–236.

Babst, M., Katzmann, D.J., Snyder, W.B., Wendland, B., and Emr, S.D. (2002a). Endosome-Associated Complex, ESCRT-II, Recruits Transport Machinery for Protein Sorting at the Multivesicular Body. Dev. Cell *3*, 283–289.

Babst, M., Katzmann, D.J., Estepa-Sabal, E.J., Meerloo, T., and Emr, S.D. (2002b). ESCRT-III: An Endosome-Associated Heterooligomeric Protein Complex Required for MVB sorting. Dev. Cell *3*, 271–282.

Baldauf, H.-M., Pan, X., Erikson, E., Schmidt, S., Daddacha, W., Burggraf, M., Schenkova, K., Ambiel, I., Wabnitz, G., Gramberg, T., et al. (2012). SAMHD1 restricts HIV-1 infection in resting CD4(+) T cells. Nat. Med. *18*, 1682–1687.

Barrett, B.S., Smith, D.S., Li, S.X., Guo, K., Hasenkrug, K.J., and Santiago, M.L. (2012). A single nucleotide polymorphism in tetherin promotes retrovirus restriction in vivo. PLoS Pathog. *8*, e1002596.

Bartee, E., McCormack, A., and Früh, K. (2006). Quantitative membrane proteomics reveals new cellular targets of viral immune modulators. PLoS Pathog. *2*, e107.

Bego, M.G., Mercier, J., and Cohen, E. a (2012). Virus-activated interferon regulatory factor 7 upregulates expression of the interferon-regulated BST2 gene independently of interferon signaling. J. Virol. *86*, 3513–3527.

Bergamaschi, A., Ayinde, D., David, A., Le Rouzic, E., Morel, M., Collin, G., Descamps, D., Damond, F., Brun-Vezinet, F., Nisole, S., et al. (2009). The human immunodeficiency virus type 2 Vpx protein usurps the CUL4A-DDB1 DCAF1 ubiquitin ligase to overcome a postentry block in macrophage infection. J. Virol. *83*, 4854–4860.

Berger, A., Sommer, A.F.R., Zwarg, J., Hamdorf, M., Welzel, K., Esly, N., Panitz, S., Reuter, A., Ramos, I., Jatiani, A., et al. (2011). SAMHD1-deficient CD14+ cells from individuals with Aicardi-Goutières syndrome are highly susceptible to HIV-1 infection. PLoS Pathog. *7*, e1002425.

Besnier, C., Takeuchi, Y., and Towers, G. (2002). Restriction of lentivirus in monkeys. Proc. Natl. Acad. Sci. U. S. A. *99*, 11920–11925.

Best, S., Le Tissier, P., Towers, G., and Stoye, J.P. (1996). Positiional cloning of the mouse retrovirus restriction gene Fv1. Nature *382*, 826–829.

Billcliff, P.G., Rollason, R., Prior, I., Owen, D.M., Gaus, K., and Banting, G. (2013). CD317/tetherin is an organiser of membrane microdomains. J. Cell Sci. *126*, 1553–1564.

Binette, J., Dubé, M., Mercier, J., Halawani, D., Latterich, M., and Cohen, É. a (2007). Requirements for the selective degradation of CD4 receptor molecules by the human immunodeficiency virus type 1 Vpu protein in the endoplasmic reticulum. Retrovirology *4*, 75.

Biron, A. (1999). Initial and innate responses to viral infections in immunity or disease - pattern setting in immunity or disease. Curr. Opin. Microbiol. *2*, 374–381.

Bishop, K.N., Holmes, R.K., and Malim, M.H. (2006). Antiviral potency of APOBEC proteins does not correlate with cytidine deamination. J. Virol. *80*, 8450–8458.

Blagoveshchenskaya, A.D., Thomas, L., Feliciangeli, S.F., Hung, C.H., and Thomas, G. (2002). HIV-1 Nef downregulates MHC-I by a PACS-1- and PI3K-regulated ARF6 endocytic pathway. Cell *111*, 853–866.

Blondeau, C., Pelchen-Matthews, A., Mlcochova, P., Marsh, M., Milne, R.S.B., and Towers, G.J. (2013). Tetherin restricts herpes simplex virus 1 and is antagonized by glycoprotein M. J. Virol. *87*, 13124–13133.

Bolduan, S., Hubel, P., Reif, T., Lodermeyer, V., Höhne, K., Fritz, J. V, Sauter, D., Kirchhoff, F., Fackler, O.T., Schindler, M., et al. (2013). HIV-1 Vpu affects the anterograde transport and the glycosylation pattern of NTB-A. Virology *440*, 190–203.

Bolinger, C., Sharma, A., Singh, D., Yu, L., and Boris-Lawrie, K. (2010). RNA helicase A modulates translation of HIV-1 and infectivity of progeny virions. Nucleic Acids Res. *38*, 1686–1696.

Bonaparte, M.I., and Barker, E. (2003). Inability of natural killer cells to destroy autologous HIV-infected T lymphocytes. AIDS *17*, 487–494.

Bonifacino, J.S., and Traub, L.M. (2003). Signals for sorting of transmembrane proteins to endosomes and lysosomes. Annu. Rev. Biochem. *72*, 395–447.

Bour, S., and Strebel, K. (1996). The human immunodeficiency virus (HIV) type 2 envelope protein is a functional complement to HIV type 1 Vpu that enhances particle release of heterologous retroviruses . The Human Immunodeficiency Virus (HIV) Type 2 Envelope Protein Is a Functional Co. J. Virol. *70*, 8285–8300.

Bour, S., and Strebel, K. (2003). The HIV-1 Vpu protein: a multifunctional enhancer of viral particle release. Microbes Infect. *5*, 1029–1039.

Bour, S., Schubert, U., Strebel, K., Bour, S., and Schubert, U. (1995). The human immunodeficiency virus type 1 Vpu protein specifically binds to the cytoplasmic domain of CD4: implications for the mechanism of degradation. J. Virol. *69*, 1510–1520.

Bour, S., Akari, H., Miyagi, E., and Strebel, K. (2003). Naturally occurring amino acid substitutions in the HIV-2 ROD envelope glycoprotein regulate its ability to augment viral particle release. Virology *309*, 85–98.

Brass, A.L., Dykxhoorn, D.M., Benita, Y., Yan, N., Engelman, A., Xavier, R.J., Lieberman, J., and Elledge, S.J. (2008). Identification of host proteins required for HIV infection through a functional genomic screen. Science *319*, 921–926.

Bresnahan, P. a, Yonemoto, W., Ferrell, S., Williams-Herman, D., Geleziunas, R., and Greene, W.C. (1998). A dileucine motif in HIV-1 Nef acts as an internalization signal for CD4 downregulation and binds the AP-1 clathrin adaptor. Curr. Biol. *8*, 1235–1238.

De Breyne, S., Soto-Rifo, R., López-Lastra, M., and Ohlmann, T. (2013). Translation initiation is driven by different mechanisms on the HIV-1 and HIV-2 genomic RNAs. Virus Res. *171*, 366–381.

Briggs, J. a G., Grünewald, K., Glass, B., Förster, F., Kräusslich, H.-G., and Fuller, S.D. (2006). The mechanism of HIV-1 core assembly: insights from three-dimensional reconstructions of authentic virions. Structure *14*, 15–20.

Bruce, E. a, Abbink, T.E., Wise, H.M., Rollason, R., Galao, R.P., Banting, G., Neil, S.J., and Digard, P. (2012). Release of filamentous and spherical influenza A virus is not restricted by tetherin. J. Gen. Virol. *93*, 963–969.

Bryceson, Y.T., March, M.E., Ljunggren, H.G., and Long, E.O. (2006). Activation, co–activation, and co–stimulation of resting human NK cells. Immunol. Rev. *214*, 73–91.

Butticaz, C., Michielin, O., Wyniger, J., Telenti, A., and Rothenberger, S. (2007). Silencing of both beta-TrCP1 and HOS (beta-TrCP2) is required to suppress human immunodeficiency virus type 1 Vpu-mediated CD4 down-modulation. J. Virol. *81*, 1502–1505.

Caillet, M., Janvier, K., Pelchen-Matthews, A., Delcroix-Genête, D., Camus, G., Marsh, M., and Berlioz-Torrent, C. (2011). Rab7A is required for efficient production of infectious HIV-1. PLoS Pathog. *7*, e1002347.

Canagarajah, B.J., Ren, X., Bonifacino, J.S., and Hurley, J.H. (2013). The clathrin adaptor complexes as a paradigm for membrane-associated allostery. Protein Sci. *22*, 517–529.

Cao, W., and Bover, L. (2010). Signaling and ligand interaction of ILT7: receptor-mediated regulatory mechanisms for plasmacytoid dendritic cells. Immunol. Rev. *234*, 163–176.

Cao, W., Bover, L., Cho, M., Wen, X., Hanabuchi, S., Bao, M., Rosen, D.B., Wang, Y.-H., Shaw, J.L., Du, Q., et al. (2009). Regulation of TLR7/9 responses in plasmacytoid dendritic cells by BST2 and ILT7 receptor interaction. J. Exp. Med. *206*, 1603–1614.

Carrington, M., and Alter, G. (2012). Innate immune control of HIV. Cold Spring Harb. Perspect. Med. *2*, a007070.

Casartelli, N., Sourisseau, M., Feldmann, J., Guivel-Benhassine, F., Mallet, A., Marcelin, A.-G., Guatelli, J., and Schwartz, O. (2010). Tetherin restricts productive HIV-1 cell-to-cell transmission. PLoS Pathog. *6*, e1000955.

Cerboni, C., Neri, F., Casartelli, N., Zingoni, A., Cosman, D., Rossi, P., Santoni, A., and Doria, M. (2007). Human immunodeficiency virus 1 Nef protein downmodulates the ligands of the activating receptor NKG2D and inhibits natural killer cell-mediated cytotoxicity. J. Gen. Virol. *88*, 242–250.

Chan, D.C., Fass, D., Berger, J.M., and Kim, P.S. (1997). Core structure of gp41 from the HIV envelope glycoprotein. Cell *89*, 263–273.

Chaudhuri, R., Lindwasser, O.W., Smith, W.J., Hurley, J.H., and Bonifacino, J.S. (2007). Downregulation of CD4 by human immunodeficiency virus type 1 Nef is dependent on clathrin and involves direct interaction of Nef with the AP2 clathrin adaptor. J. Virol. *81*, 3877–3890.

Chen, P., Hübner, W., Spinelli, M. a, and Chen, B.K. (2007). Predominant mode of human immunodeficiency virus transfer between T cells is mediated by sustained Env-dependent neutralization-resistant virological synapses. J. Virol. *81*, 12582–12595.

Cherepanov, P., Maertens, G., Proost, P., Devreese, B., Van Beeumen, J., Engelborghs, Y., De Clercq, E., and Debyser, Z. (2003). HIV-1 integrase forms stable tetramers and associates with LEDGF/p75 protein in human cells. J. Biol. Chem. *278*, 372–381.

Cho, M., Ishida, K., Chen, J., Ohkawa, J., Chen, W., Namiki, S., Kotaki, A., Arai, N., Arai, K., and Kamogawa-Schifter, Y. (2007). SAGE library screening reveals ILT7 as a specific plasmacytoid dendritic cell marker that regulates type I IFN production. Int. Immunol. *20*, 155–164.

Cicala, C., Martinelli, E., McNally, J.P., Goode, D.J., Gopaul, R., Hiatt, J., Jelicic, K., Kottilil, S., Macleod, K., O'Shea, A., et al. (2009). The integrin alpha4beta7 forms a complex with cell-surface CD4 and defines a T-cell subset that is highly susceptible to infection by HIV-1. Proc. Natl. Acad. Sci. U. S. A. *106*, 20877–20882.

Le Clerc, S., Coulonges, C., Delaneau, O., Van Manen, D., Herbeck, J.T., Limou, S., An, P., Martinson, J.J., Spadoni, J.-L., Therwath, A., et al. (2011). Screening low-frequency SNPS from genome-wide association study reveals a new risk allele for progression to AIDS. J. Acquir. Immune Defic. Syndr. *56*, 279–284.

Cocka, L.J., and Bates, P. (2012). Identification of alternatively translated Tetherin isoforms with differing antiviral and signaling activities. PLoS Pathog. *8*, e1002931.

Coffin, J., and Swanstrom, R. (2013). HIV pathogenesis: dynamics and genetics of viral populations and infected cells. Cold Spring Harb. Perspect. Med. *3*, a012526.

Cohen, E., Terwilliger, E., Sodroski, J., and Haseltine, W. (1988). Identification of a protein encoded by the vpu gene of HIV-1. Nature *334*, 532–534.

Cohen, G.B., Gandhi, R.T., Davis, D.M., Mandelboim, O., Chen, B.K., Strominger, J.L., and Baltimore, D. (1999). The selective downregulation of class I major histocompatibility complex proteins by HIV-1 protects HIV-infected cells from NK cells. Immunity *10*, 661–671.

Coiras, M., López-Huertas, M.R., Pérez-Olmeda, M., and Alcamí, J. (2009). Understanding HIV-1 latency provides clues for the eradication of long-term reservoirs. Nat. Rev. Microbiol. *7*, 798–812.

Cowan, S., Hatziioannou, T., Cunningham, T., Muesing, M. a, Gottlinger, H.G., and Bieniasz, P.D. (2002). Cellular inhibitors with Fv1-like activity restrict human and simian immunodeficiency virus tropism. Proc. Natl. Acad. Sci. U. S. A. *99*, 11914–11919.

Craigie, R., and Bushman, F.D. (2012). HIV DNA integration. Cold Spring Harb. Perspect. Med. *2*, a006890.

Cribier, A., Descours, B., Valadão, A.L.C., Laguette, N., and Benkirane, M. (2013). Phosphorylation of SAMHD1 by cyclin A2/CDK1 regulates its restriction activity toward HIV-1. Cell Rep. *3*, 1036–1043.

D'Souza, V., and Summers, M.F. (2005). How retroviruses select their genomes. Nat. Rev. Microbiol. *3*, 643–655.

Dalgleish, A.G., Beverley, P.C., Claphman, P.R., Crawford, D.H., Greaves, M.F., and Weiss, R.A. (1984). The CD4 (T4) antigen is an essential component of the receptor for the AIDS retrovirus. Nature *312*, 763–767.

Van Damme, N., Goff, D., Katsura, C., Jorgenson, R.L., Mitchell, R., Johnson, M.C., Stephens, E.B., and Guatelli, J. (2008). The interferon-induced protein BST-2 restricts HIV-1 release and is downregulated from the cell surface by the viral Vpu protein. Cell Host Microbe *3*, 245–252.

Dave, V.P., Hajjar, F., Dieng, M.M., Haddad, E., and Cohen, E. a (2013). Efficient BST2 antagonism by Vpu is critical for early HIV-1 dissemination in humanized mice. Retrovirology *10*, 128.

Diaz-Griffero, F., Li, X., Javanbakht, H., Song, B., Welikala, S., Stremlau, M., and Sodroski, J. (2006). Rapid turnover and polyubiquitylation of the retroviral restriction factor TRIM5. Virology *349*, 300–315.

Dismuke, D.J., and Aiken, C. (2006). Evidence for a Functional Link between Uncoating of the Human Immunodeficiency Virus Type 1 Core and Nuclear Import of the Viral Preintegration Complex. J. Virol. *80*, 3712–3720.

Doehle, B.P., and Gale, M.J. (2012). Chapter 10. In Nucleic Acid Sensors and Antiviral Immunity, S. Sambhara, and T. Fujita, eds. (Landes Bioscience), pp. 148–166.

Douglas, J.L., Viswanathan, K., McCarroll, M.N., Gustin, J.K., Früh, K., and Moses, A. V (2009). Vpu directs the degradation of the human immunodeficiency virus restriction

factor BST-2/Tetherin via a {beta}TrCP-dependent mechanism. J. Virol. *83*, 7931–7947.

Dowlatshahi, D.P., Sandrin, V., Vivona, S., Shaler, T. a, Kaiser, S.E., Melandri, F., Sundquist, W.I., and Kopito, R.R. (2012). ALIX is a Lys63-specific polyubiquitin binding protein that functions in retrovirus budding. Dev. Cell *23*, 1247–1254.

Dube, M., Roy, B.B., Guiot-Guillain, P., Mercier, J., Binette, J., Leung, G., and Cohen, E. a. (2009). Suppression of Tetherin-Restricting Activity upon Human Immunodeficiency Virus Type 1 Particle Release Correlates with Localization of Vpu in the trans-Golgi Network. J. Virol. *83*, 4574–4590.

Dubé, M., Bego, M.G., Paquay, C., and Cohen, É. a (2010a). Modulation of HIV-1-host interaction: role of the Vpu accessory protein. Retrovirology *7*, 114.

Dubé, M., Roy, B.B., Guiot-Guillain, P., Binette, J., Mercier, J., Chiasson, A., and Cohen, E. a (2010b). Antagonism of tetherin restriction of HIV-1 release by Vpu involves binding and sequestration of the restriction factor in a perinuclear compartment. PLoS Pathog. *6*, e1000856.

Dubé, M., Paquay, C., Roy, B.B., Bego, M.G., Mercier, J., and Cohen, E. a (2011). HIV-1 Vpu antagonizes BST-2 by interfering mainly with the trafficking of newly synthesized BST-2 to the cell surface. Traffic *12*, 1714–1729.

Edeling, M. a, Smith, C., and Owen, D. (2006). Life of a clathrin coat: insights from clathrin and AP structures. Nat. Rev. Mol. Cell Biol. *7*, 32–44.

Engelman, A., and Cherepanov, P. (2012). The structural biology of HIV-1: mechanistic and therapeutic insights. Nat. Rev. Microbiol. *10*, 279–290.

Erikson, E., Adam, T., Schmidt, S., Lehmann-Koch, J., Over, B., Goffinet, C., Harter, C., Bekeredjian-Ding, I., Sertel, S., Lasitschka, F., et al. (2011). In vivo expression profile of the antiviral restriction factor and tumor-targeting antigen CD317/BST-2/HM1.24/tetherin in humans. Proc. Natl. Acad. Sci. U. S. A. *108*, 13688–13693.

Fassati, A. (2012). Multiple roles of the capsid protein in the early steps of HIV-1 infection. Virus Res. *170*, 15–24.

Federau, T., Schubert, U., Flossdorf, J., Henklein, P., Schomburg, D., and Wray, V. (1996). Solution structure of the cytoplasmic domain of the human immunodeficiency virus type 1 encoded virus protein U (Vpu). Int. J. Pept. Res. Ther. *47*, 297–310.

Fitzpatrick, K., Skasko, M., Deerinck, T.J., Crum, J., Ellisman, M.H., and Guatelli, J. (2010). Direct restriction of virus release and incorporation of the interferon-induced protein BST-2 into HIV-1 particles. PLoS Pathog. *6*, e1000701.

Flint, S., Enquist, L., Racaniello, V., and Skalka, A. (2009). Principles of Virology (Washington: ASM Press).

Ford, M., Pearse, B., Higgins, M., Vallis, Y., Owen, D., Gibson, A., Hopkins, C., Evans, P., and McMahon, H. (2001). Simultaneous binding of PtdIns(4,5)P2 and clathrin by AP180 in the nucleation of clathrin lattices on membranes. Science *291*, 1051–1055.

Forshey, B.M., Schwedler, U. Von, Sundquist, W.I., and Aiken, C. (2002). Formation of a Human Immunodeficiency Virus Type 1 Core of Optimal Stability Is Crucial for Viral Replication. J. Virol. *76*.

Foster, J.L., and Garcia, J.V. (2008). HIV-1 Nef: at the crossroads. Retrovirology *5*, 84.

Friborg, J., Ladha, A., Gottlinger, H., Haseltine, W.A., and Cohen, E.A. (1995). Functional Analysis of the Phosphorylation Sites on the Human Immunodeficiency Virus Type 1 Vpu Protein. J. Acquir. Immune Defic. Syndr. Hum. Retrovirology *8*, 10–22.

Fritz, J. V, Tibroni, N., Keppler, O.T., and Fackler, O.T. (2012). HIV-1 Vpu's lipid raft association is dispensable for counteraction of the particle release restriction imposed by CD317/Tetherin. Virology *424*, 33–44.

Fun, A., Wensing, A.M.J., Verheyen, J., and Nijhuis, M. (2012). Human Immunodeficiency Virus Gag and protease: partners in resistance. Retrovirology *9*, 63.

Gack, M.U., Shin, Y.C., Joo, C.-H., Urano, T., Liang, C., Sun, L., Takeuchi, O., Akira, S., Chen, Z., Inoue, S., et al. (2007). TRIM25 RING-finger E3 ubiquitin ligase is essential for RIG-I-mediated antiviral activity. Nature *446*, 916–920.

Galão, R.P., Le Tortorec, A., Pickering, S., Kueck, T., and Neil, S.J.D. (2012). Innate sensing of HIV-1 assembly by Tetherin induces NFκB-dependent proinflammatory responses. Cell Host Microbe *12*, 633–644.

Ganser, B.K. (1999). Assembly and Analysis of Conical Models for the HIV-1 Core. Science (80-.). *283*, 80–83.

Ganser-Pornillos, B.K., Yeager, M., and Sundquist, W.I. (2008). The structural biology of HIV assembly. Curr. Opin. Struct. Biol. *18*, 203–217.

Ganser-Pornillos, B.K., Chandrasekaran, V., Pornillos, O., Sodroski, J.G., Sundquist, W.I., and Yeager, M. (2011). Hexagonal assembly of a restricting TRIM5alpha protein. Proc. Natl. Acad. Sci. U. S. A. *108*, 534–539.

Gao, D., Wu, J., Wu, Y.-T., Du, F., Aroh, C., Yan, N., Sun, L., and Chen, Z.J. (2013). Cyclic GMP-AMP synthase is an innate immune sensor of HIV and other retroviruses. Science *341*, 903–906.

Garcia, J. V, and Miller, D. (1991). Serine phosphorylation-independent downregulation of cell-surface CD4 by nef. Nature *350*, 508–511.

Garcia, J. a, Harrich, D., Soultanakis, E., Wu, F., Mitsuyasu, R., and Gaynor, R.B. (1989). Human immunodeficiency virus type 1 LTR TATA and TAR region sequences required for transcriptional regulation. EMBO J. *8*, 765–778.

Gillick, K., Pollpeter, D., Phalora, P., Kim, E.-Y., Wolinsky, S.M., and Malim, M.H. (2013). Suppression of HIV-1 infection by APOBEC3 proteins in primary human CD4(+) T cells is associated with inhibition of processive reverse transcription as well as excessive cytidine deamination. J. Virol. *87*, 1508–1517.

Goffinet, C., Allespach, I., Homann, S., Tervo, H.-M., Habermann, A., Rupp, D., Oberbremer, L., Kern, C., Tibroni, N., Welsch, S., et al. (2009). HIV-1 antagonism of

CD317 is species specific and involves Vpu-mediated proteasomal degradation of the restriction factor. Cell Host Microbe *5*, 285–297.

Goffinet, C., Homann, S., Ambiel, I., Tibroni, N., Rupp, D., Keppler, O.T., and Fackler, O.T. (2010). Antagonism of CD317 restriction of human immunodeficiency virus type 1 (HIV-1) particle release and depletion of CD317 are separable activities of HIV-1 Vpu. J. Virol. *84*, 4089–4094.

Goh, W., Rogel, M., Kinsey, C., Michael, S., Fultz, P., Nowak, M., Hahn, B., and Emerman, M. (1998). HIV-1 Vpr increases viral expression by manipulation of the cell cycle: a mechanism for selection of Vpr in vivo. Nat. Med. *4*, 65–71.

Goldstone, D.C., Ennis-Adeniran, V., Hedden, J.J., Groom, H.C.T., Rice, G.I., Christodoulou, E., Walker, P. a, Kelly, G., Haire, L.F., Yap, M.W., et al. (2011). HIV-1 restriction factor SAMHD1 is a deoxynucleoside triphosphate triphosphohydrolase. Nature *480*, 379–382.

Goto, T., Kennel, S.J., Abe, M., Takishita, M., Kosaka, M., Solomon, a, and Saito, S. (1994). A novel membrane antigen selectively expressed on terminally differentiated human B cells. Blood *84*, 1922–1930.

Gottlieb, M.S., Schroff, R., Schanker, H.M., Weisman, J.D., Thim Fan, P., Wolf, R.A., and Saxon, A. (1981). PNEUMOCYSTIS CARINII PNEUMONIA AND MUCOSAL CANDIDIASIS IN PREVIOUSLY HEALTHY HOMOSEXUAL MEN. N. Engl. J. Med. *305*, 1426–1431.

Göttlinger, H.G., Dorfman, T., Cohen, E. a, and Haseltine, W. a (1993). Vpu protein of human immunodeficiency virus type 1 enhances the release of capsids produced by gag gene constructs of widely divergent retroviruses. Proc. Natl. Acad. Sci. U. S. A. *90*, 7381–7385.

Goujon, C., Jarrosson-Wuillème, L., Bernaud, J., Rigal, D., Darlix, J.-L., and Cimarelli, a (2006). With a little help from a friend: increasing HIV transduction of monocyte-derived dendritic cells with virion-like particles of SIV(MAC). Gene Ther. *13*, 991–994.

Goujon, C., Moncorgé, O., Bauby, H., Doyle, T., Ward, C.C., Schaller, T., Hué, S., Barclay, W.S., Schulz, R., and Malim, M.H. (2013). Human MX2 is an interferon-induced post-entry inhibitor of HIV-1 infection. Nature *502*, 559–562.

Le Grice, S.F.J. (2012). Human immunodeficiency virus reverse transcriptase: 25 years of research, drug discovery, and promise. J. Biol. Chem. *287*, 40850–40857.

Grover, J.R., Llewellyn, G.N., Soheilian, F., Nagashima, K., Veatch, S.L., and Ono, A. (2013). Roles played by capsid-dependent induction of membrane curvature and Gag-ESCRT interactions in tetherin recruitment to HIV-1 assembly sites. J. Virol. *87*, 4650–4664.

Grütter, M.G., and Luban, J. (2012). TRIM5 structure, HIV-1 capsid recognition, and innate immune signaling. Curr. Opin. Virol. *2*, 142–150.

Guha, D., and Ayyavoo, V. (2013). Innate Immune Evasion Strategies by Human Immunodeficiency Virus Type 1. Isrn Aids *2013*, 954806.

Gummuluru, S., Kinsey, C.M., and Emerman, M. (2000). An In Vitro Rapid-Turnover Assay for Human Immunodeficiency Virus Type 1 Replication Selects for Cell-to-Cell Spread of Virus. J. Virol. *74*, 10882–10891.

Gupta, R.K., Hué, S., Schaller, T., Verschoor, E., Pillay, D., and Towers, G.J. (2009a). Mutation of a Single Residue Renders Human Tetherin Resistant to HIV-1 Vpu-Mediated Depletion. PLoS Pathog. *5*, e1000443.

Gupta, R.K., Mlcochova, P., Pelchen-Matthews, A., Petit, S.J., Mattiuzzo, G., Pillay, D., Takeuchi, Y., Marsh, M., and Towers, G.J. (2009b). Simian immunodeficiency virus envelope glycoprotein counteracts tetherin/BST-2/CD317 by intracellular sequestration. Proc. Natl. Acad. Sci. U. S. A. *106*, 20889–20894.

Gustin, J.K., Douglas, J.L., Bai, Y., and Moses, A. V (2012). Ubiquitination of BST-2 protein by HIV-1 Vpu protein does not require lysine, serine, or threonine residues within the BST-2 cytoplasmic domain. J. Biol. Chem. *287*, 14837–14850.

Guy, B., Kieny, M.P., Riviere, Y., Le Peuch, C., Dott, K., Girard, M., Monyagnier, L., and Lecocq, J. (1987). HIV F/3' orf encodes a phosphorylated GTP-binding protein resembling an oncogene product. Nature *330*, 266–269.

Habermann, A., Krijnse-Locker, J., Oberwinkler, H., Eckhardt, M., Homann, S., Andrew, A., Strebel, K., and Kräusslich, H.-G. (2010). CD317/tetherin is enriched in the HIV-1 envelope and downregulated from the plasma membrane upon virus infection. J. Virol. *84*, 4646–4658.

Hammonds, J., Wang, J.-J., Yi, H., and Spearman, P. (2010). Immunoelectron microscopic evidence for Tetherin/BST2 as the physical bridge between HIV-1 virions and the plasma membrane. PLoS Pathog. *6*, e1000749.

Hammonds, J., Ding, L., Chu, H., Geller, K., Robbins, A., Wang, J.-J., Yi, H., and Spearman, P. (2012). The tetherin/BST-2 coiled-coil ectodomain mediates plasma membrane microdomain localization and restriction of particle release. J. Virol. *86*, 2259–2272.

Harris, R.S., Hultquist, J.F., and Evans, D.T. (2012). The restriction factors of human immunodeficiency virus. J. Biol. Chem. *287*, 40875–40883.

Hauser, H., Lopez, L. a, Yang, S.J., Oldenburg, J.E., Exline, C.M., Guatelli, J.C., and Cannon, P.M. (2010). HIV-1 Vpu and HIV-2 Env counteract BST-2/tetherin by sequestration in a perinuclear compartment. Retrovirology *7*, 51.

Henklein, P., Schubert, U., Kunert, O., Klabunde, S., Wray, V., Klöppel, K., Kiess, M., Portsmann, T., and Schomburg, . (1993). Synthesis and characterization of the hydrophilic C-terminal domain of the human immunodeficiency virus type 1-encoded virus protein U (Vpu). Pept. Res. *6*, 79–87.

Henne, W.M., Buchkovich, N.J., and Emr, S.D. (2011). The ESCRT pathway. Dev. Cell *21*, 77–91.

Henne, W.M., Stenmark, H., and Emr, S.D. (2013). Molecular Mechanisms of the Membrane Sculpting ESCRT Pathway. Cold Spring Harb Perspect Biol *5*, 1–12.

Hilditch, L., Matadeen, R., Goldstone, D.C., Rosenthal, P.B., Taylor, I. a, and Stoye, J.P. (2011). Ordered assembly of murine leukemia virus capsid protein on lipid

nanotubes directs specific binding by the restriction factor, Fv1. Proc. Natl. Acad. Sci. U. S. A. *108*, 5771–5776.

Hill, M.S., Ruiz, A., Schmitt, K., and Stephens, E.B. (2010). Identification of amino acids within the second alpha helical domain of the human immunodeficiency virus type 1 Vpu that are critical for preventing CD4 cell surface expression. Virology *397*, 104–112.

Hinz, A., Miguet, N., Natrajan, G., Usami, Y., Yamanaka, H., Renesto, P., Hartlieb, B., McCarthy, A. a, Simorre, J.-P., Göttlinger, H., et al. (2010). Structural basis of HIV-1 tethering to membranes by the BST-2/tetherin ectodomain. Cell Host Microbe *7*, 314–323.

Hirano, S., Kawasaki, M., Ura, H., Kato, R., Raiborg, C., Stenmark, H., and Wakatsuki, S. (2006). Double-sided ubiquitin binding of Hrs-UIM in endosomal protein sorting. Nat. Struct. Mol. Biol. *13*, 272–277.

Hirst, J., Barlow, L.D., Francisco, G.C., Sahlender, D. a, Seaman, M.N.J., Dacks, J.B., and Robinson, M.S. (2011). The fifth adaptor protein complex. PLoS Biol. *9*, e1001170.

Hofmann, W., Schubert, D., Labonte, J., Gibson, S., Scammell, J., Ferrigno, P., Sodroski, J., Bonte, J.L.A., and Munson, L. (1999). Species-Specific , Postentry Barriers to Primate Immunodeficiency Virus Infection. J. Virol. *73*, 10020–10028.

Homann, S., Smith, D., Little, S., Richman, D., and Guatelli, J. (2011). Upregulation of BST-2/Tetherin by HIV infection in vivo. J. Virol. *85*, 10659–10668.

Hotter, D., Sauter, D., and Kirchhoff, F. (2013). Emerging role of the host restriction factor tetherin in viral immune sensing. J. Mol. Biol. *425*, 4956–4964.

Hrecka, K., Gierszewska, M., Srivastava, S., Kozaczkiewicz, L., Swanson, S.K., Florens, L., Washburn, M.P., and Skowronski, J. (2007). Lentiviral Vpr usurps Cul4–DDB1[VprBP] E3 ubiquitin ligase to modulate cell cycle. Proc. Natl. Acad. Sci. *104*, 11778–11783.

Hrecka, K., Hao, C., Gierszewska, M., Swanson, S.K., Kesik-Brodacka, M., Srivastava, S., Florens, L., Washburn, M.P., and Skowronski, J. (2011). Vpx relieves inhibition of HIV-1 infection of macrophages mediated by the SAMHD1 protein. Nature *474*, 658–661.

Hu, W.-S., and Hughes, S.H. (2012). HIV-1 reverse transcription. Cold Spring Harb. Perspect. Med. *2*, .a006882.

Huotari, J., and Helenius, A. (2011). Endosome maturation. EMBO J. *30*, 3481–3500.

Hussain, A., Das, S.R., Tanwar, C., and Jameel, S. (2007). Oligomerization of the human immunodeficiency virus type 1 (HIV-1) Vpu protein – a genetic, biochemical and biophysical analysis. Virol. J. *4*, 81.

De Iaco, A., and Luban, J. (2011). Inhibition of HIV-1 infection by TNPO3 depletion is determined by capsid and detectable after viral cDNA enters the nucleus. Retrovirology *8*, 98.

Igakura, T., Tanaka, Y., Osame, M., and Bangham, C.R.M. (2003). Spread of HTLV-I Between Lymphocytes by Virus-Induced Polarization of the Cytoskeleton. Science (80-.). *299*, 1713–1716.

Ishikawa, J., Kaisho, T., Tomizawa, H., Lee, B.O., Kobune, Y., Inazawa, J., Oritani, K., Itoh, M., Ochi, T., and Ishihara, K. (1995). Molecular cloning and chromosomal mapping of a bone marrow stromal cell surface gene, BST2, that may be involved in pre-B-cell growth. Genomics *26*, 527–534.

Iwabu, Y., Fujita, H., Kinomoto, M., Kaneko, K., Ishizaka, Y., Tanaka, Y., Sata, T., and Tokunaga, K. (2009). HIV-1 accessory protein Vpu internalizes cell-surface BST-2/tetherin through transmembrane interactions leading to lysosomes. J. Biol. Chem. *284*, 35060–35072.

Jacquelin, B., Mayau, V., Targat, B., Liovat, A., Kunkel, D., Petitjean, G., Dillies, M., Roques, P., Butor, C., Silvestri, G., et al. (2009). Nonpathogenic SIV infection of African green monkeys induces a strong but rapidly controlled type I IFN response. J. Clin. Invest. *119*, 3544–3555.

Jafari, M., Guatelli, J., and Lewinski, M.K. (2014). Activities of Transmitted/Founder and Chronic Clade B HIV-1 Vpu and a C-terminal Polymorphism Specifically Affecting Virion Release. J. Virol. *10*.

Jäger, S., Kim, D.Y., Hultquist, J.F., Shindo, K., LaRue, R.S., Kwon, E., Li, M., Anderson, B.D., Yen, L., Stanley, D., et al. (2012). Vif hijacks CBF-β to degrade APOBEC3G and promote HIV-1 infection. Nature *481*, 371–375.

Jakobsen, M.R., Bak, R.O., Andersen, A., Berg, R.K., Jensen, S.B., Jin, T., Laustsen, A., Hansen, K., Østergaard, L., Fitzgerald, K.A., et al. (2013). IFI16 senses DNA forms of the lentiviral replication cycle and controls HIV-1 replication. Proc. Natl. Acad. Sci. *110*, 19651–19651.

James, L.C., Keeble, A.H., Khan, Z., Rhodes, D. a, and Trowsdale, J. (2007). Structural basis for PRYSPRY-mediated tripartite motif (TRIM) protein function. Proc. Natl. Acad. Sci. U. S. A. *104*, 6200–6205.

Janvier, K., Kato, Y., Boehm, M., Rose, J.R., Martina, J. a, Kim, B.-Y., Venkatesan, S., and Bonifacino, J.S. (2003). Recognition of dileucine-based sorting signals from HIV-1 Nef and LIMP-II by the AP-1 gamma-sigma1 and AP-3 delta-sigma3 hemicomplexes. J. Cell Biol. *163*, 1281–1290.

Janvier, K., Pelchen-Matthews, A., Renaud, J.-B., Caillet, M., Marsh, M., and Berlioz-Torrent, C. (2011). The ESCRT-0 component HRS is required for HIV-1 Vpu-mediated BST-2/tetherin down-regulation. PLoS Pathog. *7*, e1001265.

Jia, B., Serra-Moreno, R., Neidermyer, W., Rahmberg, A., Mackey, J., Fofana, I. Ben, Johnson, W.E., Westmoreland, S., and Evans, D.T. (2009). Species-Specific Activity of SIV Nef and HIV-1 Vpu in Overcoming Restriction by Tetherin/BST2. PLoS Pathog. *5*, e1000429.

Jia, X., Singh, R., Homann, S., Yang, H., Guatelli, J., and Xiong, Y. (2012). Structural basis of evasion of cellular adaptive immunity by HIV-1 Nef. Nat. Struct. Mol. Biol. *19*, 701–706.

Jolly, C., Kashefi, K., Hollinshead, M., and Sattentau, Q.J. (2004). HIV-1 cell to cell transfer across an Env-induced, actin-dependent synapse. J. Exp. Med. *199*, 283–293.

Jolly, C., Mitar, I., and Sattentau, Q.J. (2007). Adhesion molecule interactions facilitate human immunodeficiency virus type 1-induced virological synapse formation between T cells. J. Virol. *81*, 13916–13921.

Jolly, C., Booth, N.J., and Neil, S.J.D. (2010). Cell-cell spread of human immunodeficiency virus type 1 overcomes tetherin/BST-2-mediated restriction in T cells. J. Virol. *84*, 12185–12199.

Jones, K., Kadonaga, J., Luciw, P., and Tjian, R. (1986). Activation of the AIDS retrovirus promoter by the cellular transcription factor, Sp1. Science *232*, 755–759.

Joshi, A., Garg, H., Nagashima, K., Bonifacino, J.S., and Freed, E.O. (2008). GGA and Arf proteins modulate retrovirus assembly and release. Mol. Cell *30*, 227–238.

Joshi, A., Nagashima, K., and Freed, E.O. (2009). Defects in cellular sorting and retroviral assembly induced by GGA overexpression. BMC Cell Biol. *10*, 72.

Kaletsky, R.L., Francica, J.R., Agrawal-Gamse, C., and Bates, P. (2009). Tetherin-mediated restriction of filovirus budding is antagonized by the Ebola glycoprotein. Proc. Natl. Acad. Sci. U. S. A. *106*, 2886–2891.

Kane, M., Yadav, S.S., Bitzegeio, J., Kutluay, S.B., Zang, T., Wilson, S.J., Schoggins, J.W., Rice, C.M., Yamashita, M., Hatziioannou, T., et al. (2013). MX2 is an interferon-induced inhibitor of HIV-1 infection. Nature.

Karn, J., and Stoltzfus, C.M. (2012). Transcriptional and posttranscriptional regulation of HIV-1 gene expression. Cold Spring Harb. Perspect. Med. *2*, a006916.

Katzmann, D.J., Babst, M., and Emr, S.D. (2001). Ubiquitin-Dependent Sorting into the Multivesicular Body Pathway Requires the Function of a Conserved Endosomal Protein Sorting Complex, ESCRT-I. Cell *106*, 145–155.

Kim, D.Y., Kwon, E., Hartley, P.D., Crosby, D.C., Mann, S., Krogan, N.J., and Gross, J.D. (2013). CBFβ stabilizes HIV Vif to counteract APOBEC3 at the expense of RUNX1 target gene expression. Mol. Cell *49*, 632–644.

Kim, S., Byrn, R., Groopman, J., and Baltimore, D. (1989). Temporal aspects of DNA and RNA synthesis during human immunodeficiency virus infection: evidence for differential gene. J. Virol. *63*.

Kinoshita, S., Chen, B.K., Kaneshima, H., and Nolan, G.P. (1998). Host control of HIV-1 parasitism in T cells by the nuclear factor of activated T cells. Cell *95*, 595–604.

Kirchhoff, F. (2010). Immune Evasion and Counteraction of Restriction Factors by HIV-1 and Other Primate Lentiviruses. Cell Host Microbe *8*, 55–67.

Klatzmann, D., Barré-Sinoussi, F., Nugeyre, M., Danquet, C., Vilmer, E., Griscelli, C., Brun-Veziret, F., Rouzioux, C., and Gluckman, J. (1984). Selective tropism of lymphadenopathy associated virus (LAV) for helper-inducer T lymphocytes. Science *225*, 59–63.

Klimkait, T., Strebel, K., Hoggan, M.D., Martin, M., and Orenstein, J.M. (1990). The Human Immunodeficiency Virus Type 1-Specific Protein Vpu is Required for Efficient Virus Maturation and Release. J. Virol. *64*.

Kobayashi, T., Ode, H., Yoshida, T., Sato, K., Gee, P., Yamamoto, S.P., Ebina, H., Strebel, K., Sato, H., and Koyanagi, Y. (2011). Identification of amino acids in the human tetherin transmembrane domain responsible for HIV-1 Vpu interaction and susceptibility. J. Virol. *85*, 932–945.

Kohlstaedt, L., Wang, J., Friedman, J., Rice, P., and Steitz, T. (1992). Crystal structure at 3.5 A resolution of HIV-1 reverse transcriptase complexed with an inhibitor. Science *256*, 1783–1790.

Kondo, E., Mammano, F., Cohen, E.A., Göttlinger, H.G., Kondo, E., Mammano, F., and Cohen, E.A. (1995). The p6gag domain of human immunodeficiency virus type 1 is sufficient for the incorporation of Vpr into heterologous viral particles. J. Virol. *69*, 2759–2764.

König, R., Zhou, Y., Elleder, D., Diamond, T.L., Bonamy, G.M.C., Irelan, J.T., Chiang, C.-Y., Tu, B.P., De Jesus, P.D., Lilley, C.E., et al. (2008). Global analysis of host-pathogen interactions that regulate early-stage HIV-1 replication. Cell *135*, 49–60.

Koning, F. a, Newman, E.N.C., Kim, E.-Y., Kunstman, K.J., Wolinsky, S.M., and Malim, M.H. (2009). Defining APOBEC3 expression patterns in human tissues and hematopoietic cell subsets. J. Virol. *83*, 9474–9485.

Krummheuer, J., Johnson, A.T., Hauber, I., Kammler, S., Anderson, J.L., Hauber, J., Purcell, D.F.J., and Schaal, H. (2007). A minimal uORF within the HIV-1 vpu leader allows efficient translation initiation at the downstream env AUG. Virology *363*, 261–271.

Kueck, T., and Neil, S.J.D. (2012). A Cytoplasmic Tail Determinant in HIV-1 Vpu Mediates Targeting of Tetherin for Endosomal Degradation and Counteracts Interferon-Induced Restriction. PLoS Pathog. *8*, e1002609.

Kuhl, B.D., Sloan, R.D., Donahue, D. a, Bar-Magen, T., Liang, C., and Wainberg, M. a (2010). Tetherin restricts direct cell-to-cell infection of HIV-1. Retrovirology *7*, 115.

Kühl, A., Banning, C., Marzi, A., Votteler, J., Steffen, I., Bertram, S., Glowacka, I., Konrad, A., Stürzl, M., Guo, J.-T., et al. (2011). The Ebola virus glycoprotein and HIV-1 Vpu employ different strategies to counteract the antiviral factor tetherin. J. Infect. Dis. *204 Suppl* , S850–60.

Kupzig, S., Korolchuk, V., Rollason, R., Sugden, A., Wilde, A., and Banting, G. (2003). Bst-2/HM1.24 is a raft-associated apical membrane protein with an unusual topology. Traffic *4*, 694–709.

Kutluay, S.B., and Bieniasz, P.D. (2010). Analysis of the initiating events in HIV-1 particle assembly and genome packaging. PLoS Pathog. *6*, e1001200.

Kwong, P.D., Wyatt, R., Robinson, J., Sweet, R.W., Sodroski, J., and Hendrickson, W. a (1998). Structure of an HIV gp120 envelope glycoprotein in complex with the CD4 receptor and a neutralizing human antibody. Nature *393*, 648–659.

Lafer, E.M. (2002). Clathrin-protein interactions. Traffic *3*, 513–520.

Laguette, N., Sobhian, B., Casartelli, N., Ringeard, M., Chable-Bessia, C., Ségéral, E., Yatim, A., Emiliani, S., Schwartz, O., and Benkirane, M. (2011). SAMHD1 is the dendritic- and myeloid-cell-specific HIV-1 restriction factor counteracted by Vpx. Nature *474*, 654–657.

Laguette, N., Brégnard, C., Hue, P., Basbous, J., Yatim, A., Larroque, M., Kirchhoff, F., Constantinou, A., Sobhian, B., and Benkirane, M. (2014). Premature Activation of the SLX4 Complex by Vpr Promotes G2/M Arrest and Escape from Innate Immune Sensing. Cell 1–12.

Lahouassa, H., Daddacha, W., Hofmann, H., Ayinde, D., Logue, E.C., Dragin, L., Bloch, N., Maudet, C., Bertrand, M., Gramberg, T., et al. (2012). SAMHD1 restricts the replication of human immunodeficiency virus type 1 by depleting the intracellular pool of deoxynucleoside triphosphates. Nat. Immunol. *13*, 223–228.

Laplana, M., Caruz, A., Pineda, J.A., Puig, T., and Fibla, J. (2013). Association of BST-2 gene variants with HIV disease progression underscores the role of BST-2 in HIV type 1 infection. J. Infect. Dis. *207*, 411–419.

Lau, D., Kwan, W., and Guatelli, J. (2011). Role of the endocytic pathway in the counteraction of BST-2 by human lentiviral pathogens. J. Virol. *85*, 9834–9846.

Lee, K., Ambrose, Z., Martin, T.D., Oztop, I., Mulky, A., Julias, J.G., Vandegraaff, N., Baumann, J.G., Wang, R., Yuen, W., et al. (2010). Flexible use of nuclear import pathways by HIV-1. Cell Host Microbe *7*, 221–233.

Lee, K., Mulky, A., Yuen, W., Martin, T.D., Meyerson, N.R., Choi, L., Yu, H., Sawyer, S.L., and Kewalramani, V.N. (2012). HIV-1 capsid-targeting domain of cleavage and polyadenylation specificity factor 6. J. Virol. *86*, 3851–3860.

Lehmann, M., Rocha, S., Mangeat, B., Blanchet, F., Uji-I, H., Hofkens, J., and Piguet, V. (2011). Quantitative multicolor super-resolution microscopy reveals tetherin HIV-1 interaction. PLoS Pathog. *7*, e1002456.

Lehmann, M.J., Sherer, N.M., Marks, C.B., Pypaert, M., and Mothes, W. (2005). Actin- and myosin-driven movement of viruses along filopodia precedes their entry into cells. J. Cell Biol. *170*, 317–325.

Lenburg, M.E., and Landau, N.R. (1993). Vpu-induced degradation of CD4: requirement for specific amino acid residues in the cytoplasmic domain of CD4. J. Virol. *67*, 7238–7245.

Levin, J.G., Mitra, M., Mascarenhas, A., and Musier-Forsyth, K. (2010). Role of HIV-1 nucleocapsid protein in HIV-1 reverse transcription. RNA Biol. *7*, 754–774.

Liberatore, R. a, and Bieniasz, P.D. (2011). Tetherin is a key effector of the antiretroviral activity of type I interferon in vitro and in vivo. Proc. Natl. Acad. Sci. U. S. A. *108*, 18097–18101.

Lim, E.S., Malik, H.S., and Emerman, M. (2010). Ancient adaptive evolution of tetherin shaped the functions of Vpu and Nef in human immunodeficiency virus and primate lentiviruses. J. Virol. *84*, 7124–7134.

Lindwasser, O.W., Smith, W.J., Chaudhuri, R., Yang, P., Hurley, J.H., and Bonifacino, J.S. (2008). A diacidic motif in human immunodeficiency virus type 1 Nef is a novel determinant of binding to AP-2. J. Virol. *82*, 1166–1174.

Liu, J., Perkins, N.D., Schmid, R.M., and Nabel, G.J. (1992). Specific NF-kappa B subunits act in concert with Tat to stimulate human immunodeficiency virus type 1 transcription. J. Virol. *66*.

Liu, Z., Pan, Q., Ding, S., Qian, J., Xu, F., Zhou, J., Cen, S., Guo, F., and Liang, C. (2013). The interferon-inducible MxB protein inhibits HIV-1 infection. Cell Host Microbe *14*, 398–410.

Llano, M., Saenz, D.T., Meehan, A., Wongthida, P., Peretz, M., Walker, W.H., Teo, W., and Poeschla, E.M. (2006). An essential role for LEDGF/p75 in HIV integration. Science *314*, 461–464.

Lopez, C.F., Montal, M., Blasie, J.K., Klein, M.L., and Moore, P.B. (2002). Molecular Dynamics Investigation of Membrane-Bound Bundles of the Channel-Forming Transmembrane Domain of Viral Protein U from the Human Immunodeficiency Virus HIV-1. Biophys. J. *83*, 1259–1267.

Lopez, L. a, Yang, S.J., Hauser, H., Exline, C.M., Haworth, K.G., Oldenburg, J., and Cannon, P.M. (2010). Ebola virus glycoprotein counteracts BST-2/Tetherin restriction in a sequence-independent manner that does not require tetherin surface removal. J. Virol. *84*, 7243–7255.

Lopez, L. a, Yang, S.J., Exline, C.M., Rengarajan, S., Haworth, K.G., and Cannon, P.M. (2012). Anti-tetherin activities of HIV-1 Vpu and Ebola virus glycoprotein do not involve removal of tetherin from lipid rafts. J. Virol. *86*, 5467–5480.

Lori, F., Di Marzo Veronese, F., De Vico, A., Lusso, P., Reitz, M., and Gallo, R.C. (1992). virus type 1 virions . Viral DNA Carried by Human Immunodeficiency Virus Type 1 Virions. J. Virol. *66*.

Lu, Y., Spearman, P., and Ratner, L.E.E. (1993). Human Immunodeficiency Virus Type 1 Viral Protein R Localization in Infected Cells and Virions. J. Virol. *67*.

Luban, J. (2012). TRIM5 and the Regulation of HIV-1 Infectivity. Mol. Biol. Int. *2012*, 426840.

Lubben, N.B., Sahlender, D.A., Motley, A.M., Lehner, P.J., Benaroch, P., and Robinson, M.S. (2007). HIV-1 Nef-induced Down-Regulation of MHC Class I Requires AP-1 and Clathrin but Not PACS-1 and Is Impeded by AP-2. Mol. Biol. Cell *18*, 3351–3365.

Maddon, P.J., Dalgleish, A.G., Mc Dougal, S., Clapham, P.R., and Axel, R. (1986). Gene Encodes the AIDS Virus Recepto ressed in the Immune System and the Brain. Cell *47*, 333–348.

Magadán, J.G., and Bonifacino, J.S. (2012). Transmembrane domain determinants of CD4 Downregulation by HIV-1 Vpu. J. Virol. *86*, 757–772.

Magadán, J.G., Pérez-Victoria, F.J., Sougrat, R., Ye, Y., Strebel, K., and Bonifacino, J.S. (2010). Multilayered Mechanism of CD4 Downregulation by HIV-1 Vpu Involving Distinct ER Retention and ERAD Targeting Steps. PLoS Pathog. *6*, e1000869.

Maldarelli, F., Chen, M., Willey, R.L., and Strebel, K. (1993). Human immunodeficiency virus type 1 Vpu protein is an oligomeric type I integral membrane protein. J. Virol. *67*, 5056–5061.

Malim, M.H., and Bieniasz, P.D. (2012). HIV Restriction Factors and Mechanisms of Evasion. Cold Spring Harb. Perspect. Med. *2*, a006940.

Malim, M.H., Hauber, J., Le, S.-Y., Maizel, J. V, and Cullen, B.R. (1989). The HIV-1 rev trans-activator acts through a structured target sequence to activate nuclear export of unspliced viral mRNA. Nature *338*, 254–257.

Mangeat, B., Gers-Huber, G., Lehmann, M., Zufferey, M., Luban, J., and Piguet, V. (2009). HIV-1 Vpu Neutralizes the Antiviral Factor Tetherin/BST-2 by Binding It and Directing Its Beta-TrCP2-Dependent Degradation. PLoS Pathog. *5*, e1000574.

Mangeat, B., Cavagliotti, L., Lehmann, M., Gers-Huber, G., Kaur, I., Thomas, Y., Kaiser, L., and Piguet, V. (2012). Influenza virus partially counteracts restriction imposed by tetherin/BST-2. J. Biol. Chem. *287*, 22015–22029.

Mansouri, M., Viswanathan, K., Douglas, J.L., Hines, J., Gustin, J., Moses, A. V, and Früh, K. (2009). Molecular mechanism of BST2/tetherin downregulation by K5/MIR2 of Kaposi's sarcoma-associated herpesvirus. J. Virol. *83*, 9672–9681.

Margottin, F., Bour, S.P., Durand, H., Selig, L., Benichou, S., Richard, V., Thomas, D., Strebel, K., and Benarous, R. (1998). A novel human WD protein, h-beta TrCp, that interacts with HIV-1 Vpu connects CD4 to the ER degradation pathway through an F-box motif. Mol. Cell *1*, 565–574.

Marshall, N., Peng, J., Xie, Z., and Price, D. (1996). Control of RNA Polymerase II Elongation Potential by a Novel Carboxyl-terminal Domain Kinase. J. Biol. Chem. *271*, 27176–27183.

Martin-Serrano, J., and Neil, S.J.D. (2011). Host factors involved in retroviral budding and release. Nat. Rev. Microbiol. *9*, 519–531.

Mashiba, M., and Collins, K.L. (2012). Molecular mechanisms of HIV immune evasion of the innate immune response in myeloid cells. Viruses *5*, 1–14.

Masuyama, N., Kuronita, T., Tanaka, R., Muto, T., Hirota, Y., Takigawa, A., Fujita, H., Aso, Y., Amano, J., and Tanaka, Y. (2009). HM1.24 is internalized from lipid rafts by clathrin-mediated endocytosis through interaction with alpha-adaptin. J. Biol. Chem. *284*, 15927–15941.

Matreyek, K. a, and Engelman, A. (2011). The requirement for nucleoporin NUP153 during human immunodeficiency virus type 1 infection is determined by the viral capsid. J. Virol. *85*, 7818–7827.

Matsuda, A., Suzuki, Y., Honda, G., Muramatsu, S., Matsuzaki, O., Nagano, Y., Doi, T., Shimotohno, K., Harada, T., Nishida, E., et al. (2003). Large-scale identification and characterization of human genes that activate NF-kappaB and MAPK signaling pathways. Oncogene *22*, 3307–3318.

Mauxion, F., Le Borgne, R., Munier-Lehmann, H., and Hoflack, B. (1996). A Casein Kinase II Phosphorylation Site in the Cytoplasmic Domain of the Cation-dependent

Mannose 6-Phosphate Receptor Determines the High Affinity Interaction of the AP-1 Golgi Assembly Proteins with Membranes. J. Biol. Chem. *271*, 2171–2178.

McCormick-Davis, C., Zhao, L.J., Mukherjee, S., Leung, K., Sheffer, D., Joag, S. V, Narayan, O., and Stephens, E.B. (1998). Chronology of genetic changes in the vpu, env, and nef genes of chimeric simian-human immunodeficiency virus (strain HXB2) during acquisition of virulence for pig-tailed macaques. Virology *248*, 275–283.

McDougal, J., Kennedy, M., Sligh, J., Cort, S., Mawle, A., and Nicholson, J. (1986). Binding of HTLV-III/LAV to T4+ T cells by a complex of the 110K viral protein and the T4 molecule. Science *231*, 382–385.

McEwan, W. a, Tam, J.C.H., Watkinson, R.E., Bidgood, S.R., Mallery, D.L., and James, L.C. (2013). Intracellular antibody-bound pathogens stimulate immune signaling via the Fc receptor TRIM21. Nat. Immunol. *14*, 327–336.

McNatt, M.W., Zang, T., Hatziioannou, T., Bartlett, M., Fofana, I. Ben, Johnson, W.E., Neil, S.J.D., and Bieniasz, P.D. (2009). Species-Specific Activity of HIV-1 Vpu and Positive Selection of Tetherin Transmembrane Domain Variants. PLoS Pathog. *5*, e1000300.

McNatt, M.W., Zang, T., and Bieniasz, P.D. (2013). Vpu Binds Directly to Tetherin and Displaces It from Nascent Virions. PLoS Pathog. *9*, e1003299.

Melikyan, G.B. (2008). Common principles and intermediates of viral protein-mediated fusion: the HIV-1 paradigm. Retrovirology *5*, 111.

Mettenleiter, T.C., Klupp, B.G., and Granzow, H. (2006). Herpesvirus assembly: a tale of two membranes. Curr. Opin. Microbiol. *9*, 423–429.

Miller, S.G., Carnell, L., and Moore, H.H. (1992). Post-Golgi membrane traffic: brefeldin A inhibits export from distal Golgi compartments to the cell surface but not recycling. J. Cell Biol. *118*, 267–283.

Mitchell, R.S., Beitzel, B.F., Schroder, A.R.W., Shinn, P., Chen, H., Berry, C.C., Ecker, J.R., and Bushman, F.D. (2004). Retroviral DNA integration: ASLV, HIV, and MLV show distinct target site preferences. PLoS Biol. *2*, E234.

Mitchell, R.S., Katsura, C., Skasko, M. a, Fitzpatrick, K., Lau, D., Ruiz, A., Stephens, E.B., Margottin-Goguet, F., Benarous, R., and Guatelli, J.C. (2009). Vpu antagonizes BST-2-mediated restriction of HIV-1 release via beta-TrCP and endo-lysosomal trafficking. PLoS Pathog. *5*, e1000450.

Miyagi, E., Andrew, A.J., Kao, S., and Strebel, K. (2009). Vpu enhances HIV-1 virus release in the absence of Bst-2 cell surface down-modulation and intracellular depletion. Proc. Natl. Acad. Sci. U. S. A. *106*, 2868–2873.

Moll, M., Andersson, S.K., Smed-Sörensen, A., and Sandberg, J.K. (2010). Inhibition of lipid antigen presentation in dendritic cells by HIV-1 Vpu interference with CD1d recycling from endosomal compartments. Blood *116*, 1876–1884.

Moore, R.C., Lee, I.Y., Silverman, G.L., Harrison, P.M., Strome, R., Heinrich, C., Karunaratne, a, Pasternak, S.H., Chishti, M. a, Liang, Y., et al. (1999). Ataxia in prion protein (PrP)-deficient mice is associated with upregulation of the novel PrP-like protein doppel. J. Mol. Biol. *292*, 797–817.

Mothes, W., Sherer, N.M., Jin, J., and Zhong, P. (2010). Virus cell-to-cell transmission. J. Virol. *84*, 8360–8368.

Murooka, T.T., Deruaz, M., Marangoni, F., Vrbanac, V.D., Seung, E., Andrian, U.H. Von, Tager, A.M., Luster, A.D., and Mempel, T.R. (2012). HIV-infected T cells aremigratory vehicles for viral dissemination. Nature *490*, 283–287.

Mwimanzi, P., Markle, T.J., Ueno, T., and Brockman, M. a (2012). Human leukocyte antigen (HLA) class I down-regulation by human immunodeficiency virus type 1 negative factor (HIV-1 Nef): what might we learn from natural sequence variants? Viruses *4*, 1711–1730.

Nabel, G.J., and Baltimore, D. (1987). An inducible transcription factor activates expression of human immunodeficiency virus in T cells. Nature *326*, 712–713.

Nathan, J. a, and Lehner, P.J. (2009). The trafficking and regulation of membrane receptors by the RING-CH ubiquitin E3 ligases. Exp. Cell Res. *315*, 1593–1600.

Neil, S.J.D. (2013). Intrinsic Immunity (Berlin, Heidelberg: Springer Berlin Heidelberg).

Neil, S.J.D., Eastman, S.W., Jouvenet, N., and Bieniasz, P.D. (2006). HIV-1 Vpu Promotes Release and Prevents Endocytosis of Nascent Retrovirus Particles from the Plasma Membrane. PLoS Pathog. *2*, e39.

Neil, S.J.D., Sandrin, V., Sundquist, W.I., and Bieniasz, P.D. (2007). An interferon-alpha-induced tethering mechanism inhibits HIV-1 and Ebola virus particle release but is counteracted by the HIV-1 Vpu protein. Cell Host Microbe *2*, 193–203.

Neil, S.J.D., Zang, T., and Bieniasz, P.D. (2008). Tetherin inhibits retrovirus release and is antagonized by HIV-1 Vpu. Nature *451*, 425–430.

Niranjanakumari, S., Lasda, E., Brazas, R., and Garcia-Blanco, M. a (2002). Reversible cross-linking combined with immunoprecipitation to study RNA-protein interactions in vivo. Methods *26*, 182–190.

Noble, B., Abada, P., Nunez-iglesias, J., Paula, M., and Cannon, P.M. (2006). Recruitment of the Adaptor Protein 2 Complex by the Human Immunodeficiency Virus Type 2 Envelope Protein Is Necessary for High Levels of Virus Release. J. Virol. *80*.

Ohtomo, T., Sugamata, Y., Ozaki, Y., Ono, K., Yoshimura, Y., Kawai, S., Koishihara, Y., Ozaki, S., Kosaka, M., Hirano, T., et al. (1999). Molecular cloning and characterization of a surface antigen preferentially overexpressed on multiple myeloma cells. Biochem. Biophys. Res. Commun. *258*, 583–591.

Ono, A. (2010). Relationships between plasma membrane microdomains and HIV-1 assembly. Biol. Cell *102*, 335–350.

Pardieu, C., Vigan, R., Wilson, S.J., Calvi, A., Zang, T., Bieniasz, P., Kellam, P., Towers, G.J., and Neil, S.J.D. (2010). The RING-CH ligase K5 antagonizes restriction of KSHV and HIV-1 particle release by mediating ubiquitin-dependent endosomal degradation of tetherin. PLoS Pathog. *6*, e1000843.

Park, S.H., and Opella, S.J. (2005). Tilt angle of a trans-membrane helix is determined by hydrophobic mismatch. J. Mol. Biol. *350*, 310–318.

Park, S.H., Mrse, A. a., Nevzorov, A. a., Mesleh, M.F., Oblatt-Montal, M., Montal, M., and Opella, S.J. (2003). Three-dimensional Structure of the Channel-forming Trans-membrane Domain of Virus Protein “u” (Vpu) from HIV-1. J. Mol. Biol. *333*, 409–424.

Pashkova, N., Gakhar, L., Winistorfer, S.C., Sunshine, A.B., Rich, M., Dunham, M.J., Yu, L., and Piper, R.C. (2013). The Yeast Alix Homolog Bro1 Functions as a Ubiquitin Receptor for Protein Sorting into Multivesicular Endosomes. Dev. Cell 1–14.

Paxton, W., Connor, R.I., and Landau, N.R. (1993). Incorporation of Vpr into human immunodeficiency virus type 1 virions: requirement for the p6 region of gag and mutational analysis. J. Virol. *67*, 7229–7237.

Peden, A. a, Rudge, R.E., Lui, W.W.Y., and Robinson, M.S. (2002). Assembly and function of AP-3 complexes in cells expressing mutant subunits. J. Cell Biol. *156*, 327–336.

Perez-Caballero, D., Zang, T., Ebrahimi, A., McNatt, M.W., Gregory, D. a, Johnson, M.C., and Bieniasz, P.D. (2009). Tetherin inhibits HIV-1 release by directly tethering virions to cells. Cell *139*, 499–511.

Pertel, T., Hausmann, S., Morger, D., Züger, S., Guerra, J., Lascano, J., Reinhard, C., Santoni, F. a, Uchil, P.D., Chatel, L., et al. (2011). TRIM5 is an innate immune sensor for the retrovirus capsid lattice. Nature *472*, 361–365.

Pham, T.N., Lukhele, S., Hajjar, F., Routy, J.-P., and Cohen, E. a (2014). HIV Nef and Vpu protect HIV-infected CD4+ T cells from antibody-mediated cell Lysis through down-modulation of CD4 and BST2. Retrovirology *11*, 15.

Pickering, S., Hué, S., Kim, E.-Y., Reddy, S., Wolinsky, S.M., and Neil, S.J.D. (2014). Preservation of Tetherin and CD4 Counter-Activities in Circulating Vpu Alleles despite Extensive Sequence Variation within HIV-1 Infected Individuals. PLoS Pathog. *10*, e1003895.

Piguet, V., Gu, F., Foti, M., Demaurex, N., Gruenberg, J., Carpentier, J.L., and Trono, D. (1999). Nef-induced CD4 degradation: a diacidic-based motif in Nef functions as a lysosomal targeting signal through the binding of beta-COP in endosomes. Cell *97*, 63–73.

Pizzato, M., Helander, A., Popova, E., Calistri, A., Zamborlini, A., Palù, G., and Göttlinger, H.G. (2007). Dynamin 2 is required for the enhancement of HIV-1 infectivity by Nef. Proc. Natl. Acad. Sci. U. S. A. *104*, 6812–6817.

Pomerantz, R.J., Trono, D., Feinberg, M.B., and Baltimore, D. (1990). Cells nonproductively infected with HIV-1 exhibit an aberrant pattern of viral RNA expression: a molecular model for latency. Cell *61*, 1271–1276.

Popov, S., Popova, E., Inoue, M., and Göttlinger, H.G. (2009). Divergent Bro1 domains share the capacity to bind human immunodeficiency virus type 1 nucleocapsid and to enhance virus-like particle production. J. Virol. *83*, 7185–7193.

Popov, S., Strack, B., Sanchez-Merino, V., Popova, E., Rosin, H., and Göttlinger, H.G. (2011). Human immunodeficiency virus type 1 and related primate lentiviruses engage clathrin through Gag-Pol or Gag. J. Virol. *85*, 3792–3801.

Pornillos, O., Higginson, D.S., Stray, K.M., Fisher, R.D., Garrus, J.E., Payne, M., He, G.-P., Wang, H.E., Morham, S.G., and Sundquist, W.I. (2003). HIV Gag mimics the Tsg101-recruiting activity of the human Hrs protein. J. Cell Biol. *162*, 425–434.

Prabu-Jeyabalan, M., Nalivaika, E., and Schiffer, C. a (2002). Substrate shape determines specificity of recognition for HIV-1 protease: analysis of crystal structures of six substrate complexes. Structure *10*, 369–381.

Puertollano, R., and Bonifacino, J.S. (2004). Interactions of GGA3 with the ubiquitin sorting machinery. Nat. Cell Biol. *6*, 244–251.

Radoshitzky, S.R., Dong, L., Chi, X., Clester, J.C., Retterer, C., Spurgers, K., Kuhn, J.H., Sandwick, S., Ruthel, G., Kota, K., et al. (2010). Infectious Lassa virus, but not filoviruses, is restricted by BST-2/tetherin. J. Virol. *84*, 10569–10580.

Rahm, N., and Telenti, A. (2012). The role of tripartite motif family members in mediating susceptibility to HIV-1 infection. Curr. Opin. HIV AIDS *7*, 180–186.

Raiborg, C., and Stenmark, H. (2009). The ESCRT machinery in endosomal sorting of ubiquitylated membrane proteins. Nature *458*, 445–452.

Raiborg, C., Bremnes, B., Mehlum, a, Gillooly, D.J., D'Arrigo, a, Stang, E., and Stenmark, H. (2001). FYVE and coiled-coil domains determine the specific localisation of Hrs to early endosomes. J. Cell Sci. *114*, 2255–2263.

Raiborg, C., Bache, K.G., Gillooly, D.J., Madshus, I.H., Stang, E., and Stenmark, H. (2002). Hrs sorts ubiquitinated proteins into clathrin-coated microdomains of early endosomes. Nat. Cell Biol. *4*, 394–398.

Raiborg, C., Wesche, J., Malerød, L., and Stenmark, H. (2006). Flat clathrin coats on endosomes mediate degradative protein sorting by scaffolding Hrs in dynamic microdomains. J. Cell Sci. *119*, 2414–2424.

Rasaiyaah, J., Tan, C.P., Fletcher, A.J., Price, A.J., Blondeau, C., Hilditch, L., Jacques, D. a, Selwood, D.L., James, L.C., Noursadeghi, M., et al. (2013). HIV-1 evades innate immune recognition through specific cofactor recruitment. Nature *503*, 402–405.

Raymond, C., Howald-Stevenson, I., Vater, C., and Stevens, T. (1992). Morphological Classification of the Yeast Vacuolar Protein-Sorting Mutants: Evidence for a Prevacuolar Compartment in Class E vps Mutants. Mol. Biol. Cell *3*, 1389–1402.

Ren, X., and Hurley, J.H. (2010). VHS domains of ESCRT-0 cooperate in high-avidity binding to polyubiquitinated cargo. EMBO J. *29*, 1045–1054.

Ren, X., and Hurley, J.H. (2011). Proline-rich regions and motifs in trafficking: from ESCRT interaction to viral exploitation. Traffic *12*, 1282–1290.

Ren, X., Park, S.Y., Bonifacino, J.S., and Hurley, J.H. (2014). How HIV-1 Nef hijacks the AP-2 clathrin adaptor to downregulate CD4. Elife *3*, e01754.

Richard, J., and Cohen, É. a (2010). HIV-1 Vpu disarms natural killer cells. Cell Host Microbe *8*, 389–391.

Rittner, K., Churcher, M.J., Gait, M.J., and Karn, J. (1995). The human immunodeficiency virus long terminal repeat includes a specialised initiator element which is required for Tat-responsive transcription. J. Mol. Biol. *248*, 562–580.

Robinson, M.S., Sahlender, D. a, and Foster, S.D. (2010). Rapid inactivation of proteins by rapamycin-induced rerouting to mitochondria. Dev. Cell *18*, 324–331.

Rollason, R., Korolchuk, V., Hamilton, C., Schu, P., and Banting, G. (2007). Clathrin-mediated endocytosis of a lipid-raft-associated protein is mediated through a dual tyrosine motif. J. Cell Sci. *120*, 3850–3858.

Rollason, R., Korolchuk, V., Hamilton, C., Jepson, M., and Banting, G. (2009). A CD317/tetherin-RICH2 complex plays a critical role in the organization of the subapical actin cytoskeleton in polarized epithelial cells. J. Cell Biol. *184*, 721–736.

Romani, B., and Engelbrecht, S. (2009). Human immunodeficiency virus type 1 Vpr: functions and molecular interactions. J. Gen. Virol. *90*, 1795–1805.

Roux, K.J., Kim, D.I., Raida, M., and Burke, B. (2012). A promiscuous biotin ligase fusion protein identifies proximal and interacting proteins in mammalian cells. J. Cell Biol. *196*, 801–810.

Ruiz, A., Hill, M.S., Schmitt, K., Guatelli, J., and Stephens, E.B. (2008). Requirements of the membrane proximal tyrosine and dileucine-based sorting signals for efficient transport of the subtype C Vpu protein to the plasma membrane and in virus release. Virology *378*, 58–68.

Saphire, A.C.S., Bobardt, M.D., Zhang, Z., Gallay, P.A., Zhang, Z.H.E., and David, G. (2001). Syndecans Serve as Attachment Receptors for Human Immunodeficiency Virus Type 1 on Macrophages. J. Virol. *75*, 9187–9200.

Sato, K., Misawa, N., Fukuhara, M., Iwami, S., An, D.S., Ito, M., and Koyanagi, Y. (2012). Vpu augments the initial burst phase of HIV-1 propagation and downregulates BST2 and CD4 in humanized mice. J. Virol. *86*, 5000–5013.

Sattentau, Q. (2008). Avoiding the void: cell-to-cell spread of human viruses. Nat. Rev. Microbiol. *6*, 815–826.

Sauter, D., Schindler, M., Specht, A., Landford, W.N., Münch, J., Kim, K.-A., Votteler, J., Schubert, U., Bibollet-Ruche, F., Keele, B.F., et al. (2009). Tetherin-driven adaptation of Vpu and Nef function and the evolution of pandemic and nonpandemic HIV-1 strains. Cell Host Microbe *6*, 409–421.

Sauter, D., Vogl, M., and Kirchhoff, F. (2011a). Ancient origin of a deletion in human BST2/Tetherin that confers protection against viral zoonoses. Hum. Mutat. *32*, 1243–1245.

Sauter, D., Hué, S., Petit, S.J., Plantier, J.-C., Towers, G.J., Kirchhoff, F., and Gupta, R.K. (2011b). HIV-1 Group P is unable to antagonize human tetherin by Vpu, Env or Nef. Retrovirology *8*, 103.

Sauter, D., Unterweger, D., Vogl, M., Usmani, S.M., Heigele, A., Kluge, S.F., Hermkes, E., Moll, M., Barker, E., Peeters, M., et al. (2012). Human tetherin exerts strong selection pressure on the HIV-1 group N Vpu protein. PLoS Pathog. *8*, e1003093.

Schaller, T., Ocwieja, K.E., Rasaiyaah, J., Price, A.J., Brady, T.L., Roth, S.L., Hué, S., Fletcher, A.J., Lee, K., KewalRamani, V.N., et al. (2011). HIV-1 capsid-cyclophilin interactions determine nuclear import pathway, integration targeting and replication efficiency. PLoS Pathog. *7*, e1002439.

Schindler, M., Münch, J., Kutsch, O., Li, H., Santiago, M.L., Bibollet-Ruche, F., Müller-Trutwin, M.C., Novembre, F.J., Peeters, M., Courgnaud, V., et al. (2006). Nef-mediated suppression of T cell activation was lost in a lentiviral lineage that gave rise to HIV-1. Cell *125*, 1055–1067.

Schindler, M., Rajan, D., Banning, C., Wimmer, P., Koppensteiner, H., Iwanski, A., Specht, A., Sauter, D., Dobner, T., and Kirchhoff, F. (2010). Vpu serine 52 dependent counteraction of tetherin is required for HIV-1 replication in macrophages, but not in ex vivo human lymphoid tissue. Retrovirology *7*, 1.

Schmidt, S., Fritz, J. V, and Bitzegeio, J. (2011). Intrinsic Immunity Factor CD317 / Tetherin To Overcome the Virion. MBio *2*, 1–13.

Schröder, A.R.W., Shinn, P., Chen, H., Berry, C., Ecker, J.R., and Bushman, F. (2002). HIV-1 integration in the human genome favors active genes and local hotspots. Cell *110*, 521–529.

Schubert, U., and Strebel, K. (1994). Differential activities of the human immunodeficiency virus type 1-encoded Vpu protein are regulated by phosphorylation and occur in different cellular compartments. J. Virol. *68*, 2260–2271.

Schubert, H.L., Zhai, Q., Sandrin, V., Eckert, D.M., Garcia-maya, M., and Saul, L. (2010). Structural and functional studies on the extracellular domain of BST2 / tetherin in reduced and oxidized conformations. Proc. Natl. Acad. Sci. *107*, 17951–17956.

Schubert, U., Schneider, T., Henklein, P., Hoffmann, K., Berthold, E., Hauserz, H., Paul, G., and Porstmann, T. (1992). Human-immunodeficiency-virus-type-1-encoded Vpu protein is phosphorylated by casein kinase II. Eur. J. Biochem. *204*, 875–883.

Schubert, U., Clouse, K.A., and Strebel, K. (1995). Augmentation of virus secretion by the human immunodeficiency virus type 1 Vpu protein is cell type independent and occurs in cultured human primary macrophages and lymphocytes. J. Virol. *69*, 7699–7711.

Schubert, U., Ferrer-Montiel, a V, Oblatt-Montal, M., Henklein, P., Strebel, K., and Montal, M. (1996a). Identification of an ion channel activity of the Vpu transmembrane domain and its involvement in the regulation of virus release from HIV-1-infected cells. FEBS Lett. *398*, 12–18.

Schubert, U., Bour, S., Montal, M., Maldarell, F., Schubert, U., Bour, S., Ferrer-montiel, A. V, Montal, M., Maldarelli, F., and Strebel, K. (1996b). The two biological activities of human immunodeficiency virus type 1 Vpu protein involve two separable structural domains. J. Virol. *70*, 809–819.

Schwartz, S., Felber, B.K., and Pavlakis, G.N. (1990). Env and Vpu Proteins of Human Immunodeficiency Virus Type 1 Are Produced from Multiple Bicistronic mRNAs. J. Virol. *64*, 5448–5456.

Serra-Moreno, R., Jia, B., Breed, M., Alvarez, X., and Evans, D.T. (2011). Compensatory changes in the cytoplasmic tail of gp41 confer resistance to tetherin/BST-2 in a pathogenic nef-deleted SIV. Cell Host Microbe *9*, 46–57.

Serra-Moreno, R., Zimmermann, K., Stern, L.J., and Evans, D.T. (2013). Tetherin/BST-2 Antagonism by Nef Depends on a Direct Physical Interaction between Nef and Tetherin, and on Clathrin-mediated Endocytosis. PLoS Pathog. *9*, e1003487.

Shah, A.H., Sowrirajan, B., Davis, Z.B., Ward, J.P., Campbell, E.M., Planelles, V., and Barker, E. (2010). Degranulation of natural killer cells following interaction with HIV-1-infected cells is hindered by downmodulation of NTB-A by Vpu. Cell Host Microbe *8*, 397–409.

Sharp, P.M., and Hahn, B.H. (2011). Origins of HIV and the AIDS pandemic. Cold Spring Harb. Perspect. Med. *1*, a006841.

Sheehy, A.M., Gaddis, N.C., Choi, J.D., and Malim, M.H. (2002). Isolation of a human gene that inhibits HIV-1 infection and is suppressed by the viral Vif protein. Nature *418*, 646–650.

Sherer, N.M., Jin, J., and Mothes, W. (2010). Directional spread of surface-associated retroviruses regulated by differential virus-cell interactions. J. Virol. *84*, 3248–3258.

Simmons, G., Wool-lewis, R.J., Baribaud, F., Netter, R.C., and Bates, P. (2002). Ebola Virus Glycoproteins Induce Global Surface Protein Down-Modulation and Loss of Cell Adherence. J. Virol. *76*, 2518–2528.

Simon, J.H., Gaddis, N.C., Fouchier, R. a, and Malim, M.H. (1998). Evidence for a newly discovered cellular anti-HIV-1 phenotype. Nat. Med. *4*, 1397–1400.

Singh, S.K., Möckel, L., Thiagarajan-Rosenkranz, P., Wittlich, M., Willbold, D., and Koenig, B.W. (2012). Mapping the interaction between the cytoplasmic domains of HIV-1 viral protein U and human CD4 with NMR spectroscopy. FEBS J. *279*, 3705–3714.

Skasko, M., Tokarev, A., Chen, C.-C., Fischer, W.B., Pillai, S.K., and Guatelli, J. (2011). BST-2 is rapidly down-regulated from the cell surface by the HIV-1 protein Vpu: evidence for a post-ER mechanism of Vpu-action. Virology *411*, 65–77.

Skasko, M., Wang, Y., Tian, Y., Tokarev, A., Munguia, J., Ruiz, A., Stephens, E.B., Opella, S.J., and Guatelli, J. (2012). HIV-1 Vpu protein antagonizes innate restriction factor BST-2 via lipid-embedded helix-helix interactions. J. Biol. Chem. *287*, 58–67.

Sodroski, J., Patarca, R., Rosen, C., Wong-Staal, F., and Haseltine, W. (1985a). Location of the trans-activating region on the genome of human T-cell lymphotropic virus type III. Science *229*, 74–77.

Sodroski, J., Rosen, C., Wong-Staal, F., Salahuddin, S., Popovic, M., Arya, S., Gallo, R., and Haseltine, W. (1985b). Trans-acting transcriptional regulation of human T-cell leukemia virus type III long terminal repeat. Science *227*, 171–173.

Sodroski, J., Goh, W., Rosen, C., Dayton, A., Terwilliger, E., and Haseltine, W. (1986). A second post-transcriptional trans-activator gene required for HTLV-II replication. Nature *321*, 412–417.

De Souza, R.F., and Aravind, L. (2010). UMA and MABP domains throw light on receptor endocytosis and selection of endosomal cargoes. Bioinformatics *26*, 1477–1480.

Srivastava, S., Swanson, S.K., Manel, N., Florens, L., Washburn, M.P., and Skowronski, J. (2008). Lentiviral Vpx accessory factor targets VprBP/DCAF1 substrate adaptor for cullin 4 E3 ubiquitin ligase to enable macrophage infection. PLoS Pathog. *4*, e1000059.

Stacey, A.R., Norris, P.J., Qin, L., Haygreen, E. a, Taylor, E., Heitman, J., Lebedeva, M., DeCamp, A., Li, D., Grove, D., et al. (2009). Induction of a striking systemic cytokine cascade prior to peak viremia in acute human immunodeficiency virus type 1 infection, in contrast to more modest and delayed responses in acute hepatitis B and C virus infections. J. Virol. *83*, 3719–3733.

Stark, G.R., and Darnell, J.E. (2012). The JAK-STAT pathway at twenty. Immunity *36*, 503–514.

Stefani, F., Zhang, L., Taylor, S., Donovan, J., Rollinson, S., Doyotte, A., Brownhill, K., Bennion, J., Pickering-Brown, S., and Woodman, P. (2011). UBAP1 is a component of an endosome-specific ESCRT-I complex that is essential for MVB sorting. Curr. Biol. *21*, 1245–1250.

Strebel, K., Klimkait, T., and Martin, M.A. (1988). A novel gene of HIV-1, vpu, and its 16–kilodalton product. Science *241*, 1221–1223.

Strebel, K., Klimkait, T., Maldarelli, F., and Martin, M.A. (1989). Molecular and Biochemical Analyses of Human Immunodeficiency Virus Type 1 vpu Protein. J. Virol. *63*, 3784–3791.

Stremlau, M., Owens, C.M., Perron, M.J., Kiessling, M., Autissier, P., and Sodroski, J. (2004). The cytoplasmic body component TRIM5alpha restricts HIV-1 infection in Old World monkeys. Nature *427*, 848–853.

Stremlau, M., Perron, M., Lee, M., Li, Y., Song, B., Javanbakht, H., Diaz-Griffero, F., Anderson, D.J., Sundquist, W.I., and Sodroski, J. (2006). Specific recognition and accelerated uncoating of retroviral capsids by the TRIM5alpha restriction factor. Proc. Natl. Acad. Sci. U. S. A. *103*, 5514–5519.

Suhasini, M., and Reddy, T.R. (2009). Cellular proteins and HIV-1 Rev function. Curr. HIV Res. *7*, 91–100.

Sundquist, W.I., and Kräusslich, H.-G. (2012). HIV-1 assembly, budding, and maturation. Cold Spring Harb. Perspect. Med. *2*, a006924.

Swanson, C.M., and Malim, M.H. (2008). SnapShot: HIV-1 proteins. Cell *133*, 742, 742.e1.

Swanson, C.M., Sherer, N.M., and Malim, M.H. (2010). SRp40 and SRp55 promote the translation of unspliced human immunodeficiency virus type 1 RNA. J. Virol. *84*, 6748–6759.

Swiecki, M., Scheaffer, S.M., Allaire, M., Fremont, D.H., Colonna, M., and Brett, T.J. (2011). Structural and biophysical analysis of BST-2/tetherin ectodomains reveals an evolutionary conserved design to inhibit virus release. J. Biol. Chem. *286*, 2987–2997.

Von Sydow, M., Sönnerborg, a, Gaines, H., and Strannegård, O. (1991). Interferon-alpha and tumor necrosis factor-alpha in serum of patients in various stages of HIV-1 infection. AIDS Res. Hum. Retroviruses *7*, 375–380.

Sze, A., Olagnier, D., Lin, R., van Grevenynghe, J., and Hiscott, J. (2013). SAMHD1 host restriction factor: a link with innate immune sensing of retrovirus infection. J. Mol. Biol. *425*, 4981–4994.

Tavano, B., Galao, R.P., Graham, D.R., Neil, S.J.D., Aquino, V.N., Fuchs, D., and Boasso, A. (2013). Ig-like transcript 7, but not bone marrow stromal cell antigen 2 (also known as HM1.24, tetherin, or CD317), modulates plasmacytoid dendritic cell function in primary human blood leukocytes. J. Immunol. *190*, 2622–2630.

Tennant, R.W., Myer, F.E., and McGrath, L. (1974). Effect of the Fv-1 gene on leukemia virus in mouse cell heterokaryons. Int. J. Cancer *14*, 504–513.

Tervo, H.-M., Homann, S., Ambiel, I., Fritz, J. V, Fackler, O.T., and Keppler, O.T. (2011). β-TrCP is dispensable for Vpu's ability to overcome the CD317/Tetherin-imposed restriction to HIV-1 release. Retrovirology *8*, 9.

Terwilliger, E.F., Cohen, E.A., Lu, Y., Sodroski, J.G., and Haseltine, W.A. (1989). Functional role of human immunodeficiency virus type 1 vpu. Proc. Natl. Acad. Sci. U. S. A. *86*, 5163–5167.

Tiganos, E., Yao, X.J., Friborg, J., Daniel, N., and Cohen, E.A. (1997). Putative alpha-helical structures in the human immunodeficiency virus type 1 Vpu protein and CD4 are involved in binding and degradation of the CD4 molecule. J. Virol. *71*, 4452–4460.

Tokarev, A., Suarez, M., Kwan, W., Fitzpatrick, K., Singh, R., and Guatelli, J. (2013). Stimulation of NF-κB activity by the HIV restriction factor BST2. J. Virol. *87*, 2046–2057.

Tokarev, A. a, Munguia, J., and Guatelli, J.C. (2011). Serine-threonine ubiquitination mediates downregulation of BST-2/tetherin and relief of restricted virion release by HIV-1 Vpu. J. Virol. *85*, 51–63.

Le Tortorec, A., and Neil, S.J.D. (2009). Antagonism to and intracellular sequestration of human tetherin by the human immunodeficiency virus type 2 envelope glycoprotein. J. Virol. *83*, 11966–11978.

Le Tortorec, A., Willey, S., and Neil, S.J.D. (2011). Antiviral inhibition of enveloped virus release by tetherin/BST-2: action and counteraction. Viruses *3*, 520–540.

Towers, G., Bock, M., Martin, S., Takeuchi, Y., Stoye, J.P., and Danos, O. (2000). A conserved mechanism of retrovirus restriction in mammals. Proc. Natl. Acad. Sci. U. S. A. *97*, 12295–12299.

Trono, D. (1992). Partial reverse transcripts in virions from human immunodeficiency and murine leukemia viruses. J. Virol. *66*, 4893–4900.

Usami, Y., and Göttlinger, H. (2013). HIV-1 Nef responsiveness is determined by Env variable regions involved in trimer association and correlates with neutralization sensitivity. Cell Rep. *5*, 802–812.

Varthakavi, V., Smith, R.M., Bour, S.P., Strebel, K., and Spearman, P. (2003). Viral protein U counteracts a human host cell restriction that inhibits HIV-1 particle production. Proc. Natl. Acad. Sci. U. S. A. *100*, 15154–15159.

Varthakavi, V., Smith, R.M., Martin, K.L., Derdowski, A., Lapierre, L. a, Goldenring, J.R., and Spearman, P. (2006). The pericentriolar recycling endosome plays a key role in Vpu-mediated enhancement of HIV-1 particle release. Traffic *7*, 298–307.

Veillette, M., Désormeaux, A., Medjahed, H., Gharsallah, N.-E., Coutu, M., Baalwa, J., Guan, Y., Lewis, G., Ferrari, G., Hahn, B.H., et al. (2014). Interaction with Cellular CD4 Exposes HIV-1 Envelope Epitopes Targeted by Antibody-Dependent Cell-Mediated Cytotoxicity. J. Virol. *88*, 2633–2644.

Venkatesh, S., and Bieniasz, P.D. (2013). Mechanism of HIV-1 Virion Entrapment by Tetherin. PLoS Pathog. *9*, e1003483.

Vigan, R., and Neil, S.J.D. (2010a). Determinants of Tetherin Antagonism in the Transmembrane Domain of the Human Immunodeficiency Virus Type 1 Vpu Protein. J. Virol. *84*, 12958–12970.

Vigan, R., and Neil, S.J.D. (2010b). Determinants of tetherin antagonism in the transmembrane domain of the human immunodeficiency virus type 1 Vpu protein. J. Virol. *84*, 12958–12970.

Vigan, R., and Neil, S.J.D. (2011). Separable determinants of subcellular localization and interaction account for the inability of group O HIV-1 Vpu to counteract tetherin. J. Virol. *85*, 9737–9748.

Vincent, M.J., Raja, N.U., and Jabbar, M.A. (1993). Human immunodeficiency virus type 1 Vpu protein induces degradation of chimeric envelope glycoproteins bearing the cytoplasmic and anchor domains of CD4: role of the cytoplasmic domain in Vpu-induced degradation in the endoplasmic reticulum. J. Virol. *67*, 5538–5549.

Viswanathan, K., Smith, M.S., Malouli, D., Mansouri, M., Nelson, J. a, and Früh, K. (2011). BST2/Tetherin enhances entry of human cytomegalovirus. PLoS Pathog. *7*, e1002332.

Wang, G.P., Ciuffi, A., Leipzig, J., Berry, C.C., and Bushman, F.D. (2007). HIV integration site selection: analysis by massively parallel pyrosequencing reveals association with epigenetic modifications. Genome Res. *17*, 1186–1194.

Ward, J., Davis, Z., DeHart, J., Zimmerman, E., Bosque, A., Brunetta, E., Mavilio, D., Planelles, V., and Barker, E. (2009). HIV-1 Vpr triggers natural killer cell-mediated lysis of infected cells through activation of the ATR-mediated DNA damage response. PLoS Pathog. *5*, e1000613.

Watanabe, R., Leser, G.P., and Lamb, R. a (2011). Influenza virus is not restricted by tetherin whereas influenza VLP production is restricted by tetherin. Virology *417*, 50–56.

Wei, P., Garber, M.E., Fang, S.M., Fischer, W.H., and Jones, K. a (1998). A novel CDK9-associated C-type cyclin interacts directly with HIV-1 Tat and mediates its high-affinity, loop-specific binding to TAR RNA. Cell *92*, 451–462.

Welbourn, S., Dutta, S.M., Semmes, O.J., and Strebel, K. (2013). Restriction of virus infection but not catalytic dNTPase activity is regulated by phosphorylation of SAMHD1. J. Virol. *87*, 11516–11524.

Wen, X., Duus, K.M., Friedrich, T.D., and de Noronha, C.M.C. (2007). The HIV1 protein Vpr acts to promote G2 cell cycle arrest by engaging a DDB1 and Cullin4A-containing ubiquitin ligase complex using VprBP/DCAF1 as an adaptor. J. Biol. Chem. *282*, 27046–27057.

Whitcomb, J.M., Kumar, R., and Hughes, S.H. (1990). Sequence of the circle junction of human immunodeficiency virus type 1: implications for reverse transcription and integration. J. Virol. *64*, 4903–4906.

White, T.E., Brandariz-Nuñez, A., Valle-Casuso, J.C., Amie, S., Nguyen, L.A., Kim, B., Tuzova, M., and Diaz-Griffero, F. (2013). The retroviral restriction ability of SAMHD1, but not its deoxynucleotide triphosphohydrolase activity, is regulated by phosphorylation. Cell Host Microbe *13*, 441–451.

Wiegers, K., Rutter, G., Kottler, H., Tessmer, U., and Tessmer, U.W.E. (1998). Sequential Steps in Human Immunodeficiency Virus Particle Maturation Revealed by Alterations of Individual Gag Polyprotein Cleavage Sites. J. Virol. *72*, 2846–2854.

Wildum, S., Schindler, M., Münch, J., and Kirchhoff, F. (2006). Contribution of Vpu, Env, and Nef to CD4 down-modulation and resistance of human immunodeficiency virus type 1-infected T cells to superinfection. J. Virol. *80*, 8047–8059.

Wilen, C.B., Tilton, J.C., and Doms, R.W. (2012). HIV: cell binding and entry. Cold Spring Harb. Perspect. Med. *2*, a006866.

Willey, R.L., Buckler-White, A., and Strebel, K. (1994). Sequences present in the cytoplasmic domain of CD4 are necessary and sufficient to confer sensitivity to the human immunodeficiency virus type 1 Vpu protein . J. Virol. *68*, 1207–1212.

Winkler, M., Bertram, S., Gnirß, K., Nehlmeier, I., Gawanbacht, A., Kirchhoff, F., Ehrhardt, C., Ludwig, S., Kiene, M., Moldenhauer, A.-S., et al. (2012). Influenza A virus does not encode a tetherin antagonist with Vpu-like activity and induces IFN-dependent tetherin expression in infected cells. PLoS One *7*, e43337.

Wittlich, M., Koenig, B.W., Stoldt, M., Schmidt, H., and Willbold, D. (2009). NMR structural characterization of HIV-1 virus protein U cytoplasmic domain in the presence of dodecylphosphatidylcholine micelles. FEBS J. *276*, 6560–6575.

Wray, V., Federau, T., Henklein, P., Klabunde, S., Kunert, O., Schomburg, D., and Schubert, U. (1995). Solution structure of the hydrophilic region of HIV-1 encoded virus protein U (Vpu) by CD and 1H NMR spectroscopy. Int. J. Pept. Res. Ther. *45*, 35–43.

Wu, L. (2013). Cellular and Biochemical Mechanisms of the Retroviral Restriction Factor SAMHD1. ISRN Biochem. *2013*, 1–11.

Xu, L. (2003). BTBD1 and BTBD2 colocalize to cytoplasmic bodies with the RBCC/tripartite motif protein, TRIM5δ. Exp. Cell Res. *288*, 84–93.

Yamashita, M., and Emerman, M. (2004). Capsid Is a Dominant Determinant of Retrovirus Infectivity in Nondividing Cells. J. Virol. *78*, 5670–5678.

Yan, N., Regalado-Magdos, A.D., Stiggelbout, B., Lee-Kirsch, M.A., and Lieberman, J. (2010). The cytosolic exonuclease TREX1 inhibits the innate immune response to human immunodeficiency virus type 1. Nat. Immunol. *11*, 1005–1013.

Yang, H., Wang, J., Jia, X., McNatt, M.W., Zang, T., Pan, B., Meng, W., Wang, H.-W., Bieniasz, P.D., and Xiong, Y. (2010). Structural insight into the mechanisms of enveloped virus tethering by tetherin. Proc. Natl. Acad. Sci. U. S. A. *107*, 18428–18432.

Yang, S.J., Lopez, L. a, Exline, C.M., Haworth, K.G., and Cannon, P.M. (2011). Lack of adaptation to human tetherin in HIV-1 group O and P. Retrovirology *8*, 78.

Yankulov, K., and Bentley, D. (1998). Transcriptional control: Tat cofactors and transcriptional elongation. Curr. Biol. *8*, R447–9.

Yao, X.J., Gotilinger, H., Haseltine, W.A., and Cohen, E.A. (1992). Envelope Glycoprotein and CD4 Independence of vpu-Facilitated Human Immunodeficiency Virus Type 1 Capsid Export. J. Virol. *66*, 5119–5126.

Yao, X.J., Friborg, J., Checroune, F., Gratton, S., Boisvert, F., Sékaly, R.P., and Cohen, E.A. (1995). Degradation of CD4 induced by human immunodeficiency virus type 1 Vpu protein: a predicted alpha-helix structure in the proximal cytoplasmic region of CD4 contributes to Vpu sensitivity. Virology *209*, 615–623.

Yondola, M. a, Fernandes, F., Belicha-Villanueva, A., Uccelini, M., Gao, Q., Carter, C., and Palese, P. (2011). Budding capability of the influenza virus neuraminidase can be modulated by tetherin. J. Virol. *85*, 2480–2491.

Yu, X.F., Matsuda, M., Essex, M., and Lee, T.H. (1990). Open reading frame vpr of simian immunodeficiency virus encodes a virion-associated protein. J. Virol. *64*, 5688–5693.

Zenner, H.L., Mauricio, R., Banting, G., and Crump, C.M. (2013). Herpes simplex virus type-1 counteracts tetherin restriction via its virion host shutoff activity. J. Virol.

Zennou, V., Perez-caballero, D., and Bieniasz, P.D. (2004). APOBEC3G Incorporation into Human Immunodeficiency Virus Type 1 Particles APOBEC3G Incorporation into Human Immunodeficiency Virus Type 1 Particles. J. Virol. *78*, 12058–12061.

Zenzie-Gregory, B., Sheridan, P., Jones, K. a, and Smale, S.T. (1993). HIV-1 core promoter lacks a simple initiator element but contains a bipartite activator at the transcription start site. J. Biol. Chem. *268*, 15823–15832.

Zhang, F., Wilson, S.J., Landford, W.C., Virgen, B., Gregory, D., Johnson, M.C., Munch, J., Kirchhoff, F., Bieniasz, P.D., and Hatziioannou, T. (2009). Nef proteins from simian immunodeficiency viruses are tetherin antagonists. Cell Host Microbe *6*, 54–67.

Zhang, F., Landford, W.N., Ng, M., McNatt, M.W., Bieniasz, P.D., and Hatziioannou, T. (2011a). SIV Nef proteins recruit the AP-2 complex to antagonize Tetherin and facilitate virion release. PLoS Pathog. *7*, e1002039.

Zhang, F., Zang, T., Wilson, S.J., Johnson, M.C., and Bieniasz, P.D. (2011b). Clathrin facilitates the morphogenesis of retrovirus particles. PLoS Pathog. *7*, e1002119.

Zhong, P., Agosto, L.M., Ilinskaya, A., Dorjbal, B., Truong, R., Derse, D., Uchil, P.D., Heidecker, G., and Mothes, W. (2013). Cell-to-cell transmission can overcome multiple donor and target cell barriers imposed on cell-free HIV. PLoS One *8*, e53138.

Zhou, L., Sokolskaja, E., Jolly, C., James, W., Cowley, S. a, and Fassati, A. (2011). Transportin 3 promotes a nuclear maturation step required for efficient HIV-1 integration. PLoS Pathog. *7*, e1002194.

Zizioli, D., Meyer, C., Saftig, P., Figura, K. Von, Chem, J.B., Guhde, G., and Schu, P. (1999). Early Embryonic Death of Mice Deficient in γ -Adaptin. J. Biol. Chem. *274*, 5385–5390.

Appendix A. Publications

OPEN ACCESS Freely available online

PLoS PATHOGENS

A Cytoplasmic Tail Determinant in HIV-1 Vpu Mediates Targeting of Tetherin for Endosomal Degradation and Counteracts Interferon-Induced Restriction

Tonya Kueck, Stuart J. D. Neil*

Department of Infectious Disease, King's College London School of Medicine, Guy's Hospital, London, United Kingdom

Abstract

The HIV-1 accessory protein Vpu counteracts tetherin (BST-2/CD317) by preventing its incorporation into virions, reducing its surface expression, and ultimately promoting its degradation. Here we characterize a putative trafficking motif, EXXXLV, in the second alpha helix of the subtype-B Vpu cytoplasmic tail as being required for efficient tetherin antagonism. Mutation of this motif prevents ESCRT-dependent degradation of tetherin/Vpu complexes, tetherin cell surface downregulation, but not its physical interaction with Vpu. Importantly, this motif is required for efficient cell-free virion release from CD4+ T cells, particularly after their exposure to type-1 interferon, indicating that the ability to reduce surface tetherin levels and promote its degradation is important to counteract restriction under conditions that the virus likely encounters *in vivo*. Vpu EXXXLV mutants accumulate with tetherin at the cell surface and in endosomal compartments, but retain the ability to bind both β-TrCP2 and HRS, indicating that this motif is required for a post-binding trafficking event that commits tetherin for ESCRT-dependent degradation and prevents its transit to the plasma membrane and viral budding zones. We further found that while Vpu function is dependent on clathrin, and the entire second alpha helix of the Vpu tail can be functionally complemented by a clathrin adaptor binding peptide derived from HIV-1 Nef, none of the canonical clathrin adaptors nor retromer are required for this process. Finally we show that residual activity of Vpu EXXXLV mutants requires an intact endocytic motif in tetherin, suggesting that physical association of Vpu with tetherin during its recycling may be sufficient to compromise tetherin activity to some degree.

Citation: Kueck T, Neil SJD (2012) A Cytoplasmic Tail Determinant in HIV-1 Vpu Mediates Targeting of Tetherin for Endosomal Degradation and Counteracts Interferon-Induced Restriction. PLoS Pathog 8(3): e1002609. doi:10.1371/journal.ppat.1002609

Editor: Michael Emerman, Fred Hutchinson Cancer Research Center, United States of America

Received August 22, 2011; **Accepted** February 11, 2012; **Published** March 29, 2012

Funding: This study was supported by a Wellcome Trust Research Career Development Fellowship WT082274MA and MRC project grant G0801937 to SJDN. The funders had no role in study design, data collection and analysis, decision to publish, or preparation of the manuscript.

Competing Interests: The authors have declared that no competing interests exist.

* E-mail: stuart.neil@kcl.ac.uk

Introduction

The downregulation of cell-surface immunomodulatory proteins is a common theme in the evasion of innate and adaptive immune responses by mammalian viruses. One host molecule targeted by diverse enveloped viruses is tetherin (CD317/BST-2), an interferon-induced dimeric type-II membrane protein, which inhibits the release of nascent virions from the cell surface [1,2]. By virtue of an unusual topology that consists of an N-terminal transmembrane domain and a C-terminal glycophosphatidylinositol (GPI)-linkage separated by an extended parallel coiled-coil domain [3–6], tetherin partitions into budding virus particles and is thought to directly cross-link the nascent virion to the plasma membrane (PM) [7]. Tethered virions may then be endocytosed and degraded in endosomes. Tetherin itself constitutively recycles between the PM, endosomal and trans-Golgi network (TGN) compartments through a non-canonical trafficking motif (YXYXXV) in its N-terminal cytoplasmic tail, which engages clathrin adaptors AP-1 and AP-2 [8,9]. Since tetherin targets a structural component of the virion not encoded by the viral genome, namely the host-cell derived membrane, its potential importance in the innate antiviral response is highlighted by multiple examples of virally-encoded countermeasures (reviewed in [10]).

The ability to counteract tetherin is conserved among human and simian immunodeficiency viruses (HIVs/SIVs), although the viral proteins tasked with this activity vary [10]. In HIV-1 the accessory protein Vpu fulfills this role. Vpu, a small integral membrane phosphoprotein, directly associates with tetherin through interactions between the transmembrane domains of both proteins [11–14]. Vpu blocks tetherin incorporation into assembling virions [7] and leads to a reduction of tetherin levels on the plasma membrane (PM) [2]. Subsequently, tetherin is degraded, most likely in lysosomal compartments, by an ubiquitin-dependent mechanism [15,16]. Phosphorylation of Vpu on two conserved serine residues recruits a SCF β-TrCP1/2 E3 ligase complex [17] that ubiquitinates the tetherin cytoplasmic tail on multiple residues [18], and recent evidence demonstrates that this tetherin degradation is dependent on the ESCRT pathway [19]. However, tetherin degradation is not strictly required for Vpu activity [20,21]. While recruitment of the ESCRT-0 subunit HRS by Vpu counteracts tetherin activity [19], a novel core component of ESCRT-1, Ubiquitin Associated Protein 1 (UBAP1), essential for tetherin degradation induced by both Vpu and the KSHV ubiquitin ligase K5, is dispensable [22]. Coupled with recent evidence that dysregulation of the entire late endosomal compartment by mutants of Rab7a [23], this suggests

Author Summary

Tetherin inhibits the release of several diverse enveloped viruses from infected cells and is counteracted by the HIV-1 accessory gene Vpu. Vpu prevents tetherin's incorporation into nascent viral particles, promotes its downregulation from the cell surface and targets tetherin for degradation. Here we identify a determinant that resembles an acidic-dileucine-based sorting sequence in the Vpu cytoplasmic tail that is required for efficient counteraction of tetherin activity, particularly in CD4+ T cells treated with type-1 interferon. Mutation of this motif prevents cell-surface downregulation and degradation of Vpu/tetherin complexes but does not affect their interaction. Rather, in its absence, Vpu accumulates in early endosomes and at the cell surface where it becomes incorporated into assembling virions with tetherin, indicating that this motif modulates sub-cellular trafficking of tetherin. Furthermore Vpu activity is clathrin-dependent and can be reconstituted by replacing a portion of the cytoplasmic tail encompassing this motif with one derived from HIV-1 Nef that is known to bind several clathrin adaptors. Finally, we demonstrate that residual function of the mutant Vpu requires a trafficking motif in tetherin, suggesting that physical interaction of tetherin with Vpu during its recycling to the cell-surface can interfere with its function to a variable extent.

an emerging picture that Vpu alters tetherin trafficking to counteract its antiviral activity prior to lysosomal delivery. While HIV-2 and SIV tetherin antagonists Env and Nef promote tetherin internalization through their interactions with AP-2, [24–26], Vpu does not enhance the rate of tetherin endocytosis [13,16]. Rather it is thought that Vpu/tetherin interactions preclude both the recycling of tetherin back to the cell surface and the transit of newly synthesized tetherin to the PM by trapping it in intracellular compartments, notably the TGN [13]. Consistent with this, the ability of Vpu to localize to the TGN correlates with tetherin antagonism [27], and disruption of the recycling compartment by a dominant Rab11a mutant compromises Vpu activity [28]. Truncations of the Vpu cytoplasmic tail, particularly the second alpha helix, lead to aberrant localization and a reduction in its anti-tetherin activity, suggesting it harbors a domain required for Vpu function [29].

In this study we have examined the role of the second alpha helix of HIV-1 Vpu in tetherin antagonism. We identify a putative sorting signal that is required for post-binding trafficking of Vpu/tetherin complexes and inhibition of antiviral activity in primary CD4+ T cells. While this signal can be functionally replaced by a clathrin adaptor binding peptide derived form HIV-1 Nef, Vpu activity does not require the canonical adaptors AP-1, AP-2 or AP-3. Moreover, because residual activity of second helix mutants requires an intact recycling signal in tetherin, we propose that second alpha helix mutants are selectively defective for routing tetherin into an endosomal degradation pathway thereby inhibiting its transit to the PM and incorporation into nascent virions.

Results

Determinants of tetherin inactivation in the second alpha helix of the Vpu cytoplasmic tail

Truncations of the Vpu cytoplasmic tail lead to aberrant localization and a reduction in its anti-tetherin activity [29]. To further study the determinants within the second alpha helix of Vpu that account for TGN localization, we performed overlapping triple-alanine scan mutagenesis through the second alpha helix of a codon optimized HIV-1 NL4.3 Vpu construct bearing a C-terminal HA tag (Figure 1A). We then assayed these Vpu mutants for their ability to rescue Vpu-defective HIV-1 from tetherin restriction. 293T cells were transfected with wildtype HIV-1 (HIV-1 wt) or Vpu defective HIV-1 (HIV-1 delVpu) proviruses in combination with fixed doses of a human tetherin expression vector, and 25 ng of Vpu-HA or mutant thereof. 48 h after transfection cell lysates and supernatants were harvested and analyzed for physical viral yield by Western blot (Figure 1B) or supernatant infectivity of HeLa-TZMbl indicator cells (Figure 1C). As expected, in the absence of Vpu, both supernatant particle yield and infectivity of HIV-1 delVpu was profoundly reduced in the presence of tetherin, expression of Vpu *in trans* rescued virus production to wildtype levels. By contrast mutations encompassing either E59 or L63 and V64 but not the intervening or subsequent amino acids displayed defective rescue of HIV-1 delVpu (Figure 1B and C). All Vpu mutants with the exception of Vpu 67-69A-HA were expressed equivalently. Vpu 63-65A-HA appeared to display a dominant interfering activity on HIV-1wt titer, but this was not reflected as apparently in particle yield. Thus these data suggested a functional requirement for E59 and L63/V64 in tetherin antagonism by Vpu. To confirm this we mutated these residues to alanine in the context of an HIV-1 NL4.3 provirus (NL4.3 Vpu ELV) and examined viral release from 293T cells in the presence of increasing expression of tetherin. Because this part of Vpu overlaps with start of the Env open reading frame in the provirus, these mutations were rendered silent in the +1 reading frame and displayed no defect in virus release in the absence of tetherin (Figure 1D and E). In agreement with the virus rescue *in trans*, NL4.3 Vpu ELV release was markedly defective in the presence of increasing tetherin doses, although it did display a residual antagonism of tetherin when compared to the full Vpu-defective deletion (Figure 1D and E).

We next examined the phenotypic basis for the defect in tetherin antagonism by Vpu ELV. Vpu stimulates the ubiquitin-dependent degradation of tetherin, most likely in lysozomal compartments. We infected HT1080 cells stably expressing human tetherin bearing an HA-tag in the extracellular domain (HT1080/tetherin-HA) with VSV-G-pseudotyped HIV-1 wt, HIV-1 delVpu or HIV-1 Vpu ELV at an MOI of 2 to ensure >90% cell infection. 48 h later the cells were lysed and Western blotting performed for relative tetherin-HA levels (Figure 2A). As expected, cells infected with HIV-1 wt showed reduced steady state levels of tetherin that was not apparent in those infected with HIV-1 delVpu. Similarly, in cells infected with HIV-1 Vpu ELV there was no evidence of tetherin degradation, but interestingly there appeared to be enhanced levels of tetherin, perhaps suggesting stabilization of the protein in the presence of the mutant Vpu. Thus E59, L63, V64 mutations abolish the ability of Vpu to induce tetherin degradation. Since this degradation is dependent on Vpu binding to β-TrCP2 via a phosphorylated pair of serines (S52 and S56) [16,17,30], we tested whether Vpu ELV mutants were defective for interaction with β-TrCP2 in co-immunoprecipitations from transfected cells (Figure 2B). β-TrCP2 was co-immunoprecipitated with Vpu-HA and Vpu ELV-HA, but as expected, not the phospho-mutant Vpu 2/6-HA, ruling out this defect in Vpu ELV.

Recent data suggests that ESCRT-mediated degradation of tetherin in the presence of Vpu is mediated by interaction of Vpu with HRS (ESCRT-0) [19]. We could further show that both Vpu and Vpu ELV also co-precipitated with HA-HRS from transfected 293T cells (Figure 2C) indicating that an inability to recruit ESCRT-0 does not explain the defect in Vpu ELV-mediated degradation of tetherin.

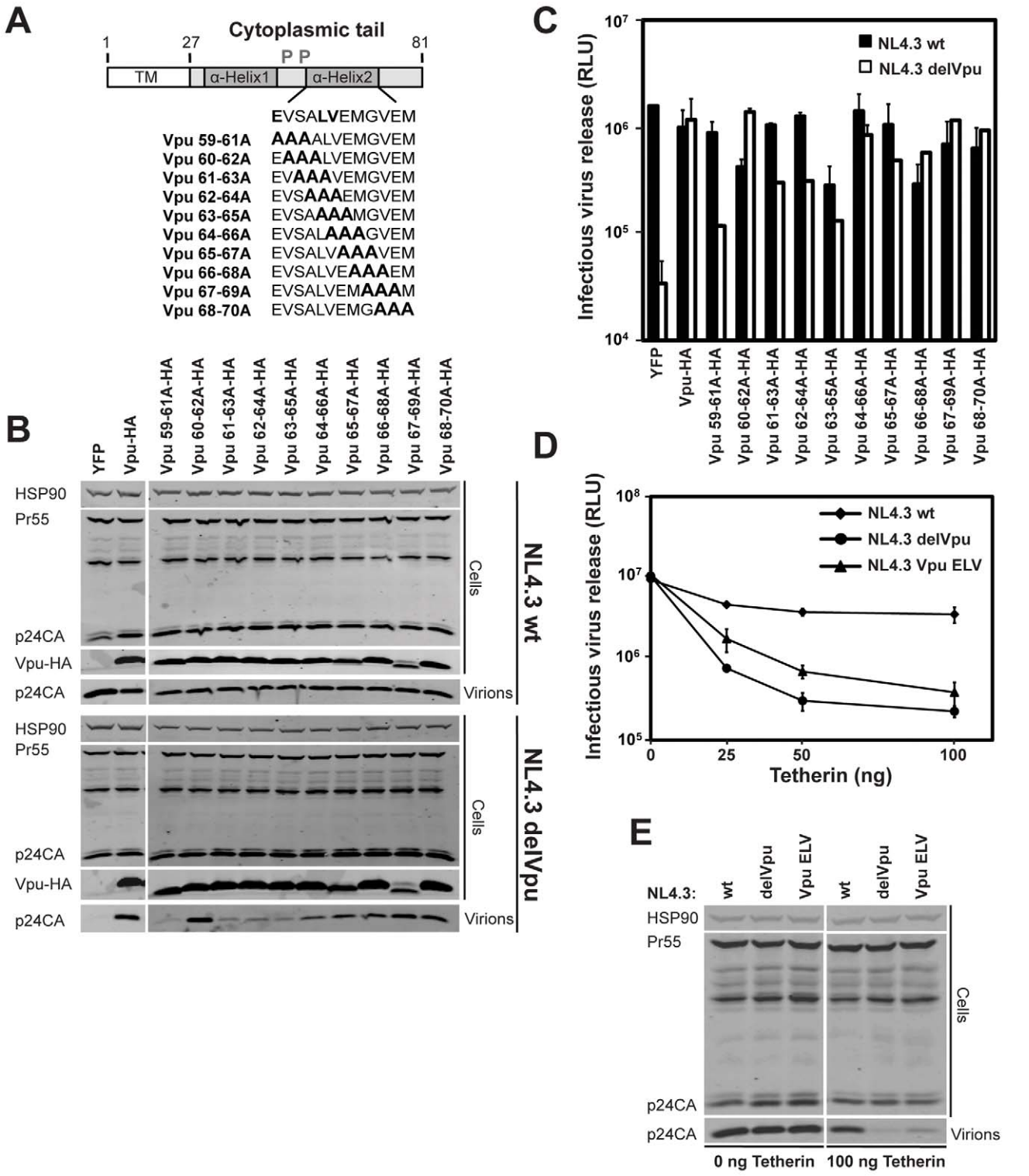

Figure 1. E59, L63 and V64 in the second alpha helix of the Vpu cytoplasmic tail are required to efficiently counteract tetherin. (**A**) Schematic representation of alanine scan mutagenesis in the second alpha helix of the codon-optimized HIV-1 NL4.3 Vpu protein. (**B**) 293T cells were transfected with NL4.3 wt or NL4.3 delVpu proviruses in combination with tetherin and the indicated pCR3.1 Vpu-HA expression vectors. 48 h post transfection, cell lysates and pelleted supernatant virions were harvested and subjected to SDS-PAGE and analyzed by Western blotting for HIV-1 p24CA, Vpu-HA and Hsp90 serving as loading control, and analyzed by LiCor quantitative imager. (**C**) Viral supernatants from **B** were assayed for infectivity using HeLa-TZMbl reporter cells. Infectious virus release is plotted on a log scale as β-galactosidase activity in relative light units (RLU). Error bars represent standard deviations of the means of three independent experiments. (**D**) E59A, L63A and V64A mutations were inserted into the *vpu* gene of the NL4.3 provirus referred to as NL4.3 Vpu ELV. 293T cells were transfected with NL4.3 wt, NL4.3 delVpu or NL4.3 Vpu ELV proviral plasmids together with increasing doses of tetherin expression vector. The resulting infectivity was determined as in **C**, error bars represent standard deviations of the means of three independent experiments. (**E**) Cell lysates and pelleted viral supernatants from 0 ng and 100 ng tetherin input from **D** were subjected to SDS-PAGE and analyzed by Western blotting for HIV-1 p24CA and Hsp90, and analyzed by LiCor quantitative imager.
doi:10.1371/journal.ppat.1002609.g001

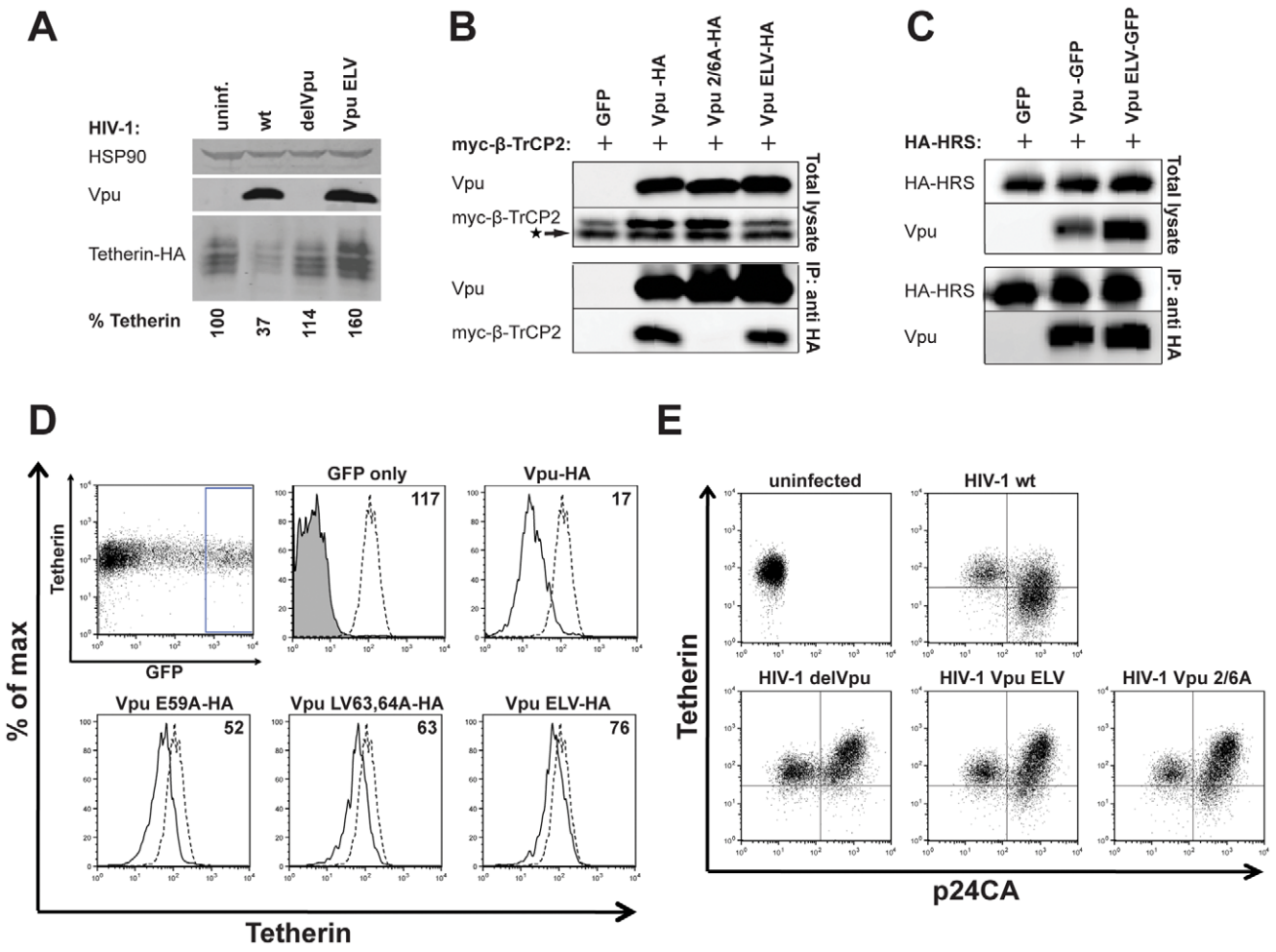

Figure 2. Vpu ELV mutants are defective for tetherin degradation and cell-surface downregulation. (**A**) HT1080 cells stably expressing tetherin-HA were infected with VSV-G-pseudotyped HIV-1 wt, HIV-1 delVpu or HIV-1 Vpu ELV at an MOI of 2. 48 h post infection, cells were harvested and subjected to SDS-PAGE and analyzed by Western blotting for tetherin-HA, Vpu and Hsp90, and analyzed by LiCor quantitative imager. Relative tetherin-HA levels are indicated below each lane. The blot shown is a representative example of 3 independent experiments. (**B**) 293T cells were transfected with pCR3.1 Vpu-HA, Vpu 2/6A-HA, or Vpu ELV-HA in combination with pCR3.1 myc-β-TrCP2. 48 h post transfection, cells were lysed and immunoprecipitated with anti-HA antibody. Lysates and precipitates were subjected to SDS-PAGE and analyzed by Western blotting for Vpu and myc-β-TrCP2, and analyzed by ImageQuant. The star represents an unspecific band. (**C**) Similarly, 293T cells were transfected with pCR3.1 HA-HRS in combination with Vpu-GFP or Vpu ELV-GFP expression constructs. Cell lysates were precipitated with an anti-HA antibody and analyzed as in **C**. (**D**) HeLa cells were co-transfected with pCR3.1 Vpu-HA or indicated Vpu mutant in combination with a GFP expression construct. Cell surface staining for endogenous tetherin was analyzed by flow cytometry 48 h post transfection. GFP positive cells were gated and tetherin levels (solid lines) were compared to those of untransfected HeLa cells (dotted lines). Numbers indicate median fluorescence intensities of surface tetherin on transfected cells. The solid peak in the upper middle histogram represents the binding of the isotype control. (**E**) Jurkat cells were infected with VSV-G-pseudotyped HIV-1 wt, HIV-1 delVpu, HIV-1 Vpu ELV or HIV-1 Vpu 2/6A at an MOI of 1. 48 h post infection, cells were stained for cell surface tetherin and intracellular p24CA, and analyzed by flow cytometry. Productively infected cells were identified by comparing with culture infected with the same MOI in the presence of 50 μM AZT to control for p24CA uptake of the inoculum (Figure S1C).
doi:10.1371/journal.ppat.1002609.g002

We then examined the ability of Vpu ELV mutants to downregulate surface tetherin levels. We first transfected HeLa cells (that express tetherin constitutively) with Vpu-HA expression vectors in combination with a GFP reporter. 48 h later surface tetherin was assayed by flow cytometry in the GFP positive cells (Figure 2D). As expected, wildtype Vpu expression reduced cell surface tetherin levels. Vpu mutants bearing E59A, LV63,64A mutations, or the full ELV mutant all displayed a reduced capacity to downregulate surface tetherin levels (Figure 2D and S1A). To confirm this in a relevant cell-type, we then infected CD4 positive Jurkat T cells with HIV-1 wt, HIV-1 delVpu, HIV-1 Vpu ELV or HIV-1 Vpu 2/6A. 48 h later, the cells were stained for surface tetherin and co-stained for intracellular p24CA as a marker of infection (Figure 2E). To discriminate between truly infected cells, and those that acquired p24+ debris by exposure of cells to high titre (MOI 1) of viral inoculum, we compared to cells exposed to virus in the presence of 50 μM AZT (Figure S1C). Cultures infected with HIV-1 wt showed clear downregulation of tetherin on the surface of p24CA positive cells. By contrast, tetherin was not downregulated from the surface of either HIV-1 delVpu, HIV-1 Vpu 2/6A or HIV-1 Vpu ELV infected cells. Rather, tetherin levels were raised on some infected cells, perhaps reflecting accumulation of tethered virions on the cell surface. A similar result was observed for HeLa cells infected with the same viral stocks (Figure S1B), although in this case we could detect no enhanced tetherin surface expression on cells infected with Vpu

mutants, likely due to their endocytic removal from the cell surface [31].

Vpu ELV mutants localize to early endosomal compartments and the cell surface

The $E_{59}XXXL_{63}V_{64}$ motif in Vpu resembles an acidic dileucine sorting signal (D/E)XXXL(L/I/M/V) found in the cytoplasmic tails of membrane proteins that traffic through endosomal compartments (reviewed in [32]). We therefore addressed whether mutation of this motif affected Vpu subcellular localization. To this end we infected 293T expressing tetherin or not, as well as Jurkat and HeLa cells with VSV-G-pseudotyped HIV-1 NL4.3 and NL4.3 Vpu ELV and stained them for Vpu in combination with several subcellular markers 48 h later. As expected, in all cells, the predominant localization of wildtype Vpu was in association with the TGN, with between 20–50% of the Vpu immunoreactivity visible in TGN46+ compartments (Figure 3A–D). The proportion of the Vpu ELV mutant in TGN46+ compartments was significantly reduced in 293T/tetherin, Jurkat and HeLa, and appeared as "endosome-like" puncta in the cytoplasm and associated on or near the plasma membrane (Figure 3A–C and E). Interestingly in the parental 293T cells, which lack tetherin expression, Vpu and Vpu ELV localization was indistinguishable, and predominantly associated with TGN46+ compartments (Figure 3D and E). Thus the difference in Vpu ELV localization appeared to be tetherin-dependent. The nature of these extra-TGN compartments was further analyzed in HeLa cells and revealed that Vpu ELV accumulated in EEA1+ early/sorting endosomal compartments, but not CD63+ late endosomes (Figure 3F). Thus mutation of the EXXXLV motif leads to endosomal and surface localization of Vpu consistent with it being required for modulating the trafficking of tetherin.

Vpu ELV mutants interact with tetherin in infected cells and are incorporated into nascent virions in a tetherin-dependent manner

As a putative trafficking signal, the EXXXLV motif may exert its effect on tetherin antagonism in two ways. Firstly, the sequence may be required to permit Vpu to traffic to a compartment where it can interact with tetherin; secondly, the sequence may be required for post-interaction trafficking of Vpu/tetherin complexes such that tetherin is not incorporated into budding virions and expression on the cell surface is reduced. A potential confounding factor in investigating however is that wildtype Vpu induces tetherin degradation, while Vpu ELV does not. Whilst a Vpu 2/6 control maybe applicable, controversies surrounding the nature of its phenotype in terms of tetherin counteraction also make it problematic. To alleviate these issues, we took advantage of our recent observations with novel ESCRT-I component, UBAP1 [22]. UBAP1 contains 3-tandem ubiquitin-binding domains and is found in complex with the core ESCRT-I components TSG101, VPS28 and VPS36. However unlike them, UBAP1 is only required for ESCRT-dependent endosomal degradation and not viral assembly or cytokinesis [22,33]. Interestingly, UBAP1 is essential for both Vpu and K5-mediated degradation of tetherin, but is not required for Vpu-mediated tetherin antagonism, implying that commitment of tetherin into a degradative pathway by Vpu, but not ESCRT-I function itself, counteracts tetherin activity [22]. We therefore first examined whether Vpu or Vpu ELV interacted with tetherin in immunoprecipitations in the presence or absence of siRNA-mediated silencing of UBAP1 by quantitative Western blotting (Figure 4A). 293T/tetherin cells were transfected twice over 48 h with either UBAP1 or control siRNA, before being infected with HIV-1 wt, HIV-1 Vpu ELV, HIV-1 delVpu, or HIV-1 Vpu A14L/W22A that contains a Vpu transmembrane mutation that abolishes tetherin interaction [14]. As expected, while tetherin levels were reduced in HIV-1 wt infected cells, they were unaffected by Vpu-defective or A14L/W22A mutants and, as in Figure 2, stabilized in cells infected with the Vpu ELV mutant. Furthermore, as expected, UBAP1 siRNA treatment rescued tetherin levels from Vpu-mediated degradation, but also further enhanced total cellular levels of tetherin [22] consistent with the known role of ESCRT in tetherin's natural turnover [19]. Interestingly, UBAP1 siRNA also enhanced the total cellular content of wildtype Vpu to that of the Vpu ELV mutant (approximately 4–5 fold). Immunoprecipitation of tetherin from the lysates from these cells revealed a similar picture. Wildtype Vpu was detected associated with residual tetherin precipitated from cells, and this was markedly increased upon UBAP1 knockdown. This data strongly suggests that Vpu itself may be co-degraded with tetherin in endosomal compartments. The Vpu ELV mutant efficiently co-precipitated with tetherin irrespective of UBAP1 knockdown, and as expected the A14L/W22A failed to co-precipitate under either condition. Interestingly, however, the ratio of relative band intensities between of Vpu or Vpu ELV precipitated with tetherin in the presence UBAP1 siRNA was equivalent, indicating that Vpu ELV was not defective for physical tetherin interaction, suggesting that the Vpu ELV mutant's defect in tetherin antagonism is due to an inability to mediate post-binding trafficking of Vpu/tetherin complexes into an ESCRT-dependent pathway in which both proteins are degraded. Consistent with this notion, Vpu ELV co-localized with tetherin in infected HeLa and 293T/tetherin, both in peripheral endosomal structures and at the cell surface (Figure 4B). By contrast, the little tetherin visible in cells infected with wildtype virus co-localized with Vpu in perinuclear areas.

Vpu is not a constituent of HIV-1 particles. We therefore reasoned that if the EXXXLV motif was required to prevent tetherin trafficking to viral budding sites and commit it for degradation, interaction with tetherin itself might lead to Vpu ELV mutant accumulation in nascent viral particles. To test this hypothesis we took advantage of a tetherin mutant lacking its GPI anchor (tetherin-delGPI), which despite its high surface expression, does not restrict virus particle release, but accumulates in virus particles and is sensitive to Vpu [7]. 293T/tetherin-delGPI cells were mock-transfected or transfected with NL4.3 wt, NL4.3 Vpu ELV, and NL4.3 delVpu. 48 h later cell supernatants were centrifuged through a sucrose cushion and analyzed for tetherin incorporation (Figure 4C and D). As expected, high levels of tetherin-delGPI could be detected in NL4.3 delVpu viral pellets, but not in pelleted supernatants from mock-transfected cells. Tetherin-delGPI incorporation was reduced in the wildtype virus consistent with tetherin removal from the cell surface. The level of tetherin incorporation in NL4.3 Vpu ELV particles was similar to that of the Vpu-defective mutant. Interestingly, NL4.3 Vpu ELV particles contained detectable levels of Vpu (in this case Vpu appears as a doublet band which we suggest may be due to exposure to active HIV-1 protease in the particle). By contrast, no Vpu was detectable in any viral particles derived from 293T cells, indicating that Vpu ELV incorporation into viral particles was tetherin-dependent. Taken together these data indicate that the EXXXLV motif is required for efficient tetherin antagonism, by modulating the trafficking of tetherin such that it cannot become efficiently incorporated into nascent viral particles.

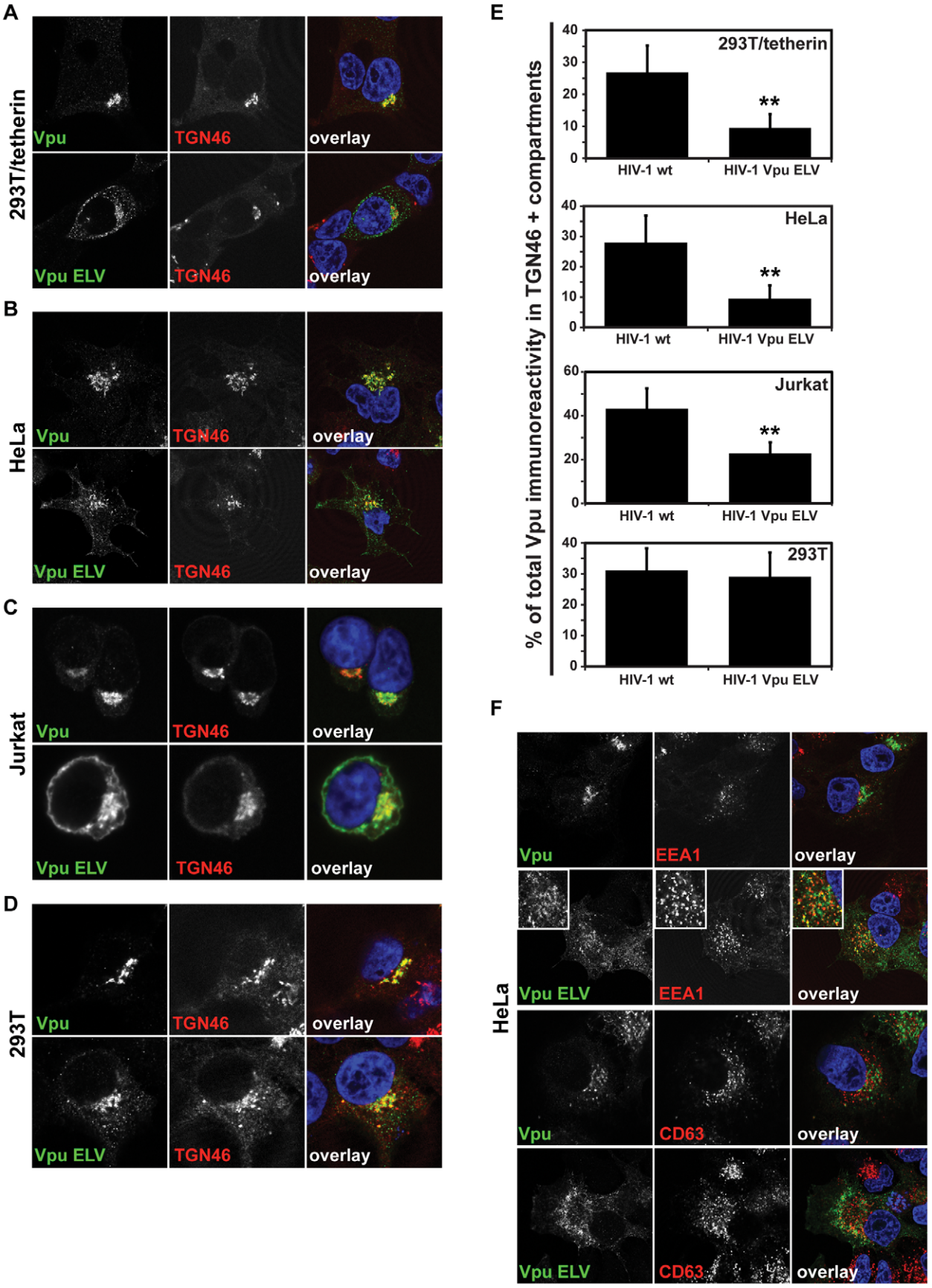
A
293T/tetherin
Vpu
TGN46
overlay
Vpu ELV
TGN46
overlay
B
HeLa
Vpu
TGN46
overlay
Vpu ELV
TGN46
overlay
C
Jurkat
Vpu
TGN46
overlay
Vpu ELV
TGN46
overlay
D
293T
Vpu
TGN46
overlay
Vpu ELV
TGN46
overlay
E
% of total Vpu immunoreactivity in TGN46 + compartments
293T/tetherin
HeLa
Jurkat
293T
HIV-1 wt
HIV-1 Vpu ELV
**
F
HeLa
Vpu
EEA1
overlay
Vpu ELV
EEA1
overlay
Vpu
CD63
overlay
Vpu ELV
CD63
overlay

Figure 3. Vpu ELV mutants localize to early endosomal compartments in tetherin-expressing cells. 293T/tetherin (**A**), HeLa (**B**), Jurkat (**C**) or parental 293T (**D**) were infected with HIV-1 wt or HIV-1 Vpu ELV at an MOI of 1. 48 h later the cells were fixed and stained for Vpu (green) and the TGN marker TGN46 (red) and examined by confocal microscopy. Panels are of representative examples. (**E**) The percentage of the total Vpu immunoreactivity localized to TGN46+ compartments was calculated for cells (n = 20) from **A–D** using the Leica Confocal Software. Results were analyzed by unpaired 2-tailed t-test - ** $P = 10^{-8}$ or lower. (**F**) HeLa cells as in **B** were stained for Vpu (green) and the early endosomal marker EEA1 or late endosomal marker CD63 (red).
doi:10.1371/journal.ppat.1002609.g003

The second alpha helix of Vpu can be complemented by a D/EXXXLL-containing peptide derived from HIV-1 Nef

Acidic-dileucine based sorting signals, D/EXXXL(L/I), act as binding sites for a hemicomplex of sigma and adaptin subunits of the canonical clathrin adaptors AP-1, AP-2 and AP-3, and are required for endocytic and endosomal/Golgi trafficking of these proteins [32]. While the requirement for the acidic and first leucine residues are absolute, the third position is less well conserved, and can be L, I or on occasion V or M. Analysis of the cytoplasmic tails of Vpu sequences from most clades of HIV-1 group M, show that a putative EXXXL(V/M/I) is well conserved in the second alpha helix (Figure S2A). In contrast to other HIV-1 subgroups, Clade C and F isolates have an EXXXLL motif juxtaposed to the plasma membrane in helix 1 (not shown), which has been previously suggested to be a determinant of Clade C Vpu localization to the PM [34]. In subgroup B, the V64 position is usually V or M, although occasional I or L residues are found at this position. We mutated position 64 to M, L or I in NL4.3 Vpu and found no defect in these proteins' ability to counteract or downregulate tetherin from the surface (Figure S2B and S2C), in agreement with the above data demonstrating that this position is the least important of the three, and consistent with the role of this motif as a sorting signal.

The Nef proteins of primate immunodeficiency viruses are also multifunctional adaptor proteins, targeting a variety of immunoregulatory cell surface molecules for downregulation and degradation [35]. Nef interacts promiscuously with AP-1, AP-2 and AP-3 through a conserved C-terminal EXXXLL motif [36,37]. The interaction of AP-2 with this site is essential for Nef targeting of CD4 for ESCRT-dependent lysozomal degradation [37], but Nef-mediated downmodulation of Class I MHC molecules requires AP-1 [38]. Importantly several SIV Nef proteins are also tetherin antagonists [39,40] and again this is dependent on the EXXXLL motif [26]. We therefore asked whether the C-terminus of HIV-1 Vpu could be functionally substituted with a known AP-binding site from these proteins. The EVSALV motif of NL4.3 Vpu was first replaced with the core AP-binding site from NL4.3 Nef, ENTSLL (Figure 5A). Since this is similar to sites already tested in the previous experiment shown in Figure S2, this Vpu was as functional as the wildtype protein in virus rescue experiments (Figure 5B and C). We then replaced the entire cytoplasmic tail of Vpu from residue 58 with a 19 amino acid stretch derived from Nef including the ENTSLL and a downstream dual-aspartic acid motif that has been previously shown to stabilize AP-2 interactions [41]. Remarkably, the Vpu/Nef chimeric protein substantially recovered tetherin antagonistic activity (Figure 5B and C). Moreover, this chimera also displayed improved tetherin downregulation from the surface of transfected HeLa cells (Figure 5D). This activity was entirely dependent on the key amino acids required for AP-interaction as a chimera in which E, LL and DD positions were mutated to alanine was unable to counteract tetherin or downregulate it from the surface (Figure 5B–D). Examination of the subcellular distribution of Vpu-Nef or the mutant fused to CherryFP suggested that the mutant was localized more prominently to the PM consistent with a defect in trafficking imparted by the mutation (Figure 5E). Thus Vpu function can be substantially recovered by replacing its entire second alpha helix with a promiscuous AP-binding (D/E)XXXL(L/I) sorting signal, indicating that linking Vpu directly to the clathrin trafficking machinery can restore its activity in absence of the second alpha helix.

Tetherin antagonism by Vpu is clathrin-dependent, but independent of canonical adaptor proteins that bind acidic di-leucine motifs

The implication of putative clathrin adaptor sites in Vpu-mediated tetherin antagonism led us to test whether inhibition of clathrin function inhibits Vpu activity. Overexpression of the C-terminal fragment of the neuronal adaptor AP180 (AP180c) that inhibits clathrin/membrane interactions [42], which was recently shown to inhibit tetherin downregulation from the surface [43], specifically blocked Vpu-dependent particle release of HIV-1 wt from 293T cells expressing tetherin (Figure 6A), indicating clathrin-dependent subcellular trafficking is essential for Vpu activity. Infectious yield could not be determined in this experiment because AP180c overexpression inhibits envelope processing and blocks clathrin incorporation into particles, which has been shown to play a role in retroviral particle infectivity [44,45]. Interestingly AP180c expression, like UBAP1 siRNA treatment, enhanced total Vpu expression levels, indicating clathrin-dependent transport is involved in the turnover of Vpu. Visualization of Vpu-YFP localization in 293T/tetherin cells overexpressing AP180c showed vesicular rather than peri-nuclear localization similar to that seen in the same cells infected with HIV-1 Vpu ELV (Figure 6B), and this was not apparent in the parental (tetherin negative) 293T cells, suggesting again this difference was driven by interaction with tetherin.

The similarities between the EXXXLV motif and acidic dileucine sorting signals, and its functional replacement with the promiscuous ENTSLL motif in HIV-1 Nef led us to test whether the major known adaptors involved in trafficking of membrane proteins between the PM, endosomes and Golgi compartments were required for Vpu-mediated tetherin antagonism. Clathrin-mediated endocytosis requires AP-2, whereas AP-3 controls early-to-late endosomal/lysosomal trafficking. AP-1 plays a role in trafficking of cargo between early endosomes and the TGN, with evidence that it can function in either direction [32]. To this end we examined the effects of siRNA-mediated silencing of AP-1 (AP-1γ1), AP-2 (AP-2μ1), AP-3 (AP-3μ1/AP-3δ1). Depletion of AP-2 by RNAi in 293T/tetherin cells had only minor effects on Vpu-dependent virus particle release, suggesting that unlike SIV Nef and HIV-2 Env, and consistent with the reports that Vpu does not enhance tetherin endocytosis, AP-2 activity is dispensable for Vpu-mediated tetherin antagonism (Figure 6C). Similarly AP-3μ1/AP-3δ1 depletion had no detectable effect on tetherin activity or Vpu-mediated counteraction (Figure 6D). Furthermore, human tetherin could also be downregulated from the surface of mouse fibroblasts defective in AP-3δ1 when transduced to express Vpu [46] (Figure S3A). For AP-1, siRNA-mediated silencing was inefficient in 293T (not shown). We therefore constructed a HeLa cell line containing a doxycycline-inducible shRNA hairpin against AP-1γ1. Induction of this hairpin coupled with simultaneous depletion of AP-1γ1 by

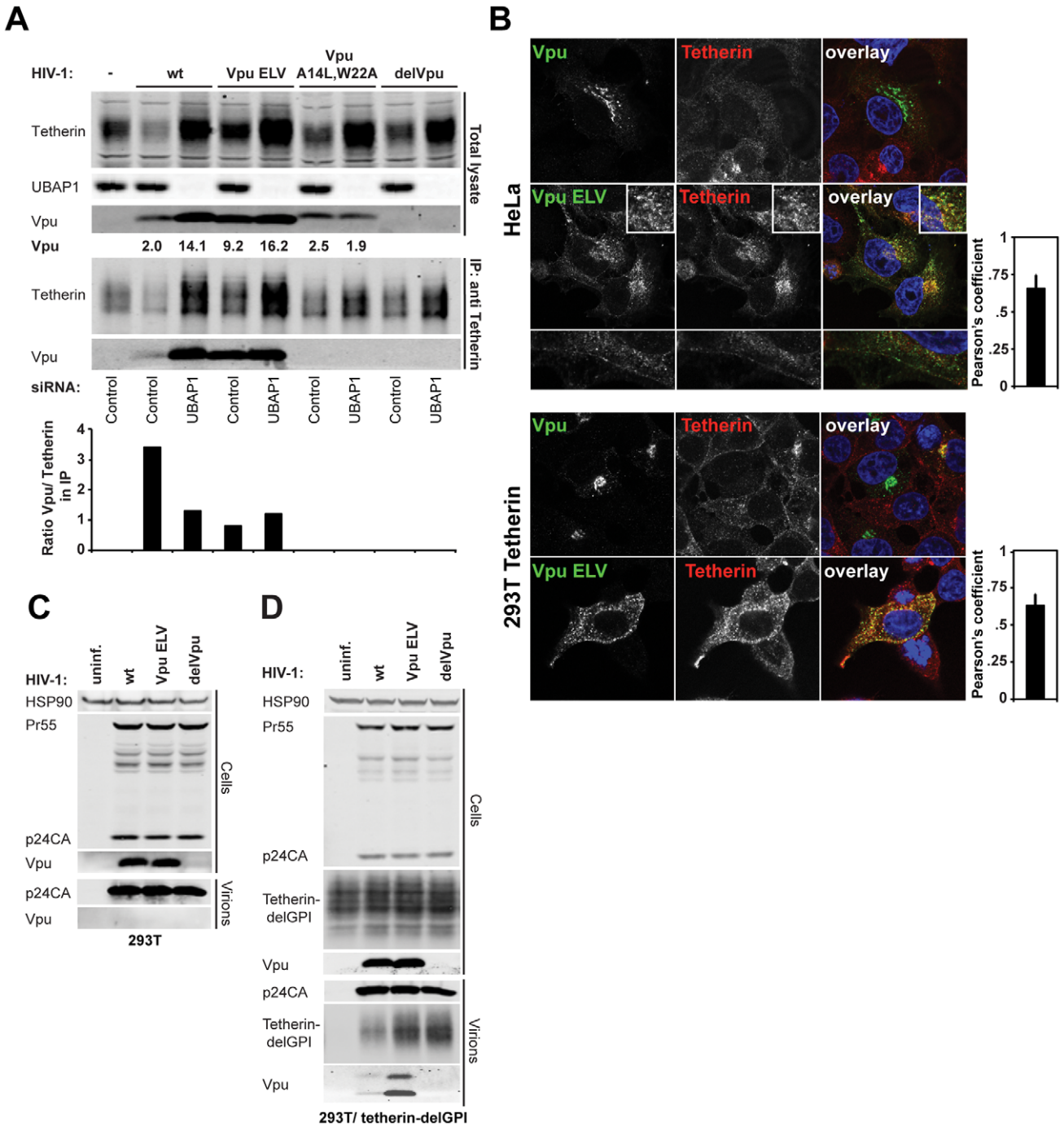

Figure 4. Vpu ELV interacts and colocalizes with tetherin, and is incorporated into nascent virions. (**A**) 293T/tetherin cells were transfected twice over 48 h with siRNA oligonucleotide directed against UBAP1 or Non-targeting control. The cells were then infected with the indicated virus at an MOI of 2. 48 h later cell lysates were immunoprecipitated with an anti-tetherin monoclonal antibody. Lysates and immunoprecipitates were separated by SDS-PAGE and blotted for tetherin, UBAP1 or Vpu using LiCor quantitative Western blotting. Numbers under the Vpu lanes of the cell lysate represent relative band intensities. The histogram below the IP represents the ratio of tetherin band intensity to that of Vpu in the co-IP. (**B**) HeLa and 293T/tetherin cells were infected as in Figure 3 and stained for Vpu (green) and tetherin (red) and examined by confocal microscopy. Adjacent histograms quantify the degree of co-localization of Vpu ELV and tetherin (Pearson's Correlation Coefficient calculated using ImageJ) for 20 individual cells. (**C**) and (**D**) 293T or 293T cells stably expressing tetherin delGPI were infected with HIV-1 wt, HIV-1 Vpu ELV or HIV-1 delVpu at an MOI of 1. 48 h post infection, cells were harvested and viral supernatants were pelleted through a 20% sucrose cushion. Cells and virions were subjected to SDS-PAGE and Western blotting for tetherin delGPI, Vpu, HIV-1 p24CA and Hsp90 and analyzed by LiCor quantitative imager.

doi:10.1371/journal.ppat.1002609.g004

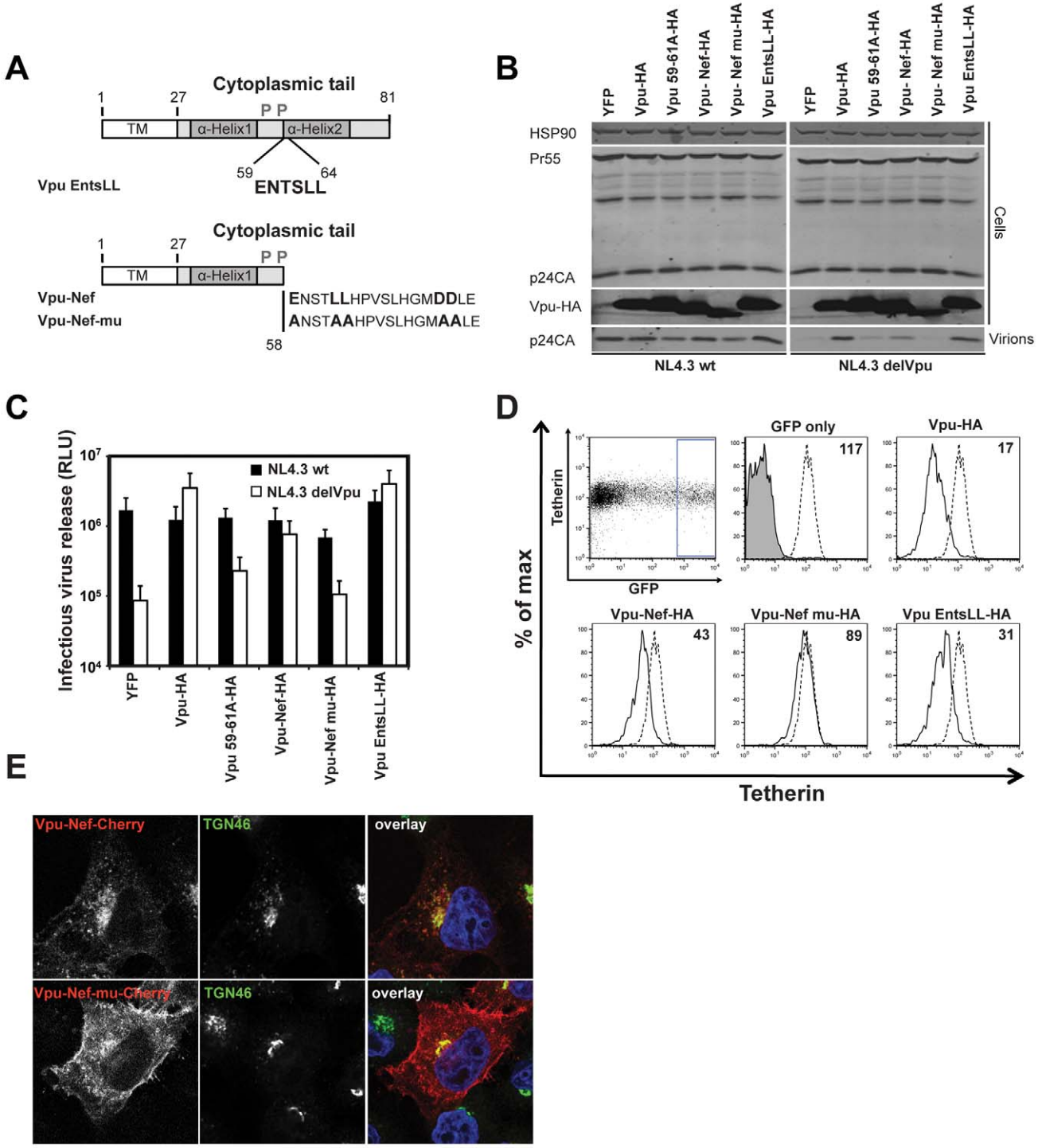

Figure 5. The second alpha helix of Vpu can be functionally replaced by the D/EXXXLL endocytic signal from HIV-1 Nef. (**A**) Schematic representation of Vpu ENTSLL and Vpu-Nef chimeric constructs. (**B**) 293T cells were transfected with NL4.3 wt of NL4.3 delVpu proviral plasmids in combination with tetherin and indicated pCR3.1 Vpu-HA or Vpu-Nef-HA chimera. 48 h post transfection, cell lysates and pelleted supernatant virions were harvested and subjected to SDS-PAGE and analyzed by Western blotting for HIV-1 p24CA, Vpu-HA and Hsp90, and analyzed by LiCor quantitative imager. (**C**) Infectivity of viral supernatants from **B** was determined on HeLa-TZMbl cells as in Figure 1B. Error bars represent standard deviation of three independent experiments. (**D**) HeLa cells were co-transfected with Vpu or indicated Vpu mutant and a GFP expression construct. Cell surface staining for endogenous tetherin was analyzed by flow cytometry 48 h post transfection, as in Figure 2D. (**E**) HeLa cells were transfected with Vpu-Nef or Vpu-Nef-mu CherryFP fusions (red) and counterstained for TGN46 (green) and DAPI (blue) and examined by confocal microscopy.

doi:10.1371/journal.ppat.1002609.g005

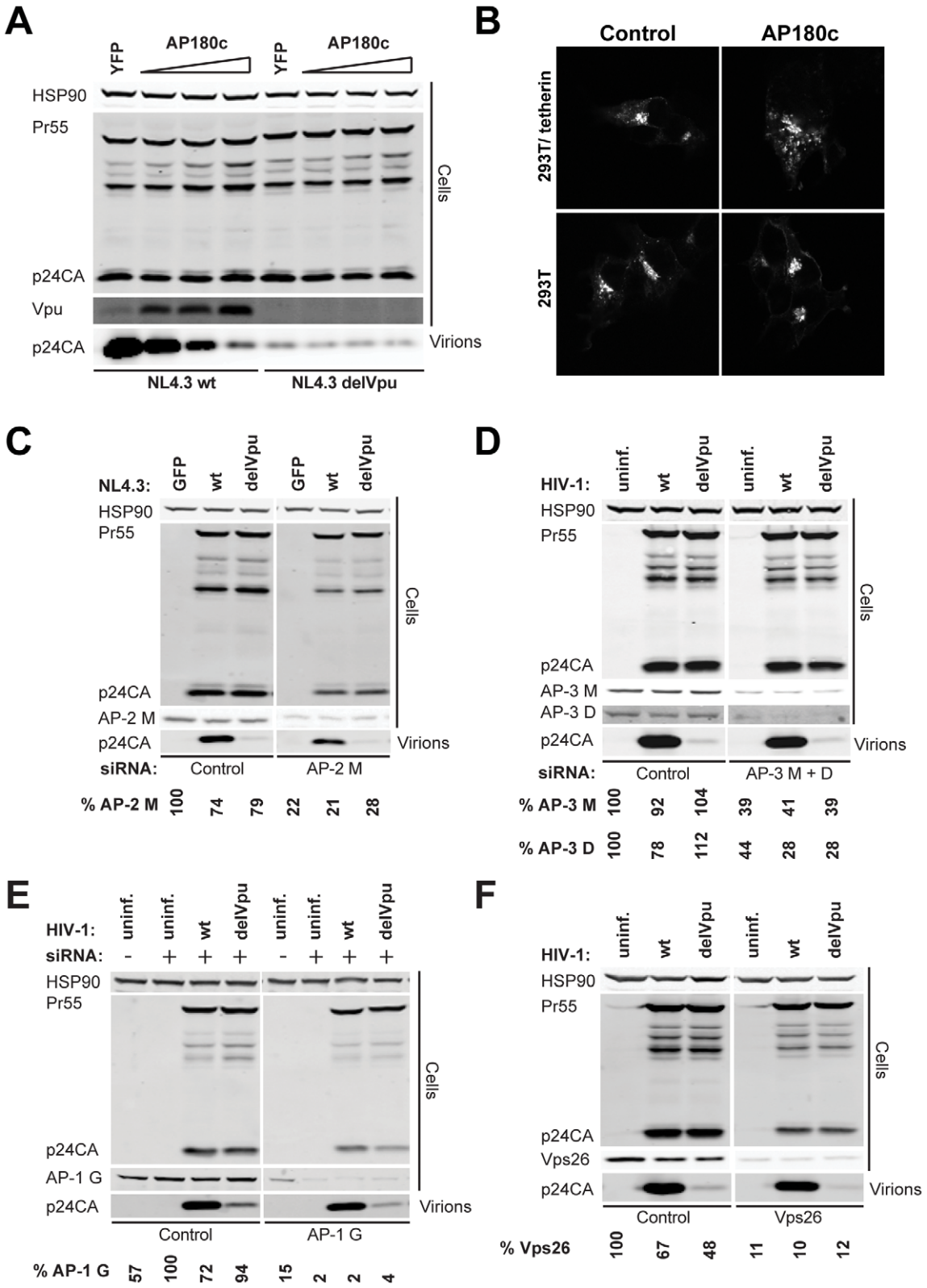

Figure 6. AP180c inhibits Vpu-mediated tetherin antagonism but AP-1, AP-2, AP-3 and retromer are dispensable. (**A**) 293T/tetherin were transfected with NL4.3 wt or NL4.3 delVpu proviral plasmids in combination with either YFP or increasing doses of an AP180c expression vector. 48 h post transfection, cell lysates and pelleted supernatant virions were harvested and subjected to SDS-PAGE and analyzed by Western blotting for HIV-1 p24CA, Vpu and Hsp90 serving as loading control, and analyzed by LiCor quantitative imager. (**B**) 293T or 293T/tetherin transfected with pCR3.1 Vpu-YFP with or without AP180c co-expression were fixed and imaged after 48 h (**C**) 293T cells stably expressing tetherin were transfected twice with pooled control or AP-2μ1 siRNAs and co-transfected with NL4.3 wt, NL4.3 delVpu or GFP expression vectors. Cell lysates and supernatants were analyzed by Western blotting 48 h later as described in Figure 1B. (**D**) 293T cells stably expressing tetherin were transfected twice with pooled control

or siRNA pools against AP-3δ1 and AP-3μ1. 4 h post the second transfection the cells were infected with VSV-G-pseudotyped HIV-1 wt or HIV-1 delVpu virus stock at an MOI of 1. Cell lysates and supernatants were analyzed by Western blotting 48 h later as described in Figure 1B. (**E**) HeLa cells expressing a doxycycline-inducible shRNA hairpin against AP-1γ1were transfected twice with pooled control or siRNA pools against AP-1γ1. The cells were infected and analyzed as in **C**. (**F**) 293T cells stably expressing tetherin were transfected twice with pooled control or siRNA pools against the retromer subunit Vps26. Cells were infected and analyzed as in **C**. In all siRNA knockdown experiments, the % knockdown of the indicated protein as determined by the relative band intensity in the western is indicated below the blot panel.
doi:10.1371/journal.ppat.1002609.g006

oligonucleotide transfection led to approximately 95% knockdown efficiency. This treatment had no specific effect on Vpu-dependent virus particle yield in HeLa cells indicating that tetherin-antagonism again was not compromised (Figure 6E), and furthermore tetherin surface downregulation was not defective in mouse AP-1γ1a −/− fibroblasts (Figure S3B) [47].

Finally, we examined whether there was any role for the retromer complex, in Vpu-mediated tetherin antagonism. Retromer regulates retrieval and recycling of endosomal proteins to the TGN and is known to act co-operatively or antagonistically with AP-1 (reviewed in [48]). The retromer complex consists of several sorting nexins (SNX), and a core complex containing cargo binding component, Vps34, and two essential co-factors, Vps26 and Vps29. We performed siRNA-mediated knockdown of Vps26 (Figure 6F). At levels of knockdown that were sufficient to relocalize the CD8-cation-independent mannose-6-phosphate receptor (CD8-CI-M6PR) (Figure S3C), disruption of retromer had no detectable effect of Vpu-mediated HIV-1 release from 293T/tetherin cells.

Taken together these data demonstrate that neither depletion of individual cellular adaptor proteins known to bind to (D/E)XXXL(L/I) motifs, nor disruption of retromer-mediated endosome-to-TGN retrieval, were sufficient to recapitulate the phenotype of the Vpu ELV mutant.

Residual function of Vpu ELV requires an intact recycling signal in tetherin

Recent data suggests that Vpu blocks both the transit of *de novo* synthesized tetherin to the cell surface as well as the recycling of tetherin endocytosed from the plasma membrane, with the relative importance of these processes currently a matter of debate. Tetherin recycling requires a dual tyrosine YXYXXV motif in its cytoplasmic tail that acts as a binding site for AP-2 (for internalization) and AP-1 (for recycling via the Golgi) [8,9]. Mutation of this site enhances tetherin's surface expression, but has minor effects on its ability to restrict virus release or its sensitivity to Vpu [11,13]. Given that the EXXXLV motif was defective for post-binding inactivation of tetherin, but retained a low residual activity against tetherin in transient transfection assays, we asked whether Vpu ELV was differentially defective against tetherin mutants bearing lesions in its own sorting sequence. We infected 293T/tetherin and 293T/tetherin Y6,8A cells with HIV-1 wt, HIV-1 delVpu and HIV-1 Vpu ELV at fixed dose (MOI 1) and measured viral release 48 h later (Figure 7A and B). Vpu-defective viral release was approximately 35-fold reduced from 293T/tetherin cells compared to the wildtype virus, and as expected NL4.3 Vpu ELV had an intermediate phenotype in this assay (6 fold less release than wt). However, in 293T/tetherin Y6,8A all residual antagonistic activity of Vpu ELV was abolished with viral release equivalent to that of the Vpu-deleted virus. By contrast the wildtype virus retained the majority of its anti-tetherin activity. This again was not due to a defect of Vpu interaction with tetherin, as immunoprecipitation of tetherin after UBAP1 siRNA treatment demonstrated equivalent levels of Vpu and Vpu ELV co-precipitation from both tetherin and tetherin Y6,8A expressing cells (Figure 7C). Thus residual activity of Vpu ELV requires that tetherin retains its capacity to recycle from the PM. These data suggest that Vpu ELV is specifically defective in blocking tetherin transit to the PM, implying that Vpu/tetherin complexes are re-routed in a Golgi-associated compartment into a pathway that ultimately results in tetherin's endosomal destruction. In the absence of the EXXXLV sequence, tetherin/Vpu ELV complexes traffic to the PM. The residual activity of Vpu ELV therefore may be reflective of steric inhibition of tetherin function.

The dominant-negative mutant of dynamin 2 (K44A) has also been described to have an intermediate effect on tetherin counteraction by Vpu, compared to the complete disruption of HIV-2 Env function which, like SIV Nef, is dependent on AP-2 and endocytosis [43]. We transfected increasing doses of HA-tagged dominant negative dynamin 2 or the wildtype protein along with HIV-1 proviruses into 293T/tetherin and parental cells (Figure S4A). In agreement with Lau et al [43] dominant negative dynamin 2, but not equivalent levels of the wild type dynamin 2 partially blocked the release of wildtype HIV-1 (Figure S4A–D). Furthermore dominant negative dynamin 2 expression levels in these assays were sufficient to block transferrin uptake in parallel cultures (Figure S4B). Interestingly dominant negative dynamin 2 also blocked residual Vpu ELV-mediated, and even the low level Vpu-defective viral release proportionally (7X, 4X and 8X for WT, Vpu-defective or Vpu ELV respectively), suggesting that this effect was independent of the ELV motif. Given that dominant negative dynamin 2 inhibits tetherin endocytosis [43], this data suggests that its effect on restriction may be due more to the build up of tetherin at the cell surface that cannot be turned over rather than a direct effect on Vpu function itself.

Vpu ELV is defective for tetherin antagonism in CD4+ T cells after treatment with type-1 interferon

The results presented hitherto have demonstrated a requirement for the Vpu ELV motif in counteracting tetherin in cells stably expressing it or mutants thereof, and that its is required in constitutively-expressing target cells such as Jurkat to reduce surface tetherin levels. However some studies have cast doubt as to whether tetherin degradation and/or surface reduction is essential for Vpu function. Furthermore, in contrast to 293T/tetherin, release of HIV-1 Vpu ELV from HeLa was only 3-fold less efficient than wildtype in one round release (Figure S5). We therefore explored whether there was a requirement for the ELV motif in HIV-1 release from physiologically relevant target cells, namely Jurkat or primary human CD4+ T cells, particularly after treatment with type-1 interferon. Infection of Jurkat at an MOI of 1 resulted in a partial defect in release of the HIV-1 Vpu ELV mutant compared to the controls (Figure 8A and B). However induction of higher tetherin expression by overnight treatment with universal type-1 interferon effectively reduced HIV-1 Vpu ELV particle release to levels similar to that of the Vpu-defective control while only reducing the wildtype release moderately. Similarly interferon treatment of purified activated human CD4+ T cells led to a selective defect in the production of cell-free HIV-1 Vpu ELV virions (Figure 8C) consistent with a concomitant upregulation of surface tetherin levels (Figure 8D), and surface tetherin downregulation (Figure 8E). Taken together with results

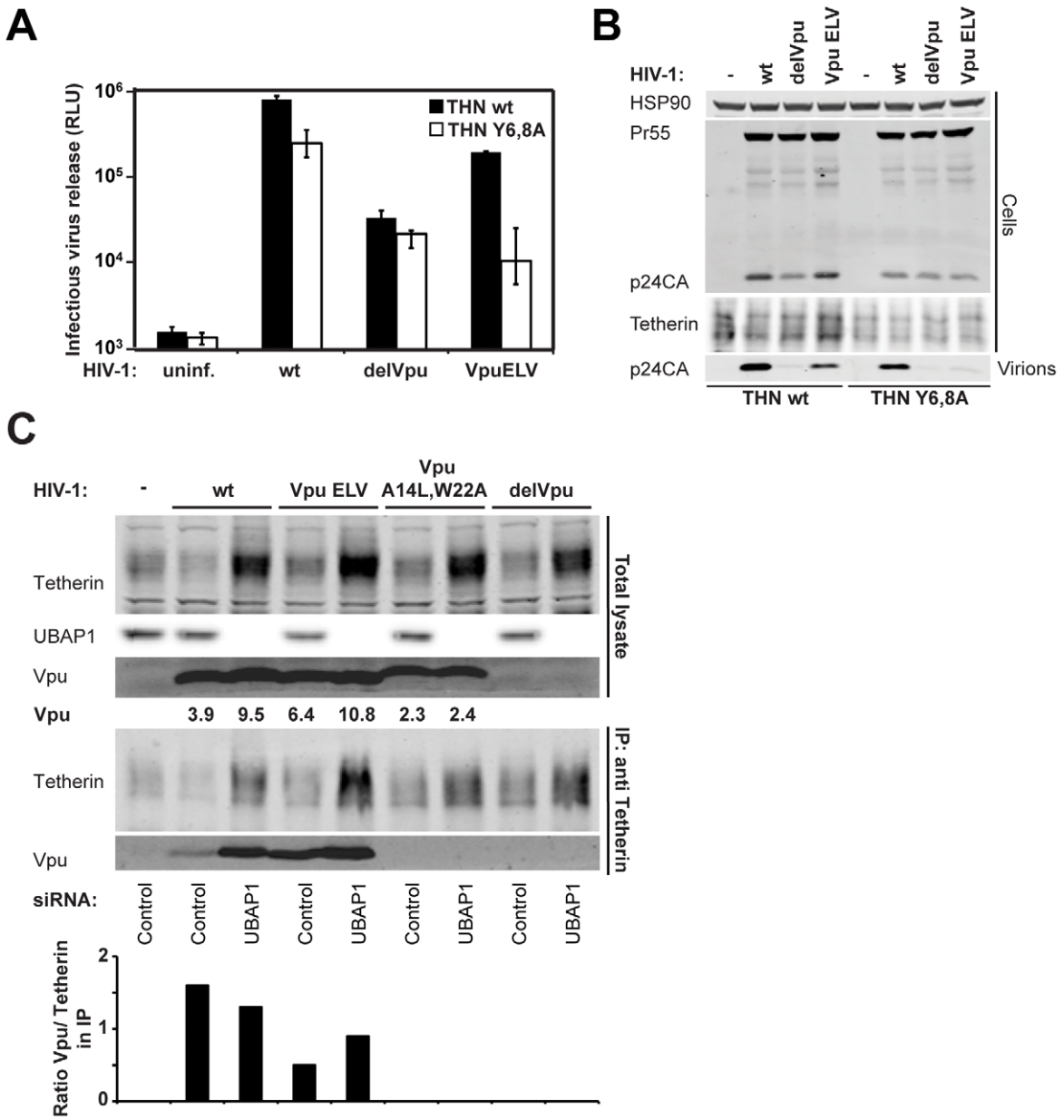

Figure 7. Residual activity of Vpu ELV requires an intact recycling signal in tetherin. (**A**) 293T/tetherin or 293T/tetherin Y6,8A mutant were infected with VSV-G-pseudotyped HIV-1 wt, HIV-1 delVpu or HIV Vpu ELV at an MOI of 0.5. Supernatants and cell lysates were harvested 48 h later and analyzed for infectious virus release on HeLa-TZMbl as in Figure 1C. (**B**) Corresponding Western blots of cell lysates and virions from **A**. (**C**) 293T/tetherin Y6,8A cells treated with control or UBAP1 specific siRNAs were infected with VSV-G-pseudotyped HIV-1 wt, HIV Vpu ELV, HIV-1 Vpu A14L/W22A or HIV-1 delVpu at an MOI of 2. 48 h post infection, cells were lysed and immunoprecipitated with an anti-tetherin antibody. Lysates and immunoprecipitates were subjected to SDS-PAGE and analyzed by Western Blotting for tetherin, UBAP1 and Vpu, and analyzed by LiCor quantitative imager. Ratios of Vpu/tetherin band intensities in the coIP are plotted on the histogram below.
doi:10.1371/journal.ppat.1002609.g007

presented above, these data demonstrate that the ability to downregulate and degrade tetherin imparted by the EXXXLV motif is required for cell-free virion release from relevant primary HIV target cells, and becomes essential when tetherin expression is enhanced by an antiviral stimulus.

Discussion

In this study we have identified a determinant within the second alpha helix of the cytoplasmic tail of HIV-1 NL4.3 Vpu, $E_{59}XXXL_{63}V_{64}$, which is required for efficient antagonism of tetherin. Mutation of this site blocks the ability of Vpu to mediate tetherin downregulation from the cell surface and its ESCRT-dependent degradation, but does not abolish its interaction with tetherin, nor recruitment of β-TrCP2 or the ESCRT-0 component HRS. Importantly, this motif is required to counteract tetherin in CD4+ T cells, particularly after their exposure to type-I interferon. Vpu ELV mutants localize to the cell surface and early/recycling endosomal compartments rather than the TGN by virtue of their interaction with tetherin. This is consistent with a role for this determinant in Vpu-mediated inhibition of the transit of newly synthesized and/or recycling tetherin to the cell surface, its

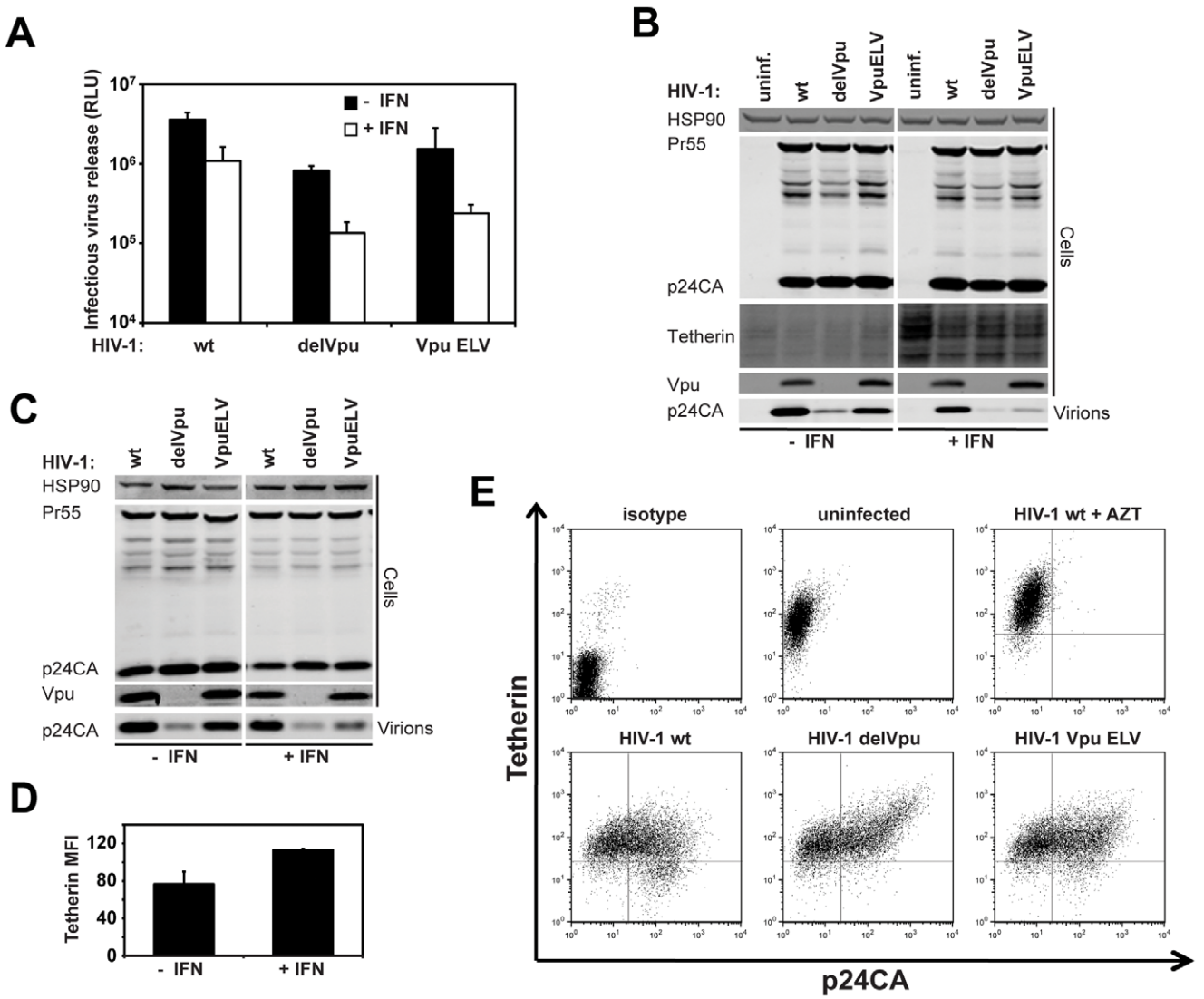

Figure 8. The EXXXLV motif is essential to counteract tetherin-mediated restriction of cell-free HIV-1 particle release from CD4+ T cells treated with type-1 interferon. Jurkat cells were infected with the indicated HIV-1 mutant at an MOI of 1. 16 h later the cells were treated or not with 5000 U/ml universal type-I interferon. Cell lysates and viral supernatants were harvested a further 24 h later and analyzed for infectivity on HeLa-TZM (**A**) or physical particle yield and cellular viral and tetherin expression by quantitative Western blotting (**B**). (**C**) A representative example of primary human CD4+ T cells treated as in (**B**) and the MFI of surface tetherin levels on these cells with or without 24 h type-I interferon treatment as analyzed by flow cytometry (**D**). (**E**) Human CD4+ T cells were infected with the indicated virus. 48 h later cells were stained for surface tetherin and intracellular p24CA and analyzed by flow cytometry.
doi:10.1371/journal.ppat.1002609.g008

internal sequestration and targeting for endo-lysosomal degradation. However, while we could functionally complement Vpu function by grafting the D/EXXX(L/I/M) motif from HIV-1 Nef in place of helix-2, we could detect no effect of depletion of the canonical clathrin adaptor proteins AP-1, AP-2 or AP-3 on Vpu-mediated tetherin antagonism. The inhibition by AP180c overexpression, however, implicates clathrin function in Vpu-mediated tetherin antagonism. Finally, residual Vpu ELV activity against tetherin was entirely dependent on an intact recycling motif in tetherin's cytoplasmic tail, suggesting that this motif differentially affects antagonism of newly synthesized tetherin rather than pre-existing pools recycling to the PM. These results are in contrast to the recent study by Lau et al who were unable to demonstrate a phenotype for an LV63,64AA mutant despite interfering with Vpu activity with AP180c [43]. Given that we have demonstrated phenotypes in several cellular systems including CD4+ T cells for the Vpu ELV mutant, the reason for this discrepancy is unclear.

There has been much debate as to whether the reduction of tetherin levels at the plasma membrane is required to counteract its antiviral activity, particularly in CD4+ T cells (reviewed in [10]). In our hands, tetherin surface levels are reduced in HIV-1 infected primary T cells and Jurkat cells. However, under these conditions, the viral release phenotype of the Vpu ELV mutant is only a few-fold different than the wildtype protein. Interestingly this changes upon treatment of the cells with type-I interferon, which upregulates tetherin expression levels. In this case Vpu ELV mutant release is reduced almost to that of the Vpu-defective virus, but only minor further reductions are observed for the wildtype virus. This therefore indicates that the requirement for surface

reduction/degradation of tetherin becomes much more important at higher expression levels of the restriction factor (something that has been suggested previously by Goffinet et al [49]). Recent conflicting data have addressed the effect of tetherin and interferon on cell-cell transmission between T cells [50,51], which when taken together show that if tetherin does restrict this mode of virion transfer, it is far less efficient than its effect on cell-free viral release. Thus, the fact that tetherin antagonism is such a highly conserved attribute amongst primate immunodeficiency viruses implies its importance in vivo. Since interferon treatment of CD4+ T cells magnifies the defective phenotype of a Vpu ELV mutant, the ability to mediate tetherin's surface reduction and target it for endosomal degradation is likely to be essential for the virus to avoid restriction under proinflammatory conditions it is likely to encounter in vivo, particularly during acute infection [52,53].

Our results are consistent with the notion that Vpu blocks delivery of tetherin to the plasma membrane [13,54] and suggest that Vpu exerts its effect on tetherin trafficking in the TGN/recycling compartment in a manner determined in part by this putative sorting sequence. It is now clear that Vpu-mediated tetherin degradation is ubiquitin-dependent and occurs in lysosomes rather than early reports of proteasomal processing [15,16], and that this process requires the ESCRT pathway [19]. Depletion of both TSG101 and Vps4 inhibits Vpu-mediated tetherin degradation, and recruitment of HRS (ESCRT-0) has been reported to be required for Vpu-mediated tetherin antagonism [19], as has ubiquitination on multiple residues in the tetherin cytoplasmic tail [18]. However tetherin's ultimate degradation itself is not essential for Vpu or other lentiviral countermeasures to inactivate it. Our recent observations with the novel ESCRT-I subunit, UBAP1, ([22] and the results presented herein), demonstrate that ESCRT-I function is unlikely to be required for tetherin antagonism, but its commitment to endosomal degradation is. Interestingly, the concomitant enhancement of wildtype Vpu levels, both co-precipitating with tetherin and at steady state, suggest that Vpu is likely co-degraded with its target.

Alongside the current literature our data suggests that Vpu interaction with tetherin leads to a differential trafficking of tetherin in the TGN and/or recycling compartments rather than enhancing tetherin internalization (Figure 9). This inhibits forward trafficking of either recycling or newly synthesized tetherin to the PM, and commits it to a pathway that ultimately targets it to endolysosomal compartments for degradation. We suggest that it is this commitment, regulated by the EXXXLV motif in second helix, rather than degradation *per se*, that is principally responsible for antagonizing tetherin. Where Vpu interacts with tetherin in the cell is likely to be related temporally to the viral replication cycle, tetherin expression level, and its natural turnover rate. Vpu is expressed "late" in replication from the same mRNA as Env [55], at the time new virions are being built. Thus Vpu must deal with two pools of tetherin; pre-existing protein in the periphery recycling via the TGN [9], and *de novo* synthesized tetherin trafficking through the Golgi *en route* from the endoplasmic reticulum (ER) to the surface. Therefore we predict that Vpu must interact with tetherin in TGN-associated compartments to engage these two pools of tetherin, although our recent data suggests that binding to newly synthesized tetherin may occur prior to this in the ER [14]. Thereafter, a clathrin-dependent sorting event determined by the helix-2 EXXXLV motif precludes Vpu/tetherin complexes transiting to the PM. This intracellular sequestration of tetherin is further coupled to late endosomal targeting and ESCRT-dependent degradation through the recruitment of HRS and tetherin ubiquitination [18,19]. In line with this, global disruption of early to late endosomal transition by dominant negative Rab7a also appears to inhibit Vpu activity [23]. Interestingly, ubiquitinated cargo destined for ESCRT-dependent degradation via HRS recruitment has been shown to partition differentially to areas of early/sorting endosomal membranes rich in flat clathrin lattices, thereby anchoring it away from the recycling machinery [56]. Recruitment of tetherin into such structures in the sorting compartment may be sufficient to antagonize its function, offering an explanation as to why clathrin is essential for Vpu activity but dynamin 2 mutants only effect the residual activity of Vpu ELV. Because Vpu activity was insensitive to retromer (Vps26) depletion, which is essential for endosome-to-TGN retrieval and recycling [48], we suggest that Vpu targets tetherin into this pathway from the TGN to endosomal compartments, and an ensuing swift degradation accounts for the observed sequestration in TGN46 positive compartments. In the absence of the EXXXLV motif, tetherin is not committed to this differential sorting in the TGN, and Vpu/tetherin complexes are targeted to the cell surface and thereafter back into the recycling system, accounting for the localization of Vpu ELV in infected cells and its incorporation into virions. Therefore in addition to acting as an adaptor for the recruitment of ESCRT-0 and E3 ubiquitin ligase activity to tetherin, we propose that through the EXXXLV motif, Vpu directly chaperones associated tetherin molecules into an endosomal compartment from which they cannot recycle to the PM.

EXXXLV mutants retain some residual antagonistic activity that is entirely dependent on the AP-1/AP-2-binding motif in tetherin. This would suggest that the action of the EXXXLV motif does not solely account for the inhibition of tetherin by Vpu. Vpu ELV still interacts with β-TrCP2, suggesting that tetherin ubiquitination, which is important for counteracting its activity [18], may still take place during the recycling process and effect antiviral function. Also physical interaction between Vpu and tetherin may be sufficient to interfere with some level tetherin function provided tetherin can still associate with the clathrin-dependent endocytic machinery. Since biochemical evidence strongly favors a direct cross-linking model for tetherin's antiviral activity [7], either of these processes could in principle affect the qualitative nature of tetherin distribution at viral assembly domains at the PM such that tethers do not form efficiently, something that is plausible in the light of Habermann et al's quantitative Cryo-EM analysis of tetherin localization at the PM in infected HeLa cells [57]. The relative efficiency of this "secondary" inhibition of tetherin activity will thus be dependent on cellular tetherin levels and the temporal stage of viral replication (ie: the expression level of Vpu). Since Vpu-defective mutants of HIV-1 in some studies show enhanced cell-to-cell transmission and that tetherin may play a role in virological synapse formation [51,58,59], such a differential effect on *de novo* synthesized versus the recycling pool tetherin may favor viral transmission during early stages of viral production, but effectively antagonize induction of tetherin expression and potent restriction by a pro-inflammatory response.

We have so far been unable to demonstrate direct interaction between the Vpu EXXXLV motif and adaptors AP-1, 2 or 3 that are known to bind acidic dileucine signals via a hemicomplex of their sigma and adaptin subunits [32]. These interactions have been demonstrated in yeast 3-hybrid assays previously for HIV-1 Nef [36,37], but not all interactions are amenable to this method and in our hands the Vpu cytoplasmic tail is a constitutive activator of transgene expression precluding its use. Furthermore, the low affinity of these interactions, their transient nature, and the complex interactions of the adaptor protein with membrane lipids

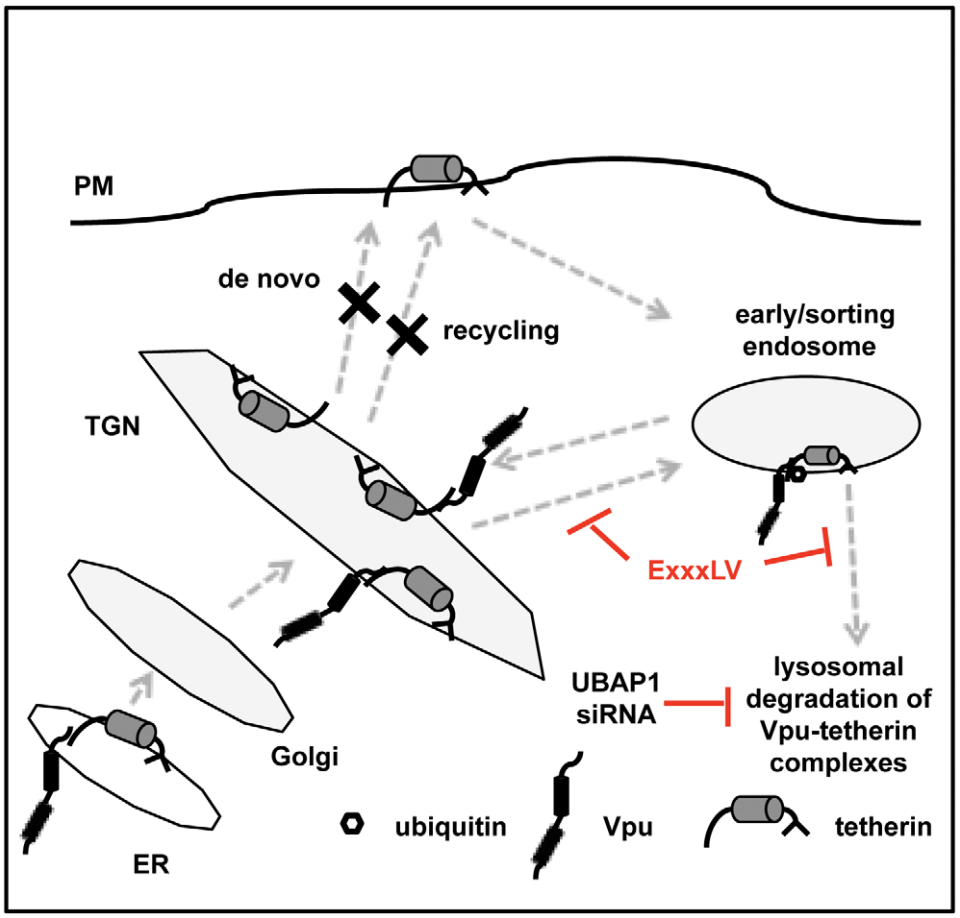

Figure 9. Model for the role of the EXXXLV motif in tetherin antagonism. Tetherin is expressed at the plasma membrane where it can become incorporated into viral particles or recycles constitutively via early/sorting endosomal compartments and the TGN. Vpu interacts with tetherin in the TGN (and perhaps earlier) through TM-domain-mediated interactions. In the presence of a functional EXXXLV motif, tetherin/Vpu complexes are prevented from trafficking to the PM and routed for ESCRT-dependent endosomal degradation via a clathrin-dependent mechanism. In the absence of an EXXXLV motif, tetherin/Vpu complexes recycle via the PM dependent on the YXYXXV sorting sequence in the tetherin cytoplasmic tail, which interacts with AP-2 and AP-1. During the recycling process, physical interaction of Vpu and/or modification by ubiquitin ligases, such as SCF-β-TrCP2, may further interfere with tetherin function to a variable degree in the absence of cell-surface downregulation.
doi:10.1371/journal.ppat.1002609.g009

means that adaptor binding is rarely measurable in co-precipitations from cells. The context dependency of (D/E)XXXL(L/I) motifs that governs which adaptor they bind to *in vivo* is poorly defined at present, meaning that RNAi-depletion is the most reliable method for identifying the cellular factor involved. While individual depletion of AP-1, 2 or 3 in our experiments had no effect on Vpu-mediated tetherin antagonism, replacement of the second alpha helix with the promiscuous AP-binding peptide from HIV-1 Nef did recover function. This site in Nef is essential for several functions including CD4 and MHC Class I downregulation, the former being AP-2-dependent [37], the latter requiring AP-1 [38]. Importantly, binding of AP-2 to this site in SIV Nef proteins is required for their counteraction of non-human primate tetherins [26]. Thus there are several possibilities. The EXXXLV motif in Vpu might be a promiscuous AP-binding site and adaptor usage may be redundant. The subcellular localization of tetherin/Vpu ELV complexes in EEA1 positive endosomes and the partial effect of dominant negative dynamin 2 would argue against a significant role for AP-2, the major regulator of clathrin-mediated transport from the PM. However toxicity associated with simultaneous knockdown of multiple adaptors has precluded us from addressing this possibility so far. Alternatively, replacement of the second alpha with the Nef peptide recovers function because it confers AP-2 binding to Vpu, thus allowing Vpu to counteract tetherin in a manner similar to SIV Nef and HIV-2/SIV Envs that both require AP-2 interactions [24–26,60]. However, these data do underscore that linking Vpu to the clathrin trafficking machinery promotes its ability to counteract tetherin.

If Vpu-mediated tetherin antagonism is clathrin-dependent, but independent of AP-1, AP-2 or AP-3 (for which the importance of clathrin is debated), what other adaptors might be important? Two further heterotetrameric adaptors, AP-4 and AP-5, have been identified, but understanding of their role in subcellular trafficking is limited and at present they are not known to bind to acidic dileucine motifs or to control clathrin-mediated transport [32,61]. The monomeric GGA (Golgi-associated, γ-ear containing, ARF-cofactors) 1–3 proteins that also function as clathrin adaptors that regulate Golgi-to-endosome transport are potentially attractive candidates, whose dysregulation has been reported to inhibit HIV-1 assembly [62]. However, known GGA-binding motifs in cellular cargoes correspond to a DXXLL consensus where the spacing of the leucines from the acidic residue is thought critical.

The (E/D)XXXL(V/M/I) motif is conserved in Vpu proteins from HIV-1 M group subtypes A, B, D, G and H (Figure S2), as

well as in Group O (www.hiv.lanl.gov). While Group O Vpus cannot antagonize tetherin [63], this maps to defective TM domain-mediated interaction and the membrane proximal hinge region. When replaced by those from a Group M Vpu these are sufficient to confer tetherin inactivation implying that C-terminal determinants retain function [64]. In Group M clades C and F, the equivalent position is (D/E)XXXL(S/A) respectively, suggesting that the site may not be functional in those Vpus, with the caveat that the second position in the dileucine motif is less important. Intriguingly both these subtypes bear EYXXL(L/I) motifs in the membrane proximal region of their cytoplasmic tails that encompass both a putative tyrosine and dileucine-based sorting sequence. Evidence from Ruiz et al [34] has shown that a model subtype C Vpu localizes to the PM rather than the TGN and that this is in part due to this motif. While LL mutations in this subtype C Vpu confer T-cell line replication phenotypes suggestive of a failure to downmodulate tetherin, no direct experiments on the role of this motif in tetherin-mediated HIV-1 release have been thus far performed, nor whether this site can bind known clathrin adaptors.

In summary our data implicate a trafficking determinant in the Vpu cytoplasmic tail that is required for tetherin downregulation, degradation and efficient antagonism, and suggest that it governs differential sorting of Vpu/tetherin complexes in the TGN to prevent forward transit of tetherin to the PM and viral budding sites.

Materials and Methods

Cells and plasmids

HEK293T, HeLa and Jurkat cells were obtained from ATCC (American Tissue Culture Collection). 293T/tetherin and 293T/tetherin-delGPI and HT1080/tetherin-HA are cell lines stably expressing human tetherin or mutant thereof, with or without a hemagglutinin (HA) epitope tag inserted at nucleotide 463, which has been previously described [1,65]. The reporter cell line HeLa-TZMbl, was kindly provided by John Kappes through the NIH AIDS Reagents Repository Program (ARRP). All adherent cells were maintained in Dulbecco's modified Eagle medium (DMEM) (Invitrogen, UK) supplemented with 10% fetal calf serum and Gentamycin; T-cell lines were grown in Roswell Park Memorial Institute medium (RPMI) supplemented with 10% fetal calf serum and Gentamycin. Murine fibroblasts from *pearl* and AP1γ1a deficient mice and derivative in which AP3μ or AP1γ1a were re-expressed were kindly provided by Andrew Peden [46] and Peter Schu [47] respectively. These cells were transduced to express HA-tagged human tetherin using pLHCX-THN-HA463 [65] and maintained in hygromycin selection.

Wildtype HIV-1 NL4.3 (obtained from NIH-ARRP), a Vpu-defective counterpart and pCR3.1 Vpu-HA containing a modified codon optimized NL4.3 Vpu has been described previously [31]. All second alpha helix mutants of Vpu and mutations in the NL4.3 proviral genome were generated by Quick-change site-directed mutagenesis PCR according to standard protocols using Phusion-II polymerase (New England Biolabs). Vpu-Nef chimeras and corresponding mutants were made with long reverse PCR primers encoding Nef clathrin adaptor binding sites, cloned into pCR3.1 expression vectors encoding tagged or untagged tetherins which have been described elsewhere [1]. β-TrCP2 was cloned from HeLa cDNA and inserted into pCR3.1 with a C-terminal myc-tag. pCR3.1 HA-HRS was kindly provided by Juan Martin-Serrano [66]. pCR3.1 dynamin 2-HA and dominant negative dynamin 2-HA have been previously described by [31].

Primary human CD4+ T cells were isolated from fresh venous blood drawn from healthy volunteers. CD4+ T cells were purified from total peripheral blood mononuclear cells (PBMC) isolated by lymphoprep (AXIS-SHIELD) gradient centrifugation using a CD4+ T cell Dynabeads isolation kit (Invitrogen). T cells were then activated for 48 h using anti-CD3/anti-CD28 magnetic beads (Invitrogen). The beads were then removed cells were then maintained in rhIL-2 (20 U/ml) (Roche).

Production of viral and vector stocks

For full-length HIV-1 stocks pseudotyped with the Vesicular Stomatitis Virus Glycoprotein (VSV-G), 293T cells were transfected with 2 μg of proviral plasmid and 200 ng of pCMV VSV-G. 48 h post-transfection, viral stocks were harvested and endpoint titers were determined on HeLa-TZMbl cells as described below [25].

Virus release assay

For transient-transfection-based virus release assays, subconfluent 293T cells were plated on 24 well plates and transfected with 500 ng proviral clone, in combination with 50 ng of tetherin and 25 ng of Vpu-HA or mutants using 1 μg/ml polyethyleneimine (Polysciences). The medium was replaced 5 h and 16 h post-transfection, cells were harvested after 48 h. The infectivity of viral supernatants was determined by infecting HeLa-TZMbl, 48 h later cells were assayed for β-galactosidase activity using the chemiluminescence Tropix GalactoStar kit (Applied Biosystems). For biochemical analysis of virus particle release, supernatants were filtered (0.22 μm) and pelleted through a 20% sucrose/PBS cushion at 20,000 g for 90 min at 4°C, and pellets were lysed in SDS-PAGE loading buffer. Virion and cell lysates were then subjected to SDS-PAGE and Western blotted for HIV-1 p24CA (monoclonal antibody 183-H12-5C; kindly provided by B Chesebro through the NIH ARRP), rabbit anti-Hsp90 (Santa Cruz Biotechnologies), monoclonal mouse anti-HA.11 (Covance), polyclonal rabbit anti-HA (Rockland) and/or Vpu (rabbit polyclonal; kindly provided by K. Strebel through the NIH ARRP [67], and visualized by LiCor apparatus using fluorophores conjugated secondary antibodies (IRDye 800 Goat anti-rabbit, IRDye 680 Goat anti-mouse).

One round viral release assay

5×10^5 cells (293T/tetherin, Jurkat or CD4+ T cells) were infected with VSV-G-pseudotyped HIV-1 wt, HIV-1 delVpu or HIV-1 Vpu ELV at an MOI of 0.5–1. 16 h post infection medium was replaced and cells (treated or not with 5000 U/ml of universal type-1 interferon (PBL InterferonSource)) were cultured for a further 24 h. The cells harvested, the infectivity of viral supernatants was determined by infecting HeLa-TZMbl and biochemical analysis of virus particle release was performed as in Virus release assay. For examining tetherin degradation HT1080 cells stably expressing tetherin-HA were infected with VSV-G-pseudotyped HIV-1 wt, HIV-1 delVpu or HIV-1 Vpu ELV virus stocks at a multiplicity of infection (MOI) of 2 to ensure that approximately 90% of the cells were infected. The medium was replaced 4 h after infection. 48 h post infection cell lysates were harvested and processed as described above.

Flow cytometry

HeLa cells were transfected with 400 ng of pCR3.1 GFP and 400 ng of pCR3.1 Vpu-HA or indicated mutants. 48 h post transfection the cells were harvested and stained for surface tetherin using a specific anti-BST2 monoclonal IgG2a antibody

(Abnova) and goat-anti-mouse IgG2a-Alexa633 conjugated secondary antibody (Molecular Probes, Invitrogen, UK). Tetherin expression on GFP positive cells was then analyzed using a FacsCalibur flow-cytometer (Becton Dickinson) and the FlowJo software. Murine fibroblasts were transduced with the pMigR1-based retroviral vector pCMS28-IRES-eGFP or a derivative expressing NL4.3 Vpu. 48 h after transduction the cells were stained for surface HA versus GFP expression. Jurkat or CD4+ T cells were infected with VSV-G-pseudotyped HIV-1 wt, HIV-1 delVpu or HIV-1 Vpu ELV at an MOI of 1. 48 h post infection cells were stained for surface tetherin expression as above, then fixed and permeabilized for 20 minutes (Cytofix/cytoperm Fixation/Permeabilization kit, BD Biosciences) and stained for intracellular HIV-1 p24CA using the KC57 antibody conjugated to PE (Beckman- Coulter).

Immunofluorescence microscopy

Cells were grown on coverslips and infected with VSV-G-pseudotyped HIV-1 wt or HIV-1 Vpu ELV, 48 h later cells were fixed in 4% paraformaldehyde/PBS, washed with 10 mM glycine/PBS, and permeabilized in 1% bovine serum albumin/0.1% Tritin-X100/PBS for 15 min. The infected cells were stained using anti-rabbit polyclonal Vpu in combination with sheep anti-human TGN46 (AbD Serotec), mouse anti-EEA1 (BD Biosciences), mouse anti-CD63 (Developmental Studies Hybridoma Bank, University of Iowa) or mouse polyclonal anti-BST-2 (Abnova) followed by the appropriate secondary antibodies conjugated to Alexa 488 or 594 fluorophores (Molecular Probes, Invitrogen). The cells were then mounted on glass slides using ProLong AntiFade- 4′,6-diamidino-2-phenylindole (DAPI) mounting solution (Molecular Probes, Invitrogen). Cells were visualized with a Leica DM-IRE2 confocal microscope. Images were analyzed using Leica Confocal Software and ImageJ.

Immunoprecipitations

293T cells stably expressing tetherin were transfected twice over 48 h with siRNA oligonucleotide against UBAP1 targeting CTCGACTATCTCTTTGCACAT or Non-targeting siRNA was used as control (Dharmacon). The cells were then infected with VSV-G-pseudotyped HIV-1 wt, HIV-1 delVpu, HIV-1 Vpu ELV or HIV-1 Vpu A14L,W22A at an MOI of 2. 48 h post infection the cells were lysed on ice for 30 min in buffer containing 50 mM Tris-HCL pH 7.4, 150 mM NaCl, complete protease inhibitors (Roche) and 1% digitonin (Calbiochem). After removal of the nuclei, the supernatants were immunoprecipitated with 5 μg/ml mouse monoclonal anti-BST2 antibody (eBiosciences) for 1.5 h at 4°C. Sepharose-protein G beads were washed in lysis buffer before they were added to the samples and incubated for further 3 h. The beads were washed extensively in lysis buffer containing 0.1% digitonin and resuspended in SDS-PAGE loading buffer. Cell lysates and immunoprecipitates were subjected to SDS-PAGE, and Western blot assays were performed using a rabbit anti-Vpu antibody (kindly provided by K Strebel through the NIH ARRP), polyclonal rabbit anti-tetherin antibody (kindly provided by K Strebel through the NIH ARRP) and polyclonal rabbit anti-UBAP1 antibody (Proteintech), and visualized by ImageQuant using corresponding HRP-linked secondary antibodies (New England Biolabs, UK). For HRS/Vpu coIP, 293T cells were co-transfected with 700 ng of pCR3.1 HA-HRS and pCR3.1 Vpu-YFP, pCR3.1 Vpu ELV-YFP or pCR3.1 YFP expression plasmids. 48 h post transfection the cells were lysed in buffer containing 0.1 M MES-NaOH pH 6.5, 1 mM magnesium acetate, 0.5 mM EGTA, 200 μM sodium ortho-vanadate, 10 mM NEM, complete protease inhibitors (Roche) and 1% digitonin. After removal of the nuclei, the supernatants were immunoprecipitated with 5 μg/ml monoclonal mouse anti-HA.11 antibody (Covance). Immunoprecipitation was performed as described above and Western blot assays were performed using a polyclonal rabbit anti-HA antibody (Rockland) and an anti-Vpu antibody.

Crosslinking IP

293T cells were co-transfected with 700 ng of pCR3.1 myc β-TrCP 2 and pCR3.1Vpu-HA, pCR3.1 Vpu ELV-HA, pCR3.1 Vpu 2/6A-HA or pCR3.1 YFP expression plasmids. 48 h post transfection, Crosslinking Immunoprecipitation was performed as previously described [68]. Cell lysates and immunoprecipitates were subjected to SDS-PAGE, and Western blot assays were performed using a rabbit anti-Vpu antibody and mouse anti-myc antibody (kindly provided by M. Malim), and visualized by ImageQuant (GE) using corresponding HRP-linked secondary antibodies (New England Biolabs).

siRNA-mediated clathrin adaptor knockdown

293T cells stable expressing tetherin or HeLa cells were seeded at a density of 2×10^5 cells per well in a 12 well plate. After 3 h, the first transfection was performed. For each well, 3 μl Oligofectamine (Invitrogen) was added to 10 μl of Opti-MEM (Life Technologies), this solution was added to 5 μl of 20 μM siRNA in 85 μl of Opti-MEM according to manufactures protocol. For AP-1 knockdown, HeLa cells stably expressing doxycycline-inducible pTRIPZ shRNA against AP-1γ1 (OpenBiosystems) were used in combination with siRNA oligonucleotide against AP-1γ1 targeting AAGAAGATAGAATTCACCTTT. For AP-2 knockdown, SMARTpool siRNA targeting the AP-2 μ1 subunit was used (Dharmacon). For AP-3 knockdown, SMARTpool siRNA targeting the AP-3 μ1 subunit was used in combination with SMARTpool siRNA targeting the AP-3δ1 subunit (Dharmacon). For Vps26 knockdown, siRNA targeting the AACCACC-TATCCTGATGTTAA sequence was used (Qiagen). On Non-targeting siRNA was used as control (Dharmafect). The cells were reseeded into a 24 well plate on day 2 and a second transfection was performed according to manufactures protocol. The cells were infected 3 h post transfection with VSV-G-pseudotyped HIV-1 wt, HIV-1 delVpu at an MOI of 0.8. The infectivity of viral supernatants was determined by infecting HeLa-TZMbl as described above. Cell lysates and viral particles were subjected to SDS-PAGE, and Western blot assays were performed using a mouse monoclonal AP-1γ1 antibody (Sigma), mouse anti-AP50 (AP-2μ1) and mouse anti-AP-3δ1antibodies (BD Bioscience), polyclonal rabbit AP-3μ1 antibody (kindly provided by M.S. Robinson) and rabbit polyclonal Vps26 antibody (Abcam).

Ethics statement

Ethical approval for the drawing of blood and preparation of leukocyte subsets from healthy donors following written informed consent was obtained through the King's College London Infectious Disease BioBank Local Research Ethics Committee (under the authority of the Southampton and South West Hampshire Research Ethics Committee – approval REC09/H0504/39), approval number SN-1/6/7/9.

Supporting Information

Figure S1 Effect of Vpu helix 2 mutants on surface tetherin expression in HeLa cells. (**A**) The full panel of helix 2 alanine scan mutants performed as described for Figure 2D. (**B**) HeLa cells were infected with the indicated VSV-G pseudotyped

HIV-1 mutant at an MOI of 0.5. 48 h later cells were stained for surface tetherin and intracellular p24CA. (**C**) Productively infected Jurkat cells in Figure 2E were discriminated from those acquiring p24+ matter from the inoculum by exposing them to the same dose of wildtype HIV-1 in presence of AZT.
(TIF)

Figure S2 Vpu EXXXL(V/M/I/L) is conserved in most HIV-1 clades. (**A**) LogoPlots of Vpu cytoplasmic tail portions encompassing the conserved phosphorylation motif (DSGNES) and helix 2 from HIV-1 subgroup M clades A,B,D,G and H generated from sequences obtained from the Los Alamos database (www.hiv.lanl.gov). (**B**) 293T cells were transfected with NL4.3 or NL4.3 delVpu proviruses in combination with tetherin and Vpu-HA, Vpu 64I-HA, Vpu 64M-HA or Vpu 64L-HA expression vectors. 48 h post transfection, cell lysates and pelleted supernatant virions were harvested and subjected to SDS-PAGE and analyzed by Western blotting for HIV-1 p24CA, Vpu-HA and Hsp90, and analyzed by LiCor quantitative imager. (**C**) HeLa cells were co-transfected with Vpu or indicated Vpu mutant and a GFP expression construct. Cell surface staining for endogenous tetherin was analyzed by flow cytometry 48 h post transfection, as in Figure 2D.
(TIF)

Figure S3 Effects of Vpu on surface expression of human tetherin in murine fibroblasts deficient for AP3 or AP1. Fibroblasts from *pearl* (AP3δ−/−) (**A**) or AP-1μ1A−/− mice (**B**) or their reconstituted counterparts were transduced to express human tetherin bearing an extracellular HA-tag. The cells were then transduced with retroviral vector constructs encoding Vpu linked to GFP via an IRES. 48 h later the cells were surface stained for human tetherin expression using anti-HA antibodies. (**C**) HeLa-CD8-CI-M6PR cells were treated with control or Vps26 siRNAs. 48 h later the cells were fixed and stained for CD8 (green) and TGN46 (red).
(TIF)

Figure S4 Effects of dominant negative dynamin 2 on Vpu-mediated HIV-1 release. 293T/tetherin cells were transfected with the indicated HIV-1 provirus and increasing doses of HA-tagged dominant negative dynamin 2 (**A**) or the wildtype protein (**B**). 48 h later, cell lysates and viral supernatants were harvested and subjected to SDS-PAGE and analyzed by Western blotting for HIV-1 p24CA, dynamin 2-HA and Hsp90, and analyzed by LiCor quantitative imager. Histograms below the blots indicate particle release efficiency compared to wildtype virus release in the absence of dynamin 2 or increasing doses of dynamin 2 expression vector. (**C**) Corresponding infectivity of viral supernatants from **A** and **B** on HeLa-TZM cells alongside those from a parallel experiment in parental 293T cells. (**D**) 293T/tetherin cells were transfected with pCR3.1 YFP with or without increasing doses of dominant negative dynamin 2. 48 h later the cells were starved in serum-free medium for 30 minutes and then treated for a further 15 minutes with 10 μg/ml Alexa-594-conjugated transferrin, before fixation and imaging.
(TIF)

Figure S5 Effect ELV mutant on HIV-1 infectious release from HeLa cells. HeLa cells were infected with VSV-G pseudotyped stocks of the indicated virus at an MOI of 0.5. 48 h later the cell supernatants were harvested and infectivity determined on HeLa-TZM cells.
(TIF)

Acknowledgments

We are grateful to all members of the Neil and Martin-Serrano Labs for support and reagents, and to John Kappes, Klaus Strebel and Bruce Chesebro for reagents obtained through the NIH-ARRP. We are particularly thankful to Scottie Robinson, Mark Peden, Peter Schu and Mark Marsh for helpful discussions and invaluable reagents.

Author Contributions

Conceived and designed the experiments: TK SJDN. Performed the experiments: TK. Analyzed the data: TK SJDN. Contributed reagents/materials/analysis tools: TK SJDN. Wrote the paper: TK SJDN.

References

1. Neil SJ, Zang T, Bieniasz PD (2008) Tetherin inhibits retrovirus release and is antagonized by HIV-1 Vpu. Nature 451: 425–430.
2. Van Damme N, Goff D, Katsura C, Jorgenson RL, Mitchell R, et al. (2008) The interferon-induced protein BST-2 restricts HIV-1 release and is downregulated from the cell surface by the viral Vpu protein. Cell Host Microbe 3: 245–252.
3. Hinz A, Miguet N, Natrajan G, Usami Y, Yamanaka H, et al. (2010) Structural basis of HIV-1 tethering to membranes by the BST-2/tetherin ectodomain. Cell Host Microbe 7: 314–323.
4. Schubert HL, Zhai Q, Sandrin V, Eckert DM, Garcia-Maya M, et al. (2010) Structural and functional studies on the extracellular domain of BST2/tetherin in reduced and oxidized conformations. Proc Natl Acad Sci U S A 107: 17951–17956.
5. Yang H, Wang J, Jia X, McNatt MW, Zang T, et al. (2010) Structural insight into the mechanisms of enveloped virus tethering by tetherin. Proc Natl Acad Sci U S A 107: 18428–18432.
6. Kupzig S, Korolchuk V, Rollason R, Sugden A, Wilde A, et al. (2003) Bst-2/HM1.24 is a raft-associated apical membrane protein with an unusual topology. Traffic 4: 694–709.
7. Perez-Caballero D, Zang T, Ebrahimi A, McNatt MW, Gregory DA, et al. (2009) Tetherin inhibits HIV-1 release by directly tethering virions to cells. Cell 139: 499–511.
8. Masuyama N, Kuronita T, Tanaka R, Muto T, Hirota Y, et al. (2009) HM1.24 is internalized from lipid rafts by clathrin-mediated endocytosis through interaction with alpha-adaptin. J Biol Chem 284: 15927–15941.
9. Rollason R, Korolchuk V, Hamilton C, Schu P, Banting G (2007) Clathrin-mediated endocytosis of a lipid-raft-associated protein is mediated through a dual tyrosine motif. J Cell Sci 120: 3850–3858.
10. Le Tortorec A, Willey S, Neil SJD (2011) Antiviral Inhibition of Enveloped Virus Release by Tetherin/BST-1: Action and Counteraction. Viruses 3: 520–540.
11. Iwabu Y, Fujita H, Kinomoto M, Kaneko K, Ishizaka Y, et al. (2009) HIV-1 accessory protein Vpu internalizes cell-surface BST-2/tetherin through transmembrane interactions leading to lysosomes. J Biol Chem 284: 35060–35072.
12. Kobayashi T, Ode H, Yoshida T, Sato K, Gee P, et al. (2011) Identification of amino acids in the human tetherin transmembrane domain responsible for HIV-1 Vpu interaction and susceptibility. J Virol 85: 932–945.
13. Dube M, Roy BB, Guiot-Guillain P, Binette J, Mercier J, et al. (2010) Antagonism of tetherin restriction of HIV-1 release by Vpu involves binding and sequestration of the restriction factor in a perinuclear compartment. PLoS Pathog 6: e1000856.
14. Vigan R, Neil SJ (2010) Determinants of Tetherin Antagonism in the Transmembrane Domain of the Human Immunodeficiency Virus Type-1 (Hiv-1) Vpu Protein. J Virol; 842412958-12970.
15. Douglas JL, Viswanathan K, McCarroll MN, Gustin JK, Fruh K, et al. (2009) Vpu Directs the Degradation of the HIV Restriction Factor BST-2/tetherin via a {beta}TrCP-dependent Mechanism. J Virol; 83167931-7947.
16. Mitchell RS, Katsura C, Skasko MA, Fitzpatrick K, Lau D, et al. (2009) Vpu antagonizes BST-2-mediated restriction of HIV-1 release via beta-TrCP and endo-lysosomal trafficking. PLoS Pathog 5: e1000450.
17. Margottin F, Bour SP, Durand H, Selig L, Benichou S, et al. (1998) A novel human WD protein, h-beta TrCp, that interacts with HIV-1 Vpu connects CD4 to the ER degradation pathway through an F-box motif. Mol Cell 1: 565–574.
18. Tokarev AA, Munguia J, Guatelli JC (2011) Serine-threonine ubiquitination mediates downregulation of BST-2/tetherin and relief of restricted virion release by HIV-1 Vpu. J Virol 85: 51–63.
19. Janvier K, Pelchen-Matthews A, Renaud JB, Caillet M, Marsh M, et al. (2011) The ESCRT-0 component HRS is required for HIV-1 Vpu-mediated BST-2/tetherin down-regulation. PLoS Pathog 7: e1001265.

20. Goffinet C, Homann S, Ambiel I, Tibroni N, Rupp D, et al. (2010) Antagonism of CD317 restriction of human immunodeficiency virus type 1 (HIV-1) particle release and depletion of CD317 are separable activities of HIV-1 Vpu. J Virol 84: 4089–4094.
21. Miyagi E, Andrew AJ, Kao S, Strebel K (2009) Vpu enhances HIV-1 virus release in the absence of Bst-2 cell surface down-modulation and intracellular depletion. Proc Natl Acad Sci U S A 106: 2868–2873.
22. Agromayor M, Soler N, Caballe A, Kueck T, Freund SM, et al. (2012) The UBAP1 subunit of ESCRT-I interacts with ubiquitin via a novel SOUBA domain. Structurein press.
23. Caillet M, Janvier K, Pelchen-Matthews A, Delcroix-Genete D, Camus G, et al. (2011) Rab7A is required for efficient production of infectious HIV-1. PLoS Pathog 7: e1002347.
24. Noble B, Abada P, Nunez-Iglesias J, Cannon PM (2006) Recruitment of the adaptor protein 2 complex by the human immunodeficiency virus type 2 envelope protein is necessary for high levels of virus release. J Virol 80: 2924–2932.
25. Le Tortorec A, Neil SJ (2009) Antagonism to and intracellular sequestration of human tetherin by the human immunodeficiency virus type 2 envelope glycoprotein. J Virol 83: 11966–11978.
26. Zhang F, Landford WN, Ng M, McNatt MW, Bieniasz PD, et al. (2011) SIV Nef proteins recruit the AP-2 complex to antagonize Tetherin and facilitate virion release. PLoS Pathog 7: e1002039.
27. Dube M, Roy BB, Guiot-Guillain P, Mercier J, Binette J, et al. (2009) Suppression of Tetherin-Restricting Activity on HIV-1 Particle Release Correlates with Localization of Vpu in the trans-Golgi Network. J Virol 83: 4574–90.
28. Varthakavi V, Smith RM, Martin KL, Derdowski A, Lapierre LA, et al. (2006) The pericentriolar recycling endosome plays a key role in Vpu-mediated enhancement of HIV-1 particle release. Traffic 7: 298–307.
29. Dube M, Roy BB, Guiot-Guillain P, Mercier J, Binette J, et al. (2009) Suppression of Tetherin-restricting activity upon human immunodeficiency virus type 1 particle release correlates with localization of Vpu in the trans-Golgi network. J Virol 83: 4574–4590.
30. Mangeat B, Gers-Huber G, Lehmann M, Zufferey M, Luban J, et al. (2009) HIV-1 Vpu neutralizes the antiviral factor Tetherin/BST-2 by binding it and directing its beta-TrCP2-dependent degradation. PLoS Pathog 5: e1000574.
31. Neil SJ, Eastman SW, Jouvenet N, Bieniasz PD (2006) HIV-1 Vpu promotes release and prevents endocytosis of nascent retrovirus particles from the plasma membrane. PLoS Pathog 2: e39.
32. Bonifacino JS, Traub LM (2003) Signals for sorting of transmembrane proteins to endosomes and lysosomes. Annu Rev Biochem 72: 395–447.
33. Stefani F, Zhang L, Taylor S, Donovan J, Rollinson S, et al. (2011) UBAP1 is a component of an endosome-specific ESCRT-I complex that is essential for MVB sorting. Curr Biol 21: 1245–1250.
34. Ruiz A, Hill MS, Schmitt K, Guatelli J, Stephens EB (2008) Requirements of the membrane proximal tyrosine and dileucine-based sorting signals for efficient transport of the subtype C Vpu protein to the plasma membrane and in virus release. Virology 378: 58–68.
35. Kirchhoff F (2010) Immune evasion and counteraction of restriction factors by HIV-1 and other primate lentiviruses. Cell Host Microbe 8: 55–67.
36. Janvier K, Kato Y, Boehm M, Rose JR, Martina JA, et al. (2003) Recognition of dileucine-based sorting signals from HIV-1 Nef and LIMP-II by the AP-1 gamma-sigma1 and AP-3 delta-sigma3 hemicomplexes. J Cell Biol 163: 1281–1290.
37. Chaudhuri R, Lindwasser OW, Smith WJ, Hurley JH, Bonifacino JS (2007) Downregulation of CD4 by human immunodeficiency virus type 1 Nef is dependent on clathrin and involves direct interaction of Nef with the AP2 clathrin adaptor. J Virol 81: 3877–3890.
38. Lubben NB, Sahlender DA, Motley AM, Lehner PJ, Benaroch P, et al. (2007) HIV-1 Nef-induced down-regulation of MHC class I requires AP-1 and clathrin but not PACS-1 and is impeded by AP-2. Mol Biol Cell 18: 3351–3365.
39. Jia B, Serra-Moreno R, Neidermyer W, Rahmberg A, Mackey J, et al. (2009) Species-specific activity of SIV Nef and HIV-1 Vpu in overcoming restriction by tetherin/BST2. PLoS Pathog 5: e1000429.
40. Zhang F, Wilson SJ, Landford WC, Virgen B, Gregory D, et al. (2009) Nef proteins from simian immunodeficiency viruses are tetherin antagonists. Cell Host Microbe 6: 54–67.
41. Lindwasser OW, Smith WJ, Chaudhuri R, Yang P, Hurley JH, et al. (2008) A diacidic motif in human immunodeficiency virus type 1 Nef is a novel determinant of binding to AP-2. J Virol 82: 1166–1174.
42. Ford MG, Pearse BM, Higgins MK, Vallis Y, Owen DJ, et al. (2001) Simultaneous binding of PtdIns(4,5)P2 and clathrin by AP180 in the nucleation of clathrin lattices on membranes. Science 291: 1051–1055.
43. Lau D, Kwan W, Guatelli J (2011) Role of the endocytic pathway in the counteraction of BST-2 by human lentiviral pathogens. J Virol 85: 9834–46.
44. Popov S, Strack B, Sanchez-Merino V, Popova E, Rosin H, et al. (2011) Human immunodeficiency virus type 1 and related primate lentiviruses engage clathrin through Gag-Pol or Gag. J Virol 85: 3792–3801.
45. Zhang F, Zang T, Wilson SJ, Johnson MC, Bieniasz PD (2011) Clathrin facilitates the morphogenesis of retrovirus particles. PLoS Pathog 7: e1002119.
46. Peden AA, Rudge RE, Lui WW, Robinson MS (2002) Assembly and function of AP-3 complexes in cells expressing mutant subunits. J Cell Biol 156: 327–336.
47. Zizioli D, Meyer C, Guhde G, Saftig P, von Figura K, et al. (1999) Early embryonic death of mice deficient in gamma-adaptin. J Biol Chem 274: 5385–5390.
48. Attar N, Cullen PJ (2010) The retromer complex. Adv Enzyme Regul 50: 216–236.
49. Goffinet C, Allespach I, Homann S, Tervo HM, Habermann A, et al. (2009) HIV-1 antagonism of CD317 is species specific and involves Vpu-mediated proteasomal degradation of the restriction factor. Cell Host Microbe 5: 285–297.
50. Casartelli N, Sourisseau M, Feldmann J, Guivel-Benhassine F, Mallet A, et al. (2010) Tetherin restricts productive HIV-1 cell-to-cell transmission. PLoS Pathog 6: e1000955.
51. Jolly C, Booth NJ, Neil SJ (2010) Cell-cell spread of human immunodeficiency virus type 1 overcomes tetherin/BST-2-mediated restriction in T cells. J Virol 84: 12185–12199.
52. Stacey AR, Norris PJ, Qin L, Haygreen EA, Taylor E, et al. (2009) Induction of a striking systemic cytokine cascade prior to peak viremia in acute human immunodeficiency virus type 1 infection, in contrast to more modest and delayed responses in acute hepatitis B and C virus infections. J Virol 83: 3719–3733.
53. Jacquelin B, Mayau V, Targat B, Liovat AS, Kunkel D, et al. (2009) Nonpathogenic SIV infection of African green monkeys induces a strong but rapidly controlled type I IFN response. J Clin Invest 119: 3544–3555.
54. Schmidt S, Fritz JV, Bitzegeio J, Fackler OT, Keppler OT (2011) HIV-1 Vpu Blocks Recycling and Biosynthetic Transport of the Intrinsic Immunity Factor CD317/Tetherin To Overcome the Virion Release Restriction. MBio 2: e00036–11.
55. Dube M, Bego MG, Paquay C, Cohen EA (2010) Modulation of HIV-1-host interaction: role of the Vpu accessory protein. Retrovirology 7: 114.
56. Raiborg C, Wesche J, Malerod L, Stenmark H (2006) Flat clathrin coats on endosomes mediate degradative protein sorting by scaffolding Hrs in dynamic microdomains. J Cell Sci 119: 2414–2424.
57. Habermann A, Krijnse-Locker J, Oberwinkler H, Eckhardt M, Homann S, et al. (2010) CD317/tetherin is enriched in the HIV-1 envelope and downregulated from the plasma membrane upon virus infection. J Virol 84: 4646–4658.
58. Gummuluru S, Kinsey CM, Emerman M (2000) An in vitro rapid-turnover assay for human immunodeficiency virus type 1 replication selects for cell-to-cell spread of virus. J Virol 74: 10882–10891.
59. Strebel K, Klimkait T, Maldarelli F, Martin MA (1989) Molecular and biochemical analyses of human immunodeficiency virus type 1 vpu protein. J Virol 63: 3784–3791.
60. Serra-Moreno R, Jia B, Breed M, Alvarez X, Evans DT (2011) Compensatory changes in the cytoplasmic tail of gp41 confer resistance to tetherin/BST-2 in a pathogenic nef-deleted SIV. Cell Host Microbe 9: 46–57.
61. Hirst J, Barlow LD, Francisco GC, Sahlender DA, Seaman MN, et al. (2011) The fifth adaptor protein complex. PLoS Biol 9: e1001170.
62. Joshi A, Garg H, Nagashima K, Bonifacino JS, Freed EO (2008) GGA and Arf proteins modulate retrovirus assembly and release. Mol Cell 30: 227–238.
63. Sauter D, Schindler M, Specht A, Landford WN, Munch J, et al. (2009) Tetherin-driven adaptation of Vpu and Nef function and the evolution of pandemic and nonpandemic HIV-1 strains. Cell Host Microbe 6: 409–421.
64. Vigan R, Neil SJ (2011) Separable Determinants of Subcellular Localization and Interaction Account for the Inability of Group O Human Immunodeficiency Virus Type 1 (Hiv-1) Vpu to Counteract Tetherin. J Virol 85: 9737–48.
65. Pardieu C, Vigan R, Wilson SJ, Calvi A, Zang T, et al. (2010) The RING-CH ligase K5 antagonizes restriction of KSHV and HIV-1 particle release by mediating ubiquitin-dependent endosomal degradation of tetherin. PLoS Pathog 6: e1000843.
66. Martin-Serrano J, Yarovoy A, Perez-Caballero D, Bieniasz PD (2003) Divergent retroviral late-budding domains recruit vacuolar protein sorting factors by using alternative adaptor proteins. Proc Natl Acad Sci U S A 100: 12414–12419.
67. Maldarelli F, Chen MY, Willey RL, Strebel K (1993) Human immunodeficiency virus type 1 Vpu protein is an oligomeric type I integral membrane protein. J Virol 67: 5056–5061.
68. Niranjanakumari S, Lasda E, Brazas R, Garcia-Blanco MA (2002) Reversible cross-linking combined with immunoprecipitation to study RNA-protein interactions in vivo. Methods 26: 182–190.

Structure
Article

The UBAP1 Subunit of ESCRT-I Interacts with Ubiquitin via a SOUBA Domain

Monica Agromayor,[1,4] Nicolas Soler,[2,4] Anna Caballe,[1] Tonya Kueck,[1] Stefan M. Freund,[2] Mark D. Allen,[2] Mark Bycroft,[2] Olga Perisic,[2] Yu Ye,[2] Bethan McDonald,[1] Hartmut Scheel,[3] Kay Hofmann,[3] Stuart J.D. Neil,[1] Juan Martin-Serrano,[1,*] and Roger L. Williams[2,*]

[1]Department of Infectious Diseases, King's College London School of Medicine, London SE1 9RT, UK
[2]MRC Laboratory of Molecular Biology, Cambridge CB2 0QH, UK
[3]Miltenyi Biotec, 51429 Bergisch-Gladbach, Germany
[4]These authors contributed equally to this work
*Correspondence: juan.martin_serrano@kcl.ac.uk (J.M.-S.), rlw@mrc-lmb.cam.ac.uk (R.L.W.)
DOI 10.1016/j.str.2011.12.013

SUMMARY

The endosomal sorting complexes required for transport (ESCRTs) facilitate endosomal sorting of ubiquitinated cargo, MVB biogenesis, late stages of cytokinesis, and retroviral budding. Here we show that ubiquitin associated protein 1 (UBAP1), a subunit of human ESCRT-I, coassembles in a stable 1:1:1:1 complex with Vps23/TSG101, VPS28, and VPS37. The X-ray crystal structure of the C-terminal region of UBAP1 reveals a domain that we describe as a solenoid of overlapping UBAs (SOUBA). NMR analysis shows that each of the three rigidly arranged overlapping UBAs making up the SOUBA interact with ubiquitin. We demonstrate that UBAP1-containing ESCRT-I is essential for degradation of antiviral cell-surface proteins, such as tetherin (BST-2/CD317), by viral countermeasures, namely, the HIV-1 accessory protein Vpu and the Kaposi sarcoma-associated herpesvirus (KSHV) ubiquitin ligase K5.

INTRODUCTION

The endosomal sorting complex required for transport (ESCRT) machinery facilitates the lysosomal degradation of ubiquitinated cell surface receptors (Hurley and Stenmark, 2011; Katzmann et al., 2001). ESCRT proteins are conserved from yeast to humans and form four multiprotein complexes termed ESCRT-0, ESCRT-I, ESCRT-II, and ESCRT-III (Henne et al., 2011; Williams and Urbé, 2007). ESCRT-0, -I, and -II capture ubiquitinated membrane proteins for sorting into intraluminal vesicles (ILV) within endosomes to form structures known as multivesicular endosomes or multivesicular bodies (MVB) (Shields and Piper, 2011).

The ESCRT machinery is also essential for resolution of the midbody during cytokinetic abscission (Carlton and Martin-Serrano, 2007; Morita et al., 2007b), a process that is topologically equivalent to MVB formation. The ability of the ESCRTs to mediate scission of a thin membranous stalk is also exploited by several enveloped viruses such as HIV-1 to facilitate their release from infected cells (Baumgärtel et al., 2011; Jouvenet et al., 2011; Martin-Serrano and Neil, 2011; Morita and Sundquist, 2004; Morita et al., 2011; Weissenhorn and Göttlinger, 2011). In particular, HIV-1 encodes a PTAP motif that recruits ESCRT-I to the sites of viral budding through a direct interaction with the UEV domain in TSG101 (Pornillos et al., 2002). Additional roles of ESCRT-I in viral pathogenesis include its cooption by gamma-herpesviruses (Nathan and Lehner, 2009) and HIV for the degradation of various antiviral cell-surface proteins such as tetherin (BST-2/CD317) (reviewed in Martin-Serrano and Neil, 2011). Tetherin is an antiviral type II membrane glycoprotein that is induced by interferons and physically inhibits enveloped virus particle release from infected cells by cross-linking nascent virions to the plasma membrane. Specifically, the HIV-1 accessory protein Vpu counteracts tetherin activity and promotes its ESCRT-dependent degradation via the lysosomal pathway (Janvier et al., 2011). Kaposi sarcoma-associated herpesvirus (KSHV) encodes K5, a membrane-bound E3 ubiquitin ligase that results in a similar effect (Bartee et al., 2006; Mansouri et al., 2009; Pardieu et al., 2010).

ESCRT-I is formed by four subunits, Vps23/TSG101, Vps28, Vps37, and Mvb12. The yeast ESCRT-I heterotetramer contains a fan-shaped headpiece formed by a heterotrimeric core consisting of the C-terminal "steadiness box" of Vps23p, the N-terminal half of Vps28p, and the C-terminal half of Vps37p (Kostelansky et al., 2006; Teo et al., 2006). This headpiece connects to an extended stalk formed by Mvb12p, Vps23p, and Vps37p. The stalk is essential for yeast ESCRT-I function in cargo sorting. The C-terminal domain of Vps28p is flexibly tethered to the headpiece and binds ESCRT-II, whereas the flexibly attached UEV domain of Vps23p binds to ESCRT-0 (Kostelansky et al., 2007). This structural organization is thought to be conserved in mammalian ESCRT-I and was used as the basis to identify, to our knowledge, novel subunits of the complex. However, in mammalian cells, ESCRT-I has evolved a much greater diversity of subunits than in yeast, including multiple isoforms of VPS37 and MVB12 (Bache et al., 2004; Eastman et al., 2005; Morita et al., 2007a; Stuchell et al., 2004).

Using our sensitive generalized profile method for sequence comparison (Bucher et al., 1996), we identified a highly significant relationship between a profile constructed from different vertebrate and invertebrate MVB12 sequences and the protein

UBAP1. An independent report also predicted a shared domain between UBAP1 and MVB12 that was named UBAP1-MVB12-associated (UMA) domain (de Souza and Aravind, 2010) (Figure 1A). The UMA domain corresponds to a region that was previously described as the ESCRT-I binding box (EBB) (Morita et al., 2007a) and is located in the C terminus of MVB12 and in the N terminus of UBAP1. UBAP1 is expressed in a wide range of tissues and is embryonic lethal when deleted in mice (http://www.sanger.ac.uk/mouseportal/search?query=ubap1). It is part of a locus that experiences a loss of heterozygosity in human nasopharyngeal cancers (Qian et al., 2001). Recently, UBAP1 was identified as a risk factor in familial frontotemporal lobar dementia (FTLD) (Rollinson et al., 2009).

In contrast to the MVB12A and MVB12B subunits, which have an N-terminal extension consisting of a MABP β-prism domain (de Souza and Aravind, 2010), UBAP1 has a greatly expanded C-terminal region, which contains three putative ubiquitin associated (UBA) domains. A number of ubiquitin-binding domains (UBDs) have been described, including CUE, UIM, NZF, UEV, GLUE, GGA, GAT, and UBA (Dikic et al., 2009). The UBA domain is the most frequently occurring UBD, with 84 sequences in the human genome according to Pfam (http://pfam.sanger.ac.uk). UBAs have about 45 residues folded into a compact three-helix bundle with a right-handed twist. UBA domains have a conserved signature motif M/L-G-Y/F in the α1/α2 loop that forms part of the interaction with ubiquitin, and there is a conserved di-leucine motif at the end of helix α3 (Hofmann and Bucher, 1996; Mueller and Feigon, 2002; Ohno et al., 2005). UBAs have been grouped in four classes according to their preference for polyubiquitin linkages: K48-linked polyubiquitin, K63-linked polyubiquitin, promiscuous recognition of multiple polyubiquitin linkages, and no ubiquitin recognition (Raasi et al., 2005). UBA domains typically also bind monoubiquitin, but generally with much lower affinity.

UBAs have important roles in many different contexts, including diverse degradative pathways. Several UBA-containing proteins, such as Rad23 and Dsk2, function as adaptors for proteasome degradation (Clague and Urbé, 2010). Degradation of polyubiquitinated protein aggregates depends on their recruitment to autophagosomes by the UBA domain of p62 (Pohl, 2009). The ESCRT complexes involved in MVB sorting in yeast contain a number of UBDs, including UIMs, VHS, NZF, and UEV domains (Shields and Piper, 2011). However, disruption of the individual UBDs in the ESCRT complexes does not block the MVB pathway and only a quadruple mutant that is completely defective for ubiquitin binding shows severe sorting defects (Shields et al., 2009). Intriguingly, UBA domains are absent from the MVB pathway in yeast.

We report here the structure of the C-terminal region of UBAP1 that folds as a solenoid of overlapping UBAs (SOUBA) domain. NMR data show that each of the three UBA domains composing SOUBA binds monoubiquitin. This is consistent with the specific role of UBAP1 in endosomal sorting of ubiquitinated membrane cargo as shown recently for EGFR by Woodman and colleagues (Stefani et al., 2011). We show that UBAP1 is required for ubiquitin-dependent degradation of the antiviral protein tetherin triggered by the viral countermeasures HIV-I protein Vpu and KSHV viral protein K5.

RESULTS

Composition and Stoichiometry of ESCRT-I Complexes Containing UBAP1

Recombinant full-length human UBAP1, when coexpressed in *Escherichia coli* together with ESCRT-I subunits VPS28, TSG101, and VPS37A, forms a stable complex with 1:1:1:1 stoichiometry of the four subunits (Figure 1B; Figure S1 available online). The cores of VPS37A, VPS37B, VPS37C, or VPS37D all give rise to stable recombinant ESCRT-I complexes with UBAP1 in *E. coli* (Figure S1A). Endogenous UBAP1 from HEK293 cell lysate eluted close to the 440 kDa marker in a complex containing TSG101 (Figure S1B). In addition, endogenous UBAP1 was efficiently copurified with TSG101 and VPS37A from a cell line stably expressing TSG101 with a One-Strep tag (OSHA-TSG101) (Figure 1C). The OSHA-TSG101 fusion is expressed at endogenous levels in these cells (McDonald and Martin-Serrano, 2008), allowing affinity purification of TSG101-binding proteins under physiological conditions. Similarly, endogenous TSG101 also bound UBAP1 and VPS28 when these proteins were overexpressed in 293T cells as GST fusions and purified with glutathione beads (Figure S1C). As observed for other ESCRT-I subunits, UBAP1 functionally recruits the ESCRT machinery in a trans-complementation assay based on the rescue of a L-domain defective HIV-1 by direct fusion of a component of the ESCRT machinery to a defective Gag protein (Martin-Serrano et al., 2001). Expression of UBAP1 fused to the C terminus of the complementing Gag protein restored infectious virus production (Figures S1E–S1H).

Deletion analysis using recombinant proteins showed that the N-terminal fragment of UBAP1 comprising residues 1 to 68 is sufficient to form a stable complex with TSG101, VPS28, and VPS37A (Figure 1D). This N-terminal construct corresponds to the UMA domain (Figure 1A). Overexpression of UMA domain constructs YFP-UBAP1$_{1\text{-}68}$ and YFP-UBAP1$_{1\text{-}92}$ in 293T cells transfected with HIV-1 proviral DNA has a dominant negative effect, resulting in approximately 5-fold inhibition of HIV-1 infectious virus release (Figure S1D). This suggests that overexpression of the UBAP1's ESCRT-I binding region disrupts the stoichiometric composition or proper localization of endogenous ESCRT-I, thus inhibiting HIV-1 budding, as previously shown for TSG101 (Martin-Serrano et al., 2003).

To identify UMA residues necessary for interaction with other ESCRT-I subunits, we tested point mutants in several conserved residues of this domain for their ability to form ESCRT-I complexes (UMA mutants M1 to M4 in Figure 1A). Given that yeast Mvb12 is involved in direct contact with Vps37 (Kostelansky et al., 2007), we tested the ability of UMA mutants to assemble into ESCRT-I complexes containing either VPS37A or VPS37B. Cells were transfected with plasmids expressing GST-TSG101, Myc-VPS28, HA-VPS37A/B, and HA-UBAP1, followed by purification using glutathione-coated beads and immunodetection of tagged ESCRT-I subunits. Alanine substitutions $L_{17}D_{18}D_{19}$/AAA and $V_{20}P_{21}F_{22}$/AAA (mutants M1 and M2) led to a complete block in ESCRT-I binding (Figure 1E, lanes 4 to 7), whereas F28A (mutant M3) did not (Figure 1E, lanes 8 and 9). Interestingly, mutation of the conserved Glu-59 (E59A, mutant M4) resulted in loss of binding to ESCRT-I when HA-VPS37B was cotransfected but not when HA-VPS37A was

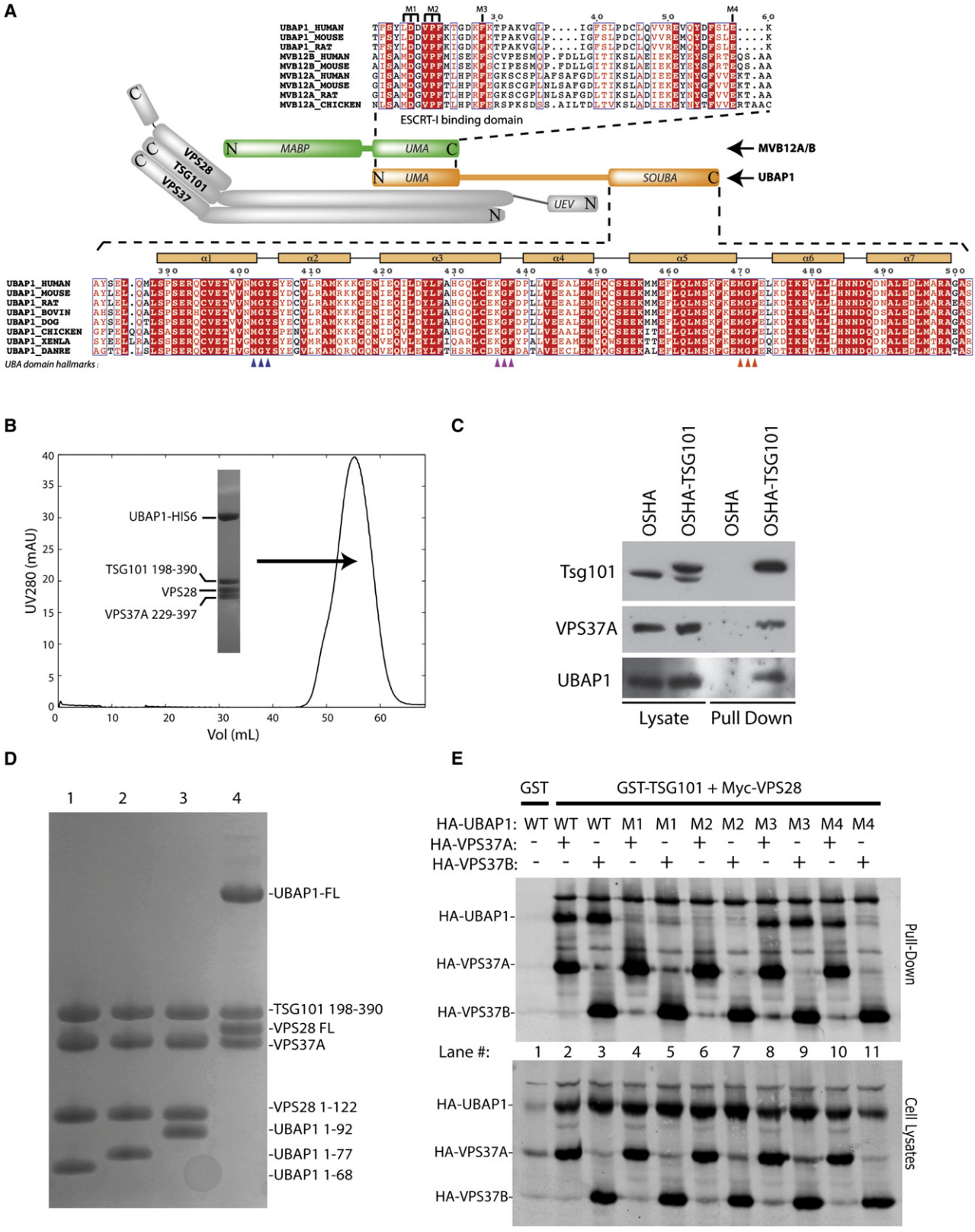

Figure 1. UBAP1 Forms a Stable Heterotetrameric Complex with ESCRT-I Subunits TSG101, VPS28, and VPS37 In Vitro and In Vivo

(A) Schematic representation of the ESCRT-I heterotetramer illustrating the putative UBAP1 arrangement relative to other ESCRT-I subunits. The top sequence alignment shows the UMA domain, also present in the C-terminal part of MVB12A and MVB12B. The bottom part shows a detailed view of the conserved

present in the protein complex (Figure 1E, lanes 10 and 11), suggesting that the VPS37 subunits interact directly with UBAP1. These results were confirmed with the HIV-1 trans-complementation assay, showing that fusing UBAP1 constructs bearing the mutations M1, M2, or M4 to Gag did not restore release of a budding deficient HIV-1 as compared to wild-type UBAP1 or M3, indicating that these residues are needed for UBAP1's interaction with ESCRT-I components (Figure S1H).

UBAP1 Functions in MVB Sorting of the Antiviral Protein Tetherin

Given the role of the ESCRT machinery in sorting ubiquitinated membrane proteins, we tested the function of UBAP1 in this process. We took advantage of the ability of several viruses to reduce cell surface expression of the antiviral protein tetherin in infected cells via the ESCRT machinery. The first experimental approach is based on HIV-1's Vpu capacity to mediate tetherin degradation. Thus, 293T cells stably expressing human tetherin (293T/tetherin) were treated with UBAP1-specific siRNA or a nontargeting control and subsequently were infected with either HIV-1 (HIV-1 wt) or Vpu-defective HIV-1 (HIV-1 delVpu) as a control. Tetherin was then immunoprecipitated, deglycosylated, and visualized by western blot. As expected, cells infected with HIV-1 wild-type have greatly reduced levels of tetherin (Figure 2A). However, this tetherin degradation was prevented in UBAP1-depleted cells infected with HIV-1 wild-type virus, and a large amount of tetherin was detected in these cells. This tetherin in UBAP1-depleted, HIV-1-infected cells is highly ubiquitinated (compare the first and second lanes in Figure 2B), suggesting that the ubiquitin-dependent sorting by the MVB pathway is inhibited in the absence of UBAP1. Tetherin levels in cells infected with a Vpu-defective HIV were high, similar to uninfected cells. Despite the restoration of tetherin levels in the UBAP1-depleted cells infected with wild-type HIV-1, viral release was not affected (Figure 2C). As expected, Vpu-defective virus release was approximately 100-fold less efficient than the wild-type virus in tetherin-expressing cells (Neil et al., 2008), and UBAP1 depletion did not affect this. These results show that, although Vpu induces targeting of tetherin for UBAP1-dependent ESCRT-mediated degradation, tetherin's ultimate destruction is not mandatory for Vpu to counteract its antiviral activity. Rather it suggests that Vpu interactions with tetherin (prior to UBAP1/ESCRT-I recruitment) inactivate the protein by committing it to an endosomal pathway from which it cannot escape back to the cell surface to inhibit virus release. Furthermore, the ability of tetherin to restrict HIV-1 delVpu release equivalently in UBAP1-depleted cells suggests that this knockdown has no significant effect on tetherin trafficking to the plasma membrane.

The second approach to determine UBAP1's function in endosomal sorting involved K5, a KSHV-encoded ubiquitin ligase that reduces cell surface expression of tetherin (Mansouri et al., 2009; Pardieu et al., 2010). We followed a knockdown approach in HT1080 cells stably expressing an HA-tetherin construct in addition to K5 (HT1080/HA-THN/K5). A quantitative western blot analysis was used to measure the total levels of HA-tetherin present in these cells. As expected, cells expressing K5 ubiquitin ligase had much lower levels of HA-tetherin (Figure 3A, lower panel). Transfection of siRNAs targeting UBAP1 prevented K5-mediated tetherin degradation, and tetherin protein levels were significantly rescued (lower panel in Figure 3A). Importantly, no changes in HA-tetherin were found when the same siRNAs were transfected into cells lacking K5. As a control, depletion of TSG101 also resulted in impairment of HA-tetherin degradation by K5 (Figure 3A). In agreement with the Vpu data, high-molecular-weight forms of tetherin, suggesting ubiquitinated species of the protein, were accumulated both in UBAP1 and TSG101 depleted cells (Figure 3A). Consistent with inhibition of endosomal sorting in UBAP1-depleted cells, HA-tetherin accumulated in intracellular punctae that display partial colocalization with the late endosomal marker CD63 and with ubiquitin (Figure 3B), a phenotype that is also observed in TSG101-depleted cells. Overall, these results show that UBAP1 is required for MVB sorting of an ubiquitinated cargo protein, namely tetherin.

UBAP1 Is Not Required for HIV-1 Budding or Cytokinesis

We also tested the role of UBAP1 in two other ESCRT-facilitated processes, namely HIV-1 budding and the resolution of the midbody during cytokinesis. Surprisingly, depletion of UBAP1 (more than 92% decrease in protein level) with two different siRNAs did not alter significantly HIV-1 budding, whereas TSG101 depletion inhibited infectious HIV-1 production as expected (Figure 4A). A similarly negative result was obtained in cytokinesis: although depletion of hIST1, an ESCRT-related protein essential for cytokinesis (Agromayor et al., 2009; Bajorek et al., 2009), resulted in cytokinesis failure and accumulation of multinucleated cells, UBAP1 depletion did not (Figure 4B). The lack of an effect of

sequence corresponding to the SOUBA domain in the C-terminal region of UBAP1 from various species. Hallmark UBA residues homologous to the conserved (M/L)-G-(Y/F) motif for the three successive UBA domains are identified by blue, pink, and orange triangles, respectively. Positions of the seven α helices mapped from the structure are shown above the alignment.

(B) Gel filtration of recombinant ESCRT-I containing UBAP1-His6 on a HiLoad 16/60 Superdex 200 column. The inset shows a Coomassie blue-stained SDS-PAGE gel of the peak fraction containing the tetrameric ESCRT-I complex including UBAP1. See also Table S1 and Figure S1.

(C) ESCRT-I protein complexes from cells stably expressing One-Strep tagged TSG101 (OSHA-TSG101) were affinity purified on a Strep-Tactin matrix and visualized by western blot. One percent of the starting cell lysate and 10% of the volume eluted from the matrix (pull-down) were analyzed by western blot with anti-TSG101, anti-VPS37A, and anti-UBAP1 antibodies. As a control for the specificity of the binding, purification from cells stably expressing an empty vector (OSHA) is also shown.

(D) Deletion analysis to determine the minimal ESCRT-I binding region on UBAP1. Recombinant UBAP1, either full length (lane 4) or N-terminal fragments (1–92, lane 3; 1–77, lane 2; or 1–68, lane 1), with a His6 tag at the C terminus were coexpressed with TSG101/VPS28/VPS37A ESCRT-I components in *E. coli* and purified by affinity chromatography and gel filtration. A Coomassie-stained SDS-PAGE of the purified complexes is shown.

(E) Coprecipitation studies to map the interaction of UBAP1 with ESCRT-I. 293T Cells were transfected with plasmids expressing GST-TSG101, Myc-VPS28, HA-VPS37A/B, and HA-UBAP1 wild-type (WT) or mutant (M1 to M4), followed by purification using glutathione-coated beads. One percent of the starting cell lysate and 10% of the volume eluted from the beads (pull-down) were analyzed by western blot with anti-HA antibody. See also Figure S1 and Table S1.

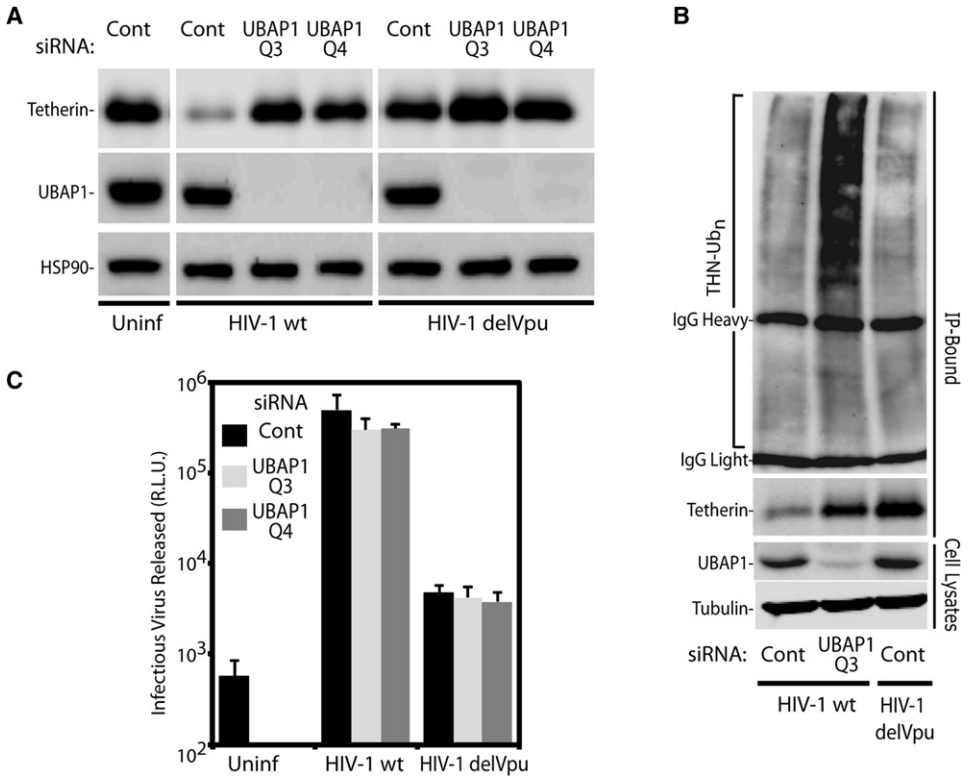

Figure 2. UBAP1 Is Essential for Degradation of Tetherin Triggered by Viral Countermeasures

(A) Tetherin was immunoprecipitated from 293T cells stably expressing tetherin. The cells were uninfected (uninf), infected with HIV-1 (HIV-1 wt), or Vpu-defective HIV-1 (HIV-1 delVpu) and were treated with irrelevant control siRNA (Cont) or with siRNAs against UBAP1 (UBAP1Q3 and UBAP1Q4). Western blots show the immunoprecipitated tetherin (upper panel), siRNA-mediated silencing of the endogenous UBAP1 (middle panel), and the HSP90 as a protein loading control (lower panel).

(B) Tetherin was immunoprecipitated from cells infected with HIV-1 (HIV-1 wt) and transfected with a plasmid expressing HA-tagged Ubiquitin and either control (cont) or UBAP1 specific siRNA (UBAP1 Q3). Tetherin ubiquitination was visualized with anti-HA antibody (top panel, THN-Ubn). As a control, the same analysis was performed in cells infected with a Vpu-defective HIV-1 (HIV-1 delVpu) and treated with an irrelevant siRNA (Cont). Bottom panels show immunoprecipitated tetherin, UBAP1 depletion and tubulin as a loading control.

(C) Infectious HIV-1 virion production was measured by inoculation of TZM-bl indicator cells and is expressed as relative luminescence units (R.L.U.). Error bars indicate the standard deviation from the mean of three independent experiments. See also Table S2.

UBAP1 depletion on cytokinesis is consistent with results recently reported (Stefani et al., 2011). One possible explanation for this lack of phenotype is that the residual amount of UBAP1 protein in siRNA treated cells might be sufficient to support ESCRT-I function but the fact that similar levels of depletion in control experiments result in endosomal defects (shown above) argues against this possibility.

UBAP1 Is a Ubiquitin-Binding ESCRT-I Subunit

The specific requirement of UBAP1 in endosomal sorting and the accumulation of ubiquitinated cargo after UBAP1 depletion from the cell suggested that UBAP1 might promote recognition of ubiquitinated cargo by ESCRT-I. We checked ubiquitin binding in solution in a label-free setup, using isothermal titration calorimetry (ITC). Using a recombinant fragment of UBAP1 consisting of the proposed UBA-containing region alone (residues 389 to 502), the Kd for the interaction with ubiquitin was about 70 μM (Figure 5A). This is on the higher-affinity end of the 20–1300 μM range commonly observed for UBA domains binding to monoubiquitin. Furthermore, this is a relatively high affinity among UBDs in the ESCRT pathway. We also measured binding of monoubiquitin to full-length UBAP1 in an ESCRT-I complex containing a TSG101 subunit with the N-terminal ubiquitin-binding UEV domain deleted in order to avoid ubiquitin binding by TSG101. The apparent Kd for the interaction between ESCRT-I/UBAP1 and monoubiquitin is about 140 μM (Figure 5B). Because many UBAs bind K48-linked diubiquitin with significantly higher affinity than monoubiquitin (typical Kds for K48-linked diubiquitin are 1–10 μM) and some UBAs bind K63-linked diubiquitin, we performed ITC experiments for label-free K48-linked or K63-linked diubiquitin binding to the SOUBA. We find that these diubiquitins bind the isolated SOUBA with an affinity comparable to that observed with monoubiquitin (Figure 5).

Structural Analysis of the C-Terminal UBA-Containing Region of UBAP1

UBAP1 has two copies of an M/L-G-F/Y motif, which have recently been shown by mutagenesis to be important for endosomal sorting (Stefani et al., 2011). To gain insight into

the organization and function of this region, we have determined its crystal structure and characterized its binding to ubiquitin in solution by NMR. Two constructs covering the UBAP1 C terminus, residues 381–502 and 389–502, produced ample protein but did not crystallize. Therefore, we used the surface entropy reduction approach (Derewenda, 2011) guided by the SERp Server (Goldschmidt et al., 2007) (http://services.mbi.ucla.edu/SER) to generate several mutants in which clusters of charged surface residues were mutated to alanine. One of these mutants, with 415-KKGE-418 mutated to AAGA, readily crystallized. The 1.65 Å resolution crystal structure of the UBA-containing C-terminal region from UBAP1 has two molecules in the asymmetric unit that are linked to each other through a disulfide bond. However, multiangle laser light scattering indicates that the molecule is a monomer in solution (data not shown). It appears that the disulfide-linked dimer is formed as the protein oxidizes during the crystallization process. The structure shows a single domain consisting of seven α helices arranged as a right-handed solenoid that contains three overlapping UBAs (UBA1, UBA2, and UBA3) (Figure 6A). We will refer to this, to our knowledge, novel domain as a solenoid of overlapping UBAs (SOUBA). The relationship of the SOUBA fold to conventional UBAs can best be described by regarding the third helix of one UBAs being also the first helix of the next UBA (Figures 6A and 6B). There are several examples of proteins that have multiple UBAs connected by linkers of low complexity that are probably structurally disordered. However, this is the first example of a rigid array of overlapping UBAs. The solenoid arrangement of the three UBAs forms a convex surface containing helices one and three from each UBA. The opposite face forms a concave surface built from the second helix from each UBA. The angles between helices in each of the UBAs are within the range observed for other UBAs. Consequently, each of the component UBAs align well with UBA structures from other proteins (Figure 6C).

Interaction of the SOUBA with Monoubiquitin

Chemical shift perturbations (CSPs) of ^{15}N-labeled ubiquitin on the addition of unlabeled SOUBA show shifts of residues in a hydrophobic patch on the surface of the ubiquitin that includes Ile44 and Val70 (Figures 7A–7C). Extensive structural analysis of diverse UBAs interacting with monoubiquitin has shown that the interaction surface on UBAs commonly includes two hydrophobic UBA patches, at the end of helix α1/loop 1 and on helix α3 (Zhang et al., 2008). Binding to K48-linked polyubiquitin typically includes an additional patch on α2 and the other side of α3. CSPs of the ^{15}N-labeled SOUBA domain on addition of three molar equivalents of unlabeled monoubiquitin indicate that each of the three overlapping UBAs is influenced by ubiquitin binding (Figures 7D–7F). The residues showing the greatest perturbation lie along the convex face of the SOUBA domain and cover an extended hydrophobic surface (Figure 7F). The signature M/L-G-F/Y motifs are located along one side of the SOUBA domain, and CSPs suggest that these residues are involved in binding ubiquitin. This is consistent with the ubiquitin binding that has been reported for UBAs from other proteins (Long et al., 2008; Ohno et al., 2005; Varadan et al., 2005; Zhang et al., 2008). The second UBA in the UBAP1 SOUBA lacks the signature motif, and instead, it has a KGF sequence in the analogous position. Nevertheless, CSP mapping suggests that this KGF motif is also involved in ubiquitin binding, because it has the highest CSP of all residues upon ubiquitin binding. In addition to residues in these signature motifs, other residues along the same face of the SOUBA also show CSPs that are greater than 0.2 ppm. For UBA1 and UBA2, almost all of these residues are at the end of the first helix and on one face of the third helix within the UBAs. Although the "di-leucine" motif in the third helix of UBA domains is a second general signature motif, the equivalent residues in SOUBA (residues 427-LF in UBA1, 461-LQ in UBA2, and 495-LM in UBA3) do not show large CSPs on ubiquitin binding. The leucine in each of these motifs is involved in helical packing in the hydrophobic core. The largest CSPs that we observe in UBA1 and UBA2 are consistent with interactions that are typical of previously characterized UBA/monoubiquitin-interacting surfaces. However, the SOUBA UBA3 has a broader distribution of residues with large CSPs on all three of its helices, including a region that has been referred to as the "backside" of the third UBA helix. This could be due to conformational changes in the third UBA on ubiquitin binding, or due to an additional ubiquitin-binding site.

Paramagnetic relaxation enhancement (PRE) measurements were performed to probe directly the binding of each of the three UBA domains in SOUBA to ubiquitin and to investigate the relative orientation of SOUBA and monoubiquitin in the complex. A paramagnetic spin label (SL) was attached to a cysteine residue replacing a lysine in ubiquitin, in order to induce a strong signal attenuation in nuclei that are near the SL. Figure 7 depicts signal attenuations in the SOUBA in a complex with ubiquitin spin-labeled at either residue 6 (K6C mutant, Figures 7G and 7H) or residue 48 (K48C mutant, Figures 7I and 7J), compared to the same complexes in which the SL probe is inactivated by ascorbic acid. The results clearly show three regions of significant attenuation for K6C-SL ubiquitin (corresponding to the end of helix 1 and the loop between helix 1 and helix 2; the end of helix 3 and the loop between helix 3 and helix 4; the end of helix 5 and the loop between helix 5 and helix 6). Four regions of attenuation were observed on SOUBA with the K48C-SL ubiquitin (the loop between helix 1 and helix 2; the end of helix 3 and the loop between helix 3 and helix 4; the end of helix 5 and the loop between helix 5 and helix 6; and the end of helix 7). The additional signal attenuation observed for K48C-SL would suggest that the spin-label in K48C ubiquitin is close in space to two regions of each UBA motif. No paramagnetic effects were observed with D39C and S57C spin-labeled monoubiquitins. A model of the SOUBA bound to three monoubiquitin molecules reveals how the SL could achieve the effects observed (Figures 7H and 7J). The PRE measurements appear to match those observed by Zhang et al. (2008) when SL were used to investigate binding of the UBA domain of ubiquilin-1 with monoubiquitin. It is worth noting that the attachment of the SL to the mutant ubiquitins did not affect their ability to interact with SOUBA. Comparison of the NMR spectra of ^{15}N-SOUBA in the presence of WT-Ub and SL-Ub (K6C, K39C, K48C, and K57C) revealed that the same CSP and relaxation regimes were observed.

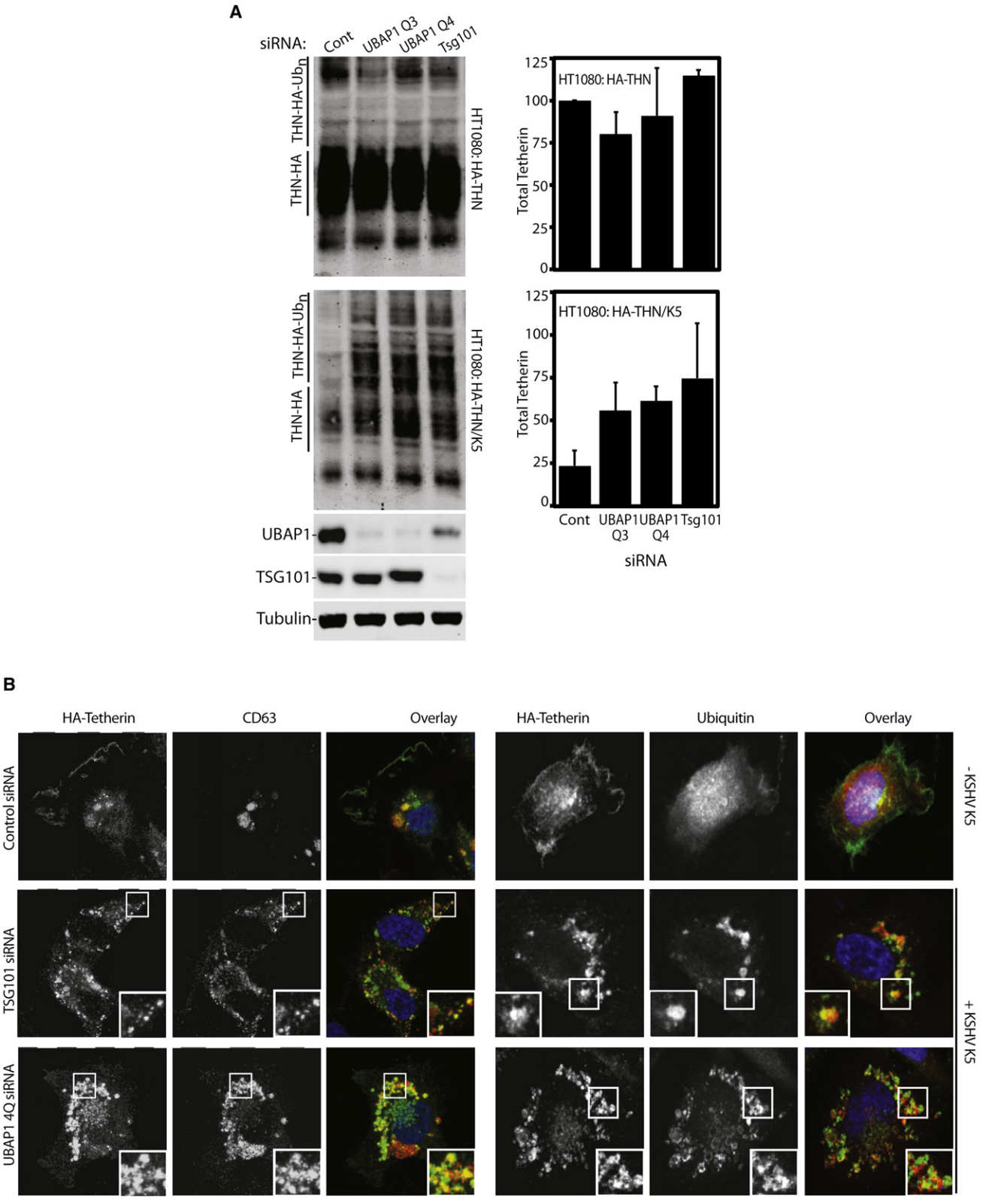

Figure 3. UBAP1 Depletion Prevents K5-Mediated Tetherin Degradation

(A) Western blots of cell lysates from HT1080 cells stably expressing HA-tetherin alone (HT1080:HA-THN) or in combination with K5 (HT1080:HA-THN/K5) and treated with siRNAs against an irrelevant control (cont), TSG101 or UBAP1. THN-HA was detected with anti-HA antibody, with tubulin as a loading control and visualized using Li-Cor fluorescently coupled 650 and 800 nm secondary antibodies. The graphs show the percentage of mature tetherin levels, normalized to

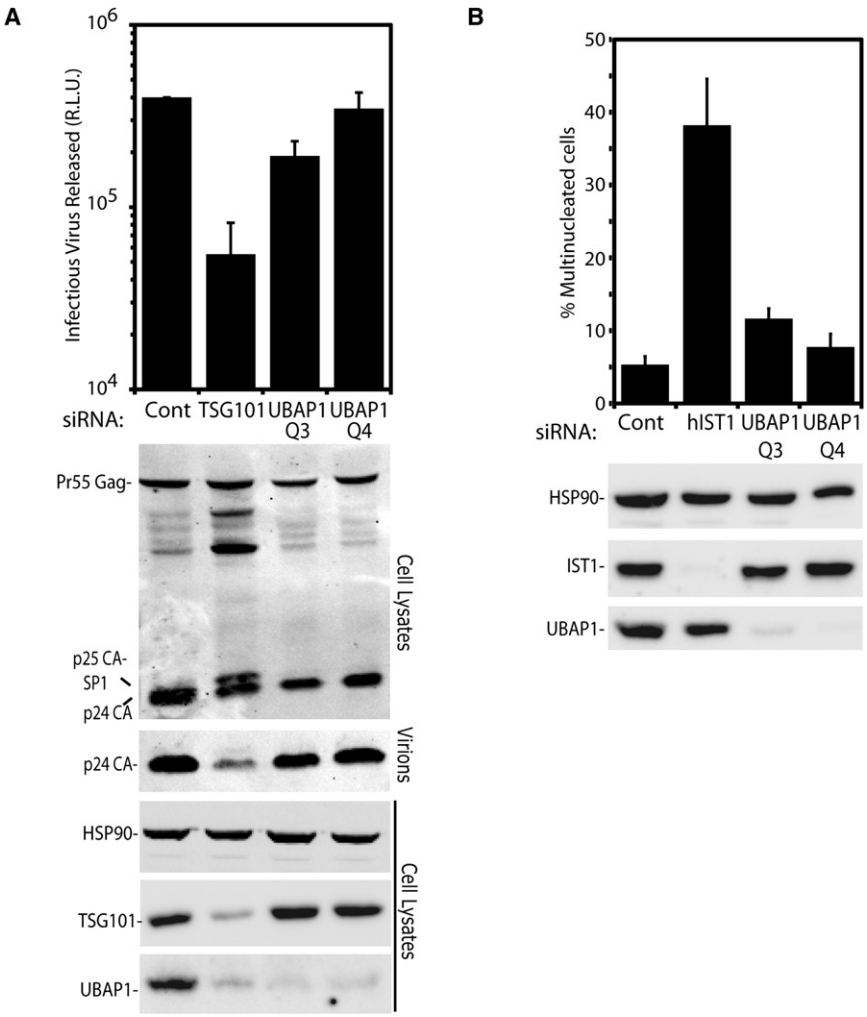

Figure 4. Role of UBAP1 in ESCRT-I Mediated HIV-1 Release and Cytokinesis

(A) Infectious virus release upon coexpression of an HIV-1 provirus with an irrelevant siRNA (Cont), siRNA against TSG101 or two different siRNAs against UBAP1. Western blots show intracellular TSG101, UBAP1, and HSP90 (protein loading control) as well as intracellular (cell lysates) and virion-associated (virions) HIV Gag protein.

(B) Quantification of cells with multiple nuclei after treatment with the irrelevant control siRNA (Cont), siRNA against hIST1 (positive control), or with either of the two different siRNAs against UBAP1. As for (A), western blots show siRNA-mediated silencing of the endogenous hIST1 and UBAP1 and HSP90 as a protein loading control. Error bars indicate the standard deviation from the mean of three independent experiments.

DISCUSSION

The results presented in this study demonstrate that recombinant UBAP1 assembles with TSG101, VPS28, and VPS37 into a complex with a 1:1:1:1 stoichiometry and, importantly, this interaction is also observed in vivo with endogenous UBAP1 and physiological levels of the remaining ESCRT-I subunits. Codepletion of TSG101 and UBAP1 in cells treated with siRNA against TSG101 suggests that endogenous UBAP1 is stabilized by its interaction with TSG101. Moreover, UBAP1's ability to functionally recruit the ESCRT machinery in a TSG101-dependent manner provides further evidence for a functional link between UBAP1 and ESCRT-I. On the basis of these observations, we propose that UBAP1 is a stable subunit of human ESCRT-I. While this manuscript was in preparation, Woodman and colleagues have reported findings that are entirely consistent with our results (Stefani et al., 2011).

In a recombinant system, UBAP1 can form heterotetrameric complexes with TSG101, VPS28, and each of the four VPS37 subunits. Our results also show that transiently transfected VPS37A and VPS37B form UBAP1-containing complexes in 293T cells. Similarly, a recent study of UBAP1 expressed in HeLa cells showed complex formation with VPS37A. However, the same study did not detect formation of UBAP1 complexes with VPS37C (Stefani et al., 2011). This could mean that additional factors such as posttranslational modifications could modulate the association between UBAP1 and VPS37 subunits in cells. Little is known about the tissue distribution and cellular abundance of different VPS37 subunits or competing MVB12A and MVB12B, all of which could affect association with UBAP1.

UBAP1's function is exclusively required for degradation of ubiquitinated endosomal cargo but not for other ESCRT-I-mediated processes such as midbody abscission or viral budding. More specifically, we show that UBAP1-containing ESCRT-I complexes are parasitized by viral immunomodulatory proteins that target host membrane proteins for endosomal degradation, in particular the targeted destruction of the antiviral protein tetherin by both HIV-1 Vpu and KSHV K5 ubiquitin ligase. The essential role of UBAP1 in K5 function is entirely consistent with previous findings showing the ESCRT-dependent destruction of tetherin via a single lysine in its cytoplasmic tail (Mansouri et al., 2009; Pardieu et al., 2010). In contrast, the pathway involved in tetherin degradation and antagonism by Vpu has

tubulin loading. Error bars indicate the standard deviation from the mean of three independent experiments. Lower panels show depletion of TSG101 and UBAP1, and tubulin as a loading control.

(B) Confocal immunofluorescence showing localization of tetherin, CD63, and ubiquitin in cells treated with either control siRNA-, TSG101-, or UBAP1-specific siRNA. A higher magnification of the boxed areas is shown in TSG101- and UBAP1-treated panels. In the overlay panels, DNA is shown in blue, tetherin in green, and CD63 or ubiquitin in red. See also Table S3.

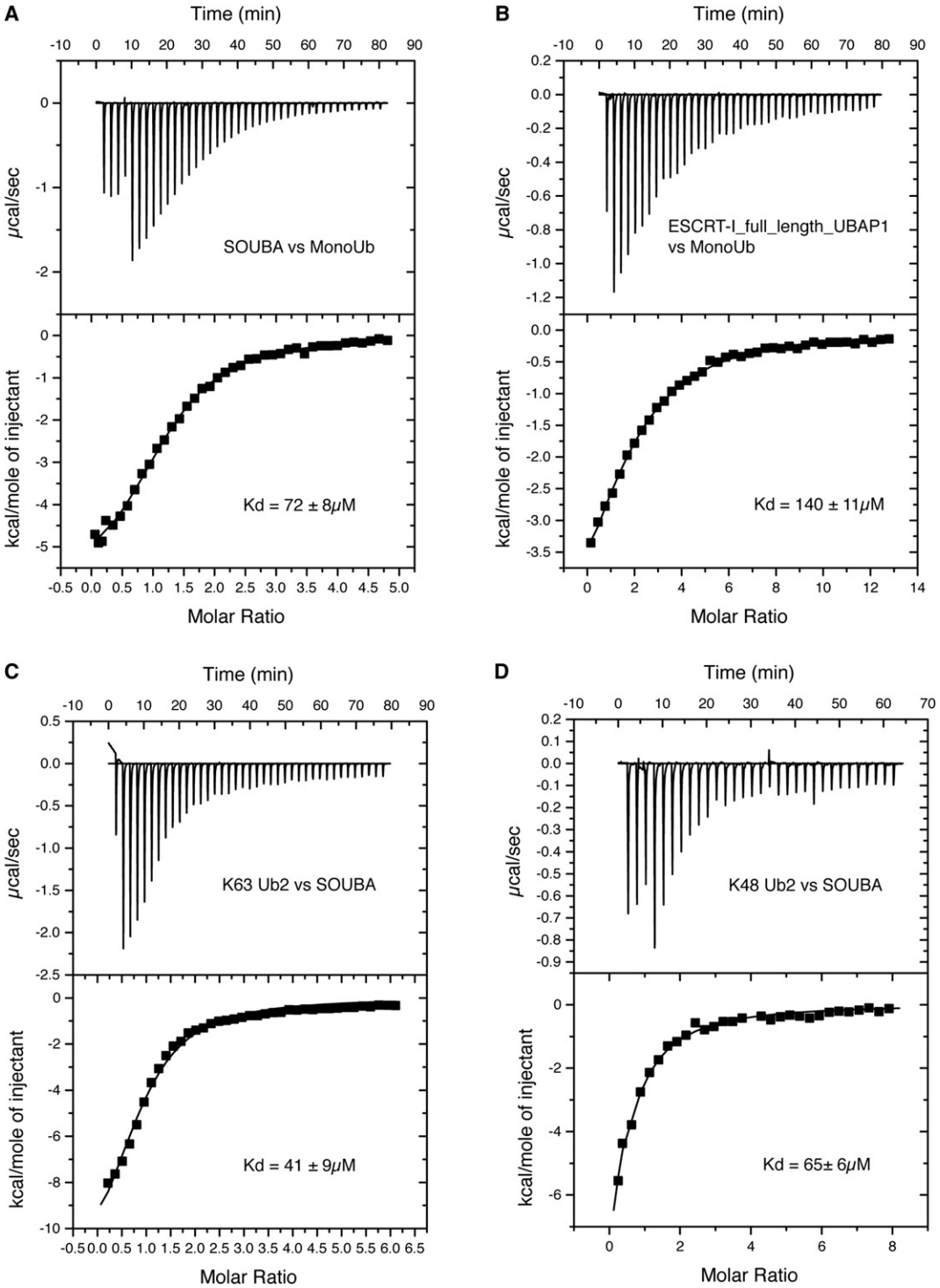

Figure 5. Ubiquitin Binding to UBAP1

Binding of human UBAP1 SOUBA domain (389–502) or UBAP1-containing ESCRT-I complex consisting of full-length UBAP1, VPS28 (full-length), TSG101 (198–390, i.e., lacking the UEV domain) and VPS37A (229–397, i.e., lacking the UEV domain). The experimental data (squares) were fit using a binding model for a single set of independent sites. The mean Kd and standard deviation were calculated from three independent measurements.

(A) ITC titration of monoubiquitin into a cell containing the UBAP1 SOUBA domain (389–502), with the thermogram shown on top and integrated peaks shown on bottom.

(B) ITC titration of monoubiquitin into a cell containing ESCRT-I with full-length UBAP1: thermogram (top) and integrated peaks (bottom).

(C) ITC titration of the SOUBA domain into a cell containing K63 diubiquitin: thermogram (top) and integrated peaks (bottom).

(D) ITC titration of the SOUBA domain into a cell containing K48 diubiquitin: thermogram (top) and integrated peaks (bottom).

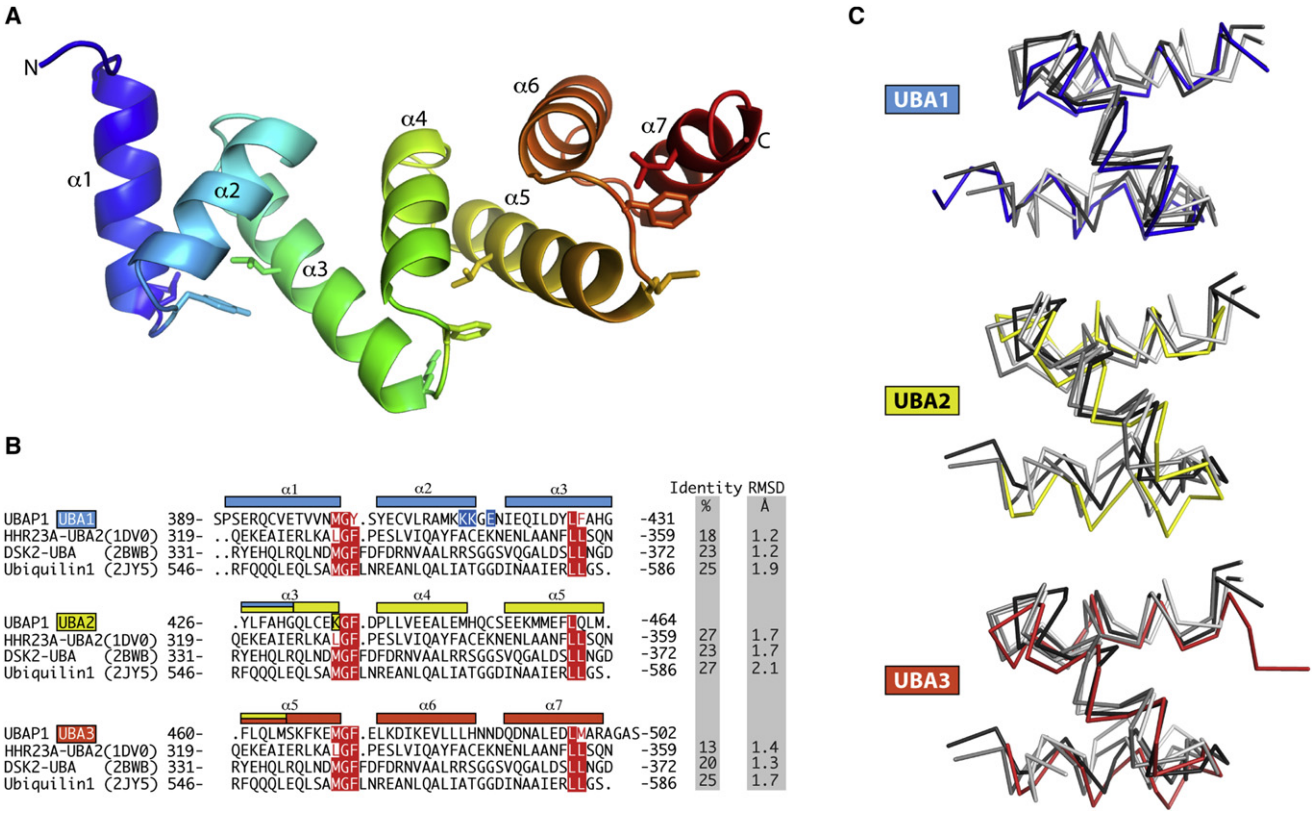

Figure 6. Overlapping UBAs Build a Compact SOUBA Domain

(A) Overview of UBAP1 SOUBA domain (389–502), showing the tandem arrangement of the three overlapping UBA domains rainbow colored from N terminus (blue) to C terminus (red).

(B) Sequence alignment of each of the three UBA domains of UBAP1 with three other well-characterized UBA domains. UBA signature motif residues are shown in red and represented as sticks in (A). Residues mutated in the SOUBA crystal structure are shown with a blue background.

(C) Structural alignment of each of the three UBAP1 UBA domains with the three previously reported UBA domains present in the sequence alignment (B), namely Ubiquilin1 (2JY5) in light gray, DSK2 UBA (2BWB) in medium gray, and HHR23A UBA2 (1DV0) in dark gray. See also Table 1.

been less clear (Martin-Serrano and Neil, 2011). Although early studies suggested that Vpu induced proteasomal degradation of tetherin (Goffinet et al., 2009), more recent reports show that, in HIV-1-infected cells, tetherin is targeted to lysosomes (Douglas et al., 2009; Iwabu et al., 2009; Mitchell et al., 2009) and its inactivation is dependent on an association with Hrs (ESCRT-0) (Janvier et al., 2011). Our demonstration that UBAP1 is essential for Vpu-induced tetherin destruction shows that tetherin is degraded in the MVB pathway rather than by the proteasome. However, it is also clear that tetherin degradation is not a prerequisite for Vpu activity. Even though tetherin is not degraded in UBAP1-depleted cells and accumulates in endosomes, Vpu is still able to efficiently counteract tetherin's antiviral activity.

A Model of Ubiquitin Binding to the SOUBA

At a mechanistic level, we demonstrate the ability of UBAP1 to promote the interaction of ESCRT-I with ubiquitin. A UBAP1-containing ESCRT-I complex is able to bind ubiquitin via the SOUBA domain located in the C-terminal region of UBAP1. The importance of this interaction is suggested by a reported frameshift mutation that precisely removes the SOUBA domain (S391Afs21X) in one case of familial frontotemporal lobar degeneration (Rollinson et al., 2009). Accordingly, mutations in the SOUBA domain disrupt sorting of endosomal cargo (Stefani et al., 2011). To our knowledge, the structure of this region shows a novel ubiquitin-binding fold, the SOUBA domain. The ability of UBAP1 to bind monoubiquitin may be important for the function of the ESCRT-I pathway, because half of conjugated ubiquitin is in the form of monoubiquitin or endcaps of polyubiquitin chains (Ziv et al., 2011), and monoubiquitination is a sufficient signal for vacuolar/lysosomal traffic (Stringer and Piper, 2011).

By superimposing the SOUBA domain on different UBAs whose structures have been solved in complexes with monoubiquitin, it is possible to generate a model of the SOUBA bound to ubiquitin. In this model, SOUBA can easily accommodate three monoubiquitins adjacent to each other, on the convex face of the domain (Figure 8). Each of the three UBAs engages with the hydrophobic patch of ubiquitin that includes Ile44 and Val70. Both the CSPs observed for ^{15}N-labeled ubiquitin upon addition of an excess of unlabelled SOUBA (Figure 7C) and the relaxation induced by a paramagnetic probe attached to ubiquitin in complex with the SOUBA (Figures 7G–7J), are

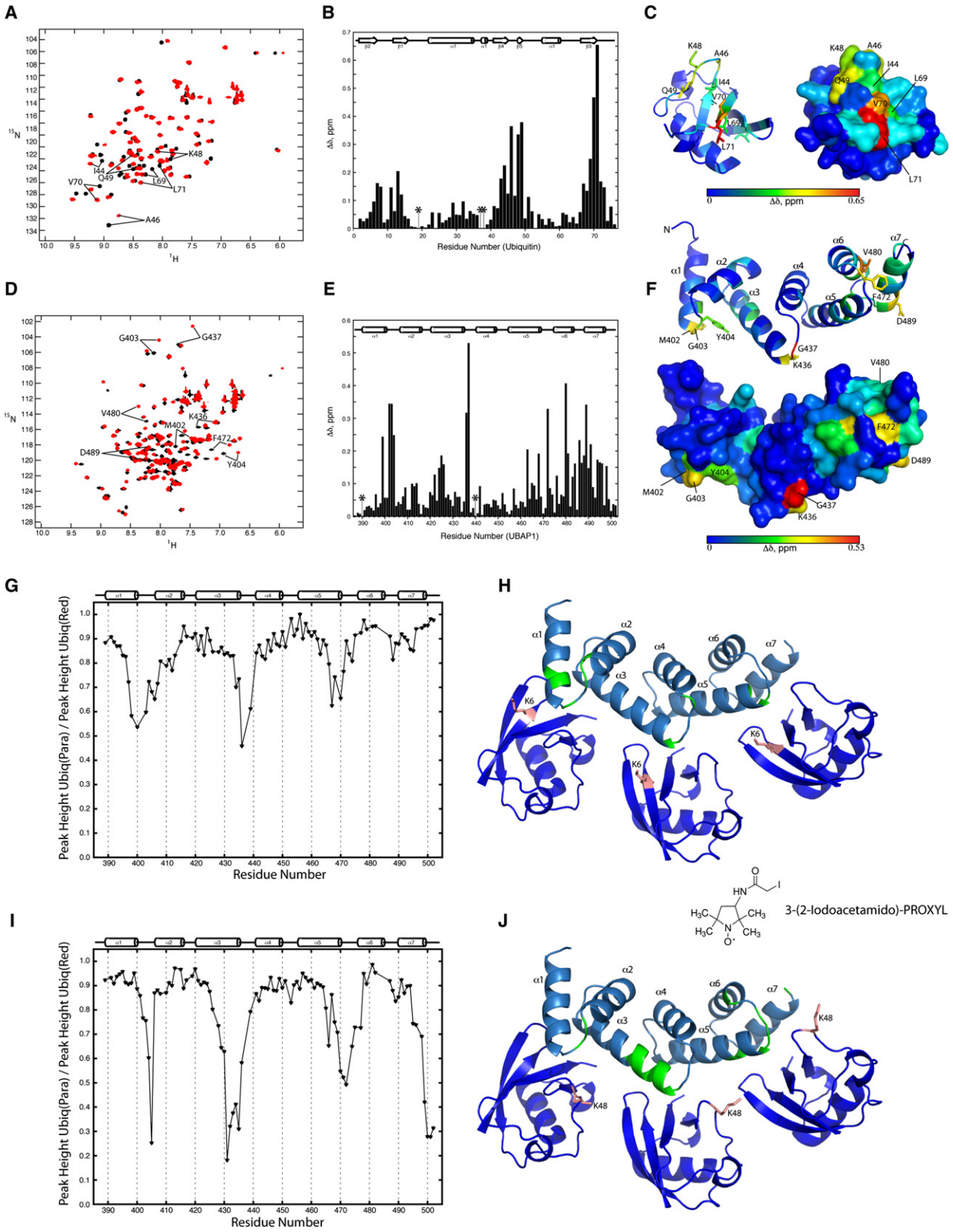

Figure 7. UBAP1 Interactions with Monoubiquitin Detected by NMR Chemical Shift Perturbations

(A) Overlay of HSQC spectra of ^{15}N-labeled monoubiquitin in the absence (black) and presence (red) of 2.5 molar equivalents of unlabeled UBAP1 SOUBA. Amide resonances with significant chemical shift changes have been annotated.

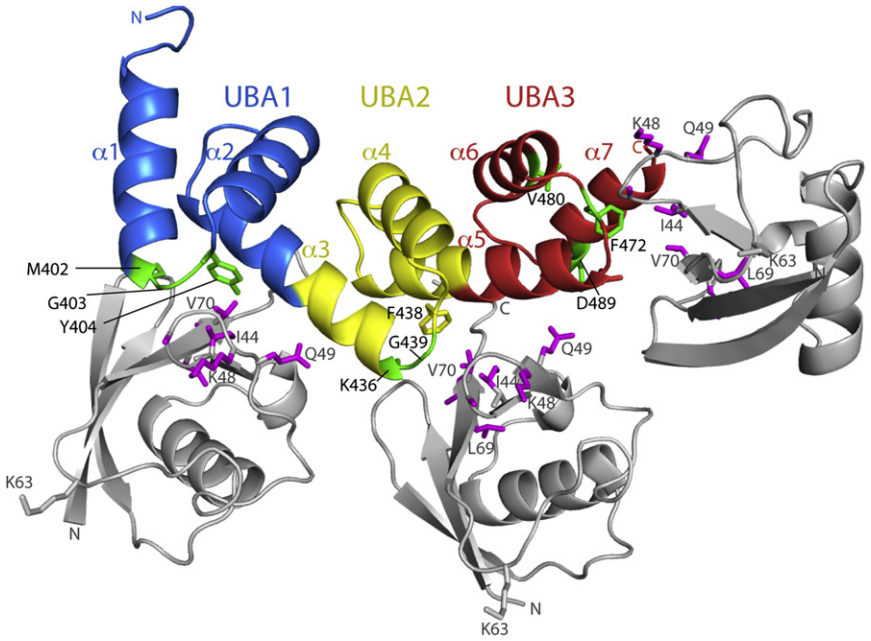

Figure 8. Model of Monoubiquitin Binding to the UBAP1 SOUBA

The UBA1, UBA2, and UBA3 are colored blue, yellow, and red, respectively. UBAP1 residues showing a CSP >0.2 ppm upon binding to monoubiquitin are shown as green sticks. Three monoubiquitins have been docked on the basis of superposition of each UBA domain with the ubiquilin UBA domain in complex with ubiquitin (PDB ID 2JY6). Ubiquitin residues with CSPs >0.2 ppm upon binding to the UBAP1 SOUBA are shown as magenta sticks. The PRE and CSP measurements show that all three UBAs bind ubiquitin. The gradual addition of substoichiometric amounts of ubiquitin causes chemical shifts for residues in all three UBA motifs, suggesting that there is no preference for the binding of ubiquitin to one site versus another. The NMR data indicated that binding occurs at each of the sites, but cannot distinguish whether one, two, or three molecules are bound at the same time. Nevertheless, there appear to be no steric clashes in the model that would prevent all three ubiquitins binding simultaneously.

consistent with this model of ubiquitin binding. In this model, the orientations of the ubiquitins would not appear to allow the ubiquitins occupying adjacent sites on the SOUBA to be linked to each other either through K48 or K63 isopeptide bonds. This is consistent with our ITC results suggesting that these linkages bind no better than monoubiquitin to the SOUBA (Figure 5). Previous NMR studies of UBAs from several different proteins in the presence of K48-linked diubiquitin suggest a second binding site for the second ubiquitin involving a separate interface on the UBA (Sims et al., 2009; Song et al., 2009; Trempe et al., 2005; Varadan et al., 2005). The solenoid arrangement of the SOUBA would appear to block this type of binding, at least for the first two UBAs.

The NMR data demonstrate that each of the three UBAs is involved in ubiquitin binding, but it remains to be shown whether all three UBAs can bind ubiquitin simultaneously. We tried investigating the affinity of each UBA for ubiquitin by generating double point mutants in the (M/K)G(F/Y) motifs: we constructed three mutant SOUBAs, each having only one functional UBA. However, NMR HSQC spectra revealed that each of these mutants was unstructured, preventing further study. ITC results for the full-length UBAP1 in the ESCRT-I complex show a lower affinity for monoubiquitin than the isolated SOUBA domain. This might suggest a more restricted access to the SOUBA in the ESCRT-I complex. Because of the difficulties associated with producing sufficient quantities of diubiquitin, it was not possible to determine the affinity of UBAP1-containing ESCRT-I for K63-linked and K48-linked diubiquitin by ITC.

Because the shape of the SOUBA domain and the interaction sites mapped by NMR lead to a model in which three bound ubiquitins are aligned and close enough to be attached via some other type of linkage than K48 or K63, it will be exciting to examine UBAP1 affinities for other polyubiquitin linkages. Alternatively, in addition to providing a grip on monoubiquitinated cargo, the SOUBA domain could enable avid interaction with multiply monoubiquitinated cargoes, or monoubiquitinated clustered cargoes. All of these are frequent passengers in the ESCRT-dependent sorting to MVBs.

EXPERIMENTAL PROCEDURES

Plasmid Construction

Human *UBAP1* was amplified by PCR from IMAGE clone 40011243. All deletions and point mutant derivatives were generated by PCR in a similar way. All of the constructs used in the study are listed in Table S1.

Expression and Purification of Recombinant ESCRT-I Proteins

Genes coding for human VPS28 (full length or 1-122), TSG101 (198-390), VPS37A (229-397), and UBAP1 (full length or deletion variants with a C-terminal His6-tag) were cloned in a polycistronic coexpression vector as described

(B) Plot of chemical shift perturbations (CSPs) for ^{15}N-labeled monoubiquitin as a function of residue number. Proline residues (for which no data are available) have been assigned a value of 0 ppm and are marked by an asterisk.
(C) CSPs for monoubiquitin mapped onto its structure.
(D) Overlay of HSQC spectra of ^{15}N-labeled SOUBA in the absence (black) and presence (red) of three molar equivalents of unlabeled monoubiquitin.
(E) Plot of CSPs for ^{15}N-labeled SOUBA as a function of residue number.
(F) CSPs for SOUBA mapped onto its structure.
(G–J) Paramagnetic relaxation enhancement effects in the SOUBA/Ub complex induced by the spin label attached to the K6C (G) and K48C (I) mutant ubiquitins. The graphs plot experimental PREs observed in SOUBA upon addition of the SL-ubiquitin against residue number. Significant paramagnetic effects are illustrated in green on a model of SOUBA bound to three molecules of ubiquitin for K6C-SL (H) and K48C-SL (J). The side chains of K6 and K48 (mutated to a Cys for spin labeling) are shown as salmon sticks.

elsewhere (Teo et al., 2006). The constructs expressed are listed in Table S1. The expression and purification was performed as described in Supplemental Experimental Procedures.

Expression and Purification of SOUBA

Human SOUBA domain (UBAP1 389-502) either wild-type or containing the K415A, K416A, and E418A triple mutation was cloned in the pOPTH(tev) expression vector downstream of an N-terminal His_6-tag followed by a TEV protease cleavage site. The expression and purification were performed as described in Supplemental Experimental Procedures.

Crystallization, Data Collection, and Refinement of SOUBA

Seleno-methionine crystals of the human SOUBA domain (UBAP1 389-502) with the K415A, K416A, and E418A triple mutation designed to reduce surface enthropy charge (using SERp server: http://services.mbi.ucla.edu/SER/) were used for crystallization (see Supplemental Experimental Procedures and Table 1).

Isothermal Titration Calorimetry

Assays were performed using a Microcal ITC200, in 20 mM Tris-HCl (pH 7.5), 100 mM NaCl, and 1 mM TCEP. The ITC cell contained either the SOUBA domain (UBAP1(389-502)) at 150 μM or full-length UBAP1 associated with VPS28 (full-length), TSG101 (198-390, i.e., lacking the UEV domain), and VPS37A (229-397, i.e., lacking the UEV domain), at 75 μM and was titrated with 38 injections of monoubiquitin (SIGMA U6253) at 3 mM. Assays on K63-linked and K48-linked diubiquitins were performed having diubiquitin in the cell at 100 μM, titrated by 38 injections of the SOUBA domain at 2.3 mM. Data were fit with a binding model employing a single set of independent sites.

Expression and purification of paramagnetically labeled monoubiquitin was performed as described in Supplemental Experimental Procedures.

NMR Spectroscopy

Wild-type SOUBA (UBAP1_389-502) samples prepared for NMR spectroscopy experiments were typically 1.0 mM in 90% H2O and 10% D2O in PBS with 10 mM DTT. All spectra were acquired with either a Bruker Advance 700 or a DRX600 spectrometer at 20°C, and referenced relative to external sodium 2,2-dimethyl-2-silapentane-5-sulfonate (DSS) for proton and carbon signals, or liquid ammonium for nitrogen. Assignments were obtained using standard NMR methods with $^{13}C/^{15}N$-labeled and ^{15}N-labeled samples. Backbone assignments were obtained using the following standard set of 2D and 3D heteronuclear spectra: ^{1}H-^{15}N HSQC, HNCACB, CBCA(CO)NH, HACACO, HNCO, CCCONH, and ^{1}H-^{13}C HSQC. HSQC titrations were performed using 0.5 mM ^{15}N-labeled UBAP1 and varying concentrations of unlabeled ubiquitin. Similar titrations were performed with 0.3 mM ^{15}N-labeled ubiquitin and unlabeled UBAP1. Amide CSPs were calculated as follows:

$$\Delta\delta = \left[(\Delta\delta_H)^2 + \left(\frac{\Delta\delta_N}{5}\right)^2\right]^{1/2},$$

where $\Delta\delta_H$ and $\Delta\delta_N$ are the observed chemical shift changes for ^{1}H and ^{15}N, respectively. Paramagnetic experiments were performed using sample containing 0.3 mM SOUBA and 0.3 mM chemically modified monoubiquitin.

Generation of Stable Cell Lines

HT1080/THN-HA K5 cells have been described elsewhere (Pardieu et al., 2010). To generate HeLa OSHA-TSG101, 293T cells were transfected with 100 ng of pHIT-VSVG, 700 ng of MLV-GagPol, and 200 ng of the pCMS28 retroviral packaging vector for 48 hr. Viral-containing supernatants were collected and used to transduce HeLa. Selection with puromycin (200 ng/ml) was applied 48 hr later, and cells were passaged under continual selection.

Coprecipitation Assays

These were performed as described in Supplemental Experimental Procedures.

Table 1. Crystallographic Statistics

	Se-Met Crystal For Structure Refinement
Data collection	
Space group	P1
Cell dimensions	
a, *b*, *c* (Å)	34.40, 43.48, 59.41
α, β, γ (°)	102.57, 96.47, 113.24
Wavelength	0.98
Resolution (Å)	38.3 (1.65)[a]
R_{sym} or R_{merge}	0.055 (0.54)
I / σI	9.9 (1.9)
Completeness (%)	95.9 (94.4)
Redundancy	3.9 (3.9)
Refinement	
Resolution (Å)	1.65
No. reflections	36253
R_{work} / R_{free}	0.1494/0.1907
No. atoms	2101
Protein	1822
Ligand/ion	37
Water	242
B-factors	34
Protein	32
Ligand/ion	66
Water	47
R.m.s deviations	
Bond lengths (Å)	0.0165
Bond angles (°)	1.536

[a]The values in parentheses are for the highest resolution shell, 1.74 Å to 1.65 Å.

HIV Infectivity Assays

Cells (293T) were transfected with 250 ng of the YFP fusions and 300 ng of pNL/HXB using polyethylenimine. Culture supernatants, collected 48 hr after transfection, were clarified by low-speed centrifugation, and particles present in 250 μl were obtained by centrifugation through a 20% sucrose cushion at 14,000 rpm for 2 hr. Viral protein content in cell and particle lysates was analyzed by western blotting with an anti-Gag antibody. Alternatively, indicator HeLa-TZM-bl cells ($CD4^+$, $CXCR4^+$, $CCR5^+$, HIV-1 LTR- LacZ) (Derdeyn et al., 2000) were infected with 1 μl of supernatant and 48 hr later, β-galactosidase activities in cell lysates were measured using the chemiluminescent detection reagent Galacto-Star (Applied Biosystems).

To assay inhibition of viral production by siRNA-mediated depletion of cellular UBAP1, 293T cells were initially transfected with 50 pmol of siRNA using Dharmafect1 (Dharmacon) and were split the next day. Forty-eight hours after initial transfection, cells were cotransfected with 50 pmol of siRNA and the HIV proviral plasmid using lipofectamine 2000 (Invitrogen). The detailed sequence of the siRNA oligos used is provided in Table S2. The plasmids and method for the trans-complementation assay have been described previously (Martin-Serrano et al., 2001).

Multinucleation Assays

The multinucleation assays for HeLa cells were performed as described in Supplemental Experimental Procedures.

Vpu-Mediated Tetherin Degradation Assay

Subconfluent 293T cells stably expressing tetherin were seeded in a six-well plate and 2 hr after plating were transfected with 50 pmol of siRNA using

Dharmafect-1 (Dharmacon). Forty-eight hours later, cells were reseeded and transfected again with 50 pmol of siRNA. Six hours after the second RNAi transfection, cells were infected with HIV-1 wild-type or Vpu-deficient at an MOI of 2. At 48 hr after infection, the cells were lysed on ice for 30 min in buffer containing 50 mM Tris-HCl (pH 7.4), 150 mM NaCl, complete protease inhibitors (Roche), and 1% digitonin (Calbiochem). After removal of the nuclei, the resulting supernatants were incubated with 1 μg/ml mouse anti-tetherin (eBiosciences) for 2 hr at 4°C before addition of 40 μl of protein G-agarose (Invitrogen) for a further 3 hr. The beads were then washed four times in lysis buffer containing 0.1% digitonin. After the final wash, beads were resuspended in water and treated with the protein deglycosylation kit from New England Biolabs under denaturing conditions as specified by the supplier. Samples were resuspended in SDS-PAGE loading buffer and cell lysates and immunoprecipitates were then western blotted for tetherin using rabbit anti-BST2 (kindly provided by K. Strebel through the NIH ARRP).

K5-Mediated Tetherin Degradation Assay

Total tetherin-HA levels were analyzed by western blot of cell lysates after siRNA treatment of HT1080 cells stably expressing HA-tetherin alone (HT1080:HA-THN) or in combination with K5 (HT1080:HA-THN/K5). Tetherin-HA was detected with anti-HA antibody, with tubulin as a loading control, and visualized using Li-Cor fluorescently coupled 650 and 800 nm secondary antibodies.

Western Blot Analysis

Cell extracts, as well as virion lysates, were separated on 10% or 12% polyacrylamide gels and transferred to nitrocellulose membranes. A list of antibodies used is provided in Table S3.

Immunofluorescence Microscopy

HT1080:HA-THN and HT1080:HA-THN/K5 cells were treated with siRNA as described above for the multinucleation assays. At 24 hr after transfection, the cells were fixed in 4% paraformaldehyde, permeabilized in 0.1% Triton X-100, and immunostained using a rabbit anti-HA antibody (Rockland) and mouse anti-CD63 (Developmental studies Hybridoma Bank. University of Iowa) or mouse anti-Mono and polyubiquitylated conjugates (clone FK2) (Enzo Life Sciences) followed by the appropriate donkey secondary antibodies coupled to Alexa 488 and 594 fluorophores (Invitrogen). Nuclei were visualized using Hoechst 33258 and coverslips were mounted in Mowiol. Images were taken using a Leica AOBS SP2 confocal microscope.

SUPPLEMENTAL INFORMATION

Supplemental Information includes one figure, three tables, and Supplemental Experimental Procedures and can be found with this article online at doi:10.1016/j.str.2011.12.013.

ACKNOWLEDGMENTS

J.M.S. is funded by the Lister Institute, the EMBO Young Investigator Programme, and the Medical Research Council (grant G0802777). J.M.S. and M.A. are funded by the Wellcome Trust (grant WT093056MA). R.L.W. is funded by the Wellcome Trust (grant 083639/Z/07/Z) and the Medical Research Council (file reference U105184308). We thank Michael Hadders for comments on the manuscript, Chris Johnson for help with ITC, and Stephen McLaughlin for help with Octet measurements. We thank David Cobessi and Elspeth Gordon for help with data collection at ESRF beamlines BM30A and ID23-1, respectively.

Received: August 22, 2011
Revised: December 13, 2011
Accepted: December 30, 2011
Published: March 6, 2012

REFERENCES

Agromayor, M., Carlton, J.G., Phelan, J.P., Matthews, D.R., Carlin, L.M., Ameer-Beg, S., Bowers, K., and Martin-Serrano, J. (2009). Essential role of hIST1 in cytokinesis. Mol. Biol. Cell *20*, 1374–1387.

Bache, K.G., Slagsvold, T., Cabezas, A., Rosendal, K.R., Raiborg, C., and Stenmark, H. (2004). The growth-regulatory protein HCRP1/hVps37A is a subunit of mammalian ESCRT-I and mediates receptor down-regulation. Mol. Biol. Cell *15*, 4337–4346.

Bajorek, M., Morita, E., Skalicky, J.J., Morham, S.G., Babst, M., and Sundquist, W.I. (2009). Biochemical analyses of human IST1 and its function in cytokinesis. Mol. Biol. Cell *20*, 1360–1373.

Bartee, E., McCormack, A., and Früh, K. (2006). Quantitative membrane proteomics reveals new cellular targets of viral immune modulators. PLoS Pathog. *2*, e107.

Baumgärtel, V., Ivanchenko, S., Dupont, A., Sergeev, M., Wiseman, P.W., Kräusslich, H.G., Bräuchle, C., Müller, B., and Lamb, D.C. (2011). Live-cell visualization of dynamics of HIV budding site interactions with an ESCRT component. Nat. Cell Biol. *13*, 469–474.

Bucher, P., Karplus, K., Moeri, N., and Hofmann, K. (1996). A flexible motif search technique based on generalized profiles. Comput. Chem. *20*, 3–23.

Carlton, J.G., and Martin-Serrano, J. (2007). Parallels between cytokinesis and retroviral budding: a role for the ESCRT machinery. Science *316*, 1908–1912.

Clague, M.J., and Urbé, S. (2010). Ubiquitin: same molecule, different degradation pathways. Cell *143*, 682–685.

de Souza, R.F., and Aravind, L. (2010). UMA and MABP domains throw light on receptor endocytosis and selection of endosomal cargoes. Bioinformatics *26*, 1477–1480.

Derdeyn, C.A., Decker, J.M., Sfakianos, J.N., Wu, X., O'Brien, W.A., Ratner, L., Kappes, J.C., Shaw, G.M., and Hunter, E. (2000). Sensitivity of human immunodeficiency virus type 1 to the fusion inhibitor T-20 is modulated by coreceptor specificity defined by the V3 loop of gp120. J. Virol. *74*, 8358–8367.

Derewenda, Z.S. (2011). It's all in the crystals…. Acta Crystallogr. D Biol. Crystallogr. *67*, 243–248.

Dikic, I., Wakatsuki, S., and Walters, K.J. (2009). Ubiquitin-binding domains—from structures to functions. Nat. Rev. Mol. Cell Biol. *10*, 659–671.

Douglas, J.L., Viswanathan, K., McCarroll, M.N., Gustin, J.K., Früh, K., and Moses, A.V. (2009). Vpu directs the degradation of the human immunodeficiency virus restriction factor BST-2/Tetherin via a betaTrCP-dependent mechanism. J. Virol. *83*, 7931–7947.

Eastman, S.W., Martin-Serrano, J., Chung, W., Zang, T., and Bieniasz, P.D. (2005). Identification of human VPS37C, a component of endosomal sorting complex required for transport-I important for viral budding. J. Biol. Chem. *280*, 628–636.

Goffinet, C., Allespach, I., Homann, S., Tervo, H.M., Habermann, A., Rupp, D., Oberbremer, L., Kern, C., Tibroni, N., Welsch, S., et al. (2009). HIV-1 antagonism of CD317 is species specific and involves Vpu-mediated proteasomal degradation of the restriction factor. Cell Host Microbe *5*, 285–297.

Goldschmidt, L., Cooper, D.R., Derewenda, Z.S., and Eisenberg, D. (2007). Toward rational protein crystallization: a Web server for the design of crystallizable protein variants. Protein Sci. *16*, 1569–1576.

Henne, W.M., Buchkovich, N.J., and Emr, S.D. (2011). The ESCRT pathway. Dev. Cell *21*, 77–91.

Hofmann, K., and Bucher, P. (1996). The UBA domain: a sequence motif present in multiple enzyme classes of the ubiquitination pathway. Trends Biochem. Sci. *21*, 172–173.

Hurley, J.H., and Stenmark, H. (2011). Molecular mechanisms of ubiquitin-dependent membrane traffic. Annu. Rev. Biophys. *40*, 119–142.

Iwabu, Y., Fujita, H., Kinomoto, M., Kaneko, K., Ishizaka, Y., Tanaka, Y., Sata, T., and Tokunaga, K. (2009). HIV-1 accessory protein Vpu internalizes cell-surface BST-2/tetherin through transmembrane interactions leading to lysosomes. J. Biol. Chem. *284*, 35060–35072.

Janvier, K., Pelchen-Matthews, A., Renaud, J.B., Caillet, M., Marsh, M., and Berlioz-Torrent, C. (2011). The ESCRT-0 component HRS is required for

HIV-1 Vpu-mediated BST-2/tetherin down-regulation. PLoS Pathog. *7*, e1001265.

Jouvenet, N., Zhadina, M., Bieniasz, P.D., and Simon, S.M. (2011). Dynamics of ESCRT protein recruitment during retroviral assembly. Nat. Cell Biol. *13*, 394–401.

Katzmann, D.J., Babst, M., and Emr, S.D. (2001). Ubiquitin-dependent sorting into the multivesicular body pathway requires the function of a conserved endosomal protein sorting complex, ESCRT-I. Cell *106*, 145–155.

Kostelansky, M.S., Sun, J., Lee, S., Kim, J., Ghirlando, R., Hierro, A., Emr, S.D., and Hurley, J.H. (2006). Structural and functional organization of the ESCRT-I trafficking complex. Cell *125*, 113–126.

Kostelansky, M.S., Schluter, C., Tam, Y.Y., Lee, S., Ghirlando, R., Beach, B., Conibear, E., and Hurley, J.H. (2007). Molecular architecture and functional model of the complete yeast ESCRT-I heterotetramer. Cell *129*, 485–498.

Long, J., Gallagher, T.R., Cavey, J.R., Sheppard, P.W., Ralston, S.H., Layfield, R., and Searle, M.S. (2008). Ubiquitin recognition by the ubiquitin-associated domain of p62 involves a novel conformational switch. J. Biol. Chem. *283*, 5427–5440.

Mansouri, M., Viswanathan, K., Douglas, J.L., Hines, J., Gustin, J., Moses, A.V., and Früh, K. (2009). Molecular mechanism of BST2/tetherin downregulation by K5/MIR2 of Kaposi's sarcoma-associated herpesvirus. J. Virol. *83*, 9672–9681.

Martin-Serrano, J., and Neil, S.J. (2011). Host factors involved in retroviral budding and release. Nat. Rev. Microbiol. *9*, 519–531.

Martin-Serrano, J., Zang, T., and Bieniasz, P.D. (2001). HIV-1 and Ebola virus encode small peptide motifs that recruit Tsg101 to sites of particle assembly to facilitate egress. Nat. Med. *7*, 1313–1319.

Martin-Serrano, J., Zang, T., and Bieniasz, P.D. (2003). Role of ESCRT-I in retroviral budding. J. Virol. *77*, 4794–4804.

McDonald, B., and Martin-Serrano, J. (2008). Regulation of Tsg101 expression by the steadiness box: a role of Tsg101-associated ligase. Mol. Biol. Cell *19*, 754–763.

Mitchell, R.S., Katsura, C., Skasko, M.A., Fitzpatrick, K., Lau, D., Ruiz, A., Stephens, E.B., Margottin-Goguet, F., Benarous, R., and Guatelli, J.C. (2009). Vpu antagonizes BST-2-mediated restriction of HIV-1 release via beta-TrCP and endo-lysosomal trafficking. PLoS Pathog. *5*, e1000450.

Morita, E., and Sundquist, W.I. (2004). Retrovirus budding. Annu. Rev. Cell Dev. Biol. *20*, 395–425.

Morita, E., Sandrin, V., Alam, S.L., Eckert, D.M., Gygi, S.P., and Sundquist, W.I. (2007a). Identification of human MVB12 proteins as ESCRT-I subunits that function in HIV budding. Cell Host Microbe *2*, 41–53.

Morita, E., Sandrin, V., Chung, H.Y., Morham, S.G., Gygi, S.P., Rodesch, C.K., and Sundquist, W.I. (2007b). Human ESCRT and ALIX proteins interact with proteins of the midbody and function in cytokinesis. EMBO J. *26*, 4215–4227.

Morita, E., Sandrin, V., McCullough, J., Katsuyama, A., Baci Hamilton, I., and Sundquist, W.I. (2011). ESCRT-III protein requirements for HIV-1 budding. Cell Host Microbe *9*, 235–242.

Mueller, T.D., and Feigon, J. (2002). Solution structures of UBA domains reveal a conserved hydrophobic surface for protein-protein interactions. J. Mol. Biol. *319*, 1243–1255.

Nathan, J.A., and Lehner, P.J. (2009). The trafficking and regulation of membrane receptors by the RING-CH ubiquitin E3 ligases. Exp. Cell Res. *315*, 1593–1600.

Neil, S.J., Zang, T., and Bieniasz, P.D. (2008). Tetherin inhibits retrovirus release and is antagonized by HIV-1 Vpu. Nature *451*, 425–430.

Ohno, A., Jee, J., Fujiwara, K., Tenno, T., Goda, N., Tochio, H., Kobayashi, H., Hiroaki, H., and Shirakawa, M. (2005). Structure of the UBA domain of Dsk2p in complex with ubiquitin molecular determinants for ubiquitin recognition. Structure *13*, 521–532.

Pardieu, C., Vigan, R., Wilson, S.J., Calvi, A., Zang, T., Bieniasz, P., Kellam, P., Towers, G.J., and Neil, S.J. (2010). The RING-CH ligase K5 antagonizes restriction of KSHV and HIV-1 particle release by mediating ubiquitin-dependent endosomal degradation of tetherin. PLoS Pathog. *6*, e1000843.

Pohl, C. (2009). Dual control of cytokinesis by the ubiquitin and autophagy pathways. Autophagy *5*, 561–562.

Pornillos, O., Alam, S.L., Davis, D.R., and Sundquist, W.I. (2002). Structure of the Tsg101 UEV domain in complex with the PTAP motif of the HIV-1 p6 protein. Nat. Struct. Biol. *9*, 812–817.

Qian, J., Yang, J., Zhang, X., Zhang, B., Wang, J., Zhou, M., Tang, K., Li, W., Zeng, Z., Zhao, X., Shen, S., et al. (2001). Isolation and characterization of a novel cDNA, UBAP1, derived from the tumor suppressor locus in human chromosome 9p21-22. J. Cancer Res. Clin. Oncol. *127*, 613–618.

Raasi, S., Varadan, R., Fushman, D., and Pickart, C.M. (2005). Diverse polyubiquitin interaction properties of ubiquitin-associated domains. Nat. Struct. Mol. Biol. *12*, 708–714.

Rollinson, S., Rizzu, P., Sikkink, S., Baker, M., Halliwell, N., Snowden, J., Traynor, B.J., Ruano, D., Cairns, N., Rohrer, J.D., et al. (2009). Ubiquitin associated protein 1 is a risk factor for frontotemporal lobar degeneration. Neurobiol. Aging *30*, 656–665.

Shields, S.B., and Piper, R.C. (2011). How ubiquitin functions with ESCRTs. Traffic *12*, 1306–1317.

Shields, S.B., Oestreich, A.J., Winistorfer, S., Nguyen, D., Payne, J.A., Katzmann, D.J., and Piper, R. (2009). ESCRT ubiquitin-binding domains function cooperatively during MVB cargo sorting. J. Cell Biol. *185*, 213–224.

Sims, J.J., Haririnia, A., Dickinson, B.C., Fushman, D., and Cohen, R.E. (2009). Avid interactions underlie the Lys63-linked polyubiquitin binding specificities observed for UBA domains. Nat. Struct. Mol. Biol. *16*, 883–889.

Song, J., Park, J.K., Lee, J.J., Choi, Y.S., Ryu, K.S., Kim, J.H., Kim, E., Lee, K.J., Jeon, Y.H., and Kim, E.E. (2009). Structure and interaction of ubiquitin-associated domain of human Fas-associated factor 1. Protein Sci. *18*, 2265–2276.

Stefani, F., Zhang, L., Taylor, S., Donovan, J., Rollinson, S., Doyotte, A., Brownhill, K., Bennion, J., Pickering-Brown, S., and Woodman, P. (2011). UBAP1 is a component of an endosome-specific ESCRT-I complex that is essential for MVB sorting. Curr. Biol. *21*, 1245–1250.

Stringer, D.K., and Piper, R.C. (2011). A single ubiquitin is sufficient for cargo protein entry into MVBs in the absence of ESCRT ubiquitination. J. Cell Biol. *192*, 229–242.

Stuchell, M.D., Garrus, J.E., Müller, B., Stray, K.M., Ghaffarian, S., McKinnon, R., Kräusslich, H.G., Morham, S.G., and Sundquist, W.I. (2004). The human endosomal sorting complex required for transport (ESCRT-I) and its role in HIV-1 budding. J. Biol. Chem. *279*, 36059–36071.

Teo, H., Gill, D.J., Sun, J., Perisic, O., Veprintsev, D.B., Vallis, Y., Emr, S.D., and Williams, R.L. (2006). ESCRT-I core and ESCRT-II GLUE domain structures reveal role for GLUE in linking to ESCRT-I and membranes. Cell *125*, 99–111.

Trempe, J.F., Brown, N.R., Lowe, E.D., Gordon, C., Campbell, I.D., Noble, M.E., and Endicott, J.A. (2005). Mechanism of Lys48-linked polyubiquitin chain recognition by the Mud1 UBA domain. EMBO J. *24*, 3178–3189.

Varadan, R., Assfalg, M., Raasi, S., Pickart, C., and Fushman, D. (2005). Structural determinants for selective recognition of a Lys48-linked polyubiquitin chain by a UBA domain. Mol. Cell *18*, 687–698.

Weissenhorn, W., and Göttlinger, H. (2011). Essential ingredients for HIV-1 budding. Cell Host Microbe *9*, 172–174.

Williams, R.L., and Urbé, S. (2007). The emerging shape of the ESCRT machinery. Nat. Rev. Mol. Cell Biol. *8*, 355–368.

Zhang, D., Raasi, S., and Fushman, D. (2008). Affinity makes the difference: nonselective interaction of the UBA domain of Ubiquilin-1 with monomeric ubiquitin and polyubiquitin chains. J. Mol. Biol. *377*, 162–180.

Ziv, I., Matiuhin, Y., Kirkpatrick, D.S., Erpapazoglou, Z., Leon, S., Pantazopoulou, M., Kim, W., Gygi, S.P., Haguenauer-Tsapis, R., Rein, N., et al. (2011). A perturbed ubiquitin landscape distinguishes between ubiquitin in trafficking and in proteolysis. Mol. Cell Proteomics *10*, M111.009753.

Cell Host & Microbe
Article

Innate Sensing of HIV-1 Assembly by Tetherin Induces NFκB-Dependent Proinflammatory Responses

Rui Pedro Galão,[1,2] Anna Le Tortorec,[1,2,3] Suzanne Pickering,[1,2] Tonya Kueck,[1] and Stuart J.D. Neil[1,*]
[1]Department of Infectious Disease, King's College London School of Medicine, Guy's Hospital, London SE1 9RT, UK
[2]These authors contributed equally to this study
[3]Present address: INSERM, IRSET, U1085, Rennes 35042, France
*Correspondence: stuart.neil@kcl.ac.uk
http://dx.doi.org/10.1016/j.chom.2012.10.007

SUMMARY

Antiviral proteins that recognize pathogen-specific or aberrantly located molecular motifs are perfectly positioned to act as pattern-recognition receptors and signal to the immune system. Here we investigated whether the interferon-induced viral restriction factor tetherin (CD317/BST2), which is known to inhibit HIV-1 particle release by physically tethering virions to the cell surface, has such a signaling role. We find that upon restriction of Vpu-defective HIV-1, tetherin acts as a virus sensor to induce NFκB-dependent proinflammatory gene expression. Signaling requires both tetherin's extracellular domain involved in virion retention and determinants in the cytoplasmic tail, including an endocytic motif, although signaling is independent of virion endocytosis. Furthermore, recruitment of the TNF-receptor-associated factor TRAF6 and activation of the mitogen-activated protein kinase TAK1 are critical for signaling. Human tetherin's ability to mediate efficient signaling may have arisen as a result of a five amino acid deletion that occurred in hominids after their divergence from chimpanzees.

INTRODUCTION

Tetherin is a broadly acting antiviral membrane protein that blocks the release of diverse mammalian viruses from the surface of infected cells and reduces retroviral pathogenesis in vivo (Liberatore and Bieniasz, 2011; Martin-Serrano and Neil, 2011). Tetherin partitions into assembling virions, cross-linking them to the plasma membrane (PM) by virtue of its unique topology. The potential importance of tetherin in innate antiviral immunity is underscored by examples of virally encoded proteins that counteract its activity, the prototype being the accessory gene product Vpu of human immunodeficiency virus type 1 (HIV-1) (Le Tortorec et al., 2011). Vpu interacts with human tetherin in infected cells, blocking its transit to viral assembly sites on the PM (Dubé et al., 2011; Kueck and Neil, 2012; Schmidt et al., 2011) and promoting its endosomal degradation (Agromayor et al., 2012; Janvier et al., 2011). Among the primate lentiviruses, the species-specific targeting of tetherin is widespread, even though the *vpu* gene is restricted to a subset of simian immunodeficiency viruses (SIVs). In SIVs in which Vpu is absent, the Nef accessory protein performs the role, and the sensitivity of primate tetherins to SIV Nefs is determined by a five amino acid patch in the protein's cytoplasmic tail that was deleted after hominids and chimpanzees diverged (Jia et al., 2009; Zhang et al., 2009).

Accumulating evidence indicates that tetherin imposes a powerful selective pressure on primate lentiviruses and that its counteraction is essential for HIV/SIV replication and spread in vivo. Adaptation of the SIVcpz Vpu to target human tetherin efficiently is a feature of the major group (Group M) of HIV-1 that is responsible for the HIV/AIDS pandemic, but not the separate SIVcpz species jumps that led to the N, O, and P groups that have remained geographically restricted (Sauter et al., 2009). Zoonotic spread of the Vpu(−) SIV of sooty mangabeys (SIVsm) to become HIV-2, whose Nef protein cannot target human tetherin, resulted in tetherin counteraction developing in the envelope protein (Env) (Le Tortorec and Neil, 2009). Furthermore, a similar adaptation in Env has been observed in macaques experimentally infected with a Nef-defective SIVmac that reverted to pathogencity (Serra-Moreno et al., 2011).

While tetherin potently blocks cell-free virion release, its ability to block cell-to-cell transfer is controversial, and where it has been observed, weak (Casartelli et al., 2010; Jolly et al., 2010). In cultured primary CD4+ T cells, Vpu-defective viruses have even been observed to spread faster through the culture in a tetherin-dependent manner (Jolly et al., 2010). These superficially paradoxical observations between viral replication in culture and the evolutionary conservation of tetherin counteraction in primate lentiviruses suggest that tetherin's contribution to the antiviral immune response is not limited to physical inhibition of virion release. Interestingly, prior to its identification as an antiviral factor, tetherin (BST2) was identified as an inducer of NFκB activation in a whole-genome transfection screen (Matsuda et al., 2003). Furthermore, tetherin has been implicated as a regulator of Toll-like receptor (TLR) function in plasmacytoid dendritic cells through the activation of the inhibitory leukocyte receptor ILT7 (Cao et al., 2009). We therefore hypothesized that tetherin, like the retroviral restriction factor TRIM5α, might act as a sensor for the presence of viral infection coupled to its antiviral activity (Pertel et al., 2011). In this study we tested this hypothesis.

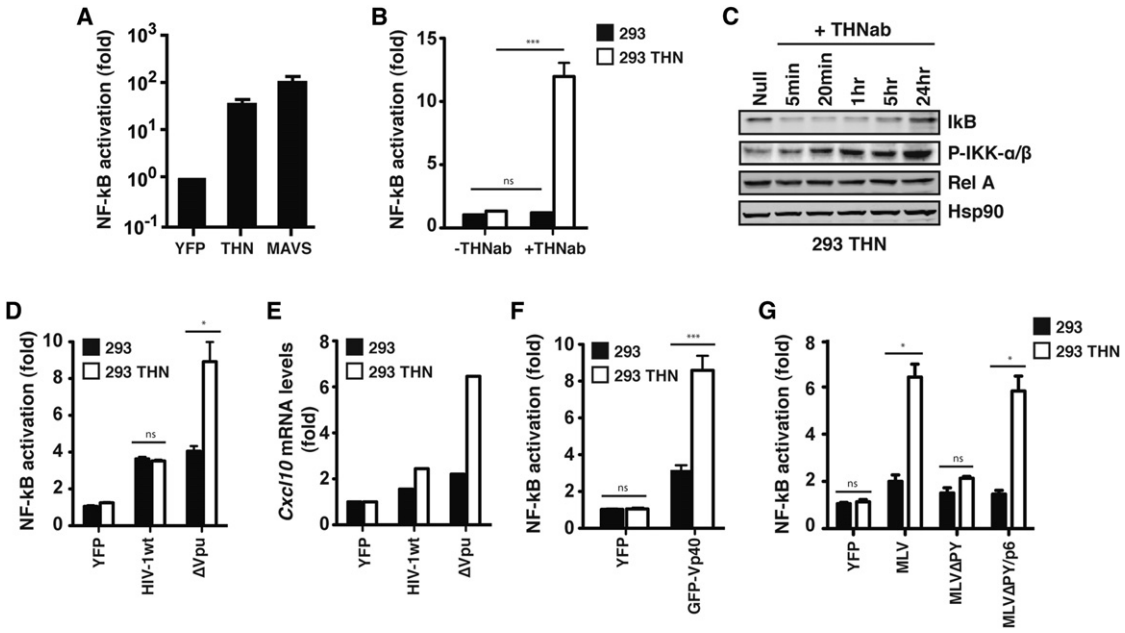

Figure 1. Tetherin Induces NFκB-Dependent Responses upon Overexpression, Crosslinking, and Restriction of Virion Release

(A) Fold activation of a firefly-luciferase NFκB reporter gene in 293 cells transiently cotransfected with tetherin, MAVS, or control YFP vectors.

(B) Fold activation of the same reporter in 293 or 293THN cells treated for 24 hr with a rabbit anti-tetherin polyclonal serum and a secondary anti-rabbit antibody.

(C) Time course of endogenous IκB degradation and IKKα/β phosphorylation in 293THN cells after antibody crosslinking.

(D and E) (D) Fold increases in NFκB-reporter activity in 293 and 293THN cells transfected with wild-type and Vpu(−) HIV-1 proviruses and (E) fold changes in *Cxcl10* mRNA levels compared to YFP transfection calculated relative to *Gapdh* by qRT-PCR.

(F and G) NFκB-reporter fold activation in 293 and 293THN cells transfected with GFP-fused Ebolavirus VP40 expression vector (F) or MLV provirus or derivatives (MLVΔPY and MLVΔPY/p6) (G). Fold changes relative to 293 cells transfected with YFP control (A, D–G) or 293 nontreated cells (B). *p > 0.05 and ***p > 0.001 as determined by two-tailed t test. All error bars represent ±SEM of three independent experiments.

RESULTS

Restriction of Enveloped Virus Particle Release by Human Tetherin Induces NFκB-Dependent Gene Expression

We first sought to confirm whether tetherin was capable of inducing NFκB activation when overexpressed. Transient transfection of human tetherin into 293 cells potently induced the activation of an NFκB-dependent firefly luciferase reporter construct to levels similar to those seen with the MAVS/IPS1/Cardif component of the cytoplasmic viral RNA-sensing pathway (Takeuchi and Akira, 2010), confirming the previous observation from the genomic screen (Matsuda et al., 2003) (Figure 1A). We then examined whether crosslinking of cell-surface tetherin was capable of transducing a similar signal in 293 cells stably expressing human tetherin (293THN), but not vector control 293 cells. While background level of reporter gene activation in the two cell types was less than 1.5-fold, crosslinking the surface protein with a polyclonal antibody resulted in a 10-fold increase in NFκB-dependent luciferase expression in tetherin-expressing cells (Figure 1B) and led to the concomitant phosphorylation of IKKα/β and degradation of IκB (Figure 1C). This suggested that clustering of tetherin might mediate a proinflammatory signal upon restriction of enveloped virus release. Consistent with this, budding and assembly of HIV-1 lacking the tetherin countermeasure Vpu (Neil et al., 2008), or encoding a point mutant of Vpu (A14L) that is defective for interaction with tetherin (Vigan and Neil, 2010), specifically induced enhanced NFκB reporter activation in cells stably expressing tetherin while the wild-type virus did not, correlating with physical particle release (Figure 1D and see Figures S1A and S1B online). Furthermore, consistent with the activation of the reporter gene, we could observe induction of the mRNA of a representative NFκB-dependent target gene, the proinflammatory chemokine CXCL10, in the same cells (Figure 1E).

Since tetherin restricts the release of a variety of mammalian viruses, we then sought to determine whether other tetherin-sensitive viral particles could activate the NFκB reporter. We observed similar reporter activation by producing tetherin-sensitive filoviral-like particles (VLPs) derived from the Ebolavirus matrix protein VP40 (Jouvenet et al., 2009; Neil et al., 2007) (Figure 1F and Figure S1C). Furthermore, since previous studies have demonstrated that tetherin restricts the release of fully assembled virions that have separated their membranes from that of the host cell, we then examined whether assembly-defective retroviral particles could trigger tetherin-dependent NFκB activation. For this we used a murine leukemia virus (MLV) provirus, or derivatives with mutations in the $p12^{Gag}$ late-domain sequence (MLVΔPY) that facilitates virion budding and membrane scission by recruiting the ESCRT-pathway (Martin-Serrano and Neil, 2011). As expected, wild-type MLV release was restricted in 293THN cells, whereas MLVΔPY release was

defective in both cell types (Figure S1D). Production of wild-type MLV virions triggered enhanced NFκB reporter activity in 293THN cells, but the assembly-defective MLVΔPY did not (Figure 1G). Interestingly, MLVΔPY/p6, where the p12 late domain has been replaced with one derived from HIV-1 $p6^{gag}$, recovered both virion production and the enhanced NFκB reporter activation in 293THN cells (Figure 1G and Figure S1D). Therefore activation of NFκB in tetherin-expressing cells requires full virion assembly and scission of the cellular and virion membranes. Together these data show that in cells constitutively expressing tetherin, the restriction of enveloped virion release triggers a proinflammatory response.

Tetherin-Sensitive HIV-1 Mutants Induce Enhanced Proinflammatory Cytokine Expression in Infected CD4+ T Cells

We then asked whether tetherin-mediated restriction of HIV-1 particle release in primary human CD4+ T cells would induce proinflammatory gene expression. Purified CD4+ T cells from three donors were infected with wild-type HIV-1, Vpu(−) HIV-1, or HIV-1 encoding tetherin binding-defective mutant Vpu-A14L that retains all other known Vpu functions. As expected, cell-free virus release of the Vpu mutant HIV-1s was impaired compared to wild-type in all donors (Figures 2A and 2B). Interestingly, cultures infected with both Vpu(−) and Vpu-A14L HIV-1 mutants led to increased levels of mRNAs for proinflammatory cytokines CXCL10 and IL-6 (Figure 2C). In two of the donors, increased levels of *Ifnb* mRNA were also detected (Figure 2C). Furthermore, these increases in mRNA levels were reflected in significant increases in the concentrations of CXCL10, IL-6, and bioactive type-1 IFN in the supernatant (Figure 2D). The induction of type 1 IFN expression implied the activation of interferon regulatory factors (IRFs) 3 or 7 in addition to NFκB. In parallel reporter gene experiments to those described above, however, tetherin overexpression, crosslinking, or Vpu(−) HIV-1 assembly could not activate an IFNβ-promoter-luciferase reporter construct in 293THN cells. Neither did we observe any induction of *ifnb* mRNA or phosphorylation of IRF3 in this system (Figures S2A–S2C). However, in CD4+ T cells we could detect IRF3 phosphorylation after 48 hr of HIV-1 infection. In contrast to the induction of the NFκB-dependent *Cxcl10* mRNA in T cells or tetherin-mediated reporter gene activation in 293THN cells, this IRF3 phosphorylation and the concomitant IFNβ expression could be suppressed by inhibition of the TLR3 adaptor TRIF (Figures S2D–S2G), suggesting that tetherin-mediated viral retention may additionally augment viral recognition by other host PRRs. Therefore, to confirm the tetherin dependency of all these data, we transduced primary CD4+ T cells with lentiviral vectors encoding shRNA hairpins against tetherin (shTHN) or an irrelevant target (GFP) 24 hr prior to infection with the above viruses. As expected, shTHN transduction reduced surface tetherin levels and rescued the release of Vpu(−) and Vpu-A14L mutant viruses to wild-type levels (Figures S2H and S2I). It also concomitantly reduced both *Cxc10* and *Ifnb* mRNA induction in the same cells (Figure 2E), demonstrating that proinflammatory gene expression induced by Vpu(−) HIV-1 in target cells is tetherin dependent. We thus provide evidence that interaction of tetherin with HIV-1 induces proinflammatory gene expression consistent with a direct signaling role.

Structural Determinants of Tetherin-Mediated Signaling

We then mapped the determinants of NFκB activation in human tetherin. The primary sequence of the tetherin cytoplasmic tail does not affect the protein's antiviral activity (data not shown). However, we reasoned that the cytoplasmic tail likely played a role in signaling and screened a series of tetherin cytoplasmic tail mutants for NFκB-dependent reporter gene activation (Figure 3A). This revealed defects in signaling that mapped to the conserved YXY site that mediates tetherin's endocytic recycling to the PM (Rollason et al., 2007), as well as an adjacent CRV motif. Mutations encompassing the two membrane-proximal lysine residues, which can serve as ubiquitylation targets (Le Tortorec et al., 2011), were also defective for signaling. However, these alanine mutants appeared immature in SDS-PAGE, suggesting a trafficking defect, and mutation of the individual lysine residues to arginine preserved signaling capacity (Figure S3A). Stable cell lines expressing tetherin Y6,8A and 10-12A failed to mediate reporter-gene activation in response to Vpu(−) HIV-1, yet they retained potent viral particle restriction, consistent with the hypothesis that these motifs are required for transducing a signal initiated by virion retention (Figures 3B). By contrast, the antiviral activity of tetherin depends upon the structural integrity of its extracellular domain, particularly in its C-terminal GPI-linked membrane anchor, its dimeric state, and its extracellular coiled-coil domain (Perez-Caballero et al., 2009). Mutations in the coiled coil (L123P), the extracellular cysteine residues that mediate dimerization, or deletion of the GPI anchor, all of which render tetherin unable to inhibit viral release, reduced the ability of tetherin to promote NFκB-reporter gene activation both in transient transfections and in stably expressing cells transfected with tetherin-sensitive and -insensitive HIV-1 (Figure 3C and Figure S3B). Thus tetherin's ability to mediate NFκB activation requires the extracellular determinants essential for multimerization and virion retention, and cytoplasmic tail motifs required to transduce a signal dependent on this retention.

Tetherin-Mediated Signaling Is Independent of Virion Endocytosis

Tetherin-mediated retention of Vpu(−) HIV-1 virions leads to their accumulation in late endosomal compartments (Martin-Serrano and Neil, 2011). The implication of the YXY motif, which has been previously shown to interact with both AP1 and AP2 clathrin adaptors, suggested that endocytosis of virions might be required for signaling. Consistent with this, a lower proportion of cells exhibited distinct endosomal accumulations of HIV-1 Gag-GFP in 293THN-Y6,8A compared to 293THN 24 hr post-transfection (48% versus 74%), suggesting that the YXY motif may play a role in virion uptake (Figures 4A and 4B). Recent evidence suggests that YXY mutants of tetherin are impaired but not fully defective for endocytosis (Lau et al., 2011), potentially accounting for this partial phenotype. However, siRNA depletion of AP2μ1 reduced endosomal virion localization to levels comparable to the parental 293 cells, similar to the expected result observed by cotransfecting a dominant inhibitory mutant S34N of the early endocytic GTPase Rab5a (Neil et al., 2008). As a control, the proportion of transfected cells with observable endosomal Gag-GFP was unchanged when using the dominantly active mutant, Rab5a(Q79L), with Gag-GFP VLPs accumulating in the lumen of swollen Rab5+ve endosomes.

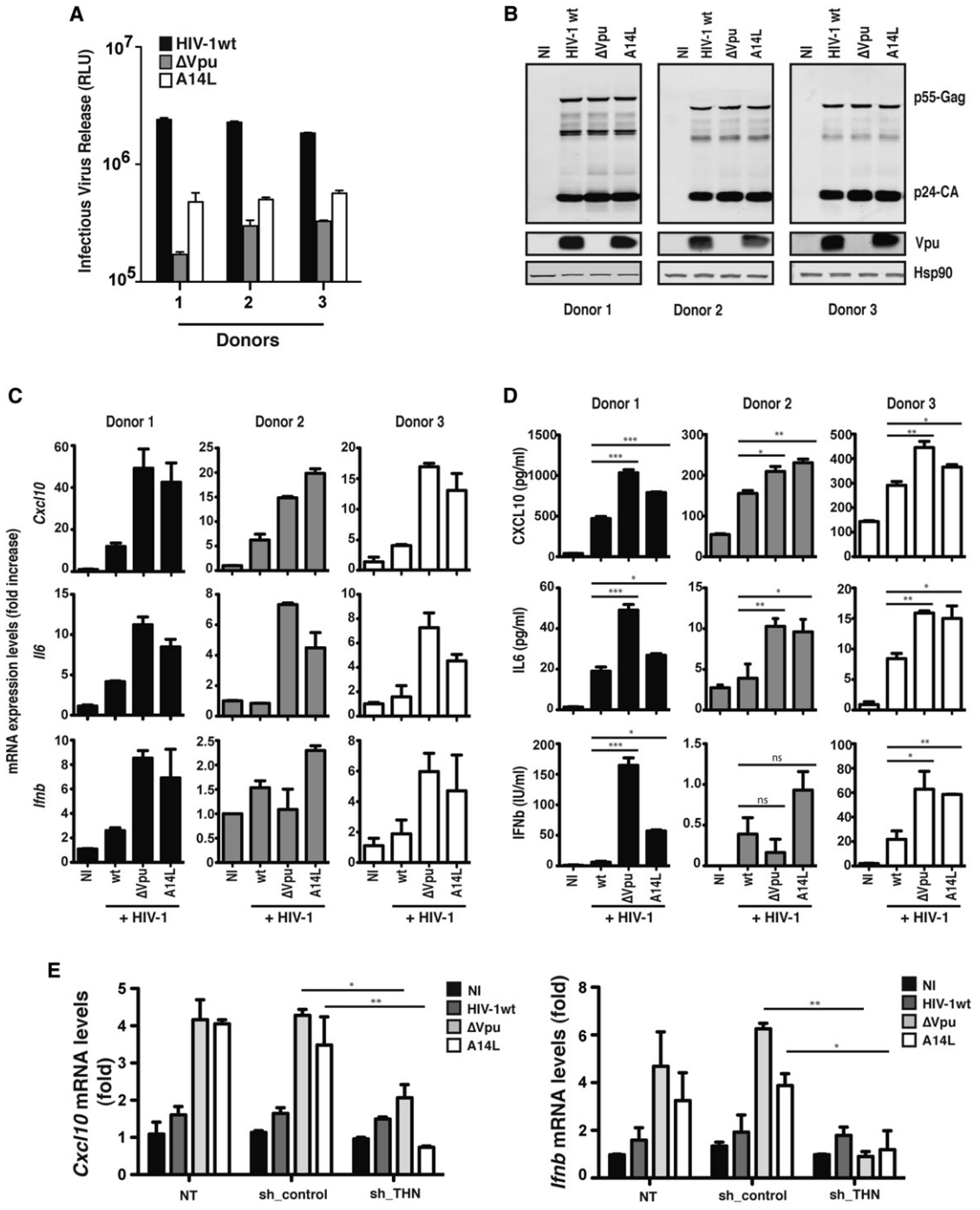

Figure 2. Restriction of Tetherin-Sensitive HIV-1 Mutant Release from Infected CD4+ T Cells Induces Proinflammatory Gene Expression

(A and B) Purified CD4+ T cells from three independent donors were infected with the indicated virus at an moi of 5, and 48 hr later viral release was determined by infection of HeLa-TZM reporter cell lines (A) and western blot of cell lysates (B).

(C) Total RNA from three biological replicates of parallel cultures infected as in (A) was analyzed for *Cxcl10*, *IL6*, and *Ifnb* mRNA levels relative to *Gapdh* by qRT-PCR.

(D) Protein levels in the supernatants from (A) were determined by ELISA (CXCL10 and IL-6) or by HEK-Blue indicator cells (IFNβ).

(E) Activated CD4+ T cells were transduced with lentiviral vectors encoding short hairpin against GFP (sh-control) or against tetherin (shTHN) 24 hr prior to infection as in (A). Total RNA from three biological replicates of parallel cultures was analyzed for *Cxcl10* and *Ifnb* mRNA levels relative to *Gapdh* by qRT-PCR. Fold changes relative to noninfected cells (C and E). *p > 0.05, **p > 0.01, and ***p > 0.001 as determined by two-tailed t test. All error bars represent ±SEM.

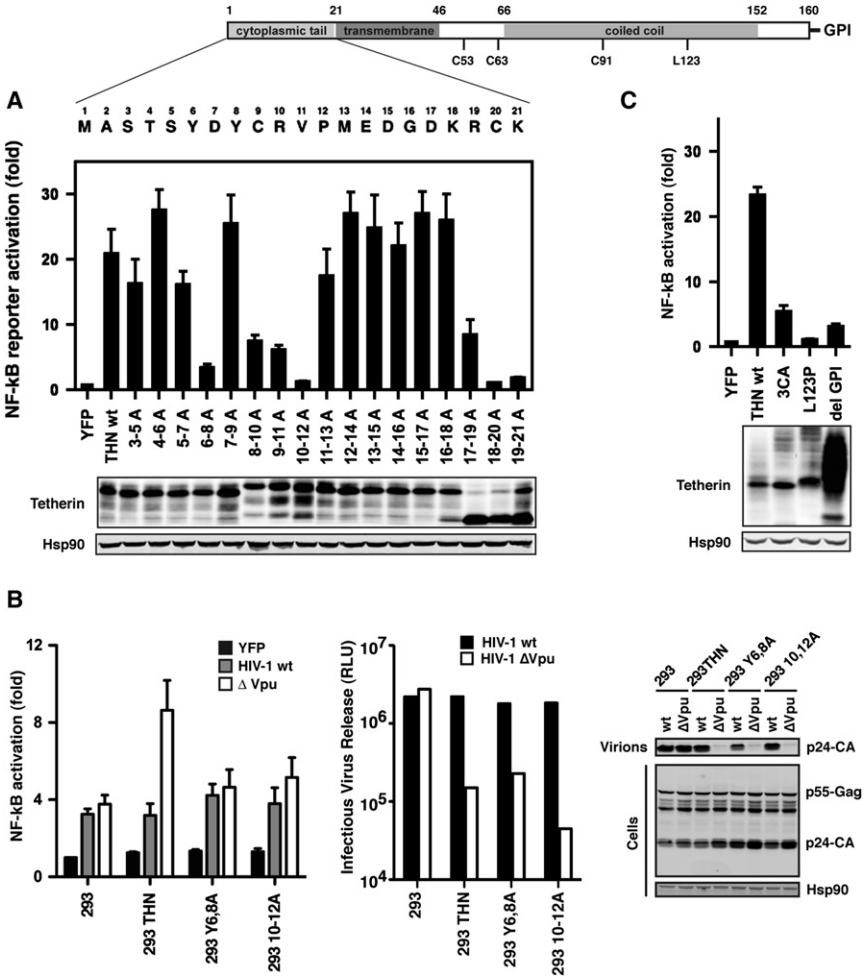

Figure 3. Determinants of Tetherin-Mediated Signaling

(A) A series of alanine scan mutants in the cytoplasmic tail of human tetherin were assessed for the ability to induce NFκB-Luc reporter activation in transiently transfected 293 cells. Mutations encompassing residues 17–21 of the cytoplasmic tail were discounted due to aberrant localization (data not shown), and further mutants are presented in Figure S3. Error bars are ±SEM.

(B) 293 cells stably expressing the Y6,8A and 10-12A mutants were further assessed for their ability to induce NFκB-Luc reporter activation upon transfection with wild-type or Vpu(−) HIV-1 proviral plasmids. Infectious virus release was determined on HeLa-TZM indicator cells and physical particle yield analyzed by western blot of cell lysates and pelleted supernatants using an anti-p24 monoclonal antibody.

(C) Mutations in the extracellular domain of tetherin defective for inhibiting viral release (cysteine-less 3CA, the coiled-coil point mutant L123P, or a truncation lacking the GPI anchor) were assayed for NFκB-Luc reporter activation in transfected 293 cells. Fold changes ±SEM relative to 293 cells transfected with YFP control (B and C).

We then examined the effects of these treatments on virion-induced NFκB-reporter activation in 293THN cells. As expected, Vpu(−) HIV-1 induced an increase in reporter activation compared to wild-type virus. However, in the presence of AP2μ1 depletion or Rab5a(S34N) overexpression, Vpu(−) virus-induced signaling was significantly increased in 293THN cells (Figures 4C and 4D). These data suggest that while the YDYCRV motif is essential for virion-induced signaling, virion uptake is not, and blockade of their delivery to late endosomes potentiates reporter gene expression. Together, they suggest that tetherin-dependent accumulation of virions on the cell surface triggers NFκB activation.

TAK1 Activation and Recruitment of TRAF6 Are Required for Tetherin-Mediated Signaling

Proinflammatory activation of NFκB from TNF receptors and membrane-associated and cytosolic PRRs is mediated through the mitogen-activated protein kinase TAK1 (MAP3K7) (Skaug et al., 2009). We therefore asked whether there were similarities between tetherin-mediated NFκB activation and that of other viral PRRs. Depletion of TAK1 by siRNA completely abolished the NFκB-reporter gene activation induced by tetherin overexpression or Vpu(−) HIV-1 in 293THN cells (Figure 5A), implicating the activation of TAK1 as critical in tetherin-mediated signaling. TAK1 activation by host PRRs depends on the upstream recruitment of family members of the TNF-receptor-associated factor (TRAF) family of E3 ubiquitin ligases, particularly TRAF2 and TRAF6, and the E2 ligase Ubc13 (UBE2N), which act to polymerize K63-linked ubiquitin chains (Skaug et al., 2009). RNAi depletion of these factors similarly inhibited tetherin-mediated NFκB reporter activity (Figure 5B). Interestingly, while the human tetherin cytoplasmic tail has a putative TRAF6 consensus-binding motif (PXEXX-aromatic/acidic), disruption of this sequence by mutagenesis did not impair tetherin signaling (Figure 3). However, tetherin could be specifically coimmunoprecipitated with an HA-tagged TRAF6 dependent on the presence of the YCRV motif that is conserved in ape tetherins and partially overlaps the protein's endocytic motif (Figure 5C and Figure S4), although whether this interaction is direct is unknown. Furthermore, mutation of residues 10–12 (RVP) retained TRAF6 interaction despite losing signaling activity, indicating that in conjunction with the RNAi data, TRAF6 is necessary but not sufficient for tetherin signaling. These data suggest that virion aggregation by tetherin leads to YDYCRV-dependent recruitment of a signaling complex that includes TRAF6 to induce TAK1-dependent NFκB activation when viral release is restricted.

Signaling Is a Feature of Human and Chimpanzee Tetherins and Is Augmented by a Hominid-Specific Deletion in the Tetherin Cytoplasmic Tail

Tetherin's antiviral activity is conserved in mammals. Surprisingly, however, murine and old world monkey tetherins showed

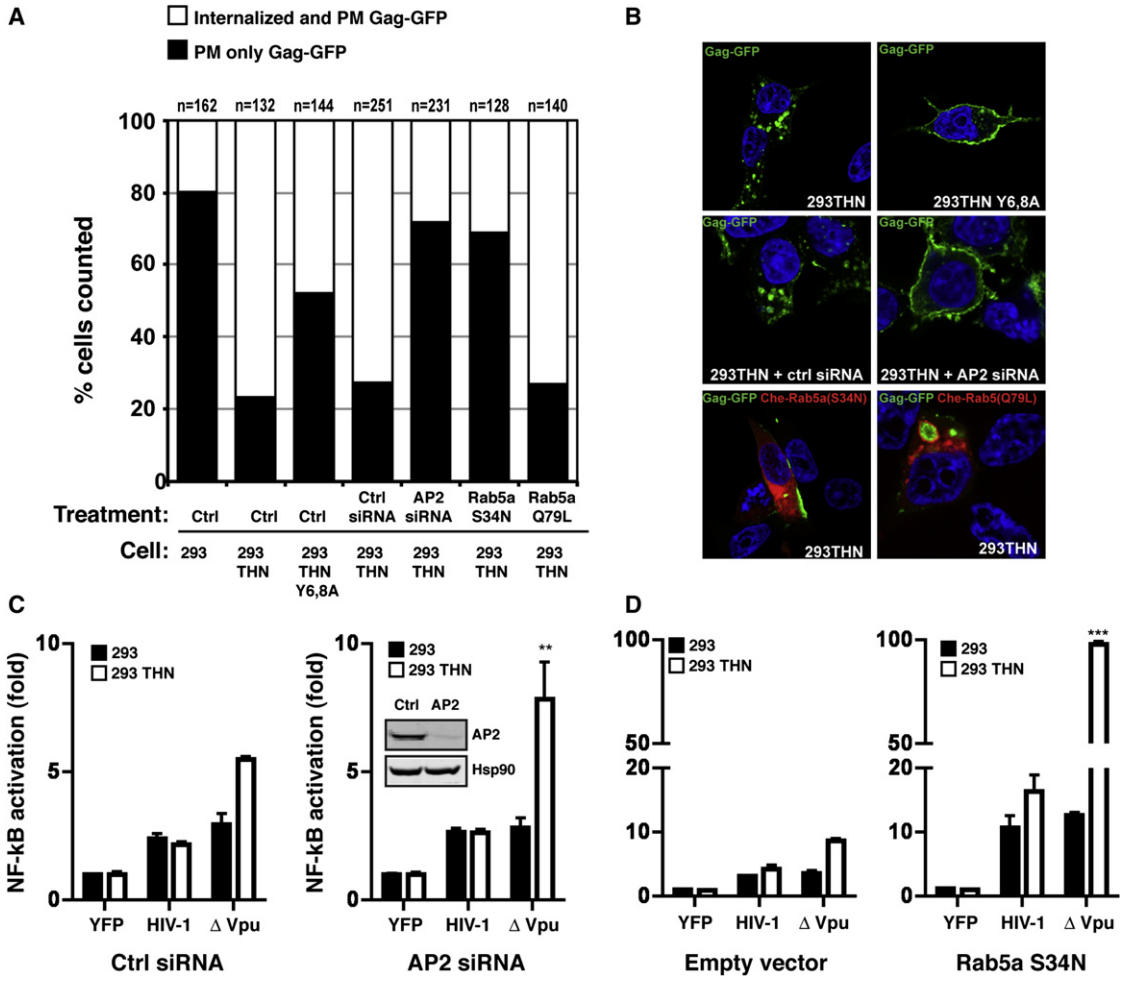

Figure 4. Inhibition of Virion Endocytosis Enhances Tetherin-Dependent NFκB Activation

(A and B) The indicated cell lines were transfected with an HIV-1 Gag-GFP expression vector, with or without either pretreatment with control siRNA or AP2μ1 for 48 hr or cotransfection with Cherry-FP fused mutants of Rab5a (S34N or Q79L). Twenty-four hours later, the cells were fixed and ten random fields were enumerated on the basis of whether transfected cells displayed plasma-membrane only Gag-GFP localization or PM and distinct endsomal accumulation (A) and imaged by confocal microscopy (B).

(C and D) The effects of AP2μ1 siRNAs and Che-Rab5a-S34N on HIV-1 proviral-induced NFκB reporter gene activation were determined as above. Fold changes relative to 293 cells transfected with YFP control with error bars representing ±SEM.

negligible ability to induce NFκB reporter activity despite potently restricting HIV-1 particle release (Figure 6A). Chimpanzee tetherin (cpz-tetherin), while capable of inducing reporter gene activation, was less potent than the human protein (Figure 6A). Informed by our mutagenesis studies (Figure 3), we identified three regions of species-specific changes between the cytoplasmic tails of human, chimpanzee, and rhesus tetherins that might contribute to the differences in signaling. First, a major difference between human and other primate proteins is the presence of a G/DDIWK motif that is absent in *Homo sapiens*. The tryptophan in this motif is under high evolutionary positive selection and determines the sensitivity of primate tetherins to the Nef proteins of SIVs (Lim et al., 2010). Second, while the two tyrosine residues in the YXYXXV endocytic motif are highly conserved throughout mammalian evolution, differences occur between humans/chimpanzees and old world monkeys at positions 9–11, a region we have identified as critical to human tetherin's signaling ability. Both the C9 (Gupta et al., 2009; Lim et al., 2010) and R10 (Gupta et al., 2009; McNatt et al., 2009) positions have been previously ascribed to be under positive selection throughout primate evolution. Third, in human and chimpanzee tetherins a repeated glycine-isoleucine pair extends the tetherin transmembrane helix, and is an important determinant of sensitivity to HIV-1 Vpu (McNatt et al., 2009). A further difference between human, chimpanzee, and rhesus encompasses an ubiquitination site (STS) (Tokarev et al., 2011), although our alanine mutagenesis suggests that this motif is not important.

Transfection of increasing amounts of hu- and cpz-tetherin plasmids revealed that at low expression levels human tetherin was markedly more efficient at inducing NFκB-reporter activation, and high levels of the chimpanzee protein never achieved parity (Figure 6B). Deletion of the DDIWK motif enhanced cpz-tetherin-mediated NFκB reporter gene activation to the level of human protein, and its reintroduction into the human protein

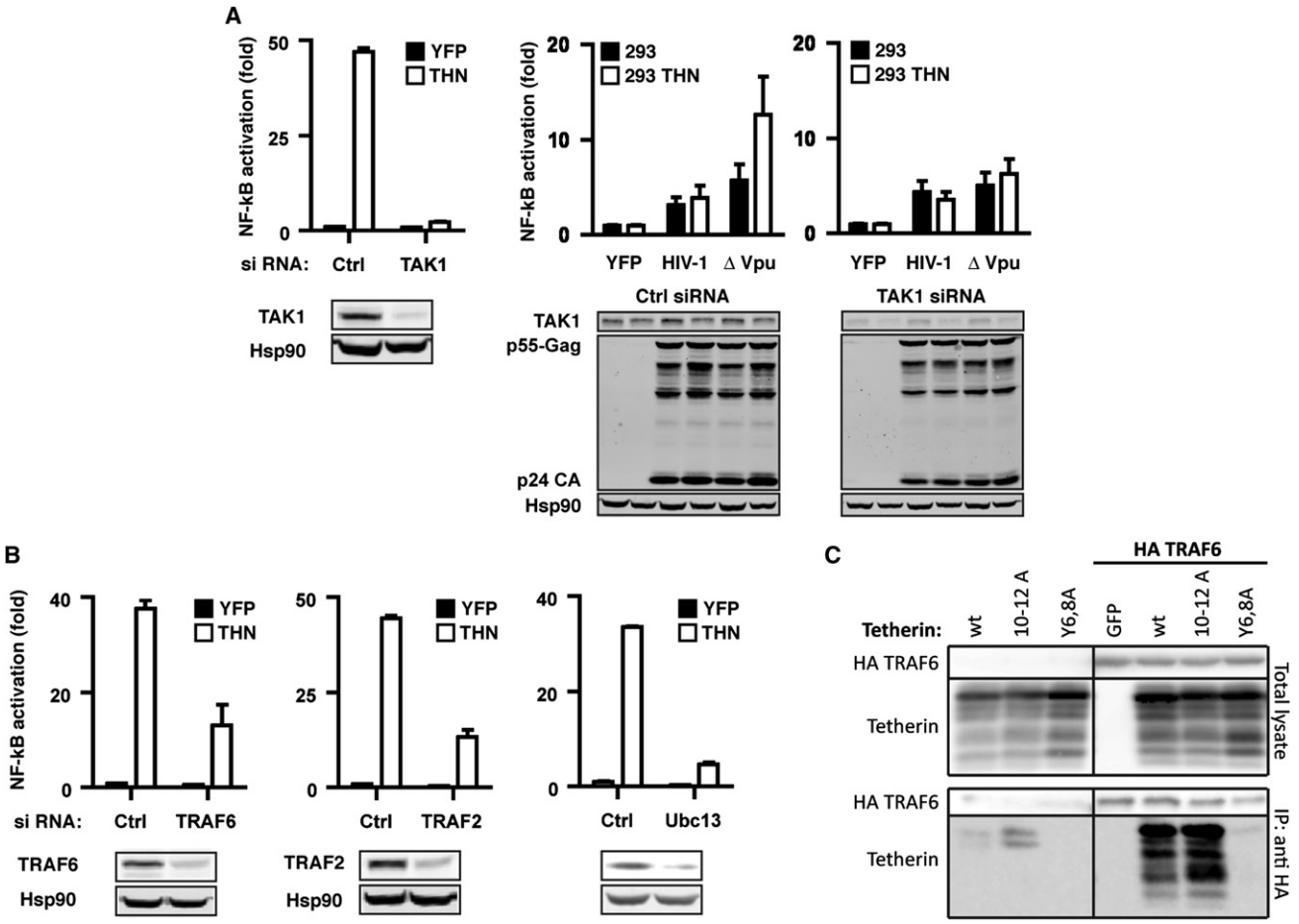

Figure 5. Mechanistic Aspects of Tetherin-Mediated Signaling

(A) Depletion of TAK1 by siRNA in either 293 cells transfected with tetherin, or in 293 and 293THN cells transfected with Vpu(−) HIV-1 proviral plasmid, abolishes NFκB-Luc reporter activation but has no effect on Gag production.

(B) Impairment of NFκB-Luc reporter activation by siRNA depletion of TRAF6, TRAF2, or Ubc13 in 293 cells transfected with tetherin.

(C) Coimmunoprecipitation of tetherin and tetherin(10-12A) but not tetherin Y6,8A with HA-TRAF6 in transiently transfected 293 cells. All error bars are ±SEM of three independent experiments.

severely impaired signaling. Neither of these changes affected either expression, restriction of Vpu(−) HIV-1 release, or TRAF6 association (Figure 6B and Figure S5). Therefore efficiency of NFκB activation between hu-tetherin and cpz-tetherin appears to be an evolutionarily recent acquisition that has coincided with the deletion of a motif known to act as a target for SIV tetherin countermeasures.

We then turned our attention to rh-tetherin. In rhesus macaques, position 9 is polymorphic (either a C or an R), and neither variant could mediate NFκB-reporter activity. Similarly, a C9R change in human tetherin had no effect on signaling ability (data not shown). Introduction of KM-to-RV changes into rh-tetherin did not endow it with any signaling activity, but the corresponding RV-to-KM swap in human tetherin severely reduced its NFκB-reporter induction without compromising antiviral activity, confirming that these residues are necessary in human, but not sufficient to explain the lack of rhesus signaling (Figure 6B). To determine the minimal changes in rh-tetherin that could confer signaling activity, we constructed chimeras between rh-tetherin and cpz-tetherin. Again all proteins were capable of restricting virion release. Surprisingly, only a chimera bearing the cpz-tetherin cytoplasmic tail including the additional TM-domain GI residues (rh-cpz 31) recovered any NFκB activation (Figure 6B). These results suggest multiple context-dependent adaptations have resulted in human tetherin's signaling capacity. First, changes in the previously identified YXYXXV motif in conjunction with a lengthened TM domain, which itself may be expected to alter the conformation of the cytoplasmic tail, are required to confer levels of signaling activity seen in cpz-tetherin. Second, deletion of the DDIWK motif in human ancestors greatly enhanced the efficiency of this activity.

DISCUSSION

In this study we have demonstrated that human tetherin can transduce a proinflammatory signal when it restricts virion production. This appears to be coupled to cell-surface aggregation of virions, resulting in the TAK1-dependent activation of NFκB

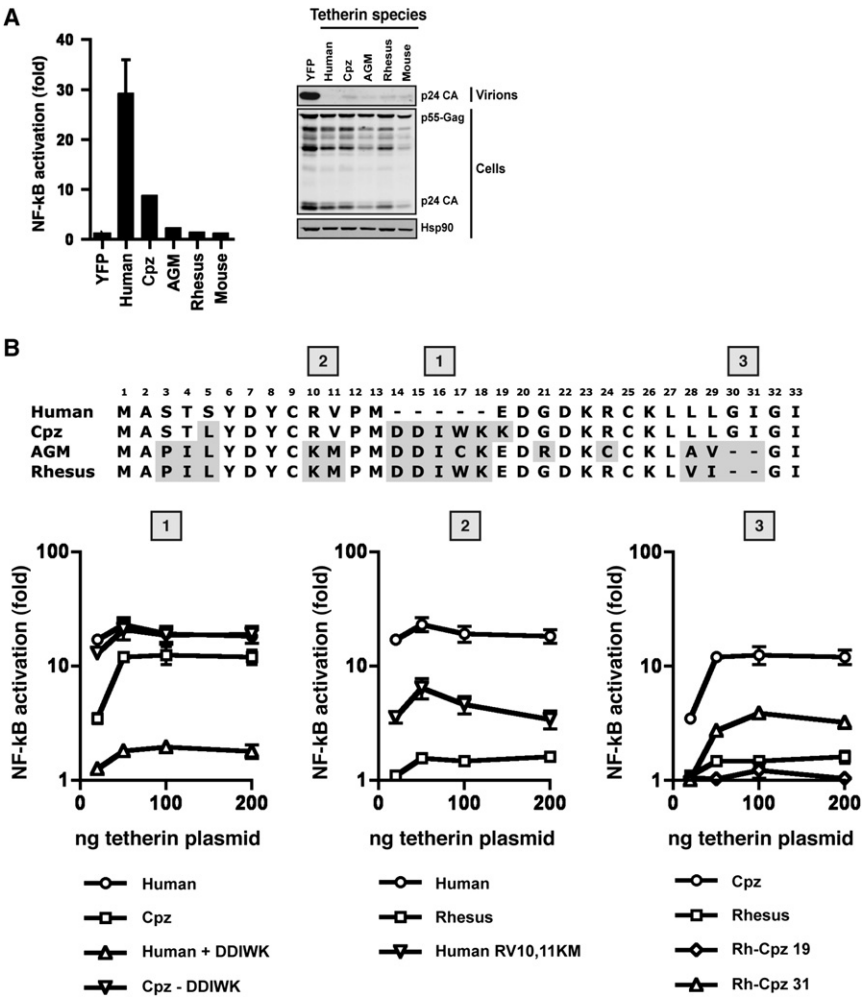

Figure 6. Tetherin's Signaling Activity Is a Recent Acquisition in Primate Evolution

(A) NFκB-Luc reporter activation in 293 cells transiently transfected with murine, rhesus, AGM, chimpanzee, and human tetherins and their respective ability to restrict Vpu-defective virus release.

(B) Alignment of the cytoplasmic tails of primate tetherins with regions differing from human shown in gray. Species-specific changes were made according to major differences indicated at positions 1, 2, and 3 and tested for NFκB-Luc reporter activation at varying expression levels. All error bars represent ±SEM of three independent experiments.

and subsequent cytokine production. Importantly, we could show that tetherin-sensitive mutants of HIV-1 induce enhanced proinflammatory cytokine production in infected CD4+ T cells. This suggests that the action of tetherin senses enveloped virus assembly, and that the infected cell responds by releasing mediators that can attract innate and adaptive immune cells to the site of infection to augment the antiviral response. Thus we suggest that in the context of an infected cell, a budding enveloped virion constitutes a pathogen-associated molecular pattern, and in addition to physically restricting virion release, tetherin acts as the cognate PRR.

Mechanistically, tetherin signaling has similarities to TLRs and other viral PRRs, including another retroviral restriction factor, TRIM5α (Pertel et al., 2011; Skaug et al., 2009; Takeuchi and Akira, 2010). NFκB is activated through the upstream kinase TAK1. PRR-mediated TAK1 activation depends on the association of its accessory factors TABs 1–3 with free polyubiquitin chains bearing K63 linkages, which in turn are synthesized by the concerted action of TRAF E3 ligases with E2 complex of Ubc13/UBE1. TRAFs, particularly TRAFs 2, 3, 5, and 6, play key roles in signal transduction from a host of proinflammatory cell-surface receptors, and TRAF2 and TRAF6 are also essential cofactors for cytoplasmic RIG-I-like helicases. We found that RNAi-mediated knockdown of TRAF2, TRAF6, and Ubc13 inhibited tetherin activation of NFκB, for which TAK1 was also essential. Furthermore we could observe an interaction between tetherin and TRAF6. While the human tetherin cytoplasmic tail contains a predicted TRAF6 binding site, we found that this interaction was actually determined by the adjacent endocytic motif YDYCRV. How the YDYCRV motif recruits TRAF6, and how this relates to its endocytic function, remains to be determined. While signaling is dependent on this signal, which appears also to play a partial role in virion internalization, blockade of virion uptake itself by AP2μ siRNAs or Rab5(S34N) potentiates NFκB activation. Since these treatments do not affect tetherin's physical antiviral activity per se, these data strongly suggest that large surface virion accumulations are the primary trigger of tetherin-mediated signaling.

TRAF6 recruitment is not sufficient to explain tetherin-mediated signal transduction, as mutation of residues 10–12 (RVP) or reinsertion of the primate DDIWK motif also impairs signaling while retaining TRAF6 binding ability. Interestingly, both the cysteine (Lim et al., 2010) and the arginine (Gupta et al., 2009; McNatt et al., 2009) residues have been reported to be under positive selection in primates, and the YCRV motif is only found in great apes. While the cysteine appears not to be required, mutation of the R and V to the K and M found in macaques impaired human tetherin signaling. Furthermore, the context dependency on the insertion of the glycine-isoluecine pair in the TM domain that allows gain of function of the rh-tetherin when fused to the cpz-tetherin tail suggests that a global structural change in the orientation of the tetherin cytoplasmic tail was a prerequisite for the acquisition of signaling capacity. One caveat to the interpretation of these observations is that at present they have not been performed in the cells from their cognate primate species. Thus it is unknown whether any of the context dependency reflects species-specific differences in downstream cellular partners. Also whether similar signaling

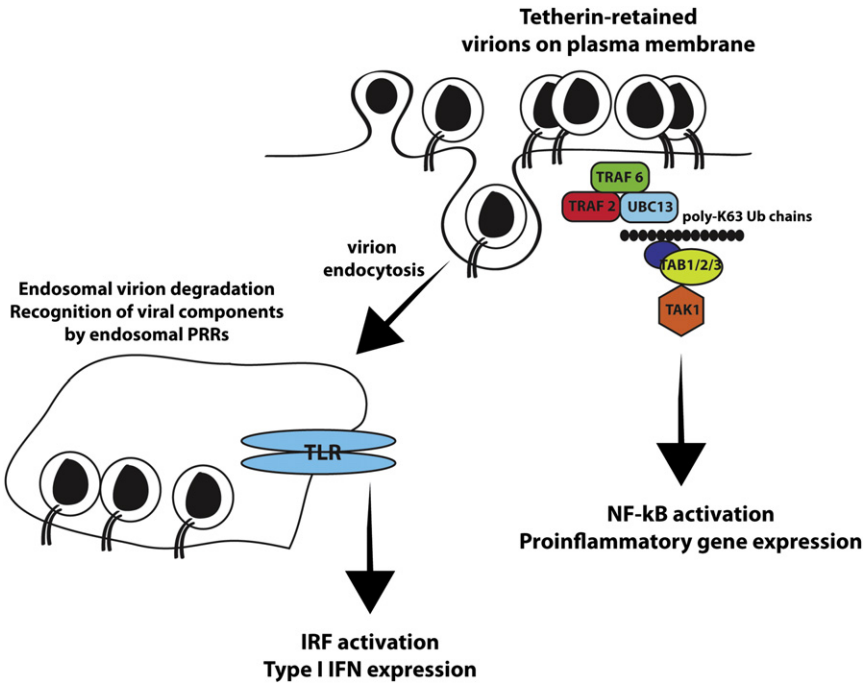

Figure 7. Model for Tetherin's Proinflammatory Activity

Clustering of tetherin dimers upon restriction of viral release promotes the recruitment of a signaling complex that includes TRAF6, and potentially TRAF2 and Ubc13 dependent on the YDYCRV motif in tetherin. This leads to the activation of TAK1, NFκB, and enhanced proinflammatory gene expression by the infected cells. Additionally, in primary HIV-1 target cells, virion retention and uptake potentially targets restricted virions to compartments where viral components are amenable to recognition by TLRs or other PRRs, thereby indirectly inducing type 1 IFN responses through the activation of IRFs.

attributes have developed in mammalian tetherins other than those tested here remains to be determined.

We propose the following model (Figure 7): tetherin-mediated virion retention triggers clustering of surface tetherin, targeting it for endocytic uptake. Coupled to this surface clustering, a signaling complex containing TRAF6 and perhaps TRAF2 is recruited to the tetherin cytoplasmic tail. What other factors are present in this complex, or whether it directly interacts with tetherin itself or an associated factor, remains to be determined. The recruited complex then activates TAK1 through the polymerization of ubiquitin chains dependent on Ubc13, which in turn leads to IKK phosphorylation, IκB degradation, and translocation of NFκB to the nucleus to activate proinflammatory gene expression. The data presented herein showing that late-domain mutants of retroviral particles cannot trigger tetherin signaling indicate that partitioning of tetherin into virions initiates signaling dependent on the physical separation of budding virions from the cell membrane. The topology of tetherin dimers that form the physical tether is not entirely clear (Perez-Caballero et al., 2009), but the evidence that they can transduce a signal implies that at least some tetherin dimers must remain with their cytoplasmic tails in the cytoplasm. Recently it was demonstrated that HIV-1 gp41 can also activate TAK1-dependent NFκB signaling to potentiate viral replication in CD4+ T cells (Postler and Desrosiers, 2012). Whether this underlies the lower level of responses that we see in wild-type infected cells is unknown, but may suggest that HIV-1 strikes a balance between maintaining sufficient NFκB activation for viral gene expression and suppressing proinflammatory responses derived from factors such as tetherin.

While tetherin activated only NFκB reporter genes in 293 cells, in some donors' T cells, tetherin-sensitive HIV-1 also induced detectable type 1 interferon secretion. Again this was tetherin dependent, as shRNAs against tetherin abolished it. Since Vpu is not a constituent of incoming viral particles, this tetherin dependence of type 1 IFN induction indicates that it requires a productive round of viral replication, rather than direct sensing of virion components from the inoculum. The upregulation of IFNβ by Vpu(−) HIV-1 and HIV-1 Vpu-A14L, but not CXCL10, was reduced by inhibitory peptides against TRIF, strongly suggesting TLR3 as the source, which is known to be expressed on some T cell subsets (Holm et al., 2009). As TLR3 resides primarily in endosomes(Takeuchi and Akira, 2010), these data suggest that immobilization and endocytic uptake of virions by tetherin may also lead to augmented recognition of viral components by membrane-associated PRRs expressed in primary HIV-1 target cells (for example, virion-associated RNA molecules that may be liberated upon virion degradation). Low levels of activated IRF3 could be detected in all virus-infected T cells 48 hr after infection, contrary to a recent study that suggested IRF3 itself is degraded by Vpu (Doehle et al., 2012). While purified HIV-1 particles do not directly induce strong inflammatory responses in most target cells, a recent study has indicated that HIV-infected cells can trigger interferon release from bystanders through the activation of IRF3 (Lepelly et al., 2011). This appears to be related to cell-to-cell transmission of fusion-competent virions, something that could conceivably be further augmented in this case by tetherin-mediated virion retention (Jolly et al., 2010). Finally, tetherin's identification as a regulator of TLR7 activity in plasmacytoid dendritic cells via the inhibitory leukocyte receptor ILT7 suggests that its signaling properties may have further roles in host-cell pattern recognition (Cao et al., 2009). The further characterization of virus-induced tetherin signaling in primary cells and the cellular factors involved will therefore determine the importance of this attribute in innate immunity.

Tetherin counteraction is conserved among human and primate lentiviruses, but the viral protein that performs this role varies (Le Tortorec et al., 2011). While tetherin restricts cell-free viral release, it poorly inhibits cell-to-cell viral transfer between CD4+ T cells (Casartelli et al., 2010; Jolly et al.,

2010), which likely represents a major route of viral spread in vivo (Jolly and Sattentau, 2004). This suggests that avoidance of tetherin-mediated restriction is required for initial viral transmission, and/or tetherin's antiviral activity imposes an additional inhibition of viral replication in vivo beyond simply blocking cell-free viral production. For example, accumulation of virions on cell surfaces by tetherin may promote recognition of infected cells through the deposition of antibodies and subsequent clearance by phagocytes. The acquisition of the coupling of tetherin activity to direct proinflammatory gene expression via NFκB activation may therefore significantly augment this by attracting other leukocytes to a site of infection. The threshold cellular levels of tetherin that can induce signaling may well be lower than those required for potent virion retention, providing further impetus for human viruses to efficiently remove tetherin from the PM. We note with interest that while the Nef and Env countermeasures of SIVs and HIV-2 do not promote tetherin degradation, HIV-1 Vpu does (Le Tortorec et al., 2011). Moreover, only Vpu proteins from the pandemic M Group of HIV-1 have acquired efficient tetherin counteraction (Sauter et al., 2009). Thus we speculate that the signaling activity of human tetherin that we have uncovered contributes to its role in the early innate response to HIV-1 and other viral infections, and may provide further selective pressure on enveloped viral pathogens to counteract its activity. The findings presented herein provide an intriguing example of a functional activity within a mediator of intrinsic viral defense that may have arisen to augment its overall potency in response to pressure by viral proteins that target its antiviral activity.

EXPERIMENTAL PROCEDURES

Plasmids and Cells

The molecular clones of HIV-1 NL4.3 and derived Vpu mutants have been described previously (Neil et al., 2006; Vigan and Neil, 2010). Tetherin mutants and species orthologs were made in pCR3.1 by standard molecular biological methods. Chimpanzee tetherin was provided by G. Towers (UCL). pCR3.1-GFP-EBoV Vp40, pMLV NCS (MLV), pMLVp6py, and pMLV NCS Δpy plasmids were provided by J. Martin-Serrano (KCL) (Martin-Serrano et al., 2004). The NFκB-dependent 3xkB-pCONA-FLuc reporter construct, the CMV-RLuc control plasmid, and human TRAF6 cDNAs were provided by A. MacDonald (Mankouri et al., 2010) (University of Leeds). TRAF6 was subcloned with an N-terminal HA tag into pCR3.1. The MAVS expression vector was provided by J. Luban (University of Geneva) and the IFNβ-promoter luciferase vectors by M. Malim.

293 and 293T cells were obtained from the ATCC, while the reporter cell line HeLa-TZMbl was provided by John Kappes through the NIH AIDS Reagents Repository Program (ARRP). All adherent cells were maintained in DMEM supplemented with 10% fetal calf serum (FCS) and gentamicin. Derivatives stably expressing human tetherin or mutants thereof were produced by transducing the cells with MLV-based retroviral vectors packaging a pLHCX (Clontech) vector genome encoding the tetherin construct and selecting the cells in hygromycin (Invitrogen).

Peripheral blood mononuclear cells were isolated from freshly drawn whole blood on Lymphoprep (Axis-Shield). CD4+ T cells were then purified using an Untouched CD4+ T cell Dynabead kit (Invitrogen), and then activated for 48 hr with anti-CD3/anti-CD28 Dynabeads (Invitrogen) prior to use and cultured in RPMI/10% FCS/gentamicin and 30 U/ml recombinant IL-2. CD4 and tetherin expression were determined by flow cytometry using anti-CD4 APC (Becton Dickinson) or anti-human BST2-PE (eBiosciences). HIV-1 infection of T cells was monitored by flow cytometry using an intracellular anti-p24-PE (Beckam Coulter) staining.

Reporter Gene Assays

For transient reporter gene assays, 10^5 293 cells were transfected with 50 ng of pCR3.1 tetherin plasmid or control pCR3.1 YFP in combination with 10 ng of 3xκB-pCONA-FLuc or IFNβ-luciferase reporter and 5 ng pCMV-RLuc. Forty-eight hours after transfection, firefly and Renilla luciferase activity in cell lysates was measured using a dual luciferase kit (Promega) and normalized. For antibody crosslinking experiments, 293 or 293THN cells were transfected with 10 ng of 3xκB-pCONA-FLuc and 5 ng pCMV-RLuc. Six hours later, the cells were treated with a 1:100 dilution of rabbit-anti-BST2 polyclonal Ab (Miyagi et al., 2009) (provided by K. Strebel through the NIH ARPP) followed by addition of a donkey anti-rabbit secondary. Cell lysates were taken at various time points thereafter and subjected to SDS-PAGE and western blot with rabbit anti-IκB-α (Cell Signaling), rabbit monoclonal anti-Phospho-IKKα/β (Ser176/180-clone 16A6, Cell Signaling), rabbit monoclonal anti-IRF3 (clone D83B9, Cell Signaling), rabbit monoclonal anti-Phospho-IRF3 (clone S396, Cell Signaling), rabbit anti-RelA, and rabbit anti-hsp90 (Santa Cruz Biotechnologies) and visualized either by Li-Cor apparatus using fluorophore-conjugated secondary antibody (IRDye 800 Goat anti-rabbi IRDye 680 Goat anti-mouse) or by ImageQuant using anti-rabbit HRP-linked secondary antibodies (NEB, UK). Luciferase activities were determined at 24 hr posttreatment.

For viral-mediated reporter gene assays, 293 or 293THN cells were transfected with 10 ng of 3xkB-pCONA-FLuc (or IFNβ luciferase reporter) and 5 ng pCMV-RLuc in combination with 500 ng pNL4.3, pNL4.3 Vpu mutant, pCR3.1-GFP-EBoV VP40), MLV, MLVΔPY, or MLVΔPY/p6 (Martin-Serrano et al., 2001. For experiments with MLV or derivatives, 200 ng of pCNCG and 100 ng of pVSV-G were cotransfected. Luciferase activities were measured 48 hr posttransfection. Infectivity of viral supernatants and biochemical analysis of cell lysates and viral particles were performed as described below in "Virus Stocks and Release Assays."

For transient knockdown of signaling components, 105 cells were seeded per well of a 24-well plate, and 6 hr later the cells were transfected with 50 pmol of siRNA in complex with Dharmofect-1 (Dharmacon). Forty-eight hours later, cells were reseeded and 6 hr later cotransfected with a second dose of siRNA alongside reporter constructs as per the transient reporter gene assays. The following siRNAs were used: from QIAGEN, MAP3K7_5 (TAK1) (SI00300741); TRAF2_7 (SI03096009) for TRAF2; TRAF6_7 and _8 (SI03046043 and SI03050145) for TRAF6; Dharmacon ON-TARGETplus SMARTpools for human AP2M1 (L-008170-00-0005) for AP2 and human UBE2N (L-003920-00-0005) for Ubc13 and siControl nontargeting pool (D-001810-10-20) as the siRNA control. Protein knockdowns were verified by western blot using the following antibodies: rabbit anti-TAK1, rabbit anti-TRAF2 (c192), rabbit anti-Ubc13 (Cell Signaling Technology), rabbit anti-TRAF6 (H274, Santa Cruz), and mouse anti-AP2μ1 (BD Biosciences).

Virus Stocks and Release Assays

HIV-1 NL4.3 and Vpu mutant viral stocks were produced in 293T cells by transient transfection, and endpoint titers were determined on HeLa-TZM indicator cells as described previously (Le Tortorec and Neil, 2009). For primary cell infections, viral stocks were treated for 2 hr with 10 U/ml DNase-I (Roche) and then concentrated by ultracentrifugation through a 20% sucrose/PBS cushion (30,000 rpm on a Sorvall SW41 rotor for 90 min) and resuspended in RPMI.

For viral release assays, CD4+ T cells were infected with HIV-1 NL4.3 or Vpu mutant at the required multiplicity, and washed. Forty-eight hours later, cell lysates and filtered viral supernatants were harvested. The infectivity of viral supernatants was determined on HeLa-TZMbl cells as described (Le Tortorec and Neil, 2009). MLV titers were determined by transducing 293T cells and enumerating the GFP-positive cells by FACS 48 hr later. HIV-1 particle release was determined by quantitative western blot, as described (Vigan and Neil, 2010).

Primary Cell Infections

5×10^5 activated CD4+ T cells were infected at a multiplicity of infection (moi) of 5 to ensure >90% p24+ cells 48 hr postinfection. Cells and supernatants were then harvested and assayed for viral gene expression, and virus particle production as described above. Cells were also harvested for total RNA and supernatants for cytokine production. When required, equal amounts of activated CD4+ T cells were transduced with lentiviral vectors (pCSGW) encoding

U6-driven shRNA-GFP, 5′-GUUCAUCUGCACCACCGGCAAGCUUCGGCUU GCCGGUGGUGCAGAUACUU-3′; or shRNA-THN, 5′-GGAGTTCTGGTG TTCCTGATTATTTCGATGATCAGGAGCACCGAATTCC-3′, provided by G. Towers (UCL) at an input equivalent to a moi of 5 when titered on 293T cells. The transduced cells were infected 24 hr later and harvested as described above. Surface tetherin levels were determined by flow cytometry at 48 hr posttransduction. For TLR inhibition studies, infected cells were cultured in the presence of 40 μM of control, TRIF, and MyD88-inhibitory peptides (Invivogen).

Quantitative RT-PCR

Total RNA was isolated and purified from transfected or infected cells using a QIAGEN RNeasy kit, and 50 ng of RNA was reverse transcribed by random hexamer priming using a High Capacity cDNA Reverse Transcription kit (ABI). Of the reaction, 5 μl was subjected to quantitative PCR using ABI primer/probe sets for human *Cxcl10*, *IL6*, *Ifnb*, and *Gapdh* in an ABIPrism 7900HT Sequence Detections System. Ct data was processed relative to the GAPDH control using the ABI RQ Manager 1.2 software.

Cytokine Production

Supernatants for infected T cells were analyzed for CXCL10 and IL-6 protein levels using specific Quantikine ELISAs (R+D Systems). Levels of bioactive type-I IFN were determined using HEK-Blue indicator cells (InVivoGen).

Immunoprecipitations

293 cells were transfected with 700 ng of HA-TRAF6 in combination with equal quantities of pCR3.1-GFP or pCR3.1 tetherin constructs. Forty-eight hours posttransfection, cells were lysed in 1% digitonin in 50 mM Tris-HCL (pH 7.4)/150 mM NaCl with protease inhibitors (Roche) and N-ethymaleimide. Postnuclear supernatants were immunoprecipitated with 5 μg of anti-HA.11 mAb (Covance) and protein G agarose beads (Invitrogen). Cell lysates and IPs were subjected to SDS-PAGE and western blots performed using rabbit anti-HA (Rockland) and rabbit anti-BST2 antibodies and visualized by Image-Quant using HRP-linked anti-rabbit secondary Abs (NEB, UK).

Ethics Statement

Ethical approval for the drawing of blood and preparation of leukocyte subsets from healthy donors following written informed consent was obtained through the King's College London Infectious Disease BioBank Local Research Ethics Committee (under the authority of the Southampton and South West Hampshire Research Ethics Committee—approval REC09/H0504/39), approval number SN-1/6/7/9.

SUPPLEMENTAL INFORMATION

Supplemental Information includes five figures and can be found with this article at http://dx.doi.org/10.1016/j.chom.2012.10.007.

ACKNOWLEDGMENTS

We thank Mike Malim, Juan Martin-Serrano, Caroline Goujon, and Sandra Diebold for helpful discussions, and Greg Towers, Jeremy Luban, Klaus Strebel, and the NIH ARRP for reagents. This study was funded by a Wellcome Research Career Development Fellowship (WT082274MA), an MRC project grant (G0801937), and latterly an ERC Starter Grant (to S.J.D.N.). R.P.G., A.L., S.P., and S.J.D.N. conceived the study. R.P.G., A.L., S.P., and T.K. performed the experiments. All authors analyzed the data. R.P.G., S.P., and S.J.D.N. wrote the manuscript.

Received: May 17, 2012
Revised: August 4, 2012
Accepted: October 1, 2012
Published: November 14, 2012

REFERENCES

Agromayor, M., Soler, N., Caballe, A., Kueck, T., Freund, S.M., Allen, M.D., Bycroft, M., Perisic, O., Ye, Y., McDonald, B., et al. (2012). The UBAP1 subunit of ESCRT-I interacts with ubiquitin via a SOUBA domain. Structure *20*, 414–428.

Cao, W., Bover, L., Cho, M., Wen, X., Hanabuchi, S., Bao, M., Rosen, D.B., Wang, Y.H., Shaw, J.L., Du, Q., et al. (2009). Regulation of TLR7/9 responses in plasmacytoid dendritic cells by BST2 and ILT7 receptor interaction. J. Exp. Med. *206*, 1603–1614.

Casartelli, N., Sourisseau, M., Feldmann, J., Guivel-Benhassine, F., Mallet, A., Marcelin, A.G., Guatelli, J., and Schwartz, O. (2010). Tetherin restricts productive HIV-1 cell-to-cell transmission. PLoS Pathog. *6*, e1000955. http://dx.doi.org/10.1371/journal.ppat.1000955.

Doehle, B.P., Chang, K., Rustagi, A., McNevin, J., McElrath, M.J., and Gale, M., Jr. (2012). Vpu mediates depletion of interferon regulatory factor 3 during HIV infection by a lysosome-dependent mechanism. J. Virol. *86*, 8367–8374.

Dubé, M., Paquay, C., Roy, B.B., Bego, M.G., Mercier, J., and Cohen, E.A. (2011). HIV-1 Vpu antagonizes BST-2 by interfering mainly with the trafficking of newly synthesized BST-2 to the cell surface. Traffic *12*, 1714–1729.

Gupta, R.K., Hué, S., Schaller, T., Verschoor, E., Pillay, D., and Towers, G.J. (2009). Mutation of a single residue renders human tetherin resistant to HIV-1 Vpu-mediated depletion. PLoS Pathog. *5*, e1000443. http://dx.doi.org/10.1371/journal.ppat.1000443.

Holm, C.K., Petersen, C.C., Hvid, M., Petersen, L., Paludan, S.R., Deleuran, B., and Hokland, M. (2009). TLR3 ligand polyinosinic:polycytidylic acid induces IL-17A and IL-21 synthesis in human Th cells. J. Immunol. *183*, 4422–4431.

Janvier, K., Pelchen-Matthews, A., Renaud, J.B., Caillet, M., Marsh, M., and Berlioz-Torrent, C. (2011). The ESCRT-0 component HRS is required for HIV-1 Vpu-mediated BST-2/tetherin down-regulation. PLoS Pathog. *7*, e1001265. http://dx.doi.org/10.1371/journal.ppat.1001265.

Jia, B., Serra-Moreno, R., Neidermyer, W., Rahmberg, A., Mackey, J., Fofana, I.B., Johnson, W.E., Westmoreland, S., and Evans, D.T. (2009). Species-specific activity of SIV Nef and HIV-1 Vpu in overcoming restriction by tetherin/BST2. PLoS Pathog. *5*, e1000429. http://dx.doi.org/10.1371/journal.ppat.1000429.

Jolly, C., and Sattentau, Q.J. (2004). Retroviral spread by induction of virological synapses. Traffic *5*, 643–650.

Jolly, C., Booth, N.J., and Neil, S.J. (2010). Cell-cell spread of human immunodeficiency virus type 1 overcomes tetherin/BST-2-mediated restriction in T cells. J. Virol. *84*, 12185–12199.

Jouvenet, N., Neil, S.J., Zhadina, M., Zang, T., Kratovac, Z., Lee, Y., McNatt, M., Hatziioannou, T., and Bieniasz, P.D. (2009). Broad-spectrum inhibition of retroviral and filoviral particle release by tetherin. J. Virol. *83*, 1837–1844.

Kueck, T., and Neil, S.J. (2012). A cytoplasmic tail determinant in HIV-1 Vpu mediates targeting of tetherin for endosomal degradation and counteracts interferon-induced restriction. PLoS Pathog. *8*, e1002609. http://dx.doi.org/10.1371/journal.ppat.1002609.

Lau, D., Kwan, W., and Guatelli, J. (2011). Role of the endocytic pathway in the counteraction of BST-2 by human lentiviral pathogens. J. Virol. *85*, 9834–9846.

Le Tortorec, A., and Neil, S.J. (2009). Antagonism to and intracellular sequestration of human tetherin by the human immunodeficiency virus type 2 envelope glycoprotein. J. Virol. *83*, 11966–11978.

Lepelly, A., Louis, S., Sourriseau, M., Law, H.K., Pothlichet, J., Schilte, C., Chaperot, L., Plumas, J., Randall, R.E., Si-Tahar, M., et al. (2011). Innate sensing of HIV-infected cells. PLoS Pathog. *7*, e10011284. http://dx.doi.org/10.1371/journal.ppat.1001284.

Le Tortorec, A., Willey, S., and Neil, S.J. (2011). Antiviral inhibition of enveloped virus release by tetherin/BST-2: action and counteraction. Viruses *3*, 520–540.

Liberatore, R.A., and Bieniasz, P.D. (2011). Tetherin is a key effector of the antiretroviral activity of type I interferon in vitro and in vivo. Proc. Natl. Acad. Sci. USA *108*, 18097–18101.

Lim, E.S., Malik, H.S., and Emerman, M. (2010). Ancient adaptive evolution of tetherin shaped the functions of Vpu and Nef in human immunodeficiency virus and primate lentiviruses. J. Virol. *84*, 7124–7134.

Mankouri, J., Fragkoudis, R., Richards, K.H., Wetherill, L.F., Harris, M., Kohl, A., Elliott, R.M., and Macdonald, A. (2010). Optineurin negatively regulates

the induction of IFNbeta in response to RNA virus infection. PLoS Pathog. *6*, e1000778. http://dx.doi.org/10.1371/journal.ppat.1000778.

Martin-Serrano, J., and Neil, S.J. (2011). Host factors involved in retroviral budding and release. Nat. Rev. Microbiol. *9*, 519–531.

Martin-Serrano, J., Zang, T., and Bieniasz, P.D. (2001). HIV-1 and Ebola virus encode small peptide motifs that recruit Tsg101 to sites of particle assembly to facilitate egress. Nat. Med. *7*, 1313–1319.

Martin-Serrano, J., Perez-Caballero, D., and Bieniasz, P.D. (2004). Context-dependent effects of L domains and ubiquitination on viral budding. J. Virol. *78*, 5554–5563.

Matsuda, A., Suzuki, Y., Honda, G., Muramatsu, S., Matsuzaki, O., Nagano, Y., Doi, T., Shimotohno, K., Harada, T., Nishida, E., et al. (2003). Large-scale identification and characterization of human genes that activate NF-kappaB and MAPK signaling pathways. Oncogene *22*, 3307–3318.

McNatt, M.W., Zang, T., Hatziioannou, T., Bartlett, M., Fofana, I.B., Johnson, W.E., Neil, S.J., and Bieniasz, P.D. (2009). Species-specific activity of HIV-1 Vpu and positive selection of tetherin transmembrane domain variants. PLoS Pathog. *5*, e1000300. http://dx.doi.org/10.1371/journal.ppat.1000300.

Miyagi, E., Andrew, A.J., Kao, S., and Strebel, K. (2009). Vpu enhances HIV-1 virus release in the absence of Bst-2 cell surface down-modulation and intracellular depletion. Proc. Natl. Acad. Sci. USA *106*, 2868–2873.

Neil, S.J., Eastman, S.W., Jouvenet, N., and Bieniasz, P.D. (2006). HIV-1 Vpu promotes release and prevents endocytosis of nascent retrovirus particles from the plasma membrane. PLoS Pathog. *2*, e39. http://dx.doi.org/10.1371/journal.ppat.0020039.

Neil, S.J., Sandrin, V., Sundquist, W.I., and Bieniasz, P.D. (2007). An interferon-alpha-induced tethering mechanism inhibits HIV-1 and Ebola virus particle release but is counteracted by the HIV-1 Vpu protein. Cell Host Microbe *2*, 193–203.

Neil, S.J., Zang, T., and Bieniasz, P.D. (2008). Tetherin inhibits retrovirus release and is antagonized by HIV-1 Vpu. Nature *451*, 425–430.

Perez-Caballero, D., Zang, T., Ebrahimi, A., McNatt, M.W., Gregory, D.A., Johnson, M.C., and Bieniasz, P.D. (2009). Tetherin inhibits HIV-1 release by directly tethering virions to cells. Cell *139*, 499–511.

Pertel, T., Hausmann, S., Morger, D., Züger, S., Guerra, J., Lascano, J., Reinhard, C., Santoni, F.A., Uchil, P.D., Chatel, L., et al. (2011). TRIM5 is an innate immune sensor for the retrovirus capsid lattice. Nature *472*, 361–365.

Postler, T.S., and Desrosiers, R.C. (2012). The cytoplasmic domain of the HIV-1 glycoprotein gp41 induces NF-κB activation through TGF-β-activated kinase 1. Cell Host Microbe *11*, 181–193.

Rollason, R., Korolchuk, V., Hamilton, C., Schu, P., and Banting, G. (2007). Clathrin-mediated endocytosis of a lipid-raft-associated protein is mediated through a dual tyrosine motif. J. Cell Sci. *120*, 3850–3858.

Sauter, D., Schindler, M., Specht, A., Landford, W.N., Münch, J., Kim, K.A., Votteler, J., Schubert, U., Bibollet-Ruche, F., Keele, B.F., et al. (2009). Tetherin-driven adaptation of Vpu and Nef function and the evolution of pandemic and nonpandemic HIV-1 strains. Cell Host Microbe *6*, 409–421.

Schmidt, S., Fritz, J.V., Bitzegeio, J., Fackler, O.T., and Keppler, O.T. (2011). HIV-1 Vpu blocks recycling and biosynthetic transport of the intrinsic immunity factor CD317/tetherin to overcome the virion release restriction. MBio *2*, e00036-e11. http://dx.doi.org/10.1128/mBio.00036-11, Print 2011.

Serra-Moreno, R., Jia, B., Breed, M., Alvarez, X., and Evans, D.T. (2011). Compensatory changes in the cytoplasmic tail of gp41 confer resistance to tetherin/BST-2 in a pathogenic nef-deleted SIV. Cell Host Microbe *9*, 46–57.

Skaug, B., Jiang, X., and Chen, Z.J. (2009). The role of ubiquitin in NF-kappaB regulatory pathways. Annu. Rev. Biochem. *78*, 769–796.

Takeuchi, O., and Akira, S. (2010). Pattern recognition receptors and inflammation. Cell *140*, 805–820.

Tokarev, A.A., Munguia, J., and Guatelli, J.C. (2011). Serine-threonine ubiquitination mediates downregulation of BST-2/tetherin and relief of restricted virion release by HIV-1 Vpu. J. Virol. *85*, 51–63.

Vigan, R., and Neil, S.J. (2010). Determinants of tetherin antagonism in the transmembrane domain of the human immunodeficiency virus type 1 Vpu protein. J. Virol. *84*, 12958–12970.

Zhang, F., Wilson, S.J., Landford, W.C., Virgen, B., Gregory, D., Johnson, M.C., Munch, J., Kirchhoff, F., Bieniasz, P.D., and Hatziioannou, T. (2009). Nef proteins from simian immunodeficiency viruses are tetherin antagonists. Cell Host Microbe *6*, 54–67.